frontiers | Research Topics

Ecological distribution, functional diversity, and the biogeochemical cycle of microorganisms in karst

Edited by
Hongchen Jiang, Xiangyu Guan, Werner W. E. Müller and Qiang Li

Published in
Frontiers in Microbiology

ISSN 1664-8714
ISBN 978-2-8325-3350-5
DOI 10.3389/978-2-8325-3350-5

About Frontiers

Frontiers is more than just an open access publisher of scholarly articles: it is a pioneering approach to the world of academia, radically improving the way scholarly research is managed. The grand vision of Frontiers is a world where all people have an equal opportunity to seek, share and generate knowledge. Frontiers provides immediate and permanent online open access to all its publications, but this alone is not enough to realize our grand goals.

Frontiers journal series

The Frontiers journal series is a multi-tier and interdisciplinary set of open-access, online journals, promising a paradigm shift from the current review, selection and dissemination processes in academic publishing. All Frontiers journals are driven by researchers for researchers; therefore, they constitute a service to the scholarly community. At the same time, the *Frontiers journal series* operates on a revolutionary invention, the tiered publishing system, initially addressing specific communities of scholars, and gradually climbing up to broader public understanding, thus serving the interests of the lay society, too.

Dedication to quality

Each Frontiers article is a landmark of the highest quality, thanks to genuinely collaborative interactions between authors and review editors, who include some of the world's best academicians. Research must be certified by peers before entering a stream of knowledge that may eventually reach the public - and shape society; therefore, Frontiers only applies the most rigorous and unbiased reviews. Frontiers revolutionizes research publishing by freely delivering the most outstanding research, evaluated with no bias from both the academic and social point of view. By applying the most advanced information technologies, Frontiers is catapulting scholarly publishing into a new generation.

What are Frontiers Research Topics?

Frontiers Research Topics are very popular trademarks of the *Frontiers journals series*: they are collections of at least ten articles, all centered on a particular subject. With their unique mix of varied contributions from Original Research to Review Articles, Frontiers Research Topics unify the most influential researchers, the latest key findings and historical advances in a hot research area.

Find out more on how to host your own Frontiers Research Topic or contribute to one as an author by contacting the Frontiers editorial office: frontiersin.org/about/contact

Ecological distribution, functional diversity, and the biogeochemical cycle of microorganisms in karst

Topic editors

Hongchen Jiang — China University of Geosciences Wuhan, China

Xiangyu Guan — China University of Geosciences, China

Werner W. E. Müller — University Medical Centre, Johannes Gutenberg University Mainz, Germany

Qiang Li — Institute of Karst Geology, Chinese Academy of Geological Sciences, China

Citation

Jiang, H., Guan, X., Müller, W. W. E., Li, Q., eds. (2023). *Ecological distribution, functional diversity, and the biogeochemical cycle of microorganisms in karst*. Lausanne: Frontiers Media SA. doi: 10.3389/978-2-8325-3350-5

Table of contents

frontiers | Frontiers in Microbiology

TYPE Editorial
PUBLISHED 11 August 2023
DOI 10.3389/fmicb.2023.1265640

OPEN ACCESS

EDITED AND REVIEWED BY
Paola Grenni,
National Research Council, Italy

*CORRESPONDENCE
Xiangyu Guan
guanxy@cugb.edu.cn

RECEIVED 23 July 2023
ACCEPTED 02 August 2023
PUBLISHED 11 August 2023

CITATION
Guan X, Li Q, Jiang H and Müller WEG (2023) Editorial: Ecological distribution, functional diversity, and the biogeochemical cycle of microorganisms in karst.
Front. Microbiol. 14:1265640.
doi: 10.3389/fmicb.2023.1265640

Editorial: Ecological distribution, functional diversity, and the biogeochemical cycle of microorganisms in karst

Xiangyu Guan[1]*, Qiang Li[2], Hongchen Jiang[1] and Werner E. G. Müller[3]

[1]School of Ocean Sciences, China University of Geosciences (Beijing), Beijing, China, [2]Key Laboratory of Karst Ecosystem and Treatment of Rocky Desertification, Ministry of Natural Resources, Key Laboratory of Karst Dynamics, Ministry of Natural Resources & Guangxi, Institute of Karst Geology, Chinese Academy of Geological Sciences, Guilin, China, [3]ERC Advanced Investigator Grant Research Group at the Institute for Physiological Chemistry, University Medical Center of the Johannes Gutenberg University, Mainz, Germany

KEYWORDS

microbiology community, bacteria, archaea, fungi, virus, diversity of functions, biomineralization, desertification

Editorial on the Research Topic
Ecological distribution, functional diversity, and the biogeochemical cycle of microorganisms in karst

Karst ecosystems are an important part of the Earth surface system, and contribute significantly to global and regional climate and environmental changes. Karst ecosystems are inhabited by abundant and diverse microorganisms, which are extensively involved in the biogeochemical cycle of elements. Therefore, it is vital to investigate the identity, functions, interactions with environments, and ecological roles of microorganisms in Karst ecosystems. Recently, with the use of new technologies (next-generation sequencing, different omics) and the intersection with other disciplines (such as mineralogy and geochemistry), the research on microbial ecology and biogeochemistry in these ecosystems has made ever-changing achievements in many aspects, such as the formation mechanism of microbial community, microbial interactions, biogeochemical cycle processes of elements mediated by microorganisms and their influence on mineralization and weathering of carbonate rock surface, changes of karst landform caused by microbial action, and microbial involvement in carbon cycle and its environmental impact and feedback. In short, microorganisms play an important role in the material and energy cycles in karst systems. Therefore, the study of microbial community composition and ecological function in karst system has attracted extensive attention. Without knowing the CO_2 balance in the atmosphere, especially over the karst-rich areas, like in Spain or in China, it is not possible to set up a reliable prediction of eco-commercial predictions.

In this Research Topic, 13 articles are here included, 10 and 3 articles on soil and water environments in karst ecosystems, respectively. We are grateful to all authors who contributed to this Research Topic. We are also grateful to all reviewers, handling editors and editorial staff who contributed during the editing and article production processes.

Among the articles related to studies on karst soil environments, Cheng et al. characterized and analyzed microbial communities, keystone taxa and the predicted ecological functions from three niches including weathered rock, sediment, and drip water inside the Heshang Cave (Central China) and three types of soils overlying the cave (forest soil, farmland soil, and pristine karst soil). Li Q. et al. investigated microbial structure patterns from bulk soil in A layer (0–10 cm) and B layer (10–20 cm) along altitudinal gradients in one karst graben basin of Yunnan-Kweichow Plateau. Jiang et al. reported that the structure, keystone taxa, assembly mechanism of bacterial and fungal communities and their relationships with environmental factors in one unique karst Tiankeng environment (the world's deepest sinkhole and the largest in the Shaanxi cluster, located in Fengjie County of Chongqing, southwestern China). Chen et al. reveal that soil nutrient content differences play an important role in regulating the cyanobacterial diversity and composition for further research and application of soil ecological restoration of cyanobacteria in biological soil crusts of karst desertification areas (in the Guizhou Plateau, southwestern China). Zhang et al. found that soil types played a predominant role in shaping rhizosphere microbial communities in northern tropical karst and non-karst seasonal rainforests. Sun et al. proposed that the different variations in microbial communities during bamboo invasion may be related to the influence of invasive bamboo on the soil properties such as pH, contents of organic matter and total phosphorus at different invasion stages. Hu et al. indicated that the magnesium-modified citrus peel biochar inhibited the organic carbon mineralization in citrus orchard soils and was more favorable to the increase of soil organic carbon fraction. Pu et al. investigated the effects of mixed application of different ratios of N fertilizer and green manure on the soil microbial community and rice yield in one karst paddy area, and found that the combined application of N fertilizer and green manure reduced the complexity of soil microbial network. On the basis of the rice yield, the authors recommend that nitrogen application should be reduced by 20–40% for rice production in ecologically sensitive karst areas. Li Y. et al. investigated soil chemical properties and microbial community stability in karst mountain soils, and showed that organ mineral fertilizer could replace chemical fertilizers or common organic fertilizers in terms of improving soil fertility and increasing crop yield and quality. Ning et al. showed that bacteria including coliforms can survive for a long time in karst soils overlying karst rocks and were unable to prevent bacteria from infiltrating into groundwater.

Among the articles related to studies on karst water environments, Liang et al. disclosed that microbial activity or the input of anthropogenic acids potentially affect carbonate dissolution, eventually altering the hydraulic properties of karst aquifers. Guan et al. revealed that there were significant annual and seasonal changes in the physicochemical properties and microbial communities of karst river, and antibiotics and inorganic nitrogen pollution indirectly affected the cycles of nitrogen and sulfur elements through microbial ecological modules. Zhong et al. found that in karst groundwater, the community assembly of a few abundant taxa was shaped by deterministic processes, especially homogeneous selection, while that of a large number of rare taxa was controlled by stochastic processes.

The collection of papers on the important karst terrestrial and biotic cycles will surely contribute to a further awareness of those beautiful, natural and biotic communities.

We are delighted to publish this Research Topic in Frontiers in Microbiology. We hope that this Research Topic will be interesting and useful to the readers of the journal, and broaden the knowledge of karst environment. The findings presented in this Research Topic are exciting, but still limited. In the future, the application of innovative research technologies and intensive and in-depth international collaboration will undoubtedly unveil more exciting aspects of karst ecosystem. Based on the data given in the papers research on karst biocoenosis will achieve and surpass new frontiers.

Author contributions

XG: Writing—original draft. QL: Writing—review and editing. HJ: Writing—review and editing. WM: Writing—review and editing.

Funding

This work was supported by the National Natural Science Foundation of China (Project Nos: 42172336 awarded to XG and 42172341 awarded to QL) and the Key Research and Development Program of Guangxi (GuiKeAD20297091).

Conflict of interest

The authors declare that the research was conducted in the absence of any commercial or financial relationships that could be construed as a potential conflict of interest.

Publisher's note

frontiers | Frontiers in Microbiology

TYPE Original Research
PUBLISHED 19 October 2022
DOI 10.3389/fmicb.2022.1002198

OPEN ACCESS

EDITED BY
Xiangyu Guan,
China University of Geosciences, China

REVIEWED BY
J. D. Lewis,
Fordham University, United States
Hongmei Wang,
China University of Geosciences Wuhan, China
Yu Shi,
Henan University, China

*CORRESPONDENCE
Wei Shui
shuiwei@fzu.edu.cn

SPECIALTY SECTION
This article was submitted to Terrestrial Microbiology, a section of the journal Frontiers in Microbiology

RECEIVED 24 July 2022
ACCEPTED 01 September 2022
PUBLISHED 19 October 2022

CITATION
Jiang C, Liu Y, Li H, Zhu S, Sun X, Wu K and Shui W (2022) The characterization of microbial communities and associations in karst tiankeng.
Front. Microbiol. 13:1002198.
doi: 10.3389/fmicb.2022.1002198

The characterization of microbial communities and associations in karst tiankeng

Cong Jiang[1], Yuanmeng Liu[2], Hui Li[2], Sufeng Zhu[3], Xiang Sun[2], Kexing Wu[2] and Wei Shui[2]*

[1]College of Urban and Environmental Sciences, Peking University, Beijing, China, [2]College of Environment and Safety Engineering, Fuzhou University, Fuzhou, China, [3]Ecology and Nature Conservation Institute, Chinese Academy of Forestry, Beijing, China

The karst tiankeng is a special and grand negative terrain on the surface, that maintains a unique ecosystem. However, knowledge about bacterial and fungal communities in karst tiankengs is still limited. Therefore, soil samples from five karst tiankengs were collected and subjected to high-throughput sequencing of 16S rRNA and ITS genes, and multivariate statistical analysis. The results showed abundant and diversified bacterial and fungal communities in karst tiankeng. The bacterial communities were dominated by *Proteobacteria* and *Acidobacteria*, and the fungal communities were dominated by *Ascomycota* and *Basidiomycota*. Statistical analysis revealed significant differences in bacterial and fungal communities among the five karst tiankengs, which may indicate that the distribution of bacterial and fungal communities was driven by separate karst tiankengs. The co-occurrence network structure was characterized by highly modularized assembly patterns and more positive interactions. The keystone taxa were mainly involved in nutrient cycling and energy metabolism. The null model analysis results showed that the stochastic process, especially dispersal limitation, tended to be more important in controlling the development of bacterial and fungal communities in karst tiankeng. The bacterial community structure was significantly associated with soil properties (SWC, TN, AN, and BD), while the fungal community structure was significantly associated with soil properties (SWC and TP) and plant diversity. These results can expand our knowledge of the karst tiankeng microbiome.

KEYWORDS

unique habitat, co-occurrence network, amplicon sequencing, karst tiankeng, microbiome

Introduction

Carbonate rocks are the material basis for the development of karst landforms, with a total distribution area of 3.44 million km^2 in China, accounting for approximately 1/3 of the country's land area (Yuan, 2005). China has the largest karst region in the world (Zhu and Chen, 2005). The karst tiankeng is a typical karst landscape that develops in specific

karst geological, geomorphological, climatic, and hydrological environments (Zhu and Waltham, 2005; Shui et al., 2015). The latest research defines karst tiankengs as karst closed pits with a width and depth of more than 100 m, a small ratio of diameter to depth, a continuous circumference, and vertical or subvertical walls (Gunn, 2019). It can be seen that karst tiankeng is a large-scale negative topographic geological wonder on the surface. China is the karst tiankeng kingdom, accounting for more than 70% of the total number of karst tiankengs (Pu et al., 2017). Karst tiankeng tends to appear in groups and form complex cave-hydrogeological systems with underground rivers and caves (Xu et al., 2009; Shui et al., 2015).

Because karst tiankengs are characterized deep into the surface and cliffs, the internal habitat of karst tiankengs is relatively independent of the land surface environment, with unique hydrothermal conditions and primitive microclimates (Zhu and Chen, 2005; Pu et al., 2019). The unique habitat of karst tiankengs serves as an environment for an abundant and unique resource of animals, plants, and microorganisms (Batori et al., 2017; Su et al., 2017; Jian et al., 2018; Jiang et al., 2022a). Karst ecosystems are well known to be characterized by soil erosion, poor soil nutrients, and biodiversity loss (Clements et al., 2006). The karst tiankeng are similar to "oases" in degraded landscapes and play an important role in karst ecosystems. Existing studies have demonstrated that karst tiankengs are important repositories for plant diversity conservation (Su et al., 2017; Chen et al., 2018b; Shui et al., 2022). As the engine of biogeochemical cycles, the role of soil microorganisms in karst tiankengs cannot be ignored (Balser and Firestone, 2005; Fierer, 2017). Meta-analyses have shown that microbial communities are significantly affected by the habitat environment (Delmont et al., 2011; Wang et al., 2013). Due to their nutrient-rich conditions, microbial communities thrive in karst tiankengs, with higher alpha diversity of microbial communities than land surface habitats (Pu et al., 2019; Jiang et al., 2021). The DSE (dark septate endophyte) resources in Dashiwei karst tiankeng were abundant and some of them possess positive effects on plant growth (Lan et al., 2017). In addition, karst tiankengs resemble a natural open top chamber (OTC) and are ideal for studying the response of terrestrial ecosystems, especially fragile karst ecosystems, to climate warming (Yang et al., 2019). Climate warming will alter soil microbial community structure and activities, which is critical to ecosystem functioning and stability (Yuan et al., 2021). The study of microbial communities in karst tiankeng ecosystems can deepen our understanding of global microbial diversity.

The preliminary study of microorganisms in karst tiankeng focused on the macrofungal species and plant fungi (Deng and Wu, 2014; Lan et al., 2017). Jiang et al. (2014) isolated strains with high keratinase yield in karst tiankeng soil through traditional culture techniques, which had the best effect on feather protein degradation. With the advent of high-throughput sequencing technology, the soil microbial community structure and functionality in karst tiankengs have been gradually discovered (Pu et al., 2019; Jiang et al., 2022a,b). The soil microbial communities of karst tiankeng exhibit significant habitat heterogeneity. However, these studies tend to be limited to characterizing soil microbial communities in karst tiankeng, ignoring the interactions of karst tiankeng microbes. In isolated karst tiankeng ecosystems, microbial community survival activity and interactions are critical to ecosystem stability. However, our understanding of the characterization of the microbiome and interactions of karst tiankeng remains poorly understood. Molecular ecological network (MEN) models based on stochastic matrix theory (RMT) can better simulate the interaction between different species in the community (Deng et al., 2012; Yuan et al., 2021). Microbial interactions constrain their ecological functions *via* competition, syntrophism, or symbiosis (He et al., 2017; de Vries et al., 2018). The abundant soil nutrients, plant cover, and unique microclimates may distinguish the microbial trophic structures of karst tiankeng ecosystems from those of general terrestrial ecosystems. Understanding how microbial co-occurrence patterns occur in separate karst tiankeng ecosystems is urgently needed.

In this study, soil samples were collected from five karst tiankengs in the Zhanyi karst tiankeng group and subjected to high-throughput sequencing of bacterial 16S rRNA and fungal ITS1 genes and multivariate statistical analysis. The main purposes of this study were: (i) to determine the taxonomic composition and structure of microbial communities in karst tiankeng, (ii) to evaluate the microbial co-occurrence patterns and assembly processes of bacterial and fungal communities in karst tiankeng, and (iii) to determine the key factors driving bacterial and fungal communities in karst tiankeng.

Materials and methods

Sample collection and measurement

We carried out this study in 2021 in Zhanyi District, Qujing City, Yunnan Province, China; the study was performed at Haifeng Natural Reserve (25°35′-25°57′N, 103°29′-103°39′E). The Zhanyi karst tiankeng group includes dozens of karst tiankengs of varying sizes. The annual precipitation ranges from 1073.5 to 1089.7 mm and is affected by the subtropical highland monsoon climate. The annual temperatures ranges from 13.8 to 14.0°C. The soil type was Yunnan red soil.

Among the Zhanyi karst tiankeng group, we selected five karst tiankengs, including Bajiaxiantang (BJXT), Shaojiaxiantang (SJXT), Shenxiantang (SXT), Wangjiaxiantang (WJXT), and Xiaotiankeng (XTK; Supplementary Figure 1). All five karst tiankengs are scattered in inaccessible areas, and only local residents occasionally enter these karst tiankengs, so they are largely kept in pristine conditions. The morphological characteristics of these five karst tiankengs are listed in Supplementary Table 1. Since the XTK slope is a vertical cliff, the seven sampling sites are all located at the bottom of the karst tiankeng. Of the other four karst tiankengs, the eight sampling sites include two at the bottom of the tiankeng and six at the slope

of the tiankeng. Each sampling ($10 \times 10\,m^2$) included three randomly established quadrats ($1 \times 1\,m^2$). The plant species richness (*R*) and Shannon-Wiener (*H′*) index were calculated (Pan et al., 2014). The soil samples (0–15 cm soil layer) were collected and mixed as a composite soil sample. The soil samples were sieved (2 mm), divided into two parts, and transferred at 4°C. One part was for DNA extraction, and the other part was for soil physicochemical analyses. The ring sampler weighing method was used to measure the soil bulk density (BD). The soil water content (SWC) was determined by the gravimetric method. Soil pH was determined using a glass electrode meter (InsMark™ IS126, Shanghai, China) in a 1:2.5 soil:water (w/v) mixture. The soil organic carbon (SOC) and soil total nitrogen (TN) were determined by potassium dichromate oxidation and the Kjeldahl method, respectively. The available nitrogen (AN) was measured by the alkali-diffusion method. Soil determination of total phosphorus (TP) and available phosphorus (AP) was performed by alkali fusion-Mo-Sb anti-spectrophotometric and sodium hydrogen carbonate solution-Mo-Sb anti-spectrophotometric methods, respectively. The total potassium (TK) was determined by alkali fusion-atomic absorption spectrophotometry methods. The available potassium (AK) was measured by the acid fusion-atomic absorption spectrophotometry method.

DNA extraction and PCR amplification

Total DNA was extracted using the CTAB method in accordance with the instructions. The concentration and purity of DNA were examined with 1% agarose gel. The primer set of 515F (5'-GTGCCAGCMGCCGCGGTAA-3′) and 806R (5'-GGACTACHVGGGTWTCTAAT-3′) targeting the bacterial 16S rRNA V4 region and ITS3F (5'-GCATCGATGAAGAACGCAGC) and ITS4R (5'-TCCTCCGCTTATTGATATGC) targeting the fungal IST2 region were used for bacterial and fungal genes sequencing, respectively (Caporaso et al., 2012; Jamil et al., 2020). The bacterial and fungal genes were amplified on Phusion® High-Fidelity PCR Master Mix (New England Biolabs). All the raw sequence reads were conducted using an Illumina NovaSeq 6,000 PE250 platform (Illumina, San Diego, CA, United States). All sequence data are deposited on the NCBI and accessible *via* BioProject IDs of PRJNA851199 for 16S sequences and PRJNA861802 for ITS sequences.

Data processing and bioinformatics analysis

The QIIME2 system was used for raw data FASTQ files filtered and analyzed (Vazquez-Baeza et al., 2013; Bokulich et al., 2018). The demultiplexed sequences were quality filtered, trimmed, denoised, and merged, and then the chimeric sequences were obtained. After identification and removal by the QIIME2 dada2 plugin, the bacterial ASVs were obtained. Vsearch (2.15.1) software was used to identify the optimized sequences with 95% similarity into fungal OTUs. The representative bacterial sequences were taxonomically classified by alignment against the GREENGENES database. The fungal sequences were taxonomically classified by alignment against the UNITE database (Nilsson et al., 2019).

A Venn diagram was drawn using the R (v 4.1.2) package "plotrix." The Sankey diagram was generated using the JShare online platform.[1] The microbial diversity index (Shannon-Wiener and Chao1) was calculated by a core-diversity plugin of QIIME2. The analysis of similarities (ANOSIM) and nonmetric multidimensional scaling (NMDS) were performed using the R (v 4.1.2) package "vegan" (Dixon, 2003). The construction of the molecular ecological networks (MEN) of bacterial and fungal communities was based on the principle of the Molecular Ecological Network Analyses Pipeline (Zhou et al., 2010; Deng et al., 2012). Random matrix theory (RMT) was used to determine the appropriate similarity threshold (St) of molecular ecological networks (Deng et al., 2012). The calculation order follows the rules of decreasing the cutoff from the top, and scan speed refers to the method of regress Poisson distribution only. Cytoscape software (v 3.9.0) was used to visualize the co-occurrence microbial network. The within-module connectivity (Zi) and among-module connectivity (Pi) represent the ecological attributes of the network nodes (Rottjers and Faust, 2018). The network node topologies were classified as peripherals ($Zi < 2.5$ and $Pi < 0.62$), connectors ($Zi < 2.5$ and $Pi \geq 0.62$), module hubs ($Zi \geq 2.5$ and $Pi \leq 0.62$), and network hubs ($Zi \geq 2.5$ and $Pi \geq 0.62$). The connectors, module hubs, and network hubs acted as keystone taxa in the co-occurrence microbial network (He et al., 2017). To determine the ecological processes, phylogenetic and null model analyses were performed (Stegen et al., 2012, 2013). The phylogenic turnover across soil samples was measured by the weighted β-nearest taxon index (βNTI) using the R (v 4.1.2) package "picante" (Kembel et al., 2010). Ecological processes were divided into deterministic processes with $|\beta NTI|$ values above 2 and stochastic processes with $|\beta NTI|$ values below 2. If $\beta NTI > 2$, variable selection plays crucial roles in shaping microbial communities. If $\beta NTI < -2$, homogeneous selection is the key assembly process in the microbial community. To further discern the stochastic processes, the Raup–Crick matrix (RCbray) was analyzed *via* the "vegan" package. The conditions of $RCbray > 0.95$, $|RCbray| < 0.95$, and $RCbray < -0.95$ indicated drift, undominated processes, and homogenizing dispersal, respectively. Redundancy analysis (RDA) of bacterial or fungal communities and soil and plant properties was conducted in the R (v 4.1.2) package "vegan." The selection principle of the RDA or CCA model was based on the results of DCA analysis; if the length was >4.0, the CCA model was chosen. Otherwise, the RDA model should be selected. In this study, the value of bacterial sample data was <4.0; thus, RDA was selected. A fungal sample date >4.0 was chosen; thus, CCA was

1 https://jshare.com.cn/demos/eYEsqk

chosen. The Mantel test was used to discern correlations among the bacterial and fungal communities and soil and plant properties based on the Spearman correlation coefficient, and was performed using the R (v 4.1.2) package "vegan." The data were assessed for normality and homogeneity of variances, and ANOVAs were performed at the 95% confidence level. The ANOVAs were carried out using SPSS (v10.0).

Results

Soil and plant characteristics of the five karst tiankengs

Except for AK and AP, the physicochemical parameters of soils varied significantly between different tiankengs (Table 1). The SWC, TN, and AN were significantly higher in XTK. The SOC content was significantly higher in SJXT. The soil TK content ranged from 3.50 to 5.54. All tiankeng soils were slightly acidic, with pH values ranging from 6.19 to 6.67. The plant diversity of karst tiankengs was indicated by Shannon-Wiener (*H*) and richness (*R*) indices and differed among the five karst tiankengs (Supplementary Table 2). The plant species diversity was significantly higher in WJXT ($p < 0.05$).

Structures of bacterial and fungal communities in karst tiankeng

After quality control, a total of 2,123,723 bacterial clean sequences and 2,508,449 fungal clean sequences were obtained. These sequences were grouped into 19,466 bacterial ASVs and 14,414 fungal OTUs (97% similarity threshold). Only 1,137 bacterial ASVs (5.8% of the total bacterial ASVs) and 195 fungal OTUs (1.4% of the total fungal OTUs) were shared by all karst tiankeng soils (Supplementary Figure 2). At the phylum of bacteria, *Proteobacteria* (39.3%–45.0.97%), *Acidobacteria* (17.2–24.8%), and *Actinobacteria* (14.9–22.1%) were predominant in all karst tiankeng soils (Figure 1A). Proteobacteria were represented by the classes *Alphaproteobacteria* (18.0–23.5%), *Betaproteobacteria* (8.7–11.3%), and *Deltaproteobacteria* (4.8–7.2%). *Actinobacteria* were represented by the classes *Thermoleophilia* (6.5–10.4%) and *Actinobacteria* (5.2–8.3%). In addition, the archaeal phyla *Crenarchaeota* and *Euryarchaeota* were also detected in the karst tiankeng soils. At the phyla of fungal, *Basidiomycota* (23.8–50.5%) and *Ascomycota* (36.2–63.6%) were predominant in all karst tiankeng soils. *Ascomycota* was mainly represented by the classes *Eurotiomycetes* (8.5–20.9%), *Sordariomycetes* (7.3–24.1%), and *Dothideomycetes* (3.5–16.2%; Figure 1B).

The alpha diversity of karst tiankeng microbial communities was indicated by the Shannon and Chao1 indices. There was no significant difference in the bacterial community Chao1 index among the five karst tiankengs ($p = 0.25$), whereas a significant difference was observed in the bacterial community Shannon index among the five karst tiankengs ($p < 0.05$). A significant difference was observed in fungal community alpha diversity among the five karst tiankengs ($p < 0.05$; Supplementary Figure 3). The analysis of similarities (ANOSIM; bacterial: $R = 0.804$, $p = 0.001$; fungal: $R = 0.489$, $p = 0.001$) revealed that bacterial and fungal communities from the different karst tiankengs significantly differed from each other (Supplementary Figure 4). The nonmetric multidimensional scaling (NMDS) plot showed that the bacterial communities in BJXT and SXT were closely clustered, while the fungal communities in BJXT, SJXT, SXT, and WJXT were closely clustered and separated from those in XTK (Figure 2).

Microbial networks and keystone taxa in karst tiankeng

The microbial random molecular ecological network (MENs) identified the microbe-microbe interactions in karst tiankeng. The karst tiankeng microbial network was a scale-free network ($R^2 = 0.923$) and exhibited a good modular structure (modularity

TABLE 1 The soil properties of the five karst tiankengs.

	BJXT	SJXT	SXT	WJXT	XTK
BD	1.07 ± 0.27a	0.72 ± 0.10b	0.96 ± 0.20ab	1.05 ± 0.28a	0.76 ± 0.24b
SWC	0.34 ± 0.05b	0.28 ± 0.08b	0.28 ± 0.05b	0.20 ± 0.07c	0.50 ± 0.09a
SOC (g kg^{-1})	38.48 ± 30.65bc	66.24 ± 26.38a	43.49 ± 17.95ab	17.99 ± 9.71c	57.54 ± 22.01ab
TN (g kg^{-1})	3.00 ± 1.96b	4.16 ± 1.67ab	3.17 ± 1.15ab	0.87 ± 0.50c	4.76 ± 1.79a
TP (mg kg^{-1})	850.10 ± 383.33a	540.27 ± 105.81b	630.00 ± 128.50ab	218.38 ± 76.01c	835.11 ± 399.44a
TK (g kg^{-1})	4.05 ± 1.24ab	3.50 ± 1.02b	5.54 ± 1.76a	5.40 ± 1.99a	3.69 ± 1.00b
AK (mg kg^{-1})	172.61 ± 65.49a	162.71 ± 44.42a	169.79 ± 28.75a	145.48 ± 46.58a	178.75 ± 48.84a
AP (mg kg^{-1})	1.06 ± 0.17a	1.04 ± 0.03a	1.01 ± 0.02a	1.05 ± 0.05a	1.09 ± 0.06a
AN (mg kg^{-1})	193.31 ± 109.78b	306.32 ± 91.28a	201.75 ± 78.38b	172.01 ± 109.96b	352.27 ± 59.05a
pH	6.19 ± 0.24b	6.19 ± 0.44b	6.36 ± 0.23b	6.36 ± 0.44b	6.76 ± 0.46a

BJXT: Bajiaxiantang, SJXT: Shaojiaxiantang, SXT: Shenxiantang, WJXT: Wangjiaxiantang, XTK: Xiaotiankeng; BD: bulk density, SOC: soil organic carbon, TN: total nitrogen, TP: total phosphorous, TK: total potassium, AK: available potassium, AP: available phosphorous, AN: available nitrogen; Values are mean ± standard error; Different minuscule alphabet means divergence is significant at 0.05 levels.

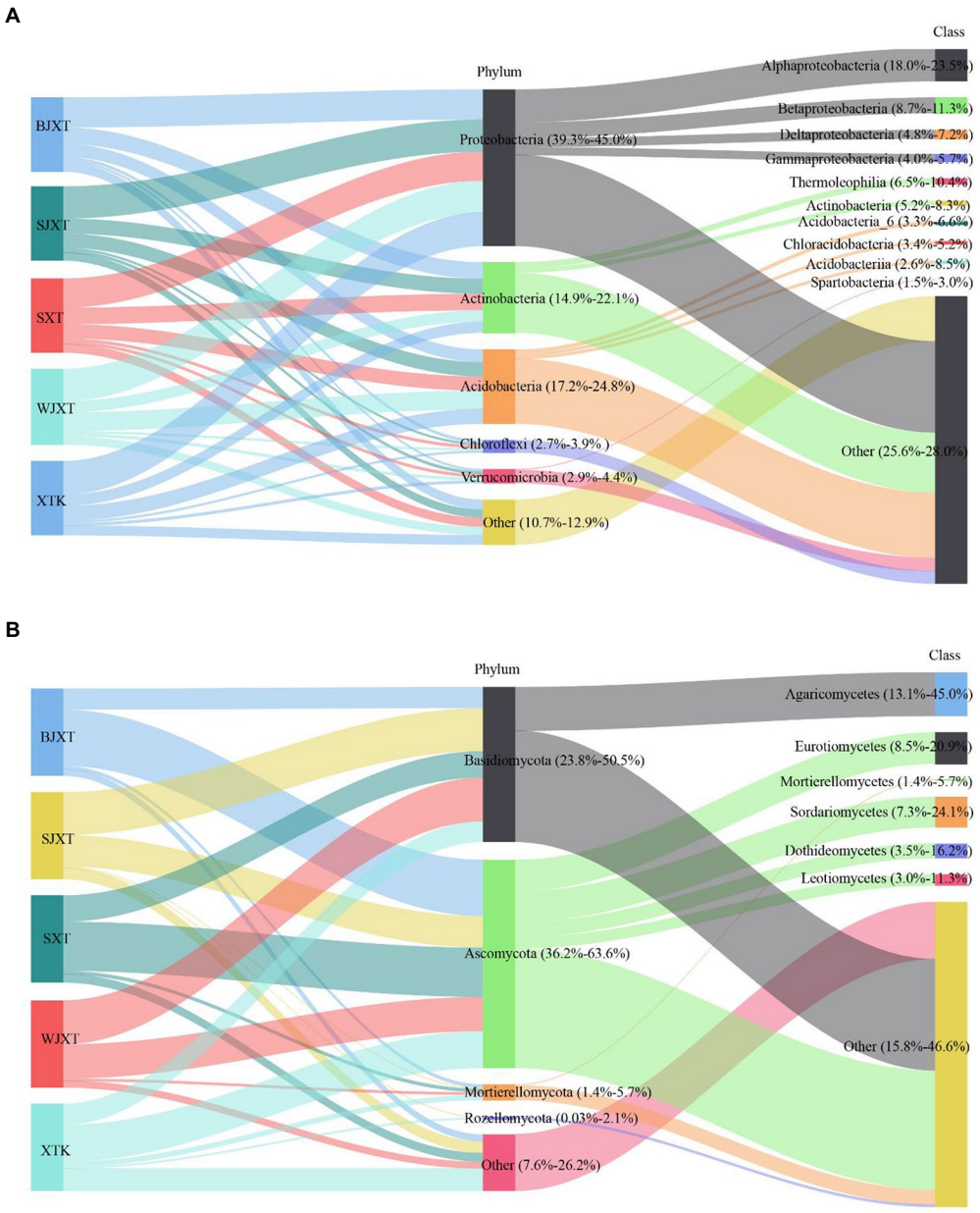

FIGURE 1
The Sankey diagram of the composition of bacterial **(A)** and fungal **(B)** communities at phylum and class level in five karst tiankengs. BJXT: Bajiaxiantang, SJXT: Shaojiaxiantang, SXT: Shenxiantang, WJXT: Wangjiaxiantang, XTK: Xiaotiankeng.

>0.4; Table 2). The karst tiankeng microbial network consisted of 185 nodes and 238 edges. More positive interaction edges (52.52%) were observed in the karst tiankeng microbial network. In the network of karst tiankeng soils, most nodes were grouped into six major modules (Figure 3A). Bacteria and fungi accounted for 90.58 and 9.42% of the total nodes, respectively (Figure 3B). The largest modules contain 17.84% of the total nodes. *Proteobacteria* (bacteria), *Acidobacteria* (bacteria), and *Ascomycota* (fungi) dominated in the major modules. Bacteria dominated in all the major modules, and fungi were mainly located in modules 0 and 1 (Figure 3C).

Among all nodes, 96.22% belonged to peripherals in karst tiankengs (Figure 4). Seven keystone taxa (five bacteria keystone taxa and two fungi keystone taxa) were identified in the karst tiankeng network, including six module hubs (3.24%) and one connector (0.54%). The dominant keystone taxa were *Proteobacteria* (bacteria) with an abundance of 42.86% of all keystone taxa. Bacteria of *Bradyrhizobium* (genus), *Steroidobacter* (genus), *Micrococcales* (order), *Ellin6513* (order), and fungi of *Umbelopsis* (genus) and *Fusarium* (genus) were the keystone taxa in the karst tiankeng network (Supplementary Table 3). All fungal keystone taxa of the karst tiankeng network were located in module 0.

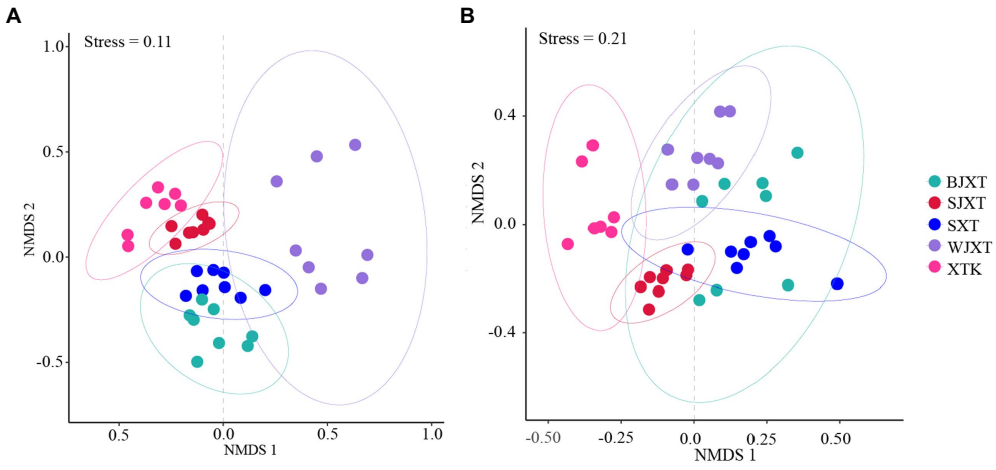

FIGURE 2
The non-metric multidimensional scaling (NMDS) analysis of bacterial **(A)** and fungal **(B)** communities in five karst tiankengs. BJXT: Bajiaxiantang, SJXT: Shaojiaxiantang, SXT: Shenxiantang, WJXT: Wangjiaxiantang, XTK: Xiaotiankeng.

TABLE 2 Topological properties of microbial networks in five karst tiankengs.

	St	Nodes	Edges	R^2 of power-law	*avgCC*	*GD*	*HD*	*avgK*	Density	Modularity
Karst Tiankeng	0.710	185	238	0.923	0.088	5.490	4.182	2.573	0.014	0.729

avgCC: Average clustering coefficient; GD: Average path distance; HD: Harmonic geodesic distance; avgK: Average degree.

Microbial communities assembly in karst tiankeng

The median phylogenetic turnover was between −2 and 2, which indicated that stochastic processes controlled the bacterial community assembly. Dispersal limitation was the key process in bacterial community assembly, with a contribution of 92.5%. Similarly, stochastic processes are crucial assembly processes in fungal community composition. Dispersal limitation and undominated processes contributed 89.5 and 9.8%, respectively, to the fungal community assembly (Figure 5).

Relationships between microbial communities and soil and plant variables

RDA was conducted to investigate the impact of soil properties and plant properties (richness and Shannon-Wiener) on bacterial and fungal communities. Among all the variables investigated, TN, AN, SWC, and BD had significant relationships with the bacterial communities (Figure 6A). SWC, *R*, TP, and TN were significantly associated with fungal communities (Figure 6B). The Mantel test results showed that BD, SWC, TN, TP, AP, and AN had significant relationships with the bacterial communities, while SWC, TN, AN, and *H′* had significant relationships with the fungal communities ($p < 0.05$, Supplementary Table 4). Significant correlations were also observed between the main microbial phylum and soil or plant variables (Supplementary Table 5).

Discussion

Characteristics of microbial communities in karst tiankeng

The constant physicochemical and microclimate conditions in the subsurface support a stable ecosystem in karst tiankeng. The bacterial communities in karst tiankeng were dominated by *Proteobacteria* and *Acidobacteria*. Similar results were reported for Shenmu karst tiankeng located in Guangxi, southwestern China (Pu et al., 2019). *Proteobacteria* are considered to play an important role in phylogenetic and ecological values and have highly diverse metabolic capabilities (Kang et al., 2019; von Borzyskowski et al., 2019). *Acidobacteria* species are considered to play a key role in nutrient cycles and perform the function of organic matter decomposition (Eichorst et al., 2018). In addition, the other abundant phyla included *Actinobacteria*, *Chloroflexi*, and *Verrucomicrobia*. *Actinobacteria* are considered the most important source of bioactive compounds, especially commercially available antibiotics (Barka et al., 2016; Rangseekaew and Pathom-aree, 2019). *Actinobacteria* (14.9–22.1%) ranked the third most abundant phyla in the karst tiankeng, which may indicate that *Actinobacteria* in the unique habitat of karst tiankeng are expected to be a good source of bioactive compound discovery. *Chloroflexi* and *Verrucomicrobia* are regarded as having a strong ability to survive in poor nutrient conditions (Pan et al., 2014; Yang et al., 2021), which may help karst tiankeng microbial communities resist external environmental disturbances. The fungal

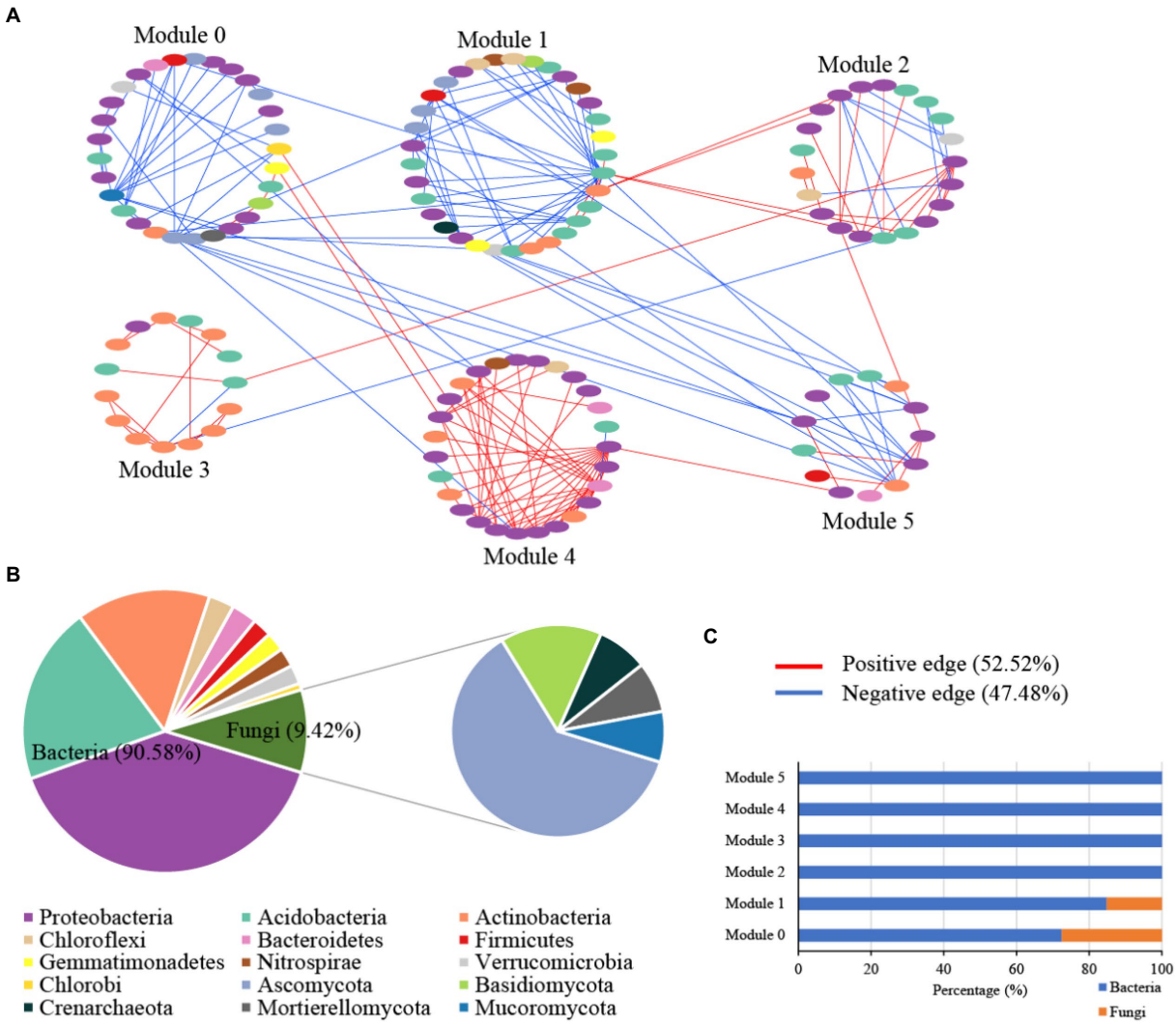

FIGURE 3
The microbial networks of bacterial and fungal communities of Zhanyi Karst Tiankeng Group by modules **(A)**; The proportion of microbial composition (phylum level) in main module **(B)**; The proportion of bacterial ASVs and fungal OTUs in main module **(C)**.

communities in karst tiankeng were dominated by *Ascomycota* and *Basidiomycota*. Previous research has shown that *Ascomycota* and *Basidiomycota* have a strong ability to decompose cellulose, and improve rock weathering in karst habitats (Baldrian et al., 2012; Xiao et al., 2022). Some of the fungal classes observed in our study were also detected in karst caves, such as *Sordariomycetes* and *Dothideomycetes* (Zhang et al., 2017; Man et al., 2018). The underground drainage system of karst landscapes is characterized by karst tiankengs and caves (Legatzki et al., 2011). The intricate hydrological system of the karst system links two unique habitats.

However, the shared bacterial ASVs and fungal OTUs among the five karst tiankengs accounted for less than 10% (Supplementary Table 1), indicating significant differences among bacterial and fungal communities among the five karst tiankengs. Different niches between karst tiankengs drive the evolution of microbial communities and maintain unique microbial populations. The results of the NMSD analysis also confirmed significant differences in bacterial and fungal communities in different karst tiankengs (Figure 2). Karst tiankengs, as isolated habitats, have a distinct island-like effect (Itescu, 2019). The isolation effect of the vertical cliff may vary between different karst tiankengs (Shui et al., 2018), leading to differences in microbial community evolution, composition, and genetic diversity. Affected by geological conditions, the external environment, and isolation effects (Wang et al., 2020), the different habitats between karst tiankengs may maintain diverse microbial communities.

Microbial co-occurrence network in karst tiankeng

Our study constructed an integrated microbial network by using different samples from five karst tiankengs, which suggests

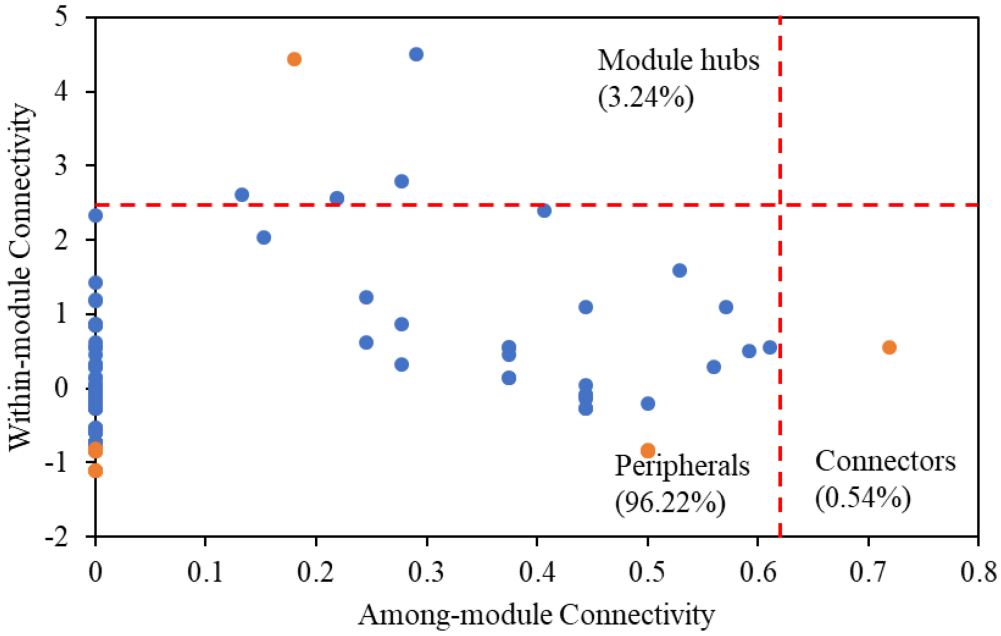

FIGURE 4
The ZP-plots shows distribution of ASVs/OTUs according to their module-based topological roles in the networks of five karst tiankengs. Each blue or orange dot represents a bacterial ASVs or fungal OTUs, respectively.

that the karst tiankeng microbial communities have more interactions within the niche (Figure 3). In the unique habitat of karst tiankengs, microbes may adopt different survival strategies (Jiang et al., 2022a). The inner microbial interactions play an important role in community stability and are determined by the basic dynamics of species to promote their survival (Zhou et al., 2011; Banerjee et al., 2018). A higher proportion of positive interaction edges of microbial networks (52.52%) suggested that bacterial and fungal communities form a tight organization through cooperation, thereby enhancing the complexity of the community structure and the stability of the karst tiankeng ecosystem (Wang Y. et al., 2022). Additionally, the collaboration between autotrophic and heterotrophic microorganisms contributes to their growth and metabolism and probably enhances community functions (Nadell et al., 2016). The microbial network showed good modularity, indicating nonrandom patterns of microbial interactions in karst tiankeng (Olesen et al., 2007).

The dominant phyla in the microbial network were *Proteobacteria* (bacteria) and *Ascomycota* (fungi), which are also the main soil microbial groups in various habitats (Sun et al., 2017; Cui et al., 2019). Based on the main functions of these microbial groups, it can be inferred that microbes involved in nutrient cycles and energy metabolism can survive well in karst tiankeng. Keystones are considered to play an important role in maintaining the stability of the microbial community (Mondav et al., 2017). A total of five bacterial keystones and two fungal keystones were identified in the karst tiankeng network (Supplementary Table 2). Previous studies demonstrated that *Bradyrhizobium* bacteria closely interact with plant roots and is abundantly present at high levels of plant diversity (Berg and Smalla, 2009; Xiao et al., 2021). *Bradyrhizobium* serves as a keystone in the network, which may be related to the abundant vegetation of karst tiankeng. As a member of *Proteobacteria*, *Steroidobacter* can access C and nutrients in oligotrophic conditions (Jeewani et al., 2020). The keystones of *Bradyrhizobium* and *Steroidobacter* play a key role in organic matter decomposition and nutrient cycling by connecting other microbial members in the network. In addition, fungal keystones of *Fusarium* are ubiquitous in karst ecosystems (Wang et al., 2016). *Fusarium* can secrete cellulase to decompose carbon, and participate in the dissolution of soil insoluble phosphorus, effectively improving the acquisition of phosphorus by plants (Yang et al., 2018). In general, keystones play a key role in maintaining the ecological function of the karst tiankeng ecosystem.

Community assembly processes and the impact of environmental variables on microbial communities

The assembly of bacterial and fungal communities is mainly a stochastic process, with the dominance of dispersal limitation in five karst tiankengs, indicating the spatial heterogeneity of karst tiankengs. The occurrence of dispersal limitation in the karst tiankeng indicates a weakening selection, which may result from the barrier of the vertical cliff. Most previous studies suggested that deterministic processes have a greater impact on the formation of bacterial communities (Cheng et al., 2021; Han et al.,

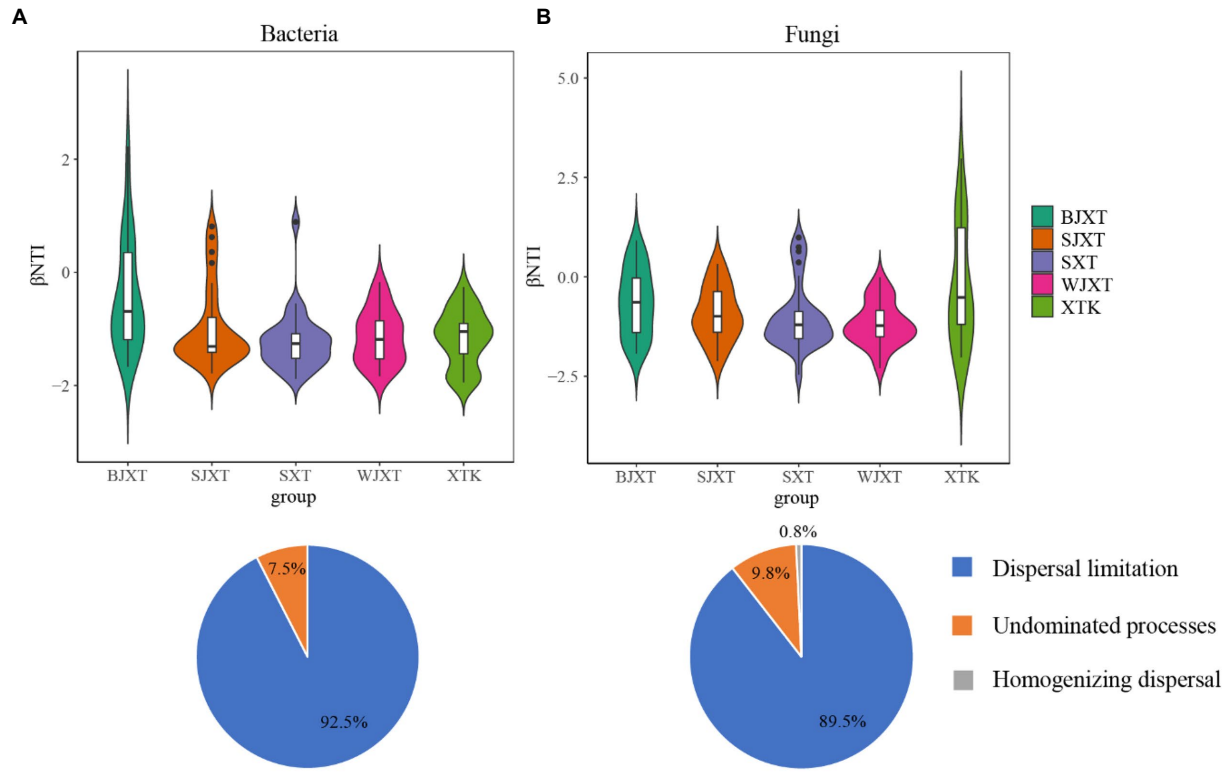

FIGURE 5
Phylogenetic and null model analyses revealing assembly processes of bacterial **(A)** and fungal **(B)** communities in five karst tiankeng tested by βNTI values, and percentage of each ecological process contributed to the assembly of bacterial and fungal communities in five karst tiankengs.

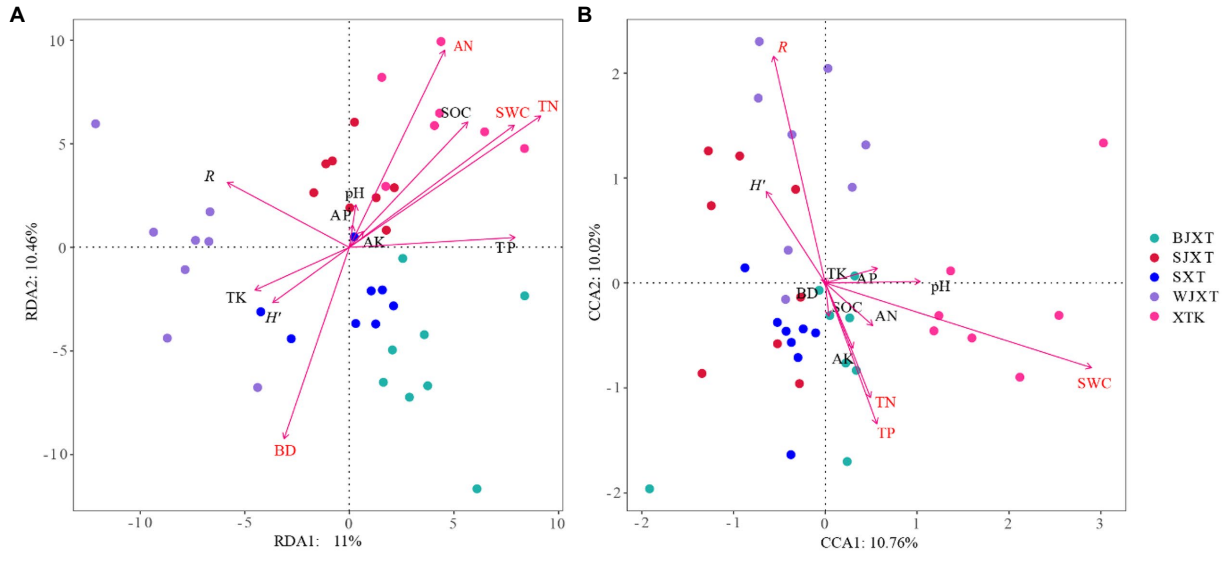

FIGURE 6
The redundancy analysis (RDA) of the bacterial **(A)** and fungal **(B)** communities with soil and plant properties in five karst tiankengs. Mark the significant factors in red font.

2022; Wang H. et al., 2022). Our results may be explained by the complex environment in the karst tiankeng. The abundant vegetation cover of karst tiankeng leads to a large accumulation of vegetation litter, which enriches soil nutrients and ultimately promotes the abundance of bacterial communities (Liu et al., 2021). The nutrient-rich soil environment allows bacterial

communities can thrive in the unique habitat of karst tiankengs. Additionally, bacterial communities can be transferred through the karst hydrological system (Mulec et al., 2019). These ecological processes were mixed to increase the stochastic process of bacterial community assembly in karst tiankeng. Deterministic processes were usually dominant in habitats with steep environmental gradients (Huang et al., 2022). Although the environments of these five karst tiankengs exhibit differences, it does not meet the characteristics of a steep environmental gradient. On the contrary, the interior of karst sinkholes maintains a relatively stable environment due to the effect of pit wall isolation. Thus, stochastic processes play a leading role in the construction of fungal communities in karst tiankengs. The dispersal limitation of fungal communities was consistent with previous studies (Li et al., 2020). The spread of fungal spores is usually limited to short distances, and the unique topography of karst tiankengs significantly reduces the spread of fungal spores. It is important to note that stochastic processes tend to occur before stable microbial communities form; our results may reflect that bacterial and fungal communities in karst tiankengs are still in an unstable state.

The soil and plant properties of the five karst tiankengs showed high habitat heterogeneity. Environmental variables are closely related to microbial diversity and community composition (Gao et al., 2017; Song et al., 2018). The RDA and mental test results showed that soil and plant properties were significantly associated with bacterial and fungal communities of the five karst tiankengs (Figure 6; Supplementary Table 1). SWC has been widely demonstrated to construct soil bacterial and fungal communities (Kaisermann et al., 2015; Long et al., 2021; Lin et al., 2022). Soil moisture content can directly affect the survival activity of microbes, and affect microbial growth by indirectly regulating the distribution of soil nutrients (Clark et al., 2009; Manzoni et al., 2014). For fungal communities, the soil water may help the expansion of soil hyphal networks (Hawkes et al., 2011). Our previous studies also indicated that the abundant soil water content in the karst tiankeng may make it easy for microorganisms to colonize (Jiang et al., 2022a). High SOC contents in karst regions, and soil nitrogen contents are more critical for bacterial communities (e.g., *Proteobacteria*; Li et al., 2022). Previous studies have indicated that soil structure with different bulk densities affects the spread and activity of bacteria in soil (Juyal et al., 2021). The high heterogeneity of karst habitats may affect bacterial communities by altering soil bulk density. Karst areas are generally limited by phosphorus (Chen et al., 2018a) and thus affect microbial communities. Liu et al. (2012) studies also reported that soil TP content is the limiting factor of microbial growth. Yang et al. (2017) study found that soil phosphorus has a more important effect on soil fungal communities than soil carbon-nitrogen ratios, which is consistent with our results. Fungal communities have a close relationship with plant diversity (He et al., 2008). Fungal communities are a key player in breaking down plant litter (Voriskova and Baldrian, 2013). The abundant plants in the karst tiankeng underground forest provide a high-quality environment for fungal communities.

Conclusion

This study provides a comprehensive assessment of the bacterial and fungal communities in karst tiankeng. The dominant phyla in the five karst tiankengs were mainly included *Proteobacteria*, *Acidobacteria* (bacterial), *Ascomycota,* and *Basidiomycota* (fungal). The diversity and composition of bacterial and fungal communities significantly differed among the five karst tiankengs. The co-occurrence network indicated that microorganisms preferred to survive in karst tiankengs in a modular manner, and abundant taxa relied more on partnerships to adapt to the environment. The keystones might play a critical role in nutrient cycles and energy metabolism. The bacterial communities were mainly related to SWC, TN, AN, and BD, while the fungal communities were mainly related to SWC, TP, and plant diversity. These observations provide improved knowledge about the structure, composition, community assembly processes, and co-occurrence patterns of bacterial and fungal communities in karst tiankeng ecosystems. This study contributes to further studies of the diversity and interaction patterns of bacterial and fungal communities in karst tiankeng worldwide and explores the value of the biodiversity conservation pool of karst tiankeng.

Data availability statement

The datasets presented in this study can be found in online repositories. The names of the repository/repositories and accession number(s) can be found in the article/supplementary material.

Author contributions

CJ and WS designed the study. CJ, XS, YL, KW, and HL carried out field sampling and plot surveys. CJ performed the experiments, analyzed the data, and wrote the manuscript. SZ provided technical support to this study. WS provided critical comments and edited the manuscript. All authors contributed to the article and approved the submitted version.

Funding

This work was supported by the National Natural Science Foundation of China (41871198).

Conflict of interest

The authors declare that the research was conducted in the absence of any commercial or financial relationships that could be construed as a potential conflict of interest.

Publisher's note

All claims expressed in this article are solely those of the authors and do not necessarily represent those of their affiliated organizations, or those of the publisher, the editors and the reviewers. Any product that may be evaluated in this article, or claim that may be made by its manufacturer, is not guaranteed or endorsed by the publisher.

Supplementary material

The Supplementary material for this article can be found online at: https://www.frontiersin.org/articles/10.3389/fmicb.2022.1002198/full#supplementary-material

References

Baldrian, P., Kolarik, M., Stursova, M., Kopecky, J., Valaskova, V., Vetrovsky, T., et al. (2012). Active and total microbial communities in forest soil are largely different and highly stratified during decomposition. *ISME J.* 6, 248–258. doi: 10.1038/ismej.2011.95

Balser, T. C., and Firestone, M. K. (2005). Linking microbial community composition and soil processes in a California annual grassland and mixed-conifer forest. *Biogeochemistry* 73, 395–415. doi: 10.1007/s10533-004-0372-y

Banerjee, S., Schlaeppi, K., and van der Heijden, M. G. A. (2018). Keystone taxa as drivers of microbiome structure and functioning. *Nat. Rev. Microbiol.* 16, 567–576. doi: 10.1038/s41579-018-0024-1

Barka, E. A., Vatsa, P., Sanchez, L., Gaveau-Vaillant, N., Jacquard, C., Meier-Kolthoff, J. P., et al. (2016). Taxonomy, physiology, and natural products of Actinobacteria (vol 80, pg 1, 2016). *Microbiol. Mol. Biol. Rev.* 80:III. doi: 10.1128/mmbr.00044-16

Batori, Z., Vojtko, A., Farkas, T., Szabo, A., Havadtoi, K., Vojtko, A. E., et al. (2017). Large- and small-scale environmental factors drive distributions of cool-adapted plants in karstic microrefugia. *Ann. Bot.* 119, 301–309. doi: 10.1093/aob/mcw233

Berg, G., and Smalla, K. (2009). Plant species and soil type cooperatively shape the structure and function of microbial communities in the rhizosphere. *FEMS Microbiol. Ecol.* 68, 1–13. doi: 10.1111/j.1574-6941.2009.00654.x

Bokulich, N. A., Kaehler, B. D., Rideout, J. R., Dillon, M., Bolyen, E., Knight, R., et al. (2018). Optimizing taxonomic classification of marker-gene amplicon sequences with QIIME 2 ' s q2-feature-classifier plugin. *Microbiome* 6:90. doi: 10.1186/s40168-018-0470-z

Caporaso, J. G., Lauber, C. L., Walters, W. A., Berg-Lyons, D., Huntley, J., Fierer, N., et al. (2012). Ultra-high-throughput microbial community analysis on the Illumina HiSeq and MiSeq platforms. *ISME J.* 6, 1621–1624. doi: 10.1038/ismej.2012.8

Chen, Y. P., Jiang, C., Jian, X. M., Shui, W., Hu, Y., Ma, T., et al. (2018b). Spatial distribution characteristics of grassland plant communities in a moderately degraded tiankeng in Zhanyi. *Yunnan. Acta Ecol Sin* 38, 134–147.

Chen, H., Li, D. J., Xiao, K. C., and Wang, K. L. (2018a). Soil microbial processes and resource limitation in karst and non-karst forests. *Funct. Ecol.* 32, 1400–1409. doi: 10.1111/1365-2435.13069

Cheng, X., Yun, Y., Wang, H., Ma, L., Tian, W., Man, B., et al. (2021). Contrasting bacterial communities and their assembly processes in karst soils under different land use. *Sci. Total Environ.* 751:142263. doi: 10.1016/j.scitotenv.2020.142263

Clark, J. S., Campbell, J. H., Grizzle, H., Acosta-Martinez, V., and Zak, J. C. (2009). Soil microbial community response to drought and precipitation variability in the Chihuahuan Desert. *Microb. Ecol.* 57, 248–260. doi: 10.1007/s00248-008-9475-7

Clements, R., Sodhi, N. S., Schilthuizen, M., and Ng, P. K. L. (2006). Limestone karsts of Southeast Asia: imperiled arks of biodiversity. *Bioscience* 56, 733–742. doi: 10.1641/0006-3568(2006)56[733:Lkosai]2.0.Co;2

Cui, Y., Fang, L., Guo, X., Wang, X., Wang, Y., Zhang, Y., et al. (2019). Responses of soil bacterial communities, enzyme activities, and nutrients to agricultural-to-natural ecosystem conversion in the loess plateau. *China. J. Soils Sediments* 19, 1427–1440. doi: 10.1007/s11368-018-2110-4

de Vries, F. T., Griffiths, R. I., Bailey, M., Craig, H., Girlanda, M., Gweon, H. S., et al. (2018). Soil bacterial networks are less stable under drought than fungal networks. *Nat. Commun.* 9:3033. doi: 10.1038/s41467-018-05516-7

Delmont, T. O., Malandain, C., Prestat, E., Larose, C., Monier, J.-M., Simonet, P., et al. (2011). Metagenomic mining for microbiologists. *ISME J.* 5, 1837–1843. doi: 10.1038/ismej.2011.61

Deng, Y., Jiang, Y.-H., Yang, Y., He, Z., Luo, F., and Zhou, J. (2012). Molecular ecological network analyses. *Bmc Bioinformatics* 13:113. doi: 10.1186/1471-2105-13-113

Deng, C., and Wu, X. (2014). The component and assessment of macro-fungi in Leye County, Guangxi autonomous region. *China. Guizhou Sci* 32, 1–18.

Dixon, P. (2003). VEGAN, a package of R functions for community ecology. *J. Veg. Sci.* 14, 927–930. doi: 10.1111/j.1654-1103.2003.tb02228.x

Eichorst, S. A., Trojan, D., Roux, S., Herbold, C., Rattei, T., and Woebken, D. (2018). Genomic insights into the Acidobacteria reveal strategies for their success in terrestrial environments. *Environ. Microbiol.* 20, 1041–1063. doi: 10.1111/1462-2920.14043

Fierer, N. (2017). Embracing the unknown: disentangling the complexities of the soil microbiome. *Nat. Rev. Microbiol.* 15, 579–590. doi: 10.1038/nrmicro.2017.87

Gao, C., Shi, N.-N., Chen, L., Ji, N.-N., Wu, B.-W., Wang, Y.-L., et al. (2017). Relationships between soil fungal and woody plant assemblages differ between ridge and valley habitats in a subtropical mountain forest. *New Phytol.* 213, 1874–1885. doi: 10.1111/nph.14287

Gunn, J. (2019). Tiankeng (giant doline) definitions with particular reference to the Hanzhong depressions, Shaanxi, China. *Cave Karst Sci* 46, 51–60.

Han, S., Tan, S., Wang, A., Chen, W., and Huang, Q. (2022). Bacterial rather than fungal diversity and community assembly drive soil multifunctionality in a subtropical forest ecosystem. *Environ. Microbiol. Rep.* 14, 85–95. doi: 10.1111/1758-2229.13033

Hawkes, C. V., Kivlin, S. N., Rocca, J. D., Huguet, V., Thomsen, M. A., and Suttle, K. B. (2011). Fungal community responses to precipitation. *Glob. Chang. Biol.* 17, 1637–1645. doi: 10.1111/j.1365-2486.2010.02327.x

He, D., Shen, W., Eberwein, J., Zhao, Q., Ren, L., and Wu, Q. L. (2017). Diversity and co-occurrence network of soil fungi are more responsive than those of bacteria to shifts in precipitation seasonality in a subtropical forest. *Soil Biol. Biochem.* 115, 499–510. doi: 10.1016/j.soilbio.2017.09.023

He, X.-Y., Wang, K.-L., Zhang, W., Chen, Z.-H., Zhu, Y.-G., and Chen, H.-S. (2008). Positive correlation between soil bacterial metabolic and plant species diversity and bacterial and fungal diversity in a vegetation succession on karst. *Plant Soil* 307, 123–134. doi: 10.1007/s11104-008-9590-8

Huang, L., Bai, J., Wang, J., Zhang, G., Wang, W., Wang, X., et al. (2022). Different stochastic processes regulate bacterial and fungal community assembly in estuarine wetland soils. *Soil Biol. Biochem.* 167:108586. doi: 10.1016/j.soilbio.2022.108586

Itescu, Y. (2019). Are island-like systems biologically similar to islands? *A review of the evidence. Ecography* 42, 1298–1314. doi: 10.1111/ecog.03951

Jamil, A., Yang, J.-Y., Su, D.-F., Tong, J.-Y., Chen, S.-Y., Luo, Z.-W., et al. (2020). Rhizospheric soil fungal community patterns of Duchesnea indica in response to altitude gradient in Yunnan, Southwest China. *Can. J. Microbiol.* 66, 359–367. doi: 10.1139/cjm-2019-0589

Jeewani, P. H., Gunina, A., Tao, L., Zhu, Z., Kuzyakov, Y., Van Zwieten, L., et al. (2020). Rusty sink of rhizodeposits and associated keystone microbiomes. *Soil Biol. Biochem.* 147:107840. doi: 10.1016/j.soilbio.2020.107840

Jian, X. M., Shui, W., Wang, Y. N., Wang, Q. F., Chen, Y. P., Jiang, C., et al. (2018). Species diversity and stability of grassland plant community in heavily-degraded karst tiankeng: a case study of Zhanyi tiankeng in Yunnan, China. *Acta Ecologica Sinica* 38, 4704–4714. doi: 10.5846/stxb201706281163

Jiang, C., Feng, J., Zhu, S. F., and Shui, W. (2021). Characteristics of the soil microbial communities in different slope positions along an inverted stone slope in a degraded karst Tiankeng. *Biology-Basel* 10:474. doi: 10.3390/biology10060474

Jiang, Z., Lu, B., Zhan, B., and Lu, Q. (2014). Screening, identification and enzyme-producing conditions of strains with high keratinase yield. *Guizhou Agric Sci* 42, 139–141.

Jiang, C., Sun, X.-R., Feng, J., Zhu, S.-F., and Shui, W. (2022a). Metagenomic analysis reveals the different characteristics of microbial communities inside and outside the karst tiankeng. *BMC Microbiol.* 22:115. doi: 10.1186/s12866-022-02513-1

Jiang, C., Zhu, S., Feng, J., and Shui, W. (2022b). Slope aspect affects the soil microbial communities in karst tiankeng negative landforms. *BMC ecology and evolution* 22:54. doi: 10.1186/s12862-022-01986-y

Juyal, A., Otten, W., Baveye, P. C., and Eickhorst, T. (2021). Influence of soil structure on the spread of Pseudomonas fluorescens in soil at microscale. *Eur. J. Soil Sci.* 72, 141–153. doi: 10.1111/ejss.12975

Kaisermann, A., Maron, P. A., Beaumelle, L., and Lata, J. C. (2015). Fungal communities are more sensitive indicators to non-extreme soil moisture variations than bacterial communities. *Appl. Soil Ecol.* 86, 158–164. doi: 10.1016/j.apsoil.2014.10.009

Kang, C. S., Dunfield, P. F., and Semrau, J. D. (2019). The origin of aerobic methanotrophy within the Proteobacteria. *FEMS Microbiol. Lett.* 366:096. doi: 10.1093/femsle/fnz096

Kembel, S. W., Cowan, P. D., Helmus, M. R., Cornwell, W. K., Morlon, H., Ackerly, D. D., et al. (2010). Picante: R tools for integrating phylogenies and ecology. *Bioinformatics* 26, 1463–1464. doi: 10.1093/bioinformatics/btq166

Lan, T., Chen, Y., Huang, C., Zhang, W., Xie, L., Shi, G., et al. (2017). Community constituent of dark septate endophytic fungi in Dashiwei Doline group and their effects on Pioneer Plants'Drought resistance capability. *J. Mirobiol.* 37, 26–34.

Legatzki, A., Ortiz, M., Neilson, J., Dominguez, S., Andersen, G. L., Toomey, R. S., et al. (2011). Bacterial and archaeal community structure of two adjacent calcite speleothems in Kartchner caverns, Arizona, USA. *Geomicrobiol J.* 28, 99–117. doi: 10.1080/01490451003738465

Li, Y., Gong, J., Liu, J., Hou, W., Moroenyane, I., Liu, Y., et al. (2022). Effects of different land use types and soil depth on soil nutrients and soil bacterial communities in a karst area, Southwest China. *Soil Systems* 6:20. doi: 10.3390/soilsystems6010020

Li, S.-P., Wang, P., Chen, Y., Wilson, M. C., Yang, X., Ma, C., et al. (2020). Island biogeography of soil bacteria and fungi: similar patterns, but different mechanisms. *ISME J.* 14, 1886–1896. doi: 10.1038/s41396-020-0657-8

Lin, Y., Kong, J., Yang, L., He, Q., Su, Y., Li, J., et al. (2022). Soil bacterial and fungal community responses to Throughfall reduction in a eucalyptus plantation in southern China. *Forests* 13:37. doi: 10.3390/f13010037

Liu, L., Gundersen, P., Zhang, T., and Mo, J. (2012). Effects of phosphorus addition on soil microbial biomass and community composition in three forest types in tropical China. *Soil Biol. Biochem.* 44, 31–38. doi: 10.1016/j.soilbio.2011.08.017

Liu, M., Li, X., Zhu, R., Chen, N., Ding, L., and Chen, C. (2021). Vegetation richness, species identity and soil nutrients drive the shifts in soil bacterial communities during restoration process. *Environ. Microbiol. Rep.* 13, 411–424. doi: 10.1111/1758-2229.12913

Long, H., Wu, X., Wang, Y., Yan, J., Guo, X., An, X., et al. (2021). Effects of revegetation on the composition and diversity of bacterial and fungal communities of sandification land soil, in southern China. *Environ. Monit. Assess.* 193:706. doi: 10.1007/s10661-021-09508-x

Man, B., Wang, H., Yun, Y., Xiang, X., Wang, R., Duan, Y., et al. (2018). Diversity of fungal communities in Heshang cave of Central China revealed by Mycobiome-sequencing. *Front. Microbiol.* 9:1400. doi: 10.3389/fmicb.2018.01400

Manzoni, S., Schaeffer, S. M., Katul, G., Porporato, A., and Schimel, J. P. (2014). A theoretical analysis of microbial eco-physiological and diffusion limitations to carbon cycling in drying soils. *Soil Biol. Biochem.* 73, 69–83. doi: 10.1016/j.soilbio.2014.02.008

Mondav, R., McCalley, C. K., Hodgkins, S. B., Frolking, S., Saleska, S. R., Rich, V. I., et al. (2017). Microbial network, phylogenetic diversity and community membership in the active layer across a permafrost thaw gradient. *Environ. Microbiol.* 19, 3201–3218. doi: 10.1111/1462-2920.13809

Mulec, J., Petric, M., Kozelj, A., Brun, C., Batagelj, E., Hladnik, A., et al. (2019). A MULTIPARAMETER analysis of environmental gradients related to hydrological conditions in a binary karst system (underground course of the PIVKA river, SLOVENIA). *Acta Carsologica* 48, 313–327. doi: 10.3986/ac.v48i3.7145

Nadell, C. D., Drescher, K., and Foster, K. R. (2016). Spatial structure, cooperation and competition in biofilms. *Nat. Rev. Microbiol.* 14, 589–600. doi: 10.1038/nrmicro.2016.84

Nilsson, R. H., Larsson, K.-H., Taylor, A. F. S., Bengtsson-Palme, J., Jeppesen, T. S., Schigel, D., et al. (2019). The UNITE database for molecular identification of fungi: handling dark taxa and parallel taxonomic classifications. *Nucleic Acids Res.* 47, D259–D264. doi: 10.1093/nar/gky1022

Olesen, J. M., Bascompte, J., Dupont, Y. L., and Jordano, P. (2007). The modularity of pollination networks. *Proc. Natl. Acad. Sci. U. S. A.* 104, 19891–19896. doi: 10.1073/pnas.0706375104

Pan, Y., Cassman, N., de Hollander, M., Mendes, L. W., Korevaar, H., Geerts, R. H. E. M., et al. (2014). Impact of long-term N, P, K, and NPK fertilization on the composition and potential functions of the bacterial community in grassland soil. *FEMS Microbiol. Ecol.* 90, 195–205. doi: 10.1111/1574-6941.12384

Pu, G. Z., Lv, Y. N., Dong, L. N., Zhou, L. W., Huang, K. C., Zeng, D. J., et al. (2019). Profiling the bacterial diversity in a typical karst Tiankeng of China. *Biomol. Ther.* 9:187. doi: 10.3390/biom9050187

Pu, G. Z., Lv, Y. N., Xu, G. P., Zeng, D. J., and Huang, Y. Q. (2017). Research Progress on karst Tiankeng ecosystems. *Bot. Rev.* 83, 5–37. doi: 10.1007/s12229-017-9179-0

Rangseekaew, P., and Pathom-aree, W. (2019). Cave Actinobacteria as producers of bioactive metabolites. *Front. Microbiol.* 10:387. doi: 10.3389/fmicb.2019.00387

Rottjers, L., and Faust, K. (2018). From hairballs to hypotheses biological insights from microbial networks. *Fems Microbiol. Rev.* 10. doi: 10.3389/fmicb.2019.00387

Shui, W., Chen, Y., Jian, X., Jiang, C., Wang, Q., and Guo, P. (2018). Spatial pattern of plant community in original karst tiankeng: a case study of Zhanyi tiankeng in Yunnan, China. *J. applied ecology* 29, 1725–1735. doi: 10.13287/j.1001-9332.201806.010

Shui, W., Chen, Y., Jian, X., Jiang, C., Wang, Q., Zeng, Y., et al. (2022). Original karst tiankeng with underground virgin forest as an inaccessible refugia originated from a degraded surface flora in Yunnan, China. *Sci. Rep.* 12:9408. doi: 10.1038/s41598-022-13678-0

Shui, W., Chen, Y. P., Wang, Y. W., Su, Z. A., and Zhang, S. (2015). Origination, study progress and prospect of karst tiankeng research in China. *Acta Geograph. Sin.* 70, 431–446. doi: 10.11821/dlxb201503007

Song, M., Peng, W., Zeng, F., Du, H., Peng, Q., Xu, Q., et al. (2018). Spatial patterns and drivers of microbial taxa in a karst broadleaf Forest. *Front. Microbiol.* 9:1691. doi: 10.3389/fmicb.2018.01691

Stegen, J. C., Lin, X., Fredrickson, J. K., Chen, X., Kennedy, D. W., Murray, C. J., et al. (2013). Quantifying community assembly processes and identifying features that impose them. *ISME J.* 7, 2069–2079. doi: 10.1038/ismej.2013.93

Stegen, J. C., Lin, X., Konopka, A. E., and Fredrickson, J. K. (2012). Stochastic and deterministic assembly processes in subsurface microbial communities. *ISME J.* 6, 1653–1664. doi: 10.1038/ismej.2012.22

Su, Y. Q., Tang, Q. M., Mo, F. Y., and Xue, Y. G. (2017). Karst tiankengs as refugia for indigenous tree flora amidst a degraded landscape in southwestern China. *Sci. Rep.* 7:4249. doi: 10.1038/s41598-017-04592-x

Sun, S., Li, S., Avera, B. N., Strahm, B. D., and Badgley, B. D. (2017). Soil bacterial and fungal communities show distinct recovery patterns during Forest ecosystem restoration. *Appl. Environ. Microbiol.* 83:17. doi: 10.1128/aem.00966-17

Vazquez-Baeza, Y., Pirrung, M., Gonzalez, A., and Knight, R. (2013). EMPeror: a tool for visualizing high-throughput microbial community data. *Gigascience* 2:16. doi: 10.1186/2047-217x-2-16

von Borzyskowski, L. S., Severi, F., Krueger, K., Hermann, L., Gilardet, A., Sippel, F., et al. (2019). Marine Proteobacteria metabolize glycolate via the beta-hydroxyaspartate cycle. *Nature* 575:500. doi: 10.1038/s41586-019-1748-4

Voriskova, J., and Baldrian, P. (2013). Fungal community on decomposing leaf litter undergoes rapid successional changes. *ISME J.* 7, 477–486. doi: 10.1038/ismej.2012.116

Wang, Y., Cheng, X., Wang, H., Zhou, J., Liu, X., and Tuovinen, O. H. (2022). The characterization of microbiome and interactions on weathered rocks in a subsurface karst cave, Central China. *Front. Microbiol.* 13:909494. doi: 10.3389/fmicb.2022.909494

Wang, P., Li, S.-P., Yang, X., Zhou, J., Shu, W., and Jiang, L. (2020). Mechanisms of soil bacterial and fungal community assembly differ among and within islands. *Environ. Microbiol.* 22, 1559–1571. doi: 10.1111/1462-2920.14864

Wang, P. C., Mo, B. T., Chen, Y., Zeng, Q. F., and Wang, L. B. (2016). Effect of karst rocky desertification on soil fungal communities in Southwest China. *Genet. Mol. Res.* 15:460. doi: 10.4238/gmr.15038460

Wang, H., Qi, Z., Zheng, P., Jiang, C., and Diao, X. (2022). Abundant and rare microbiota assembly and driving factors between mangrove and intertidal mudflats. *Appl. Soil Ecol.* 174:104438. doi: 10.1016/j.apsoil.2022.104438

Wang, J., Shen, J., Wu, Y., Tu, C., Soininen, J., Stegen, J. C., et al. (2013). Phylogenetic beta diversity in bacterial assemblages across ecosystems: deterministic versus stochastic processes. *ISME J.* 7, 1310–1321. doi: 10.1038/ismej.2013.30

Xiao, D., Chen, Y., He, X., Xu, Z., Bai, S. H., Zhang, W., et al. (2021). Temperature and precipitation significantly influence the interactions between arbuscular mycorrhizal fungi and diazotrophs in karst ecosystems. *For. Ecol. Manag.* 497:119464. doi: 10.1016/j.foreco.2021.119464

Xiao, D., He, X., Zhang, W., Hu, P., Sun, M., and Wang, K. (2022). Comparison of bacterial and fungal diversity and network connectivity in karst and non-karst forests in Southwest China. *Sci. Total Environ.* 822:153179. doi: 10.1016/j.scitotenv.2022.153179

Xu, S., Zhang, Y., Huang, B., and Chen, W. (2009). Comparative analysis on value of typical geological trace landscapes of Guangxi Fengshan karst National Geopark. *J. Mountain Res.* 27, 373–380.

Yang, T., Adams, J.M., and Shi, Y., He, J.-s., Jing, X., Chen, L., et al. (2017). Soil fungal diversity in natural grasslands of the Tibetan plateau: associations with plant diversity and productivity. *New Phytol.* 215, 756–765. doi:10.1111/nph.14606

Yang, L., Barnard, R., Kuzyakov, Y., and Tian, J. (2021). Bacterial communities drive the resistance of soil multifunctionality to land-use change in karst soils. *Eur. J. Soil Biol.* 104:103313. doi: 10.1016/j.ejsobi.2021.103313

Yang, G., Peng, C. H., Liu, Y. Z., and Dong, F. Q. (2019). Tiankeng: an ideal place for climate warming research on forest ecosystems. *Environ. Earth Sci.* 78. doi: 10.1007/s12665-018-8033-y

Yang, S., Yang, T., Lin, B., Liu, X., and Xiang, M. (2018). Isolation and evaluation of two phosphate-dissolving fungi. *Acta Microbiol Sin.* 58, 264–273.

Yuan, D. (2005). The development of Morden karstology in China. *Sci. Foundation in China* 19, 139–141.

Yuan, M. M., Guo, X., Wu, L., Zhang, Y., Xiao, N., Ning, D., et al. (2021). Climate warming enhances microbial network complexity and stability. *Nat. Clim. Chang.* 11, 343–348. doi: 10.1038/s41558-021-00989-9

Zhang, Z. F., Liu, F., Zhou, X., Liu, X. Z., Liu, S. J., and Cai, L. (2017). Culturable mycobiota from karst caves in China, with descriptions of 20 new species. *Persoonia* 39, 1–31. doi: 10.3767/persoonia.2017.39.01

Zhou, J., Deng, Y., Luo, F., He, Z., Tu, Q., and Zhi, X. (2010). Functional molecular ecological networks. *MBio* 1:10. doi: 10.1128/mBio.00169-10

Zhou, J., Deng, Y., Luo, F., He, Z., and Yang, Y. (2011). Phylogenetic molecular ecological network of soil microbial communities in response to elevated CO2. *MBio* 2:11. doi: 10.1128/mBio.00122-11

Zhu, X., and Chen, W. (2005). Tiankengs in the karst of China. *Cave and Karst Science* 32, 55–56.

Zhu, X., and Waltham, T. (2005). Tiankeng: Definition and description. *Cave Karst Sci.* 32, 75–79. doi: 1001-4810(2006)S-0035-08

frontiers | Frontiers in Microbiology

TYPE Original Research
PUBLISHED 24 November 2022
DOI 10.3389/fmicb.2022.1058067

OPEN ACCESS

EDITED BY
Hongchen Jiang,
China University of Geosciences Wuhan, China

REVIEWED BY
Xiaojing Hu,
Northeast Institute of Geography and Agroecology (CAS), China
Xiubing Gao,
Guizhou Tea Research Institute, China

*CORRESPONDENCE
Xiuming Liu
liuxiuming@vip.skleg.cn
Bin Lian
bin2368@vip.163.com

†These authors have contributed equally to this work and share first authorship

SPECIALTY SECTION
This article was submitted to Terrestrial Microbiology, a section of the journal Frontiers in Microbiology

RECEIVED 30 September 2022
ACCEPTED 08 November 2022
PUBLISHED 24 November 2022

CITATION
Li Y, Shen Q, An X, Xie Y, Liu X and Lian B (2022) Organomineral fertilizer application enhances *Perilla frutescens* nutritional quality and rhizosphere microbial community stability in karst mountain soils. *Front. Microbiol.* 13:1058067. doi: 10.3389/fmicb.2022.1058067

Organomineral fertilizer application enhances *Perilla frutescens* nutritional quality and rhizosphere microbial community stability in karst mountain soils

Ying Li[1,2†], Qi Shen[3†], Xiaochi An[2], Yuanhuan Xie[1], Xiuming Liu[1*] and Bin Lian[2*]

[1]State Key Laboratory of Environmental Geochemistry, Institute of Geochemistry, Chinese Academy of Sciences, Guiyang, China, [2]College of Life Sciences, College of Marine Science and Engineering, Nanjing Normal University, Nanjing, China, [3]Institute of Medical Plant Physiology and Ecology, School of Pharmaceutical Sciences, Guangzhou University of Chinese Medicine, Guangzhou, China

Introduction: Applications of organomineral fertilizer (OMF) are important measures for developing organic agriculture in karst mountain areas. However, the influence of OMF on the structure and function of soil microbial diversity and their relationship with crop yield and quality are still unclear.

Methods: Based on soil science, crop science, and high-throughput sequencing methods, we investigated the changes of rhizosphere soil microbial communities of *Perilla frutescens* under different fertilization measures. Then, the relationship between *P. frutescens* yield and quality with soil quality was analyzed.

Results: The results showed that the addition of OMF increased the amount of total carbon and total potassium in soil. OF, especially OMF, improved *P. frutescens* yield and quality (e.g., panicle number per plant, main panicle length, and unsaturated fatty acid contents). Both OF and OMF treatments significantly increased the enrichment of beneficial microorganism (e.g., *Bacillus*, *Actinomadura*, *Candidatus_Solibacter*, *Iamia*, *Pseudallescheria*, and *Cladorrhinum*). The symbiotic network analysis demonstrated that OMF strengthened the connection among the soil microbial communities, and the community composition became more stable. Redundancy analysis and structural equation modeling showed that the soil pH, available phosphorus, and available potassium were significantly correlated with soil microbial community diversity and *P. frutescens* yield and quality.

Discussion: Our study confirmed that OMF could replace *CF* or common OF to improve soil fertility, crop yield and quality in karst mountain soils.

KEYWORDS

karst soil, organomineral fertilizer, *Perilla frutescens*, nutritional quality, rhizosphere microbial community

Introduction

Application of chemical fertilizers (CFs) can significantly increase soil fertility and crop yield in a short time. However, long-term excessive application of CFs damages soil microbial communities and biological activities, which results in decreased soil quality, increased dependence of crop growth on fertilizer nutrients, and aggravated agricultural surface source pollution (Gomiero et al., 2011; Kour et al., 2020; Ren et al., 2020). To reduce the negative effects caused by excessive application of CFs, organic fertilizers (OFs) are usually used to replace or partially replace CFs to protect soil biodiversity and maintain soil ecological balance (Megali et al., 2013; Steffen et al., 2015). Increased OFs application can increase soil carbon storage and plant nutrients, and improve soil biological activity, which are of great significance for mitigating climate warming and developing sustainable agricultural production (Gattinger et al., 2012; Seufert et al., 2012). Many studies have shown that OFs application is an effective way to improve crop yield and quality (Liu et al., 2020, 2021; Du et al., 2022), and increase soil microbial richness and diversity (Zhou et al., 2015; Cui et al., 2018; Li et al., 2020). However, the contents of mineral nutrients such as nitrogen, phosphorus, and potassium in OFs are low, and the increased amount of fertilizer needed increases the cost and application difficulty. Therefore, it is very necessary to improve the contents of mineral elements in traditional OFs.

As a new fertilizer combining the advantages of organic fertilizer and inorganic fertilizer, the nutrient release effect of OMFs occurs simultaneously with the crop growth process, making the agronomic efficiency higher when compared with the inorganic fertilizer (Kiehl, 2008). Compared with CFs, OMFs can reduce the loss of some nutrients, such as nitrogen volatilization, phosphorus fixation and potassium leaching (Aguilar et al., 2019). Compared with common OFs, OMFs are rich in mineral elements necessary for crop growth. OMFs are usually composed of natural organic matter sources and inorganic element sources. Organomineral fertilizer ingredients are mostly agricultural wastes such as chicken manure, coffee shell, wood waste, sewage sludge and sugarcane cake, combined with urea, calcium superphosphate, potassium chloride, magnesium silicate, calcium sulfate and other inorganic chemical fertilizers (Efanov et al., 2001; Carvalho et al., 2014; Grohskopf et al., 2019; Gonçalves et al., 2021; Hawrot-Paw et al., 2022; Ngo et al., 2022). According to the published articles, the research on the application effect of organic mineral fertilizer mainly focuses on the agronomic efficiency of crops. Compared with the crop response to inorganic fertilizers, the response to organomineral fertilizers is quite variable. The reported results are gains (Efanov et al., 2001; Deeks et al., 2013; Carvalho et al., 2014; Sakurada et al., 2016; Vollú et al., 2018; Ngo et al., 2022), losses (Antille et al., 2017; Frazão et al., 2019), or equivalent efficiency (Corrêa et al., 2018; Dias et al., 2020; Mumbach et al., 2020). Those varied results may be related to the different ingredients of OMFs, the amount of fertilizer applied and the environment of the study sites. Limited research literature showed that OMF, as a source of organic carbon and mineral elements, had a positive effect on the quantity and activity of soil microorganisms (Hawrot-Paw et al., 2022), but had little effect on the rhizosphere bacterial diversity of crops (Vollú et al., 2018).

The staggering production of cuttings and quarry by-products from mining activities results in a huge environmental burden; however, the combined use of these cuttings and low-grade mineral rocks can help reduce this pollution (Basak et al., 2021; Syed et al., 2021). The OMF formed by the combination fermentation of low-grade mineral powder and agricultural waste can more fully reflect the production concept of energy saving and environmental protection, and reduce the cost in the production process of inorganic fertilizers such as urea and phosphate fertilizer. Previous studies have shown that OMF produced by mixing rock powder containing potassium and phosphate with OF or mixing rock powder during OF fermentation can provide beneficial mineral nutrients for crop growth without introducing toxic heavy metal pollution (Theodoro and Leonardos, 2006; Biswas et al., 2009; Lian et al., 2020; Basak et al., 2021; Syed et al., 2021). As an important support of soil quality, soil microorganisms are sensitive to fertilization managements (Wang et al., 2020; Bello et al., 2021). However, there have been no reports on the effects of OMFs application on soil microbial community diversity and composition in karst mountain soils.

P. frutescens is an annual herb in the Labiaceae family and is a widely cultivated cash crop in Asian countries (Hu et al., 2010; Yu et al., 2017). In China, it has traditionally been used in medicine and food, and has been cultivated for more than 2000 years (Lee and Kim, 2007). The oil-rich seeds of *P. frutescens* are used to make condiments in traditional Asian cuisines (Luitel et al., 2017). As the raw material of cooking oil, perilla grains are rich in unsaturated fatty acids and have a high content of α-linolenic acid, up to 50–70%; this is the highest α-linolenic acid content known in plants (Yu et al., 2017). In addition to value as a food item, *P. frutescens* is also used in traditional Chinese medicine, and as food decoration and a coloring agent (Tian et al., 2014). Moreover, *P. frutescens* is an important agricultural crop in karst areas of southwest China (Tian et al., 2017).

Potassium is one of the main elements necessary for plant growth. According to the standard of the Second Soil Survey of China (China Soil Science Database[1]), the soil in karst areas is in a state of potassium deficiency (total $K < 10\,g{\cdot}kg^{-1}$ and available $K < 100\,mg{\cdot}kg^{-1}$). Therefore, potassium supplementation is necessary to improve soil fertility in karst areas of southwest China. For this reason, our OMF was fermented from potassium-containing rocks (potassium feldspar) together with agricultural wastes such as chicken manure and straw. We hypothesized that the application of potassium-containing OMF was beneficial to improving *P. frutescens* quality and yield, and had positive effects on the distribution and structure of soil microbial communities. To test this hypothesis, the yield, quality, and rhizosphere soil

1 http://vdb3.soil.csdb.cn/

microbial community characteristics of *P. frutescens* were analyzed and studied based on soil science, crop science, and high-throughput sequencing technology methods. The aim of this study was to reveal: (1) differences in soil microbial diversity and community structure of the *P. frutescens* rhizosphere under different fertilization treatments; (2) the relationship among *P. frutescens* yield and quality, soil characteristics, and microbial community under different fertilization treatments; and (3) the effects of OMF on soil and crop quality. This study investigated for the first time the feasibility of using OMFs to improve the quality of *P. frutescens* and the abundance of soil beneficial microbial community in the potassium-deficient karst areas. The results will be conducive to the application of new OMFs in karst areas, and improve the yield and quality of *P. frutescens* which is widely cultivated in this area.

Materials and methods

Experimental design and sample collection

The experimental field site was located in Changzhai Village, Changshun County, Guizhou Province, China (26°01′25″ N, 106°30′55″ E; elevation, 1,004 m). The strata are mainly light-colored limestone of the Permian Qixia Formation and Maokou Formation. The soil type is yellow soil according to the Chinese soil classification system (Gong, 1999) and Orthic Acrisols according to the World Reference Base (WRB) soil classification system (USS Working Group WRB, 2015). The region has a subtropical monsoon humid climate. The annual average temperature is 15.1°C, the annual average precipitation is 1396.7 mm, the annual sunshine duration is 1202.1 h, and the annual frost-free period is 275 days.

Four treatments were set up in the field experiment: blank control group (CK), no fertilization; *CF* group, compound *CF* was applied; OF group, ordinary OF was applied; OMF group, potassium-containing OMF was applied. Four parallel plots (5 m × 5 m) were set for each treatment group (total, 16 plots). The randomized complete block design was used to divide the sample area blocks (Supplementary Figure S1). On 7 May 2019, *P. frutescens* was planted and fertilized. The *P. frutescens* seeds were the 1st generation hybrids cultivated by the Oil Materials Research Institute of Guizhou Academy of Agricultural Sciences (China).

The fertilizer specifications used were as follows:

The raw materials for OF fermentation were mushroom residue, distiller's grains, straw, and chicken manure, which were mixed according to a mass ratio of 1:1:1:2 and EM microbial agent was added for fermentation (1 kg bacterial agent was added for every 10 T substrate). The mixture was then fermented in a fermentation tank for 30 days with periodic stirring. The total nutrient content ($N + P_2O_5 + K_2O$) was 7.2%, among which the content ratio of N:P_2O_5:K_2O was 0.9%:2.9%:3.4%, organic matter was 48.3%, and pH was 7.7.

Potassium-containing OMF was made by mixing the raw fermentation materials of the OF and potassium-containing rock powder, which contained 76% potassium feldspar, and passing the mixture through a 2-mm sieve. In accordance with a mass ratio of 3:1, the chemical composition was as follows: Al_2O_3, 17.11%; SiO_2, 54.06%; K_2O, 9.09%; CaO, 1.9%; Fe_2O_3, 6.15%; and MgO, 3.41% (Sun et al., 2019). Then, EM microbial agent was added for fermentation (1 kg bacterial agent per 10 T substrate). The raw materials were thoroughly mixed and fermented for 30 days with periodic stirring. The total nutrient content of OMF was 6.4%, with a content ratio of N: P_2O_5: K_2O of 1.6%:1.1%:3.7%, the content of organic matter was 56.4%, and the pH was 7.6. OF and OMF were produced by Guizhou Guifu Ecological Fertilizer Co., LTD. (China).

The compound *CF* was produced by Guizhou Xiyang Fertilizer Co., LTD. (China) and had a total nutrient content ≥45%, N:P_2O_5:K_2O content ratio was 15%:15%:15%. Urea was produced by Guizhou Chitianhua Tongzi Chemical Co., LTD. (China) with a total N ≥ 46.4%. Phosphate fertilizer was produced by Fuda Phosphorus Chemical Co., LTD. (China) with P_2O_5 ≥ 12%. The proportions of N, P, and K in OF and OMF groups were balanced by urea and phosphate fertilizer. All treatment groups had fertilizer applied with a content ratio of N:P_2O_5:K_2O of 15:15:15, and application amounts are shown in Table 1.

Rhizosphere soil sampling was conducted on 19 August 2019, which was the 105th day of *P. frutescens* growth. Rhizosphere soil samples were arbitrarily collected from eight *P. frutescens* plants in each plot and mixed into one sample. A total of 16 mixed soil samples were collected. When collecting rhizosphere soil, the whole plant was first dug up, and the scattered soil at the root was gently shaken off. The remaining soil attached to the root system was considered the rhizosphere soil (Sun et al., 2021). The soil samples were frozen and transported to the laboratory on dry ice, passed through a 2-mm sterile sieve, and the plant roots were removed. Each sample was divided into two parts: one part was naturally air-dried to determine physicochemical properties, and the other was stored in a −80°C freezer for DNA extraction.

Soil physicochemical analysis

Soil pH was analyzed by vibrating slurry with a water:soil ratio of 2.5:1 (v/w) and determined using a pH meter (Mettler-Toledo FE28, Switzerland; Marcos et al., 2019). Soil total organic carbon (TOC), total organic nitrogen (TON), total carbon (TC), and total nitrogen (TN) were determined using an elemental analyzer (Vario MACRO Cube, Germany; Liu et al., 2014). Total phosphorus (TP) and total potassium (TK) were determined by sodium hydroxide melting flame spectrophotometry (Ren et al., 2016). Available phosphorus (AP) was determined by the $NaHCO_3$ method, and available potassium (AK) was determined by ammonium acetate extraction–flame spectrophotometry (Lu, 1999).

TABLE 1 Fertilization doses of different treatment groups.

Treatments	Base fertilizer				
	Inorganic compound fertilizer kg.hm^{-1}	Conventional organic fertilizer kg.hm^{-1}	Organomineral fertilizer kg.hm^{-1}	Urea (N) kg.hm^{-1}	Calcium superphosphate (P_2O_5) kg.hm^{-1}
CK	0	0	0	0	0
CF	225.00	0	0	0	0
OF	0	993.35	0	53.48	40.37
OMF	0	0	912.47	41.28	197.55

CK is the control blank group; CF is conventional inorganic compound fertilizer group; OF is conventional organic fertilizer group; OMF is organomineral fertilizer group.

P. frutescens yield and quality analysis

On 21 September 2019, *P. frutescens* were harvested on the 137th day of growth. The *P. frutescens* yield was measured after harvest. The main indicators were plant height, biomass per plant, number of stem nodes, number of effective branches at one time, length of effective branches at one time, number of branch angles, number of panicles per plant, length of the main panicle, number of fruits in a single row of the main panicle, number of fruits on the main ear, and number of grains in the 10 main ears. After the perilla seeds were harvested, seed quality was inferred by determining fatty acid content (e.g., palmitic acid content, stearic acid content, oleic acid content, linoleic acid content, and linolenic acid content), total lipid content, and crude protein content. The fatty acid content was determined by gas chromatography–mass spectrometry (GCMS-QP2010, Schimadzu, Japan; Javier et al., 2018; Ko et al., 2018). Fat content was determined by sequential Soxhlet extraction according to ISO 659:2009 (Kourimska et al., 2018). The crude protein content was determined by the Kjeldahl method, the nitrogen concentration of the sample was calculated with a conversion factor (6.25), and the total nitrogen and protein mass were determined to obtain the crude protein content (Yaldiz and Camlica, 2020).

DNA extraction and high-throughput sequencing

Total soil DNA was extracted from 0.5 g soil according to the manufacturer's instructions for the E.Z.N.A.® Soil DNA Kit (Omega Bio-Tek, USA). The DNA extraction quality was detected using 1% agarose gel electrophoresis, and the DNA concentration and purity were determined using a NanoDrop2000 spectrophotometer (Thermo Fisher Scientific Co., LTD., USA). Using the extracted DNA as a template, the V3–V4 region of the bacterial 16 s rRNA gene was amplified using the primers 338F (5′-ACTCCTACGGGAGGCAGCAG-3′) and 806R (5′-GGACTACHVGGGTWTCTAAT-3′; Xu et al., 2016). The fungal ITS region was amplified using the primers ITS1F (5′-CTTGGTCATTTAGAGGAAGTAA-3′) and ITS2R (5′-GCTGCGTTCTTCATCGATGC-3′; Adams et al., 2013). PCR amplification conditions and high-throughput sequencing were conducted as described in Li et al. (2021). Sequencing was performed on Illumina's MiSeq PE300 platform (Shanghai Majorbio Bio-pharm Technology Co., LTD., China). The raw sequence data reported in this paper were deposited in the NCBI SRA database (serial numbers: bacteria, PRJNA836163; fungi, PRJNA836186).

Trimmomatic (version 0.33[2]) was used for quality control of the original sequences (Bolger et al., 2014), and FLASH (version 1.2.11[3]) was used for splicing (Magoc and Salzberg, 2011). The splicing sequence data were analyzed using UPARSE (version 7.1;[4] Edgar, 2013), and sequences with a similarity of ≥97% were assigned to the same operational taxonomic unit (OTU). After quality control and concatenation of the original sequences of all samples, 1,088,672 and 976,526 high-quality sequences of bacteria and fungi were obtained, respectively. At the 97% sequence similarity level, the sequences clustered into 5,685 and 2,585 OTUs, respectively. For each representative sequence, the SILVA (bacteria[5]) and UNITE (fungi[6]) databases were used to annotate taxonomic information (Fan et al., 2020; Kang et al., 2022).

Statistical analysis

Mean value, standard deviation, and variance analysis of soil physicochemical properties and *Perilla* yield and quality were analyzed using Microsoft Excel 2010 and SPSS Statistics (version 20.0, IBM, USA). Differences between mean values were determined by one-way ANOVA and LSD post-hoc test ($p < 0.05$). All bioinformatic analyses were performed using R (version 3.6.1; https://cran.r-project.org/bin/windows/base/old/3.6.1/).

2 http://www.usadellab.org/cms/?page=trimmomatic
3 https://ccb.jhu.edu/software/FLASH/
4 http://drive5.com/uparse/
5 http://www.arb-silva.de
6 http://unite.ut.ee

The alpha diversity (Sobs, Chao, and Shannon indices) of *Perilla* rhizosphere soil microbial communities was estimated based on OTUs. All indices were calculated by the "vegan" (Dixon, 2003) and "picante" (Kembel et al., 2010) packages in R (version 3.6.3). The linear discriminant analysis (LDA) effect size (LEfSe) method was used to assess potential bacterial and fungal biomarkers (from phylum to genus) within soil microbiomes that were specifically enriched under different fertilization management types based on $p < 0.05$ and an LDS score > 4.0 (Segata et al., 2011). Principal coordinates analysis (PCoA) was performed to calculate the gradient of compositional changes for bacterial and fungal microbial communities (based on Weighted-Unifrac distance matrix) using the ggplot2 package (Lozupone and Knight, 2005). Differences in bacterial and fungal communities between different samples were analyzed by Adonis test.

After variance inflation factor (VIF) analysis, pH, TC, TOC, TN, TK, AP, and AK with a VIF threshold less than 10 were selected for redundancy analysis (RDA) between environmental factors and soil microbial communities. Variance partitioning analysis (VPA) was used to quantitatively evaluate the individual and common explainability of environmental factor variables for microbial community differences. In addition, FAPROTAX (Louca et al., 2016) and FUNGuild (Nguyen et al., 2016) were used to analyze the ecological functions of soil bacteria and fungi, respectively. Kruskal–Wallis H test was used to test the significance of differences between groups.

Co-occurrence network analysis

To study the effect of different fertilization management techniques on the relationship of soil microbial communities, soil bacterial and fungal communities were combined based on fertilization management technique, and a soil microbial co-occurrence network based on genus classification was constructed. The co-occurrence network was constructed with genera that had a relative abundance greater than 0.1% based on random matrix theory (Deng et al., 2012). To simplify the networks for better visualization, a Spearman's correlation between the two genera was considered statistically significant if the Spearman's correlation coefficient (r) was >0.6 and the p value was <0.05. Moreover, p values were adjusted using the Benjamini–Hochberg FDR method (Benjamini and Hochberg, 1995). Spearman's correlation and network attributes were calculated using the WGCNA, Psych, Igraph, and fdrci packages in R (version 3.6.3) (Csardi and Nepusz, 2006). The network attributes included the number of edges, average clustering coefficient, average degree, modularity, average path length, graph density, and betweenness centrality. Higher numbers of nodes and edges, graph density, average degree, and lower average path length indicate a more complex and connected network (Ma et al., 2016; Jiao et al., 2021). The higher the betweenness centrality value of microbial species, the greater the critical role of the species in the network. The Fruchterman–Reingold layout algorithm was used in the interactive platform Gephi (version 0.9.2[7]) for network visualization and network topology parameter calculation (Bastian et al., 2009). The network stability was evaluated by removing the nodes in the static network to estimate the speed of robustness decline, and the network robustness was evaluated by the natural connectivity of the nodes (Yuan et al., 2021; Zhu et al., 2022).

Structural equation model analysis

A structural equation model (SEM) was used to identify the direct and indirect effects of soil physicochemical properties (such as pH, TC, AK, and AP) on bacterial and fungal diversity (Shannon index), and *P. frutescens* yield (biomass per plant) and quality (linoleic acid content). To reduce SEM complexity, the representative indices of soil physicochemical properties were calculated by PCoA (Sun et al., 2021). All variables were standardized using Z-transformation (mean = 0, standard deviation = 1; Du et al., 2022).

The theoretical model assumed that: (1) soil pH has a direct impact on soil nutrient content, microbial community diversity, and *P. frutescens* quality or yield, (2) the soil available phosphorus, potassium, and total carbon had direct or indirect effects on the *P. frutescens* quality and yield and the soil microbial community, and (3) the *P. frutescens* yield has a direct effect on the soil microbial community. Model fitting was performed using root mean square error of approximation (RMSEA), probability level p value, Bentler comparative fit index (CFI), maximum likelihood goodness of fit (χ^2), and degrees of freedom (df) tests (Du et al., 2022). The SEM was constructed using Amos Graphics (version 24.0, IBM Corp., USA; Liu, L. et al., 2019).

Results

Soil physicochemical properties

Compared with the CK group, the OMF group significantly increased soil TC and TK contents ($p < 0.05$; Table 2). Fertilization also significantly increased soil AK content ($p < 0.05$; Table 2). In addition, there were no significant differences in the physicochemical properties between the different fertilization treatment groups. The measurement results of different fertilization treatment groups indicated that short-term fertilization treatments may not significantly improve soil physicochemical properties. However, numerical analysis demonstrated that OF and OMF treatments tended to produce better results than no fertilization and *CF* treatment.

7 https://gephi.org/

TABLE 2 Soil chemical properties under different fertilization treatments.

Chemical factor	CK	*CF*	OF	OMF
pH	5.98 ± 0.19a	5.91 ± 0.07a	6.04 ± 0.10a	6.00 ± 0.13a
TOC	15.73 ± 0.79a	16.12 ± 0.72a	16.31 ± 0.78a	16.49 ± 1.14a
TON	0.14 ± 0.01a	0.15 ± 0.01a	0.15 ± 0.01a	0.15 ± 0.01a
TC	20.43 ± 0.50b	20.78 ± 0.66ab	20.86 ± 0.29ab	21.16 ± 0.34a
TN	1.92 ± 0.06a	1.97 ± 0.05a	1.95 ± 0.04a	1.93 ± 0.03a
TP	0.80 ± 0.05a	0.81 ± 0.04a	0.82 ± 0.04a	0.81 ± 0.04a
TK	5.59 ± 0.14b	5.68 ± 0.20ab	5.70 ± 0.19ab	5.84 ± 0.09a
AP	28.51 ± 6.65a	35.24 ± 5.88a	30.89 ± 5.73a	30.42 ± 5.61a
AK	92.75 ± 20.35b	99.5 ± 44.44a	98.50 ± 31.29a	109.75 ± 30.83a

pH stands for soil pH; TOC represents soil total organic carbon content, g·kg^{-1}; TON stands for soil total organic nitrogen content, g·kg^{-1}; TC stands for soil total carbon content, g·kg^{-1}; TN stands for soil total nitrogen content, g·kg^{-1}; TP represents soil total phosphorus content, g·kg^{-1}; TK represents soil total potassium content, g·kg^{-1}; AP stands for soil available phosphorus content, mg·kg^{-1}; AK stands for soil available potassium content, mg·kg^{-1}. Different letters (a, b) on the same row indicate values that are significantly different ($p < 0.05$) based on one-way ANOVA and LSD post-hoc test.

P. frutescens yield and quality

The analysis of *P. frutescens* yield during the harvest period showed that, compared with the CK group, the *CF*, OF, and OMF groups all significantly improved the yield indicators, including the number of stem nodes, number of effective branches at one time, and number of branch angles. However, there were no significant differences among the three fertilization treatments (Table 3). In addition, the number of panicles per plant and length of the main panicle in the OMF group were significantly greater than those in the other treatment groups.

Analysis of *P. frutescens* seed quality showed that the contents of oleic acid, linoleic acid, α-linolenic acid, and fat in the OF and OMF groups were significantly higher than those in the CK and *CF* groups. Additionally, the OMF group had the highest contents of oleic acid, α-linolenic acid, and fat (Figure 1). The crude protein content of the OMF group was significantly higher than that of the other treatment groups ($p < 0.05$). This indicated that the application of OFs, especially OMF, helped improve *P. frutescens* quality.

Effects of fertilization treatments on soil microbial community composition

Alpha diversity analysis showed that different fertilization treatments did not significantly affect soil bacterial community richness and diversity, whereas OMF significantly increased soil fungal community richness (Figure 2). PCoA showed that there was no clear distinction between samples from different treatment groups on the PC1 and PC2 axes (Figures 3A,B); this indicated that there was no significant difference in soil bacterial community and fungal community composition among different fertilizer treatment groups in the short term.

TABLE 3 *Perilla frutescens* yield indexes under different fertilization treatments.

Fertilizer regimes	Individual plant biomass (g)	Plant height (cm)	Nodes on main stem	Number of once effective branches	Once effective branch length	Number of pod angles on branches	Spike number per plant	Length of main spike (cm)	Number of main spike per row	Number of pod horns in main ear	Grain number of 10 main spike
CK	365.56 ± 77.36a	130.81 ± 8.80a	10.06 ± 1.00b	18.81 ± 2.34b	109.06 ± 11.39a	26.25 ± 4.28b	51.31 ± 10.93c	27.56 ± 2.63b	32.13 ± 2.80a	128.50 ± 11.21a	35.94 ± 3.38ab
CF	383.31 ± 64.18a	130.88 ± 9.14a	10.69 ± 0.60ab	20.94 ± 1.24a	110.13 ± 11.63a	28.44 ± 3.52ab	55.25 ± 11.53bc	27.13 ± 2.19b	31.88 ± 1.59a	127.50 ± 6.35a	35.56 ± 2.85b
OF	433.31 ± 163.47a	134.25 ± 12.08a	10.63 ± 1.02ab	20.94 ± 1.65a	115.63 ± 15.13a	29.69 ± 2.87ab	59.63 ± 9.53ab	28.06 ± 2.52b	33.25 ± 1.84a	133.00 ± 7.38a	38.44 ± 1.09a
OMF	426.31 ± 68.00a	133.31 ± 5.58a	10.88 ± 1.02a	20.81 ± 2.26a	114.06 ± 8.98a	30.31 ± 2.87a	64.94 ± 11.33a	30.50 ± 2.50a	32.94 ± 2.49a	131.75 ± 9.96a	37.88 ± 1.71ab

Different letters (a, b) on the same column indicate values that are significantly different ($P < 0.05$) based on one-way ANOVA and LSD post-hoc test.

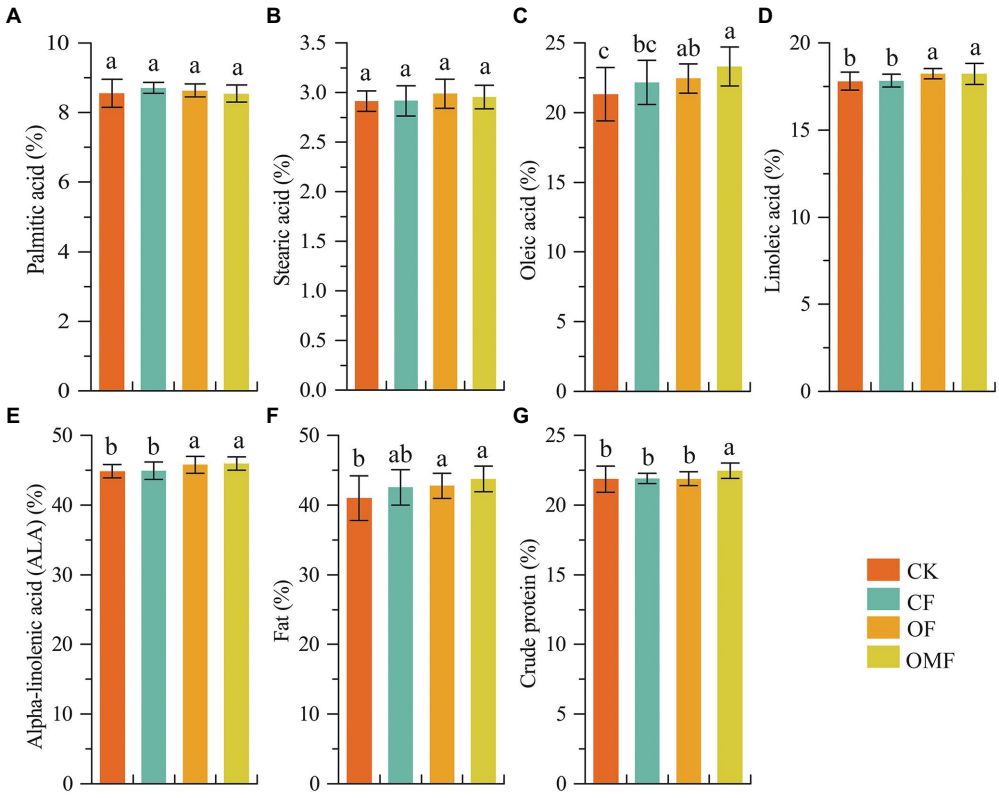

FIGURE 1
Perilla frutescens quality index under different fertilization treatments. Based on one-way ANOVA and LSD post hoc test, different letters (a,b) indicated significant differences among fertilization treatment groups ($P < 0.05$).

Fertilization management did not cause significant changes in phylum-level bacterial composition ($p > 0.05$, ANOVA analysis; Figure 3C). Proteobacteria, Actinobacteria, Acidobacteria, and Chloroflexi were the main dominant bacterial phyla in each fertilization treatment group. Fertilization management also did not significantly affect the fungal community composition at the phylum level ($p > 0.05$, ANOVA; Figure 3D). Ascomycota, Mortierellomycota, Basidiomycota, and Glomeromycota were the dominant fungal phyla in each treatment group. The taxonomic analysis of the dominant bacterial genera with relative abundance >1% showed that different short-term fertilization treatments had no obvious effect on most dominant bacterial genera (Supplementary Table S1). However, the relative abundances of *Bacillus* and *Candidatus_Solibacter* significantly increased after fertilization, especially in the OF and OMF groups; the relative abundance of *Bryobacter* significantly decreased in the OF and OMF groups. The relative abundances of *Clonostachys* and *Gonytrichum* in the OMF group were significantly lower than those in the other groups, and the relative abundance of *Penicillium* in the OF group was significantly lower than that in the other treatment groups. In addition, there were no significant differences in other dominant fungal genera among the treatment groups (Supplementary Table S2).

The LEFSe results showed that *Bryobacter* was significantly enriched in the CK group; the nitrogen-fixing bacteria *Saccharimonadia* and iron-reducing bacteria *Desulfobacca* were significantly enriched in the *CF* group; *Actinomadura*, *Nakamurellaceae* and *Nakamurella* were significantly enriched in the OF group; and *Iamia* and *Iamiaceae* was significantly enriched in the OMF group (Figure 4A). The LEFSe analysis of the fungal community showed (Figure 4B) that Cyphellaceae, Piskurozymaceae, Filobasidiales, *Solicoccozyma*, and *Funneliformis* were mainly enriched in the CK group, and Mycosphaerellaceae, Didymosphaeriaceae, *Paraphaeosphaeria*, and *Pseudopithomyces* were mainly enriched in the *CF* group. Helotiales, Glomerales, *Cladorrhinum*, and *Pseudallescheria* in the OF group, and Phaeosphaeriaceae, Bulleribasidiaceae, and *Sodiomyces* were mainly enriched in the OMF group.

Co-occurrence network analysis of soil microbial communities under different fertilization management techniques

Analysis of the topological indicators of the bacterial community co-occurrence network revealed that the OMF group had the highest increase in the number of network edges and average degree (Table 4). The OF group had the highest modularity index, followed by the OMF group. This finding indicated that the application of OF and OMF could enhance the association of soil

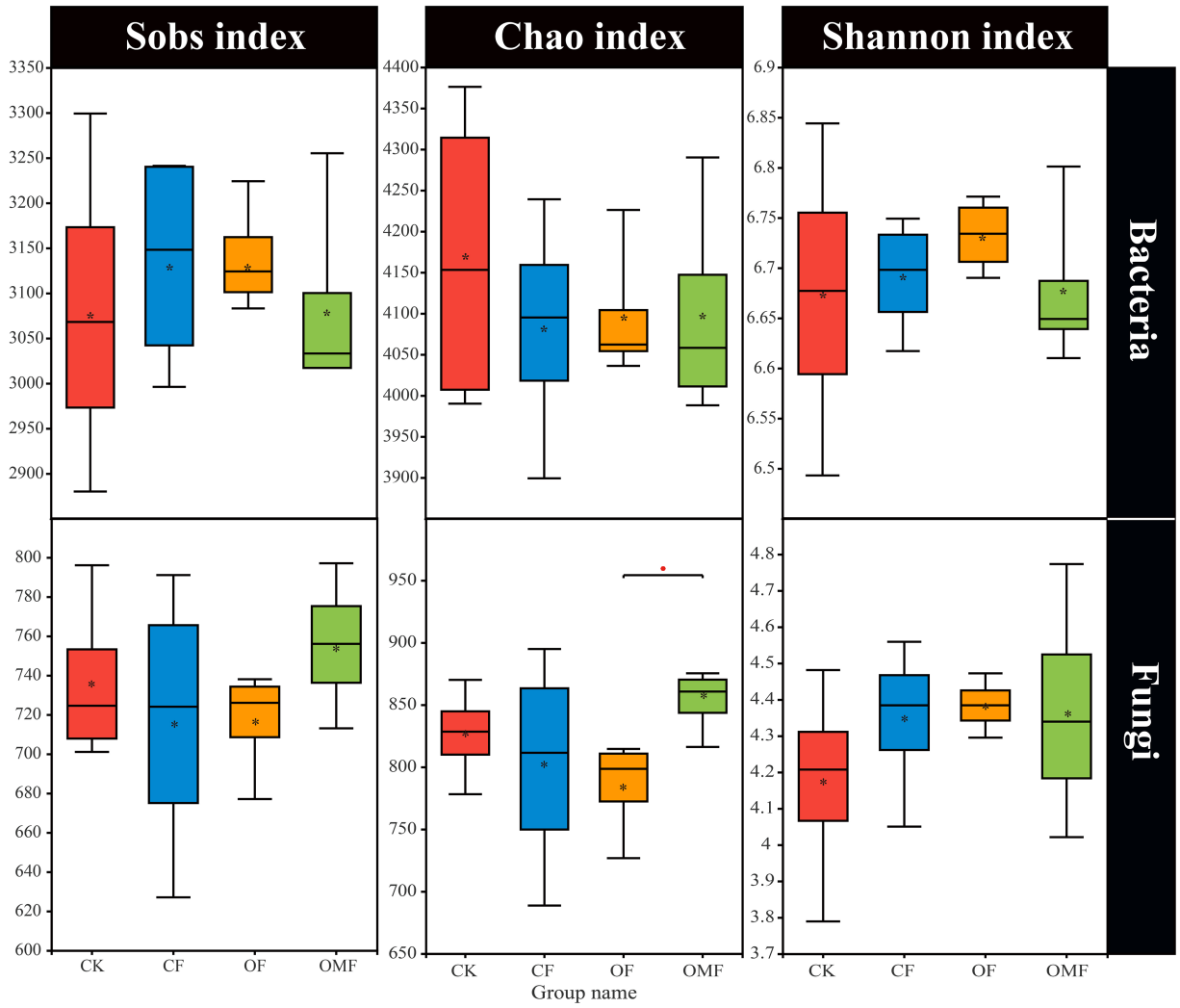

FIGURE 2
Alpha diversity index of soil microbial community in different treatment groups. *indicates a significant difference at the level of $0.01<p\leq0.05$ (Student *t* test).

bacterial communities because the degree of modularity was higher. The robustness analysis results showed that the robustness of OF and OMF treatment groups were higher than that of CK and OF groups, and OMF groups was highest (Figure 5C).

Analysis of the network topology indicators of the fungal community showed that, compared with other treatment groups, the OMF group significantly increased the total number of edges in the network, number of positive correlation edges, number of nodes, graph density, and average degree (Table 4). The OMF group had the highest modularity index; this demonstrated that OMF can improve the association of fungal communities, and OMF can make the fungal community structure more modular and more stable. The robustness analysis results showed that the robustness of OMF and *CF* groups had little difference, but was higher than that of CK and OF groups (Figure 5D).

Analysis of the scale proportions of the top three modules in each group revealed that the proportion of the top three modules of bacterial and fungal communities was greatest in the OF group followed by the OMF group (Supplementary Figure S2). This indicated that the bacterial communities and the fungal communities of the OF and OMF groups were more closely related.

The main nodes in the bacterial community network of each treatment group belonged to Proteobacteria, Actinobacteria, Acidobacteria, Chlorobacteria, Bacteroidetes, and Firmicutes; the main nodes in the fungal community network belonged to Ascomycota, Basidiomycota, and Glomeromycota. This finding indicated that these bacterial and fungal phyla were keystone microbiota in all treatment groups (Figure 5). According to the analysis of the betweenness centrality values (Supplementary Table S3), the top 10 genus-level species were different in each treatment group, which indicated that the genus-level microbiota that played a key role in the co-occurrence network differed among treatment groups.

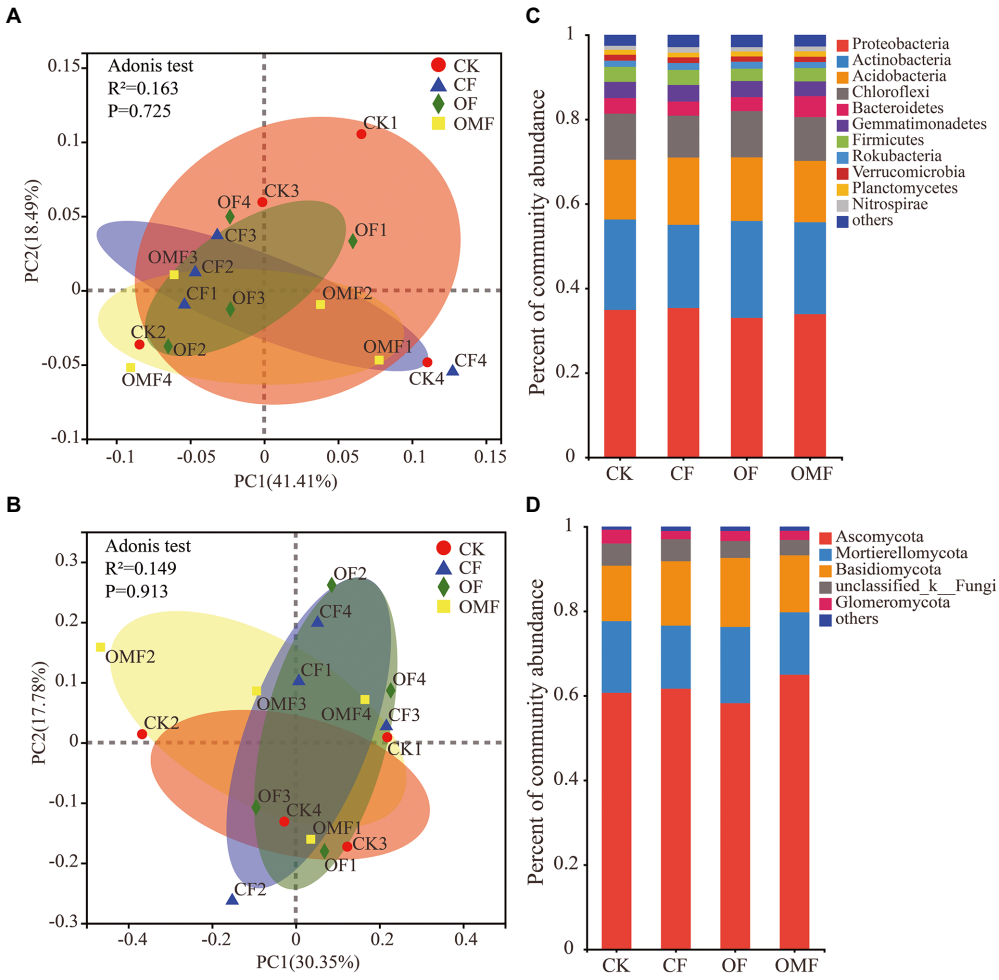

FIGURE 3
Principal coordinates analysis of the Weighted-Unifrac distance matrix for bacteria **(A)**, and fungi **(B)**, in different fertilizer treatment groups. Bar plots of relative abundance of bacterial phyla **(C)**, and fungal phyla **(D)**, in different fertilization groups.

Effects of different fertilizer treatments on the ecological function of soil microbial communities

According to FAPROTAX functional analysis, chemoheterotrophy, aerobic chemoheterotrophy, nitrification, aerobic ammonia oxidation, and nitrogen fixation were the top five bacterial community functions in each treatment group (Figure 6A). Among the top 50 functions, only human pathogens all significantly differed among different treatments, and the OF and OMF treatments reduced the proportion of human pathogenic bacteria in soil compared with CK and *CF* treatments. There were no significant differences in other bacterial community functions among different treatment groups.

FUNGuild functional analysis indicated that Saprotroph, Saprotroph–Symbiotroph, Pathotroph–Saprotroph–Symbiotroph, Pathotroph, and Symbiotroph were the top five trophic modes of the fungal community (Figure 6B). Analysis of the relative abundance of arbuscular mycorrhizal fungi (AMF) in symbiotic trophic fungi showed that the AMF abundance was significantly reduced in the *CF* group (Supplementary Figure S3A); this indicated that CFs inhibited AMF growth. F_unclassified_o_Paraglomerales, Glomeraceae, Diversisporales_fam_Incertae_sedis, f_unclassified_o_GS24, and Paraglomeraceae were the dominant families in AMF, but there were significant differences in their relative abundances among different fertilization treatments groups (Supplementary Figure S3B).

Effects of soil environmental factors on microbial community composition and diversity, and *P. frutescens* yield and quality

RDA indicated that the selected environmental factors explained 38.20% of the total change in bacterial communities (Figure 7A) and 31.32% of total changes in fungal communities (Figure 7B). The results of RDA showed that pH (ANOVA,

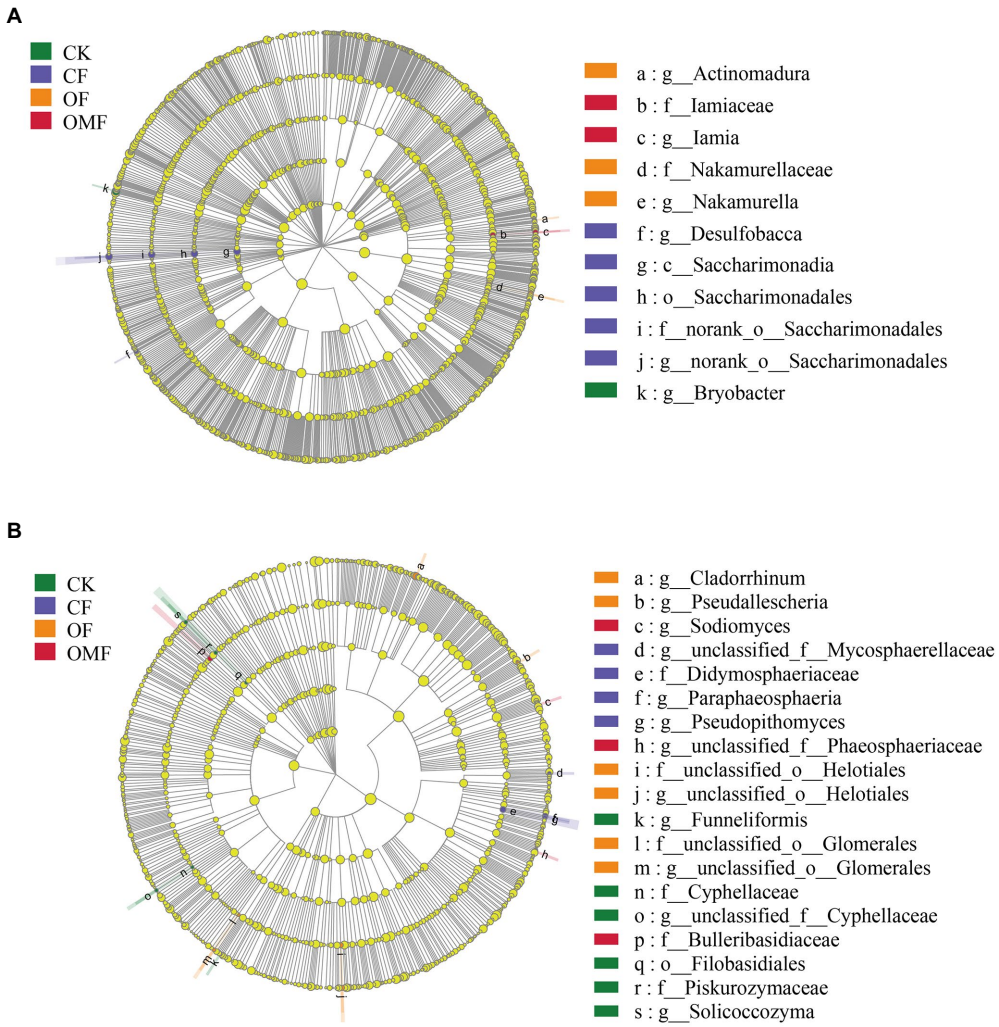

FIGURE 4
Effects of different fertilization treatments on the relative abundance of soil bacterial **(A)**, and fungal **(B)**, lineages. The linear discriminant analysis (LDA) effect size analysis was performed to identify the indicator taxa representing each group, and the values were significant ($p<0.05$) when the LDA score was greater than 4. There are five rings in the cladogram, that represent the phylum, class, order, family, and genus from inside to outside, respectively. The different color nodes (except yellow, which indicates no significant changes) on the ring represent significant changes in taxonomic composition due to the treatments. Abbreviations for classification levels: P, phylum; C class; O, order; F, family; G, genus.

TABLE 4 Topological indices of each co-occurrence network in Figure 5.

	Bacteria				Fungi			
	CK	*CF*	OF	OMF	CK	*CF*	OF	OMF
No. of edges[1]	1,629	1,915	1,833	1,985	411	473	420	659
Modularity[2]	3.702	5.209	7.045	5.807	1.154	1.190	1.584	1.808
Graph density[3]	0.065	0.077	0.070	0.076	0.075	0.080	0.071	0.097
Average degree[4]	14.480	17.175	15.939	17.336	7.829	8.679	7.706	11.265
Average path length[5]	4.508	4.306	4.274	4.390	7.941	7.498	5.829	3.252
Average clustering coefficient[6]	0.660	0.666	0.648	0.659	0.752	0.760	0.703	0.778

[1]Number of connections/correlations obtained by Gephi software.
[2]Capability of the nodes to form highly connected communities, that is, a structure with high density of between nodes connections.
[3]Measure network integrity. A complete graph with all possible edges, that is, any two nodes with edge connections, has a density of 1.
[4]Average number of connections per node in the network, that is, the node connectivity.
[5]Average network distance between all pair of nodes or the average length off all edges in the network.
[6]How nodes are embedded in their neighborhood and the degree to which they tend to cluster together.

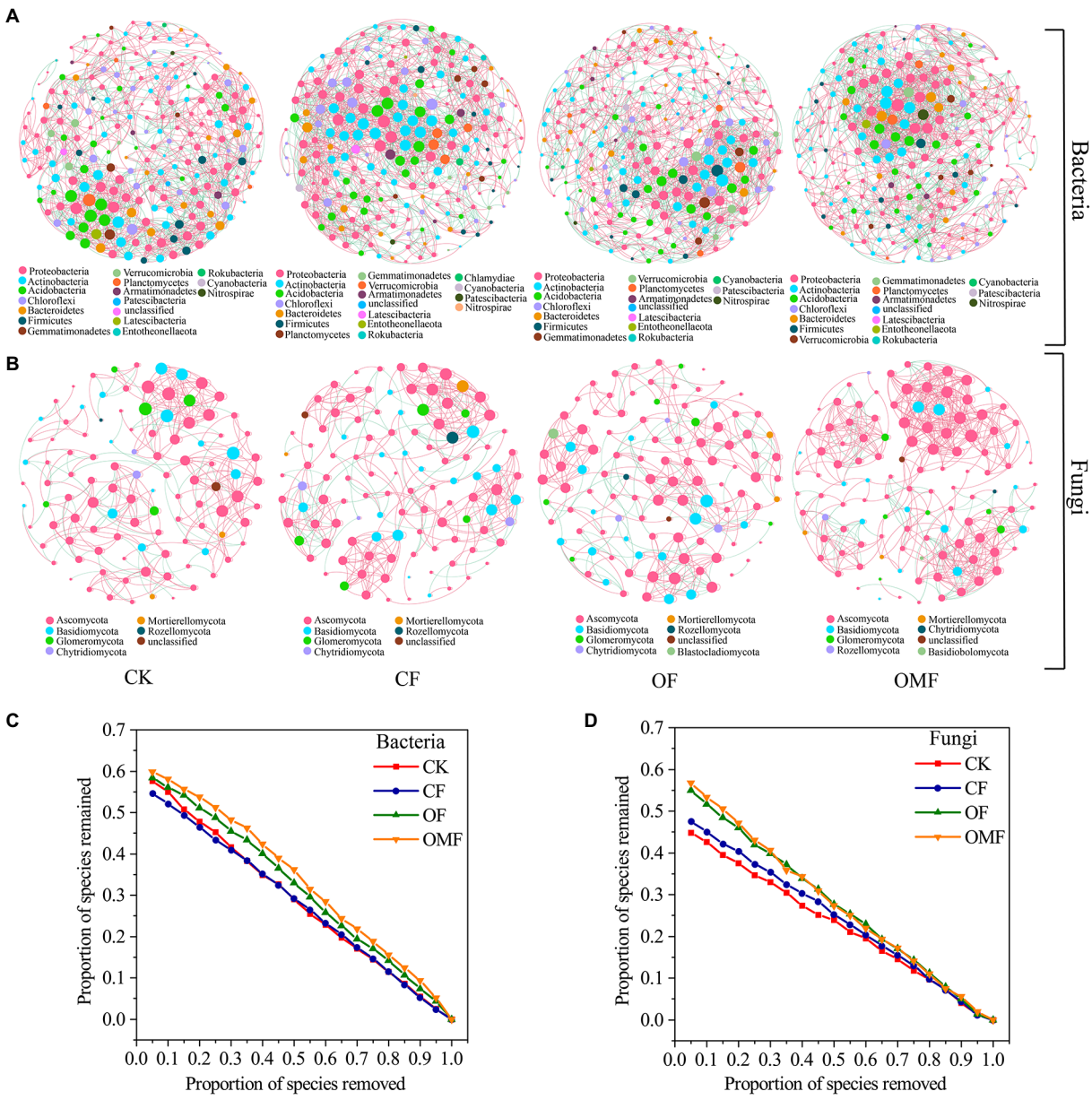

FIGURE 5
Co-occurrence networks of the soil microbial communities at the genus level in different fertilization treatment groups **(A,B)**; and the robustness of bacterial network **(C)**, and fungal network **(D)**. The node size is proportional to the taxon abundance, and the nodes represent bacterial or fungi taxa at the genus level (genera with relative abundances greater than 0.1%). The node colors represent different bacterial and fungal phyla. The edges are colored according to interaction types; positive correlations are labeled in pink and negative correlations are labeled in green.

$p = 0.021$) and AP (ANOVA, $p = 0.024$) were the main factors affecting the soil bacterial community composition, and pH (ANOVA, $p = 0.034$) and AK (ANOVA, $p = 0.011$) were the main factors affecting the soil fungal community composition (Figure 7).

The SEM fit the measured data well (bacteria, $\chi^2/df = 0.658$, $p = 0.764$, CFI = 1.000, RMSEA = 0.000; fungi, $\chi^2/df = 1.493$, $p = 0.135$, CFI = 0.920, RMSEA = 0.181); this indicated high consistency between the hypothesized model and the observed data (Figure 8). The SEM showed that soil physicochemical properties accounted for 68% of *P. frutescens* quality, among which AK and TC were significantly positively correlated with *P. frutescens* quality, and pH and AP were significantly negatively correlated with *P. frutescens* quality (Figure 8). AK and AP were significantly positively correlated with bacterial diversity, and *P. frutescens* yield was significantly negatively correlated with bacterial diversity; these factors accounted for 68% of bacterial diversity (Figure 8A). AP was significantly positively correlated with and explained 61% of *P. frutescens* yield. TC and *P. frutescens* yield were directly and significantly positively correlated with fungal community diversity, whereas AK was directly and

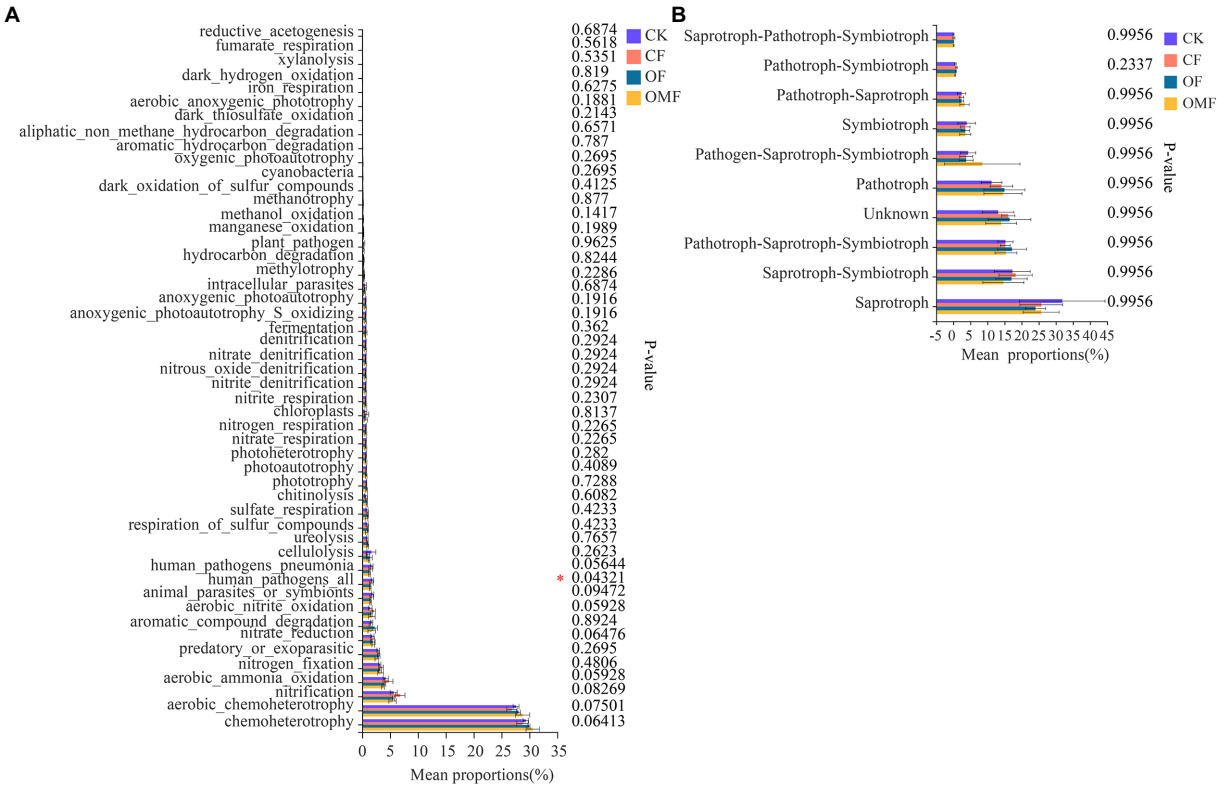

FIGURE 6
Functional analysis of soil microbial community in different treatment groups. FAPROTAX function analysis of bacterial communities **(A)**, and FUNGuild function analysis of fungal communities **(B)**. The abscissa indicates the function name, the ordinate indicates the percentage value of a function abundance of the sample, and different colors indicate different groups. Based on Kruskal–Wallis H test, the rightmost values represent *p* values, where *indicates $0.01<p\leq0.05$.

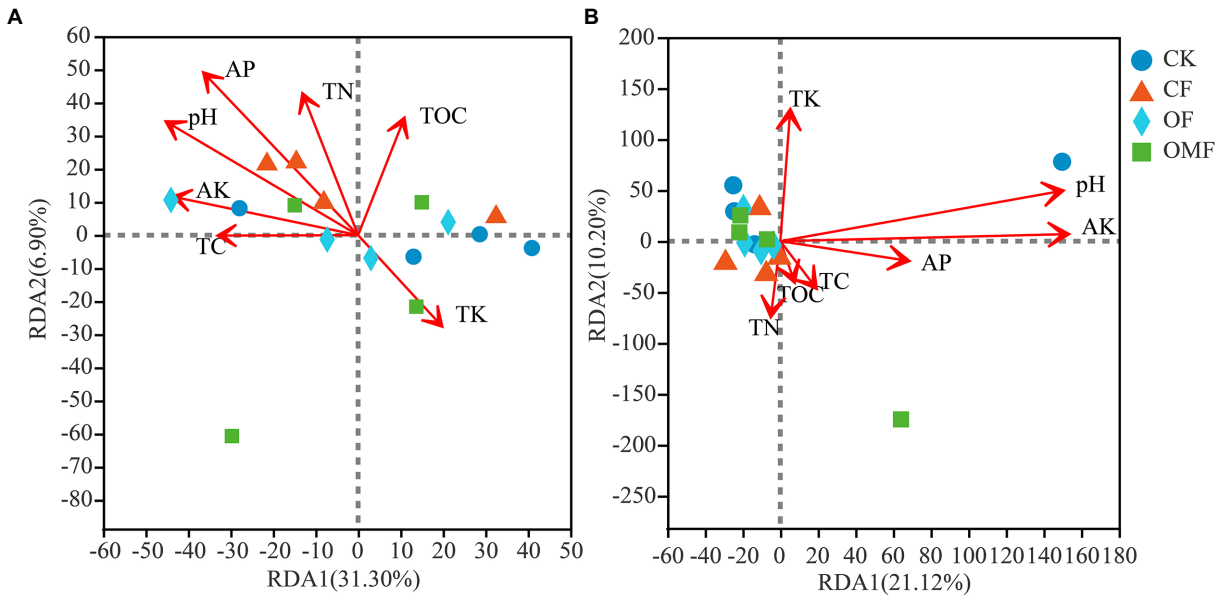

FIGURE 7
Distance-based redundancy analysis (RDA) among bacterial **(A)**, or fungal **(B)**, communities and environmental factors.

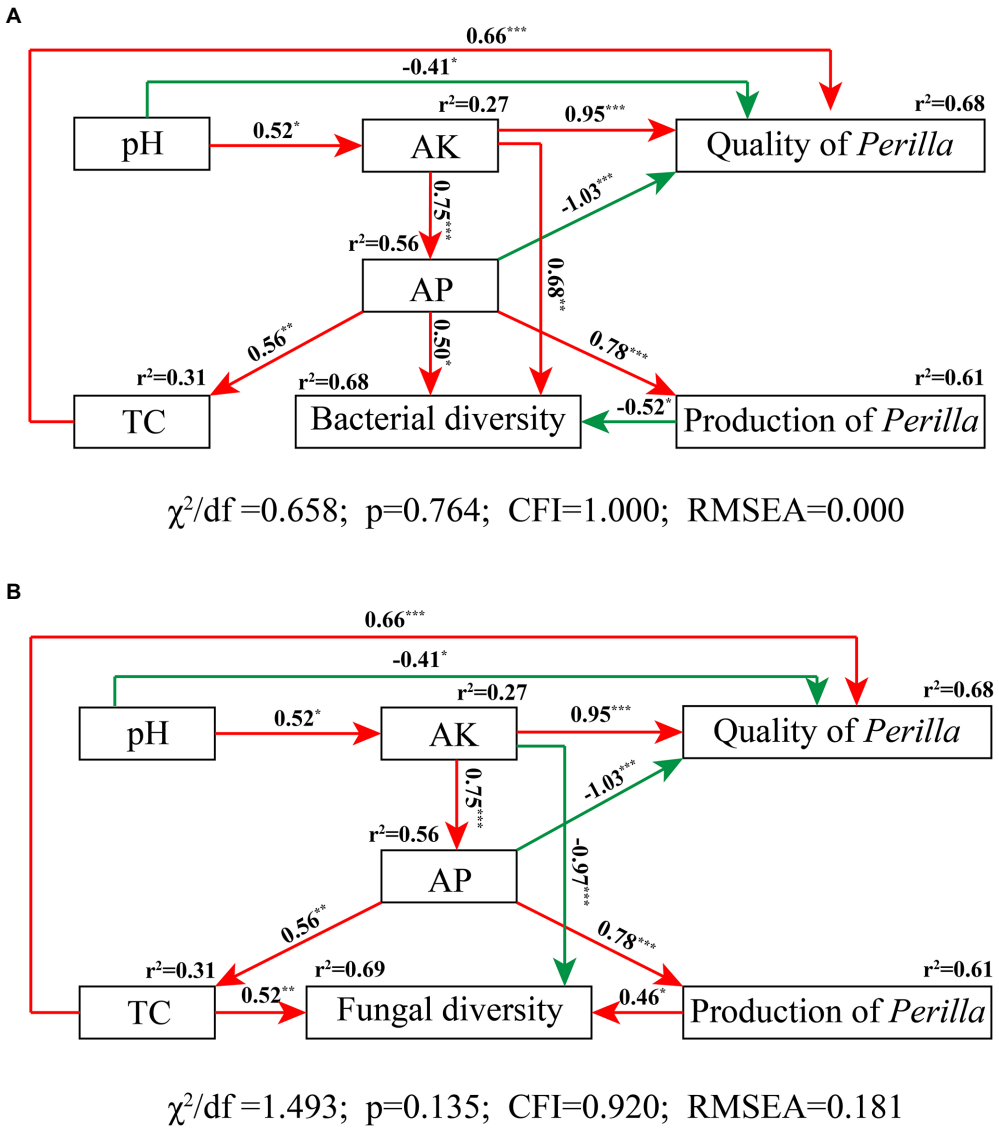

FIGURE 8
Structural equation modeling results describing the relationship among soil nutrients, microbial diversity, and *P. frutescens* yield and quality. The relationship among soil pH value, total soil carbon content (TC), available potassium (AK), available phosphorus (AP), *P. frutescens* production, and *P. frutescens* quality with bacterial diversity **(A)**, and fungal diversity **(B)**. Red lines: positive correlation; green lines: negative correlation. The numbers above the arrows indicate correlation strength. r^2 values indicate the proportion of variance explained for each variable. χ^2, Chi-square; df, degrees of freedom; p, probability level; RMSEA, goodness-of-fit statistics for each model. Significance levels of each predictor are shown as *for $p<0.05$, **for $p<0.01$, and ***for $p<0.001$.

significantly negatively correlated with fungal community diversity (Figure 8B).

Discussion

Effects of organomineral fertilizer on soil properties and *P. frutescens* yield and quality

Compared with the CK group, OMF application significantly increased the TC and TK contents of the soil (Table 2). The experiment proved that although short-term application of OMF could not significantly improve most of the soil physicochemical properties, it could guarantee the same effect as the same amount of inorganic fertilizer. Numerical analysis showed that OF especially OMF application had a trend of improving soil fertility compared with no fertilization and *CF* application, which was consistent with previous continuous fertilization results (Zhao et al., 2016; Du et al., 2022).

The yield test results of *P. frutescens* at harvest showed that the number of panicles per plant and length of the main panicle were significantly greater in the OMF group compared with the other treatment groups (Table 3); this indicated that OMF

increased *P. frutescens* yield to a certain extent. The quality inspection results of *P. frutescens* showed that OF and OMF treatments significantly increased the contents of unsaturated fatty acids, total fat, and total protein in *P. frutescens*, and the OMF treatment values were higher (Figure 1). These results were similar to those of a previous study that investigated the effect of OMF on *Purslane* growth, which also showed that OMF treatment increased unsaturated fatty acid content (Yang et al., 2020). The SEM results also demonstrated that soil AK content was significantly positively correlated with *P. frutescens* quality (Figure 8). Therefore, OMF application was beneficial for improving *P. frutescens* quality.

Effects of different fertilization treatments on soil microbial communities

Microorganisms are the driver of soil fertility changes; they can directly indicate soil quality and play an important role in plant growth and crop yield (Fan et al., 2020; Finkel et al., 2020). In this study, short-term fertilization treatments did not significantly affect alpha diversity (Figure 2). Similar studies also showed that soil microbial alpha diversity was stable and not easily affected by agricultural management practices (Coller et al., 2019; Gui et al., 2021; Kang et al., 2022). How fertilization management affects soil microbial diversity depends on soil properties (Mendes et al., 2015), such as soil pH, which is generally considered a decisive factor underlying microbial diversity (Bissett et al., 2011).

Actinobacteria and Firmicutes are generally considered to be beneficial microorganisms for plants (Yang et al., 2017). Actinobacteria can control plant bacterial diseases by producing various antibiotics, secreting cell wall-degrading enzymes, and inducing host resistance (Conn et al., 2008; Chater et al., 2010; Liu et al., 2012). LEFSe analysis showed that the treatment of OF and OMF promoted the enrichment of some bacteria belong to Actinobacteria, including *Actinomadura*, *Nakamurellaceae*, *Nakamurella*, *Iamiaceae*, and *Iamia* (Figure 4). *Actinomadura* can produce several antibiotics that inhibit the growth of soil pathogens and reduce the occurrence of crop diseases and insect pests (Li et al., 2022). *Bacillus* and *Candidatus_Solibacter* were also significantly increased in OF and OMF groups (Supplementary Table S1). *Bacillus* is commonly formulated as biocontrol agents because they secrete antibiotics or antimicrobial proteins (Ahimou et al., 2000; Weller et al., 2002; Moyne et al., 2004), and improve soil fertility by increasing soil mineral nutrient availability (Chen et al., 2016). Additionally, *Candidatus_Solibacter* is a bacterium that decomposes organic matter (Rime et al., 2015).

LEFSe analysis showed that the main enriched fungal species (e.g., Glomerales, *Cladorrhinum*, and *Pseudallescheria*) in the OF groups belonged to the phyla Ascomycota and Glomeromycota (Figure 4B). Among them, *Pseudallescheria* is a biocontrol fungus; it is an important natural enemy of some plant parasitic nematodes that can parasitize eggs and infect larvae and females, and can significantly reduce the damage of plant nematode diseases such as those caused by root-knot, cyst, and stem nematodes of various crops (Wang et al., 1997; Ko et al., 2010; Zhu et al., 2020). *Cladorrhinum* is an effective biocontrol fungus for controlling the soil-borne *Rhizoctonia solani* pathogen (Liu, H. et al., 2019). Ascomycota is a key driver of the degradation of organic residues in soil (Richardson, 2009; Ma et al., 2013); therefore, the Ascomycota abundance may increase with increasing organic matter content (Du et al., 2022). Glomeromycota can undergo symbiosis with terrestrial plants to form arbuscular mycorrhizae, and this symbiosis can help plants absorb inorganic salts in soil, especially phosphorus (Smith and Read, 2008; Calaca and Bustamante, 2022). Our results showed that, OF treatments promoted increase in the number of beneficial fungi in the karst soil.

In conclusion, short-term fertilization treatments affected soil microbial communities, and OF and OMF had advantages over *CF*. However, compared with previous long-term experimental results, some differences in this study were not significant. Therefore, extending the fertilization period and intensifying fertilization may produce significant fertilization effects (Kox et al., 2020).

OMF treatment increased connectivity and structural stability of soil microbial communities

There is a complex association network among soil microbial communities, and they do not exist alone. When soil microbial community composition changes because of fertilization management, the microbial co-occurrence network also changes (Kang et al., 2022). The OF and OMF groups had higher modularity indices, which indicated that OF and OMF improved the soil microbial community connectivity and made the community connected more closely (Figure 5; Supplementary Figure S2; Table 4). This result is generally consistent with those of other studies on OF application (Ling et al., 2016; Wang et al., 2017; Liu et al., 2020; Kang et al., 2022).

Complex networks with higher connectivity are more tolerant of environmental disturbances than simple networks with lower connectivity (Santolini and Barabási, 2018). In this study, the network connectivity of both bacterial and fungal communities was highest in the OMF group (Table 4); this indicated that OMF treatment resulted in higher anti-interference ability of soil microorganisms. As the core components of soil organic matter degradation, bacteria and fungi usually form different functional groups and change the interaction between their ecological networks because of the decomposition or utilization of organic and inorganic nutrients (Wang et al., 2017; Dai et al., 2018; Samaddar et al., 2019), and they tend to maintain a complex network structure (Kang et al., 2022). The robustness analysis

showed that the application of OF, especially OMF, could improve the stability of bacterial and fungal network structures (Figures 5C,D).

Keystone microbial groups play an important role in maintaining ecosystem homeostasis (Banerjee et al., 2018; Fan et al., 2020). According to the degree values of the network nodes, it was found that the key bacterial and fungal phyla in the nodes were not significantly different among the treatment groups (Figure 5); this was consistent with the composition and distribution of dominant species in the community (Figures 3C,D). At the phylum level, microorganisms had strong stability and were not easily affected by fertilization management. The genera with the highest betweenness centrality scores are generally considered keystone taxa (González et al., 2010; Vick-Majors et al., 2014). In this study, the keystone genera differed among fertilization treatment groups. The keystone genus of the bacterial community in the OMF group was *Pseudomonas*, and the keystone genus of the fungal community was *Metarhizium* (Supplementary Table S3), both of which are recognized as biocontrol microorganisms. *Pseudomonas* can adsorb heavy metals in soil and promote plant growth (Costa-Gutierrez et al., 2020; Ghorbanzadeh et al., 2020; Wu et al., 2022), whereas *Metarhizium* can kill plant pests and mitigate plant diseases (Riguetti Zanardo Botelho et al., 2019; Gebremariam et al., 2021; González-Pérez et al., 2022). In conclusion, this study demonstrated that the application of organic fertilizer, especially OMF, can not only enhance the connectivity, cohesiveness and stability of microbial community network structure, but also increase the abundance of beneficial microorganisms.

Relationship among soil physicochemical properties, soil microbial community, and *P. frutescens* yield and quality

The RDA results showed that soil pH was the most important factor affecting bacterial and fungal communities (Figure 7). This results was consistent with the previous study (Cho et al., 2016; Gu et al., 2019). Changes in soil pH can alter soil structure, fertility, and vegetation communities, thereby directly or indirectly affecting soil microbial community composition (Lauber et al., 2009; Qi et al., 2018). In addition, in this study, AP was also the main factor affecting bacterial communities, and AK was the main factor affecting fungal communities (Figure 7). Fertilizers may be absorbed and used by plants after entering the soil, or they may remain in the soil, leading to changes in the composition of bacterial communities (Sun et al., 2016) and fungal communities (Zhou et al., 2016). Therefore, different fertilization treatments affected soil microbial community composition by mediating the effects of soil physicochemical properties, especially pH, and AP and AK.

SEM results showed that both soil TC and AK content was positively correlated to the quality (linoleic acid content) of *P. frutescens* (Figure 8), indicated that improve soil carbon and available potassium content could improve the quality of *P. frutescens*. There was a direct and significant positive correlation between *P. frutescens* yield and AP (Figure 8); this indicated that *P. frutescens* yield was mainly affected by the AP content in soil, and increasing the AP content can improve *P. frutescens* yield. Soil bacterial diversity was significantly positively correlated with soil AK (Figure 8A), but fungal diversity was significantly negatively correlated with soil AK (Figure 8B). Some previous studies showed that soil bacteria and fungi exhibited different patterns in response to fertilization treatments (Álvarez-Martín et al., 2016; Ai et al., 2018), and our study also supported this conclusion. Fungi are generally considered more closely related to plants and they are able to provide nutrients to plants in a symbiotic relationship (Chen et al., 2017), whereas bacteria are more affected by soil properties and environmental factors (Singh et al., 2008; Delgado-Baquerizo et al., 2016, 2018); our study obtained similar results (Figures 7, 8). In this study, we found that soil bacterial diversity was significantly negatively correlated with *P. frutescens* yield, and fungal diversity was significantly positively correlated with *P. frutescens* yield. This result may be opposite to many previous long-term fertilization studies. Because, in this study, short-term application of OF and OMF significantly increased *P. frutescens* yield (biomass per plant), but there was no significant change in bacterial diversity (Shannon index), and the value of OMF group even showed a downward trend (Figure 2). The application of organic fertilizer may stimulate the rapid growth of some dominant bacteria and beneficial bacteria in soil in a short time, while the abundance of some oligotrophic microorganisms that are not adapted to the existence of organic fertilizer will decline, resulting in the decrease of bacterial diversity. Through the correlation analysis among soil physicochemical properties, microbial communities and *P. frutescens* agronomic efficiency, it can be concluded that the application of OF or OMFs can improve the physicochemical properties of soil, especially the contents of total carbon, available potassium and available phosphorus, which can promote the quality and yield of *P. frutescens*.

Conclusion

The results of this study demonstrated that, under short-term fertilization management, OMF increased the total carbon and total potassium contents of soil. OF, especially OMF, improved measures of *P. frutescens* yield and quality, including the number of panicles per plant, length of the main panicle, and contents of unsaturated fatty acids such as α-linolenic acid, total fat, and total protein, while significantly increasing the number of beneficial microbial communities in the soil. The co-occurrence network analysis also revealed that OF and OMF improved the connectivity and stability of soil microbial communities. In conclusion, application of OF,

especially OMF, is a good strategy to shape the composition of beneficial bacterial communities in the soil, and to improve soil fertility and crop yield and quality in karst areas.

Data availability statement

The datasets presented in this study can be found in online repositories. The names of the repository/repositories and accession number(s) can be found at: https://www.ncbi.nlm.nih.gov/, PRJNA836163; https://www.ncbi.nlm.nih.gov/, PRJNA836186.

Author contributions

BL and XL designed the study and modified the manuscript. YL and QS did the experimental work, carried out the data analysis, and wrote the manuscript. XA and YX contributed to the data analysis and original draft writing. All authors contributed to the article and approved the submitted version.

Funding

This work was supported by the Strategic Priority Research Program of the Chinese Academy of Science (XDA23060102), the Project on Social Development by Department of Science and Technology of Guizhou Province (SY-[2014]3041), the talents of Guizhou Science and Technology Cooperation Platform (2016-5648) and the Opening Fund of the State Key Laboratory of Environmental Geochemistry (SKLEG2021XXX).

Acknowledgments

Thanks to the editors and reviewers for their professional revision suggestions, which greatly improved the quality of this manuscript. We thank Mallory Eckstut, PhD, from Liwen Bianji (Edanz) (www.liwenbianji.cn) for editing the English text of a draft of this manuscript.

Conflict of interest

The authors declare that the research was conducted in the absence of any commercial or financial relationships that could be construed as a potential conflict of interest.

Publisher's note

All claims expressed in this article are solely those of the authors and do not necessarily represent those of their affiliated organizations, or those of the publisher, the editors and the reviewers. Any product that may be evaluated in this article, or claim that may be made by its manufacturer, is not guaranteed or endorsed by the publisher.

Supplementary material

The Supplementary material for this article can be found online at: https://www.frontiersin.org/articles/10.3389/fmicb.2022.1058067/full#supplementary-material

References

Adams, R. I., Miletto, M., Taylor, J. W., and Bruns, T. D. (2013). Dispersal in microbes: fungi in indoor air are dominated by outdoor air and show dispersal limitation at short distances. *ISME J.* 7, 1262–1273. doi: 10.1038/ismej.2013.28

Aguilar, A. S., Cardoso, A. F., Lima, L. C., Luz, J. M. Q., Rodrigues, T., and Lana, R. M. Q. (2019). Influence of organomineral fertilization in the development of the potato crop CV. Cupid. *Biosci. J.* 35, 199–210. doi: 10.14393/BJ-v35n1a2019-41740

Ahimou, F., Jacques, P., and Deleu, M. (2000). Surfactin and iturin a effects on *Bacillus subtilis* surface hydrophobicity. *Enzyme Microb. Technol.* 27, 749–754. doi: 10.1016/S0141-0229(00)00295-7

Ai, C., Zhang, S., Zhang, X., Guo, D., Zhou, W., and Huang, S. (2018). Distinct responses of soil bacterial and fungal communities to changes in fertilization regime and crop rotation. *Geoderma* 319, 156–166. doi: 10.1016/j.geoderma.2018.01.010

Álvarez-Martín, A., Hilton, S. L., Bending, G. D., Rodriguez-Cruz, M. S., and SanchezMartin, M. J. (2016). Changes in activity and structure of the soil microbial community after application of azoxystrobin or pirimicarb and an organic amendment to an agricultural soil. *Appl. Soil Ecol.* 106, 47–57. doi: 10.1016/j.apsoil.2016.05.005

Antille, D. L., Godwin, J., Sakrabani, R., Seneweera, S., Tyrrel, S. F., and Johnstron, A. E. (2017). Field-scale evaluation of biosolids derived organomineral fertilizers applied to winter wheat in England. *Agron. J.* 109, 654–674. doi: 10.2134/agronj2016.09.0495

Banerjee, S., Schlaeppi, K., and van der Heijden, M. G. A. (2018). Keystone taxa as drivers of microbiome structure and functioning. *Nat. Rev. Microbiol.* 16, 567–576. doi: 10.1038/s41579-018-0024-1

Basak, B. B., Sarkar, B., and Naidu, R. (2021). Environmentally safe release of plant available potassium and micronutrients from organically amended rock mineral powder. *Environ. Geochem. Health* 43, 3273–3286. doi: 10.1007/s10653-020-00677-1

Bastian, M., Heymann, S., and Jacomy, M. (2009). "Gephi: an open source software for exploring and manipulating networks." In *The Third International AAAI Conference on Weblogs and Social Media LCWSM*, San Jose, 361–362.

Bello, A., Wang, B., Zhao, Y., Yang, W., Ogundeji, A., Deng, L., et al. (2021). Composted biochar affects structural dynamics, function and co-occurrence network patterns of fungi community. *Sci. Total Environ.* 775:145672. doi: 10.1016/j.scitotenv.2021.145672

Benjamini, Y., and Hochberg, Y. (1995). Controlling the false discovery rate - a practical and powerful approach to multiple testing. *J. R. Stat. Soc. B* 57, 289–300. doi: 10.1111/j.2517-6161.1995.tb02031.x

Bissett, A., Richardson, A. E., Baker, G., and Thrall, P. H. (2011). Long-term land use effects on soil microbial community structure and function. *Appl. Soil Ecol.* 51, 66–78. doi: 10.1016/j.apsoil.2011.08.010

Biswas, D. R., Narayanasamy, G., Datta, S. C., Singh, G., Begum, M., Maiti, D., et al. (2009). Changes in nutrient status during preparation of enriched organomineral fertilizers using rice straw, low-grade rock phosphate, waste mica, and phosphate solubilizing microorganism. *Commun. Soil Sci. Plant Anal.* 40, 2285–2307. doi: 10.1080/00103620902961243

Bolger, A. M., Lohse, M., and Usadel, B. (2014). Trimmomatic: a flexible trimmer for Illumina sequence data. *Bioinformatics* 30, 2114–2120. doi: 10.1093/bioinformatics/btu170

Calaca, F. J. S., and Bustamante, M. M. C. (2022). Richness of arbuscular mycorrhizal fungi (*Glomeromycota*) along a vegetation gradient of Brazilian Cerrado: responses to seasonality, soil types, and plant communities. *Mycol. Prog.* 21:27. doi: 10.1007/s11557-022-01785-1

Carvalho, R. P., Moreira, R. A., Cruz, M. C. M., Fernandes, D. R., and Oliveira, A. F. (2014). Organomineral fertilization on the chemical characteristics of Quartzarenic Neosol cultivated with olive tree. *Sci. Hortic.* 176, 120–126. doi: 10.1016/j.scienta.2014.07.006

Chater, K. F., Biro, S., Lee, K. J., Palmer, T., and Schrempf, H. (2010). The complex extracellular biology of *Streptomyces*. *FEMS Microbiol. Rev.* 34, 171–198. doi: 10.1111/j.1574-6976.2009.00206.x

Chen, L., Liu, Y., Wu, G., Veronican Njeri, K., Shen, Q., Zhang, N., et al. (2016). Induced maize salt tolerance by rhizosphere inoculation of *Bacillus amyloliquefaciens* SQR9. *Physiol. Plant.* 158, 34–44. doi: 10.1111/ ppl.12441

Chen, Y. L., Xu, T. L., Veresoglou, S. D., Hu, H. W., Hao, Z. P., Hu, Y. J., et al. (2017). Plant diversity represents the prevalent determinant of soil fungal community structure across temperate grasslands in northern China. *Soil Biol. Biochem.* 110, 12–21. doi: 10.1016/j.soilbio.2017.02.015

Cho, S. J., Kim, M. H., and Lee, Y. O. (2016). Effect of pH on soil bacterial diversity. *J. Environ. Prot. Ecol.* 40, 75–83. doi: 10.1186/s41610-016-0004-1

Coller, E., Cestaro, A., Zanzotti, R., Bertoldi, D., Pindo, M., Larger, S., et al. (2019). Microbiome of vineyard soils is shaped by geography and management. *Microbiome* 7:170. doi: 10.1186/s40168-019- 0758-7

Conn, V., Walker, A., and Franco, C. (2008). Endophytic actinobacteria induce defense pathways in *Arabidopsis thaliana*. *Mol. Plant-Microbe Interact.* 21, 208–218. doi: 10.1094/MPMI-21-2-0208

Corrêa, J. C., Rebellatto, A., Grohskopf, M. A., Cassol, P. C., Hentz, P., and Rigo, A. Z. (2018). Soil fertility and agriculture yield with the application of organomineral or mineral fertilizers in solid and fluid forms. *Pesqui. Agropecu. Bras.* 53, 633–640. doi: 10.1590/S0100-204X2018000500012

Costa-Gutierrez, S. B., Raimondo, E. E., Lami, M. J., Vincent, P. A., Espinosa-Urgel, M., and de Cristóbal, R. E. (2020). Inoculation of *Pseudomonas* mutant strains can improve growth of soybean and corn plants in soils under salt stress. *Rhizosphere* 16:100255. doi: 10.1016/j.rhisph.2020.100255

Csardi, G., and Nepusz, T. (2006). The igraph software package for complex network research. *InterJ. Complex Syst.* 1695, 1–9.

Cui, X., Zhang, Y., Gao, J., Peng, F., and Gao, P. (2018). Long-term combined application of manure and chemical fertilizer sustained higher nutrient status and rhizospheric bacterial diversity in reddish paddy soil of Central South China. *Sci. Rep.* 8:16554. doi: 10.1038/s41598-018-34685-0

Dai, Z., Su, W., Chen, H., Barberán, A., Zhao, H., Yu, M., et al. (2018). Long-term nitrogen fertilization decreases bacterial diversity and favors the growth of *Actinobacteria* and *Proteobacteria* in agroecosystems across the globe. *Glob. Chang. Biol.* 24, 3452–3461. doi: 10.1111/gcb.14163

Deeks, L., Chaney, K., Murray, C., Sakrabani, R., Gedara, S., Le, M., et al. (2013). A new sludge-derived organo-mineral fertilizer gives similar crop yields as conventional fertilizers. *Agron. Sustain. Dev.* 33, 539–549. doi: 10.1007/s13593-013-0135-z

Delgado-Baquerizo, M., Oliverio, A. M., Brewer, T. E., Benavent-Gonzalez, A., Eldridge, D. J., Bardgett, R. D., et al. (2018). A global atlas of the dominant bacteria found in soil. *Science* 359, 320–325. doi: 10.1126/science.aap9516

Delgado-Baquerizo, M., Reich, P. B., Khachane, A. N., Campbell, C. D., Thomas, N., Freitag, T. E., et al. (2016). It is elemental: soil nutrient stoichiometry drives bacterial diversity. *Environ. Microbiol.* 19, 1176–1188. doi: 10.1111/1462-2920.13642

Deng, Y., Jiang, Y. H., Yang, Y. F., He, Z. L., Luo, F., and Zhou, J. Z. (2012). Molecular ecological network analyses. *BMC Bioinf.* 13:113. doi: 10.1186/1471-2105-13-113

Dias, M. A. D., Lana, R. M. Q., Mageste, J. G., Marques, O. J., Silva, A. D., Lemes, E. M., et al. (2020). Mineral and organomineral sources of nitrogen to maize agronomic performance. *Biosci. J.* 36, 1528–1534. doi: 10.14393/BJ-v36n5a2020-45632

Dixon, P. (2003). VEGAN, a package of R functions for community ecology. *J. Veg. Sci.* 14, 927–930. doi: 10.1111/j.1654-1103.2003.tb02228.x

Du, T. Y., He, H. Y., Zhang, Q., Lu, L., Mao, W. J., and Zhai, M. Z. (2022). Positive effects of organic fertilizers and biofertilizers on soil microbial community composition and walnut yield. *Appl. Soil Ecol.* 175:104457. doi: 10.1016/j.apsoil.2022.104457

Edgar, R. C. (2013). UPARSE: highly accurate OTU sequences from microbial amplicon reads. *Nat. Methods* 10, 996–998. doi: 10.1038/Nmeth.2604

Efanov, M. V., Galochkin, A. I., Schott, P. R., Dudkin, D. V., and Klepikov, A. G. (2001). Nitrogen-containing organomineral fertilizer based on wood waste. *Russ. J. Appl. Chem.* 74, 1774–1776. doi: 10.1023/A:1014850528793

Fan, K., Delgado-Baquerizo, M., Guo, X., Wang, D., Zhu, Y., and Chu, H. (2020). Biodiversity of key-stone phylotypes determines crop production in a 4-decade fertilization experiment. *ISME J.* 15, 550–561. doi: 10.1038/s41396-020-00796-8

Finkel, O. M., Salas-Gonzalez, I., Castrillo, G., Conway, J. M., Law, T. F., Teixeira, P. J. P. L., et al. (2020). A single bacterial genus maintains root growth in a complex microbiome. *Nature* 587, 103–108. doi: 10.1038/s41586-020-2778-7

Frazão, J. J., Benites, V. M., Ribeiro, J. V. S., Pierobon, V. M., and Lavres, J. (2019). Agronomic effectiveness of a granular poultry litter-derived organomineral phosphate fertilizer in tropical soils: soil phosphorus fractionation and plant responses. *Geoderma* 337, 582–593. doi: 10.1016/j.geoderma.2018.10.003

Gattinger, A., Muller, A., Haeni, M., Skinner, C., Fliessbach, A., Buchmann, N., et al. (2012). Enhanced top soil carbon stocks under organic farming. *Proc. Natl. Acad. Sci. U. S. A.* 109, 18226–18231. doi: 10.1073/pnas.1209429109

Gebremariam, A., Chekol, Y., and Assefa, F. (2021). Phenotypic, molecular, and virulence characterization of entomopathogenic fungi, *Beauveria bassiana* (Balsam) Vuillemin, and *Metarhizium anisopliae* (Metschn.) Sorokin from soil samples of Ethiopia for the development of mycoinsecticide. *Heliyon* 7:e07091. doi: 10.1016/j.heliyon.2021.e07091

Ghorbanzadeh, N., Mahsefat, M., Farhangi, M. B., Khalili Rad, M., and Proietti, P. (2020). Short-term impacts of pomace application and *Pseudomonas* bacteria on soil available phosphorus. *Biocatal. Agric. Biotechnol.* 28:101742. doi: 10.1016/j.bcab.2020.101742

Gomiero, T., Pimentel, D., and Paoletti, M. G. (2011). Environmental impact of different agricultural management practices: conventional vs. organic agriculture. *Crit. Rev. Plant Sci.* 30, 95–124. doi: 10.1080/07352689.2011.554355

Gonçalves, C. A., de Camargo, R., de Sousa, R. T. X., Soares, N. S., de Oliveira, R. C., Stanger, M. C., et al. (2021). Chemical and technological attributes of sugarcane as functions of organomineral fertilizer based on filter cake or sewage sludge as organic matter sources. *PLoS One* 16:e0236852. doi: 10.1371/journal.pone.0236852

Gong, Z. T. (1999). Soil system classification in China-theory, method and practice*Beijing: Science press*.

González, A. M. M., Dalsgaard, B., and Olesen, J. M. (2010). Centrality measures and the importance of generalist species in pollination networks. *Ecol. Complex.* 7, 36–43. doi: 10.1016/j.ecocom.2009.03.008

González-Pérez, E., Ortega-Amaro, M. A., Bautista, E., Delgado-Sanchez, P., and Jimenez-Bremont, J. F. (2022). The entomopathogenic fungus *Metarhizium anisopliae* enhances *Arabidopsis*, tomato, and maize plant growth. *Plant Physiol. Biochem.* 176, 34–43. doi: 10.1016/j.plaphy.2022.02.008

Grohskopf, M. A., Corrêa, J. C., Fernandes, D. M., Teixeira, P. C., and Mota, S. C. A. (2019). Mobility of nitrogen in the soil due to the use of organomineral fertilizers with different concentrations of phosphorus. *Commun. Soil Sci. Plant Anal.* 51, 208–220. doi: 10.1080/00103624.2019.1705321

Gu, S., Hu, Q., Cheng, Y., Bai, L., Liu, Z., Xiao, W., et al. (2019). Application of organic fertilizer improves microbial community diversity and alters microbial network structure in tea (*Camellia sinensis*) plantation soils. *Soil Tillage Res.* 195:104356. doi: 10.1016/j.still.2019.104356

Gui, H., Fan, L., Wang, D., Yan, P., Li, X., Zhang, L., et al. (2021). Organic management practices shape the structure and associations of soil bacterial communities in tea plantations. *Appl. Soil Ecol.* 163:103975. doi: 10.1016/j.apsoil.2021.103975

Hawrot-Paw, M., Mikiciuk, M., Koniuszy, A., and Meller, E. (2022). Influence of organomineral fertiliser from sewage sludge on soil microbiome and physiological parameters of maize (*Zea mays* L.). *Agronomy* 12:1114. doi: 10.3390/agronomy12051114

Hu, Y., Sun, L. W., Mokgolodi, N. C., Zhang, Y. X., Wen, C. X., Xie, X. L., et al. (2010). Primary identifications and palynological observations of *Perilla* in China. *J. Syst. Evol.* 48, 133–145. doi: 10.1111/j.1759-6831.2010.00067.x

Javier, S., Canales, F., Tweed, J., and Lee, M. (2018). Fatty acid profile changes during gradual soil water depletion in oats suggests a role for jasmonates in coping with drought. *Front. Plant Sci.* 9:1007. doi: 10.3389/fpls.2018.0107

Jiao, S., Lu, Y., and Wei, G. (2021). Soil multitrophic network complexity enhances the link between biodiversity and multifunctionality in agricultural systems. *Glob. Chang. Biol.* 28, 140–153. doi: 10.1111/gcb.15917

Kang, Y., Ma, Y., Wu, W., Zeng, S., Jiang, S., Yang, H., et al. (2022). Bioorganic and silicon amendments alleviate early defoliation of pear trees by improving the soil nutrient bioavailability, microbial activity, and reshaping the soil microbiome network. *Appl. Soil Ecol.* 173:104383. doi: 10.1016/j.apsoil.2021.104383

Kembel, S. W., Cowan, P. D., Helmus, M. R., Cornwell, W. K., Morlon, H., Ackerly, D. D., et al. (2010). Picante: R tools for integrating phylogenies and ecology. *Bioinformatics* 26, 1463–1464. doi: 10.1093/bioinformatics/btq166

Kiehl, E. J. (2008). *Fertilizantes organominerais. 4. ed*. Piracicaba, SP: Degaspari, 160 p.

Ko, O., Jn, O., and Hc, O. (2018). Pharmacological potentials, characterization and fatty acids profile of *Persea americana* mill. (*Avocardo*) seed oil using gas

chromatography-mass spectroscopy. *Biochem. Anal. Biochem.* 7, 1–3. doi: 10.4172/2161-1009.100036

Ko, W. H., Tsou, Y. J., Ju, Y. M., Hsieh, H. M., and Ann, P. J. (2010). Production of a fungistatic substance by *Pseudallescheria boydii* isolated from soil amended with vegetable tissues and its significance. *Mycopathologia* 169, 125–131. doi: 10.1007/s11046-009-9237-1

Kour, D., Rana, K. L., Yadav, A. N., Yadav, N., Kumar, M., Kumar, V., et al. (2020). Microbial biofertilizers: bioresources and ecofriendly technologies for agricultural and environmental sustainability. *Biocatal. Agric. Biotechnol.* 23:101487. doi: 10.1016/j.bcab.2019.101487

Kourimska, L., Sabolova, M., Horcicka, P., Rys, S., and Bozik, M. (2018). Lipid content, fatty acid profile, and nutritional value of new oat cultivars. *J. Cereal Sci.* 84, 44–48. doi: 10.1016/j.jcs.2018.09.012

Kox, M., Elzen, E., Lamers, L. P. M., Jetten, M. S. M., and Kessel, M. (2020). Microbial nitrogen fixation and methane oxidation are strongly enhanced by light in *Sphagnum* mosses. *AMB Expr.* 10:61. doi: 10.1186/s13568-020-00994-9

Lauber, C. L., Hamady, M., Knight, R., and Fierer, N. (2009). Pyrosequencing–based assessment of soil pH as a predictor of soil bacterial community structure at the continental scale. *Appl. Environ. Microbiol.* 75, 5111–5120. doi: 10.1128/AEM.00335-09

Lee, J. K., and Kim, N. S. (2007). Genetic diversity and relationships of cultivated and weedy types of *Perilla frutescens* collected from East Asia revealed by SSR markers. *Korean J. Breed. Sci* 39:491–499.

Li, Y., Liu, X. M., Yin, Z. Y., Chen, H., Cai, X. L., Xie, Y. H., et al. (2021). Changes in soil microbial communities from exposed rocks to arboreal rhizosphere during vegetation succession in a karst mountainous ecosystem. *J. Plant Interact.* 16, 550–563. doi: 10.1080/17429145.2021.2002955

Li, Y., Liu, X. M., Zhang, L., Xie, Y. H., Cai, X. L., Wang, S. J., et al. (2020). Effects of short-term application of chemical and organic fertilizers on bacterial diversity of cornfield soil in a karst area. *J. Soil Sci. Plant Nut.* 20, 2048–2058. doi: 10.1007/s42729-020-00274-2

Li, Q., Zhang, D., Song, Z., Ren, L., Jin, X., Fang, W., et al. (2022). Organic fertilizer activates soil beneficial microorganisms to promote strawberry growth and soil health after fumigation. *Environ. Pollut.* 295:118653. doi: 10.1016/j.envpol.2021.118653

Lian, B., Xiao, B., Xiao, L. L., Wang, W. J., and Sun, Q. B. (2020). Molecular mechanism and carbon sink effects of microbial transformation in potassium-bearing rocks. *Earth Sci. Front.* 27, 238–246. doi: 10.13745/j.esf.sf.2020.5.38

Ling, N., Zhu, C., Xue, C., Chen, H., Duan, Y., Peng, C., et al. (2016). Insight into how organic amendments can shape the soil microbiome in long-term field experiments as revealed by network analysis. *Soil Biol. Biochem.* 99, 137–149. doi: 10.1016/j.soilbio.2016.05.005

Liu, X., Bolla, K., Ashforth, E. J., Zhou, Y., Gao, H., and Huang, P. (2012). Systematics-guided bioprospecting for bioactive microbial natural products. *Antonie Van Leeuwenhoek* 101, 55–66. doi: 10.1007/s10482-011-9671-1

Liu, L., Chen, H., Liu, M., Yang, J. R., Xiao, P., Wilkinson, D. M., et al. (2019). Response of the eukaryotic plankton community to the *cyanobacterial* biomass cycle over 6 years in two subtropical reservoirs. *ISME J.* 13, 2196–2208. doi: 10.1038/s41396-019-0417-9

Liu, Z., Guo, Q., Feng, Z. Y., Liu, Z. D., Li, H. Y., Sun, Y. F., et al. (2020). Long-term organic fertilization improves the productivity of kiwifruit (*Actinidia chinensis* Planch.) through increasing rhizosphere microbial diversity and network complexity. *Appl. Soil Ecol.* 147:103426. doi: 10.1016/j.apsoil.2019.103426

Liu, H., Pan, F., Han, X., Song, F., Zhang, Z., Yan, J., et al. (2019). Response of soil fungal community structure to long-term continuous soybean cropping. *Front. Microbiol.* 9:3316. doi: 10.3389/fmicb.2018.03316

Liu, J., Shu, A., Song, W., Shi, W., and Gao, Z. (2021). Long-term organic fertilizer substitution increases rice yield by improving soil properties and regulating soil bacteria. *Geoderma* 404:115287. doi: 10.1016/j.geoderma.2021.115287

Liu, J., Sui, Y., Yu, Z., Shi, Y., Chu, H., Jin, J., et al. (2014). High throughput sequencing analysis of biogeographical distribution of bacterial communities in the black soils of Northeast China. *Soil Biol. Biochem.* 70, 113–122. doi: 10.1016/j.soilbio.2013.12.014

Louca, S., Parfrey, L. W., and Doebeli, M. (2016). Decoupling function and taxonomy in the global ocean microbiome. *Science* 353, 1272–1277. doi: 10.1126/science.aaf4507

Lozupone, C., and Knight, R. (2005). UniFrac: a new phylogenetic method for comparing microbial communities. *Appl. Environ. Microbiol.* 71, 8228–8235. doi: 10.1128/AEM.71.12.8228-8235.2005

Lu, R. K. (1999). *Methods of agrochemical soil analysis vol* China Agricultural Science Press, Beijing.

Luitel, B. P., Ko, H. C., Hur, O. S., Rhee, J. H., Baek, H. J., Ryu, K. Y., et al. (2017). Variation for morphological characters in cultivated and weedy types of *Perilla frutescens* Britt. germplasm. *Korean J. Plant Resour.* 30, 298–310. doi: 10.7732/kjpr.2017.30.3.298

Ma, B., Wang, H. Z., Dsouza, M., Lou, J., He, Y., Dai, Z. M., et al. (2016). Geographic patterns of co-occurrence network topological features for soil microbiota at continental scale in eastern China. *ISME J.* 10, 1891–1901. doi: 10.1038/ismej.2015.261

Ma, A., Zhuang, X., Wu, J., Cui, M., Lv, D., Liu, C., et al. (2013). *Ascomycota* members dominate fungal communities during straw residue decomposition in arable soil. *PLoS One* 8:e66146. doi: 10.1371/journal.pone.0066146

Magoc, T., and Salzberg, S. L. (2011). FLASH: fast length adjustment of short reads to improve genome assemblies. *Bioinformatics* 27, 2957–2963. doi: 10.1093/bioinformatics/btr507

Marcos, M. S., Bertiller, M. B., and Olivera, N. L. (2019). Microbial community composition and network analyses in arid soils of the Patagonian Monte under grazing disturbance reveal an important response of the community to soil particle size. *Appl. Soil Ecol.* 138, 223–232. doi: 10.1016/j.apsoil.2019.03.001

Megali, L., Glauser, G., and Rasmann, S. (2013). Fertilization with beneficial microorganisms decreases tomato defenses against insect pests. *Agron. Sustain. Dev.* 34, 649–656. doi: 10.1007/s13593-013-0187-0

Mendes, L. W., de Lima Brossi, M. J., Kuramae, E. E., and Tsai, S. M. (2015). Land-use system shapes soil bacterial communities in southeastern Amazon region. *Appl. Soil Ecol.* 95, 151–160. doi: 10.1016/j.apsoil.2015.06.005

Moyne, A. L., Cleveland, T. E., and Tuzun, S. (2004). Molecular characterization and analysis of the operon encoding the antifungal lipopeptide bacillomycin D. *FEMS Microb. Lett.* 234, 43–49. doi: 10.1016/j.femsle.2004.03.011

Mumbach, G. L., Gatiboni, L. C., Bona, F. D., Schmitt, D. E., Corrêa, J. C., Gabriel, C. A., et al. (2020). Agronomic efficiency of organomineral fertilizer in sequential grain crops in southern Brazil. *Agron. J.* 112, 3037–3049. doi: 10.1002/agj2.20238

Ngo, H. T. T., Watts-Williams, S. J., Panagaris, A., Baird, R., McLaughlin, M. J., and Cavagnaro, T. R. (2022). Development of an organomineral fertiliser formulation that improves tomato growth and sustains arbuscular mycorrhizal colonisation. *Sci. Total Environ.* 815:151977. doi: 10.1016/j.scitotenv.2021.151977

Nguyen, N. H., Song, Z. W., Bates, S. T., Branco, S., Tedersoo, L., Menke, J., et al. (2016). FUNGuild: an open annotation tool for parsing fungal community datasets by ecological guild. *Fungal Ecol.* 20, 241–248. doi: 10.1016/j.funeco.2015.06.006

Qi, D., Wieneke, X., Tao, J., Zhou, X., and Desilva, U. (2018). Soil pH is the primary factor correlating with soil microbiome in karst rocky desertification regions in the Wushan County, Chongqing, China. *Front. Microbiol.* 9:1027. doi: 10.3389/fmicb.2018.01027

Ren, H., Qin, X., Huang, B., Fernández-García, V., and Lv, C. (2020). Responses of soil enzyme activities and plant growth in a eucalyptus seedling plantation amended with bacterial fertilizers. *Arch. Microbiol.* 202, 1381–1396. doi: 10.1007/s00203-020-01849-4

Ren, C. J., Zhao, F. Z., Kang, D., Yang, G. H., Han, X. H., Tong, X. G., et al. (2016). Linkages of C:N:P stoichiometry and bacterial community in soil following afforestation of former farmland. *Forest Ecol. Manag.* 376, 59–66. doi: 10.1016/j.foreco.2016.06.004

Richardson, M. (2009). The ecology of the *zygomycetes* and its impact on environmental exposure. *Clin. Microbiol. Infect.* 15, 2–9. doi: 10.1111/j.1469-0691.2009.02972.x

Riguetti Zanardo Botelho, A. B., Alves-Pereira, A., Colonhez Prado, R., Zucchi, M. I., and Delalibera Júnior, I. (2019). *Metarhizium* species in soil from Brazilian biomes: a study of diversity, distribution, and association with natural and agricultural environments. *Fungal Ecol.* 41, 289–300. doi: 10.1016/j.funeco.2019.07.004

Rime, T., Hartmann, M., Brunner, I., Widmer, F., Zeyer, J., and Frey, B. (2015). Vertical distribution of the soil microbiota along a successional gradient in a glacier forefield. *Mol. Ecol.* 24, 1091–1108. doi: 10.1111/mec.13051

Sakurada, L. R., Batista, M. A., Inoue, T. T., Muniz, A. S., and Pagliari, P. H. (2016). Organomineral phosphate fertilizers: agronomic efficiency and residual effect on initial corn development. *Agron. J.* 108, 2050–2059. doi: 10.2134/agronj2015.0543

Samaddar, S., Truu, J., Chatterjee, P., Truu, M., Kim, K., Kim, S., et al. (2019). Long-term silicate fertilization increases the abundance of actinobacterial population in paddy soils. *Biol. Fertil. Soils* 55, 109–120. doi: 10.1007/s00374-018-01335-6

Santolini, M., and Barabási, A. L. (2018). Predicting perturbation patterns from the topology of biological networks. *Proc. Natl. Acad. Sci. U. S. A.* 115, E6375–E6383. doi: 10.1073/pnas.1720589115

Segata, N., Izard, J., Waldron, L., Gevers, D., Miropolsky, L., Garrett, W. S., et al. (2011). Metagenomic biomarker discovery and explanation. *Genome Biol.* 12:R60. doi: 10.1186/gb-2011-12-6-r60

Seufert, V., Ramankutty, N., and Foley, J. A. (2012). Comparing the yields of organic and conventional agriculture. *Nature* 485, 229–232. doi: 10.1038/nature11069

Singh, B. K., Nunan, N., Ridgway, K. P., McNicol, J., Young, J. P. W., Daniell, T. J., et al. (2008). Relationship between assemblages of mycrorrhizal fungi and bacteria on grass roots. *Environ. Microbiol.* 10, 534–541. doi: 10.1111/j.1462-2920.2007.01474.x

Smith, S. E., and Read, D. J. (2008). "The symbionts forming arbuscular mycorrhizas," in *Mycorrhizal Symbiosis*. eds. S. E. Smith and D. J. Read (San Diego: Academic Press), 13–41.

Steffen, W., Richardson, K., Rockstrom, J., Cornell, S. E., Fetzer, I., Bennett, E. M., et al. (2015). Planetary boundaries: guiding human development on a changing planet. *Science* 347:1259855. doi: 10.1126/science.1259855

Sun, R., Dsouza, M., Gilbert, J. A., Guo, X., Wang, D., Guo, Z., et al. (2016). Fungal community composition in soils subjected to long-term chemical fertilization is most influenced by the type of organic matter. *Environ. Microbiol.* 18, 5137–5150. doi: 10.1111/1462-2920.13512

Sun, A., Jiao, X. Y., Chen, Q., Wu, A. L., Zheng, Y., Lin, Y. X., et al. (2021). Microbial communities in crop phyllosphere and root endosphere are more resistant than soil microbiota to fertilization. *Soil Biol. Biochem.* 153:108113. doi: 10.1016/j.soilbio.2020.108113

Sun, Q. B., Ruan, Y. L., Chen, P., Wang, S. J., Liu, X. M., and Lian, B. (2019). Effects of mineral-organic fertilizer on the biomass of green Chinese cabbage and potential carbon sequestration ability in karst areas of Southwest China. *Acta Geochim.* 38, 430–439. doi: 10.1007/s11631-019-00320-6

Syed, S., Wang, X., Prasad, T. N. V. K. V., and Lian, B. (2021). Bio-organic-mineral fertilizer for sustainable agriculture: current trends and future perspectives. *Fortschr. Mineral.* 11:1336. doi: 10.3390/ min11121336

Theodoro, S. H., and Leonardos, O. H. (2006). The use of rocks to improve family agriculture in Brazil. *An. Acad. Bras. Cienc.* 78, 721–730. doi: 10.1590/S0001-37652006000400008

Tian, S. G., Guo, P., Shen, Q., Wang, X. P., Yang, S., Shang, Z. W., et al. (2017). Main traits and quality of seven *Perilla frutescens* varieties (lines) in Guizhou. *Guizhou Agric. Sci.* 45, 107–109.

Tian, J., Zeng, X., Zhang, S., Wang, Y., Zhang, P., Lü, A., et al. (2014). Regional variation in components and antioxidant and antifungal activities of *Perilla frutescens* essential oils in China. *Ind. Crop. Prod.* 59, 69–79. doi: 10.1016/j.indcrop.2014.04.048

USS Working Group WRB. (2015). *World reference base for soil resources 2014, update 2015 international soil classification system for naming soils and creating legends for soil maps*. World Soil Resources Reports No. 106. FAO, Rome.

Vick-Majors, T. J., Priscu, J. C., and Amaral-Zettler, L. A. (2014). Modular community structure suggests metabolic plasticity during the transition to polar night in ice-covered Antarctic lakes. *ISME J.* 8, 778–789. doi: 10.1038/ismej.2013.190

Vollú, R. E., Cotta, S. R., Jurelevicius, D., Leite, D. C. A., Parente, C. E. T., Malm, O., et al. (2018). Response of the bacterial communities associated with maize rhizosphere to poultry litter as an organomineral fertilizer. *Front. Environ. Sci.* 6:118. doi: 10.3389/fenvs.2018.00118

Wang, Y., Chen, G. W., Sun, Y. F., Zhu, K., Jin, Y., Li, B. G., et al. (2020). Different agricultural practices specify bacterial community compositions in the soil rhizosphere and root zone. *Soil Ecol. Lett.* 4, 18–31. doi: 10.1007/s42832-020-0058-y

Wang, L., Li, J., Yang, F., E, Y., Raza, W., Huang, Q., et al. (2017). Application of bioorganic fertilizer significantly increased apple yields and shaped bacterial community structure in orchard soil. *Microb. Ecol.* 73, 404–416. doi: 10.1007/s00248-016-0849-y

Wang, C. J., Song, C. Y., Zhang, X. D., Xie, Y. Q., Liu, X. Z., and Wang, M. Z. (1997). Sustainable control efficacy of *Paecilomyces lilacinus* against *Heterodera glycines*. *Chin. J. Biol. Contr.* 13:26.

Weller, D., Raaijmakers, J., Gardener, B., and Thomashow, L. (2002). Microbial populations responsible for specific soil suppressiveness to plant pathogens. *Annu. Rev. Phytopathol.* 40, 309–348. doi: 10.1146/annurev. phyto.40.030402.110010

Wu, S., Zhou, Z., Zhu, L., Zhong, L., Dong, Y., Wang, G., et al. (2022). Cd immobilization mechanisms in a *Pseudomonas* strain and its application in soil Cd remediation. *J. Hazard. Mater.* 425:127919. doi: 10.1016/j.jhazmat.2021.127919

Xu, N., Tan, G. C., Wang, H. Y., and Gai, X. P. (2016). Effect of biochar additions to soil on nitrogen leaching, microbial biomass and bacterial community structure. *Eur. J. Soil Biol.* 74, 1–8. doi: 10.1016/j.ejsobi.2016.02.004

Yaldiz, G., and Camlica, M. (2020). Yield components and some quality properties of fenugreek cultivar and lines. Banat's. *J. Biotechnol.* XI, 40–47. doi: 10.7904/2068-4738-XI(22)-40

Yang, H. W., Li, J., Xiao, Y. H., Gu, Y. B., Liu, H. W., and Liang, Y. L. (2017). An integrated insight into the relationship between soil microbial community and tobacco bacterial wilt disease. *Front. Microbiol.* 8:2179. doi: 10.3389/fmicb.2017.02179

Yang, Y. R., Syed, S., Mao, S. X., Li, Q., Ge, F., Lian, B., et al. (2020). Bioorganic–mineral fertilizer can remediate chemical fertilizer-oversupplied soil: Purslane planting as an example. *J. Soil Sci. Plant Nutr.* 20, 892–900. doi: 10.1007/s42729-020-00175-4

Yu, H., Qiu, J. F., Ma, L. J., Hu, Y. J., Li, P., and Wan, J. B. (2017). Phytochemical and phytopharmacological review of *Perilla frutescens* L. (Labiatae), a traditional edible-medicinal herb in China. *Food Chem. Toxicol.* 108, 375–391. doi: 10.1016/j.fct.2016.11.023

Yuan, M. M., Guo, X., Wu, L., Zhang, Y., Xiao, N., Ning, D., et al. (2021). Climate warming enhances microbial network complexity and stability. *Nat. Clim. Chang.* 11, 343–348. doi: 10.1038/s41558-021-00989-9

Zhao, J., Ni, T., Li, J., Lu, Q., Fang, Z., Huang, Q., et al. (2016). Effects of organic–inorganic compound fertilizer with reduced chemical fertilizer application on crop yields, soil biological activity and bacterial community structure in a rice–wheat cropping system. *Appl. Soil Ecol.* 99, 1–12. doi: 10.1016/j.apsoil.2015.11.006

Zhou, J., Guan, D., Zhou, B., Zhao, B., Ma, M., Qin, J., et al. (2015). Influence of 34-years of fertilization on bacterial communities in an intensively cultivated black soil in Northeast China. *Soil Biol. Biochem.* 90, 42–51. doi: 10.1016/j.soilbio.2015.07.005

Zhou, J., Jiang, X., Zhou, B. K., Zhao, B. S., Ma, M. C., Guan, D. W., et al. (2016). Thirty-four years of nitrogen fertilization decreases fungal diversity and alters fungal community composition in black soil in Northeast China. *Soil Biol. Biochem.* 95, 135–143. doi: 10.1016/j.soilbio.2015.12.012

Zhu, J., Ren, Z., Huang, B., Cao, A., Wang, Q., Yan, D., et al. (2020). Effects of fumigation with allyl isothiocyanate on soil microbial diversity and community structure of tomato. *J. Agric. Food Chem.* 68, 1226–1236. doi: 10.1021/acs.jafc.9b07292

Zhu, W., Zhu, M., Liu, X., Xia, J., Yin, H., and Li, X. (2022). Different responses of bacteria and microeukaryote to assembly processes and co-occurrence pattern in the coastal upwelling. *Microb. Ecol* doi: 10.1007/s00248-022-02093-7. Epub ahead of print.

frontiers | Frontiers in Microbiology

TYPE Original Research
PUBLISHED 22 December 2022
DOI 10.3389/fmicb.2022.1054667

OPEN ACCESS

EDITED BY
Yongxing Cui,
Peking University,
China

REVIEWED BY
Lie Xiao,
Xi'an University of Technology, China
Javad Gharechahi,
Baqiyatallah University of Medical Sciences, Iran

*CORRESPONDENCE
Qiang Li
✉glqiangli@hotmail.com

SPECIALTY SECTION
This article was submitted to Terrestrial Microbiology, a section of the journal Frontiers in Microbiology

RECEIVED 27 September 2022
ACCEPTED 02 December 2022
PUBLISHED 22 December 2022

CITATION
Li Q, Qiu J, Liang Y and Lan G (2022) Soil bacterial community changes along elevation gradients in karst graben basin of Yunnan-Kweichow Plateau.
Front. Microbiol. 13:1054667.
doi: 10.3389/fmicb.2022.1054667

Soil bacterial community changes along elevation gradients in karst graben basin of Yunnan-Kweichow Plateau

Qiang Li[1,2]*, Jiangmei Qiu[1,2], Yueming Liang[1,2] and Gaoyong Lan[1,2]

[1]Key Laboratory of Karst Ecosystem and Treatment of Rocky Desertification, MNR, Key Laboratory of Karst Dynamics, MNR & GZAR, Institute of Karst Geology, Chinese Academy of Geological Sciences, Guilin, China, [2]International Research Center on Karst under the Auspices of UNESCO, Guilin, China

Elevation gradients could provide natural experiments to examine geomorphological influences on biota ecology and evolution, however little is known about microbial community structures with soil depths along altitudinal gradients in karst graben basin of Yunnan-Kweichow Plateau. Here, bulk soil in A layer (0~10 cm) and B layer (10~20 cm) from two transect Mounts were analyzed by using high-throughput sequencing coupled with physicochemical analysis. It was found that the top five phyla in A layer were Proteobacteria, Acidobacteria, Actinobacteria, Bacteroidetes, and Verrucomicrobia, and the top five phyla in B layer were Proteobacteria, Acidobacteria, Actinobacteria, Verrucomicrobia, and Chloroflexi in a near-neutral environment. Edaphic parameters were different in two layers along altitudinal gradients. Besides that, soil microbial community compositions varied along altitudinal gradient, and soil organic carbon (SOC) and total nitrogen (TN) increased monotonically with increasing elevation. It was further observed that Shannon indexes with increasing altitudes in two transect Mounts decreased monotonically with significant difference (p=0.001), however beta diversity followed U-trend with significant difference (p=0.001). The low proportions of unique operational taxonomic units (OTUs) appeared at high altitude areas which impact the widely accepted elevation Rapoport's rules. The dominant *Bradyrhizobium* (alphaproteobacterial OTU 1) identified at high altitudes in two layers constitutes the important group of free-living diazotrophs and could bring fixed N into soils, which simultaneously enhances SOC and TN accumulation at high altitudes (p<0.01). Due to different responses of bacterial community to environmental changes varying with soil depths, altitudinal gradients exerted negative effects on soil bacterial communities *via* soil physical properties and positive effects on soil bacterial diversities *via* soil chemical properties in A layer, however the results in B layer were opposite. Overall, our study is the first attempt to bring a deeper understanding of soil microbial structure patterns along altitudinal gradients at karst graben basin areas.

KEYWORDS

karst graben basin, Yunnan-Kweichow Plateau, elevation gradients, soil bacterial structure patterns, *Bradyrhizobium*

Introduction

Complex landforms shaped by nature as an aspect of the combined and interacting influences of geology, climate, time, biota and the secondary composite products of those interactions provide the habitat for life on earth (Phillips, 2016). Moreover, landforms can be distributed following an altitudinal gradient, which result in environmental changes such as temperature and humidity. Consequently, altitudinal gradients provide the most powerful 'natural experiments' for examining the hypothesis about geomorphological influences on biota ecology and evolution (Körner, 2007). The research on characteristics, origin and evolution of fauna and flora along altitudinal gradients has long been the focus (Brown, 2001; Sundqvist et al., 2013; Bhat et al., 2020). Based on 441 group data of fauna and flora along altitudinal gradients across Northern and Southern hemispheres, it was found that most elevational diversity curves were skewed positively, that is maximum diversity below the middle of the gradient (Guo et al., 2013). Though soil microorganisms play important roles in material cycles and energy flow in nature, only few studies were did to examine their diversity patterns along altitudinal gradients and soil microbes do not follow elevational diversity patterns of plants and animals (Bryant et al., 2008; Fierer et al., 2011; Keller, 2022).

The distribution patterns of soil microbiome along altitudinal gradients are multiple, complex and changeable. For example, the taxon richness and phylogenetic diversities of soil bacteria decreased monotonically with increasing elevation in Colorado and Southwestern Tibetan Plateau (Bryant et al., 2008; Shen et al., 2019), however Cai et al. (2020) found that soil bacterial and fungal community diversities increased monotonically in northwest Yunnan plateau, China. Moreover, the hump-backed trend in bacterial diversities from Mount Fuji (Singh et al., 2012) as well as declines, increases, mid-elevation or no discernable trend in soil microbial diversities (Looby and Martin, 2020) were found. Moreover, it is a common belief that the number of endemic species decreased and their proportions increased with increasing altitude (Vetaas and Grytnes, 2002; Zhou et al., 2019). However, Grau et al. (2007) found that the proportion of endemic bryophytes with other plant groups in Nepal at the highest altitudes decreased. The multiple microbe patterns along altitudinal gradients may have been due to edaphic factors that shaped the microbial diversities and community compositions varying with the changed sampling areas. Secondly, the responses of soil microorganisms to above-and below-ground ecosystems were out of sync. Consequently, these studies have not uncovered the soil microbial patterns along altitudinal gradients on global scales, especially without representative samples from karst area (Bryant et al., 2008; Singh et al., 2012; Shen et al., 2019; Cai et al., 2020; Looby and Martin, 2020). Therefore, more work is still needed to address soil microbiome patterns along altitudinal gradients to better understand microbial ecology and function (Looby and Martin, 2020).

Despite less reports of soil microbial ecology along karst altitudinal gradients, Hu et al. (2022) and Yan et al. (2022) pointed out the soil microbial diversity, composition and assembly along vegetation succession sequence or calcareous succession process from karst montane areas. Knowing that calcareous soil originating from weathering products of carbonate rocks (limestone, dolomite or marble) has calcium-rich and alkaline characteristics with scales, spatial heterogeneity and temporal dynamics (Yuan, 2001), karst soil microbiome would exhibit different lifestyles and adaptive strategies from non-karst soil. Then, studying their distribution patterns and community characters may reveal the distinctive groups from karst montane areas. Moreover, the response of bacterial community to environmental change varies with surface soil depths (Barbour et al., 2022). Due to greatest number and largest spatial distribution sites with sampling depths from 0 to 10 cm (Wieder et al., 2021) and most karst soil with depths of 0 ~ 20 cm (Yan et al., 2022), the previous studies mainly focused on soil microbial ecology with depths of 0 ~ 10 cm (defined as A layer) or 0 ~ 20 cm. To provide more information on their vertical variability (Qiu et al., 2020) and identify the bacterial community patterns along elevation gradients in karst graben basin of Yunnan-Kweichow Plateau, bulk soil from two layers (A layer and 10 ~ 20 cm defined as B layer) were collected, respectively, for analysis by using high-throughput sequencing coupled with physicochemical analysis. To reduce the knowledge gap, we focus on the following issues in this study: (i) The diversity pattern of soil bacteria in two layers along altitudinal gradients is different. (ii) The proportions of endemic bacteria increase or decrease along altitudinal gradients. (iii) What are the relationships among altitudinal gradients, soil physical/chemical properties, and soil bacterial communities?

Materials and methods

Study sites

Eighty soil samples were collected in Xibeile Village from Mengzi City of Yunnan-Kweichow Plateau, China. At this area, karst intermountain basins, namely karst graben basins are typical due to the subsidence and dissolution of fault blocks caused by Cenozoic tectonic uplift. The geomorphic zones are distinct, neotectonic movements are intense, water resource distribution is uneven, soil and vegetation zonings are prominent, vertical climate variations are significant, and regional differences in human activities are large (Wang, Y. et al., 2017). Moreover, red calcareous soil with high Fe_2O_3, Al_2O_3, and SiO_2 contents is widely distributed at this area. Due to uneven depths of calcareous soil, 45 soil samples from A layer and 35 soil samples from B layer were collected, respectively. Because intense neotectonic movements resulted in discontinuous elevation, two transects with altitude interval of 505 m between Mount Cuomodi (CMD, altitude from 1,844 to 1,997 m) and Mount Wugongshan (WGS, altitude from 1,290 to 1,339 m) were investigated at this area (Table 1). The plant

TABLE 1 Environmental parameters with soil depth changes along altitudinal gradients in karst graben basin of Yunnan-Kweichow Plateau.

		Altitude (m)	T (°C)	EC (ms/m)	SM (%)	SOC (g/kg)	TN (g/kg)	TP (g/kg)	AK (g/kg)	pH
(0–10 cm) A layer	CMD1	1997	6.13 ± 0.6d	45.25 ± 6.55f	12.75 ± 2.21d	127.81 ± 45.91a	8.25 ± 3.31a	0.68 ± 0.04c	199.03 ± 55.85c	6.41 ± 0.07c
	CMD2	1966	5.18 ± 0.43e	60 ± 3.56e	17.6 ± 1.72d	91.32 ± 65.08b	7.33 ± 5.04ab	0.77 ± 0.23bc	122.35 ± 51.06 cd	6.4 ± 0.22c
	CMD3	1947	5.43 ± 0.76ed	73.5 ± 4.12d	32.6 ± 2.87bc	17.28 ± 3.75c	1.62 ± 0.25c	0.3 ± 0.08d	68 ± 19.26d	6.73 ± 0.23ab
	CMD4	1934	7.5 ± 0.79c	70.5 ± 1.73de	34.78 ± 2.2b	20.05 ± 0.83c	1.83 ± 0.1c	0.61 ± 0.22c	55 ± 6.55d	6.55 ± 0.09bc
	CMD5	1873	6.06 ± 0.77d	96.8 ± 6.3c	45.1 ± 8.08a	38.21 ± 13.41c	3.43 ± 1.17bc	0.92 ± 0.06b	265.18 ± 53.73bc	6.65 ± 0.07b
	CMD6	1844	6.88 ± 0.35 cd	96.75 ± 7.59c	48.33 ± 1.36a	20.86 ± 0.65c	1.71 ± 0.03c	0.71 ± 0.02c	352.75 ± 48.2b	6.6 ± 0.19bc
	WGS1	1,339	12.65 ± 0.17b	112.5 ± 5.2bc	22.45 ± 6.22 cd	62.78 ± 3.62bc	4.87 ± 0.48b	0.83 ± 0.08bc	169.08 ± 84.08 cd	6.66 ± 0.24ab
	WGS2	1,324	14.5 ± 0.44a	111.25 ± 8.5bc	25.48 ± 10.19c	48.84 ± 17.88c	3.07 ± 0.32bc	0.67 ± 0.07c	193.5 ± 12.04c	6.68 ± 0.04ab
	WGS3	1,312	13.33 ± 0.46b	101.25 ± 4.03c	14.48 ± 5.02d	45.67 ± 12.21c	3.89 ± 1.35bc	0.68 ± 0.12c	279.55 ± 178.92bc	6.6 ± 0.18bc
	WGS4	1,299	13.88 ± 0.5ab	120.75 ± 5.25b	34.85 ± 2.28b	17.73 ± 1.39c	1.51 ± 0.12c	0.64 ± 0.03c	127.38 ± 10.74 cd	6.86 ± 0.07a
	WGS5	1,290	12.6 ± 0.27b	153.25 ± 20.68a	24.95 ± 0.82c	24.34 ± 1.29c	1.85 ± 0.27c	1.17 ± 0.31a	574.25 ± 140.62a	6.32 ± 0.09c
(10–20 cm) B layer	CMD1	1997	8.5 ± 1.83e	56.67 ± 5.86c	21.67 ± 7.44c	112.82 ± 59.74a	7.6 ± 4.29a	0.51 ± 0.07c	80.13 ± 8.64bc	6.55 ± 0.26ab
	CMD2	1966	8.1 ± 0.71e	73.5 ± 17.68c	23.35 ± 12.09c	31.05 ± 6.13bc	2.35 ± 0.2bc	0.55 ± 0.01c	42.3 ± 16.12bc	6.21 ± 0.1b
	CMD3	1947	8.93 ± 0.36de	73 ± 4.08c	48.2 ± 4.21ab	9.9 ± 6.56c	1.07 ± 0.47c	0.22 ± 0.02d	30.95 ± 10.75c	6.58 ± 0.08ab
	CMD4	1934	9.63 ± 0.31d	67.5 ± 6.35c	47.48 ± 3.18ab	11.26 ± 0.86c	1.08 ± 0.19c	0.51 ± 0.02c	31.75 ± 10.98c	6.66 ± 0.19a
	CMD5	1873	8.3 ± 0.62e	109.6 ± 9.45b	52.32 ± 4.8a	23.24 ± 8.92c	2.1 ± 0.61bc	0.82 ± 0.09b	119.72 ± 28.13b	6.8 ± 0.12a
	CMD6	1844	8.43 ± 0.55e	97.75 ± 3.59b	51.88 ± 1.96a	12.4 ± 0.27c	1.07 ± 0.04c	0.57 ± 0.03c	126.08 ± 13.69b	6.57 ± 0.22ab
	WGS1	1,339	14.87 ± 0.15b	106.33 ± 4.16b	21.63 ± 6.19c	52.33 ± 5.4b	3.49 ± 0.73b	0.72 ± 0.1bc	140.07 ± 22.98b	6.63 ± 0.05ab
	WGS2	1,324	16.55 ± 0.07a	111.5 ± 0.71b	36 ± 0bc	33.66 ± 0.6bc	2.05 ± 0.04bc	0.61 ± 0c	129.5 ± 22.77b	6.64 ± 0.09ab
	WGS4	1,299	15.73 ± 0.13ab	116.5 ± 15.46b	42.13 ± 1.56b	9.11 ± 2.35c	0.84 ± 0.21c	0.52 ± 0.02c	73.95 ± 6.76bc	6.62 ± 0.27ab
	WGS5	1,290	13.45 ± 0.26c	168.5 ± 30.73a	28.78 ± 3.2c	21.75 ± 1.25c	1.55 ± 0.19bc	0.96 ± 0.18a	370.78 ± 169.2a	6.41 ± 0.14b

Different lower case letters represent significant difference from different sampling sites in the same soil layer ($p < 0.05$). Data are means ± standard error. Five duplicates in CMD5 and four repetitions in other sample sites from A layer. Three duplicates in WGS1, WGS2, CMD1, and CMD2, no samples in WGS3, and the same repetitions in other sample sites from B layer as in A layer.

10.3389/fmicb.2022.1054667

species at here were *Arundinella setosa*, *Dodonaea viscosa* (L.) Jacq., *Bothriochloa ischaemum* (L.) Keng., *Bidens pilosa* L., *Hedera nepalensis* var. *sinensis* (Tobl.) Rehd., *Parthenium hysterophorus* L., and *Alnus ferdinandi-coburgii* Schneid. The bare rock rates at this area were 2.7–28.9% (Yin et al., 2020). Moreover, the average annual rainfall at this area was 2026.5 mm and the average annual temperature was 16.3°C.

Soil sample collection

Six sampling sites in Mount CMD and 5 sampling sites in Mount WGS were investigated in January 2018. At each randomly selected sampling site almost without man-made management to avoid pseudo-replication, at least three replicates of soil samples with 5 m distances in every soil layer were randomly collected along S-shapes. If soil layer was less than 20 cm, only soil samples in A layer were collected. If soil layer was more than 20 cm, soil samples in two layers were simultaneously collected. After substance invasion removed, the soil samples were evenly divided into two parts and kept in sterile polyethylene bags for future work. One part was used for edaphic analysis and another part was kept in −80°C for soil bacterial community analysis. The detailed sampling information is listed in Supplementary Table S1.

Edaphic analysis

Soil organic carbon (SOC) and total nitrogen (TN) were determined on SerCon Integra 2 Elemental Analyzer (Sercon Ltd., England). Soil pH, total phosphorus (TP) and available potassium (AK) were determined according to the methods described in Hu et al. (2022) and Yan et al. (2022). Soil temperature (T), soil moisture (SM), and electrical conductivity (EC) were measured *in situ* by soil three-parameter tachometer (UK three-parameter tachometer HH2/WET).

Sequencing of 16S rRNA genes and bioinformatic analysis

Soil DNA extraction and high-throughput sequencing were performed in Magigene Ltd., China. Their detailed protocols were described in Hu et al. (2022) and Yan et al. (2022). The V3-V4 region of 16S rRNA gene was amplified using PCR primers of 338F and 806R (Wang, J. et al., 2017) and sequenced on the Illumina HiSeq 2,500 platform (Illumina Inc., San Diego, CA, United States). The sequence reads were deposited in the NCBI Sequence Read Archive under the accession number PRJNA514872.

Raw sequencing reads were processed on QIIME 1.9.1. About 4,637,609 raw reads of 80 soil samples filtered with length less than 300 bp or average base quality score more than 20 resulted in 1,446,651 high-quality and chimera-free reads, with a minimum sequencing depth of 8,138 reads per sample, according to Silva v.123 16S rRNA database. All clean sequences were grouped into operational taxonomic units (OTUs) based on a genetic similarity of 97%. Alpha diversities (Chao 1, Simpson, Shannon, observed OTUs, PD whole tree and Goods coverage) and beta diversity based on Bray-Curtis metrics were calculated based on rarefied OTU tables. The Goods coverage of all samples was more than 93% indicating that the achieved sequencing depth was sufficient for sequential studies. The detailed data are shown in Supplementary Table S1.

Statistical analysis

One-way ANOVA and Pearson's correlation analyses (two-tailed test) were carried out with SPSS 19.0. to perform statistical analysis. The Origin 8.5 software was used to illustrate the variations of mean relative abundances at phylum level and the alpha diversities, as well as the influence of altitudinal gradients on Shannon index.

Moreover, principal coordinate analysis (PCoA) was used to assess the influence of altitudinal gradients on the similarity/dissimilarity of soil bacterial communities by using beta diversity data based on Bray-Curtis metrics. Redundancy analysis (RDA) was carried out by Canoco 5 software to display the relationships between environmental factors and identified phyla in our study. The heat map was performed by using R studio 2.15.1 to detect the relationships between the most abundant OTUs and environmental factors, as well as the relative frequency of the most abundant OTUs in each sampling site. To explore the influence of altitudinal gradients on the proportions of shared and unique OTUs, the OTUs with more than five sequences were used to sort the shared and unique OTUs at different altitudes for network-based visualization generated with Cytoscape 3.6.1 (Shen et al., 2019). The partial least squares path model (PLS-PM) and PASSaGE 2 software was used to detect the relationships between altitudinal gradients, soil physical/chemical properties, soil bacterial communities based on the most abundant OTUs, and soil bacterial alpha diversities. Partial Mantel test was carried to recognize the influence of altitudinal gradients and soil physical/chemical properties on soil bacterial communities. Moreover, analysis of similarity (ANOSIM) test was performed with the vegan R package to determine the statistical differences of beta diversities along altitudinal gradients (Anderson and Walsh, 2013).

Results

Edaphic parameters along altitudinal gradients

In general, the monotonically increased SOC and TN had no obvious changes (Table 1). In our study, soil pH was in a near-neutral environment. T, SM and EC in A layer were lower than

those in B layer, however TP, AK, SOC and TN in A layer were higher than those in B layer. Besides that, altitudinal gradients had significantly negative effects on T, EC and AK in different soil layers ($p < 0.05$), and had significantly negative and positive effects on TP and SM, respectively, in B layer ($p < 0.05$, Supplementary Table S2). Despite all this, the influence of altitudinal gradients on edaphic parameters in the two transects was different. Altitudinal gradients had significantly positive effects on TN and SOC in A layer from Mount WGS ($p < 0.05$), and in the two layers from Mount CMD ($p < 0.05$), and had significantly negative effects on pH in A layer from Mount CMD ($p < 0.05$).

Soil microbial community structures and diversities along altitudinal gradients

Of all the reads, ≥94.7% were assigned to 10 phyla (e.g., Proteobacteria, Acidobacteria, Actinobacteria, Firmicutes, Bacteroidetes, Gemmatimonadetes, Chloroflexi, Verrucomicrobia, Planctomycetes, and Nitrospirae) in A layer, and ≥95.1% were assigned to 11 phyla (e.g., Acidobacteria, Actinobacteria, Proteobacteria, Verrucomicrobia, Firmicutes, Chloroflexi, Gemmatimonadetes, Bacteroidetes, Planctomycetes, Nitrospirae, and Latescibacteria) in B layer. Moreover, their abundances in the two layers along altitudinal gradients were different (Figure 1). The top five phyla with mean relative abundances in A layer were Proteobacteria (24%~43%), Acidobacteria (17%~34%), Actinobacteria (4%~21%), Bacteroidetes (4%~13%) and Verrucomicrobia (2%~13%), and the top five phyla in B layer were Proteobacteria (19%~38%), Acidobacteria (20%~32%), Actinobacteria (5%~36%), Verrucomicrobia (2%~34%), and Chloroflexi (2%~15%). The mean relative abundances of Proteobacteria followed U-shaped patterns, Actinobacteria, Firmicutes, Bacteroidetes, Chloroflexi, Planctomycetes, and Nitrospirae had hump-shaped patterns, Gemmatimonadetes decreased monotonically while Verrucomicrobia and Acidobacteria increased monotonically with increasing altitudes in A layer (Supplementary Figure S1). By contrast, the mean relative abundances of Acidobacteria, Proteobacteria, and Bacteroidetes followed U-shaped patterns, Firmicutes, Chloroflexi, Planctomycetes, Nitrospirae, Latescibacteria, and Actinobacteria had hump-shaped patterns, Verrucomicrobia increased monotonically as well as Gemmatimonadetes decreased monotonically with increasing altitudes in B layer.

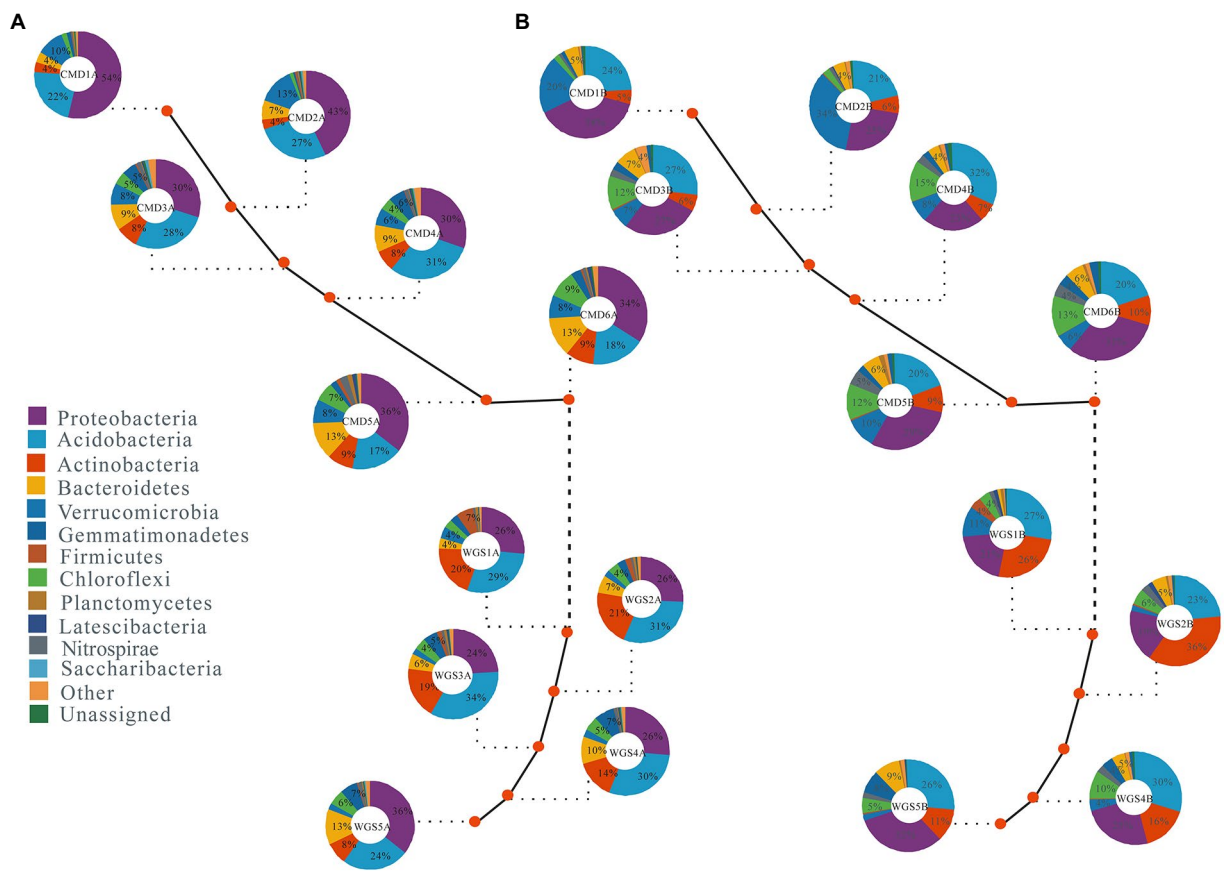

FIGURE 1
The mean relative abundance (≥0.1%) of dominant soil bacterial phyla in karst graben basin of Yunnan-Kweichow Plateau **(A)** indicating A layer and **(B)** indicating B layer. The mean relative abundance less than 0.1% were classified into other.

The alpha diversities along altitudinal gradients were higher in Mount CMD than those in Mount WGS, and were also higher in A layer than those in B layer (Figure 2). Considering that Shannon diversity usually was recommended to analyze microbial diversity, it was selected as the metric to investigate the effects of altitudinal gradients on alpha diversities. It was found that Shannon indexes decreased monotonically with increased elevation in Mount CMD and Mount WGS (Figure 3). Moreover, similar variations were also found in the two layers. The similarities and differences in soil bacterial community structures can be described by using beta diversity based on Bray-Curtis distances. The results indicated that two independent bacteria groups from A layer and B layer were identified in Mount CMD and Mount WGS, and U-trend was formed, though no monotonic changes appeared with increasing altitude (Figure 4). Moreover, ANOSIM revealed that altitudinal gradients exerted significantly influences on soil bacteria diversities (Alpha diversities—$R = 0.399$, $P = 0.001$ in A layer, alpha diversities—$R = 0.597$, $P = 0.001$ in B layer, beta diversity based on Bray-Curtis—$R = 0.862$, $P = 0.001$ in A layer, and beta diversity based on Bray-Curtis—$R = 0.985$, $P = 0.001$ in B layer), as seen in Supplementary Figure S2.

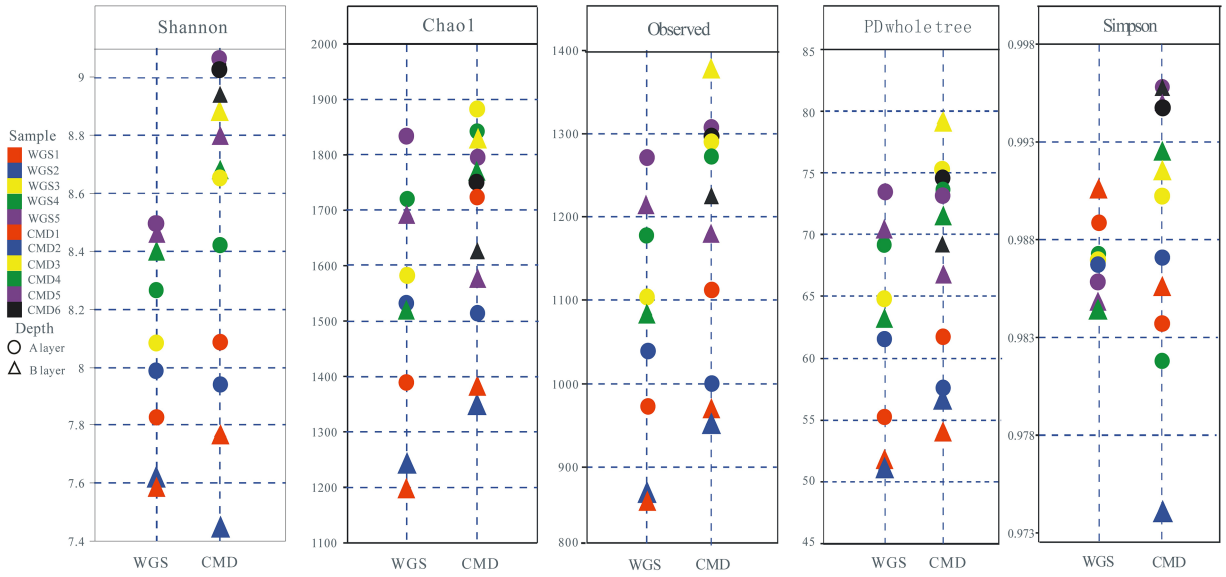

FIGURE 2
Alpha diversity of soil bacteria from Mount WGS and Mount CMD in karst graben basin of Yunnan-Kweichow Plateau.

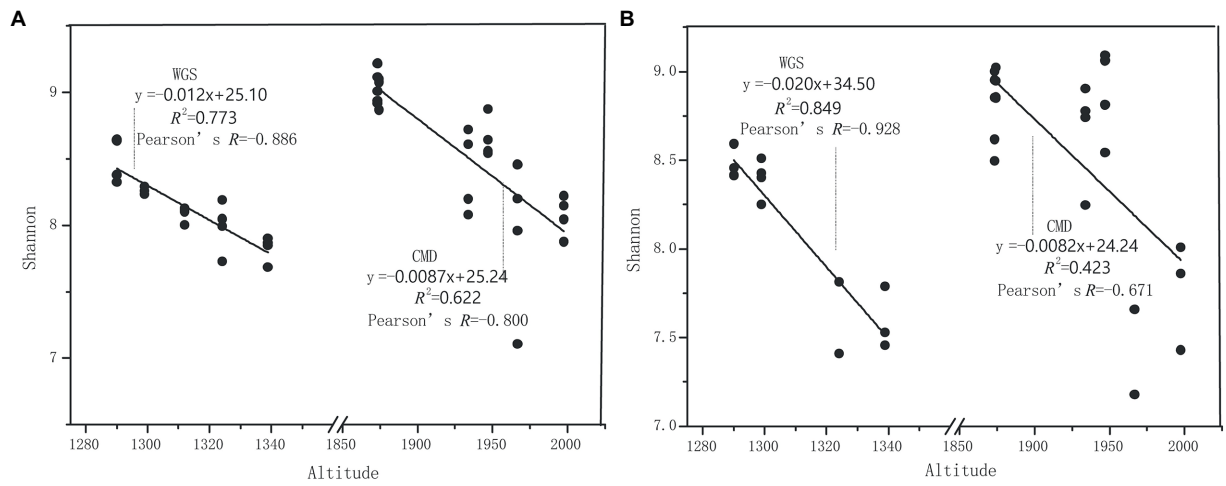

FIGURE 3
The relationships between altitudinal gradients and Shannon indexes in karst graben basin of Yunnan-Kweichow Plateau **(A)** indicating A layer and **(B)** indicating B layer.

To better evaluate the similarity and difference of bacterial communities along altitudinal gradients, network-based visualization with the proportions of shared and unique OTUs was applied. The proportions of shared OTUs in A layer and B layer were 12.56% (shared OTUs = 496, total OTUs = 3,948) and 11.27% (shared OTUs = 383, total OTUs = 3,407) respectively (Figure 5). The proportions of unique OTUs with increasing altitude exhibited the similar variation trend to Shannon diversities in Mount CMD and Mount WGS. Moreover, the proportions of unique OTUs in Mount CMD were lower than those in Mount WGS. In any case, the low proportion value of unique OTUs appeared in the joint area of Mount CMD and Mount WGS.

Among the most frequent OTUs, only *Rubrobacter* (actinobacterial OTU 12), *Arthrobacter* (actinobacterial OTU 15),

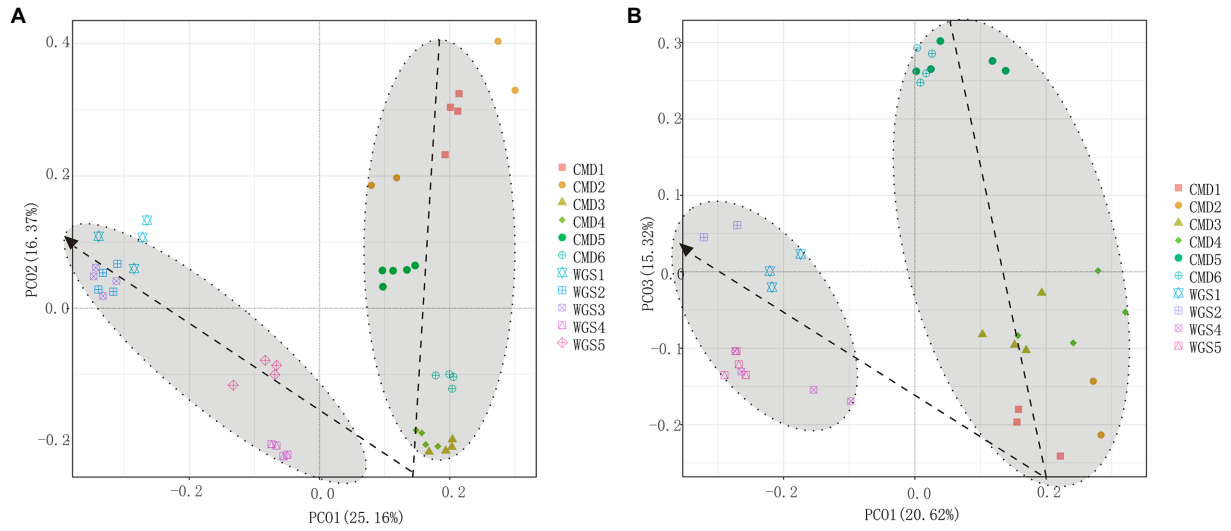

FIGURE 4
PCoA plots indicating influences of altitudinal gradients on the similarity/dissimilarity of soil bacterial communities by using beta diversity data based on Bray-Curtis metrics **(A)** indicating A layer and **(B)** indicating B layer.

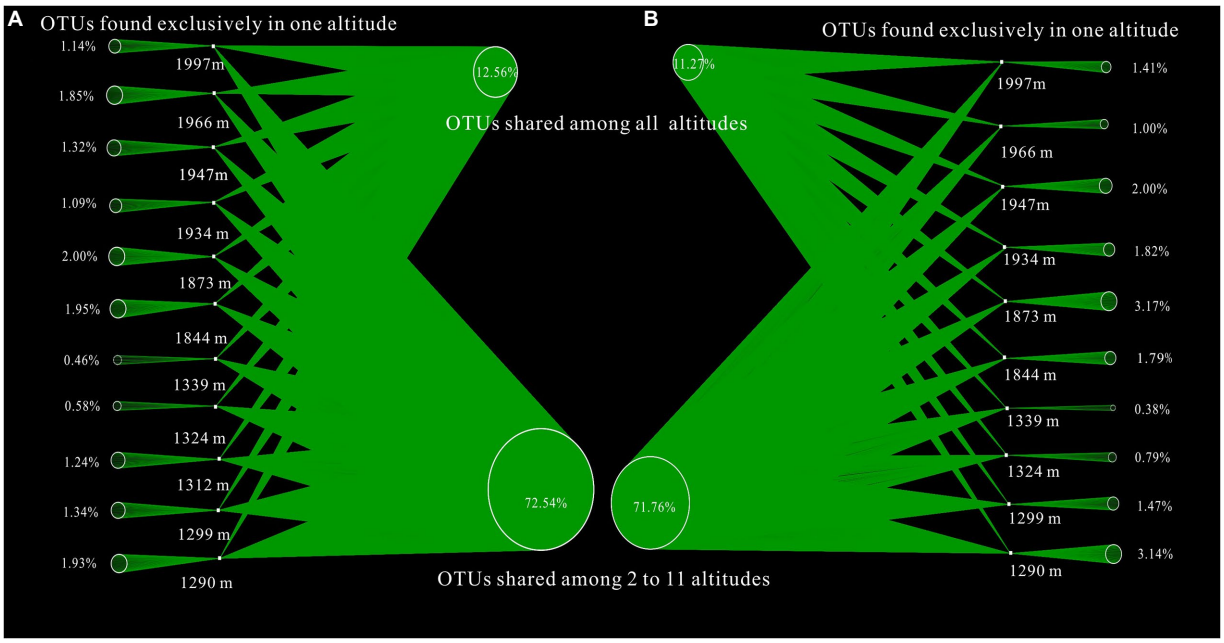

FIGURE 5
Influences of altitudinal gradients on the proportions of shared and unique OTUs based on network-based visualization **(A)** indicating A layer and **(B)** indicating B layer.

Bradyrhizobium (alphaproteobacterial OTU 1), and *Sphingomonas* (alphaproteobacterial OTUs 2, 37 and 182) were classified at the genus level in A layer (Figures 6C,D). In contrast, only *Bradyrhizobium* (alphaproteobacterial OTU 1), *Sphingomonas* (alphaproteobacterial OTU 9), and *Ferruginibacter* (Bacteroidetes OTU 28) were classified at the genus level in B layer. The altitudinal gradients had obvious effects on them (Figures 6A,B). In A layer, Actinobacteria-related OTUs (12 and 15) were dominant at low altitudes, and Proteobacteria-related OTUs (1 and 182) were dominant at high altitudes. In contrast, only Proteobacteria-related OTU1 was dominant at high altitudes in B layer.

Relationships between soil microbial communities and environmental parameters

Heatmap was drawn to reveal relationships between environmental parameters and the most frequent OTUs as well as dominant phyla in this study (Figure 6). In general, only SM showed significantly negative correlations with some OTU clusters in the two layers ($p < 0.05$), and other environmental factors had significantly negative or positive correlations with some OTU clusters ($p < 0.05$, Supplementary Table S3). Moreover, altitudinal gradients, T, EC, SM, SOC, TN, TP, AK and pH had significantly negative or positive correlations with some dominant phyla ($p < 0.05$, Figures 6E,F; Supplementary Table S4).

Instead of focusing on the relationships between individual environmental factors and soil bacterial communities, partial Mantel test was used to reveal the inter-relationships among altitudinal gradients, soil physical/chemical properties and soil bacterial communities (Table 2). Altitudinal gradients had significant influence on microbial communities from A layer and B layer ($p < 0.01$). Moreover, PLS-PM indicated that altitudinal gradients exerted negative effects on soil physical properties, and exerted positive effects on soil chemical properties *via* soil physical properties (Figure 7). Altitudinal gradients exerted negative effects on soil bacterial communities *via* soil physical properties and positive effects on soil bacterial diversities *via* soil chemical properties in A layer, however the results in B layer were opposite.

Discussion

This study showed the results of bacterial community characters, and the relationships between them and environmental factors along altitudinal gradients in karst graben basin of Yunnan-Kweichow Plateau.

Influence of altitudinal gradients on edaphic parameters

As previous report, climate, topography, and parent material are natural factors affecting SOC storage and distribution (Baveye et al., 2020). The maximum value of SOC was observed at high altitude which also may be due to the low microbial activities or the contributions of endemic microorganism at this area. Soil microorganisms performing SOC cycles involve two main stages: (i) *ex vivo* modification of organics relating to extracellular enzymes, and (ii) *in vivo* turnover of substances controlled by soil microorganisms (Liang et al., 2017). Then, the decreased activities of specific enzymes *via* microbial secretion at high altitude may contribute to high SOC accumulation in karst graben basin of Yunnan-Kweichow Plateau (Kumar et al., 2019), though we did not assess the exoenzyme activities. The contribution of endemic microorganism to SOC accumulation at high altitude will be discussed later in this article. It was well known that 96–98% soil N existed as complex and insoluble polymers which can be broken down by specific soil enzymes produced by specific soil microorganisms (Van Der Heijden et al., 2008). Coupled with the significant correlation between SOC and TN ($p < 0.01$, Supplementary Table S2), high soil TN was found at high altitude.

Moreover, the environmental features at high altitude are typical of low temperature and arid (Li et al., 2019). Consequently, SM and T decreased with increasing altitude. As to EC, it was usually used to indicate soil salt content or chemical supply which decreased with increasing altitudes due to weathering product from carbonate rocks easily transported and carried away by runoff. This phenomenon also occurred in TP and AK, which may be relating to soil drying and re-wetting significantly affecting P and K leached from soils (Gao et al., 2020; Amin et al., 2021). Except for the lower SM and T in A layer reflecting the direct influence of climate change (Kardol et al., 2010), the decreased SOC, TN, TP, AK and EC in deep soil correlates to previous studies (Pham et al., 2018). The high input of plant residues and plant activity could explain their higher levels in top soils (Jobbágy and Jackson, 2001; Pham et al., 2018).

Influence of altitudinal gradients on soil bacterial communities

Considering that environmental conditions determine soil bacterial compositions (Xun et al., 2015), and the occurrence and functioning of soil bacteria depend on their niches (Banerjee et al., 2018), soil bacterial abundances (e.g., Acidobacteria, Actinobacteria, Proteobacteria, Verrucomicrobia, Firmicutes, Chloroflexi, Gemmatimonadetes, Bacteroidetes, Planctomycetes, Nitrospirae, and Latescibacteria) can follow hump-shaped, decreasing, increasing or U-shaped patterns along altitudinal gradients. These bacteria followed the above patterns due to them at their own optimum conditions though the responses of their ecological lifestyles to altitudinal gradients remain unclear (Nottingham et al., 2018; Dai et al., 2021). Besides that, the different distribution patterns of bacteria taxa in two layers may be due to their response depending on soil depth (Barbour et al., 2022).

The monotonically decreased Shannon indexes with elevation increasing in Mount CMD and Mount WGS indicate that inducible mutations in easily accessed low-altitude areas may

10.3389/fmicb.2022.1054667

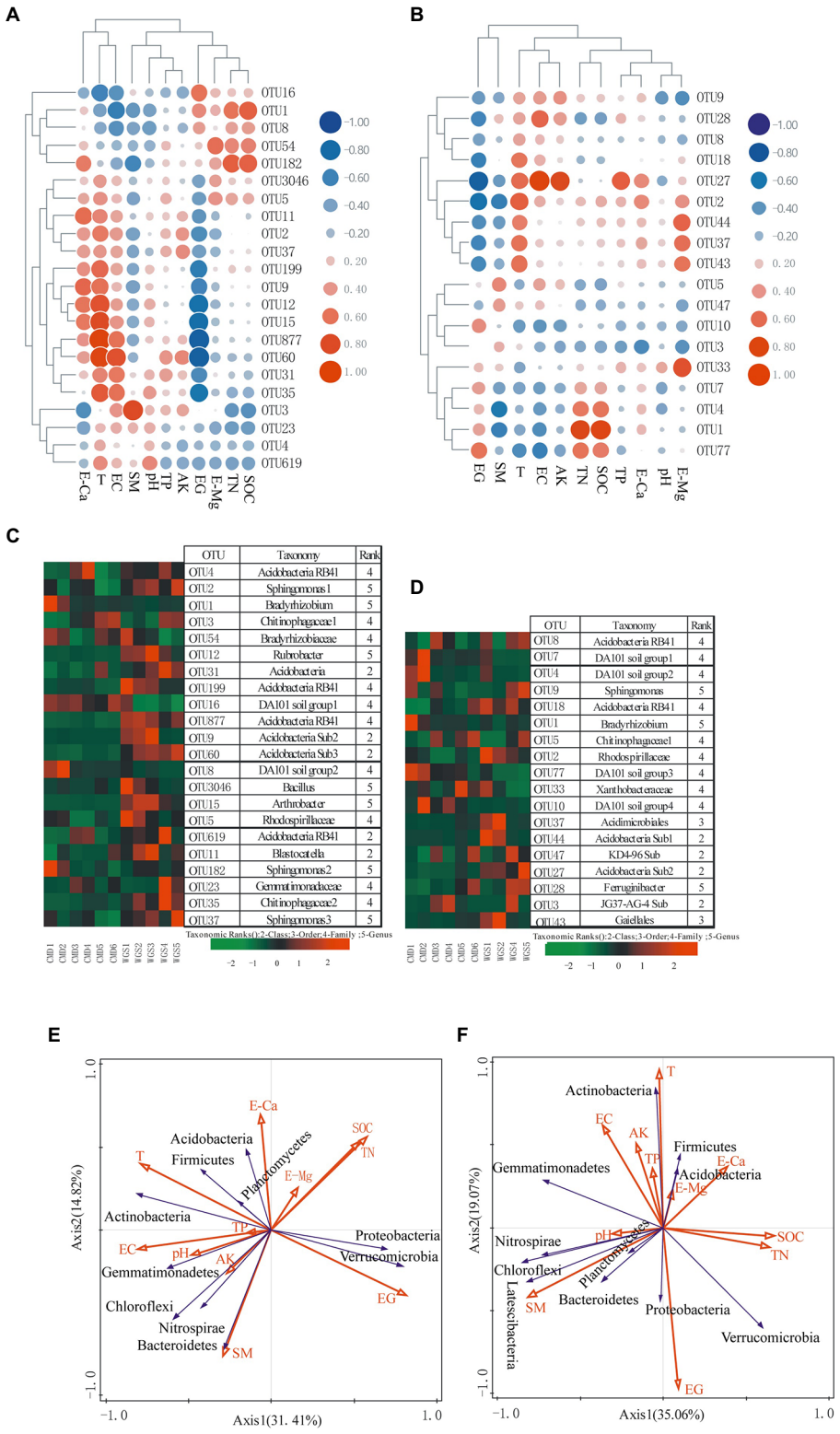

FIGURE 6
Heat map representing relationships between the most abundant OTUs (>0.5%) and environmental factors **(A)** from A layer and **(B)** from B layer, as well as the relative frequency of the most abundant OTUs (>0.5%) in each sampling site **(C)** from A layer and **(D)** from B layer. RDA plots displaying the relationships between environmental factors and the identified phyla **(E)** from A layer and **(F)** from B layer. EG indicating altitudinal gradient.

TABLE 2 Influence of altitudinal gradients and soil physical/chemical properties on soil bacterial communities by partial Mantel test with soil depth changes in karst graben basin of Yunnan-Kweichow Plateau.

	Effect of	a	a	a	a	b	b	b	b
A layer	Controlling for		b	c	bc		a	c	ac
	Bacterial communities	*r*	*r*	*r*	*r*	*r*	*r*	*r*	*r*
		0.642	0.263	0.638	0.266	0.643	0.266	0.633	0.245
B layer	Effect of	a	a	b	b	b	b		
	Controlling for		c		a	c	ac		
	Bacterial communities	*r*	*r*	*r*	*r*	*r*	*r*		
		0.418	0.408	0.517	0.336	0.5	0.318		

All *p* values are less than 0.01. a. Altitudinal gradients; b. Soil physical properties (T, EC and SM); c. Soil chemical properties (SOC, TP, AK, pH, and TN).

promote the enormous appearance of unique/endemic species, especially rare bacterial species (Fitzgerald and Rosenberg, 2019). By contrast, in the harsh environments at high altitudes, only few rare taxa adapting to this environment can be induced. Though unique/endemic species restricted in specific habitats are important contributors to soil microbial diversities (Lynch and Neufeld, 2015), our result was contrary to previous reports that endemic species decreased with elevation increasing (Zhou et al., 2019). Second, and more speculatively, red calcareous soil with spatial heterogeneity and temporal dynamics in Yunnan-Kweichow Plateau may drive the occurrence of high Shannon indexes at low altitude areas because rare taxa acting as 'seed bank' could become dominant under proper conditions (Yuan, 2001; Lennon and Jones, 2011; Jiao and Lu, 2020). These reasons also were applied to the variations of other alpha diversities. Moreover, based on independent-monotonically decreasing Shannon indexes from Mount CMD and Mount WGS, it can be speculated that the coordinated patterns of Shannon indexes may be monotonically decreased with elevation increasing though karst graben basin caused sampling discontinuous. Considering that nutrients (e.g., SOC and TN) in surface soils are usually high than those in sub-surface soils (Hayat et al., 2021), and high nutrient accessibilities could cause the imbalances of soil microbial communities and the appearance of atypical nutrient substrates favoring unique bacterial strains (Leeming et al., 2019; Mirmohamadsadeghi et al., 2021), the alpha diversities were higher in A layer than those in B layer. As to higher alpha diversities in Mount CMD than those in Mount WGS, perhaps spatiotemporal heterogeneity at high altitude areas may be the major drivers of microorganism alpha diversity (Banerjee et al., 2018). Though vegetation type has been reported to influence soil bacterial community diversity and composition (Karimi et al., 2018), alpha diversities in our study has no obvious changes with vegetation type variations (Supplementary Figure S3).

It is should be noted that alpha diversity was used as a measure of species richness and beta diversity was used to indicate the compositional dissimilarity at community levels. Though alpha diversities (e. g. Shannon indexes) may be monotonically decreased with elevation increasing, the U-trend of beta diversity in our study was in accordance with previous studies (Nottingham et al., 2018). These results suggested that though the dissimilarity of soil bacterial communities was affected by multiple environmental factors (Dai et al., 2021), changeable conditions at low or high elevation area sustained higher biodiversity than that at long-term stability environment in middle elevation area (Simpson, 1980). Moreover, if continuous samplings were obtained in karst graben basin of Yunnan-Kweichow Plateau, the real changing rules may be not U-trend. Then, beta diversity was the suitable indicator of karst soil bacterial structure patterns along altitudinal gradients in Yunnan-Kweichow Plateau.

Though it is a common belief that endemic species decreased and their proportions increased with elevation increasing (Zhou et al., 2019), the monotonically decreased proportions of unique OTUs with elevation increasing in Mount CMD and Mount WGS might impact the widely accepted opinions, namely elevation Rapoport's rules (Stevens, 1992). The reason is that soil microbial communities usually contain a large number of low-abundance species (usually referred as the unique/endemic species) and a small number of high-abundance species at low altitude areas, and only few rare taxa at high altitude areas can be induced (Lennon and Jones, 2011; Jiao and Lu, 2020). In this respect, high proportions of unique OTUs appear at low altitude areas, and low proportions of unique OTUs appear at high altitude areas. This result conforms to the changed regularities of Shannon indexes. Moreover, due to high proportions of unique OTUs appearing at low altitude areas, the proportions of unique OTUs in Mount CMD were lower than those in Mount WGS, which in general followed hump-shaped patterns along altitudinal gradients perhaps due to the discontinuous ridge at his area. In spite of this, their ecology mechanisms which are contrary to elevation Rapoport's rules in karst graben basin of Yunnan-Kweichow Plateau are not well clear and further research is needed.

The interactions between environmental factors and soil bacterial communities along altitudinal gradients

At phylum level, the associations between environmental factors and soil bacterial taxa varied, which may have been due to

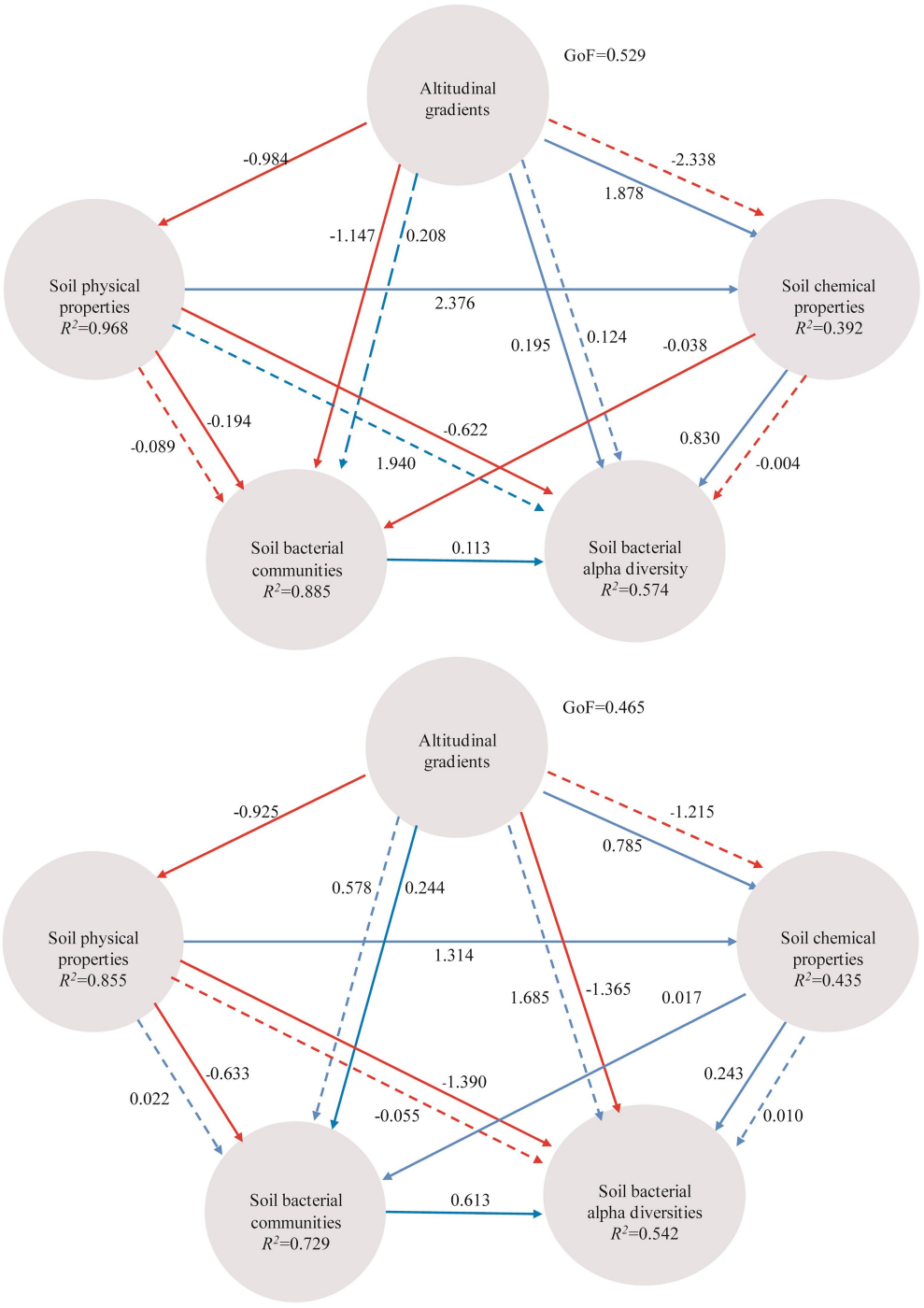

FIGURE 7
PLS-PM indicating the relationships between altitudinal gradients, soil physical properties (T, EC, and SM), chemical properties (SOC, TP, AK, pH, and TN), soil bacterial communities based on the most abundant OTUs and soil bacterial alpha diversities (Shannon, Simpson and observed OTUs). The path coefficients and the explained variability (R^2) are calculated after 999 bootstraps and reflected in the arrows with blue and red indicating positive and negative effects, respectively (solid line represents direct effect and dotted line represents indirect effect). Models with different structures were assessed using the Goodness of Fit (GoF) statistic, a measure of the overall prediction performance.

environmental filtering. That is, specific environmental factors favor the formation of particular soil bacterial communities (Delgado-Baquerizo et al., 2018; Nottingham et al., 2018). In this respect, a certain environmental factor may promote the fast-growth of some bacteria but could restrict the growth of other bacteria (Delgado-Baquerizo et al., 2018; Langenheder and Lindström, 2019). Consequently, the most frequent OTUs, especially those classified at the genus level had the significantly negative or positive

correlations with environmental factors in our study ($p < 0.05$). Significantly, *Bradyrhizobium* (alphaproteobacterial OTU 1) appearing in all layers had significantly positive relationships with SOC and TN ($p < 0.01$), which may have been due to them performing free-living N_2 fixation (Tao et al., 2021). Tao et al. (2021) also have reported that *Bradyrhizobium* could constitute the important group of free-living diazotrophs and potentially bring a amount of fixed N into soils, which simultaneously enhances SOC accumulation. Moreover, *Bradyrhizobium* could be tolerant to stressors due to them harboring *HspQ* gene which encodes a chaperone protein to combat detrimental effects (Shimuta et al., 2004; Tao et al., 2021). Consequently, Proteobacteria-related OTU1 was dominant at high altitudes in all layers.

Though a particular factor can be examined by experiments to obtain their role in microbial ecology, the studies about soils reacting to multifactor changes at a time are less (Rillig et al., 2019). In fact, soils are usually influenced by multiple-factors due to their spatial heterogeneity and temporal dynamics (Baldrian, 2019; Rillig et al., 2019). Understanding the impacts of multiple factors acting in concert is important because they can display the intrinsic characters in soil microbial ecology. To address the effects of multiple-factors on soil bacteria, partial Mantel test and PLS-PM have been used in our study. Altitudinal gradients had the significant effects on soil bacteria community compositions, supported by the fact that, altitude gradients associating with abiotic changes, including temperature and precipitation, can build soil bacterial communities in their corresponding habitat (Sundqvist et al., 2013). Besides that, soil physical changes along altitudinal gradients had directly adverse effects on microbial community compositions and diversities, and the soil chemical properties in their corresponding habitat were favorable to the appearing of specific species relating to the microbial community diversity changes (Ogola et al., 2021; Anselmo and Rizzioli, 2022). In this respect, soil physical changes had negative effects on microbial community compositions and diversities, and soil chemical property changes had positive effects on microbial community diversities. However, soil physical and chemical properties usually change with depths so that different soil layer harbors distinct microbial communities and the response of bacterial community to environmental changes depends on soil depth (Barbour et al., 2022). Consequently, the responses of microbial community compositions to soil chemical property changes were different, and altitudinal gradients had different effects on soil microbial community compositions and diversities in all layers. In spite of this, there still has some knowledge gaps existed on the responses of bacteria to altitudinal gradients. Then, future work should be focusing on their evolutionary and physiological processes in response to elevation gradient changes that could usefully move the understanding of soil microbial ecology forward.

Conclusion

Our results showed that soil microbial community compositions varied along altitudinal gradient in Yunnan karst graben basin due to environmental filtering. Because unique/endemic species restricted in specific habitats could become dominant under proper conditions and are important contributors to soil microbial diversities, high Shannon indexes were found in low altitude areas with changing environment conditions. The monotonically decreased Shannon indexes with elevation increasing in Mount CMD and Mount WGS also demonstrated that the coordinated patterns of Shannon indexes may be monotonically decreased along altitudinal gradients. Considering that unique species are not enormous in high altitude areas, the low proportions of unique OTUs appear at high altitude areas, which conforms to the changed regularities of Shannon indexes and impacts the widely accepted elevation Rapoport's rules. Moreover, edaphic parameters were different in all layers, and SOC and TN increased monotonically with elevation increasing. The dominant *Bradyrhizobium* (alphaproteobacterial OTU 1) identified at high altitudes in all layers constitutes the important group of free-living diazotrophs and could bring fixed N into soils, which simultaneously enhances SOC and TN accumulation at high altitudes. Due to the responses of bacterial community to environmental changes varying with soil depths, the altitudinal gradients had different effects on soil microbial community compositions and diversities in all layers. Though it is the primary work about soil microbial community structure and diversity varying along altitudinal gradients in karst graben basin of Yunnan-Kweichow Plateau, our finding provides powerful information that can improve our better understanding of soil microbial ecology along altitudinal gradients at karst areas.

Data availability statement

The datasets presented in this study can be found in online repositories. The names of the repository/repositories and accession number(s) can be found in the article/Supplementary material.

Author contributions

QL designed the study and wrote the paper. QL, YL, and GL collected the soil samples. QL and JQ conducted the experiments and data analysis. All authors critically commented on and contributed to the manuscript.

Funding

This study was supported by the National Key Research and Development Program of China (2016YFC0502501) and the Key Research and Development Program of Guangxi (GuikeAD20297091).

Conflict of interest

The authors declare that they have no known competing financial interests or personal relationships that could have appeared to influence the work reported in this paper.

Publisher's note

All claims expressed in this article are solely those of the authors and do not necessarily represent those of their affiliated organizations, or those of the publisher, the editors and the reviewers. Any product that may be evaluated in this article, or claim that may be made by its manufacturer, is not guaranteed or endorsed by the publisher.

Supplementary material

The Supplementary material for this article can be found online at: https://www.frontiersin.org/articles/10.3389/fmicb.2022.1054667/full#supplementary-material

References

Amin, M. M., Akter, A., Jahangir, M. M. R., and Ahmed, T. (2021). Leaching and runoff potential of nutrient and water losses in rice field as affected by alternate wetting and drying irrigation. *J. Environ. Manag.* 297:113402. doi: 10.1016/j.jenvman.2021.113402

Anderson, M. J., and Walsh, D. C. (2013). PERMANOVA, ANOSIM, and the mantel test in the face of heterogeneous dispersions: what null hypothesis are you testing? *Ecol. Monogr.* 83, 557–574. doi: 10.1890/12-2010.1

Anselmo, L., and Rizzioli, B. (2022). The small range and the great threat: extinction risk assessment of the narrow endemism *Carabus cychroides* under climate change. *J. Insect Conserv.* 26, 17–27. doi: 10.1007/s10841-021-00357-0

Baldrian, P. (2019). The known and the unknown in soil microbial ecology. *FEMS Microbiol. Ecol.* 95:fiz005. doi: 10.1093/femsec/fiz005

Banerjee, S., Schlaeppi, K., and van der Heijden, M. G. (2018). Keystone taxa as drivers of microbiome structure and functioning. *Nat. Rev. Microbiol.* 16, 567–576. doi: 10.1038/s41579-018-0024-1

Barbour, K. M., Weihe, C., Allison, S. D., and Martiny, J. B. (2022). Bacterial community response to environmental change varies with depth in the surface soil. *Soil Biol. Biochem.* 172:108761. doi: 10.1016/j.soilbio.2022.108761

Baveye, P. C., Schnee, L. S., Boivin, P., Laba, M., and Radulovich, R. (2020). Soil organic matter research and climate change: merely re-storing carbon versus restoring soil functions. *Front. Env. Sci.* 8:579904. doi: 10.3389/fenvs.2020.579904

Bhat, J. A., Kumar, M., Negi, A. K., Todaria, N. P., Malik, Z. A., Pala, N. A., et al. (2020). Species diversity of woody vegetation along altitudinal gradient of the Western Himalayas. *Glob. Ecol. Conserv.* 24:e01302. doi: 10.1016/j.gecco.2020.e01302

Brown, J. H. (2001). Mammals on mountainsides: Elevational patterns of diversity. *Glob. Ecol. Biogeogr.* 10, 101–109. doi: 10.1046/j.1466-822x.2001.00228.x

Bryant, J. A., Lamanna, C., Morlon, H., Kerkhoff, A. J., Enquist, B. J., and Green, J. L. (2008). Microbes on mountainsides: contrasting elevational patterns of bacterial and plant diversity. *Proc. Natl. Acad. Sci. U.S.A.* 105, 11505–11511. doi: 10.1073/pnas.0801920105

Cai, Z., Wang, X., Bhadra, S., and Gao, Q. (2020). Distinct factors drive the assembly of quinoa-associated microbiomes along elevation. *Plant Soil* 448, 55–69. doi: 10.1007/s11104-019-04387-1

Dai, Z., Zang, H., Chen, J., Fu, Y., Wang, X., Liu, H., et al. (2021). Metagenomic insights into soil microbial communities involved in carbon cycling along an elevation climosequences. *Environ. Microbiol.* 23, 4631–4645. doi: 10.1111/1462-2920.15655

Delgado-Baquerizo, M., Oliverio, A. M., Brewer, T. E., Benavent-González, A., Eldridge, D. J., Bardgett, R. D., et al. (2018). A global atlas of the dominant bacteria found in soil. *Science* 359, 320–325. doi: 10.1126/science.aap9516

Fierer, N., McCain, C. M., Meir, P., Zimmermann, M., Rapp, J. M., Silman, M. R., et al. (2011). Microbes do not follow the elevational diversity patterns of plants and animals. *Ecology* 92, 797–804. doi: 10.1890/10-1170.1

Fitzgerald, D. M., and Rosenberg, S. M. (2019). What is mutation? A chapter in the series: how microbes "jeopardize" the modern synthesis. *PLoS Genet.* 15:e1007995. doi: 10.1371/journal.pgen.1007995

Gao, D., Bai, E., Li, M., Zhao, C., Yu, K., and Hagedorn, F. (2020). Responses of soil nitrogen and phosphorus cycling to drying and rewetting cycles: a meta-analysis. *Soil Biol. Biochem.* 148:107896. doi: 10.1016/j.soilbio.2020.107896

Grau, O., Grytnes, J. A., and Birks, H. J. B. (2007). A comparison of altitudinal species richness patterns of bryophytes with other plant groups in Nepal, Central Himalaya. *J. Biogeogr.* 34, 1907–1915. doi: 10.1111/j.1365-2699.2007.01745.x

Guo, Q., Kelt, D. A., Sun, Z., Liu, H., Hu, L., Ren, H., et al. (2013). Global variation in elevational diversity patterns. *Sci. Rep.* 3:3007. doi: 10.1038/srep03007

Hayat, W., Khan, S., Hayat, M. T., Pervez, R., Ahmad, S., and Iqbal, A. (2021). The effect of deforestation on soil quality in lesser-Himalayan community forests of Abbottabad, Pakistan. *Arab. J. Geosci.* 14, 1–14. doi: 10.1007/s12517-021-08271-0

Hu, L., Li, Q., Yan, J., Liu, C., and Zhong, J. (2022). Vegetation restoration facilitates belowground microbial network complexity and recalcitrant soil organic carbon storage in Southwest China karst region. *Sci. Total Environ.* 820:153137. doi: 10.1016/j.scitotenv.2022.153137

Jiao, S., and Lu, Y. (2020). Soil pH and temperature regulate assembly processes of abundant and rare bacterial communities in agricultural ecosystems. *Environ. Microbiol.* 22, 1052–1065. doi: 10.1111/1462-2920.14815

Jobbágy, E. G., and Jackson, R. B. (2001). The distribution of soil nutrients with depth: global patterns and the imprint of plants. *Biogeochemistry* 53, 51–77. doi: 10.1023/A:1010760720215

Kardol, P., Cregger, M. A., Campany, C. E., and Classen, A. T. (2010). Soil ecosystem functioning under climate change: plant species and community effects. *Ecology* 91, 767–781. doi: 10.1890/09-0135.1

Karimi, B., Terrat, S., Dequiedt, S., Saby, N. P. A., Horrigue, W., Lelièvre, M., et al. (2018). Biogeography of soil bacteria and archaea across France. *Sci. Adv.* 4:eaat1808. doi: 10.1126/sciadv.aat1808

Keller, S. (2022). Vegetation and soil microbial diversity along alpine elevation and snow gradients [dissertation/master's thesis]. [Winterthur(IL)]: ZHAW Zürcher Hochschule für Angewandte Wissenschaften. doi: 10.21256/zhaw-25202

Körner, C. (2007). The use of 'altitude' in ecological research. *Trends Ecol. Evol.* 22, 569–574. doi: 10.1016/j.tree.2007.09.006

Kumar, S., Suyal, D. C., Yadav, A., Shouche, Y., and Goel, R. (2019). Microbial diversity and soil physiochemical characteristic of higher altitude. *PLoS One* 14:e0213844. doi: 10.1371/journal.pone.0213844

Langenheder, S., and Lindström, E. S. (2019). Factors influencing aquatic and terrestrial bacterial community assembly. *Environ. Microbiol. Rep.* 11, 306–315. doi: 10.1111/1758-2229.12731

Leeming, E. R., Johnson, A. J., Spector, T. D., and Le Roy, C. I. (2019). Effect of diet on the gut microbiota: rethinking intervention duration. *Nutrients* 11:2862. doi: 10.3390/nu11122862

Lennon, J. T., and Jones, S. E. (2011). Microbial seed banks: the ecological and evolutionary implications of dormancy. *Nat. Rev. Microbiol.* 9, 119–130. doi: 10.1038/nrmicro2504

Li, L., Zhang, Y., Wu, J., Li, S., Zhang, B., Zu, J., et al. (2019). Increasing sensitivity of alpine grasslands to climate variability along an elevational gradient on the Qinghai-Tibet Plateau. *Sci. Total Environ.* 678, 21–29. doi: 10.1016/j.scitotenv.2019.04.399

Liang, C., Schimel, J. P., and Jastrow, J. D. (2017). The importance of anabolism in microbial control over soil carbon storage. *Nat. Microbiol.* 2:17105. doi: 10.1038/nmicrobiol.2017.105

Looby, C. I., and Martin, P. H. (2020). Diversity and function of soil microbes on montane gradients: the state of knowledge in a changing world. *FEMS Microbiol. Ecol.* 96:fiaa122. doi: 10.1093/femsec/fiaa122

Lynch, M. D., and Neufeld, J. D. (2015). Ecology and exploration of the rare biosphere. *Nat. Rev. Microbiol.* 13, 217–229. doi: 10.1038/nrmicro3400

Mirmohamadsadeghi, S., Karimi, K., Azarbaijani, R., Yeganeh, L. P., Angelidaki, I., Nizami, A. S., et al. (2021). Pretreatment of lignocelluloses for enhanced biogas

production: a review on influencing mechanisms and the importance of microbial diversity. *Renew. Sust. Energ. Rev.* 135:110173. doi: 10.1016/j.rser.2020.110173

Nottingham, A. T., Fierer, N., Turner, B. L., Whitaker, J., Ostle, N. J., McNamara, N. P., et al. (2018). Microbes follow Humboldt: temperature drives plant and soil microbial diversity patterns from the Amazon to the Andes. *Ecology* 99, 2455–2466. doi: 10.1002/ecy.2482

Ogola, H. J. O., Selvarajan, R., and Tekere, M. (2021). Local geomorphological gradients and land use patterns play key role on the soil bacterial community diversity and dynamics in the highly endemic indigenous afrotemperate coastal scarp forest biome. *Front. Microbiol.* 12:592725. doi: 10.3389/fmicb.2021.592725

Pham, T. G., Nguyen, H. T., and Kappas, M. (2018). Assessment of soil quality indicators under different agricultural land uses and topographic aspects in Central Vietnam. *Int. Soil Water Conse.* 6, 280–288. doi: 10.1016/j.iswcr.2018.08.001

Phillips, J. D. (2016). Landforms as extended composite phenotypes. *Earth Surf. Process. Landf.* 41, 16–26. doi: 10.1002/esp.3764

Qiu, J., Cao, J., Lan, G., Liang, Y., Wang, H., and Li, Q. (2020). The influence of land use patterns on soil bacterial community structure in the karst graben basin of Yunnan province, China. *Forests* 11:51. doi: 10.3390/f11010051

Rillig, M. C., Ryo, M., Lehmann, A., Aguilar-Trigueros, C. A., Buchert, S., Wulf, A., et al. (2019). The role of multiple global change factors in driving soil functions and microbial biodiversity. *Science* 366, 886–890. doi: 10.1126/science.aay2832

Shen, C., Shi, Y., Fan, K., He, J. S., Adams, J. M., Ge, Y., et al. (2019). Soil pH dominates elevational diversity pattern for bacteria in high elevation alkaline soils on the Tibetan Plateau. *FEMS Microbiol. Ecol.* 95:fiz003. doi: 10.1093/femsec/fiz003

Shimuta, T. R., Nakano, K., Yamaguchi, Y., Ozaki, S., Fujimitsu, K., Matsunaga, C., et al. (2004). Novel heat shock protein *HspQ* stimulates the degradation of mutant DnaA protein in Escherichia coli. *Genes Cells* 9, 1151–1166. doi: 10.1111/j.1365-2443.2004.00800.x

Simpson, G. G. (1980). *Splendid isolation: The curious history of south American mammals* Yale Univ. Press.

Singh, D., Takahashi, K., Kim, M., Chun, J., and Adams, J. M. (2012). A hump-backed trend in bacterial diversity with elevation on Mount Fuji, Japan. *Microb. Ecol.* 63, 429–437. doi: 10.1007/s00248-011-9900-1

Stevens, G. C. (1992). The elevational gradient in altitudinal range: an extension of Rapoport's latitudinal rule to altitude. *Am. Nat.* 140, 893–911. doi: 10.1086/285447

Sundqvist, M. K., Sanders, N. J., and Wardle, D. A. (2013). Community and ecosystem responses to elevational gradients: processes, mechanisms, and insights for global change. *Annu. Rev. Ecol. Evol. Syst.* 44, 261–280. doi: 10.1146/annurev-ecolsys-110512-135750

Tao, J., Wang, S., Liao, T., and Luo, H. (2021). Evolutionary origin and ecological implication of a unique nif island in free-living Bradyrhizobium lineages. *ISME J.* 15, 3195–3206. doi: 10.1038/s41396-021-01002-z

Van Der Heijden, M. G., Bardgett, R. D., and Van Straalen, N. M. (2008). The unseen majority: soil microbes as drivers of plant diversity and productivity in terrestrial ecosystems. *Ecol. Lett.* 11, 296–310. doi: 10.1111/j.1461-0248.2007.01139.x

Vetaas, O. R., and Grytnes, J. A. (2002). Distribution of vascular plant species richness and endemic richness along the Himalayan elevation gradient in Nepal. *Glob. Ecol. Biogeogr.* 11, 291–301. doi: 10.1046/j.1466-822X.2002.00297.x

Wang, J., Gong, B., Wang, Y., Wen, Y., Zhou, J., and He, Q. (2017). The potential multiple mechanisms and microbial communities in simultaneous nitrification and denitrification process treating high carbon and nitrogen concentration saline wastewater. *Bioresour. Technol.* 243, 708–715. doi: 10.1016/j.biortech.2017.06.131

Wang, Y., Zhang, H., Zhang, G., Wang, B., Peng, S. H., He, R. S., et al. (2017). Zoning of environmental geology and functions in karst fault-depression basins. *Carsol. Sin.* 36, 283–295. (In Chinese with English abstract) doi: 10.11932/karst20170316

Wieder, W. R., Pierson, D., Earl, S., Lajtha, K., Baer, S. G., Ballantyne, F., et al. (2021). SoDaH: the SOils DAta harmonization database, an open-source synthesis of soil data from research networks, version 1.0. *Earth Syst. Sci. Data* 13, 1843–1854. doi: 10.5194/essd-13-1843-2021

Xun, W., Huang, T., Zhao, J., Ran, W., Wang, B., Shen, Q., et al. (2015). Environmental conditions rather than microbial inoculum composition determine the bacterial composition, microbial biomass and enzymatic activity of reconstructed soil microbial communities. *Soil Biol. Biochem.* 90, 10–18. doi: 10.1016/j.soilbio.2015.07.018

Yan, J., Li, Q., Hu, L., Wang, J., Zhou, Q., and Zhong, J. (2022). Response of microbial communities and their metabolic functions to calcareous succession process. *Sci. Total Environ.* 825:154020. doi: 10.1016/j.scitotenv.2022.154020

Yin, Z., Shan, Z. J., Qin, W., Yu, Y., Guo, Q. K., Li, B., et al. (2020). Preliminary research on a method of outcrops extraction on karst gabin ecosystem based on digital image processing: the case of the Mengzi Gabin Basin. *Forest. Environ. Sci.* 36, 26–33. (In Chinese with English abstract) doi: 10.3969/j.issn.1006-4427.2020.06.005

Yuan, D. X. (2001). On the karst ecosystem. *Acta Geol. Sin.* 75, 336–338. doi: 10.1111/j.1755-6724.2001.tb00541.x

Zhou, Y., Ochola, A. C., Njogu, A. W., Boru, B. H., Mwachala, G., Hu, G., et al. (2019). The species richness pattern of vascular plants along a tropical elevational gradient and the test of elevational Rapoport's rule depend on different life-forms and phytogeographic affinities. *Ecol. Evol.* 9, 4495–4503. doi: 10.1002/ece3.5027

frontiers | Frontiers in Microbiology

TYPE Original Research
PUBLISHED 09 January 2023
DOI 10.3389/fmicb.2022.1070876

OPEN ACCESS

EDITED BY
Xiangyu Guan,
China University of Geosciences,
China

REVIEWED BY
Jia Liu,
Jiangxi Academy of
Agricultural Sciences (CAAS),
China
Wenjie Ren,
Institute of Soil Science,
Chinese Academy of Sciences (CAS),
China
Zhen Wang,
Yulin Normal University,
China
Manoj Kumar Solanki,
University of Silesia in Katowice,
Poland

*CORRESPONDENCE
Zhongyi Li
✉ lizhongyi2007@163.com
Tieguang He
✉ tghe118@163.com

SPECIALTY SECTION
This article was submitted to
Terrestrial Microbiology,
a section of the journal
Frontiers in Microbiology

RECEIVED 15 October 2022
ACCEPTED 12 December 2022
PUBLISHED 09 January 2023

CITATION
Pu J, Li Z, Tang H, Zhou G, Wei C, Dong W, Jin Z and He T (2023) Response of soil microbial communities and rice yield to nitrogen reduction with green manure application in karst paddy areas. *Front. Microbiol.* 13:1070876. doi: 10.3389/fmicb.2022.1070876

Response of soil microbial communities and rice yield to nitrogen reduction with green manure application in karst paddy areas

Junyu Pu[1,2], Zhongyi Li[1]*, Hongqin Tang[1], Guopeng Zhou[3], Caihui Wei[1], Wenbin Dong[1], Zhenjiang Jin[2] and Tieguang He[1]*

[1]Agricultural Resource and Environment Research Institute, Guangxi Academy of Agricultural Sciences/Guangxi Key Laboratory of Arable Land Conservation, Nanning, Guangxi, China, [2]The Guangxi Key Laboratory of Theory and Technology for Environmental Pollution Control, College of Environmental Science and Engineering, Guilin University of Technology, Guilin, Guangxi, China, [3]Institute of Agricultural Resources and Regional Planning, Chinese Academy of Agricultural Sciences, Beijing, China

Fertilizer application practices are one of the major challenges facing agroecology. The agrobenefits of combined application of green manure and chemical fertilizers, and the potential of green manure to replace chemical fertilizers are now well documented. However, little is known about the impact of fertilization practices on microbial communities and tice yield. In this study, the diversity of bacterial and fungal communities, symbiotic networks and their relationship with soil function were analyzed in five fertilization treatments (N: 100% nitrogen fertilizer alone; M: green manure alone; MN_{60}: green manure couple with 60% nitrogen fertilizer, MN_{80}: green manure couple with 80% nitrogen fertilizer; and MN_{100}: green manure couple with 100% nitrogen fertilizer). First, early rice yield was significantly higher by 12.6% in MN_{100} treatment in 2021 compared with N. Secondly, soil bacterial diversity showed an increasing trend with increasing N fertilizer application after green manure input, however, the opposite was true for fungal diversity. Microbial interaction analysis showed that different fertilizer applications changed soil microbial network complexity and fertilizer-induced changes in soil microbial interactions were closely related to soil environmental changes. Random forest models further predicted the importance of soil environment, microorganisms and rice yield. Overall, nitrogen fertilizer green manure altered rice yield due to its effects on soil environment and microbial communities. In the case of combined green manure and N fertilizer application, bacteria and fungi showed different responses to fertilization method, and the full amount of N fertilizer in combination with green manure reduced the complexity of soil microbial network. In contrast, for more ecologically sensitive karst areas, we recommend fertilization practices with reduced N by 20–40% for rice production.

KEYWORDS

green manure, karst area, soil microorganisms, dominant taxa, random forest model, rice yield

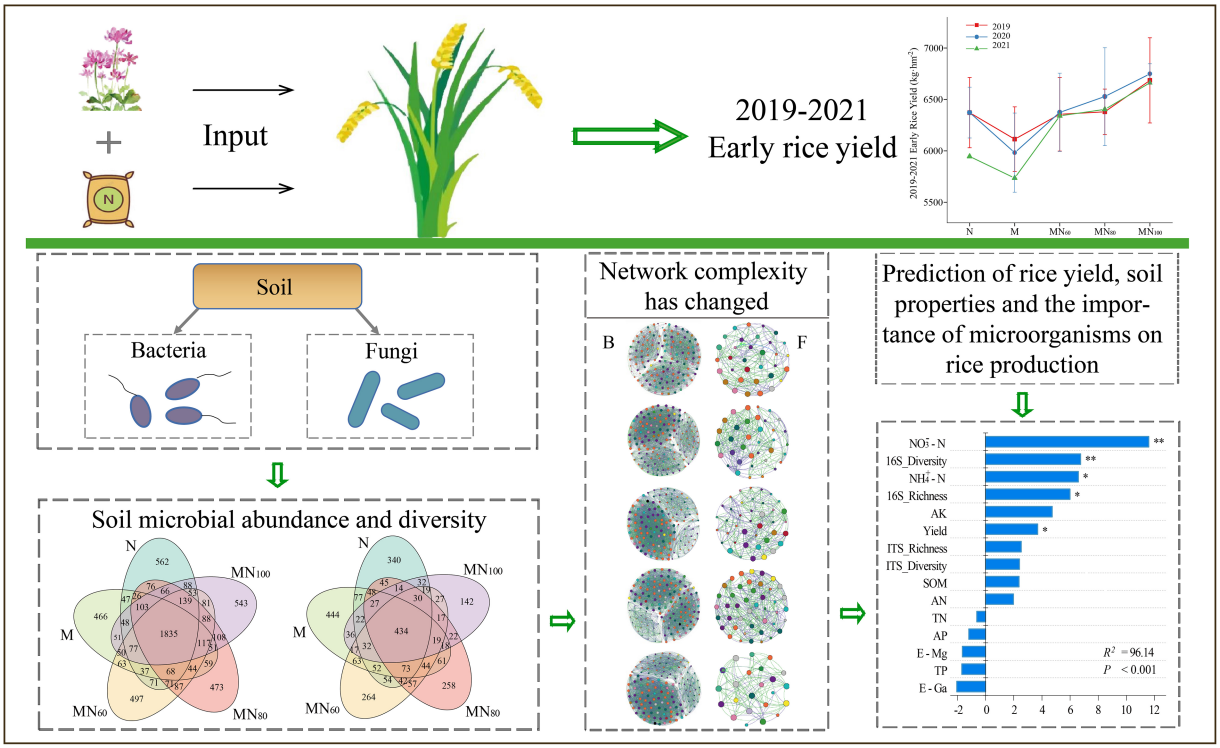

GRAPHICAL ABSTRACT

Introduction

China is a major rice producer, accounting for about 30% of the world's total rice production (Chen et al., 2020). Fertilizers play an important role in maintaining crop yields and are one of the most rapid and effective ways to increase crop yields. However, long-term application of large amounts of single fertilizer can threaten soil quality, which ultimately feeds into crop yield stability (Chen et al., 2011; Liu et al., 2013). Therefore, improving the agro-ecological environment and promoting sustainable crop growth has become a hot research topic.

Green manure is a completely biological nutrient that has gradually become an important alternative fertilizer for zero-growth chemical fertilizer program, which is of great significance to agricultural development (Bao et al., 2018; Zhang et al., 2023). In rice areas of southern China, the scattering of green manure crops such as Chinese milk vetch (*Astragalus sinicus* L.) in winter can make reasonably use of light and heat resources and provide a large number of organic nutrients for subsequent rice crop, and its role in reducing fertilizer and enhancing efficiency has been widely recognized (Gao et al., 2020). Previous experiments have shown that green manure is important for increasing yields, saving fertilizer, enriching soil, and improving soil nutrient absorption (Li et al., 2019; Yang et al., 2019; Zhou et al., 2020).

Soil bacteria and fungi are important components of agro-ecosystems and drivers of soil nutrient cycling and sensitive indicators for assessing soil environment (van der Heijden et al., 2008). The type and effectiveness of soil matrix is an important factor influencing microbial community changes including microbial community abundance, diversity and their functions (Sofo et al., 2019). Previous research has shown that climatic conditions (Pan et al., 2016), crop types (Guo et al., 2015) and fertilization regimes (Zhang X. et al., 2017) could interact with soil nutrients to influence microbial composition and function. Long-term input of mineral fertilizers may lead to a decrease in soil microbial diversity and abundance, resulting in decrease in soil fertility (Gao et al., 2021). Green manure planting in winter can promote crop growth and improve nutrient utilization by changing soil nutrient patterns, thus affecting microbial community's composition and structure (Xie et al., 2017). Studies have shown that applying green manure with appropriate amounts of chemical fertilizers facilitated growth and reproduction of soil microorganisms (Zou et al., 2013; Gao et al., 2015), significantly increasing the numbers of bacteria, fungi and nitrogen-fixing bacteria (Wan et al., 2013; Gao et al., 2021). Moreover, green manure application altered community structures of soil root endophytes by increasing their richness and diversity (Zhang et al., 2013) and the number of beneficial bacteria which then promotes nutrient uptake by crop roots (Zhang X. et al., 2017) to effectively increase crop yields.

Soil microbial communities are often interconnected and form complex ecological relationships, such as parasitism,

mutualism, neutrality, predation and competition, which determine their ability to maintain stability or recover from disturbances (Yang et al., 2023). Therefore, an increasing number of studies are using network analysis to understand the potential interactions within a given ecosystem. That is, species associations among microbial communities elucidate the complexity and stability of communities (Deng et al., 2012; Yuan et al., 2021). It is generally accepted that microecologies with more complex networks tend to have more active metabolic processes and faster growth rates, and their community performance is higher (Jordan, 2009; Yuan et al., 2021). Therefore, we used network analysis to better understand the effects of fertilization practices on microbial communities. Previous studies have found that changes in soil environment affect microbial network complexity due to changes in land use practices (Yang et al., 2022) and soil nitrogen accumulation reducing microbial network complexity (Ma et al., 2022), etc. However, further studies on changes in soil microbial network complexity caused by fertilization practices are needed.

As a product of carbonate rock dissolution and weathering, karst soil represents an alkaline and calcium-rich soil. The soil formation rate is slow and the thickness of soil layer is thin (Yuan, 2001; Li, 2022). Studies have shown that soil microorganisms are more abundant in karst areas than in non-karst areas with similar land use, and there are differences in microbial species interactions (Gao et al., 2012). Compared with red soils at same latitude, brownish-yellow karst soils are reported to have higher water stability and erosion resistance (Hu et al., 2013). However, relatively few studies have been conducted on the effects of fertilization practices on soil microbial community changes in karst paddy fields. Based on this, we propose the scientific conjecture that fertilizer application in karst paddy ecosystems would alter soil microenvironment by affecting microbial community structure and microbial intra- and/or inter-group interactions, which would change soil ecology and benefit rice production.

In this study, we analyzed and verified green manure-regulating effects of moderate N fertilization on environmental factors and microorganisms to understand interrelationships between environment, subsurface microbial ecology, and aboveground crop productivity. A three-year field experiment was conducted on a typical brownish-yellow rice soil in karst region to elucidate how fertilization affects microbial communities and soil properties, and how microbial communities feedback to crop productivity, and to verify the optimal fertilization strategy for rice production in karst regions by comparing different N fertilizer dosages. The main objectives were to answer the following three questions: (1) What will be the effect of N fertilizer reduction with green manure on rice production, (2) How does the reduction of nitrogen fertilizer with green manure affect the diversity, community structure and network complexity of bacteria and fungi, and (3) What is the importance of soil microbial diversity and community in maintaining productivity and soil environment of karst rice.

Materials and methods

Site description

The field experiment was conducted in Dingdian village (23°0′41″N, 107°51′21″E), Natong Town, Guangxi Province, China. The area has a subtropical monsoon climate with annual average temperature of 21.6°C, precipitation of about 1,300 mm and average altitude of 64 m. The soil is brownish-yellow rice soil from karst area. The basic physical properties of soil organic matter (SOM), total N (TN), available N (AN), available P (AP), available K (AK) and pH are 31.3 g/kg, 1.90 g/kg, 136 mg/kg, 19.4 mg/kg, 161 mg/kg, and 6.81, respectively.

Experimental design and crop management

Five treatments were established in the experiments: (i) 100% nitrogen fertilizer alone (N), (ii) green manure alone (M), (iii) green manure couple with 60% nitrogen fertilizer (MN_{60}), (iv) green manure couple with 80% nitrogen fertilizer (MN_{80}), and (v) green manure couple with 100% nitrogen fertilizer (MN_{100}). We used the treatments of N, M and MN_{100} previous determined in Pu et al. (2022). Each treatment was performed in three replications and arranged in a randomized block design. Each experimental plot area was 20.7 m^2 and separated by a ridge to prevent the movement of water and nutrients between plots.

The positioning test began in October 2018 and samples were collected for test analysis in middle of July 2021. A double-cropping system for rice was adopted. The green manure variety was Chinese milk vetch (*Astragalus sinicus* L.), sowed evenly 1–2 weeks before the late rice harvest with a seeding rate of 30 kg/hm^2, and the full amount was returned to field *in situ* at the full flowering stage (March 22, 2021). The test rice (Guiyu 9) was transplanted on April 7 and harvested on July 13, 2021. The paddy field was flooded and exposed to sun for 1 week at tillering stage without irrigation of 2 weeks before harvest. The fertilizer types were urea (containing 46.4% Nitrogen), calcium superphosphate (containing 18.0% P_2O_5), and potassium chloride (containing 60% K_2O), respectively. The 100% N fertilizer treatment was applied with 180 kg/hm^2 of urea, 90 kg/hm^2 of phosphorus and 120 kg/hm^2 of potassium. Potassium fertilizer and phosphorus fertilizer were applied once to paddy fields, while nitrogen fertilizer was applied several times according to the ratio base: tillering: tapping = 4:3:3.

Rice and soil sampling

The field experiment was conducted for 3 consecutive years. Rice yield and associated factors were measured at the harvest stage of early rice. Soil samples were collected from surface soil (0–20 cm) of each plot on July 13, 2021. Five soil cores were randomly sampled from each plot and homogenized to reduce variability. Each fresh

soil sample was divided into two sub-samples. One part was used for analysis of soil microorganism and the other was air-dried and passed 10/100 mesh sieve for analysis of soil chemical properties.

Chemical analysis

Soil pH was tested with a soil-to-water ratio of 1:2.5 (*m*:*v*). Soil organic matter (SOM) was determined using potassium dichromate oxidation method. Soil total nitrogen (TN) was determined with Kjeldahl method, alkaliolytic nitrogen (AN) was determined by alkaliolytic nitrogen diffusion method with ferrous sulfate reductant, and filtrate concentrations of ammonium nitrogen (NH_4^+–N) and nitrate nitrogen (NO_3^-–N) were analyzed with a discrete auto-analyzer (SmartChem TM200, United States). Exchangeable calcium and magnesium were determined using ammonium acetate exchange-atomic absorption spectrophotometer method. Available phosphorus (AP) and available potassium (AK) were measured as previously described by Lu (2000). Available N was measured by diffusion method with ferrous sulfate reductant. Available phosphorus was determined by molybdenum-antimony counterstain method with sodium bicarbonate extraction, and available potassium was determined by ammonium acetate exchange flame photometry described by Lu (2000). Some data of pH, SOM, AP, AK, AN, TN, E-Ga and E-Mg were from our previoustreatments of N, M and MN100 (Pu et al., 2022).

Bioinformatics analysis

Soil microbial sequencing was conducted by Guangdong Meige Gene Technology Co., Ltd. on the Illumina NovaSeq high-throughput sequencing platform. The primer sequences of 515F (GTGCCAGCMGCCGCGGTAA) and 907R (CCGTCAATTCMTTTRAGTTT) were selected to amplify the V4–V5 segment of bacterial 16S rRNA gene, and the PCR amplification conditions were: denaturation 95°C, 10 s, annealing 55°C, 30 s, extension 72°C, 45 s. The cycle of denaturation–annealing–extension repeated 45 times. The primer sequences of ITS1F (TCCGTAGGTGAACCTGCGG) and ITS2-2034R (GCTGCGTTCTTCATCGATGC) were selected to amplify the ITS1-4 segment of fungal ITS gene, and the PCR amplification conditions were: denaturation 95°C, 10 s, annealing 50°C, 30 s, extension 72°C, 45 s. The cycle of denaturation-annealing-extension repeated 45 times. The sequencing results were spliced using FLASH software, and low-quality sequences were removed using the Usearch software to draw a flat with the lowest sample quality sequences. By using cluster command, a taxonomy analysis of operational taxonomic unit (OTU) representative of sequences with a 97% similarity level was performed. After randomly sampling OTU table in same sequence depth, α diversity index and β diversity distance matrix were calculated using QIIME software (Cock et al., 2010). Ultimately, a total of 9,498 bacterial OTUs (belonging to 57 phyla, 128 classes, 238 orders, 440 families and 1,204 genera), and 4,505 fungal OTUs (belonging to 8 phyla, 34 classes, 99 orders, 236 families and 548 genera) were obtained from the karst rice soil All the sequence data of the present study have been deposited in the NCBI Squence Read Archive (SRA) database under accession numbers SRR21891129-SRR21891143 (Bacteria) and SRR21901595-SRR21901609 (Fungi), and we used the treatments of N, M and MN100 previous listed in Pu et al. (2022).

Statistical analysis

Data were subjected for analysis of variance (ANOVA) according to the experimental design (Randomize Design). Significant differences in rice yield, soil properties and relative microbial abundance among each fertilization treatment were tested by one-way ANOVA followed by Fisher LSD ($p < 0.05$) test (Buyer and Sasser, 2012). The unweighted UniFrac distance for phylogenetic relationship and Bray-Curtis for microbial communities were calculated, and principal coordinate analysis (PCoA) was performed to determine the differences in microbial taxa among the samples based on the dissimilarity (R vegan package; Zhong et al., 2020). The intra- and inter-group interactions of microbial groups were investigated by network analysis to reveal OTUs in soil microbial communities interacted using the positive or negative spearman correlations under different fertilization treatments. Positive correlations indicated mutually beneficial interactions among microorganisms, while negative correlations indicated competitive relationships. OTUs of bacteria and fungi with relative abundance $\geq 0.1\%$ were defined as the dominant groups (Zhong et al., 2021; Yang et al., 2023), which were visualized using stacking histogram. *p*-values for co-occurrence networks were obtained by Gephi based on R "psych" package (R Studio Version 4.1.2; Qiu et al., 2021). Redundancy analysis (RDA) was conducted to determine correlations between dominant OTUs and soil factors, and the effects of environmental factors and microorganisms on rice yield were assessed using the Mantel test (Sunagawa et al., 2015). A random forest model was used to predict the indicative nature of important variables on crop yield with R "randomForest" package (Liaw and Wiener, 2002), and univariate linear regression models were performed to analyze the correlations between important variables and rice yield.

Results

Early rice yield and soil properties

The results of early rice yield in 2019–2021 are shown in Figure 1A. In this case, there was no significant difference of early rice yield in 2019–2020 ($p > 0.05$) under different fertilizer treatments. In 2021, MN_{100} significantly increased the yield by 12.06% over N and 16.15% over M. In addition, the rice yields of MN_{60} and MN_{80} treatments showed an increasing trend comparing

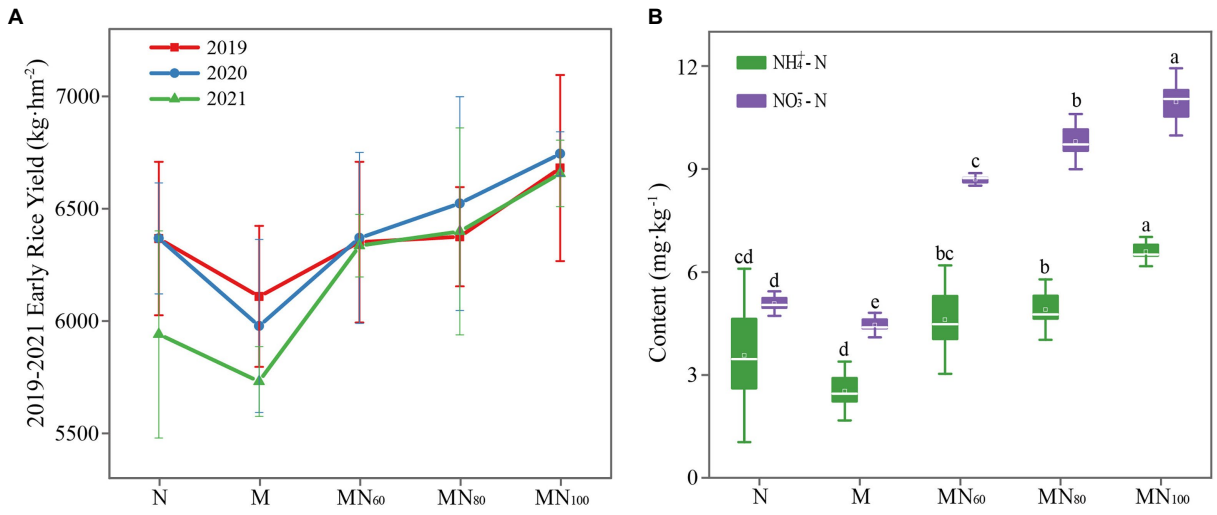

FIGURE 1
(A) Early rice yield of different fertilization treatments in 2019-2021. **(B)** Soil NH_4^+–N and NO_3^-–N contents under different treatments. NH_4^+–N: ammonium nitrogen; NO_3^-–N: nitrate nitrogen. The value is mean ± standard error, and different letters indicate significant difference between treatments ($p < 0.05$).

with N fertilizer treatments and the increases were 6.64 and 7.72%, respectively (Figure 1A).

One-way ANOVA analysis showed that the contents of SOM, AK, AN, NH_4^+–N and NO_3^-–N in paddy soils varied significantly under different fertilization treatments (Figure 1B). Among them, soil ammonium and nitrate N contents increased in MN_{60}, MN_{80} and MN_{100} treatments compared with N and M. The highest ammonium and nitrate N contents were achieved in the MN_{100} treatment. The differences in soil AK content were significant at different treatments. Compared with N and M, AK content decreased significantly under MN_{60} and MN_{80} treatments, while AK content increased significantly under MN_{100} treatment. In addition, soil TN, TP, AP, E-Ca, and E-Mg did not significantly differ under different fertilization treatments (Supplementary Table 1).

Microbial community characteristics under different fertilization treatments

Effects of fertilization on microbial communities

Figure 2 demonstrates the opposite trend of soil bacterial and fungal Shannon indices under different fertilization treatments. The highest bacterial diversity index was observed with MN_{100} treatment and the lowest value was observed with M treatment. The opposite was the fungal diversity index compared with N treatment. The soil B/F (bacteria/fungi) ratio was significantly higher at the MN_{100} treatment than those at other treatments (Figure 2A). In addition, the Venn diagram results showed the differences in OTU categories, and numbers of 16S and ITS under different fertilization treatments (Figure 2B).

To understand the effects of fertilization measures on soil microbial community structure, PCoA based on Bray–Curtis (Beta diversity) was performed (Figure 2C). The PCoA result showed that the first two axes for bacteria explained was 64.69% and fungi was 69.21%. In addition, the result of Adonis analysis showed significant difference in bacterial ($r = 0.298$, $p = 0.037$) and fungal ($r = 0.249$, $p = 0.044$) community structure among fertilization treatments.

Microbial community composition

The relative abundance of major bacteria and fungi differed slightly between fertilization treatments (Figure 3). Major bacterial phyla were Chloroflexi (27.15–47.99%), Proteobacteria (17.40–25.70%), and Acidobacteria (8.44–12.20%). The main fungal species were Ascomycota (44.27–53.62%), Basidiomycota (31.87–44.90%), and Zygomycota (8.46–15.35%). In addition, MN_{80} and MN_{100} significantly increased the relative abundance of Proteobacteria by 24.83 and 24.40%, respectively, compared with N, while the relative abundance of Crenarchaeota was decreased. At class level (Figure 3B), Anaerolineae was the most abundant taxon based on 16S rRNA genes with relative abundance of 30.18–39.40%, while the relative abundance of Deltaproteobacteria was 8.09–10.92%. According to ITS genes, Pezizomycetes (17.44–32.04%) had the greatest relative abundance at phylum level.

At the genus level (Figure 3C), the relative abundance of the major bacteriophage genus *Longilinea* decreased at the MN_{80} and MN_{100} treatments compared with the N treatment, and were

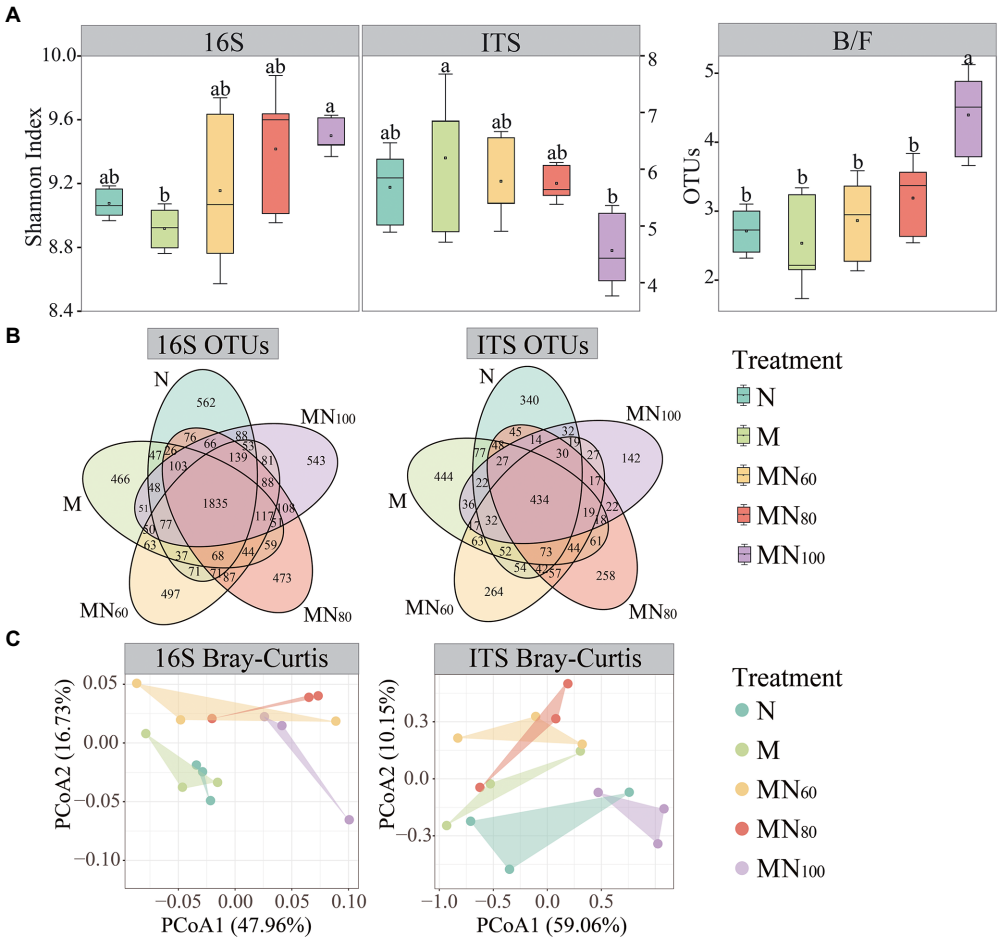

FIGURE 2
Soil microbial communities under different fertilizer treatments. **(A)** Shannon index of soil bacterial and fungal species as influenced by fertilizer treatments. Significant effects were obtained by one-way ANOVA test. Different lowercase letters indicate significant differences of bacteria and fungi among treatments, respectively ($p<0.05$). **(B)** Venn diagram of bacterial and fungal richness in different fertilization treatments. **(C)** Principal coordinate analysis (PCoA) plot of microbial community structures based on Bray–Curtis between samples of different fertilization treatments.

decreased by 16.63% (MN_{80}) and 25.64% (MN_{100}), respectively. The relative abundance of *Caldisphaera* also differed significantly among treatments. Compared with N, the relative abundance of *Caldisphaera* were decreased by 27.24, 32.07 and 6.90% for MN_{60}, MN_{80} and MN_{100} treatments, respectively. For the major fungal genera, green manure with N fertilizer reduced the relative abundance of *Bensingtonia* and the reduction of *Bensingtonia* was 15.69, 48.62 and 48.04% for MN_{60}, MN_{80} and MN_{100} treatments, respectively, compared with N. In contrast, the relative abundance of *Pucciniastrum* increased under MN_{60} and MN_{80} treatments compared with N and the increases were 65.60 and 64.54%, respectively.

Co-occurrence network of microbial communities

Network was used to analyze the dominant bacterial and fungal groups with relative abundance ≥0.1% in different fertilization treatments (Figure 4). Among them, the results of the co-occurrence network within bacterial groups showed that the green manure input increased the bacterial interactions compared with N (Figure 4A). However, the number of positively correlated edges decreases in MN_{100} compared with MN_{60} and MN_{80} (Supplementary Table 2). In contrast, the interactions within fungal groups showed the opposite trend to that of bacteria (Figure 4B). According to parameters such as number of nodes, total connected edges and modularity, the change in complexity of bacterial and fungal networks under different fertilization treatments followed the same trend as the change in bacterial diversity. Compared with N treatment, bacterial network complexity was greatest at MN_{100} and second highest at MN_{80}, while fungal networks showed the opposite trend (Figure 4). However, for bacterial-fungal interactions, network complexity appeared to be unaffected by microbial abundance.

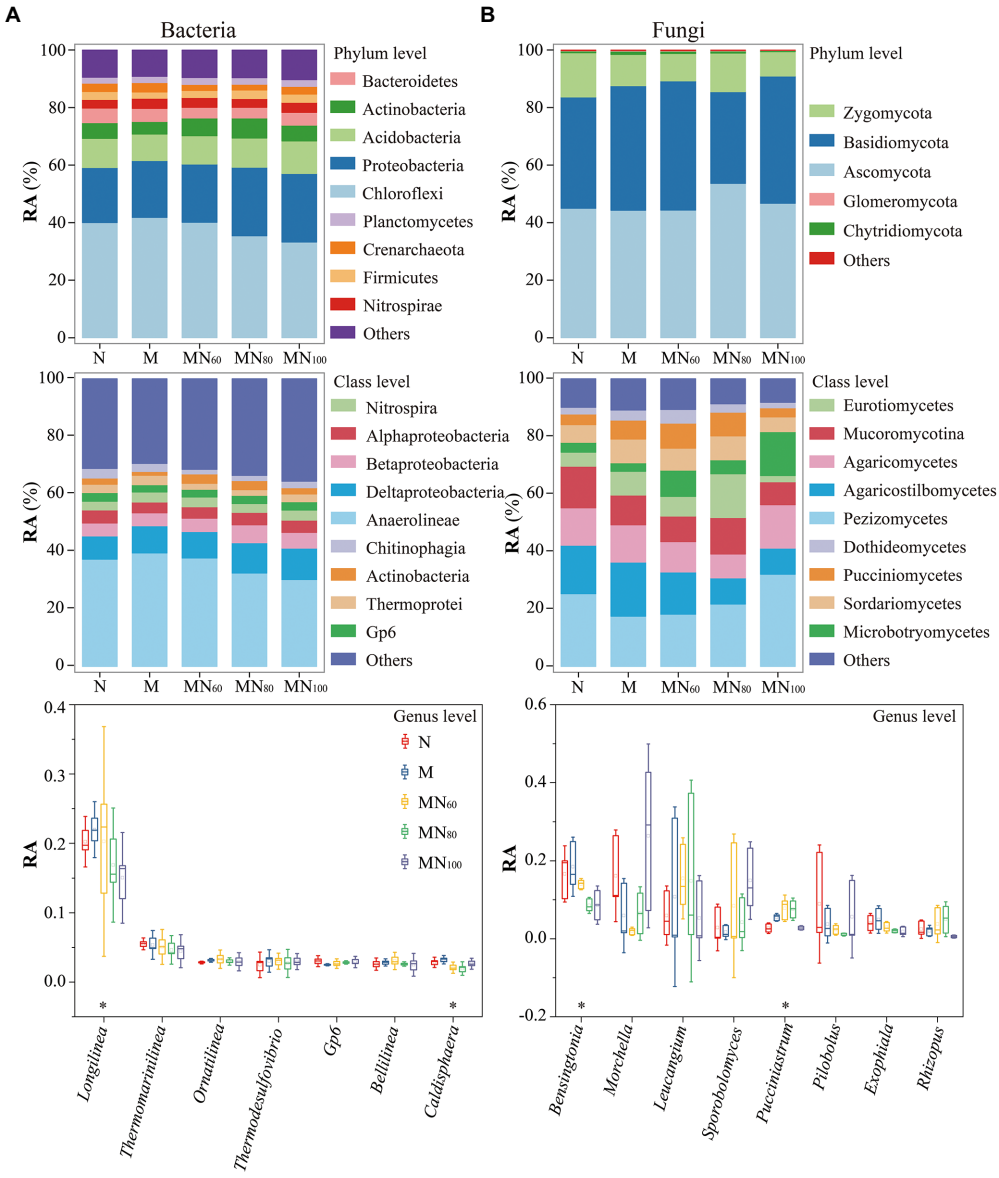

FIGURE 3
Soil microbial communities under different fertilization measures. **A,B** show the composition and abundance of soil bacteria at the taxonomic levels of phylum, order and genus, respectively. RA: Relative abundance. *p<0.05 indicates that the relative abundance of taxa at the genus level differed significantly under different fertilization treatments.

The relationships between soil properties, microbial abundance and diversity, and rice yield

Relationship between microbial community and environmental properties

The association between environmental factors and microbial communities was assessed using RDA (Figure 5A). The first two RDA dimensions showed a 67.54% variation in bacterial communities. All environmental factors except AP and TP were positively correlated with RAD1. Among them, SOM (r = 0.39, p = 0.048) and NO_3^-–N (r = 0.42, p = 0.033) were the environmental factors that significantly affected bacterial communities. And, the first two RDA dimensions explained 48.87% of the variation in bacterial communities, NO_3^-–N (r = 0.42, p = 0.033) were the most important drivers of fungal communities. The Mantel test results showed that SOM (r = 0.24, p = 0.047), NO_3^-–N (r = 0.32, p < 0.005), NH_4^+–N (r = 0.17, p = 0.024) and AK (r = 0.21, p = 0.022) were the key factors driving the changes of bacterial communities (Figure 5B).

The results of Spearman-based correlation heat map show that *Bensingtonia*, *Exophiala*, *Thanatephorus*, and *Hypocrea* showed significantly negative correlations with NH_4^+–N and NO_3^-–N. *Meanwhile*, *Pucciniastrum*, *Rhizopus*,

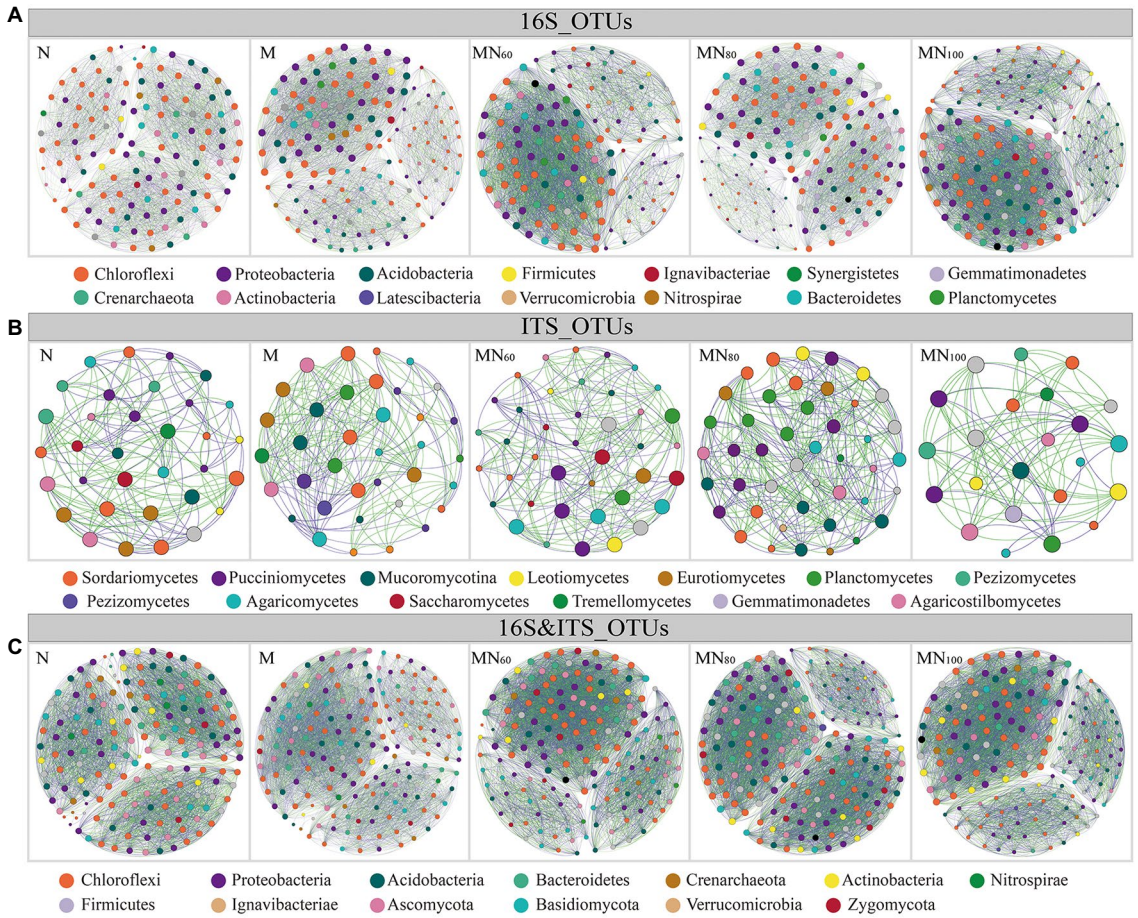

FIGURE 4
Network visualizes the interactions between soil operational taxonomic units (OTUs) in Karst paddy fields. Positive correlations are displayed in green and negative correlations were displayed in purple. The nodes are colored according to different types of species category. The size of each node is proportional to the betweenness centrality. **A–C** denote bacterial intra-group interactions, fungal intra-group interactions, and bacterial–fungal inter-group interactions, respectively.

Chrysosporium, *Neosartorya* and *Dimorphospora* also showed significantly negative correlations with AK. In contrast, *Leucangium* and *Chrysosporium* were significantly positively correlated with AP.

Potential factors affecting sustainable development of rice in karst areas

Random forest modeling was conducted to determine the relative importance of soil environment and microorganisms in predicting soil function and crop yield under different fertilization treatment conditions (Figure 6A). The model explained 96.14% of the ecological variation in soil function. The abundance and diversity of NO_3^-–N, NH_4^+–N, bacterial communities, and rice yield were predicted with greater importance than other factors. In addition, the regression analysis showed that soil properties had significantly positive linear correlation with rice yield and bacterial community abundance, and had significantly negative linear correlation with fungal community abundance (Figure 6).

Discussion

The soils in karst areas have slow soil formation rate, thin soil layer and fragile soil environment (Yan et al., 2020). Long-term application of single chemical fertilizer can seriously harm soil ecosystem of rice in karst areas. To solve these problems, we have done corresponding research to mitigate this harm expected to improve rice yield and protect soil ecological balance (Zhong et al., 2021; Pu et al., 2022). Previous studies showed that factors associated with high rice yield include climatic environment, soil nutrients and fertilization measures, as well as the regulation effects of soil microorganisms (Hayat et al., 2010; Romaniuk et al., 2011). In this study, we comprehensively characterized the relationship between soil nutrients, microbial communities and rice yield in karst paddy fields. It was reported that green manure with nitrogen fertilizer increased rice yield (Xie et al., 2016; Gao et al., 2020). Additionally, the use of green manure can effectively reduce the need for nitrogen fertilizer and even increase rice yield (Mohanty et al., 2013; Liu et al., 2021). This result related

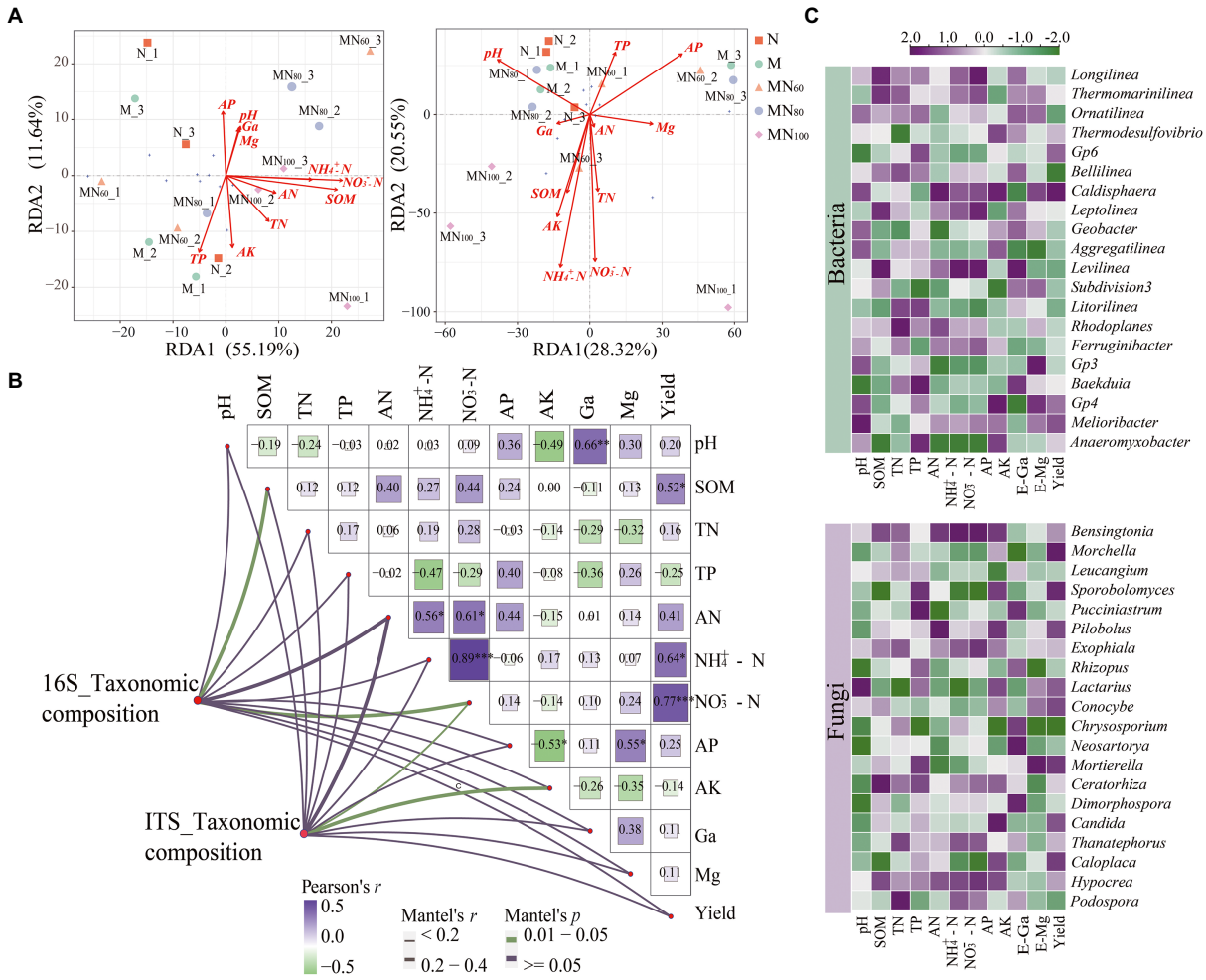

FIGURE 5
(A) RDA analysis of the effect of environmental factors on microbial composition. **(B)** Mantel test above with a Pairwise comparisons of environmental factors are shown, with a color gradient denoting Pearson's correlation coefficient. Edge width corresponds to the Mantel's R statistic for the corresponding distance correlations, and edge color denotes the statistical significance based on permutations. **(C)** Heatmap of the correlation between dominant microorganisms (genus level) and environmental factors based on Spearman correlation analysis.

toproduction of abundant nutrients from green manure decomposition, an exogenous additive that improves the soil environment (Zhang D. et al., 2017) and enhances the activity and mineralization of soil microorganisms (Liao et al., 2015; Hu et al., 2018), which ultimately affects rice yield.

Soil pH, organic matter, nitrogen, phosphorus and potassium influence crop growth, nutrient cycling and microbial processes, and are thus used as indicators of soil fertility (Guo Q. et al., 2020; Chen et al., 2021). As changes in chemical composition and concentration of soil physicochemical factors in most ecosystems are the main drivers of environmental disturbances, it is particularly important to understand the links between changes in microbial communities and the ecological environment (Lozupone et al., 2007; Hall et al., 2018). For instance, although soil pH does not directly affect microbial communities, it may directly or indirectly affect soil nutrient variables, which may change microbial structure and diversity (Lauber et al., 2009; Sagova-Mareckova et al., 2015). On the contrary, green manure inputs increase the amount of soil organic matter, which then decomposes producing many weak acids maintain the balance and stability of soil acidity and alkalinity through acid group dissociation and amino protonation (Zhao et al., 2014). In regard to soil nitrogen, green manure can effectively improve soil nitrogen capacity due to its fixation of atmospheric nitrogen (Gao et al., 2020). In this study, although we found no significant difference in soil nitrogen contents between green manure crop rotation and N fertilizer alone, the rice yield of the green manure group was higher, which may indicate that green manure application improved the absorption and utilization of nitrogen by rice (Nie et al., 2019; Qaswar et al., 2019). We also found no significant difference in rice yield between the high and reduced N (20–40%) treatments, and both were higher than N alone and green manure alone, suggesting that green manure may have a partial substitution effect on N fertilizer (Xie et al., 2016; Qaswar

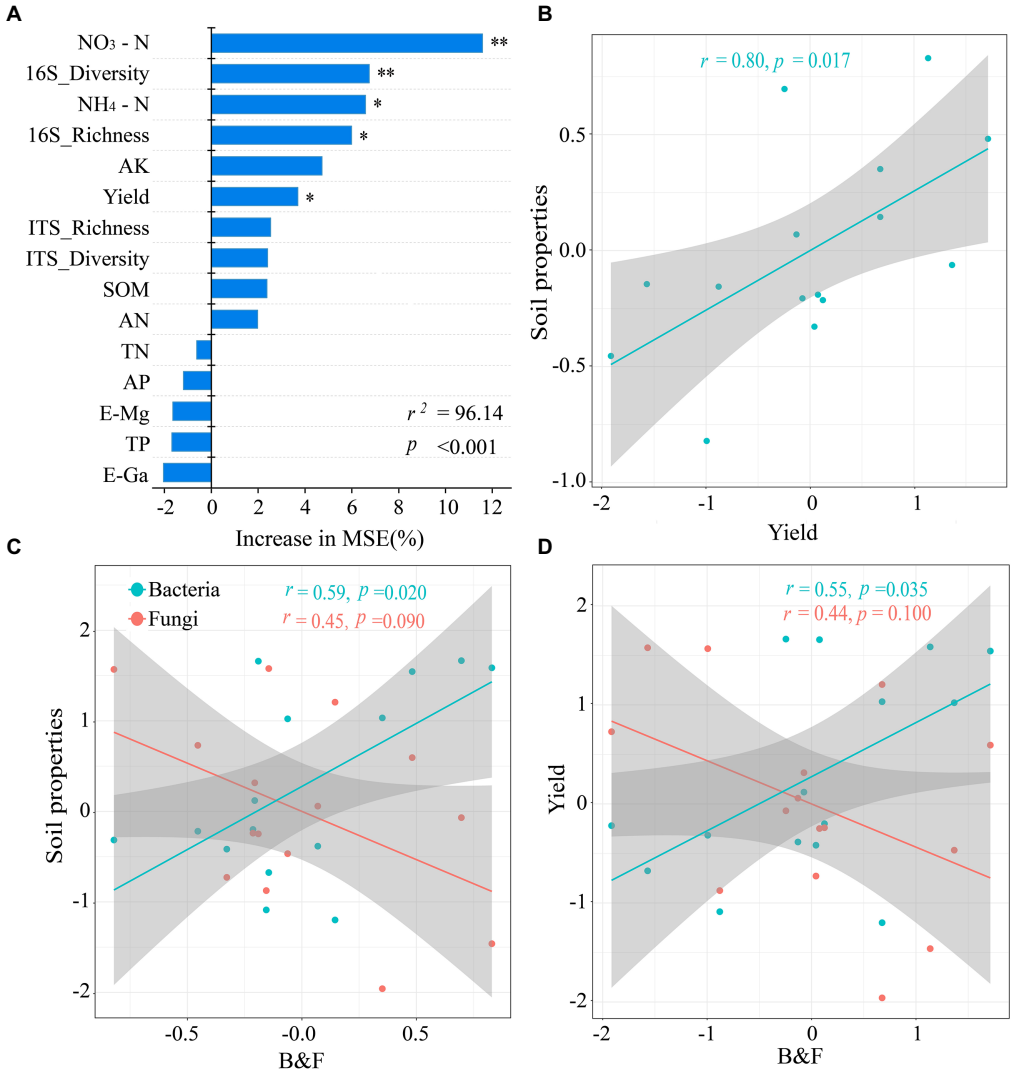

FIGURE 6
(A) Random Forest model showing the importance of predictors under different fertilization treatments. **(B–D)** Regression analysis after standardization (Z-Score) of the data showed a two-by-two linear relationship between soil properties, microorganisms and crop yield. MSE: mean square error. *$p < 0.05$, **$p < 0.01$ indicates a significant correlation between the factors.

et al., 2019; Zhou et al., 2019). Moreover, soil phosphorus and potassium are important nutrients for crop growth and development. Previous studies reported that green manure rotation reduced soil nutrient absorption and enhanced soil phosphorus and potassium content (Yang et al., 2009). However, this study found that under green manure reversion, nitrogen reduction reduced soil fast-acting potassium content, indicating that rice was more efficient in using fast-acting potassium due to the prolonged flooding of paddy fields (Chen et al., 2021).

Soil microorganisms are the basis of Earth's biosphere and play an irreplaceable role in nutrient cycling and organic matter decomposition (Balser and Firestone, 2005; Lucas et al., 2007). However, differences in response of different microbial taxa to environmental factors cause different adaptations in environmental gradients (Kivlin et al., 2014). Compared with bacterial communities, fungal communities undergo greater variations (Xu et al., 2019) probably because most fungal taxa in soils have a slower turnover pattern and decompose complex organic matter, making fungi more efficient in their use of organic matter (Waldrop and Firestone, 2006). Dominant taxa of karst paddy soil microorganisms (Figure 5C) grow together, share ecological niches, and play an important role in changing environmental factors such as soil's physical and chemical properties. For instance, Chloroflexi (bacterial taxa) is relatively abundant in agricultural soils and can ferment sugars and polysaccharide into hydrogen and organic acids, which can promote the degradation of plant residues, fix nitrite and reduce nitrate content (Rao et al., 2022). Similar to Acidobacteria, Proteobacteria play an important role in carbon and nitrogen metabolism and are both highly abundant in agricultural soil

environments (Kim et al., 2021). Actinobacteria are widely reported as symbiotic or autotrophic nitrogen-fixing colonies with potassium and phosphate solubilization and produce plant growth agents and biocontrol agents with high functional effects in agricultural production (Boubekri et al., 2022). Bacteroidetes are mainly responsible for nitrification processes, including autotrophic metabolism and subsequent nitrite oxidation (Wolinska et al., 2017). In addition, Ascomycota (fungal taxa) is closely relating to soil nitrogen effectiveness (Liu et al., 2022). Similar results were observed in this study based on the significant and positive correlation ($p < 0.05$) between soil AN and the relative abundance of Ascomycota. Basidiomycota are the group of ecologically strategic fungi with high diversity and high abundance in agricultural soils (Kjoller and Rosendahl, 2014). Zygomycota are the group of fungi employing r-strategy, similar to Ascomycota. They grow fast and effectively decompose unstable carbon, implying high C effectiveness and high relative abundance in soil environments with low C/N in agricultural soil (Liu et al., 2022).

Co-occurrence networks are often used to express the mutual co-occurrence and exclusion of microorganisms, and to identify and categorize key microorganisms that are highly relevant to soil function and crop production (Banerjee et al., 2018; Li et al., 2021) and are used to analyze the interspecific relationships of microbial communities (Barberan et al., 2012). The results showed that the network structure of microbial communities in karst paddy soils differed after reintroducing green manure. For example, 20% N reduction treatment increased the complexity of fungal network compared with N fertilization only, while MN_{100} treatment exhibited lower complexity. This result suggests that changes in microbial diversity are linked to changes in networks, i.e., increased microbial diversity increases the complexity of microbial networks (Guo J. et al., 2020). However, the results of bacterial-fungal interaction network showed that microbial network complexity decreased with full N fertilizer application. This result is in contrast to the bacterial and fungal network results, which may indicate that changes in soil microbial networks are not always associated with changes in microbial diversity, but depend on the interactions between microorganisms (Zhou et al., 2011; Yang et al., 2023). Thus, a multidimensional analysis of the uncertain relationship between diversity and network complexity highlights the importance of studying the relationships within and between microbial groups (Zhou et al., 2010). The significant differences in community composition under different fertilization treatments may explain the changes in abundance of key microorganisms (i.e., *Leptolinea*, *Syntrophorhabdus*, *Geobacter*, and *Dimorphospora*) induced by fertilizer application and alterations in rice yield. In addition, the random forest model and linear regression results showed a significant and negative linear relationship between some soil factors(i.e., NO_3^-–N, NH_4^+–N, and SOM) and rice yield in karst rice ecosystems. This is important for predicting the influencing factors on rice production.

Compared with fungi, bacteria have higher endogenous growth rates, are more resistant to external environmental disturbances (Loeuille et al., 2017), have relatively rapid nutrient turnover and recovery rates, have relatively rapid nutrient turnover and recovery rates, and have greater ecological niche width to stimulate rapid response (Blagodatskaya and Anderson, 1998). However, the dispersal ability of fungi is limited by the growth of their mycelium, which is affected by several factors, including soil particle size, thus, indicating that fungal community dynamics are often limited by more pronounced environmental factors (Fukami et al., 2010). Previous studies showed that soils with high nitrogen are not conducive to fungal growth (Six et al., 2006; Wu et al., 2014). The green manure species tested in this study was milk vetch. It is a leguminous green manure with low carbon: nitrogen ratio that can fix atmospheric nitrogen and return it to soil through biological nitrogen fixation, releasing about 90% of the nitrogen within 1 month after tilling (Zhu et al., 2014). Therefore, it may explain the apparent effect of green manure application on fungal community. Similarly, we observed that MN_{100} significantly increased B/F ratio compared with N. Additionally, we also observed that soil microbial structures after green manure application tended to be dominated by bacteria (Chen et al., 2019), which was contrary to the previous findings (Wan et al., 2013; Xie et al., 2017). Therefore, we speculate that the results may be related to habitat and climatic conditions in our study area. Therefore, a more in-depth study of these vacancies should also be conducted.

Our multidimensional analysis of environmental conditions, microbial communities and agricultural yield revealed the substitutability of green manure as chemical fertilizers in rice plantations. It could lead to reduced chemical nitrogen fertilizer (20–40% N reduction) and ensure satisfactory crop yield. Consequently, it is beneficial to environment and sustainable agricultural economy.

Conclusion

For typical karst paddy soils, fertilization practices significantly affect soil microbial community structure and alter microbial intra- and inter-group interactions. Green manure input provided more nutrients for microbial growth and development, which further drove microbial growth and material exchange. In addition, green manure with nitrogen fertilizer increased soil nitrogen, which was more favorable to soil bacterial growth, and maintained stable interactions between bacteria and fungi. Based on these findings, we recommend green manure application with reduced nitrogen fertilizer (20–40% N reduction) in karst areas. Currently, the coupling mechanism between fertilization, microorganisms and soil environment in fragile karst soil ecosystem still needs further in-depth investigations, such as

regulation of crop production by affecting certain specific microbial groups, and the relationships between dynamic characteristics of microbial communities and ecological functions during production cycle of rice. In addition, to solve these better-designed studies, combining multiple perspectives are needed in future to systematically elaborate the biogeochemical processes of soil ecology in karst paddy fields for improved sustainable rice production.

Data availability statement

The datasets presented in this study can be found in online repositories. The names of the repository/repositories and accession number(s) can be found at: https://www.ncbi.nlm.nih.gov/, SRR21891143 SRR21891142 SRR21891136 SRR21891135 SRR21891134 SRR21891133 SRR21891132 SRR21891131 SRR21891130 SRR21891129 SRR21891141 SRR21891140 SRR21891139 SRR21891138 SRR21891137. https://www.ncbi.nlm.nih.gov/, SRR21901609 SRR21901608 SRR21901607 SRR21901606 SRR21901605 SRR21901604 SRR21901603 SRR21901602 SRR21901601 SRR21901600 SRR21901599 SRR21901598 SRR21901597 SRR219015 96 SRR21901595.

Author contributions

JP and ZL conducted the experiments. HT and GZ analyzed the data. CW and WD prepared the figures and tables. ZL and TH designed the project and supervised the experiments. JP, ZL, ZJ, and TH drafted the manuscript. All authors contributed to the article and approved the submitted version.

Funding

This study was funded by the National Key Research and Development Program of China under Grant (No. 2021YFD1700200), Guangxi Key R&D Program Project under Grant (No. GuiKe AB22080068 and No. Guike AD20297091), National Natural Science Foundation of China (No. 41867008), China Agriculture Research System-Green Manure under Grant (No. CARS-22) and the Research and Development Fund of Guangxi Academy of Agricultural Sciences under Grant (No. 2021YT037 and No. 2022ZX08).

Conflict of interest

The authors declare that the research was conducted without any commercial or financial relationships that could be construed as a potential conflict of interest.

Publisher's note

All claims expressed in this article are solely those of the authors and do not necessarily represent those of their affiliated organizations, or those of the publisher, the editors and the reviewers. Any product that may be evaluated in this article, or claim that may be made by its manufacturer, is not guaranteed or endorsed by the publisher.

Supplementary material

The Supplementary material for this article can be found online at: https://www.frontiersin.org/articles/10.3389/fmicb.2022.1070876/full#supplementary-material

References

Balser, T. C., and Firestone, M. K. (2005). Linking microbial community composition and soil processes in a California annual grassland and mixed-conifer forest. *Biogeochemistry* 73, 395–415. doi: 10.1007/s10533-004-0372-y

Banerjee, S., Schlaeppi, K., and van der Heijden, M. G. A. (2018). Keystone taxa as drivers of microbiome structure and functioning. *Nat. Rev. Microbiol.* 16, 567–576. doi: 10.1038/s41579-018-0024-1

Bao, M., He, H., Ma, X., Wang, C., and Qiu, W. (2018). Effects of chemical nitrogen fertilizer and green manure on diversity and functions of soil bacteria in wheat Field. *Acta Pedol. Sin.* 55, 734–743. doi: 10.11766/trxb201710270425

Barberan, A., Bates, S. T., Casamayor, E. O., and Fierer, N. (2012). Using network analysis to explore co-occurrence patterns in soil microbial communities. *ISME J.* 6, 343–351. doi: 10.1038/ismej.2011.119

Blagodatskaya, E. V., and Anderson, T. H. (1998). Interactive effects of pH and substrate quality on the fungal-to-bacterial ratio and QCO2 of microbial communities in forest soils. *Soil Biol. Biochem.* 30, 1269–1274. doi: 10.1016/s0038-0717(98)00050-9

Boubekri, K., Soumare, A., Mardad, I., Lyamlouli, K., Ouhdouch, Y., Hafidi, M., et al. (2022). Multifunctional role of Actinobacteria in agricultural production sustainability: a review. *Microbiol. Res.* 261:127059. doi: 10.1016/j.micres.2022.127059

Buyer, J. S., and Sasser, M. (2012). High throughput phospholipid fatty acid analysis of soils. *Appl. Soil Ecol.* 61, 127–130. doi: 10.1016/j.apsoil.2012.06.005

Chen, Y., Hu, N., Zhang, Q., Lou, Y., Li, Z., Tang, Z., et al. (2019). Impacts of green manure amendment on detritus micro-food web in a double-rice cropping system. *Appl. Soil Ecol.* 138, 32–36. doi: 10.1016/j.apsoil.2019.02.013

Chen, J., Huang, Y., and Tang, Y. (2011). Quantifying economically and ecologically optimum nitrogen rates for rice production in South-Eastern China. *Agric. Ecosyst. Environ.* 142, 195–204. doi: 10.1016/j.agee.2011.05.005

Chen, X., Liu, Q., and Zhang, G. (2021). Effects of different crop rotation modes on soil fertility and rice yield in Taihu region. *Jiangsu J. Agric. Sci.* 37, 874–883. doi: 10.3969/j.issn.1000-4440.2021.04.009

Chen, J., Qin, W., Chen, X., Cao, W., Qian, G., Liu, J., et al. (2020). Application of Chinese milk vetch affects rice yield and soil productivity in a subtropical double-rice cropping system. *J. Integr. Agric.* 19, 2116–2126. doi: 10.1016/s2095-3119(19)62858-3

Cock, P. J. A., Fields, C. J., Goto, N., Heuer, M. L., and Rice, P. M. (2010). The sanger FASTQ file format for sequences with quality scores, and the Solexa/Illumina FASTQ variants. *Nucleic Acids Res.* 38, 1767–1771. doi: 10.1093/nar/gkp1137

Deng, Y., Jiang, Y., Yang, Y., He, Z., Luo, F., and Zhou, J. (2012). Molecular ecological network analyses. *BMC Bioinform.* 13:113. doi: 10.1186/1471-2105-13-113

Fukami, T., Dickie, I. A., Wilkie, J. P., Paulus, B. C., Park, D., Roberts, A., et al. (2010). Assembly history dictates ecosystem functioning: evidence from wood decomposer communities. *Ecol. Lett.* 13, 675–684. doi: 10.1111/j.1461-0248.2010.01465.x

Gao, S., Cao, W., Zhou, G., and Rees, R. M. (2021). Bacterial communities in paddy soils changed by milk vetch as green manure: a study conducted across six provinces in South China. *Pedosphere* 31, 521–530. doi: 10.1016/s1002-0160(21)60002-4

Gao, X., Wan, S., Cao, J., Hao, Y., and Huang, F. (2012). Comparative investigation of soil microbial activity in the karst and non-karst areas. *Earth Environ.* 40, 499–504. doi: 10.14050/j.cnki.1672-9250.2012.04.004

Gao, S., Zhang, R., Cao, W., Fan, Y., Gao, J., Huang, J., et al. (2015). Long-term rice-rice-green manure rotation changing the microbial communities in typical red paddy soil in South China. *J. Integr. Agric.* 14, 2512–2520. doi: 10.1016/s2095-3119(15)61230-8

Gao, S., Zhou, G., and Cao, W. (2020). Effects of milk vetch (*Astragalus sinicus*) as winter green manure on rice yield and rate of fertilizer application in rice paddies in South China. *J. Plant Nutr. Fertil.* 26, 2115–2126. doi: 10.11674/zwyf.20375

Guo, G., Kong, W., Liu, J., Zhao, J., Du, H., Zhang, X., et al. (2015). Diversity and distribution of autotrophic microbial community along environmental gradients in grassland soils on the Tibetan plateau. *Appl. Microbiol. Biotechnol.* 99, 8765–8776. doi: 10.1007/s00253-015-6723-x

Guo, Q., Liang, G., Zhou, W., Chen, J., Sun, J., Wang, X., et al. (2020). Microbiological mechanism of long-term organic fertilization on improving soil biological properties and double rice yields in red paddy soil. *J. Plant Nutr. Fertil.* 26, 492–501. doi: 10.11674/zwyf.19450

Guo, J., Ling, N., Chen, Z., Xue, C., Li, L., Liu, L., et al. (2020). Soil fungal assemblage complexity is dependent on soil fertility and dominated by deterministic processes. *New Phytol.* 226, 232–243. doi: 10.1111/nph.16345

Hall, E. K., Bernhardt, E. S., Bier, R. L., Bradford, M. A., Boot, C. M., Cotner, J. B., et al. (2018). Understanding how microbiomes influence the systems they inhabit. *Nat. Microbiol.* 3, 977–982. doi: 10.1038/s41564-018-0201-z

Hayat, R., Ali, S., Amara, U., Khalid, R., and Ahmed, I. (2010). Soil beneficial bacteria and their role in plant growth promotion: a review. *Ann. Microbiol.* 60, 579–598. doi: 10.1007/s13213-010-0117-1

Hu, L., Su, Y. R., and He, X. (2013). Characteristic of soil aggregate structure in different typical soils in karst region of Northwest Guangxi, China. *J. Guangxi Normal Univ.* 31, 213–219. doi: 10.16088/j.issn.1001-6600.2013.03.008

Hu, A., Tang, T., and Liu, Q. (2018). Nitrogen use efficiency in different rice-based rotations in southern China. *Nutr. Cycl. Agroecosyst.* 112, 75–86. doi: 10.1007/s10705-018-9930-x

Jordan, F. (2009). Keystone species and food webs. *Philos. Trans. R. Soc. B Biol. Sci.* 364, 1733–1741. doi: 10.1098/rstb.2008.0335

Kim, H. S., Lee, S. H., Jo, H. Y., Finneran, K. T., and Kwon, M. J. (2021). Diversity and composition of soil Acidobacteria and Proteobacteria communities as a bacterial indicator of past land-use change from forest to farmland. *Sci. Total Environ.* 797:148944. doi: 10.1016/j.scitotenv.2021.148944. doi: 10.1016/j.scitotenv.2021.148944

Kivlin, S. N., Winston, G. C., Goulden, M. L., and Treseder, K. K. (2014). Environmental filtering affects soil fungal community composition more than dispersal limitation at regional scales. *Fungal Ecol.* 12, 14–25. doi: 10.1016/j.funeco.2014.04.004

Kjoller, R., and Rosendahl, S. (2014). Cultivated and fallow fields harbor distinct communities of Basidiomycota. *Fungal Ecol.* 9, 43–51. doi: 10.1016/j.funeco.2014.02.005

Lauber, C. L., Hamady, M., Knight, R., and Fierer, N. (2009). Pyrosequencing-based assessment of soil pH as a predictor of soil bacterial community structure at the continental scale. *Appl. Environ. Microbiol.* 75, 5111–5120. doi: 10.1128/aem.00335-09

Li, Q. (2022). Microbial mechanism on distribution, renewal, and maintenance of soil organic carbon pool in karst area. *Acta Microbiol Sin.* 62, 2188–2197. doi: 10.13343/j.cnki.wsxb.20220010

Li, Z., He, T., Tang, H., Wei, C., and Dong, W. (2019). Knowledge mapping analysis of green manure research based on CiteSpace. *J. Chin. Agric. Mech.* 40, 157–164. doi: 10.13733/j.jcam.issn.2095-5553.2019.07.28

Li, Q., Song, A., Yang, H., and Mueller, W. E. G. (2021). Impact of rocky desertification control on soil bacterial Community in Karst Graben Basin, southwestern China. *Front. Microbiol.* 12:636405. doi: 10.3389/fmicb.2021.636405

Liao, Y., Lu, Y., Xie, J., Zhou, X., Nie, J., Tang, W., et al. (2015). Effects of combined application of controlled release nitrogen fertilizer and Chinese milk vetch on yield and nitrogen nutrient uptake of early rice. *J. Soil Water Conserv.* 29, 190–195+201. doi: 10.13870/j.cnki.stbcxb.2015.03.035

Liaw, A., and Wiener, M. (2002). Classification and regression by randomForest. *R News.* 2, 18–22.

Liu, T., Wu, C., Li, H., Ning, C., Li, Y., Zhang, X., et al. (2022). Soil quality and r–K fungal communities in plantations after conversion from subtropical forest. *Catena (Amst.)* 219:106584:106584. doi: 10.1016/j.catena.2022.106584

Liu, X., Zhang, Y., Han, W., Tang, A., Shen, J., Cui, Z., et al. (2013). Enhanced nitrogen deposition over China. *Nature* 494, 459–462. doi: 10.1038/nature11917

Liu, C., Zhang, C., Li, B., Lv, Y., Nie, L., and Zhang, L. (2021). Effects of *Astragalus sinicus* combined with chemical fertilizer on nitrogen absorption and uti-lization of rice and nitrogen distribution and residue of *Astragalus sinicus* in rice-soil system. *Chin. J. Appl. Ecol.* 32, 1791–1798. doi: 10.13287/j.1001-9332.202105.026

Loeuille, N., Le Mao, T., and Barot, S. (2017). Effects of plant evolution on nutrient cycling couple aboveground and belowground processes. *Theor. Ecol.* 10, 117–127. doi: 10.1007/s12080-016-0315-y

Lozupone, C. A., Hamady, M., Kelley, S. T., and Knight, R. (2007). Quantitative and qualitative beta diversity measures lead to different insights into factors that structure microbial communities. *Appl. Environ. Microbiol.* 73, 1576–1585. doi: 10.1128/aem.01996-06

Lu, R. (2000). *Analytical Method for Soil and Agro-chemical*. Agricultural Science and Technology Press, Beijing, China.

Lucas, R. W., Casper, B. B., Jackson, J. K., and Balser, T. C. (2007). Soil microbial communities and extracellular enzyme activity in the New Jersey pinelands. *Soil Biol. Biochem.* 39, 2508–2519. doi: 10.1016/j.soilbio.2007.05.008

Ma, X., Wang, T., Shi, Z., Chiariello, N. R., Docherty, K., Field, C. B., et al. (2022). Long-term nitrogen deposition enhances microbial capacities in soil carbon stabilization but reduces network complexity. *Microbiome.* 10:112. doi: 10.1186/s40168-022-01349-1

Mohanty, S., Nayak, A. K., Kumar, A., Tripathi, R., Shahid, M., Bhattacharyya, P., et al. (2013). Carbon and nitrogen mineralization kinetics in soil of rice-rice system under long term application of chemical fertilizers and farmyard manure. *Eur. J. Soil Biol.* 58, 113–121. doi: 10.1016/j.ejsobi.2013.07.004

Nie, J., Yi, L., Xu, H., Liu, Z., Zeng, Z., Dijkstra, P., et al. (2019). Leguminous cover crop *Astragalus sinicus* enhances grain yields and nitrogen use efficiency through increased tillering in an intensive double-cropping rice system in Sothern China. *Agronomy-Basel.* 9:554. doi: 10.3390/agronomy9090554

Pan, Y., Tian, S., Liu, D., Fang, Y., Zhu, X., Zhang, Q., et al. (2016). Reply to comment on "fossil fuel combustion-related emissions dominate atmospheric ammonia sources during severe haze episodes: evidence from N-15-stable isotope in size-resolved aerosol ammonium". *Environ. Sci. Technol.* 50, 10767–10768. doi: 10.1021/acs.est.6b04197

Pu, J., Li, Z., Zhong, J., Jin, Z., Tang, H., Wei, C., et al. (2022). Effect of the combination of green manure with nitrogen fertilizer on microbial community in karst paddy soil. *Acta Microbiol Sin.* 62, 2417–2432. doi: 10.13343/j.cnki.wsxb.20220079

Qaswar, M., Huang, J., Ahmed, W., Liu, S., Li, D., Zhang, L., et al. (2019). Substitution of inorganic nitrogen fertilizer with green manure (GM) increased yield stability by improving C input and nitrogen recovery efficiency in Rice based cropping system. *Agronomy-Basel.* 9:609. doi: 10.3390/agronomy9100609. doi: 10.3390/agronomy9100609

Qiu, L., Li, D., Zhang, J., and Zhao, B. (2021). Effects of key-stone microbe based on co-occurrence networks on wheat yield in the soils with straw returning. *Acta Pedol. Sin.*, 1, 1–13. doi: 10.11766/trxb202107200372

Rao, M. P. N., Luo, Z., Dong, Z., Li, Q., Liu, B., Guo, S., et al. (2022). Metagenomic analysis further extends the role of Chloroflexi in fundamental biogeochemical cycles. *Environ. Res.* 209:112888. doi: 10.1016/j.envres.2022.112888

Romaniuk, R., Giuffre, L., Costantini, A., and Nannipieri, P. (2011). Assessment of soil microbial diversity measurements as indicators of soil functioning in organic and conventional horticulture systems. *Ecol. Indic.* 11, 1345–1353. doi: 10.1016/j.ecolind.2011.02.008

Sagova-Mareckova, M., Cermak, L., Omelka, M., Kyselkova, M., and Kopecky, J. (2015). Bacterial diversity and abundance of a creek valley sites reflected soil pH and season. *Open Life Sci.* 10, 61–70. doi: 10.1515/biol-2015-0007

Six, J., Frey, S. D., Thiet, R. K., and Batten, K. M. (2006). Bacterial and fungal contributions to carbon sequestration in agroecosystems. *Soil Sci. Soc. Am. J.* 70, 555–569. doi: 10.2136/sssaj2004.0347

Sofo, A., Ricciuti, P., Fausto, C., Mininni, A. N., Crecchio, C., Scagliola, M., et al. (2019). The metabolic and genetic diversity of soil bacterial communities depends on the soil management system and C/N dynamics: the case of sustainable and conventional olive groves. *Appl. Soil Ecol.* 137, 21–28. doi: 10.1016/j.apsoil.2018.12.022

Sun, W., Xiao, E., Pu, Z., Krumins, V., Dong, Y., Li, B., et al. (2018). Paddy soil microbial communities driven by environment– and microbe–microbe interactions: a case study of elevation-resolved microbial communities in a rice terrace. *Sci. Total Environ.* 612, 884–893. doi: 10.1016/j.scitotenv.2017.08.275

Sunagawa, S., Coelho, L. P., Chaffron, S., Kultima, J. R., Labadie, K., Salazar, G., et al. (2015). Structure and function of the global ocean microbiome. *Science* 348, 1261359. doi: 10.1126/science.1261359

Van Der Heijden, M. G. A., Bardgett, R. D., and van Straalen, N. M. (2008). The unseen majority: soil microbes as drivers of plant diversity and productivity in terrestrial ecosystems. *Ecol. Lett.* 11, 296–310. doi: 10.1111/j.1461-0248.2007.01139.x

Waldrop, M. P., and Firestone, M. K. (2006). Response of microbial community composition and function to soil climate change. *Microb. Ecol.* 52, 716–724. doi: 10.1007/s00248-006-9103-3

Wan, S., Tang, B., Wang, Y., Zhou, H., and Guo, X. (2013). Effect of returning quantity of *Astragalus sinicus* to soil on quantity and activity of microbial in paddy soil. *Soil Fert. Sci. China.*, 4, 39–42. doi: 10.11838/sfsc. 20130409

Wolinska, A., Kuzniar, A., Zielenkiewicz, U., Izak, D., Szafranek-Nakonieczna, A., Banach, A., et al. (2017). Bacteroidetes as a sensitive biological indicator of agricultural soil usage revealed by a culture-independent approach. *Appl. Soil Ecol.* 119, 128–137. doi: 10.1016/j.apsoil.2017.06.009

Wu, K., Lin, X., and Lin, W. (2014). Advances and perspective in research on plant–soil–microbe interactions mediated by root exudates. *Chin. J. Plant Ecol.* 38, 298–310. doi: 10.3724/SP.J.1258.2014.00027

Xie, Z., He, Y., Tu, S., Xu, C., Liu, G., Wang, H., et al. (2017). Chinese Milk vetch improves plant growth, development and N-15 recovery in the Rice-based rotation system of South China. *Sci. Rep.* 7, 3577. doi: 10.1038/s41598-017-03919-y

Xie, Z., Tu, S., Shah, F., Xu, C., Chen, J., Han, D., et al. (2016). Substitution of fertilizer-N by green manure improves the sustainability of yield in double-rice cropping system in South China. *Field Crop Res.* 188, 142–149. doi: 10.1016/j.fcr.2016.01.006

Xu, Y., Dong, S., Li, S., and Shen, H. (2019). Research progress on ecological filtering mechanisms for plant community assembly. *Acta Ecol. Sin.* 39, 2267–2281. doi: 10.5846/stxb201804260946

Yan, J., Zhou, Q., Jiang, W., Chen, J., Li, Q., and Li, Z. (2020). Variation of cultivable bacterial community structure and the main influencing factors in karst paddy soil under different fertilization regimes. *Microbiol. China.* 47, 2833–2847. doi: 10.13344/j.microbiol.china.200672

Yang, Y., Chai, Y., Xie, H., Zhang, L., Zhang, Z., Yang, X., et al. (2023). Responses of soil microbial diversity, network complexity and multifunctionality to three land-use changes. *Sci. Total Environ.* 859:160255. doi: 10.1016/j.scitotenv.2022.160255

Yang, L., Li, T., and Zhou, C. (2009). Long-term fertilization effect on fraction and content of phosphorus in vegetable soil in plastic film house. *J. Soil Water Conserv.* 23, 205–208. doi: 10.13870/j.cnki.stbcxb.2009.05.049

Yang, X., You, L., Hu, H., and Chen, Y. (2022). Conversion of grassland to cropland altered soil nitrogen-related microbial communities at large scales. *Sci. Total Environ.* 816:151645. doi: 10.1016/j.scitotenv.2021.151645

Yang, L., Zhou, X., Liao, Y., Lu, Y., Nie, J., and Cao, W. (2019). Co-incorporation of rice straw and green manure benefits rice yield and nutrient uptake. *Crop Sci.* 59, 749–759. doi: 10.2135/cropsci2018.07.0427

Yuan, D. (2001). On the karst ecosystem. *Acta Geol. Sin. Eng. Edn.* 75, 336–338.

Yuan, M., Guo, X., Wu, L., Zhang, Y., Xiao, N., Ning, D., et al. (2021). Climate warming enhances microbial network complexity and stability. *Nat. Clim. Chang.* 11, 343–348. doi: 10.1038/s41558-021-00989-9

Zhang, D., Fu, B., Hu, W., Zhai, L., Liu, H., Chen, A., et al. (2017). Increasing soil nitrogen fixation capacity and crop yield of rice-rape rotation by straw returning. *Trans. Chin. Soc. Agric. Eng.* 33, 133–140. doi: 10.11975/j.issn.1002-6819.2017.09.017

Zhang, X., Gao, J., Cao, Y., Ma, X., and He, J. (2013). Long-term Rice and green manure rotation alters the endophytic bacterial communities of the Rice root. *Microb. Ecol.* 66, 917–926. doi: 10.1007/s00248-013-0293-1

Zhang, J., Nie, J., Cao, W., Gao, Y., Lu, Y., and Liao, Y. (2023). Long-term green manuring to substitute partial chemical fertilizer simultaneously improving crop productivity and soil quality in a double-rice cropping system. *Eur. J. Agron.* 142:126641. doi: 10.1016/j.eja.2022.126641

Zhang, X., Zhang, R., Gao, J., Wang, X., Fan, F., Ma, X., et al. (2017). Thirty-one years of rice-rice-green manure rotations shape the rhizosphere microbial community and enrich beneficial bacteria. *Soil Biol. Biochem.* 104, 208–217. doi: 10.1016/j.soilbio.2016.10.023

Zhao, S., Cao, C., Li, K., Qiu, S., Zhou, W., and He, P. (2014). Effects of long-term straw return on soil fertility, nitrogen pool fractions and crop yields on a fluvo-aquic soil in North China. *J. Plant Nutr. Fertil.* 20, 1441–1449. doi: 10.11674/zwyf.2014.0614

Zhong, Y., Hu, J., Xia, Q., Zhang, S., Li, X., Pan, X., et al. (2020). Soil microbial mechanisms promoting ultrahigh rice yield. *Soil Biol. Biochem.* 143:107741. doi: 10.1016/j.soilbio.2020.107741

Zhong, J., Tang, H., Li, Z., Dong, W., Wei, C., Li, Q., et al. (2021). Effects of combining green manure with chemical fertilizer on the bacterial community structure in karst paddy soil. *J. Plant Nutr. Fertil.* 27, 1746–1756. doi: 10.11674/zwyf.2021246

Zhou, J., Deng, Y., Luo, F., He, Z., Tu, Q., and Zhi, X. (2010). Functional molecular ecological networks. *MBio* 1, e00169–10. doi: 10.1128/mBio.00169-10

Zhou, J., Deng, Y., Luo, F., He, Z., and Yang, Y. (2011). Phylogenetic molecular ecological network of soil microbial communities in response to elevated CO2. *MBio* 2, e00122–11. doi: 10.1128/mBio.00122-11

Zhou, X., Liao, Y., Lu, Y., Rees, R., Cao, W., Nie, J., et al. (2020). Management of rice straw with relay cropping of Chinese milk vetch improved double -rice cropping system production in southern China. *J. Integr. Agric.* 19, 2103–2115. doi: 10.1016/S2095-3119(21)63779-6

Zhou, X., Lu, Y., Liao, Y., Zhu, Q., Cheng, H., Nie, X., et al. (2019). Substitution of chemical fertilizer by Chinese milk vetch improves the sustainability of yield and accumulation of soil organic carbon in a double-rice cropping system. *J. Integr. Agric.* 18, 2381–2392. doi: 10.1016/s2095-3119(18)62096-9

Zhu, B., Yi, L., Hu, Y., Zeng, Z., Lin, C., Tang, H., et al. (2014). Nitrogen release from incorporated N-15-labelled Chinese milk vetch (*Astragalus sinicus* L.) residue and its dynamics in a double rice cropping system. *Plant Soil* 374, 331–344. doi: 10.1007/s11104-013-1808-8

Zou, C., Wang, Y., Yang, J., Tang, B., Liu, Y., and Zhang, X. (2013). Effects of combined application of chemical fertilizer and Chinese milk vetch (*Astragalus sinicus*) on the microorganism and nutrients of paddy soil. *Soil Fert. Sci. China.*, 6, 28–31. doi: 10.11838/n20130606

frontiers | Frontiers in Microbiology

TYPE Original Research
PUBLISHED 17 January 2023
DOI 10.3389/fmicb.2022.1054295

OPEN ACCESS

EDITED BY
Qiang Li,
Chinese Academy of Geological Sciences, China

REVIEWED BY
Yanlin Zhao,
Hunan University of Science and Technology, China
Tianliang Zheng,
Chengdu University of Technology, China

*CORRESPONDENCE
Jianyao Chen
✉ chenjyao@mail.sysu.edu.cn
Lei Gao
✉ 416581541@qq.com

SPECIALTY SECTION
This article was submitted to Terrestrial Microbiology, a section of the journal Frontiers in Microbiology

RECEIVED 26 September 2022
ACCEPTED 15 December 2022
PUBLISHED 17 January 2023

CITATION
Liang Z, Li S, Wang Z, Li R, Yang Z, Chen J, Gao L and Sun Y (2023) Microbial community structure characteristics among different karst aquifer systems, and its potential role in modifying hydraulic properties of karst aquifers. *Front. Microbiol.* 13:1054295. doi: 10.3389/fmicb.2022.1054295

Microbial community structure characteristics among different karst aquifer systems, and its potential role in modifying hydraulic properties of karst aquifers

Zuobing Liang[1,2], Shaoheng Li[1], Zhuowei Wang[3], Rui Li[1], Zhigang Yang[4], Jianyao Chen[1]*, Lei Gao[5]* and Yuchuan Sun[6]

[1]School of Geography and Planning, Sun Yat-sen University, Guangzhou, China, [2]Key Laboratory of Groundwater Sciences and Engineering, Ministry of Natural Resources, Shijiazhuang, China, [3]China Institute of Water Resources and Hydropower Research, Beijing, China, [4]Department of Hydraulic Engineering, Tsinghua University, Beijing, China, [5]South China Botanical Garden, Chinese Academy of Sciences, Guangzhou, China, [6]Chongqing Key Laboratory of Karst Environment, School of Geographical Sciences, Southwest University, Chongqing, China

Little is known about how microbial activity affects the hydraulic properties of karst aquifers. To explore the potential impacts of microbial activity on the hydraulic properties of karst aquifers, microbiological analysis, heat tracer, isotope (dissolved inorganic carbon isotope, $\delta^{13}C_{DIC}$) and aqueous geochemical analyses were conducted at six monitoring wells in Northern Guangdong Province, China. Greater hydraulic conductivity corresponded to a low temperature gradient to an extent; the temperature gradient in karst groundwater aquifers can reflect the degree of dissolution. Higher HCO_3^- concentrations coupled with lower d-excess and pH values at B2 and B6 reflect potential microbial activity (e.g., *Sulfuricurvum kujiense*) causing carbonate dissolution. Microbial activity or the input of anthropogenic acids, as evidenced by significantly more positive $\delta^{13}C_{DIC}$ values, potentially affect carbonate dissolution in deep karst aquifers, which eventually alters hydraulic properties of karst aquifer. However, more direct evidence is needed to quantify the effects of microbial activity on carbonate dissolution in karst aquifers.

KEYWORDS

karst aquifer, subsurface microbiology, heat tracer, isotopes, hydraulic properties

1. Introduction

Karst regions cover 7 ~ 12% of the Earth's continental area, and their aquifers are a source of drinking water for almost one quarter of the global population (Ford and Williams, 2007). However, karst aquifers have complex characteristics that make them very different from other aquifers, because they are self-developing, dissolved bedrock

constituents are transported through and out of the system (Ford and Williams, 2007), and this unique property of the aquifer results in difficulty developing and utilizing karst groundwater (Goldscheider and Drew, 2007).

Karst aquifers can be modified by external factors, such as climate change (Loáiciga, 2009), which alter the flux of meteoric water into the system and change the pressure or temperature imparted by vertically migrating fluids and internal processes (Corbella and Ibáñez, 2003), like chemical reactions (Loáiciga, 2009) and microbial activity (Engel et al., 2004a,b). In addition, mine water produced by mining activities also accelerate the dissolution rate of rocks in karst aquifers (Zhao et al., 2020; Liu et al., 2022), and seepage-damage effect in fractured rocks of karst aquifers may also produce great influences on the conductivity of karst aquifer (Zhao et al., 2021). More studies of microbial control of karst processes have focused on the sulfidic, saline water zones of karst aquifers (Engel and Randall, 2011; Gray and Engel, 2013). However, few reports have been focused on carbonate dissolution in freshwater aquifers. Lianjiang River Basin (LRB) is located in the north of Guangdong Province, China, characterized by high spatial hydrogeological heterogeneity. The LR system belongs to the trellis drainage, extending from the northwest to the southeast of the drainage basin. In the northwest of the LRB, karst aquifers have low permeability and low water richness, fissures are not developed; in the southeast of the drainage basin, karst aquifers have high permeability, joints and fissures are relatively developed, and dissolution is obvious.

In the present study, we determined the n-Alkanes biomarkers, groundwater temperature, dissolved inorganic carbon isotope ($\delta^{13}C_{DIC}$), microbial community and hydrochemical characteristics of groundwater from the LRB to elaborate the following objectives: (1) ascertaining the structures of microbial communities in different karst aquifers; (2) exploring the effects of biogeochemical processes in modifying hydraulic properties.

2. Materials and methods

2.1. Well selection and geochemical analyses

Six monitoring wells are located in the Lianjiang River basin: B1 and B2 are upstream, B3–B5 are in midstream, and B6 is downstream (Figure 1). B1 is in an area of Cretaceous Nanxion calcareous mudstone; B2 is in an area of Devonian (Baqi/Liujiang) carbonate; B3 is in an area of Devonian Rongxian carbonate; B4 and B5 are in an area of Carboniferous Shidengzi carbonate; and B6 is in an area of Devonian Tianziling carbonate. More information about the lithology of selected boreholes was seen in attachment files (Supplementary Figure S1; Supplementary Table S1).

Groundwater from the sampling wells was sampled after pumping. Parameters, including pH, dissolved oxygen (DO) concentration, electrical conductivity (EC), and temperature (*T*) were quantified with a portable water quality analyzer (Horiba D-24, Japan). The concentration of bicarbonate (HCO_3^-) was measured *in situ* using the titration kit (Merck, Germany). Water samples were filtered after sampling using a 0.22 μm cellulose acetate filter and then stored in precleaned polypropylene bottles. Major anions (Cl^-, NO_3^-, and SO_4^{2-}) of filtered water samples were determined *via* ion chromatography (ICS 900, Dionex, United States). One aliquot of filtered water samples was acidified to pH < 2 with ultra-purified HNO_3 for analyses of major cations (K^+, Na^+, Ca^{2+}, and Mg^{2+}) measurements using inductively coupled plasma-atomic emission spectrometry (ICP-AES, IRIS-HR, United States). The $\delta^{18}O$ of ground water values were analyzed using a high-precision laser isotope analyzer (Picarro L2130-i Analyzer) with the measurement accuracy of 0.02%, and measurements were reported relative to the V-SMOW standard. $\delta^{13}C_{DIC}$ values were analyzed using a MAT-253 mass spectrometer coupled with a Gas Bench II automated device with analytical precision of ±0.15%. The results are expressed as $\delta^{13}C_{DIC}$ (%) with respect to the Vienna Pee Dee Belemnite (V-PDB) standard. Aqueous geochemical analyses and computational modeling provided saturation conditions for aquifer minerals, specifically calcite, dolomite and gypsum. The saturation index (SI) of a mineral is defined as log (IAP/Ksp), where IAP is the ion activity product and Ksp is a mineral thermodynamic equilibrium constant. A positive SI value indicates that precipitation with respect to a mineral is thermodynamically possible, whereas negative SI values indicate dissolution. A SI of 0 ± 0.5 indicates a mineral is at equilibrium within the solution (Gray and Engel, 2013). Deuterium excess (d-excess) is a second-order isotope parameter that is a function of the isotopic composition of oxygen and hydrogen in water, as defined by the Dansgaard's equation: $d\text{-excess} = \delta^2H - 8 \times \delta^{18}O$ (Dansgaard, 1964).

2.2. Groundwater temperature data collection

The temperature–depth (TD) profiles of the six wells were determined using a COMPACT-TD logger (JFE Advantech, Japan), which simultaneously records water temperature and depth automatically; this equipment has a temperature resolution of 0.001°C and depth resolution of 0.008 m for every monitoring depth. Measurements were repeated to ensure that the equipment reached equilibrium with the surrounding environment (Li et al., 2019b). 'Temperature-depth' profile in the subsurface can be divided into the surficial zone and the geothermal zone (Parsons, 1970), and within the surficial zone temperature is influenced by seasonal heating and cooling of the land surface. Temperature profiles in the surficial zone potentially provide information about seasonal recharge/discharge events from precipitation and interchange with surface water (Anderson, 2005).

2.3. Microbiological analysis

For the microbiological analysis, 2 L water samples were filtered through polycarbonate filters (pore size = 0.22 μm). Total DNA was

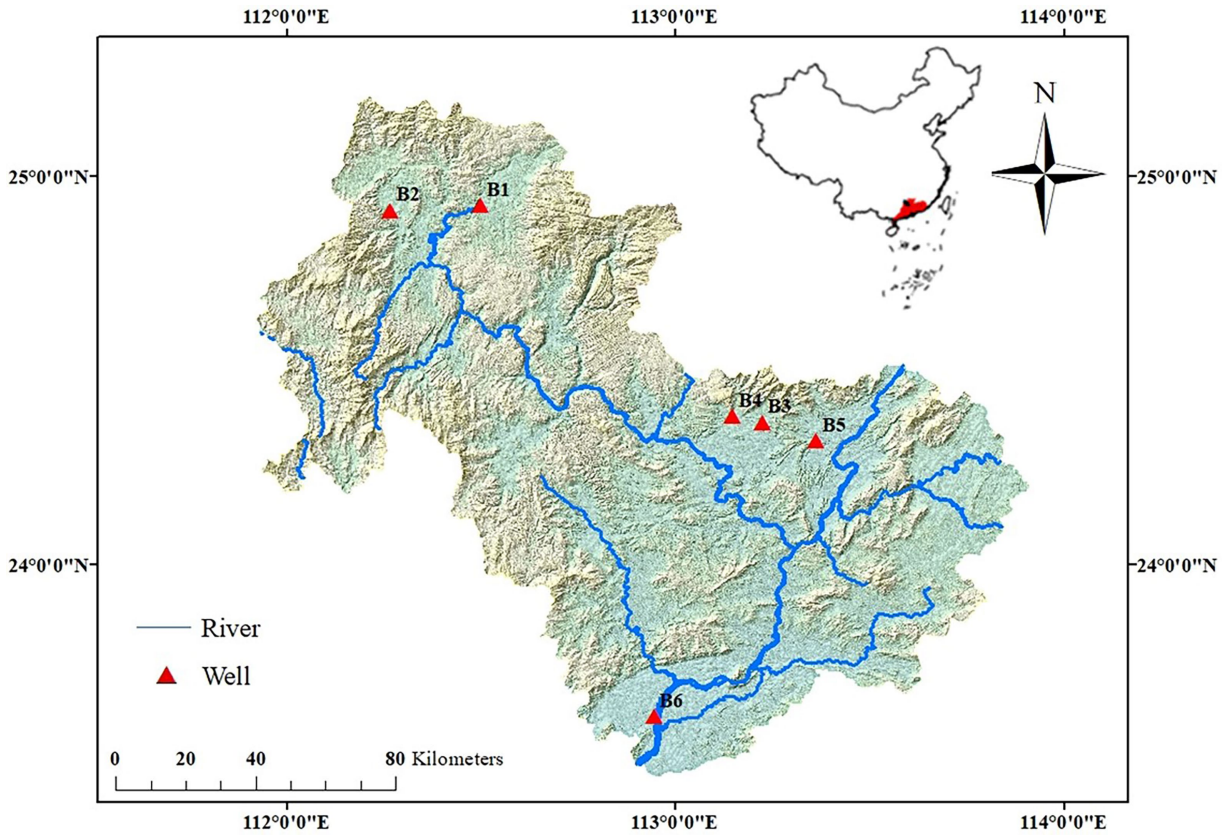

FIGURE 1
Map of the sampling sites.

extracted from the water samples using the PowerSoil DNA Isolation Kit (MO BIO Laboratories, Carlsbad, CA, USA), according to the manufacturer's instructions. The quality of the extracted DNA was checked using agarose gel electrophoresis and the DNA was stored at −20°C. DNA concentrations were determined using a Qubit® 2.0 fluorometer. Microcosms were constructed, deployed, and analyzed using a modified version of the method of Zhu et al. (2020). Briefly, the V4 region of bacterial 16S rRNA was amplified using primer pair 515F and 806R. PCR amplicons were sequenced on an Illumina MiSeq platform at Beijing Biomarker Technologies, and sequences were analyzed using QIIME and UPARSE software with the default settings to obtain effective tags and operational taxonomic units (OTUs). The UPARSE pipeline was then used for taxonomic assignment at the 97% similarity level *via* Ribosomal Database Project Naïve Bayesian Classifier v.2.2, trained on the SILVA database (ver. 123), using a 0.8 confidence level as the cutoff. The Mothur package was used to calculate the abundance-based coverage estimator (ACE) and Shannon's diversity index.

2.4. n-Alkanes

To determine n-alkanes, the pH of the samples was adjusted to 2 and they were stored at 5°C until analysis. Methanol (10%) was added to the water samples before solid-phase extraction (SPE). n-Alkanes were constructed, deployed, and analyzed using a modification of the approach of Saim et al. (2009). n-Alkanes were extracted using C18 SPE cartridges conditioned with 10 ml of methanol followed by 6 ml of ultrapure water at a rate of 1–2 ml/min. The cartridges were then dried under vacuum. A 4 L water sample was loaded into the SPE column at a rate of 6 ml/min. The cartridges were then dried under vacuum for 30 min. The n-alkanes were eluted using 2 × 3 ml of dichloromethane. The extract was blown down to 1 ml under a gentle flow of nitrogen, and then analyzed by gas chromatography–mass spectrometry (GC–MS, Agilent 7890A GC, 5975C MSD) in selected ion monitoring (SIM) modes with internal standards n-Alkanes, and Deuterated tetracosane was used as internal standard for quantifying. The analysis was carried out in Chongqing Key Laboratory of Karst Environment, School of Geographical Sciences, Southwest University.

3. Results

3.1. Aquifer geochemistry

Borehole B1 had Ca–SO_4-type water with total dissolved substances (TDS) > 1,000 mg/L; borehole B2 to B6 had Ca–HCO_3-type water with TDS < 1,000 mg/L. The groundwater

temperature varied from 23.4 to 27.1°C, i.e., did not vary markedly among boreholes; the pH ranged from 6.8 at B6 to 8.1 at B4. The d-excess also showed variation among wells, similar to the pH.

3.2. Taxonomic diversity

River water samples analyzed in this study was used to compare difference with groundwater samples. The coverage index of the sequenced samples ranged from 0.99 to 1.00; all values were >98%, indicating high reliability of the sequencing depth. The Shannon index was in the order B6 > B5 > B4 > B2 > R1 > B3 > B1, indicating a sequential decrease in microorganism diversity (Table 1). The OTUs obtained from the sequencing were analyzed taxonomically and represented 64 phyla, 200 classes, 370 orders, 540 families, 771 genera, and 814 species.

The distance measure used in CA (cluster analysis) was Pearson correlation, and the results are presented in a dendogram (Figure 2). As shown in Figure 2, the groundwater in B3 and river water in R1 were grouped together, groundwater in B4 and B2 belonged to same cluster, and B5 and B1 were grouped together. In addition, the species-level composition and abundance in groundwater *Acinetobacter lwoffii* was present in all water samples, except for B6. Its abundance in the environment was 0.27% ~ 7.21% in well water samples and 15.8% in river water samples, indicating that *A. lwoffii* was the dominant bacterium species in the studied samples. *S. kujiense* was dominant in B2 and B6, with respective abundances of 3.38 and 9.28%; similar lower abundances of *Desulfovirga adipica* were also presented in B2 and B6. However, *S. kujiense* and *Desulfovirga adipica* were not found in the river water sample (R1). *Acinetobacter venetianus*, *Pseudomonas umsongensis*, *Pseudomonas viridiflava*, and *Roseomonas lacus* were also presented.

3.3. n-Alkanes

The total dissolved n-alkane concentrations varied from 11,586 to 18,400 ng/l among the wells. Groundwater from all wells showed a unimodal distribution, with low-molecular-weight (LMW) n-alkanes having even numbers of carbons (n-C14 to n-C18) predominating; n-C16 was the dominant n-alkane (Figure 3). This indicates that the dissolved organic matter in the wells was of bacterial origin (Fang et al., 2014) and the dominant source of dissolved organic carbon in the aquifer is likely microbial primary production.

TABLE 1 Diversity and richness estimators for pyrosequence libraries.

Sample	Unique sequences	97% OTUs	Shannon	Coverage
R1	73,492	340	2.73	1.00
B1	69,975	1989	3.58	1.00
B2	76,178	1,084	3.98	1.00
B3	73,098	1769	3.94	0.99
B4	65,225	2,519	4.17	1.00
B5	74,911	1,081	4.99	1.00
B6	72,031	1,251	5.38	0.99

4. Discussion

4.1. Hydrodynamic characteristics among different karst aquifer system

Heat carried by groundwater serves as a tracer to identify flow through fractures, and flow patterns in groundwater basins (Anderson, 2005), and the groundwater flow in the preponderance flow path interferes with the normal temperature distribution of the formation, and the information of groundwater seepage in the formation can be inferred from the anomaly of the temperature curve (Chi et al., 2020). In this study, six boreholes 'temperature-depth' profile were used to characterize the hydraulic properties of aquifers, the temperature gradient in B1, B2, B3, B4, B5, and B6 were 4.3, 1.7, 1.5, 0.6, 1.8, and1.0°C/100 m, respectively (Figure 4). Among the selected boreholes, B1 belongs to non-karst aquifer and gypsum interlayer grows on it, which can also be reflected from the high SO_4^{2-} concentration in groundwater (Table 2). It also be found that lower temperature gradient was also corresponded to higher *k* values in karst aquifers (especially in B2, B3, B5 and B6).

In the karst aquifer system, there are groundwater migration channels such as pores, fissures, and cavities with large diameters. In areas where karst is not formed, rock mass is dense, and small pores are dominant, groundwater flow rate is very slow, even water-tight. It can be concluded that from borehole B2 to B6, karst aquifers are featured by vertical flow and have the characteristics of groundwater seepage. Especially, in the light of borehole profile description between wells (Supplementary Figure S1), the karst aquifer in B5 showed high permeability, karstification was well developed, and fissures and caves were found. By contrast, aquifer in B1 was not karst aquifer, and the vertical flow rate is slow. In addition, groundwater age estimation using tritium (^{3}H) only provides semi-quantitative values (Brkic et al., 2016): <0.8 TU indicates sub-modern water (recharged prior to 1950s), 0.8 to ~4 TU indicates a mix of sub-modern and modern water, 5 to 15 TU indicates modern water (<5 to 10 years),15–30 TU indicates some bomb tritium and > 30 TU indicates recharged occurred in the 1960s to 1970s. As shown in Table 2, B3 and B6 had ^{3}H values higher than 5 TU, indicating modern water (< 5 to 10 years) in above aquifers; whereas ^{3}H values in B2, B4 and B5 all higher than 0.8 TU and lower than 4 TU, showing a mix of sub-modern and modern water in above aquifers. And B1 showing ^{3}H values lower than 2, which may

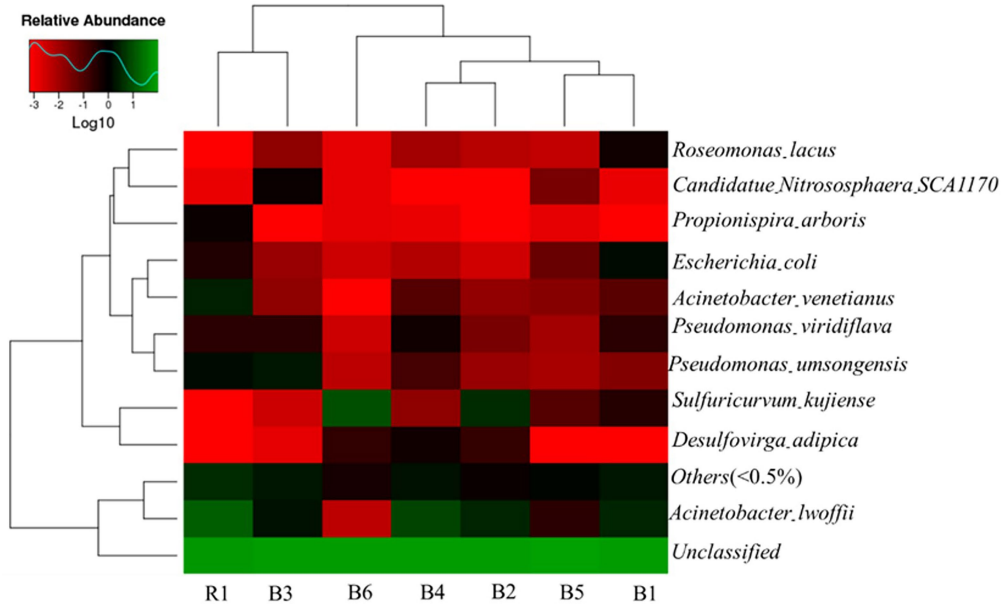

FIGURE 2
Heatmap of species relative abundance among different samples.

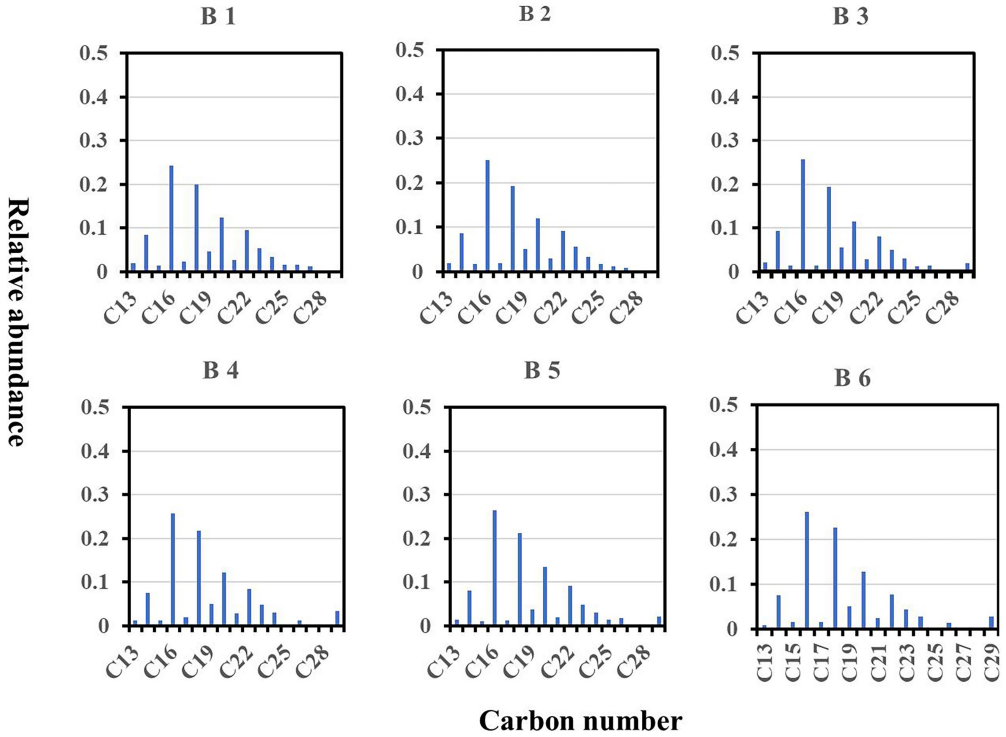

FIGURE 3
Concentration distributions of n-alkanes among wells.

indicate sub-modern water in it. Hence, combined with the 'temperature-depth' profile characteristics and ^{3}H values above in selected boreholes, it can conclude that karst aquifer in borehole B1 belongs to regional flow, karst aquifers in borehole B3 and B6 perhaps belong to local flow, and karst aquifers in borehole B2, B4 and B5 maybe belong to

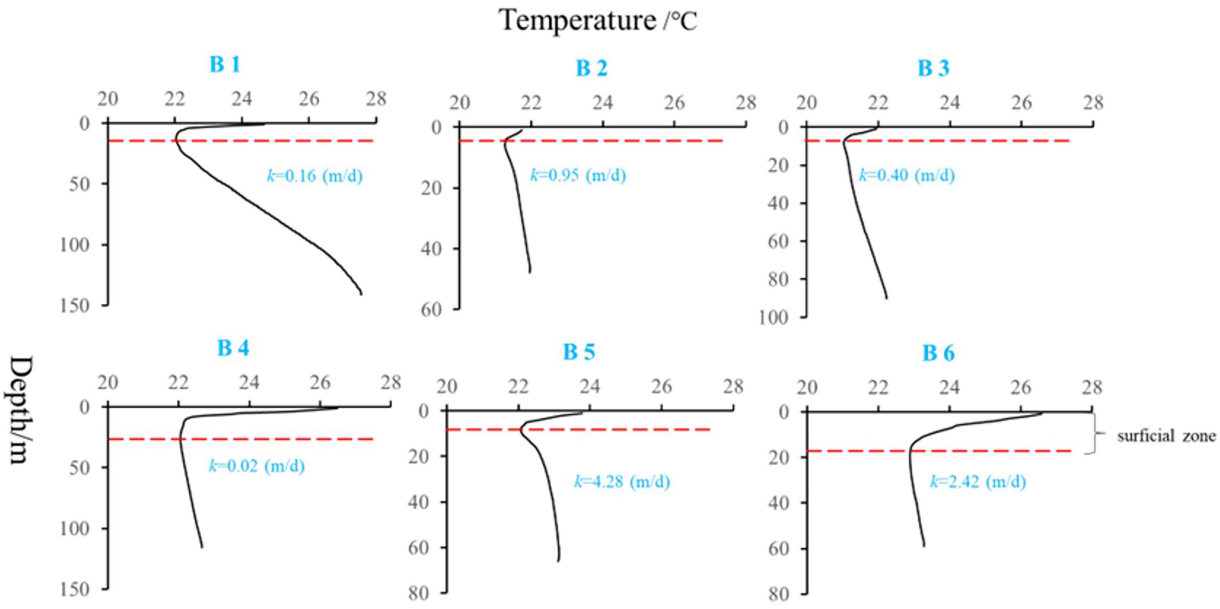

FIGURE 4
'Temperature-depth' profiles of the selected boreholes (k, hydraulic conductivity; red dashed line, surficial zone boundary).

TABLE 2 Chemical and physical properties among different wells.

Item	River	Well					
	R1	B1	B2	B3	B4	B5	B6
TDS(mg/L)	437	2,652	499	377	164	304	409
DO(mg/L)	3.2	2.1	1.9	2.2	2.1	1.8	1.5
T(°C)	25	25.8	27.1	23.4	23.6	25.8	25.6
Ph	6.9	7.3	6.9	7.5	8.1	7.7	6.8
DOC(mg/L)	0.9	0.7	0.6	0.5	0.5	1	1.6
d-excess (%)	13.3	11.3	7.8	13.1	12.8	11.7	10.1
$\delta^{13}C_{DIC}$ (%)	-	−8.19	−7.88	−8.09	−4.65	−7.88	−8.66
^{3}H (TU)	-	< 2	3.44	8.27	2.78	3.16	6.61
HCO_3^-(meq/L)	4	3	7.2	4	2.4	3.2	4.3
Cl^-(meq/L)	0.9	0.2	0.1	0.1	0	0.1	0.2
NO_3^-(meq/L)	1	BDL	0	0	0.1	0.1	BDL
SO_4^{2-}(meq/L)	0.4	42	0.3	0.5	0.2	0.5	0.6
K^+(meq/L)	0.4	0.1	0	0	0	0	0.1
Na^{2+}(meq/L)	0.8	1.7	0.1	0	0	0	0.3
Cl^-(meq/L)	0.9	0.2	0.1	0.1	0	0.1	0.2
Ca^{2+}(meq/L)	4.7	17	1.8	4.3	0.3	3.9	4.4
Mg^{2+}(meq/L)	0.2	5.7	0.2	1.4	0.1	0.4	0.7

DO, dissolved oxygen; BDL, below detection limit; DOC, dissolved organic carbon; d-excess, deuterium excess; —, missing data.

intermediate flow. In addition, similar distribution of microbe species between river water and groundwater in B3 also support that groundwater in B3 was more potentially influenced by seepage, and which should belong to local flow.

4.2. Potential factors influencing microbe activities in selected karst aquifers

Principal Component Analysis (PCA) is based on the diagonalization of the correlation matrix, which can not only

point out associations between variables that can show the global coherence of the data set, but also it will evidence the participation of the individual chemical parameters in several influence factors (Helena et al., 2000), and help to explore the dominating factors in the geochemistry (Hu et al., 2013). In this study, PCA was performed to identify potential factors influencing microbe activities in selected karst aquifers, which is a common phenomenon in hydrochemistry.

In the PCA, the first three eigenvalues were greater than one and explained more than 88% of the variance (Table 3). The first principal component (PC1) accounted for more than 47.9% of the variance in the data and had high positive loadings for *A. lwoffii*, *A. venetianus*, *Escherichia coli*, *Propionispira arboris*, EC, DO, Cl^-, NO_3^-, K^+, and Na^+. In groundwater, *E. coli* and NO_3^- are usually from the input of effluent (Dougherty et al., 2009), while K^+ and Na^+ ions can result from agricultural fertilizer use in rural and suburban areas, as well as from livestock manure and sewer leakage (Liang et al., 2018). This indicates that *A. lwoffii*, *A. venetianus*, *E. coli*, and *P. arboris* were not from the internal environment of the karst aquifer.

The second principal component (PC2) accounted for more than 24.4% of the variance and had high loadings for *P. viridiflava*, pH, and d-excess (all positive) and *S. kujiense*, temperature, and HCO_3^- (all negative). *S. kujiense* is a parthenogenetic, anaerobic, chemoautotrophic sulfur-oxidizing bacterium, and temperature and pH control sulfur-oxidizing bacterium. This indicates that the HCO_3^- concentration increased with the density of *S. kujiense*.

The third principal component (PC3) accounted for more than 16.47% of the variance and had high loadings for *P. umsongensis*, *Candidatus Nitrososphaera SCA1170*, and SO_4^{2-} (all positive) and *D. adipica* (negative), and moderate loading for *R. lacus*. This indicates that the SO_4^{2-} concentration increased with the relative abundance of *Candidatus_Nitrososphaera_SCA1170* and *P. umsongensis*, but decreased with the relative abundance of *D. adipica*.

In this study, the length of the gradient in the first axis calculated by detrended correspondence analysis (DCA) was <3, which was 2.8 in our study, the redundancy analysis (RDA) model should be selected to evaluate the potential relationship between the distribution of microbe species and environmental parameters (Chen et al., 2015), but the *p* values of environmental factors in groundwater were all higher than 0.05, which can not be used to evaluate the potential relationship between the distribution of microbe species and environmental parameters in our study. Hence, the relationship between microbe species abundance and groundwater environmental factors in six selected boreholes was evaluated by multivariate analysis (Figure 5).

As shown in Figure 5, similar relationships were found between selected microbe species (*E. coli* and *R. lacus*) and groundwater environmental factors (K^+, Na^+, Ca^{2+}, Mg^{2+}, and $SI_{dolomite}$), indicating *E. coli* and *R. lacus* may produce influence on groundwater chemistry types. And also, *S. kujiense* showed higher positive relationship with HCO_3^- ($p < 0.05$), indicating the abundance of *S. kujiense* in karst groundwater was an important factor that influencing HCO_3^- concentrations.

TABLE 3 The main component load of bacterial species and their water physics and chemical parameters.

Items	PC 1	PC 2	PC 3
Acinetobacter_lwoffii	**0.858**	0.21	−0.338
Acinetobacter_venetianus	**0.995**	0.047	−0.064
Candidatus_Nitrososphaera_SCA1170	−0.243	0.39	**0.881**
Desulfovirga_adipica	−0.423	0.256	**−0.717**
Escherichia_coli	**0.995**	0.041	−0.057
Propionispira_arboris	**0.997**	0.032	−0.046
Pseudomonas_umsongensis	0.452	0.432	**0.752**
Pseudomonas_viridiflava	0.032	**0.819**	−0.329
Roseomonas_lacus	−0.552	0.267	0.547
Sulfuricurvum_kujiense	−0.259	**−0.868**	−0.052
EC	**0.645**	−0.491	0.492
DO	**0.943**	0.258	0.024
Temperature	0.039	**−0.971**	−0.179
pH	−0.555	**0.714**	−0.316
DOC	0.547	−0.302	−0.209
d-excess	0.373	**0.895**	0.12
HCO_3^-	−0.03	**−0.87**	0.253
Cl^-	**0.999**	0.007	−0.031
NO_3^-	**0.994**	0.047	−0.09
SO_4^{2-}	0.118	0.009	**0.85**
K^+	**0.995**	−0.047	−0.052
Na^+	**0.989**	−0.092	−0.034
Eigenvalue	10.55	5.37	3.62
Total variance (%)	47.94	24.41	16.47
Cumulative variability (%)	47.94	72.35	88.82

Because the HCO_3^- concentration increased with the density of *S. kujiense*. It is necessary to assess the solubility of carbonate minerals based on bulk aquifer fluid geochemistry before considering the potential for microbially mediated carbonate dissolution. By calculating the saturation index (SI), the equilibrium state of water with respect to a particular mineral phase can be determined, and which can also be used to distinguish the hydrogeochemical evolution as well as by identifying the geochemical reactions that control the water chemistry (Li et al., 2019a; Subba Rao et al., 2022). The saturation indexes of calcite, dolomite, and gypsum were calculated to interpret the hydrogeochemical processes in the six wells (Figure 5). The

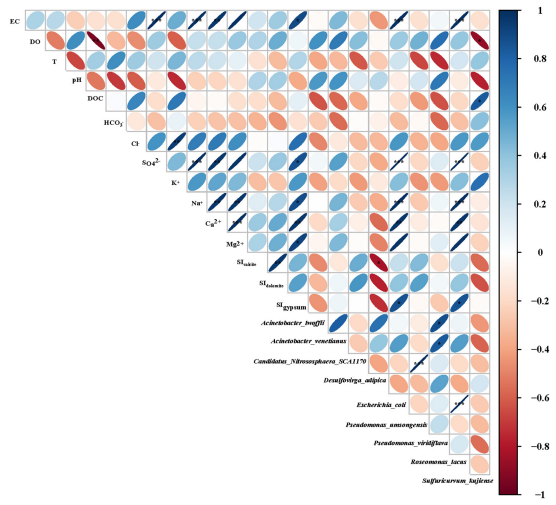

FIGURE 5
Correlation heatmap for groundwater environmental parameters and microbe species (In brief, orange and red colors indicate negative correlations, blue colors indicate positive correlations and the strength of color indicates the magnitude of correlation coefficient, as shown on the correlation spectrum, insert right; *p <0.05, **p <0.01, ***p <0.001).

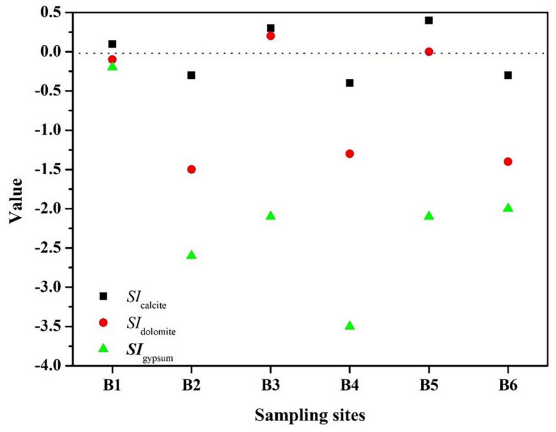

FIGURE 6
Saturation indexes of the major minerals at the different boreholes. The relative abundance of *S. kujiense* among the different wells roughly matched the HCO_3^- concentrations (Figure 5), especially in B2 and B6 (Figure 7).

saturation indexes of calcite, dolomite and gypsum in B1 were all around 0, indicating hydrogeochemical processes at B1 was saturated state; B2, B4, and B6 were undersaturated with respect to calcite, dolomite, and gypsum and had higher relative abundances of *S. kujiense* (B2, 3.38%; B4, 0.02%; B6, 9.23%), while the saturation indexes of calcite, dolomite, and gypsum were all less than 0 in B2, B4 and B6, indicating an unsaturated state in all groundwaters. Besides, the saturation indexes of gypsum in B3 and B5 were all less than 0, indicating unsaturated state, but the saturation indexes of calcite and dolomite were all higher than or equal to 0, indicating 'rapid dissolution' to 'dissolution equilibrium' state. In multiple groundwater flow systems, related study found that carbonate dissolution dominated the local flow, carbonate dissolution and gypsum dissolution coexisted in the intermediate flow, and gypsum dissolution dominated the regional flow (Wang et al., 2022). Combined with the groundwater flow characteristics based on 'temperature-depth' profile characteristics and age dating of the boreholes (Figure 4), it can be concluded that the karst aquifers in B3 and B6 (which belong to local flow) have higher saturation indexes (with the saturation indexes of calcite and dolomite all higher than 0); the karst aquifers in B2, B4 and B5 (which belong to intermediate flow) have lower saturation indexes (with the saturation indexes of calcite and dolomite all less than 0); aquifer in borehole B1 (which belong to regional flow) with the saturation indexes of calcite, dolomite and gypsum all around 0 (Figures 6, 7).

In groundwater, d-excess reflects the extent of water/rock oxygen isotope exchange on a regional scale and indicates its variability, the stronger the water/rock interaction the lower the d-excess (Liu et al., 2016). It was listed in Table 2 that, higher d-excess values were presented in B3, B4 and B5, while lower d-excess values were found in B2 and B6, which indicated that the stronger water/rock interaction were happened in B2 and B6. Study found sulfur-oxidizing bacteria consume reduced-sulfur compounds and produce sulfuric acid, which decreases the surface pH locally and promotes carbonate dissolution near a shallow groundwater table (Macalady et al., 2006). They can also influence aquifer-scale geochemical processes because they are metabolically active at low oxygen tensions under completely anaerobic conditions (Goldscheider et al., 2006). Microbially promoted carbonate dissolution is enhanced by a local decrease in pH at the cell–mineral interface (Sjöberg and Rickard, 1984; MacInnis and Brantley, 1992), and *S. kujiense* is a parthenogenetic, anaerobic, chemoautotrophic sulfur-oxidizing bacterium, the temperature and pH control sulfur-oxidizing bacterium, therefore, lower pH values in B2 and B6 perhaps enhance the carbonate dissolution medicated by *S. kujiense*, and lower d-excess values in B2 and B6 reflected the higher degree of carbonate dissolution medicated by *S. kujiense*.

n-Alkanes of bacterial origin are characterized by a predominance of even numbers of carbon atoms (14, 16 or 18; Derrien et al., 2017), which matches our results that the organic matter in the studied wells is predominately caused by autochthonous microbial activity and seldom no allochthonous organic matter input. Because *S. kujiense* is a chemoautotrophic sulfur-oxidizing bacterium, which is no need to require organic substrates to get their carbon for growth and development in karst aquifers. Which also supports that *S. kujiense* potentially mediated carbonate dissolution in the karst aquifers of B2 and B6, and it should be noted that higher dissolution and caves in karst aquifer were also found in B6 (Supplementary Figure S1).

In addition to the effects of microbial activity on karst aquifers, chemical reactions play an important role in internal

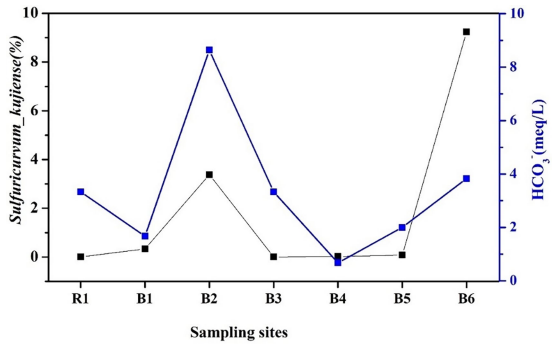

FIGURE 7
Variation in bicarbonate concentrations and the relative abundance of bacterial species at different boreholes.

processes. For instance, carbonic acid and anthropogenic acids (e.g., sulfuric and nitric acid) increase the dissolution of carbonate and HCO_3^- concentration in groundwater (Huang et al., 2017). Carbon isotopes in groundwater ($\delta^{13}C_{DIC}$) can be used to identify different acids affecting carbonate dissolution (Ali and Atekwana, 2011). In the study area, the rainwater was typically acidic, with a volume-weighted mean pH of 4.49 (Cao et al., 2009), which indicates that atmospheric CO_2 makes a negligible contribution to dissolved inorganic carbon (DIC). The DIC in the study area likely has two primary sources: the weathering of carbonate minerals and the dissolution of CO_2 in soil (Eq. 1).

$$Ca_{(1-x)}Mg_xCO_3 + H_2CO_3 = (1-x)Ca^{2+} + xMg^{2+} + 2HCO_3^- \quad (1)$$

Open-system carbonate weathering mediated solely by carbonic acid requires that the isotopic composition of DIC is continuously in equilibrium with the gaseous phase of a given pCO_2, and that continuous isotopic exchange occurs between CO_2 and the aqueous solution. Thus, $\delta^{13}C_{DIC}$ is controlled mainly by the hydrolysis of CO_2 in soil (Jiang et al., 2013; Huang et al., 2017). Therefore, the $\delta^{13}C_{DIC}$ in karst groundwater under open-system conditions should be around −14% (i.e., −23% plus +9%; Jiang et al., 2013). In a closed-system, the amount of soil-derived CO_2 decreases gradually over time during carbonic acid-driven carbonate dissolution; as the carbon in our groundwater samples was produced from carbonate and soil-derived CO_2 in approximately equal amounts, the $\delta^{13}C_{DIC}$ should approach a value of −11.5% [i.e., 0.5 × (−23% + 0)] (Jiang et al., 2013). When carbonate dissolution is facilitated by other acids (e.g., sulfuric, nitric, or organic acid), all DIC is derived from non-carbonic acid carbonate dissolution (Eq. 2), so it has a $\delta^{13}C$ value (0%) identical to that of the constituent carbonate minerals (Li et al., 2008; Jiang et al., 2013).

$$3Ca_{(1-x)}Mg_xCO_3 + H_2SO_4 + HNO_3 \rightleftharpoons 3(1-x)Ca^{2+} + 3xMg^{2+} + SO_4^{2-} + NO_3^- + 3HCO_3^- \quad (2)$$

For the groundwater analyzed, the $\delta^{13}C_{DIC}$ values were in the range − 8.66% to −4.65% with a mean value of −7.56%, which is significantly more positive than −11.5% (Table 2). This suggests that carbonate dissolution in the study area was likely facilitated by additional acids. Because groundwater recharge areas have vast areas of fertile agricultural land, higher levels of domestic sewage and nitrogenous fertilizers percolate through the topsoil and enter the karst aquifers, which can increase carbonate dissolution (Yamanaka, 2012). The larger range of $\delta^{13}C_{DIC}$ values is strongly related to enhanced carbonate dissolution by nitric and sulfuric acids.

5. Conclusion

The main conclusion of this study is that carbonate dissolution in the deep karst aquifer was potentially influenced by microbial activity (e.g., *S. kujiense*) and the input of anthropogenic acids, as evidenced by significantly more positive $\delta^{13}C_{DIC}$ values. This ultimately changes the hydraulic properties of karst aquifers. However, more studies are needed to quantify the effect of microbial activity on carbonate dissolution in the karst aquifer.

Data availability statement

The data presented in the study are deposited in the NCBI repository, accession number PRJNA917210.

Author contributions

ZL wrote the manuscript. SL, ZW, RL, and ZY performed the data collection and the bioinformatic analysis. JC and LG conceived the idea and supervised the work. YS performed the lipids biomarker analysis. All authors contributed to the article and approved the submitted version.

Funding

This work was financially supported by Natural Science Foundation of Guangdong Province of China (2021A1515110505), Open Funding Project of the Key Laboratory of Groundwater Sciences and Engineering, Ministry of Natural Resources (SK202102), National Natural Science Foundation of China (41961144027 and 41771027), China Postdoctoral Science Foundation (2021M703657), Scientific and Technological

Innovation Project of the Water Sciences Department of Guangdong Province (2020–09), and Asia-Pacific Network for Global Change Research (APN; CRRP2019-09MY-Onodera).

Acknowledgments

We thank Lixiang Cao for the help with manuscript formatting the valuable technical help.

Conflict of interest

The authors declare that the research was conducted in the absence of any commercial or financial relationships that could be construed as a potential conflict of interest.

Publisher's note

Supplementary material

The Supplementary material for this article can be found online at: https://www.frontiersin.org/articles/10.3389/fmicb.2022.1054295/full#supplementary-material

References

Ali, H. N., and Atekwana, E. A. (2011). The effect of sulfuric acid neutralization on carbonate and stable carbon isotope evolution of shallow groundwater. *Chem. Geol.* 284, 217–228. doi: 10.1016/j.chemgeo.2011.02.023

Anderson, M. P. (2005). Heat as a ground water tracer. *Ground Water* 43, 951–968. doi: 10.1111/j.1745-6584.2005.00052.x

Brkic, Z., Briski, M., and Markovic, T. (2016). Use of hydrochemistry and isotopes for improving the knowledge of groundwater flow in a semiconfined aquifer system of the Eastern Slavonia (Croatia). *Catena* 142, 153–165. doi: 10.1016/j.catena.2016.03.010

Cao, Y.-Z., Wang, S., Zhang, G., Luo, J., and Lu, S. (2009). Chemical characteristics of wet precipitation at an urban site of Guangzhou, South China. *Atmos. Res.* 94, 462–469. doi: 10.1016/j.atmosres.2009.07.004

Chen, H., Liu, S., Xu, X. R., Zhou, G. J., Liu, S. S., Yue, W. Z., et al. (2015). Antibiotics in the coastal environment of the Hailing Bay region, South China Sea: spatial distribution, source analysis and ecological risks. *Mar. Pollut. Bull.* 95, 365–373. doi: 10.1016/j.marpolbul.2015.04.025

Chi, G., Xing, L., Xing, X., Li, C., and Dong, F. (2020). Seepage characteristics of karst water system using temperature tracer technique. *Earth Space Sci.* 7:e2019EA000712. doi: 10.1029/2019EA000712

Corbella, M., and Ibáñez, C. A. (2003). Role of fluid mixing in deep dissolution of carbonates. *Geol. Acta* 1, 305–313. doi: 10.1344/105.000001618

Dansgaard, W. (1964). Stable isotopes in precipitation. 16, 436–468. doi: 10.1111/j.2153-3490.1964.tb00181.x,

Derrien, M., Yang, L., and Hur, J. (2017). Lipid biomarkers and spectroscopic indices for identifying organic matter sources in aquatic environments: a review. *Water Res.* 112, 58–71. doi: 10.1016/j.watres.2017.01.023

Dougherty, M. C., Thevathasan, N. V., Gordon, A. M., Lee, H., and Kort, J. (2009). Nitrate and Escherichia coli NAR analysis in tile drain effluent from a mixed tree intercrop and monocrop system. *Agric. Ecosyst. Environ.* 131, 77–84. doi: 10.1016/j.agee.2008.09.011

Engel, A. S., Porter, M. L., Stern, L. A., Quinlan, S., and Bennett, P. C. (2004a). Bacterial diversity and ecosystem function of filamentous microbial mats from aphotic (cave) sulfidic springs dominated by chemolithoautotrophic "Epsilonproteobacteria". *FEMS Microbiol. Ecol.* 51, 31–53. doi: 10.1016/j.femsec.2004.07.004%

Engel, A. S., and Randall, K. W. (2011). Experimental evidence for microbially mediated carbonate dissolution from the saline water zone of the edwards aquifer, Central Texas. *Geomicrobiol J.* 28, 313–327. doi: 10.1080/01490451.2010.500197

Engel, A. S., Stern, L. A., and Bennett, P. C. (2004b). Microbial contributions to cave formation: new insights into sulfuric acid speleogenesis. *Geology* 32, 369–372. doi: 10.1130/G20288.1

Fang, J., Wu, F., Xiong, Y., Li, F., du, X., An, D., et al. (2014). Source characterization of sedimentary organic matter using molecular and stable carbon isotopic composition of n-alkanes and fatty acids in sediment core from Lake Dianchi, China. *Sci. Total Environ.* 473-474, 410–421. doi: 10.1016/j.scitotenv.2013.10.066

Ford, D., and Williams, P. (2007). Dissolution: chemical and kinetic behaviour of the karst rocks. *Karst Hydrogeol. Geomorphol.* 3, 39–76. doi: 10.1002/9781118684986.ch3

Goldscheider, N., and Drew, D. (2007). *Methods in karst hydrogeology*. London: CRC Press.

Goldscheider, N., Hunkeler, D., and Rossi, P. (2006). Review: microbial biocenoses in pristine aquifers and an assessment of investigative methods. *Hydrogeol. J.* 14, 926–941. doi: 10.1007/s10040-005-0009-9

Gray, C. J., and Engel, A. S. (2013). Microbial diversity and impact on carbonate geochemistry across a changing geochemical gradient in a karst aquifer. *ISME J.* 7, 325–337. doi: 10.1038/ismej.2012.105

Helena, B., Pardo, R., Vega, M., Barrado, E., Fernandez, J. M., and Fernandez, L. (2000). Temporal evolution of groundwater composition in an alluvial aquifer (Pisuerga River, Spain) by principal component analysis. *Water Res.* 34, 807–816. doi: 10.1016/S0043-1354(99)00225-0

Hu, S., Luo, T., and Jing, C. (2013). Principal component analysis of fluoride geochemistry of groundwater in Shanxi and Inner Mongolia, China. *J. Geochem. Explor.* 135, 124–129. doi: 10.1016/j.gexplo.2012.08.013

Huang, Q.-B., Qin, X.-Q., Liu, P.-Y., Zhang, L.-K., and Su, C.-T. (2017). Impact of sulfuric and nitric acids on carbonate dissolution, and the associated deficit of CO2 uptake in the upper–middle reaches of the Wujiang River, China. *J. Contam. Hydrol.* 203, 18–27. doi: 10.1016/j.jconhyd.2017.05.006

Jiang, Y., Hu, Y., and Schirmer, M. (2013). Biogeochemical controls on daily cycling of hydrochemistry and δ13C of dissolved inorganic carbon in a karst spring-fed pool. *J. Hydrol.* 478, 157–168. doi: 10.1016/j.jhydrol.2012.12.001

Li, S.-L., Calmels, D., Han, G., Gaillardet, J., and Liu, C.-Q. (2008). Sulfuric acid as an agent of carbonate weathering constrained by δ13CDIC: examples from Southwest China. *Earth Planet. Sci. Lett.* 270, 189–199. doi: 10.1016/j.epsl.2008.02.039

Li, S., Dong, L., Chen, J., Li, R., Yang, Z., and Liang, Z. (2019b). Vertical groundwater flux estimation from borehole temperature profiles by a numerical model, RFLUX. *Hydrol. Process.* 33, 1542–1552. doi: 10.1002/hyp.13420

Li, P., He, X., and Guo, W. (2019a). Spatial groundwater quality and potential health risks due to nitrate ingestion through drinking water: a case study in Yan'an City on the Loess Plateau of Northwest China. *Hum. Ecol. Risk Assess. Int. J.* 25, 11–31. doi: 10.1080/10807039.2018.1553612

Liang, Z., Chen, J., Jiang, T., Li, K., Gao, L., Wang, Z., et al. (2018). Identification of the dominant hydrogeochemical processes and characterization of potential contaminants in groundwater in Qingyuan, China, by multivariate statistical analysis. *RSC Adv.* 8, 33243–33255. doi: 10.1039/C8RA06051G

Liu, K., Qiao, X., Li, B., Sun, Y., Li, Z., and Pu, C. (2016). Characteristics of deuterium excess parameters for geothermal water in Beijing. *Environ. Earth Sci.* 75:1485. doi: 10.1007/s12665-016-6285-y

Liu, J., Zhao, Y., Tan, T., Zhang, L., Zhu, S., and Xu, F. (2022). Evolution and modeling of mine water inflow and hazard characteristics in southern coalfields of China: a case of Meitanba mine. *Int. J. Min. Sci. Technol.* 32, 513–524. doi: 10.1016/j.ijmst.2022.04.001

Loáiciga, H. A. (2009). Long-term climatic change and sustainable ground water resources management. *Environ. Res. Lett.* 4:035004. doi: 10.1088/1748-9326/4/3/035004

Macalady, J. L., Lyon, E. H., Koffman, B., Albertson, L. K., Meyer, K., Galdenzi, S., et al. (2006). Dominant microbial populations in limestone-corroding stream biofilms, Frasassi Cave System, Italy. *Appl. Environ. Microbiol.* 72, 5596–5609. doi: 10.1128/AEM.00715-06

MacInnis, I. N., and Brantley, S. L. (1992). The role of dislocations and surface morphology in calcite dissolution. *Geochim. Cosmochim. Acta* 56, 1113–1126. doi: 10.1016/0016-7037(92)90049-O

Parsons, M. L. (1970). Groundwater thermal regime in a glacial complex. *Water Resour. Res.* 6, 1701–1720. doi: 10.1029/WR006i006p01701

Saim, N., Osman, R., Sari Abg Spian, D. R., Jaafar, M. Z., Juahir, H., Abdullah, M. P., et al. (2009). Chemometric approach to validating faecal sterols as source tracer for faecal contamination in water. *Water Res.* 43, 5023–5030. doi: 10.1016/j.watres.2009.08.052

Sjöberg, E. L., and Rickard, D. T. (1984). Calcite dissolution kinetics: surface speciation and the origin of the variable pH dependence. *Chem. Geol.* 42, 119–136. doi: 10.1016/0009-2541(84)90009-3

Subba Rao, N., Dinakar, A., and Sun, L. (2022). Estimation of groundwater pollution levels and specific ionic sources in the groundwater, using a comprehensive approach of geochemical ratios, pollution index of groundwater, unmix model and land use/land cover - a case study. *J. Contam. Hydrol.* 248:103990. doi: 10.1016/j.jconhyd.2022.103990

Wang, Z., Guo, X., Kuang, Y., Chen, Q., Luo, M., and Zhou, H. (2022). Recharge sources and hydrogeochemical evolution of groundwater in a heterogeneous karst water system in Hubei Province, Central China. *Appl. Geochem.* 136:105165. doi: 10.1016/j.apgeochem.2021.105165

Yamanaka, M. (2012). Contributions of C3/C4 organic materials and carbonate rock to dissolved inorganic carbon in a karst groundwater system on Miyakojima Island, southwestern Japan. *J. Hydrol.* 412-413, 151–169. doi: 10.1016/j.jhydrol.2011.07.046

Zhao, Y., Liu, Q., Zhang, C., Liao, J., Lin, H., and Wang, Y. (2021). Coupled seepage-damage effect in fractured rock masses: model development and a case study. *Int. J. Rock Mech. Min. Sci.* 144:104822. doi: 10.1016/j.ijrmms.2021.104822

Zhao, Y., Zhang, L., Liao, J., Wang, W., Liu, Q., and Tang, L. (2020). Experimental study of fracture toughness and subcritical crack growth of three rocks under different environments. *Int. J. Geomech.* 20:04020128. doi: 10.1061/(ASCE)GM.1943-5622.0001779

Zhu, A., Yang, Z., Liang, Z., Gao, L., Li, R., Hou, L., et al. (2020). Integrating hydrochemical and biological approaches to investigate the surface water and groundwater interactions in the hyporheic zone of the Liuxi River basin, southern China. *J. Hydrol.* 583:124622. doi: 10.1016/j.jhydrol.2020.124622

frontiers | Frontiers in Microbiology

TYPE Original Research
PUBLISHED 27 January 2023
DOI 10.3389/fmicb.2023.1109272

OPEN ACCESS

EDITED BY
Qiang Li,
Institute of Karst Geology,
Chinese Academy of Geological Sciences,
China

REVIEWED BY
Manish Kumar,
University of Palermo,
Italy
Izhar Ali,
Guangxi University,
China

*CORRESPONDENCE
Hua Deng
✉ denghua@mailbox.gxnu.edu.cn
Ke Li
✉ likeniko@126.com

SPECIALTY SECTION
This article was submitted to Terrestrial Microbiology, a section of the journal Frontiers in Microbiology

RECEIVED 27 November 2022
ACCEPTED 04 January 2023
PUBLISHED 27 January 2023

CITATION
Hu L, Huang R, Zhou L, Qin R, He X, Deng H and Li K (2023) Effects of magnesium-modified biochar on soil organic carbon mineralization in citrus orchard. *Front. Microbiol.* 14:1109272. doi: 10.3389/fmicb.2023.1109272

Effects of magnesium-modified biochar on soil organic carbon mineralization in citrus orchard

Lening Hu[1,2,3]*, Rui Huang[1,2], Liming Zhou[1,2], Rui Qin[1,2], Xunyang He[4], Hua Deng[1,2]* and Ke Li[5]*

[1]Key Laboratory of Ecology of Rare and Endangered Species and Environmental Protection, Guangxi Normal University, Ministry of Education, Guilin, China, [2]College of Environment and Resources, Guangxi Normal University, Guilin, China, [3]Key Laboratory of Geospatial Technology for Middle and Lower Yellow River Regions, Henan University, Ministry of Education, Kaifeng, China, [4]CAS Key Laboratory of Agro-ecological Processes in Subtropical Region, Institute of Subtropical Agriculture, Changsha, China, [5]College of Civil Engineering and Architecture, Guilin University of Technology, Guilin, China

In order to investigate the carbon sequestration potential of biochar on soil, citrus orchard soils with a forest age of 5years was taken as the research object, citrus peel biochar (OBC) and magnesium-modified citrus peel biochar (OBC-mg) were selected as additive materials, and organic carbon mineralization experiments were carried out in citrus orchard soil. OBC and OBC-Mg were applied to citrus orchard soils at four application rates (0, 1, 2, and 4%), and incubated at a constant temperature for 100days. Compared with CK, the cumulative mineralization of soil organic carbon decreased by 5.11% with 1% OBC and 2.14% with 1% OBC-Mg. The application of OBC and OBC-Mg significantly increased the content of soil organic carbon fraction, while the content of soil organic carbon fraction was higher in OBC-Mg treated soil than in OBC treated soil. Meanwhile, the cumulative mineralization of soil organic carbon was significantly and positively correlated with the activities of soil catalase, urease and sucrase. The enzyme activities increased with the cumulative mineralization of organic carbon, and the enzyme activities of the OBC-Mg treated soil were significantly higher than those of the OBC treated soil. The results indicated that the OBC-Mg treatment inhibited the organic carbon mineralization in citrus orchard soils and was more favorable to the increase of soil organic carbon fraction. The Mg-modified approach improved the carbon sequestration potential of biochar for citrus orchard soils and provided favorable support for the theory of soil carbon sink in orchards.

KEYWORDS

Mg-modified citrus peel biochar, mineralization, organic carbon fraction, enzyme activity, soil physical and chemical properties

1. Introduction

In recent years, the excessive emission of greenhouse gas has led to a series of serious environmental problems and posed a great threat to the survival of human beings. China is a large agricultural country, and agricultural soil is an important source of greenhouse gas emissions (Stefaner et al., 2021). Carbon dioxide is one of the most important greenhouse gases (Perez-Quezada et al., 2021). Scientists estimate that by 2050, atmospheric CO_2 levels will reach 550 mg/l (Du et al., 2022). Carbon sequestration through soil to achieve emission reduction is one of the important directions of environmental research today. Soil organic carbon (SOC) is one of the most important indicators of soil quality (Masto et al., 2013a). Soil organic carbon affects the global carbon cycle process by influencing the release or sequestration of atmospheric CO_2 from soil. Soil

organic carbon mineralization is an important process for the conversion of carbon to CO_2 in soil (Gan et al., 2020), therefore it is important to study the effect of soil organic carbon mineralization on the soil carbon cycle.

Previously, many materials have been used in the study of agricultural soil, and studies have shown that the application of dolomite and different biochar can reduce soil greenhouse gas emissions (Oo et al., 2018). The application of rice straw biochar at high CO_2 concentration and air temperature can suppress soil NO_2 emissions (Sun et al., 2018), which indicates that biochar has a better impact on reducing greenhouse gas emissions from agricultural soil (Korai et al., 2018; Wu et al., 2018). Biochar is a solid material with high carbon content prepared by high-temperature pyrolysis of biomass under oxygen-limited or oxygen-isolated conditions (Chen, W. et al., 2019). The effects of biochar application in soil have been extensively studied (Kuo et al., 2020; Rubin et al., 2020). Studies have shown that the application of biochar to soil reduces greenhouse gas emissions; and has a positive impact in terms of soil moisture retention, soil nitrogen and phosphorus retention (Bashir et al., 2020; Lu et al., 2020). At the same time, the application of biochar to soil can provide nutrients and habitat for microorganisms, thus directly or indirectly affecting the function and composition of microbial communities (Abhishek et al., 2022). In addition, the application of biochar increases the microbial pool of carbon and nitrogen in the soil and provides organic substrate for soil enzymes, thus changing the enzyme activity (Ullah et al., 2020). Therefore, applying biochar to the soil is important to improve soil nutrient dynamics and maintain the soil organic carbon pool.

Modification of biochar can improve its properties and enhance the stability of biochar (Liu et al., 2021). Mg is used for biochar modification because of its abundant reserves, non-toxicity, and high affinity for anions (Jiao et al., 2022), Mg is often used to make modified biochar. Yin et al. (2018) modified biochar with Mg and used it to treat PO_4^{3-} and NO_3^- contaminated eutrophic water bodies, and the results showed that Mg-modified biochar can improve water quality. The results of Wu et al. (2019) showed that application of MgO modified biochar to saline soil could increase soil effective phosphorus content and crop yield. Shan et al. (2022) applied Mg-modified peanut shell biochar to soil and effectively increased soil pH and reduced soil bioeffective state Cd content. Khan et al. (2022) even showed that Mg-modified biochar could slow down soil greenhouse gas emissions. Soil calcium and magnesium deficiencies are common in citrus soils (Chen, H. et al., 2019), and applying Mg-modified biochar to citrus soils can effectively improve the soil Mg deficiency. At present, the application of Mg-modified biochar to citrus soils has not been extensively studied, so the study of the effect of Mg-modified biochar on organic carbon mineralization in citrus soils is of great value.

Guangxi is the province with the largest citrus planting area and yield of citrus in China (Xie et al., 2021; Qiao et al., 2021). Bad and waste fruits as well as peel residues from citrus orchard cause a lot of wasted resources, and burning citrus peels into carbon applied to soil may be an important way to make efficient and reasonable utilization of waste *in situ*. Therefore, in this study, citrus peel biochar was modified to prepare Mg-modified citrus peel biochar, and citrus peel biochar and Mg-modified citrus peel biochar were applied to citrus orchard soils at different proportions. The effects on soil organic carbon mineralization, organic carbon and its active components in citrus orchard soils were investigated through a 100-day incubation experiment in a constant temperature incubation room. The effects and mechanisms of adding biochar on soil organic carbon mineralization were explored through the characteristics of changes in various indicators under different treatments.

2. Materials and methods

2.1. Experimental materials

The test soil was obtained in December 2021 from the core demonstration base of citrus cultivation at the Encounter Dragon River, Yangshuo County, Guilin City, Guangxi Zhuang Autonomous Region (24°48′17″N, 110°22′16″E). The area has a subtropical monsoon climate with an average annual temperature of 19.1°C and an average annual rainfall of 1887.6 mm. The soil type is red soil. Soil samples were collected from 0 to 20 cm surface layer of citrus orchards according to the principle of random multi-point mixing. Soil samples were removed from plant and animal residues and gravels, naturally dried and passed through 2 mm sieve for subsequent experiments. The basic physical and chemical properties of the test soils are shown in Table 1.

Citrus peels and soil were taken from the same citrus orchard. The citrus peels were dried at 70°C for 24 h, then crushed with a crusher and passed through a 60 mesh screen, and carbonized at 500°C for 2 h under oxygen limitation to prepare citrus peel biochar (OBC). The sieved citrus peel powder was mixed with 1 mol/l $MgCl_2$–$6H_2O$ solution at a solid–liquid ratio of 1:10 for 24 h (That is, every 100 g of citrus peel powder mixed with 1 l of $MgCl_2$–$6H_2O$ solution). The dried powder was filtered through a filter and dried at 60°C for 24 h. The Mg-modified citrus peel biochar (OBC-Mg) was prepared by limiting oxygen carbonization at 500°C for 2 h. The basic physicochemical properties of OBC and OBC-Mg are shown in Table 2.

2.2. Experimental design

There were seven treatments with three replications for each treatment, and the experiment was set up with four application rates, i.e., 0% (CK), 1, 2, and 4% of soil mass of the applied material, as shown in Table 3.

Culture test: 1,000 g of soil was placed in 2 l polyethylene bottles. Citrus peel biochar and magnesium modified citrus peel biochar were applied according to the experimental design (Table 3). After the soil was mixed well with the materials, deionized water was added to keep the field water holding capacity at about 60%. The polyethylene bottles were incubated in a constant temperature incubator at 25°C for 100 days and soil samples were collected for analysis on days 1, 3, 5, 10, 15, 20, 30, 40, 60, 80, and 100, respectively. Another batch of soil samples of the same treatment was set up and incubated under the same conditions with a soil weight of 50 g. A 10 ml beaker containing 0.1 mol L^{-1} sodium hydroxide solution was placed in a polyethylene bottle and analyzed for soil organic carbon mineralization on days 1, 3, 5, 10, 15, 20, 30, 40, 60, 80, and 100 (Xu et al., 2019).

2.3. Measurement method

The pH was determined by potentiometric method (water–soil ratio 2.5:1; Zhang et al., 2021). Available phosphorus was determined by sodium bicarbonate extraction-molybdenum antimony anti-spectrophotometric method (Wang, H. et al., 2021). Available potassium was determined by 1 mol/l ammonium acetate extraction-flame

TABLE 1 Basic physical and chemical properties of the test soil.

pH	Ec (Sm^{-1})	AP ($mgkg^{-1}$)	AK ($mgkg^{-1}$)	SOC (gkg^{-1})	Mechanical composition (%)	
4.36 ± 0.01	53.8 ± 2.07	27.13 ± 0.56	38.24 ± 1.21	6.78 ± 0.27	Sand (0.2–0.02 mm)	25.6
					Silt (0.02–0.002 mm)	47.1
					Clay (<0.002 mm)	27.3

Mean ± standard deviation of each index of the test soil ($n = 3$). EC, conductivity; AP, available phosphorus; AK, available potassium; SOC, soil organic carbon. The values followed by the same superscript letters within a row are not significantly different ($p <= 0.05$) between relevant treatments.

TABLE 2 Basic properties and elemental contents of two biochar.

	pH	Productivity (%)	C/N	C/H	Elemental contents (%)			
					C	H	N	S
OBC	10.04	38.13	36.72	114.59	63.77	0.556	1.74	0.009
OBC-Mg	10.19	46.26	35.87	73.07	23.81	0.326	0.66	0.029

photometric method (Rong et al., 2021). Soil cation exchange capacity (CEC) was determined by the barium chloride-sulfuric acid forced exchange method (Zhang et al., 2010). Soil organic carbon (SOC) was determined by the potassium dichromate oxidation-spectrophotometric method (Hu et al., 2020). Soil dissolved organic carbon (DOC) content was determined by TOC total organic carbon analyzer (Huang et al., 2018). Soil microbial biomass carbon (MBC) was determined by fumigation method (Gao et al., 2017).Soil readily organic carbon (ROC) was determined by 333 mmol/l potassium permanganate oxidation method (Jien et al., 2018). Soil catalase was determined by the potassium permanganate titration method (Zhao et al., 2020), soil urease activity was determined by the indophenol blue colorimetric method (Sarma et al., 2017), and soil sucrase activity was determined by the 3,5-dinitrosalicylic acid colorimetric method (Xu et al., 2019). Soil CO_2 emissions were determined by the titrimetric method (Pei et al., 2017). The surface morphological characteristics of biochar were observed by FEI Inspect F5 field emission scanning electron microscope (SEM) at a magnification of 500–40,000× and an acceleration voltage of 20 kV of the electron beam, and its composition was analyzed by mapping (Deng et al., 2022).

2.4. Calculation methods

(1) Soil organic carbon mineralization (in terms of CO_2).

$$CO_2\left(\mathrm{mg}\cdot\mathrm{kg}^{-1}\right) = \left\{\left[\left(V_0 - V\right)\times c\times 0.022\times\left(22.4/44\right)\times 1000\right]\times 2\times 1000\right\}/m.$$

(2) Soil organic carbon mineralization rate.

Soil organic carbon mineralization rate ($mg\,kg^{-1}\,d^{-1}$) = organic carbon mineralization/Δt (2).

(3) Cumulative soil organic carbon mineralization (total soil CO_2 release from the beginning of cultivation to a certain time point).

$$\text{Cumulative mineralization} = \sum_{1}^{n} CO_2.$$

(4) Mineralization fitting calculation.

The first level kinetic equation was applied to fit the soil carbon mineralization under different treatments.

$$C_t = C_0\left(1 - e^{-kt}\right)$$

where V_0 is the volume of standard hydrochloric acid consumed during the blank titration, V is the volume of standard hydrochloric acid consumed during the sample titration, c is the concentration of standard hydrochloric acid, 0.022 is the molar mass of carbon dioxide ($1/2CO_2$), M ($1/2CO_2$) = 0.022 g $mmol^{-1}$, 22.4 × 1000/44 is the number of milliliters per gram of CO_2 in the standard state; $\triangle$t is the incubation interval (d); C_t is the cumulative mineralization at incubation time t (d), C_0 is the potential mineralization of soil carbon, C ($mg{\bullet}kg^{-1}$); k is the rate constant of soil carbon mineralization, d^{-1}; t is the incubation time, day (d) (Hu et al., 2020).

2.5. Statistical analysis

Excel 2020 and SPSS 25.0 (IBM Corporation, United States) were used for statistical analysis of the data. One-way analysis of variance (ANOVA) was used to compare the differences between treatments, and the least significant difference (LSD) method was used to test the significance of differences at the level of significance ($p <= 0.05$). Figures were plotted by origin2022 (OriginLab Corporation, United States). The correlation heat map was plotted using the Correlation Plot App in origin 2022, with red representing positive correlations and blue representing negative correlations, and color shades representing the magnitude of correlation coefficients; the darker the color, the stronger the correlation.

3. Results

3.1. Characterization of biochar

Figure 1 shows the SEM-EDS patterns of OBC and OBC-Mg. The morphological structures of OBC and OBC-Mg are significantly different. The surface structure of OBC in the figure presents a complete blocky structure with smooth surface and well-developed pore structure.

TABLE 3 Experiment design.

Number	1	2	3	4	5	6	7
Treatment	CK	1%OBC	2%OBC	4%OBC	1%OBC-Mg	2%OBC-Mg	4%OBC-Mg

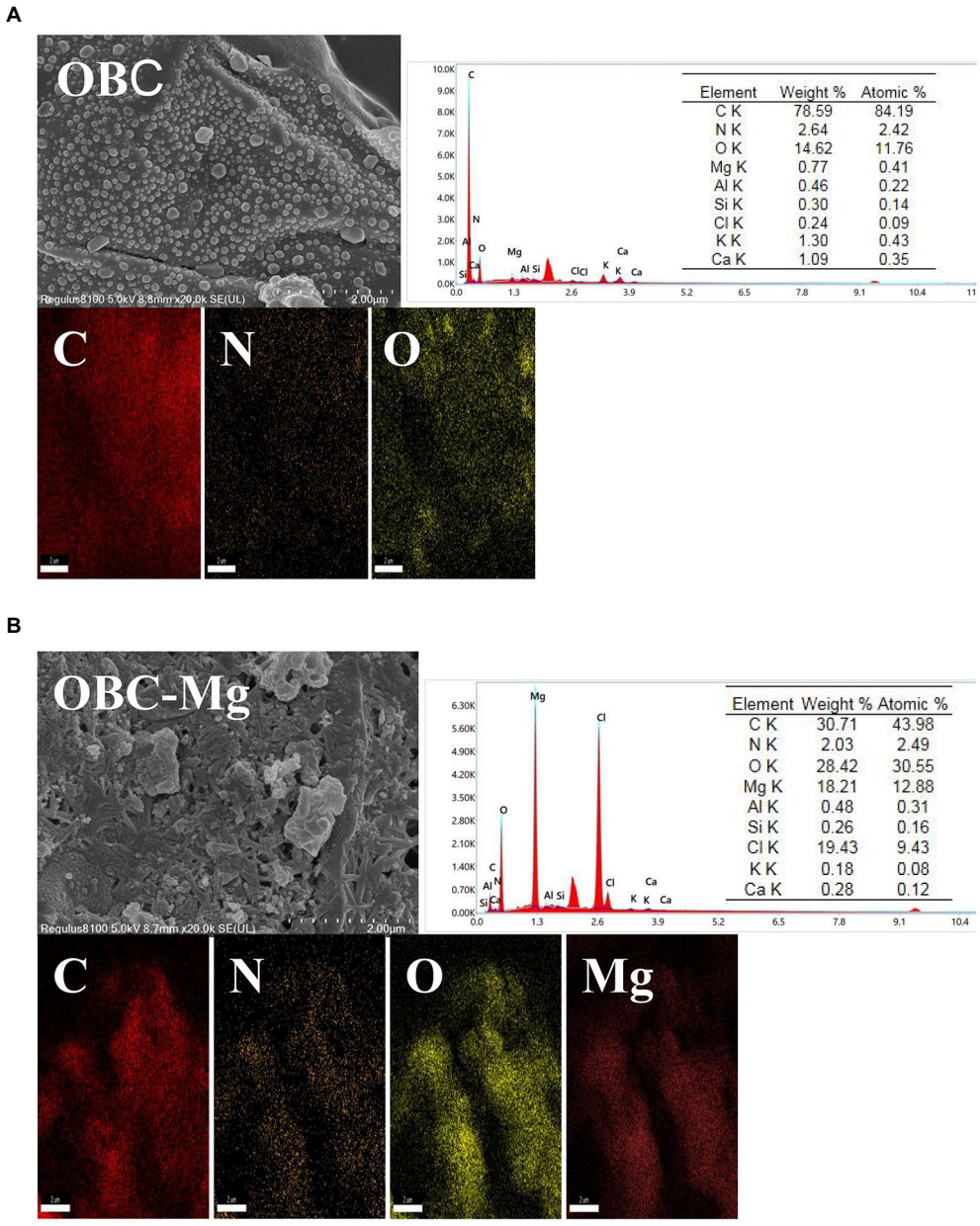

FIGURE 1
scanning electron microscopy–energy dispersive X-ray spectroscopy (SEM–EDS) analysis of **(A)** citrus peel biochar (OBC) and **(B)** magnesium-modified citrus peel biochar (OBC-Mg).

The surface structure of OBC-Mg was broken, with increased specific surface area and irregular granular flocs on the surface. The rough flake morphology on the surface of OBC-Mg may be due to the formation of MgO from $MgCl_2$–$6H_2O$ after intense dehydration in pyrolysis (Zhang et al., 2012; Li et al., 2017). The results of EDS analysis showed that that the elemental C content of the modified biochar surface decreased from 78.59 to 30.71% compared to OBC-Mg. The decrease in carbon content may be due to the absorption of Mg into the surface of carbon (Li et al., 2016). EDS analysis also showed that the content of Mg in OBC-Mg was significantly higher compared to OBC, which also indicated that the impregnation modification successfully loaded Mg. In addition, EDS analysis also revealed Al, Si, Cl, K, and *Ca*.

3.2. Effect of the OBC and OBC-Mg on soil physiochemical properties

3.2.1. Impact of OBC and OBC-Mg on soil pH

The effects of OBC and OBC-Mg on soil pH are shown in Figure 2. The ANOVA/statistical indicators are shown in Supplementary Tables 1–3.

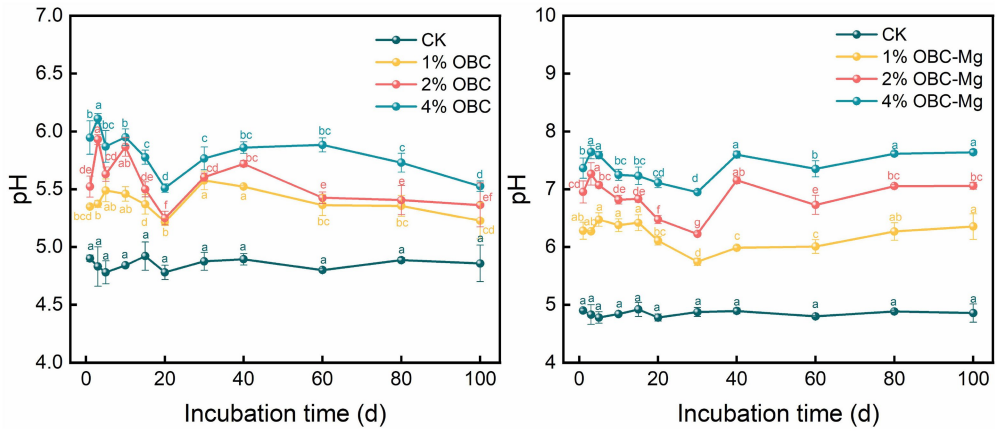

FIGURE 2
Changes in soil pH after the amendment of OBC and OBC-Mg.

The pH of CK without biochar application did not change significantly during the incubation period; the soil pH of OBC and OBC-Mg application increased significantly, and the soil pH of the same treatment increased significantly with the incubation time, and the improvement effect on soil acidity was shown as 4% > 2% > 1% > CK in both cases. After OBC application, the soil pH increased with the increase of application rate at the end of incubation compared with the control by 0.37, 0.51, and 0.67 units, respectively. After OBC-Mg application, soil pH increased by 1.50, 2.20, and 2.78 units at the end of the incubation compared to the CK. With the increase in the application rate, the difference between the different application rates was significant. The application of OBC-Mg was more effective in improving the acidity of the soil compared to other treatments.

3.2.2. Impact of OBC and OBC-Mg on soil cation exchange capacity (CEC)

During the incubation period, the overall soil CEC showed a decreasing trend after the application of OBC and OBC-Mg with the increase of incubation time (Figure 3). Among them, CK soil had the highest CEC value at the 15th day of incubation and the lowest at the end of incubation; after applying OBC, 4% OBC increased soil CEC, 2% OBC and 1% OBC were partially slightly lower than CK at the 1st–30th days of incubation, and both were higher than CK after 30 days, and the difference of soil CEC of the same treatment with increasing incubation time was significant, and the effect on soil CEC was shown as 4% OBC > 2% OBC > 1% OBC. After OBC application, compared with CK at the end of incubation with the increase of the application rate, the soil CEC increased by 74.57, 146.49 and 72.88%, respectively. The application of OBC-Mg significantly increased the soil CEC, and the effect on CEC was 4% OBC-Mg > 2% OBC-Mg > 1% OBC-Mg. After the application of OBC-Mg, at the end of the incubation with the increase of the applied proportion compared to CK, the soil CEC increased by 125.74, 165.85, and 207.80%, respectively, and the difference between different applied proportions was significant. OBC-Mg was more effective in enhancing soil CEC compared to other treatments.

3.2.3. Impact of OBC and OBC-Mg on soil available phosphorus (AP)

The effects of OBC and OBC-Mg application on AP in citrus orchard soil are shown in Figure 4. After the application of OBC, the AP content of each treatment first increased, then decreased and gradually stabilized, reaching the highest level at the 15th day of incubation. At the end of the incubation, the AP content was higher than that of CK under different rates of OBC. The size of AP content in different rates of OBC application was 4% > 2% > 1% > CK. With the increase of application rate, the AP content increased by 28.62, 44.52 and 48.82% compared with CK. The trend of AP content in each treatment was similar to that of OBC, which first increased, then decreased and gradually stabilized, and reached the highest value at day 20 of incubation. The AP content of OBC-Mg applied at different rates was positively correlated with the application rate. Compared with CK, the AP content increased by 96.98, 108.11 and 114.47%, respectively. In a comprehensive comparison, OBC-Mg applied to citrus orchard soil increased the AP content better than OBC.

3.2.4. Impact of OBC and OBC-Mg on soil available potassium (AK)

The effects of OBC and OBC-Mg application on AK in citrus orchard soil are shown in Figure 5. After applying OBC-Mg to the soil, the AK content in the soil increased with the increase of the applied proportion. The AK content was 4% OBC > 2% OBC > 1% OBC > CK from the largest to the smallest. Compared with CK, at the end of the incubation, the AK content increased by 14.98, 18.61, and 19.12%, respectively, with the increase of the applied proportion. After applying different proportions of OBC-Mg to the soil, the AK content in the soil was CK > 1% OBC-Mg > 2% OBC-Mg > 4% OBC-Mg. Compared with CK, at the end of the incubation, the CK content decreased by 14.98, 18.61, and 19.12%, respectively, with the increase of the applied proportion.

3.3. Effect of the OBC and OBC-Mg on soil mineralization

3.3.1. Impact of OBC and OBC-Mg on soil mineralization rate

As shown in Figure 6, the application of OBC and OBC-Mg to citrus orchard soil significantly affected the rate of soil organic carbon mineralization in citrus orchards. Throughout the incubation period, the soil organic carbon mineralization rates after applying different rates of OBC and OBC-Mg were higher than those of the CK. On the first day

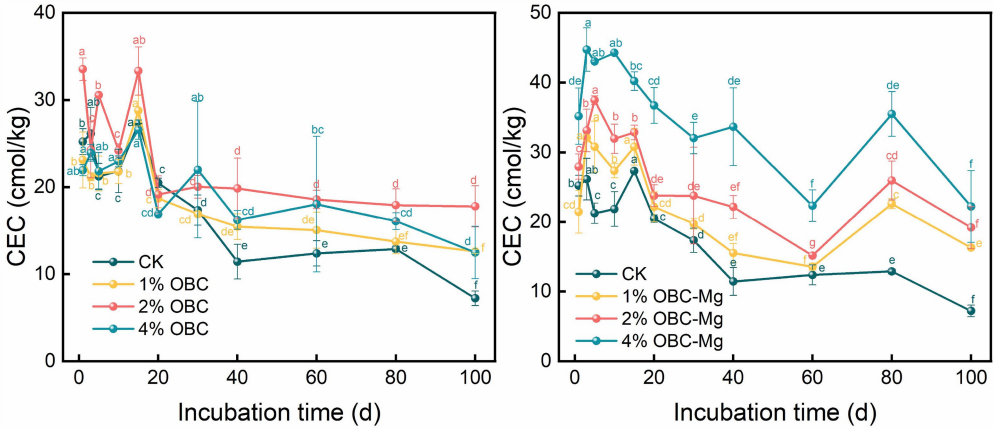

FIGURE. 3
Changes in soil cation exchange capacity (CEC) after the amendment of OBC and OBC-Mg.

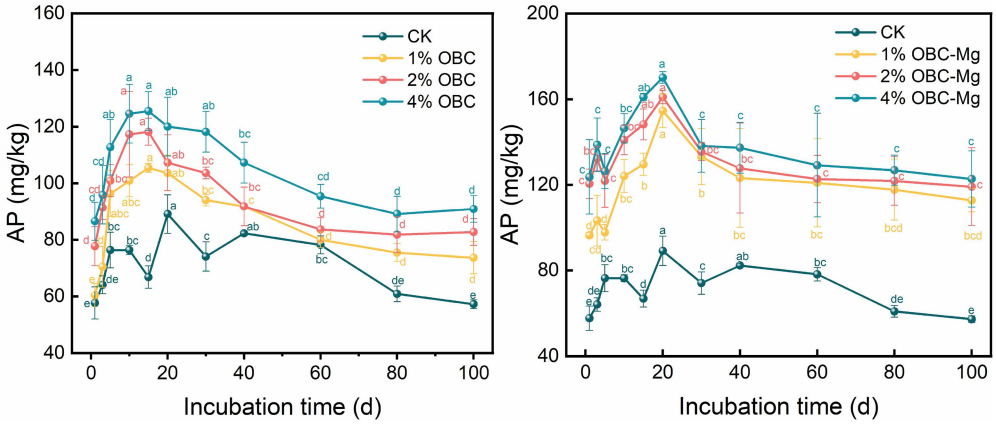

FIGURE 4
Changes in soil available phosphorus (AP) after the amendment of OBC and OBC-Mg.

of incubation, the rates of soil organic carbon mineralization with 1, 2 and 4% OBC were 1.32, 1.58 and 1.52 times higher than those with CK, respectively. And the rates of soil organic carbon mineralization with 1, 2 and 4% OBC-Mg were 1.39, 1.52 and 1.65 times higher than those with CK. The soil mineralization rate decreased in all treatments from 0 to 10 days of incubation, and showed an increasing trend in all treatments from 10 to 20 days of incubation. The organic carbon mineralization rate decreased with increasing incubation time in all treatments after 20 days of incubation. At the end of incubation, compared with CK, soil organic carbon mineralization rates increased by 11.72, 41.21, and 78.45% with 1, 2, and 4% OBC applied; and increased by 33.45, 55.17, and 55.17% with 1, 2, and 4% OBC-Mg applied. In summary, all soil organic carbon mineralization rates decreased with increasing incubation time. The rates were at a high level in the early incubation period, decreased with increasing time, and stabilized in the late incubation period.

3.3.2. Impact of OBC and OBC-Mg on soil cumulative mineralization

As shown in Figure 7, the application of OBC and OBC-Mg significantly increased the cumulative soil organic carbon mineralization. The cumulative mineralization of soil organic carbon in CK was the lowest among the treatments from 0 to 40 days of incubation, and after 40 days of incubation, the cumulative mineralization of soil organic carbon in CK was higher than that in 1% OBC and 1% OBC-Mg. The cumulative mineralization of soil organic carbon in each treatment increased with the increase of incubation time. After the application of OBC, the cumulative mineralization of 1% OBC decreased by 5.11, 2% OBC and 4% OBC increased by 6.18 and 15.68%, respectively, compared with CK. The cumulative mineralization of soil organic carbon showed an overall increase of 4% OBC > 2% OBC > 1% OBC with the increase of the application ratio. At the end of incubation, the cumulative mineralization of 1% OBC-Mg decreased by 2.14, 2% OBC-Mg and 4% OBC-Mg increased by 15.20 and 10.93%, respectively. The cumulative mineralization showed 4% OBC-Mg > 2% OBC-Mg > 1% OBC-Mg at days 0–40 of incubation, and 2% OBC-Mg > 4% OBC-Mg > 1% OBC-Mg at days 40–100 of incubation. The application of 1% of two biochar to citrus orchard soils could slow down the emission of soil CO_2 to some extent.

The dynamic changes between the cumulative mineralization of soil organic carbon and incubation days in citrus orchards after the application of OBC and OBC-Mg were fitted using the quasi-level kinetic equation $C_t = C_0(1-e^{-kt})$, and the model fitted well with a

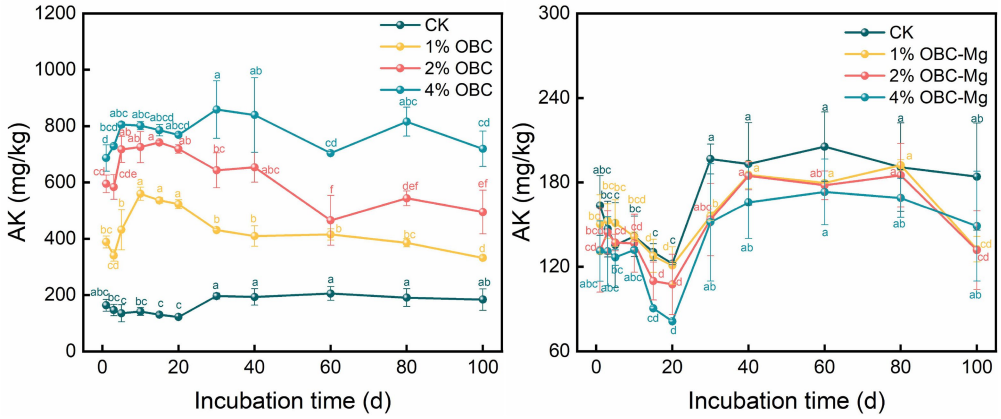

FIGURE 5
Changes in soil available potassium (AK) after the amendment of OBC and OBC-Mg.

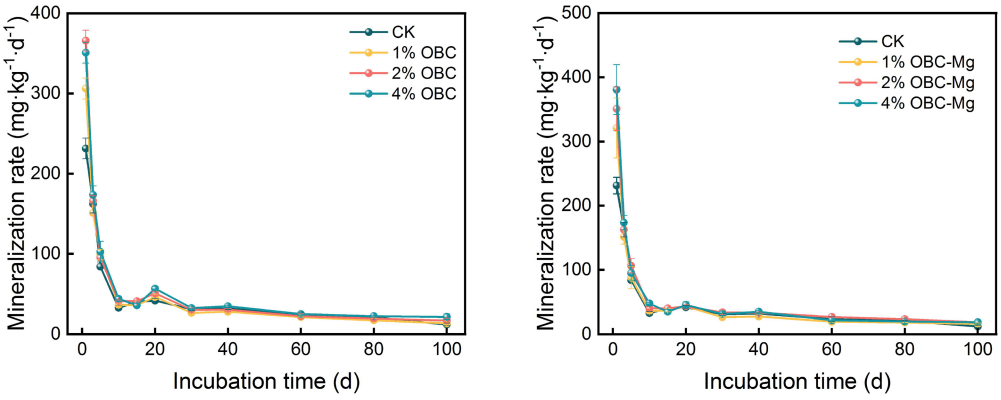

FIGURE 6
Changes in soil mineralization rate after the amendment of OBC and OBC-Mg.

correlation coefficient $R^2 > 0.933$ (Table 4). The results showed that after the application of OBC, the C_0 of potential mineralization of organic carbon in 1% OBC and 2% OBC soils was lower than that of CK. The potential mineralization of organic carbon in 4% OBC soils was higher than that of CK. The organic carbon turnover rate constant k was significantly higher than that of CK, its C_0 increased with the increase of the application ratio. After the application of OBC-Mg, the potential mineralization of organic carbon in 1% OBC-Mg soil C_0 was lower than that of CK, the potential mineralization of organic carbon in 2% OBC-Mg and 4% OBC-Mg soil was higher than that of CK, the organic carbon turnover rate constant k was significantly higher than that of CK, its C_0 increased with the increase of the application rate.

3.4. Effect of the OBC and OBC-Mg on soil active organic carbon components

3.4.1. Impact of OBC and OBC-Mg on soil organic carbon

Application of OBC and OBC-Mg to citrus orchard soil was able to significantly increase SOC content (Figure 8). The overall effect of OBC and OBC-Mg on the dynamics of soil SOC content showed 4% > 2% > 1% > CK, and the difference in the same application rate was not significant with increasing incubation time. Compared with CK, at the end of incubation, 1% OBC was 1.20 times, 2% OBC was 1.28 times and 4% OBC was 1.43 times of CK, 1% OBC-Mg was 1.64 times, 2% OBC-Mg was 1.89 times and 4% OBC-Mg was 2.14 times of CK. Compared with OBC, OBC-Mg applied to citrus orchard soil could better improve the SOC content in the soil.

3.4.2. Impact of OBC and OBC-Mg on soil microbial biomass carbon

As shown in Figure 9, the application of OBC and OBC-Mg to citrus orchard soil significantly changed the soil MBC content. After applying OBC to citrus orchard soils, soil MBC content gradually decreased from 0 to 20 days of incubation and gradually increased after 20 days, but some treatments still had less MBC than CK. At the end of incubation, 1% OBC increased by 6.77, 2% OBC increased by 9.92, and 4% OBC increased by 5.12% compared to CK. Overall, the application of 2% OBC could better increase soil MBC. After applying OBC-Mg to citrus orchard soil, soil MBC content changed repeatedly during the first 20 days of incubation and gradually increased from 30 to 100 days of incubation. At the end of incubation, the MBC content was greater than CK at all rates. At the end of incubation, 1% OBC-Mg increased by 18.95, 2% OBC-Mg

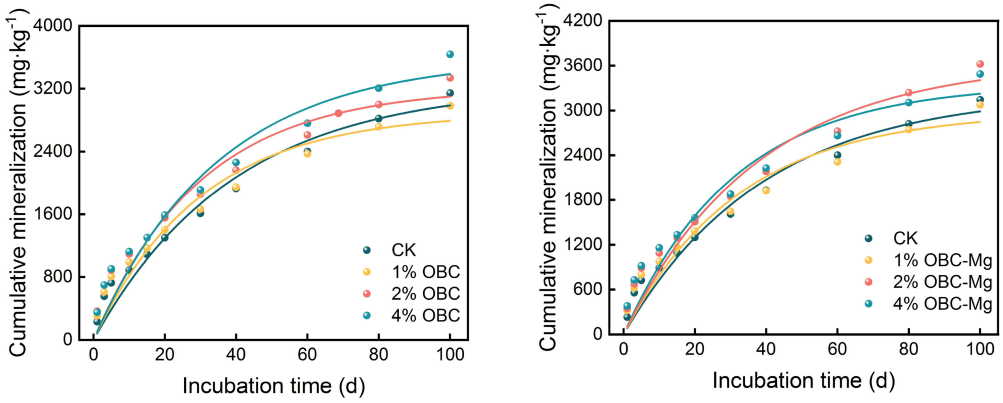

FIGURE 7
Changes in soil cumulative mineralization after the amendment of OBC and OBC-Mg.

TABLE 4 Soil carbon mineralization kinetic parameters.

Treatment	Fitting parameters		
	C_0/mgkg^{-1}	k/d^{-1}	R^2
CK	3,239 ± 257.40	0.026 ± 0.004	0.962
1% OBC	2,894 ± 208.92	0.033 ± 0.006	0.944
2% OBC	3,215 ± 240.54	0.033 ± 0.006	0.939
4% OBC	3,586 ± 294.67	0.029 ± 0.005	0.945
1% OBC-Mg	2,983 ± 248.38	0.031 ± 0.006	0.935
2% OBC-Mg	3,362 ± 274.01	0.032 ± 0.006	0.933
4% OBC-Mg	3,662 ± 330.20	0.027 ± 0.005	0.945

increased by 17.50, and 4% OBC-Mg increased by 18.78% compared to CK.

3.4.3. Impact of OBC and OBC-Mg on soil dissolved organic carbon

As shown in Figure 10, the application of OBC and OBC-Mg to citrus orchard soil changed the DOC content in the soil. All treatments showed a decreasing trend with the increase of incubation time. After the application of OBC, each proportion of DOC showed a decreasing trend, but there were still some treatments with DOC less than CK, and at the end of incubation each applied proportion of DOC was greater than CK. Compared with CK, the DOC content increased by 25.67% (1% OBC), 17.26% (2% OBC), and 22.58% (4% OBC), respectively. After the application of OBC-Mg, DOC gradually increased in all ratios and at the end of the incubation, all treatments were greater than CK, and DOC content increased by 12.26% (1% OBC-Mg), 20.91% (2% OBC-Mg), and 25.28% (4% OBC-Mg), respectively.

3.4.4. Impact of OBC and OBC-Mg on soil readily oxidized organic carbon

As shown in Figure 11, the application of OBC and OBC-Mg to citrus orchard soil significantly changed the soil ROC content. After applying OBC to citrus orchard soils, the soil ROC content showed a decreasing trend throughout the incubation period, but some treatments still had less ROC than CK. At the end of incubation, the ROC content in 1% OBC soil was the same as CK, while 2% OBC increased by 26.56 and 4% OBC increased by 43.75% compared to CK. After applying OBC-Mg to citrus orchard soils, soil ROC content decreased on 0–5 days of incubation, gradually increased on 5–20 days, and increased after decreasing on 20–60 days. At the end of incubation, the ROC content of each treatment was greater than that of CK, 1% OBC-Mg increased by 151.56, 2% OBC-Mg increased by 87.50, and 4% OBC-Mg increased by 187.50% compared to CK.

3.5. Effect of the OBC and OBC-Mg on soil enzyme activity

3.5.1. Impact of OBC and OBC-Mg on soil catalase activity

As shown in Figure 12, application of OBC and OBC-Mg to citrus orchard soils increased the activity of catalase in the soil. Compared with CK, after the application of OBC, the catalase activity in soil increased from 0 to 30 days of incubation, but some treatments still had less catalase activity than CK. Throughout the incubation period, the catalase activity first increased to reach the highest value at 30th day, then decreased and then stabilized. At the end of incubation, with the application ratio with an overall performance of 4% OBC > 2% OBC > 1% OBC > CK, it increased by 26.67, 40 and 56.67%, respectively, with the increase of applied ratio. After the application of OBC-Mg, the catalase activity in the soil increased significantly compared with CK, and the change trend was similar to that of OBC. With the increase of incubation time, the catalase activity first increased to reach the highest value at 30th day and then decreased and then stabilized. At the end of incubation, 1% OBC-Mg, 2% OBC-Mg, and 4% OBC-Mg increased by 73.33, 100.00, and 116.67%, respectively, and the catalase activity increased with the increase of applied percentage.

3.5.2. Impact of OBC and OBC-Mg on soil urease activity

As shown in Figure 13, the application of OBC and OBC-Mg to citrus orchard soils significantly increased the urease activity in the soil. After the application of OBC, the overall trend of increasing urease activity of each proportion with incubation time was observed, and at the end of incubation, the urease activity of each proportion was higher than that of CK, 1% OBC was 1.61 times, 2% OBC was 1.72 times, and

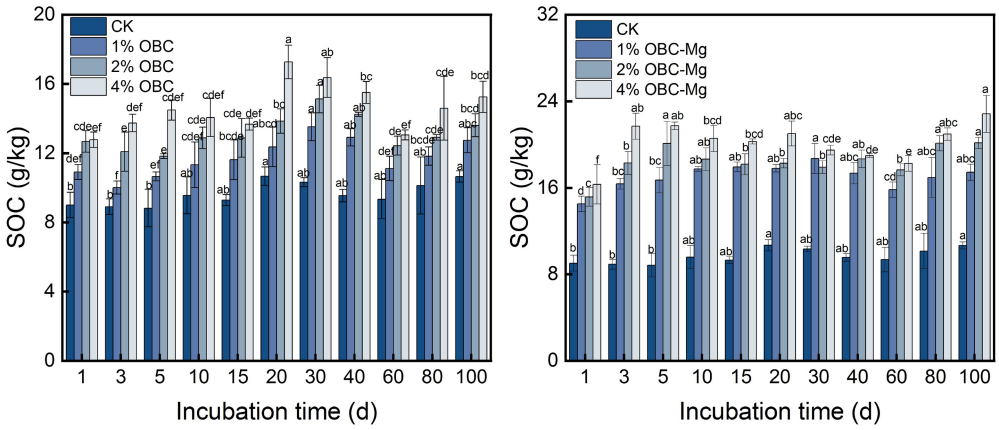

FIGURE 8
Changes in soil organic carbon (SOC) after the amendment of OBC and OBC-Mg.

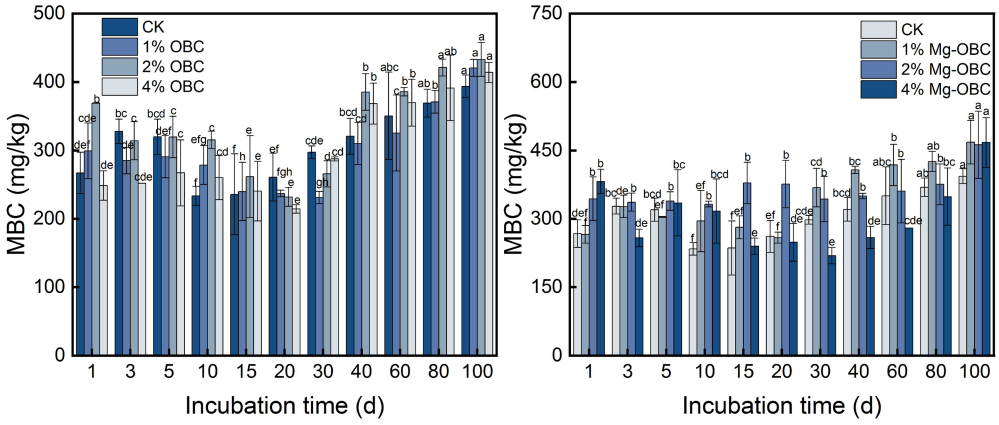

FIGURE 9
Changes in microbial biomass carbon (MBC) after the amendment of OBC and OBC-Mg.

4% OBC was 1.92 times than that of CK. Throughout the incubation period, the urease activity of each applied ratio showed 4% OBC > 2% OBC > 1% OBC > CK. After the application of OBC-Mg, the urease activity of each ratio gradually increased after decreasing from 0 to 5 days. At the end of the incubation, the urease activity increased by 252.49% for 1% OBC-Mg, 279.91% for 2% OBC-Mg and 206.80% for 4% OBC-Mg compared to CK. The urease activity of each treatment showed 4% OBC-Mg > 2% OBC-Mg > 1% OBC-Mg > CK on 0–10 days of incubation, and the urease activity of each applied percentage showed 2% OBC-Mg > 1% OBC-Mg > 4% OBC > CK after 20 days of incubation.

3.5.3. Impact of OBC and OBC-Mg on soil sucrase activity

As shown in Figure 14, the application of OBC and OBC-Mg to citrus orchard soils increased the sucrase activity in the soil. The application of OBC showed an overall trend of increasing sucrase activity with incubation time. At the end of incubation, the urease activity was higher than that of CK for all proportions, with an increase of 108.21 for 1% OBC, 158.03 for 2% OBC, and 243.05% for 4% OBC compared to CK. The sucrase activity of each treatment increased with the applied percentage throughout the incubation period. After the application of OBC-Mg, the sucrase activity increased with the increase of incubation time for each percentage. At the end of incubation, such enzyme activity increased by 517.60% for 1% OBC-Mg, 490.18% for 2% OBC-Mg and 489.65% for 4% OBC-Mg compared to CK. The sucrase activity of each ratio decreased with the increase of applied ratio, 1% OBC-Mg > 2% OBC-Mg > 4% OBC > CK.

3.6. Correlation analysis

In Figure 15A, it can be seen that after applying OBC to citrus orchard soils, soil pH was significantly positively correlated ($p <= 0.05$) with AK, SOC and DOC, and negatively correlated with AP. Soil CEC content was positively correlated with DOC, ROC, and organic carbon mineralization rate. It was negatively correlated with MBC, cumulative mineralization of organic carbon, catalase, urease, and sucrase. AP content was negatively correlated with AK, SOC, urease and sucrase. DOC was positively correlated with ROC and organic carbon mineralization rate, and negatively correlated with MBC, organic carbon mineralization, catalase, urease and sucrase. MBC was positively correlated with organic carbon mineralization, urease and sucrase, and

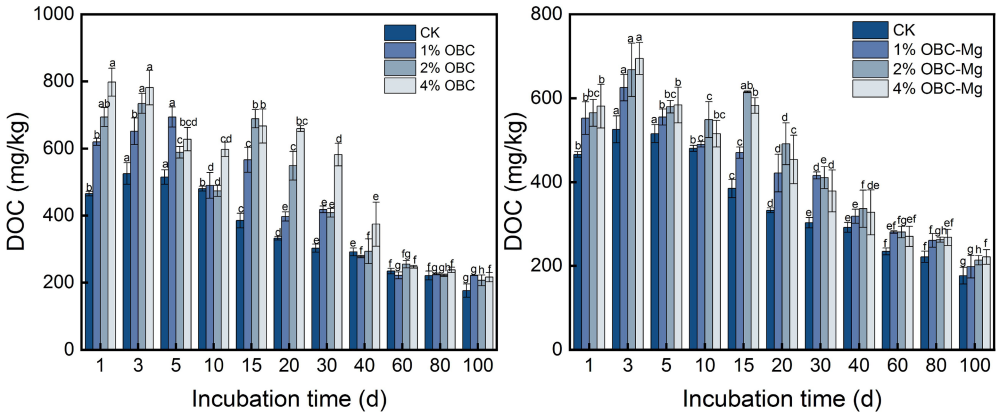

FIGURE 10
Changes in dissolved organic carbon (DOC) after the amendment of OBC and OBC-Mg.

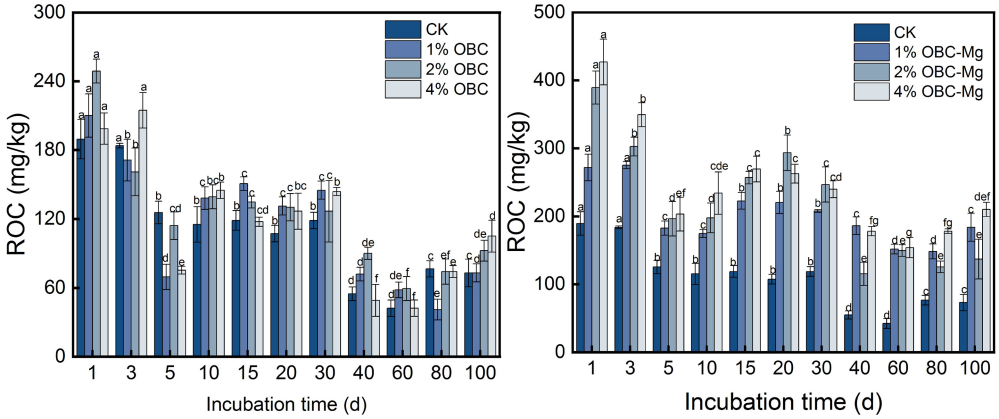

FIGURE 11
Changes in readily oxidized organic carbon (ROC) after the amendment of OBC and OBC-Mg.

negatively correlated with ROC. The ROC was positively correlated with the rate of organic carbon mineralization and negatively correlated with the cumulative mineralization of organic carbon, catalase and sucrase. The rate of organic carbon mineralization was negatively correlated with the cumulative mineralization of organic carbon, catalase, and sucrase. Cumulative mineralization of organic carbon was positively correlated with catalase, urease and sucrase. Catalase was positively correlated with urease and sucrase. Urease was positively correlated with sucrase.

As seen in Figure 15B, soil pH was significantly and positively correlated ($p <= 0.05$) with CEC after application of OBC-Mg to citrus orchard soil. Soil CEC content was positively correlated with DOC and ROC, and negatively correlated with AK, MBC, accumulated organic carbon mineralization and sucrose. AP was positively correlated with catalase and negatively correlated with AK, MBC and organic carbon mineralization rate. SOC was negatively correlated with ROC and organic carbon mineralization rate. DOC was positively correlated with ROC and organic carbon mineralization rate, and negatively correlated with MBC, organic carbon mineralization, urease and sucrase. The ROC was positively correlated with the rate of organic carbon mineralization and negatively correlated with the cumulative mineralization of organic carbon and sucrase. The organic carbon mineralization rate was negatively correlated with the accumulated organic carbon mineralization, catalase, and sucrase. The cumulative mineralization of organic carbon was positively correlated with catalase, urease and sucrase. Meanwhile, urease was positively correlated with sucrase.

4. Discussion

4.1. Effect of biochar on soil physicochemical properties

The application of OBC and OBC-Mg significantly increased soil pH compared to CK. The increase in pH after OBC application may be due to the fact that biochar contains soluble organic and inorganic bases, making it highly alkaline (Fidel et al., 2017; Shi et al., 2019). Applying biochar to acidic soil neutralized soil acidity, thus increasing soil pH. Whereas the increase in pH after OBC-Mg application was greater than that of OBC, probably due to the fact that the Mg-modified biochar surface was loaded with more Mg^{2+} and other alkaline cations, which are converted to oxides, hydroxides and carbonates after pyrolysis, resulting in higher pH of Mg-modified biochar and thus better increase in soil pH. Similarly, Khan et al. (2022) used pristine and Mg-modified rice straw biochar applied to

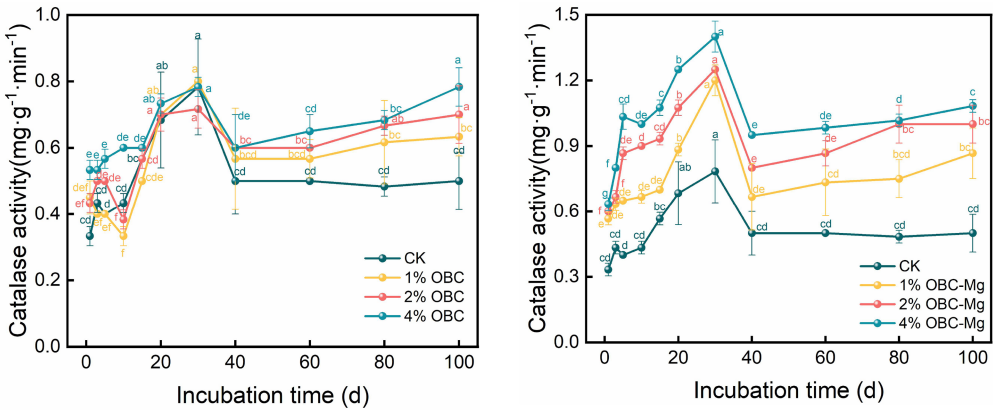

FIGURE 12
Changes in soil catalase activity after the amendment of OBC and OBC-Mg.

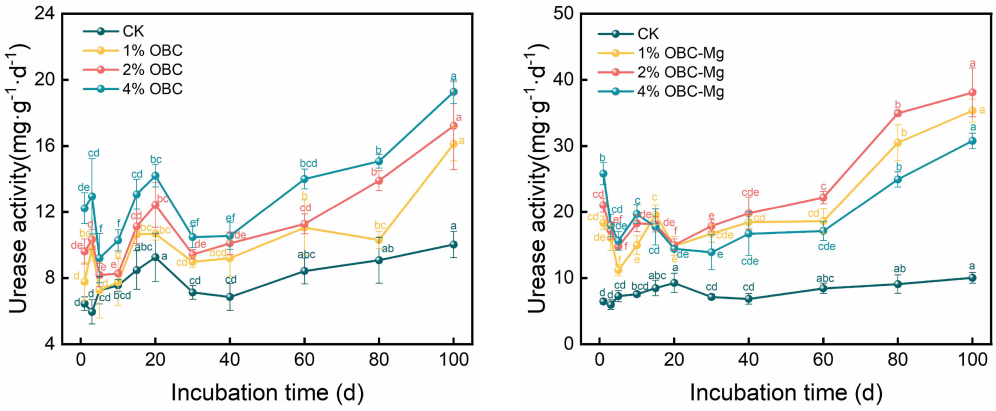

FIGURE 13
Changes in soil urease activity after the amendment of OBC and OBC-Mg.

the soil and an increase in soil pH occurred, which is consistent with the results of this study. In this study, the application of OBC and OBC-Mg to citrus soils significantly increased soil pH, which was mainly due to the alkalinity of biochar, indicating that both applications could improve soil acidity.

Cation exchange capacity (CEC) reflects the amount of negative charge in the soil that can be neutralized by exchangeable cations such as Mg and Ca (Wu et al., 2020). Application of OBC-Mg to citrus orchard soils increased the CEC content of the soil, partly because of the adsorption of oxides such as Al and Fe by biochar and the decrease in the zero point charge of the soil (Hailegnaw et al., 2019), and partly because of the presence of oxygen-containing functional groups on the surface of biochar (Yadav et al., 2019). The application of OBC to citrus orchard soils reduced the CEC content of the soil, and a similar phenomenon was found in the study of Seokjoon's (2005), which suggested that the reduction of CEC after biochar application might be mainly due to the enrichment of humic and xanthic acids in the soil by organic matter, thus blocking the internal pores of the biochar from the next physical sorption step and thus reducing the CEC. OBC and OBC-Mg applied to the soil differed in their effect on cation exchange mainly due to the higher Mg content in OBC-Mg, which can neutralize more with negative charges and increase soil CEC. The effect of OBC-Mg on pH and CEC in this study was significantly positively correlated, with higher pH and higher CEC in OBC-Mg soil, which is consistent with the findings of Heikkinen et al. (2019). Also correlation analysis showed that soil CEC was significantly negatively correlated with cumulative mineralization, indicating that the elevated cumulative mineralization of soil organic carbon by OBC and OBC-Mg applied to the soil led to a decrease in CEC.

A study by Li, S. et al. (2018) found that the application of biochar to the soil was effective in reducing N leaching and increasing K content. The application of OBC and OBC-Mg resulted in a significant increase in AP content, which is consistent with the findings of other studies. Kamran et al. (2018) applied three types of biochar, chicken manure bochar, pig manure biochar and peat moss biochar to soil, the results showed a significant increase in soil AP, and the change in AP content was related to the amount of biochar applied. The increase in AP was due to three reasons. On the one hand, biochar contains a certain amount of phosphorus itself and thus directly increases soil effective phosphorus (Hong and Lu, 2018). On the other hand, biochar increases soil pH and changes the activity of cations such as Al^{3+}, Fe^{3+}, and Ca^{2+}, thus reducing P adsorption or increasing P desorption, making phosphorus more effective (Yang and Lu, 2022). Finally, because biochar applied to the soil, causing changes in the soil microbial environment

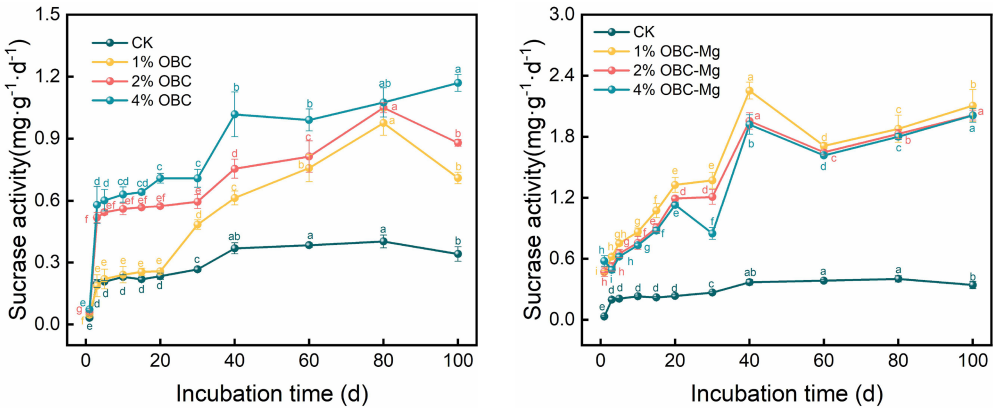

FIGURE 14
Changes in soil sucrase activity after the amendment of OBC and OBC-Mg.

and increasing the phosphorus fixation capacity of the soil (Tian et al., 2021). The main reason of the decrease in AP content with increasing incubation time is that the fixation of phosphorus by the soil leads to a decrease in effective phosphorus (Kahura et al., 2018). The application of alkaline biochar in acidic soils can better improve the bioeffectiveness of phosphorus (Chintala et al., 2014), and the difference in the effect of OBC and OBC-Mg application to soil on AP content may be due to the inconsistent chemical composition and surface characteristics of biochar. In this study, the application of OBC-Mg could better increase the content of fast-acting phosphorus, mainly because OBC-Mg was loaded with more cations on the surface, which increased the effectiveness of phosphorus. Furthermore, it is also reported that biochar can improve the relative abundance of proteobacteria in soil which plays a significant role in improving soil properties (Zhang et al., 2022). Correlation analysis showed that AP content was significantly and negatively correlated with AK content, indicating that AP content increased with the decrease of AK in the soil.

Citrus peel biochar (OBC) application to soil significantly increased soil AK content and increased with increasing application rate. This is consistent with the findings of Yao et al. (2021), which found a significant increase in AK after biochar application in heavily salinized paddy fields. The increase in AK content may be due to the interaction of biochar with soil minerals that affects the release of nutrients from the soil, which results in an increase in AK (El-Naggar et al., 2019). Analysis of the EDS of biochar showed that the K content of Mg-modified biochar was significantly lower, which led to a better increase of the AK content by OBC, while the effect of OBC-Mg on AK was smaller.

4.2. Effect of biochar on soil organic carbon mineralization in citrus orchards

The stimulatory effect of biochar on soil CO_2 emissions is governed by various factors, such as biochar physicochemical properties, biochar stability and soil properties (Song et al., 2019), and microorganisms in biochar may also affect soil CO_2 emissions (Wang, L. et al., 2021). Some studies have shown that, the more biochar applied, the faster respiration rate of soil microorganisms was and the more total CO_2 released at the beginning of incubation (Steiner et al., 2008). And when the amount of biochar applied is higher, soil microorganisms are more likely to decompose water-soluble organic matter in biochar for microbial activity, thus releasing more CO_2 (Zhang et al., 2020). The rate of soil organic carbon mineralization in different treatments has a similar pattern. And in this study, the application of OBC and OBC-Mg in citrus orchard soil promoted CO_2 emission in the early incubation period, then decreased and stabilized with increasing incubation time, it is consistent with the findings of Ameloot et al. (2013). This is due to the application of biochar to the soil, which stimulates the native carbon pool, and the stimulation of soil organisms leading to the biodegradation of biochar components, resulting in enhanced CO_2 release (Blagodatskaya and Kuzyakov, 2008). Similarly, Orlova et al. (2019) made biochar from birch and poplar wood at 550°C and injected it into the soil, showing that 1% biochar increased mineralization by 15–18%, while a study by El-Naggar et al. (2018) showed that rice straw biochar and sludge biochar promoted mineralization for 3 and 1.5 months. Whereas CO_2 emissions decreased in the later stages of incubation due to biochar, which added higher carbon content and richer aromatic structure, thus enhancing resistance to biodegradation and ultimately leading to a potential negative excitation effect. Also, the inhibition of soil mineralization by biochar generally occurred in the later stages of incubation (Rasul et al., 2022), which is consistent with our findings. Similar effective reduction of soil CO_2 emissions by biochar has been reported in other studies (Hua et al., 2014; Rubin et al., 2020). The cumulative mineralization of organic carbon was significantly and positively correlated with catalase, urease, and sucrase activities. In this study, the stimulation of microbial activity in the soil led to the increase in soil organic carbon mineralization, which resulted in an increase in soil enzyme activity.

4.3. Effect of biochar on different carbon fractions in citrus orchard soils

The application of OBC and OBC-Mg to citrus orchard soils not only increased soil SOC content, but also showed a positive correlation with the percentage of biochar application, which is consistent with the findings of Novak et al. (2010). The increase in soil SOC content may be due to the high carbon content of biochar itself, and the application of biochar to soil is equivalent to the application of exogenous organic carbon (Li, Y. et al., 2018). The refractory nature of biochar allows it to persist in the soil, which contributes to the increase in organic carbon (Rasul et al., 2022). Similarly, Dong et al. (2018) applied different amounts of rice husk and cotton seed hull biochar to the soil to observe

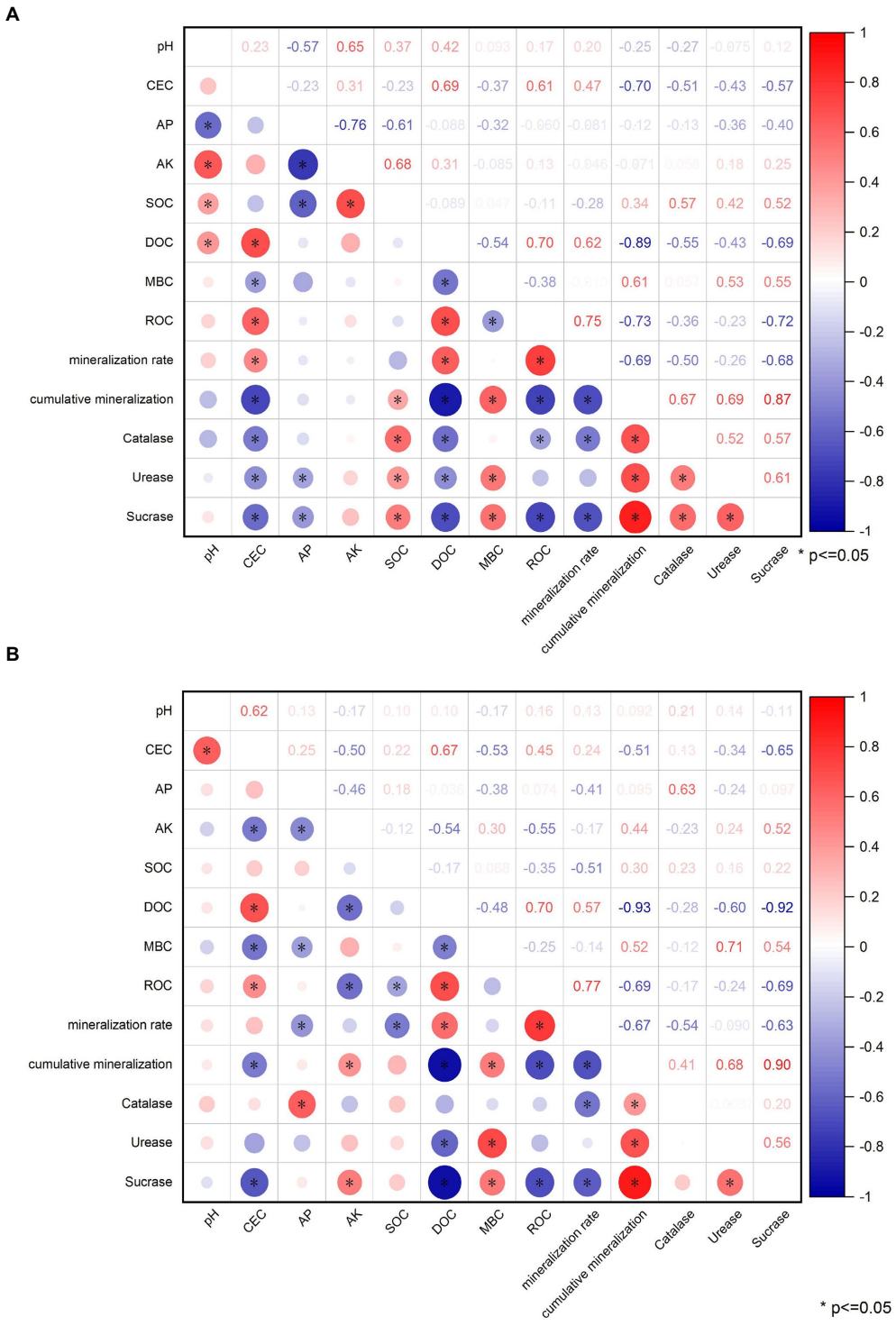

FIGURE 15
Correlation between physical and chemical properties, carbon composition, enzyme activity and mineralization of **(A)** OBC-Mg and **(B)** OBC-Mg.

organic carbon changes and showed that biochar significantly increased SOC content and SOC increased with increasing biochar amount.

Soil microbial biomass carbon (MBC), DOC, and ROC are reactive organic carbon in soils and usually respond rapidly to soil changes (Wang, X. et al., 2021). Soil MBC is derived from the hydrolysis of soil organic matter, soil microorganisms themselves and their metabolites (Zhang et al., 2018). In this study, application of OBC and OBC-Mg to citrus orchard soil increased or decreased MBC content compared to CK. The decrease in MBC in the early stages of incubation was mainly due to the depletion and mineralization of unstable components of organic carbon, resulting in a decrease in MBC (Huang et al., 2021). While the gradual increase in MBC in the later stages may be due to a stable and less disturbed soil environment in the later stages, where microbial activity increases leading to an increase in MBC. In this study,

the MBC was significantly and positively correlated with the cumulative mineralization of organic carbon, indicating that the mineralization of soil organic carbon also affects the MBC.

Soil dissolved organic carbon (DOC) is the most active component of SOC and an important source of organic carbon and an important indicator of soil microbial effectiveness (Hu et al., 2022). In this study, application of OBC and OBC-Mg to citrus orchard soil increased DOC content and showed an overall decreasing trend with increasing incubation time. The increase in DOC content may be due to the release of the active organic carbon fraction from biochar into the soil after biochar application. This induced the conversion of SOC to DOC, thus leading to an increase in soil DOC content (Ye and Horwath, 2017). And the decrease in DOC content with increasing incubation time is because the stabilized organic carbon from biochar makes the soil SOC increase. And the decomposed active organic carbon, leading to a decrease in DOC content (Zhang et al., 2017). Compared with OBC, OBC-Mg has a better effect on the enhancement of soil DOC content mainly because OBC-Mg has a better effect on the improvement of soil acidity. And the increase of soil pH leads to the deprotonation process of weakly acidic functional groups in soluble organic carbon molecules. This increases the surface charge density of soil soluble organic carbon molecules and enhances hydrophilicity, promoting the solubilization of soil soluble organic carbon (Smebye et al., 2016). In this study, DOC content was significantly and negatively correlated with the accumulated mineralization of organic carbon.

Soil readily oxidized organic carbon (ROC) is the more reactive and easily oxidized carbon fraction of the organic carbon pool (Yang et al., 2017). In this study, OBC and OBC-Mg increased the ROC content in the soil compared to CK, and the ROC content decreased with increasing incubation time. ROC is the same active organic carbon as DOC, and the reason for its change is similar to DOC. Biochar applied to citrus orchard soil increased the soil microbial activity leading to an increase in ROC (Abiven et al., 2015). With increasing incubation time, the active organic carbon of biochar was decomposed and the ROC content decreased. In this study, the ROC content was significantly and negatively correlated with the cumulative mineralization of organic carbon. The ROC content decreased as the cumulative mineralization of organic carbon increased, which is consistent with the changes in DOC in the previous paper. This indicated that the active organic carbon components such as soil DOC and ROC are susceptible to the cumulative mineralization of organic carbon.

4.4. Effect of biochar on soil enzyme activity in citrus orchards

Soil enzyme activity is an important biological indicator of soil quality, and changes in microbial activity are mainly due to changes in the physicochemical properties of the soil. Biochar surface has a high potential to adsorb organic molecules, including enzymes and substrates, thus altering enzyme activity (Foster et al., 2018). Application of OBC and OBC-Mg to citrus orchard soil resulted in a significant increase in soil enzyme activity compared to the CK. Catalase is an important enzyme that indicates the redox potential of soil (Yang et al., 2016). And biochar as an additional carbon source effectively improves the survival environment of microorganisms in soil by providing more nutrients and increasing the number and activity of microorganisms, which leads to more secretion of catalase by microorganisms. Masto et al. (2013b) applied water hyacinth biochar to soil, the results showed that catalase activity increased with the amount of biochar applied, which is consistent with the findings of this study. The effect of OBC on soil catalase was less than that of OBC-Mg because catalase is stable and not easily affected by environmental conditions, but OBC-Mg caused changes in the physicochemical properties of biochar and increased the impact on the soil environment (Yang et al., 2016). The catalase activity of the 1% OBC and 2% OBC fractions was lower than that of CK on 0–30 days of incubation, which may be due to the large availability of soil organic matter and microbial community in the pre-culture period, resulting in lower catalase activity (Ullah et al., 2020). Soil urease catalyzes the hydrolysis of phthalate bonds in organic molecules and promotes the conversion of soil organic N to active N (Gao et al., 2017). Application of OBC and OBC-Mg significantly increased urease activity compared to CK because urease activity is associated with microbial growth and the application of biochar stimulated soil microbial activity, thus leading to an increase in soil urease activity (Yadav et al., 2019). Jing et al. (2020) studied the application of three types of straw biochar from wheat, rice, and maize to soil and showed an increase in urease activity of 42.5–94.2%. Both biochar applied to soil also increased soil sucrase activity, this is because sucrose can be broken down by sucrase into glucose and fructose. Glucose and fructose are important carbon source for microorganisms, and the higher carbon to nitrogen ratio in soil is, the more enzyme substrate it can provide, thus increasing sucrase activity (Tang et al., 2022). Meanwhile, catalase, urease and sucrase activities were all significantly and positively correlated with the cumulative mineralization of soil organic carbon, and soil enzyme activity increased with the increase in cumulative mineralization of organic carbon.

5. Conclusion

In this study, we investigated the effects of OBC and OBC-Mg on soil organic carbon mineralization in citrus orchards by applying them to citrus orchard soils at different rate. The results showed that there was a significant difference between OBC and OBC-Mg on soil organic carbon mineralization, and OBC-Mg significantly increased soil organic carbon content with a significantly higher enhancement effect than OBC. 1% OBC-Mg reduced soil organic carbon mineralization and had good potential for soil carbon sequestration and reduction. Meanwhile, with the increase of cumulative soil organic carbon mineralization, OBC-Mg treatment more significantly increased the activities of soil catalase, urease and sucrase than OBC treatment. In conclusion, Mg-modified citrus peel biochar had better carbon sequestration effect on citrus orchard soil. We will continue our metagenomic measurements and conduct an in-depth mechanistic study on the application of Mg-modified citrus peel biochar to citrus soil.

Data availability statement

The raw data supporting the conclusions of this article will be made available by the authors, without undue reservation.

Author contributions

LH: conceptualization and data curation. RH: software, writing original draft preparation and data curation. LZ, RQ, and XH: data curation and supervision. HD: writing review and editing. KL: funding

acquisition. All authors contributed to the article and approved the submitted version.

Funding

This work was supported by Guangxi Surface project, grant no. 2022GXNSFAA035555. The Key Laboratory of Ecology of Rare and Endangered Species and Environmental Protection (Guangxi Normal University), Ministry of Education, China, grant no. ERESEP2022Z13; Open Fund of Key Laboratory of Geospatial Technology for the Middle and Lower Yellow River Regions (Henan University), Ministry of Education, grant no. GTYR202103; Guangxi Key Research and development Program, grant no. AB22080097.

Acknowledgments

We thank Yulong River Citrus Planting Core Demonstration Base in Yangshuo County, Guilin for providing us with experimental materials and all the people who helped us during the experiment.

Conflict of interest

The authors declare that the research was conducted in the absence of any commercial or financial relationships that could be construed as a potential conflict of interest.

Publisher's note

Supplementary material

The Supplementary material for this article can be found online at: https://www.frontiersin.org/articles/10.3389/fmicb.2023.1109272/full#supplementary-material

References

Abhishek, K., Shrivastava, A., Vimal, V., Gupta, A. K., Bhujbal, S. K., Biswas, J. K., et al. (2022). Biochar application for greenhouse gas mitigation, contaminants immobilization and soil fertility enhancement: a state-of-the-art review. *Sci. Total Environ.* 853:158562. doi: 10.1016/j.scitotenv.2022.158562

Abiven, S., Hund, A., Martinsen, V., and Cornelissen, G. (2015). Biochar amendment increases maize root surface areas and branching: a shovelomics study in Zambia. *Plant Soil* 395, 45–55. doi: 10.1007/s11104-015-2533-2

Ameloot, N., Graber, E. R., Verheijen, F. G. A., and De Neve, S. (2013). Interactions between biochar stability and soil organisms: review and research needs. *Eur. J. Soil Sci.* 64, 379–390. doi: 10.1111/ejss.12064

Bashir, S., Hussain, Q., Zhu, J., Fu, Q., Houben, D., and Hu, H. (2020). Efficiency of KOH-modified rice straw-derived biochar for reducing cadmium mobility, bioaccessibility and bioavailability risk index in red soil. *Pedosphere* 30, 874–882. doi: 10.1016/S1002-0160(20)60043-1

Blagodatskaya, E., and Kuzyakov, Y. (2008). Mechanisms of real and apparent priming effects and their dependence on soil microbial biomass and community structure: critical review. *Biol. Fertil. Soils* 45, 115–131. doi: 10.1007/s00374-008-0334-y

Chen, W., Meng, J., Han, X., Lan, Y., and Zhang, W. (2019). Past, present, and future of biochar. *Biochar.* 1, 75–87. doi: 10.1007/s42773-019-00008-3

Chen, H., Wang, Y., Zhang, L., Luo, L., Ye, X., Li, Y., et al. (2019). Advances in magnesium nutritional status and its mechanisms of physiological and molecule in citrus. *J. Fruit Sci.* 36, 1578–1590. doi: 10.13925/j.cnki.gsxb.20190210

Chintala, R., Schumacher, T. E., McDonald, L. M., Clay, D. E., Malo, D. D., Papiernik, S.-K., et al. (2014). Phosphorus sorption and availability from biochars and soil/biochar mixtures. *CLEAN Soil Air Water* 42, 626–634. doi: 10.1002/clen.201300089

Deng, H., Zhang, J., Huang, R., Wang, W., Meng, M., Hu, L., et al. (2022). Adsorption of malachite green and Pb^{2+} by $KMnO_4^-$Modified biochar: insights and mechanisms. *Sustainability* 14. doi: 10.3390/su14042040

Dong, X., Singh, B. P., Li, G., Lin, Q., and Zhao, X. (2018). Biochar application constrained native soil organic carbon accumulation from wheat residue inputs in a long-term wheat-maize cropping system. *Agric. Ecosyst. Environ.* 252, 200–207. doi: 10.1016/j.agee.2017.08.026

Du, Y., Guo, X., Li, J., Liu, Y., Luo, J., Liang, Y., et al. (2022). Elevated carbon dioxide stimulates nitrous oxide emission in agricultural soils: a global meta-analysis. *Pedosphere* 32, 3–14. doi: 10.1016/S1002-0160(21)60057-7

El-Naggar, A., El-Naggar, A. H., Shaheen, S. M., Sarkar, B., Chang, S. X., Tsang, D. C. W., et al. (2019). Biochar composition-dependent impacts on soil nutrient release, carbon mineralization, and potential environmental risk: a review. *J. Environ. Manag.* 241, 458–467. doi: 10.1016/j.jenvman.2019.02.044

El-Naggar, A., Lee, S. S., Awad, Y. M., Yang, X., Ryu, C., Rizwan, M., et al. (2018). Influence of soil properties and feedstocks on biochar potential for carbon mineralization and improvement of infertile soils. *Geoderma* 332, 100–108. doi: 10.1016/j.geoderma.2018.06.017

Fidel, R. B., Laird, D. A., Thompson, M. L., and Lawrinenko, M. (2017). Characterization and quantification of biochar alkalinity. *Chemosphere* 167, 367–373. doi: 10.1016/j.chemosphere.2016.09.151

Foster, E., Fogle, E., and Cotrufo, M. (2018). Sorption to biochar impacts β-glucosidase and phosphatase enzyme activities. *Agriculture* 8. doi: 10.3390/agriculture8100158

Gan, H. Y., Schöning, I., Schall, P., Ammer, C., and Schrumpf, M. (2020). Soil organic matter mineralization as driven by nutrient stoichiometry in soils under differently managed Forest stands. *Front. For. Global Change* 3:99. doi: 10.3389/ffgc.2020.00099

Gao, S., Hoffman-Krull, K., and DeLuca, T. H. (2017). Soil biochemical properties and crop productivity following application of locally produced biochar at organic farms on Waldron Island. *Biogeochemistry* 136, 31–46. doi: 10.1007/s10533-017-0379-9

Hailegnaw, N. S., Mercl, F., Pračke, K., Száková, J., and Tlustoš, P. (2019). Mutual relationships of biochar and soil pH, CEC, and exchangeable base cations in a model laboratory experiment. *J. Soils Sediments* 19, 2405–2416. doi: 10.1007/s11368-019-02264-z

Heikkinen, J., Keskinen, R., Soinne, H., Hyväluoma, J., Nikama, J., Wikberg, H., et al. (2019). Possibilities to improve soil aggregate stability using biochars derived from various biomasses through slow pyrolysis, hydrothermal carbonization, or torrefaction. *Geoderma* 344, 40–49. doi: 10.1016/j.geoderma.2019.02.028

Hong, C., and Lu, S. (2018). Does biochar affect the availability and chemical fractionation of phosphate in soils? *Environ. Sci. Pollut. Res. Int.* 25, 8725–8734. doi: 10.1007/s11356-018-1219-8

Hu, L., Huang, R., Deng, H., Li, K., Peng, J., Zhou, L., et al. (2022). Effects of different intercropping methods on soil organic carbon and aggregate stability in sugarcane field. *Pol. J. Environ. Stud.* 31, 3587–3596. doi: 10.15244/pjoes/147187

Hu, L., Li, S., Li, K., Huang, H., Wan, W., Huang, Q., et al. (2020). Effects of two types of straw biochar on the mineralization of soil organic carbon in farmland. *Sustainability* 12. doi: 10.3390/su122410586

Hua, L., Lu, Z., Ma, H., and Jin, S. (2014). Effect of biochar on carbon dioxide release, organic carbon accumulation, and aggregation of soil. *Environ. Prog. Sustain. Energy* 33, 941–946. doi: 10.1002/ep.11867

Huang, R., Lan, T., Song, X., Li, J., Ling, J., Deng, O., et al. (2021). Soil labile organic carbon impacts C:N:P stoichiometry in urban park green spaces depending on vegetation types and time after planting. *Appl. Soil Ecol.* 163:103926. doi: 10.1016/j.apsoil.2021.103926

Huang, R., Tian, D., Liu, J., Lv, S., He, X., and Gao, M. (2018). Responses of soil carbon pool and soil aggregates associated organic carbon to straw and straw-derived biochar addition in a dryland cropping mesocosm system. *Agric. Ecosyst. Environ.* 265, 576–586. doi: 10.1016/j.agee.2018.07.013

Jiao, Y., Wang, T., He, M., Liu, X., Lin, C., and Ouyang, W. (2022). Simultaneous stabilization of Sb and as co-contaminated soil by FeMg modified biochar. *Sci. Total Environ.* 830:154831. doi: 10.1016/j.scitotenv.2022.154831

Jien, S. H., Chen, W. C., Ok, Y. S., Awad, Y. M., and Liao, C. S. (2018). Short-term biochar application induced variations in C and N mineralization in a compost-amended tropical soil. *Environ. Sci. Pollut. Res. Int.* 25, 25715–25725. doi: 10.1007/s11356-017-9234-8

Jing, Y., Zhang, Y., Han, I., Wang, P., Mei, Q., and Huang, Y. (2020). Effects of different straw biochars on soil organic carbon, nitrogen, available phosphorus, and enzyme activity in paddy soil. *Sci. Rep.* 10:8837. doi: 10.1038/s41598-020-65796-2

Kahura, M. W., Min, H., Kim, M. S., and Kim, J. G. (2018). Assessing phosphorus availability in a high pH, biochar amended soil under inorganic and organic fertilization. *Ecol. Resilient Infrastruct.* 5, 11–18. doi: 10.1016/j.scitotenv.2022.158562

Kamran, M. A., Jiang, J., Li, J. Y., Shi, R. Y., Mehmood, K., Baquy, M. A. A., et al. (2018). Amelioration of soil acidity, Olsen-P, and phosphatase activity by manure- and peat-derived biochars in different acidic soils. *Arab. J. Geosci.* 11:272. doi: 10.1007/s12517-018-3616-1

Khan, M. N., Li, D., Shah, A., Huang, J., Zhang, L., Nunez-Delgado, A., et al. (2022). The impact of pristine and modified rice straw biochar on the emission of greenhouse gases from a red acidic soil. *Environ. Res.* 208:112676. doi: 10.1016/j.envres.2022.112676

Korai, P. K., Xia, X., Liu, X., Bian, R., Omondi, M. O., Nahayo, A., et al. (2018). Extractable pool of biochar controls on crop productivity rather than greenhouse gas emission from a rice paddy under rice-wheat rotation. *Sci. Rep.* 8:802. doi: 10.1038/s41598-018-19331-z

Kuo, Y. L., Lee, C. H., and Jien, S. H. (2020). Reduction of nutrient leaching potential in coarse-textured soil by using biochar. *Water* 12:2012. doi: 10.3390/w12072012

Li, Y., Li, Y., Chang, S. X., Yang, Y., Fu, S., Jiang, P., et al. (2018). Biochar reduces soil heterotrophic respiration in a subtropical plantation through increasing soil organic carbon recalcitrancy and decreasing carbon-degrading microbial activity. *Soil Biol. Biochem.* 122, 173–185. doi: 10.1016/j.soilbio.2018.04.019

Li, R., Wang, J. J., Zhou, B., Awasthi, M. K., Ali, A., Zhang, Z., et al. (2016). Enhancing phosphate adsorption by mg/Al layered double hydroxide functionalized biochar with different mg/Al ratios. *Sci. Total Environ.* 559, 121–129. doi: 10.1016/j.scitotenv.2016.03.151

Li, R., Wang, J. J., Zhou, B., Zhang, Z., Liu, S., Lei, S., et al. (2017). Simultaneous capture removal of phosphate, ammonium and organic substances by MgO impregnated biochar and its potential use in swine wastewater treatment. *J. Clean. Prod.* 147, 96–107. doi: 10.1016/j.jclepro.2017.01.069

Li, S., Zhang, Y., Yan, W., and Shangguan, Z. (2018). Effect of biochar application method on nitrogen leaching and hydraulic conductivity in a silty clay soil. *Soil Tillage Res.* 183, 100–108. doi: 10.1016/j.still.2018.06.006

Liu, Z., Tang, J., Ren, X., and Schaeffer, S. M. (2021). Effects of phosphorus modified nZVI-biochar composite on emission of greenhouse gases and changes of microbial community in soil. *Environ. Pollut.* 274:116483. doi: 10.1016/j.envpol.2021.116483

Lu, Y., Silveira, M. L., O'Connor, G. A., Vendramini, J. M. B., Erickson, J. E., Li, Y. C., et al. (2020). Biochar impacts on nutrient dynamics in a subtropical grassland soil: 1. Nitrogen and phosphorus leaching. *J. Environ. Qual.* 49, 1408–1420. doi: 10.1002/jeq2.20139

Masto, R. E., Ansari, M. A., George, J., Selvi, V. A., and Ram, L. C. (2013a). Co-application of biochar and lignite fly ash on soil nutrients and biological parameters at different crop growth stages of Zea mays. *Ecol. Eng.* 58, 314–322. doi: 10.1016/j.ecoleng.2013.07.011

Masto, R. E., Kumar, S., Rout, T. K., Sarkar, P., George, J., and Ram, L. C. (2013b). Biochar from water hyacinth (Eichornia crassipes) and its impact on soil biological activity. *Catena* 111, 64–71. doi: 10.1016/j.catena.2013.06.025

Novak, J. M., Busscher, W. J., Watts, D. W., Laird, D. A., Ahmedna, M. A., and Niandou, M. A. S. (2010). Short-term CO_2 mineralization after additions of biochar and switchgrass to a typic Kandiudult. *Geoderma* 154, 281–288. doi: 10.1016/j.geoderma.2009.10.014

Oo, A. Z., Sudo, S., Akiyama, H., Win, K. T., Shibata, A., Yamamoto, A., et al. (2018). Effect of dolomite and biochar addition on N_2O and CO_2 emissions from acidic tea field soil. *PLoS One* 13:e0192235. doi: 10.1371/journal.pone.0192235

Orlova, N., Abakumov, E., Orlova, E., Yakkonen, K., and Shahnazarova, V. (2019). Soil organic matter alteration under biochar amendment: study in the incubation experiment on the podzol soils of the Leningrad region (Russia). *J. Soils Sediments* 19, 2708–2716. doi: 10.1007/s11368-019-02256-z

Pei, J., Zhuang, S., Cui, J., Li, J., Li, B., Wu, J., et al. (2017). Biochar decreased the temperature sensitivity of soil carbon decomposition in a paddy field. *Agric. Ecosyst. Environ.* 249, 156–164. doi: 10.1016/j.agee.2017.08.029

Perez-Quezada, J. F., Urrutia, P., Olivares-Rojas, J., Meijide, A., Sánchez-Cañete, E. P., et al. (2021). Long term effects of fire on the soil greenhouse gas balance of an old-growth temperate rainforest. *Sci. Total Environ.* 755:142442. doi: 10.1016/j.scitotenv.2020.142442

Qiao, J., Li, X., and Shi, R. (2021). Research on the industry of three citrus producing areas in China – taking Guangxi, Hunan and Hubei as examples. *Yunnan Sci. Technol. Manag.* 01, 45–49. doi: 10.19774/j.cnki.53-1085.2021.01.012

Rasul, M., Cho, J., Shin, H. S., and Hur, J. (2022). Biochar-induced priming effects in soil via modifying the status of soil organic matter and microflora: a review. *Sci. Total Environ.* 805:150304. doi: 10.1016/j.scitotenv.2021.150304

Rong, G., Zhang, X., Wu, H., Ge, N., Yao, Y., and Wei, X. (2021). Changes in soil organic carbon and nitrogen mineralization and their temperature sensitivity in response to afforestation across China's loess plateau. *Catena* 202:105226. doi: 10.1016/j.catena.2021.105226

Rubin, R. L., Anderson, T. R., and Ballantine, K. A. (2020). Biochar simultaneously reduces nutrient leaching and greenhouse gas emissions in restored wetland soils. *Wetlands* 40, 1981–1991. doi: 10.1007/s13157-020-01380-8

Sarma, B., Borkotoki, B., Narzari, R., Kataki, R., and Gogoi, N. (2017). Organic amendments: effect on carbon mineralization and crop productivity in acidic soil. *J. Clean. Prod.* 152, 157–166. doi: 10.1016/j.jclepro.2017.03.124

Seokjoon, K. (2005). Effect of natural organic substances on the surface and adsorptive properties of environmental black carbon (char): pseudo pore blockage by model lipid components and its implications for N2-probed surface properties of natural sorbents. *Environ. Sci. Technol.* 39, 7932–7939. doi: 10.1021/es050976h

Shan, R., Li, W., Chen, Y., and Sun, X. (2022). Effects of mg-modified biochar on the bioavailability of cadmium in soil. *Bioresources* 15, 8008–8025. doi: 10.15376/biores.15.4.8008-8025

Shi, R. Y., Li, J. Y., Ni, N., and Xu, R. K. (2019). Understanding the biochar's role in ameliorating soil acidity. *J. Integr. Agric.* 18, 1508–1517. doi: 10.1016/S2095-3119(18)62148-3

Smebye, A., Alling, V., Vogt, R. D., Gadmar, T. C., and Mulder, J. (2016). Cornelissen, G., et al. Biochar amendment to soil changes dissolved organic matter content and composition. *Chemosphere* 142, 100–105, doi: 10.1016/j.chemosphere.2015.04.087.

Song, Y., Li, Y., Cai, Y., Fu, S., Luo, Y., Wang, H., et al. (2019). Biochar decreases soil N_2O emissions in Moso bamboo plantations through decreasing labile N concentrations, N-cycling enzyme activities and nitrification/denitrification rates. *Geoderma* 348, 135–145. doi: 10.1016/j.geoderma.2019.04.025

Stefaner, K., Ghosh, S., Mohd Yusof, M. L., Ibrahim, H., Leitgeb, E., Schindlbacher, A., et al. (2021). Soil greenhouse gas fluxes from a humid tropical forest and differently managed urban parkland in Singapore. *Sci. Total Environ.* 786:147305. doi: 10.1016/j.scitotenv.2021.147305

Steiner, C., Das, K. C., Garcia, M., Förster, B., and Zech, W. (2008). Charcoal and smoke extract stimulate the soil microbial community in a highly weathered xanthic Ferralsol. *Pedobiologia* 51, 359–366. doi: 10.1016/j.pedobi.2007.08.002

Sun, X., Han, X., Ping, F., Zhang, L., Zhang, K., Chen, M., et al. (2018). Effect of rice-straw biochar on nitrous oxide emissions from paddy soils under elevated CO_2 and temperature. *Sci. Total Environ.* 628-629, 1009–1016.

Tang, B., Xu, H., Song, F., Ge, H., Chen, L., Yue, S., et al. (2022). Effect of biochar on immobilization remediation of cd rectanglecontaminated soil and environmental quality. *Environ. Res.* 204:111840. doi: 10.1016/j.envres.2021.111840

Tian, J., Kuang, X., Tang, M., Chen, X., Huang, F., Cai, Y., et al. (2021). Biochar application under low phosphorus input promotes soil organic phosphorus mineralization by shifting bacterial phoD gene community composition. *Sci. Total Environ.* 779:146556. doi: 10.1016/j.scitotenv.2021.146556

Ullah, S., Liang, H., Ali, I., Zhao, Q., Iqbal, A., Wei, S., et al. (2020). Biochar coupled with contrasting nitrogen sources mediated changes in carbon and nitrogen pools, microbial and enzymatic activity in paddy soil. *J. Saudi Chem. Soc.* 24, 835–849. doi: 10.1016/j.jscs.2020.08.008

Wang, L., Gao, C., Yang, K., Sheng, Y., Xu, J., Zhao, Y., et al. (2021). Effects of biochar aging in the soil on its mechanical property and performance for soil CO_2 and N_2O emissions. *Sci. Total Environ.* 782:146824. doi: 10.1016/j.scitotenv.2021.146824

Wang, X., Li, W., Xiao, Y., Cheng, A., Shen, T., Zhu, M., et al. (2021). Abundance and diversity of carbon-fixing bacterial communities in karst wetland soil ecosystems. *Catena* 204:105418. doi: 10.1016/j.catena.2021.105418

Wang, H., Ren, T., Muller, K., Van Zwieten, L., Wang, H., Feng, H., et al. (2021). Soil type regulates carbon and nitrogen stoichiometry and mineralization following biochar or nitrogen addition. *Sci. Total Environ.* 753:141645. doi: 10.1016/j.scitotenv.2020.141645

Wu, J., Li, Z., Huang, D., Liu, X., Tang, C., Parikh, S. J., et al. (2020). A novel calcium-based magnetic biochar is effective in stabilization of arsenic and cadmium co-contamination in aerobic soils. *J. Hazard. Mater.* 387:122010. doi: 10.1016/j.jhazmat.2019.122010

Wu, L., Wei, C., Zhang, S., Wang, Y., Kuzyakov, Y., and Ding, X. (2019). MgO-modified biochar increases phosphate retention and rice yields in saline-alkaline soil. *J. Clean. Prod.* 235, 901–909. doi: 10.1016/j.jclepro.2019.07.043

Wu, S., Zhuang, G., Bai, Z., Cen, Y., Xu, S., Sun, H., et al. (2018). Mitigation of nitrous oxide emissions from acidic soils by bacillus amyloliquefaciens, a plant growth-promoting bacterium. *Glob. Chang. Biol.* 24, 2352–2365. doi: 10.1111/gcb.14025

Xie, G. X., Huang, Q. T., Yang, S. E., Qin, Z. L., Liu, L. H., and Deng, T. H. (2021). Extraction of citrus planting plots based on medium-high different images. *J. Southern Agric.* 52, 3454–3462.

Xu, H., Shao, H., and Lu, Y. (2019). Arbuscular mycorrhiza fungi and related soil microbial activity drive carbon mineralization in the maize rhizosphere. *Ecotoxicol. Environ. Saf.* 182:109476. doi: 10.1016/j.ecoenv.2019.109476

Yadav, V., Jain, S., Mishra, P., Khare, P., Shukla, A. K., Karak, T., et al. (2019). Amelioration in nutrient mineralization and microbial activities of sandy loam soil by short term field aged biochar. *Appl. Soil Ecol.* 138, 144–155. doi: 10.1016/j.apsoil.2019.01.012

Yang, X., Liu, J., McGrouther, K., Huang, H., Lu, K., Guo, X., et al. (2016). Effect of biochar on the extractability of heavy metals (cd, cu, pb, and Zn) and enzyme activity in soil. *Environ. Sci. Pollut. Res. Int.* 23, 974–984. doi: 10.1007/s11356-015-4233-0

Yang, C., and Lu, S. (2022). Straw and straw biochar differently affect phosphorus availability, enzyme activity and microbial functional genes in an Ultisol. *Sci. Total Environ.* 805:150325. doi: 10.1016/j.scitotenv.2021.150325

Yang, X., Wang, D., Lan, Y., Meng, J., Jiang, L., Sun, Q., et al. (2017). Labile organic carbon fractions and carbon pool management index in a 3-year field study with biochar amendment. *J. Soils Sediments* 18, 1569–1578. doi: 10.1007/s11368-017-1874-2

Yao, T., Zhang, W., Gulaqa, A., Cui, Y., Zhou, Y., Weng, W., et al. (2021). Effects of Peanut Shell biochar on soil nutrients, soil enzyme activity, and Rice yield in heavily saline-sodic Paddy field. *J. Soil Sci. Plant Nutr.* 21, 655–664. doi: 10.1007/s42729-020-00390-z

Ye, R., and Horwath, W. R. (2017). Influence of rice straw on priming of soil C for dissolved organic C and CH_4 production. *Plant Soil* 417, 231–241. doi: 10.1007/s11104-017-3254-5

Yin, Q., Wang, R., and Zhao, Z. (2018). Application of mg–Al-modified biochar for simultaneous removal of ammonium, nitrate, and phosphate from eutrophic water. *J. Clean. Prod.* 176, 230–240. doi: 10.1016/j.jclepro.2017.12.117

Zhang, M., Gao, B., Yao, Y., Xue, Y., and Inyang, M. (2012). Synthesis of porous MgO-biochar nanocomposites for removal of phosphate and nitrate from aqueous solutions. *Chem. Eng. J.* 210, 26–32. doi: 10.1016/j.cej.2012.08.052

Zhang, Y. X., Li, D., Zhang, Z. Y., and Liao, K. J. (2010). A comparison study of two methods for mensuration of soil cation exchange capacity. *Guizhou Forestry Sci. Technol.* 38, 45–49.

Zhang, X., Teng, Z., Zhang, H., Cai, D., Zhang, J., Meng, F., et al. (2021). Nitrogen application and intercropping change microbial community diversity and physicochemical characteristics in mulberry and alfalfa rhizosphere soil. *J. For. Res.* 32, 2121–2133. doi: 10.1007/s11676-020-01271-y

Zhang, H., Ullah, F., Ahmad, R., Ali Shah, S. U., Khan, A., and Adnan, M. (2022). Response of soil proteobacteria to biochar amendment in sustainable agriculture—a mini review. *J. Soil Plant Environ.* 1, 16–30. doi: 10.56946/jspae.v1i2.56

Zhang, Z., Wang, W., Qi, J., Zhang, H., Tao, F., and Zhang, R. (2018). Priming effects of soil organic matter decomposition with addition of different carbon substrates. *J. Soils Sediments* 19, 1171–1178. doi: 10.1007/s11368-018-2103-3

Zhang, Q., Xiao, J., Xue, J., and Zhang, L. (2020). Quantifying the effects of biochar application on greenhouse gas emissions from agricultural soils: a global meta-analysis. *Sustainability* 12:3436. doi: 10.3390/su12083436

Zhang, T., Zhu, X., Shi, L., Li, J., Li, S., Lu, J., et al. (2017). Efficient removal of lead from solution by celery-derived biochars rich in alkaline minerals. *Bioresour. Technol.* 235, 185–192. doi: 10.1016/j.biortech.2017.03.109

Zhao, Z., Zhang, C., Li, F., Gao, S., and Zhang, J. (2020). Effect of compost and inorganic fertilizer on organic carbon and activities of carbon cycle enzymes in aggregates of an intensively cultivated vertisol. *PLoS One* 15:e0229644. doi: 10.1371/journal.pone.0241371

frontiers | Frontiers in Microbiology

TYPE Original Research
PUBLISHED 06 February 2023
DOI 10.3389/fmicb.2023.1068595

OPEN ACCESS

EDITED BY
Xiangyu Guan,
China University of Geosciences, Beijing, China

REVIEWED BY
Weiguo Hou,
China University of Geosciences, Beijing, China
Meng Li,
Chinese Academy of Forestry, China

*CORRESPONDENCE
Hongmei Wang
✉ wanghmei04@163.com;
✉ hmwang@cug.edu.cn

SPECIALTY SECTION
This article was submitted to Terrestrial Microbiology, a section of the journal Frontiers in Microbiology

RECEIVED 13 October 2022
ACCEPTED 19 January 2023
PUBLISHED 06 February 2023

CITATION
Cheng X, Xiang X, Yun Y, Wang W, Wang H and Bodelier PLE (2023) Archaea and their interactions with bacteria in a karst ecosystem. *Front. Microbiol.* 14:1068595. doi: 10.3389/fmicb.2023.1068595

Archaea and their interactions with bacteria in a karst ecosystem

Xiaoyu Cheng[1,2,3], Xing Xiang[1,4], Yuan Yun[1,5], Weiqi Wang[1,2], Hongmei Wang[1,2]* and Paul L. E. Bodelier[3]

[1]State Key Laboratory of Biogeology and Environmental Geology, China University of Geosciences, Wuhan, China, [2]School of Environmental Studies, China University of Geosciences, Wuhan, China, [3]Department of Microbial Ecology, Netherlands Institute of Ecology (NIOO-KNAW), Wageningen, Netherlands, [4]College of Life Science, Shangrao Normal University, Shangrao, China, [5]College of Life Sciences, Nankai University, Tianjin, China

Karst ecosystems are widely distributed around the world, accounting for 15–20% of the global land area. However, knowledge on microbial ecology of these systems does not match with their global importance. To close this knowledge gap, we sampled three niches including weathered rock, sediment, and drip water inside the Heshang Cave and three types of soils overlying the cave (forest soil, farmland soil, and pristine karst soil). All these samples were subjected to high-throughput sequencing of V4-V5 region of 16S rRNA gene and analyzed with multivariate statistical analysis. Overall, archaeal communities were dominated by *Thaumarchaeota*, whereas *Actinobacteria* dominated bacterial communities. *Thermoplasmata*, *Nitrosopumilaceae*, *Aenigmarchaeales*, *Crossiella*, *Acidothermus*, and *Solirubrobacter* were the important predictor groups inside the Heshang Cave, which were correlated to NH_4^+ availability. In contrast, *Candidatus* Nitrososphaera, *Candidatus* Nitrocosmicus, *Thaumarchaeota* Group 1.1c, and *Pseudonocardiaceae* were the predictors outside the cave, whose distribution was correlated with pH, Ca^{2+}, and NO_2^-. Tighter network structures were found in archaeal communities than those of bacteria, whereas the topological properties of bacterial networks were more similar to those of total prokaryotic networks. Both chemolithoautotrophic archaea (*Candidatus* Methanoperedens and *Nitrosopumilaceae*) and bacteria (subgroup 7 of *Acidobacteria* and *Rokubacteriales*) were the dominant keystone taxa within the co-occurrence networks, potentially playing fundamental roles in obtaining energy under oligotrophic conditions and thus maintaining the stability of the cave ecosystem. To be noted, all the keystone taxa of karst ecosystems were related to nitrogen cycling, which needs further investigation, particularly the role of archaea. The predicted ecological functions in karst soils mainly related to carbohydrate metabolism, biotin metabolism, and synthesis of fatty acid. Our results offer new insights into archaeal ecology, their potential functions, and archaeal interactions with bacteria, which enhance our understanding about the microbial dark matter in the subsurface karst ecosystems.

KEYWORDS

karst ecosystem, karst soil, subterranean cave, archaeal community, interaction between archaea and bacteria, niche differentiation

1. Introduction

Karst ecosystems largely developed in the exposed area of soluble rocks including limestone, dolomite and gypsum, are widely distributed around the world, accounting for about 15–20% of the global land area (De Waele et al., 2009; Chalikakis et al., 2011; Di Maggio et al., 2012; Kaufmann, 2014). The overlying soil of the karst zone contains abundant organic carbon and high microbial activity in the topsoil layer (0–30 cm) (Ahmed et al., 2012). Next to this, karst forest soils show higher

decomposition, higher respiration rate, but are more carbon-limited compared to non-karst forest soils (Chen et al., 2018). Except organic matter, karst overlying soils also show high nitrogen concentration even up to nitrogen saturation especially in southwestern China (Wen et al., 2016; Chen et al., 2018). Water is the bridge linking the surface karst soils and subterranean karst caves, which transports natural organic matter and trace metals into the underground ecosystem (De Waele et al., 2009; Hartland et al., 2012). $\delta^{18}O$ of cave drip water is employed to track the processes of speleothem deposits (Bradley et al., 2010), which reflects meteoric precipitation in cool climate (mean annual temperature < 10°C) (Baker et al., 2019). Inside karst caves, the permanent darkness, saturated humidity, and potential evaporation largely differ from those in surface habitats in terms of light, energy, nutrients, weathering degree, and abiotic stability, which provide a unique oligotrophic habitat for biotic communities (Gabriel and Northup, 2013).

Studies have clearly demonstrated the evolutionary differences between macro-biota in subsurface and surface ecosystems. Underground macro-creatures evolve unique characteristics compared with surface creatures, which are solely found in a single cave or adjacent caves due to geographical isolation (Ribera et al., 2019). However, most microorganisms in caves can also be found in other ecosystems, but with different relative abundances. Quantitatively, prokaryotes inside the caves are 2–3 orders of magnitude lower than those in overlying karst soils. 16S rRNA gene copies ranged from 10^{10} to 10^{12} copies·g^{-1} soil in karst soils with different land use (croplands and wetland) (Hu et al., 2018; Liao et al., 2018; Wang X. et al., 2021). In contrast, the absolute abundance of 16S rRNA gene inside caves varies from 10^{5}–10^{9} copies·g^{-1} weathered rock to 10^{8}–10^{9} copies·g^{-1} sediment (Alonso et al., 2018; Zhao et al., 2018).

The knowledge on bacterial communities in karst ecosystems has increased recently about their involvement in elemental cycles and functional diversity. *Actinobacteria*, *Proteobacteria*, and *Acidobacteria* dominate in karst soils with different land-use (Liao et al., 2018; Cheng et al., 2021). For instance, the carbon-fixing bacterial communities of *Thiomonas*, *Bradyrhizobium*, *Ferriphaselus* and *Sulfuricaulis* are, respectively, dominant in native wetland soil, degraded wetland soil, and reclaimed farmland wetland soil of karst zone, which closely correlate to edaphic parameters such as organic carbon, dissolved organic carbon, microbial biomass carbon, and labile organic carbon (Wang X. et al., 2021). Inside karst caves, microbial diversity and elemental cycles microbes involved vary with the cave lithology. Sulfur metabolism is mostly reported in plutonic caves rich in hydrogen sulfide, where bacteria can utilize sulfur to provide metabolic energy for other cave biota (Engel et al., 2010). A large proportion of sulfate-reducing bacteria (SRB), such as *Desulfovibrio* and *Desulfomicrobium* has also been observed in Altamira Cave, suggesting potential function of sulfur reduction in supergene caves (Portillo and Gonzalez, 2009). *Acidithiobacillus*, dominated a biofilm in acid Frasassi Cave, is capable of carbon fixation, sulfur oxidation, and nitrogen assimilation, indicating the coupling of carbon and nitrogen cycling (Jones et al., 2012). Cave bacteria living on weathered rock and speleothem surfaces can fix carbon *via* Calvin-Benson-Bassham cycle, whereas those in sediments prefer the 3-hydroxypropionate/4-hydroxybutyrate (HP/HB) pathway (Ortiz et al., 2014; Yun, 2018). Furthermore, it has been demonstrated that carbon fixation by *Bacillus*, *Actinomycetes*, and *Burkholderia* increase with elevated CO_2 concentration (Ortiz et al., 2014; Yun, 2018). Other than carbon fixation, microbes can also mediate methane cycling in caves. Recently, it has been reported that high-affinity methane-oxidizing bacteria, especially those belonging to upland soil cluster γ (USCγ), are widely distributed in karst caves from southwest and central China. The *pmoA* gene abundance of USCγ in weathered rocks is higher than that in sediments (Zhao et al., 2018; Cheng et al., 2021, 2022). USCγ is a keystone taxon in co-occurrence networks of both methane functional groups and the total bacterial communities (Cheng et al., 2021). *Nitrosococcaceae* wb1-P19, *Rokubacteriales*, *Gaiellales*, and *Nitrospira* are identified as the keystone members in bacterial networks in the karst caves, which are closely linked to elemental cycles (Zhu et al., 2019; Ma et al., 2021). Fungi dominated by *Ascomycota* played a fundamental role in maintaining the microbial ecosystem on weathered rocks inside the karst cave as indicated by the cross-domain fungi-bacteria network analysis (Wang Y. et al., 2022).

In comparison to bacteria, archaea are far less studied in karst ecosystems. Recently, abundant archaeal taxa have been detected in iron-manganese cave deposits, which harbor functional genes involved in nitrogen cycling such as nitrification, dissimilatory nitrate reduction, assimilatory nitrate reduction, and denitrification (Kimble et al., 2018). The absolute abundance of ammonia-oxidizing archaea (AOA) exceeds that of ammonia-oxidizing bacteria (AOB) up to 2 orders of magnitude in cave sediments (Zhao et al., 2016). *Thaumarchaeota* at least contribute >40% to ammonia oxidation, suggesting archaea play a vital role in cave nitrogen cycle (Zhao et al., 2016). Nitrogen availability is inextricably linked to the presence of archaea and low nitrogen content increases the abundance of *Thaumarchaeota* (> 15%) (Northup et al., 2003; Hershey and Barton, 2018). Nevertheless, we still know little about archaeal distribution in different niches in karst ecosystems and how they correlate with environmental variables.

Besides microbial functional groups mediating elemental cycling, microbial interactions also play fundamental roles in maintaining the functional stability of an ecosystem. It has been demonstrated that interactions between microbial groups rather than microbial relative abundance and alpha diversity are crucial to function in the complex engineering ecosystem (Zhao et al., 2022). The well-known interaction between archaea and bacteria is the anaerobic methanotrophic archaea (ANME) with SRB. They cooperated with each other to utilize methane as the main energy source under anaerobic condition in methane seeps (Xin et al., 2022; Yu et al., 2022). Moreover, interactions between bacteria and archaea can help them to adapt the environments with heavy metal contaminations (Li et al., 2017). Other than cooperation between archaea and bacteria, competition also happens. For example, under low NH_4^+ and low dissolved O_2 conditions, AOA would compete out their counterpart AOB, and collaborate better with anammox bacteria on treating low strength nitrogen sewage (Pan et al., 2016). However, up to date, there are still knowledge gaps about archaeal functions and how archaea interact with their bacterial counterpart to sustain the karstic ecosystem.

To fill the knowledge gaps in archaeal ecology and interactions between archaea and bacteria in karst ecosystems, we sampled the forest soil, farmland soil, and pristine karst soil overlying the investigated the Heshang Cave, weathered rock, sediment, and drip water inside the Heshang Cave, central China (Yun et al., 2016). Subsequently, all these samples were sequenced for 16S rRNA gene of V4-V5 region *via* high-throughput sequencing. The purposes of this study were to (i) reveal structural differences of archaeal and bacterial communities in karst soils and inside subsurface caves, (ii) explore relationships of archaea and bacteria with environmental factors, and

(iii) understand the interaction between archaea and bacteria in karst soils and inside caves.

2. Materials and methods

2.1. Sampling description and physicochemical analysis

The 250-meter long Heshang Cave (29°40′–30°48′ N and 108°30′–111°20′ E) is a dolomite karst cave formed in Cambrian, located in Changyang County, Hubei Province, central China. The Heshang Cave is about 30 m above the water surface of the Qingjiang River with a sole entrance (Supplementary Figure 1). The average annual temperature and average precipitation are about 16.5°C and 1,118 mm, respectively, in this region (Yun et al., 2016). The highest temperature in this region is observed in July (27.5°C) and the lowest temperature is in January (4.8°C). *Pinus massoniana* and *Cinnamomum bodinieri* are dominant vegetation on the top of the Heshang Cave, whereas part of the land is reclaimed to grow potato, clover, and economical crop oilseed rape (Cheng et al., 2021). Soils overlying the Heshang Cave are divided into forest soil (FS), farmland soil (FLS), and pristine soil (PS) on the basis of land-use patterns. Surface soils were collected at a depth of <10 cm by the standard five-point sampling technique. Samples at one site were collected from the 4 vertexes of a quadrangle with an area around 1 m^2 and the central point. These samples were pooled together and homogenized. Subsequently, three subsamples were collected from the homogenized sample and served as the biological triplicate. Samples inside the cave include drip water (DW), sediments (S), and weathered rocks (W). The weathered rocks and sediments of photic zone (near the entrance), twilight zone, and dark zone were sampled separately inside cave. Surface sediment samples with a depth of 1 cm were collected with five-point sampling technique and homogenized before loading into the 50 mL sterile falcon tubes. The drip water was collected with sterile 10 L buckets and funnels, and immediately filtered with 2 μm membrane after collection. Filters with cells were preserved in sterile falcon tubes on dry ice. In total, 10 samples outside the cave (containing 4 FS, 3 FLS, and 3 PS samples), and 21 samples (containing 3 DW, 9 S and 9 W samples) inside cave were collected in the Heshang Cave karstic system. All samples were transported to the geomicrobiology lab at China University of Geosciences (Wuhan) on dry ice within 24 h and stored at −80°C upon arrival until further use. Environmental factors, such as pH, TOC (total organic carbon), Ca^{2+}, Mg^{2+}, K^+, Na^+, NH_4^+, Cl^-, NO_2^-, NO_3^-, and SO_4^{2-} concentrations were measured as reported in our previous work (Yun et al., 2016).

2.2. DNA extraction and sequencing processes

Total DNA of 0.5 g solid samples was extracted with the Power Soil® DNA Isolation Kit (MOBIO, United States), and total DNA from drip water was extracted from membrane filters with the Power Water® DNA Isolation Kit (MOBIO, United States). DNA quality and purification steps were executed as described previously (Ma et al., 2021). The prokaryotic universal primers 707f (3'-ATTAGATACCCSBGTAG TCC-5′) and 1059r (3'-GCCATGCACCWCCTCT-5′) were used to amplify V4-V5 region of 16S rRNA (Kim et al., 2018). Raw sequences were obtained from an Illumina MiSeq platform in two separate runs at Shanghai Personal Biotechnology, Co., Ltd., (Shanghai, China) and deposited in the National Omics Data Encyclopedia (NODE)[1] with the project numbers OER254939.

Raw sequences were processed with the bcl2fastq software (version 1.8.4, Illumina) to cut primers and barcodes. Subsequently, the quality and analysis of processed sequences were controlled with QIIME2 (Quantitative Insight Into Microbial Ecology, version 2019.7) software (Bolyen et al., 2019). The high-quality sequences were clustered at 97% sequence similarity to generate representative OTU (Operational Taxonomic Unit) sequences with the VSEARCH plugin, and the feature taxonomy of the 16S rRNA gene was assigned against modified SILVA database (version 132) to improve the efficiency of archaeal annotation. The sequence numbers of all samples were resampled to 60,000 reads to avoid the influence of sequencing depth on microbial diversity.

2.3. Statistical analysis

Shannon index for each sample, beta diversity of archaea and bacteria, permutational multivariate analysis of ANOVA (ADONIS), analysis of similarities (ANOSIM), and multi response permutation procedure (MRPP), mantel test, and principal coordinate analysis (PCoA) were calculated with the vegan[2] package in R software (version 4.0.3). The ADONIS, ANOSIM, and MRPP analysis of microbial community were performed based on Bray-Curtis distance, and the normalized *p* values of these analysis were adjusted by Benjamini and Hochberg method. Mantel test was performed to evaluate the correlation between environmental matrix and microbial matrix *via* Spearman's rho analysis under 9,999 permutations. To further assess the spatial patterns of beta diversity, total dissimilarity of Sørensen indices (β_{sor}), their turnover component (β_{sim}), and their nestedness component (β_{sne}) were computed *via* betapart package (Baselga and Orme, 2012). Random forest machine learning was conducted with randomForest[3] and A3[4] package to rank the impacts of microbial genus in cave ecosystem. To further understand functional inference and ecological trait assignment of microbial community in cave ecosystem (Djemiel et al., 2022), we, respectively, performed representative sequences with Tax4Fun2 package (Wemheuer et al., 2020) and Functional Annotation of Prokaryotic Taxa database (FAPROTAX, v1.2.3).[5] The boxplot, pie chart, histogram, heatmap, scatter diagram, density map, and PCoA plot were visualized with ggpubr,[6] pheatmap, and ggplot2[7] package. The analysis of variance (ANOVA), student's *t*-test (*t*-test), and Kruskal-Wallis *H* test were calculated with SPSS statistics (version 26.0).

The archaeal OTUs that had relative abundance above 0.01% and more than 20% occurrence in all samples and bacterial OTUs that had relative abundance above 0.01% and more than 50% occurrence were selected for co-occurrence networks analysis to reduce the network

1 https://www.biosino.org/node
2 https://cran.r-project.org/web/packages/vegan/index.html
3 https://cran.r-project.org/web/packages/randomForest/index.html
4 https://cran.r-project.org/web/packages/A3/index.html
5 http://www.loucalab.com/archive/FAPROTAX/lib/php/index.php?section=Download
6 https://cran.r-project.org/web/packages/pheatmap/index.htm
7 https://cran.r-project.org/web/packages/ggplot2/index.html

complexity with Hmisc[8] and igraph[9] packages. The correlations among archaeal OTUs, bacterial OTUs, and archaeal and bacterial OTUs were calculated with correlation coefficient ρ of ≥0.7 and p value of <0.01 (Benjamini and Hochberg method adjusted) based on Spearman's p correlation. Networks were visualized with the layout of Fruchterman-Reingold in Gephi (version 0.9.2) software. Nodes with high betweenness centrality values indicated that a node was capable of sustaining the nodes of community and had high connectivity with other nodes, which were considered keystone taxa in the network (Martín González et al., 2010; Vick-Majors et al., 2014; Jiao et al., 2016).

3. Results

3.1. Archaeal and bacterial community composition in the cave ecosystem

Totally, a number of 1,860,000 high-quality sequences were recovered after quality control, which were converted into 43,488 OTUs containing 1,539 archaeal OTUs, 41,665 bacterial OTUs, and 283 unassigned OTUs based on 97% similarity.

Significant differences of bacterial Shannon indices between FS and FLS, and between FS and PS were observed in the soils overlying the Heshang Cave, whereas archaeal Shannon indices were significantly different only between SP (sediments in the photic zone) and WT (weathered rocks in the twilight zone) inside the cave (Figures 1A,B). Shannon index showed an opposite pattern between archaea and bacteria. For instance, archaeal Shannon index was highest (3.48 ± 0.99) in FS, whereas bacterial Shannon values was lowest (6.26 ± 0.99) in overlying soils (Figures 1A,B). This phenomenon was also found inside the Heshang Cave. DW showed higher archaeal Shannon index (3.73 ± 0.49) and lower bacterial Shannon value (5.80 ± 0.59) compared with other cave niches (Figures 1A,B). Shannon indices of sediment samples were generally higher than those in weathered rock, especially in the photic zone (Figures 1A,B). Notably, no significant difference between archaeal and bacterial beta diversity was observed, whereas archaeal beta diversity was higher than that of bacteria (Figure 1C). Both archaeal and bacterial community were significantly dissimilar between overlying soils and samples inside the cave as verified by ADONIS, ANOSIM, and MRPP based on Bray-Curtis distances (Supplementary Table 1). The principal coordinate analysis (PCoA) showed that both bacterial and archaeal communities exhibit niche specificity (Supplementary Figure 2). The PCo1 and PCo2 axis explained 20 and 16% of the variance in the bacterial community, and 28 and 14% of the variance in the archaeal community (Supplementary Figure 2). The relative abundance of archaea in SD (sediments in the dark zone), DW, SP, and FS niches was higher than those in other niches. In contrast, bacterial relative abundance was higher than those of archaea in cave ecosystem (Figure 1D).

Thaumarchaeota dominated in all archaeal communities at the phylum level, especially in FS (18.21 ± 11.82%) and SD (21.69 ± 8.88%) niches. *Actinobacteria*, ranging from 17.79 ± 5.39% to 90.18 ± 2.31%, and *Rokubacteria*, ranging from 0.25 ± 0.13% to 24.22 ± 5.99%, were dominant in bacterial communities inside the cave (Figure 1D; Supplementary Table 2). Significant difference was observed in the relative abundance of phylum *Thaumarchaeota*, *Euryarchaeota*,

8 https://cran.r-project.org/web/packages/Hmisc/index.html

9 https://cran.r-project.org/web/packages/igraph/index.html

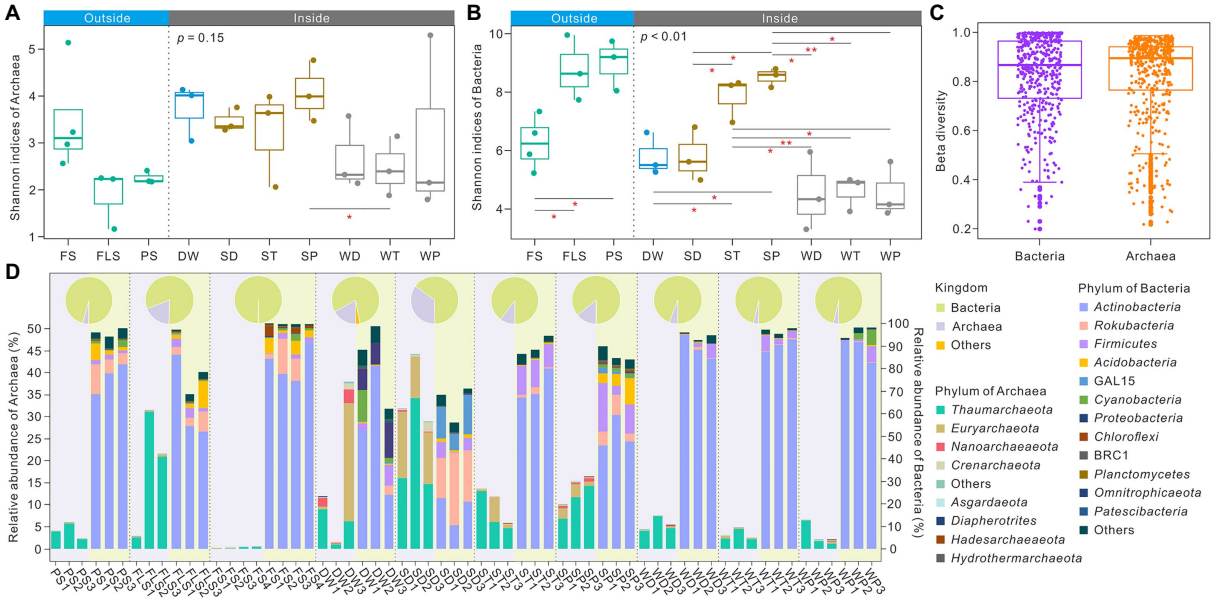

FIGURE 1
Alpha, beta diversity distribution and community composition of archaea and bacteria in cave ecosystem of the Heshang Cave, central China. Panel **(A)** and **(B)**, respectively, showed Shannon indices of archaea and bacteria in different niches inside or outside the Heshang Cave. Panel **(C)** indicated the result of beta diversity between archaea and bacteria. Panel **(D)** showed the relative abundance of archaeal phylum and bacterial phylum from different niches. Pie charts showed the relative abundance of total bacteria and archaea in an individual niche and histogram shows the relative abundances of bacterial or archaeal phyla in each sample. The relative abundance of archaea refers to the left axis scale, whereas bacterial abundance refers to the right axis scale. Histograms for archaea are located in the area highlighted in light purple, whereas those of bacteria in light green. FS, forest soil; PS, pristine soil; FLS, farmland soil; WD, weathered rocks in the dark zone; WT, weathered rocks in the twilight zone; WP, weathered rocks in the photic zone; SD, sediments in the dark zone; ST, sediments in the twilight zone; SP, sediments in the photic zone; DW, drip waters.

*Nanoarchaeaeo*ta, *Rokubacteria*, *Firmicutes*, *Acidobacteria*, GAL15, *Proteobacteria*, *Chloroflexi*, BRC1, *Planctomycetes*, *Omnitrophicaeota*, and *Patescibacteria* between overlying soils and niches inside the cave (Supplementary Table 2). *Thaumarchaeota* and BRC1 were significantly different in their relative abundances in overlying soils with different land use. Inside the cave *Thaumarchaeota*, *Nanoarchaeaeota*, *Actinobacteria*, *Rokubacteria*, *Acidobacteria*, GAL15, *Proteobacteria*, *Chloroflexi*, BRC1, *Planctomycetes*, *Omnitrophicaeota*, and *Patescibacteria* also showed significant differences in their relative abundances (Supplementary Table 2).

To infer mechanisms underlying the observed biodiversity patterns, beta diversity based on the Sørensen index were conducted to separate the turnover and nestedness components, which, respectively, indicated the processes of species replacement and species loss (or gain) in the environment (Baselga and Orme, 2012). Overall turnover components (β_{sim}) were much higher than nestedness-resultant dissimilarity (β_{sne}) (Figures 2A,B), which suggested the noteworthy substitution of microbial community in these niches and thus contributed to their community differences (Baselga and Orme, 2012). Random forest algorithm analysis was employed to understand the important rank of microbial genus under β_{sor} values (Figures 2C–F). Archaeal and bacterial genera with high percentage of increase of mean square error (MSE) were defined as the most important predictors of total microbial composition. *Thermoplasmata* (affiliated to phylum *Euryarchaeota*), *Nitrosopumilaceae* (*Thaumarchaeota*), *Aenigmarchaeales* (*Nanoarchaeaeota*), *Crossiella* (*Actinobacteria*), *Acidothermus* (*Actinobacteria*), and *Solirubrobacter* (*Actinobacteria*) were the important genera closely correlated to β_{sor} values inside the Heshang Cave (Figures 2C,D). *Candidatus* Nitrososphaera (*Thaumarchaeota*), *Candidatus* Nitrocosmicus (*Thaumarchaeota*), *Thaumarchaeota* Group 1.1c (*Thaumarchaeota*), MB-A2-108 (*Actinobacteria*), and *Pseudonocardiaceae* (*Actinobacteria*) were the important genera in the overlying soils (Figures 2E,F).

3.2. Correlations between microbial communities and environmental variables

Correlations between environmental parameters and microbial community structure were analyzed *via* Mantel test. In overlying soils, both archaeal and bacterial communities were closely correlated with pH, Ca^{2+}, and NO_2^- concentrations, whereas bacterial communities were also correlated with NH_4^+ concentration (Supplementary Table 3; Figures 3C,D). The important predictor groups identified above were found to be significantly correlated with environmental variables. For instance, relative abundance of *Thaumarchaeota* Group 1.1c and *Pseudonocardiaceae* showed a negative correlation with pH, whereas the relative abundance of *Candidatus* Nitrososphaera and MB-A2-108 positively correlated with pH (Figures 3C,D). NO_2^- concentration positively correlated with the relative abundance of *Candidatus* Nitrocosmicus and MB-A2-108, whereas negatively with the relative abundance of *Thaumarchaeota* Group 1.1c (Figures 3C,D). Within the cave, NH_4^+ concentration negatively correlated to archaeal (*Woesearchaeia*, *Thermoplasmata*, *Nitrosopumilaceae*, and *Aenigmarchaeales*) and positively correlated to bacterial communities (*Acidothermus*, *Crossiella*, *Pseudonocardiaceae*, and *Solirubrobacter*) (Figures 3A,B). Besides NH_4^+ concentration, the relative abundance of *Woesearchaeia* and *Aenigmarchaeales* negatively correlated with TOC content, and the relative abundance of *Nitrosopumilaceae* and *Thermoplasmata* showed a positive correlation with pH (Figure 3A). Relative abundances of *Solirubrobacter* and *Acidothermus* showed a positive correlation with SO_4^{2-} concentration (Figure 3B).

3.3. Microbial interactions in the cave ecosystem

To investigate underlying interactions among archaea, bacteria, and environmental variables, co-occurrence networks were conducted in the cave ecosystem. The inside-cave networks of archaea, bacteria, and total prokaryotes had 250, 181, and 194 nodes and 1,405, 521, and 523 edges, respectively (Figures 4A–C,E–G; Supplementary Table 4). In contrast, the outside networks of archaea, bacteria, and total prokaryotes had 36, 145, and 152 nodes and 80, 128, and 132 edges, respectively (Supplementary Table 4). Positive links dominated the edges in all co-occurrence networks (Figure 4). The modularity values of all networks were higher than 0.4, showing good modular structures (Supplementary Table 4). Higher average clustering coefficient, higher density, higher average degree, lower diameter, and lower average path length were observed in archaeal topological properties compared to bacterial and total networks inside the cave. Similar patterns were also observed in topological properties of outside archaeal network with exceptions in average path length and diameter values (Supplementary Table 4). Bacterial networks and total prokaryotic networks were more similar in the topological properties of (Supplementary Table 4). Concentrations of NO_2^- and Ca^{2+} were tightly correlated with nodes in the outside archaeal network (Figure 4E).

The relevance between the relative abundance of nodes and betweenness centrality revealed that keystone taxa in low relative abundance sustain the function in the co-occurrence networks (Figures 4D,H). The taxonomy of keystone taxa was significantly different between networks of total prokaryotes inside and outside the cave. Inside the cave, keystone taxa consisted of subgroup 6 (*Acidobacteria*), *Candidatus* Methanoperedens (*Euryarchaeota*), *Rokubacteriales* (*Rokubacteria*), MB-A2-108 (*Actinobacteria*), and *Nitrosopumilaceae* (*Thaumarchaeota*) (Figure 4D). In contrast, keystone taxa of the prokaryotic network outside the cave were constituted by *Solirubrobacterales*, *Ilumatobacter*, and *Gaiellales* (Figure 4H, Supplementary Table 5).

3.4. Microbial functional inference and ecological trait assignment in cave ecosystem

Microbial functional prediction consists of microbial functional inference and ecological trait assignment in general (Djemiel et al., 2022). The results of functional prediction were mainly clustered by niches (Figure 5). In the weathered rocks, chemo-heterotrophy was dominant, and WP (weathered rocks in the photic zone) particularly exhibited functional inference of cyanobacteria, oxygenic photoautotrophy, and phototrophy (Figure 5A). In sediments, SP (sediments in the photic zone) mainly showed methanogenesis, and ST (sediments in the twilight zone) and SD (sediments in the dark zone) were dominated by nitrification and aerobic ammonia oxidation, which were similar to the functions in PS and FS niches (Figure 5A). The functional inference of DW consisted of chloroplasts, fermentation, and multiple degradation of organic compounds (Figure 5A).

10.3389/fmicb.2023.1068595

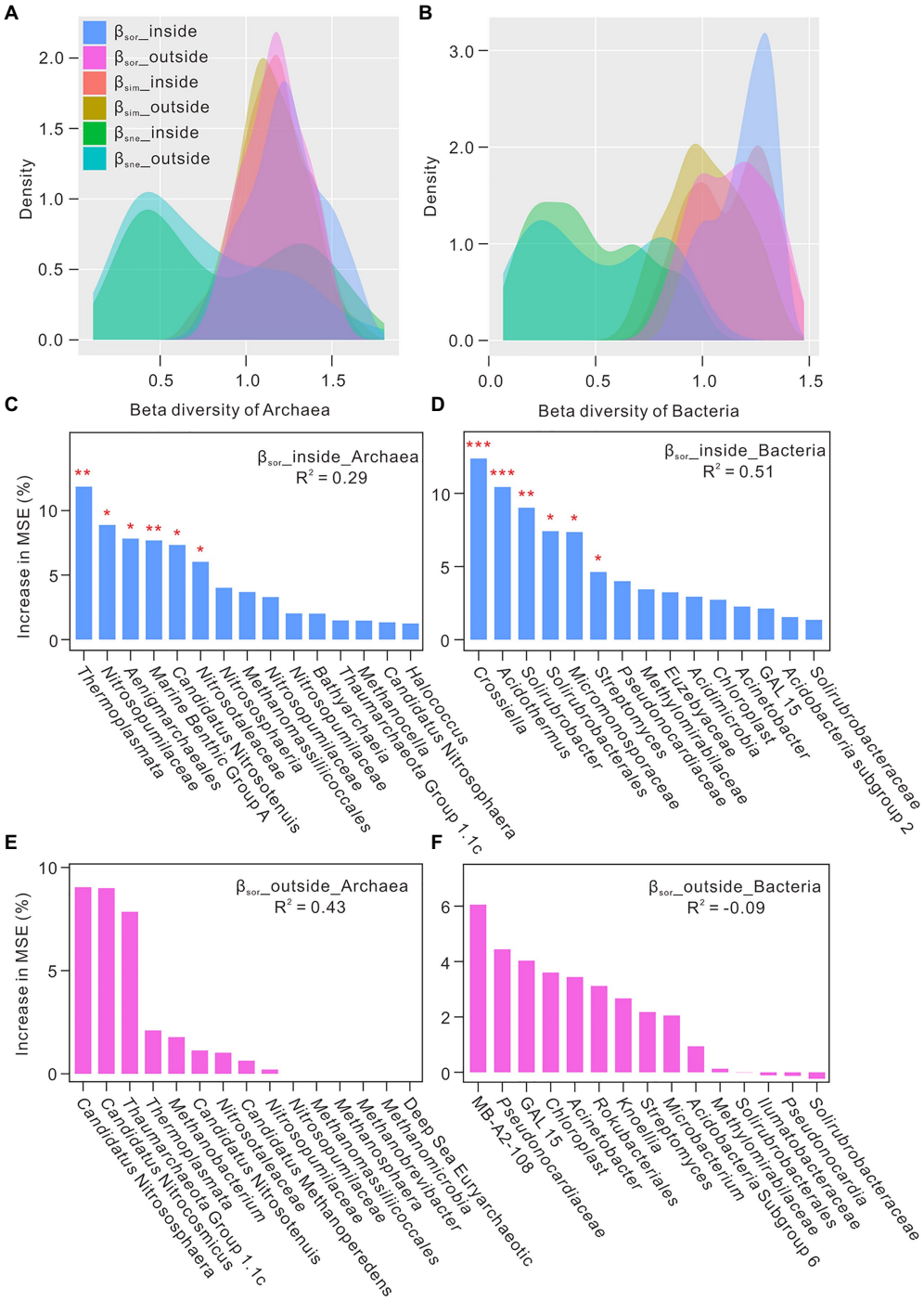

FIGURE 2
The relationship between beta diversity and microbial genus in the karst ecosystem. Panel **(A)** and **(B)** indicated the partition of β_{sor} into β_{sim} and β_{sne} inside and outside the Heshang Cave, central China. Panel **(C–F)** showed that importance ranking (percentage of increase of mean square error, MSE) of archaeal and bacterial genus under the conditions of β_{sor} values as indicated by random forest machine learning. High MSE values mean more importance of microbial genus as predictors compared with those with low MSE values. *indicated a *p* value <0.05, and **indicated a *p* value <0.01.

For the details of microbial functional inference, inside and outside niches were predominated by different metabolic pathways (Figure 5B). For specific enzymes in cave ecosystem, adenylate cyclase [EC: 4.6.1.1], 8-oxo-dGTP diphosphatase [EC: 3.6.1.55], and ABC-2 type transport system permease protein were dominant in inside the cave (Figure 5C). The proteins related to ATP binding, such as iron (III) transport system ATP-binding protein [EC: 3.6.3.30], branched-chain amino acid transport system ATP-binding protein, and putative spermidine/putrescine transport system ATP-binding protein, were dominant in DW samples (Figure 5C). Furthermore, dehydrogenase (long-chain acyl-CoA synthetase [EC: 6.2.1.3], aldehyde dehydrogenase (NAD+) [EC: 1.2.1.3], succinate-semialdehyde dehydrogenase/glutarate-semialdehyde dehydrogenase [EC: 1.2.1.16, 1.2.1.79, 1.2.1.20], and 3-hydroxybutyrate dehydrogenase [EC: 1.1.1.30]), reductase (3-oxoacyl-[acyl-carrier protein] reductase [EC: 1.1.1.100]), and synthase (Fatty-acyl-CoA synthase [EC: 6.2.1.-]) enzymes were dominant in outside samples (Figure 5C).

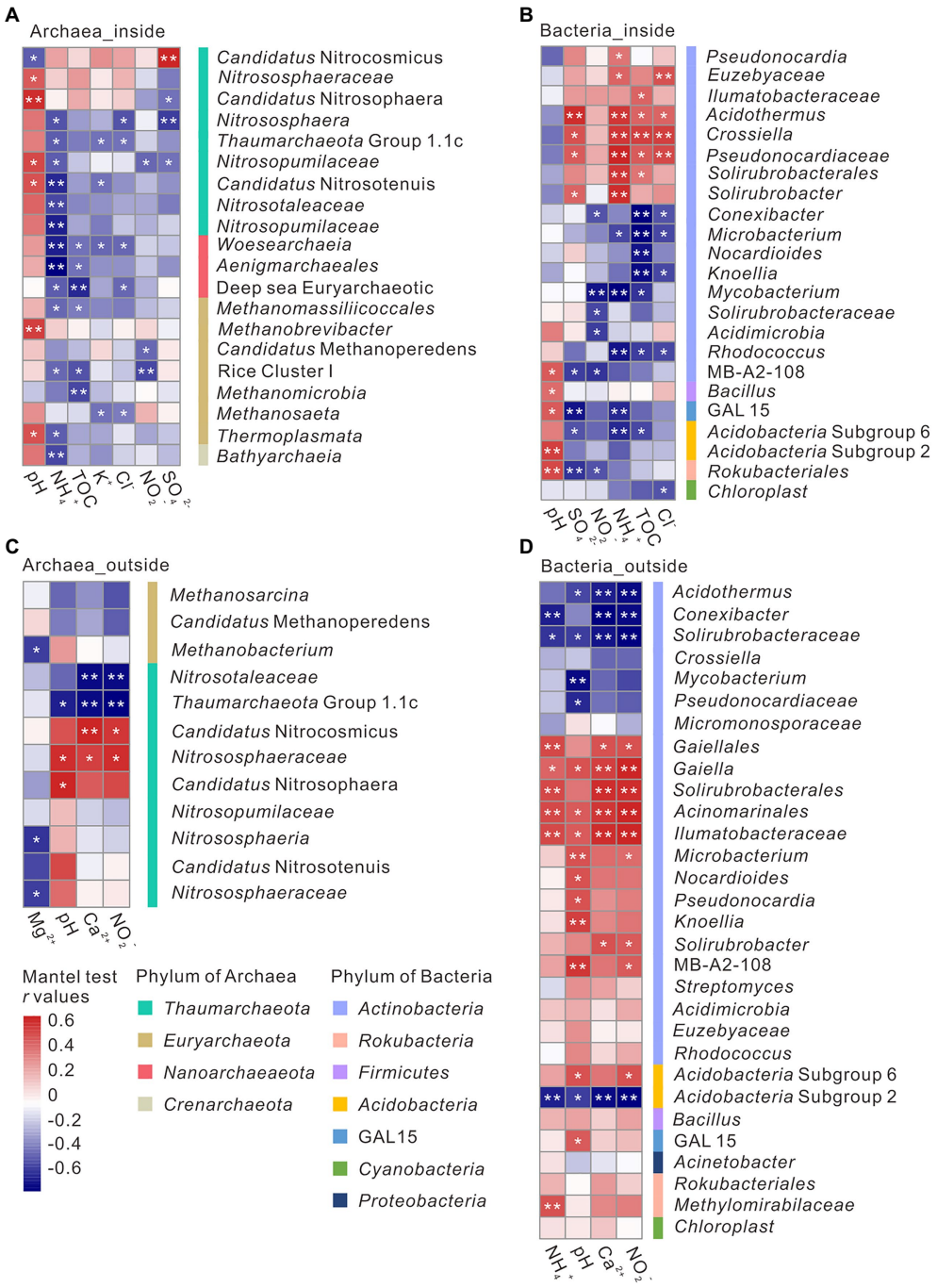

FIGURE 3
The correlations between environmental factors and microbial genus inside **(A, B)** and outside **(C, D)** the Heshang Cave under the analysis of mantel test. Positive correlations were in red and negative correlations were in blue. *indicated a *p* value <0.05, and **indicated a *p* value <0.01.

4. Discussion

4.1. Differences in prokaryotic communities within and outside the Heshang Cave

Overall, *Thaumarchaeota* and *Crenarchaeota* were reported to be dominant in karst niches, such as weathered rocks, sediments within the cave and soils outside the cave (Ai et al., 2022), which were consistent with our results mainly dominated by *Thaumarchaeota*, with a relative abundance ranging from 0.23 ± 0.14% to 21.69 ± 8.88% (Figure 1D; Supplementary Table 2). *Thaumarchaeota* might associate with the acidic environment due to their dominance in the acidic cave with a pH value ranging from 4.97 to 6.88 (Barton et al., 2014). However, wide occurrence of *Thaumarchaeota* was also observed in the biofilm on weathered rocks and stalactites in southwestern karst caves (Anda et al., 2017; Dong et al., 2020). High abundance of *Thaumarchaeota* was observed in karst farmland soils outside the cave (Figure 1D), and other farmland soils with low salinity and with heavy metal pollutions (Zheng et al., 2017; Chang et al., 2021; Hu et al., 2021). The bacterial community was dominated by *Actinobacteria* (Figure 1D; Supplementary Table 2).

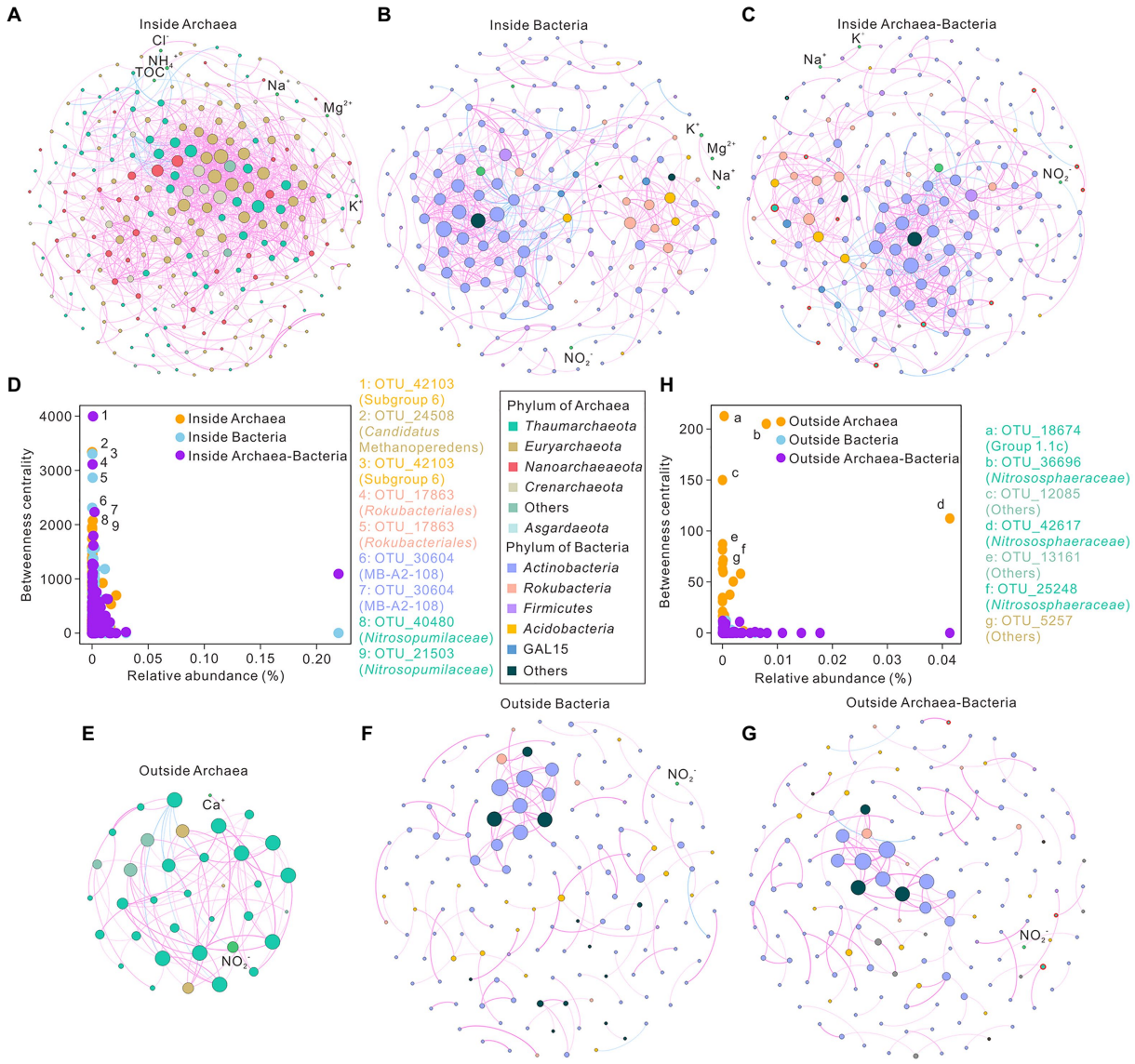

FIGURE 4
Co-occurrence networks of microbial communities in the Heshang Cave ecosystem, central China. Panel **(A–C)** indicated networks of archaeal **(A)**, bacterial **(B)**, and total prokaryotic **(C)** communities inside the Heshang Cave. Panel **(E–G)** showed networks of archaeal **(E)**, bacterial **(F)**, and total prokaryotic **(G)** communities outside the Heshang Cave. Panel **(D,H)** revealed the betweenness centrality and relative abundance of network nodes inside **(D)** and outside (H) the cave. Each node represents an OTU in the network, and the node size is proportional to the degree (connecting with other nodes). Negative links were in blue, whereas positive edges were in pink. Nodes of archaea were marked with red outer rings.

Actinobacteria are widely distributed in karst ecosystems (Fan et al., 2019; Zhu et al., 2019; Buresova-Faitova et al., 2022), and the Actinobacterial communities were significantly different between human-influenced and pristine karst caves, which were, respectively, predominated by *Nocardia*, *Mycobacterium*, and *Gaiellales* (Buresova-Faitova et al., 2022).

It should be pointed out that significant differences between microbial communities inside and outside the karst cave may result from their unique habitat characteristics. *Euryarchaeota* was predominant in DW3, located in the twilight zone, and in sediment samples across the cave, especially in the dark zone (Figure 1D). *Euryarchaeota* closely correlated with the functions of sulfur reducers, sulfate reducers, and thermophilic heterotrophs, and had been found on the surface of bat guano pile (Chroňáková et al., 2009). The sediments in the dark zone of the Heshang Cave were covered with bat guano, the dominance of *Euryarchaeota* in our cave was consistent with previous studies. Simultaneously, high Shannon indices of archaea and bacteria were observed in the Heshang Cave ecosystem (Figures 1A,B) compared with the previous reports (Ai et al., 2022; Xiao et al., 2022). SD was dominant by *Rokubacteria* (24.22 ± 5.99%) and GAL15 (13.03 ± 4.29%) (Figure 1D, Supplementary Table 2). The potential anaerobic conditions in SD samples might account for the dominance of the phylum *Rokubacteria*, which might be capable of anaerobic methane oxidation coupling with nitrite reduction (Lomakina et al., 2019; Gonzalez-Pimentel et al., 2021). GAL15 was previously proposed as rare cave biosphere due to their rare occurrence in caves (Gonzalez-Pimentel et al., 2021). However, the relative high abundance of GAL15 (13.03 ± 4.29%) in sediments in the dark zone in the Heshang Cave potentially indicated their important role in cave ecosystem, which merits further investigation.

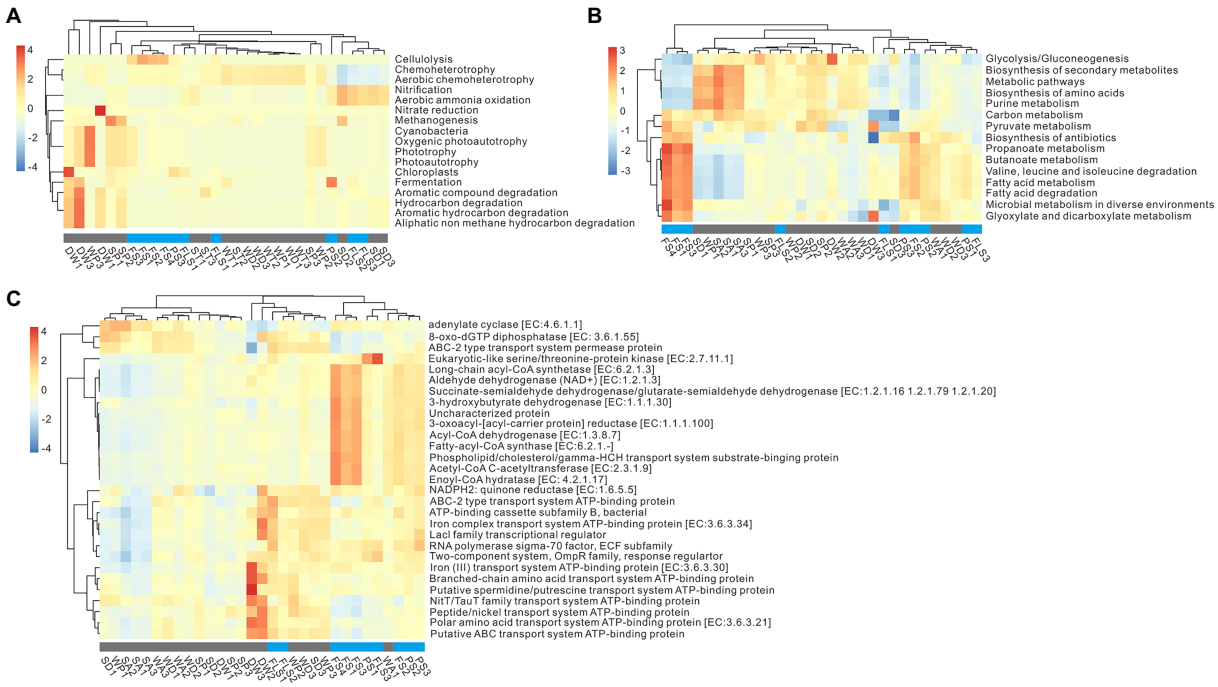

FIGURE 5
Ecological trait assignment and functional inference of microbes in the cave ecosystem. Panel **(A)** showed the top 17 results of ecological trait assignment based on the analysis of FAPROTAX. Panel **(B,C)** indicated pivotal functional inference with the Tax4Fun2 software. The relative abundance of top 15 pathways **(B)** and top 29 functional genes **(C)** in each sample. All these results were revealed with the Pearson correlation. FS, forest soil; PS, pristine soil; FLS, farmland soil; WD, weathered rocks in the dark zone; WT, weathered rocks in the twilight zone; WP, weathered rocks in the photic zone; SD, sediments in the dark zone; ST, sediments in the twilight zone; SP, sediments in the photic zone; DW, drip waters.

The results of beta diversity showed that microbial community at one site may substitute by different microbes from other sites (Baselga and Orme, 2012), which may diversify microbial community structures in karst cave ecosystems (Figures 2A,B). Inside the cave, archaeal groups such as *Thermoplasmata*, *Nitrosopumilaceae*, and *Aenigmarchaeales* (Figure 2C), and bacterial groups such as *Crossiella*, *Acidothermus*, and *Solirubrobacter* (Figure 2D) were the important taxa closely correlated to β_{sor} values, revealing their vital roles in these ecosystems. *Thermoplasmata*, one of acidophilic archaea, is reported to be present in the snottiest from the sulfide-rich Frasassi Cave (Macalady et al., 2007). Members of this group are considered only living in the aphotic environment, and played a role on obligate heterotrophs of fermenting the breakdown products of cellular decomposition with SO_4^{2-} as an electron acceptor (Barton and Luiszer, 2005). Our detection of *Thermoplasmata* with high relative abundance of 10.50 ± 2.78% in the alkaline Heshang Cave, especially in sediments of dark zone indicated their wider ecological niches in natural environments than previously thought. Their ecological functions in alkaline caves merits further investigation. *Nitrosopumilaceae* were reported to live in the active and fossil parts of the Dupnisa Cave System with the relative abundance >5% (Doğruöz-Güngör, 2020). *Nitrosopumilaceae* preferred aquatic niches (DW) in the Heshang Cave, which might process ammonia-oxidation in water samples (Toumi et al., 2021). *Aenigmarchaeales,* found in ice-capped lake and wheat-maize rotation soils, has never been reported in karst ecosystem (Wan et al., 2021; Vigneron et al., 2022). Nevertheless, low abundance of *Aenigmarchaeales* was found in DW samples (0.31 ± 0.33%), especially in DW1 with high metabolic potential in summer (Yun et al., 2018). The functions of *Aenigmarchaeales* affiliated to anaerobic DPANN archaea contained not only degradation and fermentation of cellular compounds, and sulfide and polysulfide reduction, but also coded genes of pore-forming toxins, peptidoglycan degradation, and RNA scavenging (Vigneron et al., 2022). Four *Actinobacteria* taxa were closely correlated with beta diversity inside the cave (Figure 2D). Higher abundance of *Crossiella* was previously reported in weathered rocks than in sediments from the Heshang Cave, which were also identified as the key genera and keystone taxa in weathered rocks as indicated by the analysis of least discriminant analysis effect size and network (Yun et al., 2016; Ma et al., 2021). Recent study showed that syntrophic relationship existed between *Crossiella* and nitrifying bacteria during the processes of CO_2 fixation, heterotrophic ammonification, and the moonmilk formation (Martin-Pozas et al., 2022). *Acidothermus*, detected in acidophilic and thermal environments, was found in weathered rock from a thermal karst cave, speleothems and mineral surface from an orthoquartzite cave (Mohagheghi et al., 1986; Borsodi et al., 2012; Ghezzi et al., 2021). *Solirubrobacter* was abundant in weathered rock in the twilight and dark zones, ranging from 6.98 ± 1.05% to 7.51 ± 2.28%, which preferred aerobic, neutral, and mesophilic (28–30°C) conditions (Singleton et al., 2003).

Outside the cave, substitution of microbial communities might be weak in comparison with those in caves as no microbial groups significantly contributed to β_{sor} (Figures 2E,F). *Candidatus* Nitrososphaera, *Candidatus* Nitrocosmicus, *Thaumarchaeota* Group 1.1c, MB-A2-108, and *Pseudonocardiaceae* were the important taxa (Figures 2E,F). *Candidatus* Nitrososphaera and *Candidatus* Nitrocosmicus are ammonia-oxidizing archaea (Wu et al., 2021), and *Candidatus* Nitrososphaera have been reported to be dominant in karst soils (Wang et al., 2019). The relative higher abundance of *Candidatus* Nitrocosmicus (1.26 ± 1.40%) in farmland soil than that in FS and PS

samples may result from the N-fertilization (Tanunchai et al., 2021). High relative abundance of *Thaumarchaeota* Group 1.1c (0.08%) was observed in FS samples with a pH ranging from 4.05–5.69 (Yun et al., 2016), which coincided with their dominance in acidic soils (Tripathi et al., 2013). MB-A2-108, affiliated to phylum *Actinobacteria*, was more commonly found in farmland soils compared with other karst niches, which also lived in stony meteorites (Tait et al., 2017).

4.2. Different response of prokaryotic communities to environmental factors in the karst ecosystem

Microbial communities inside and outside the cave response differently to environmental factors (Supplementary Table 3). Inside the cave, pH and NH_4^+ significantly impacted on archaeal relative abundance, whereas multiple edaphic variables such as NH_4^+, TOC, SO_4^{2-}, pH, and NO_2^- significantly correlated with the relative abundances of bacterial groups. pH positively impacted on the relative abundance of *Nitrosopumilaceae* and *Thermoplasmata*, which dominated in DW and sediment samples with a pH of 7.76–8.35 (Figure 3A). The relationship between *Nitrosopumilaceae* and pH was consistent with those observed in farmland soils and saline soils (Wan et al., 2021; Wang B. et al., 2022). The relative abundance of *Thermoplasmata* was reported negatively correlated with pH in acidic tropic soil, acidic springs, solfataras, and volcanic soils (Tripathi et al., 2013), whereas an opposite correlation was observed in our alkaline cave. The detection of *Thermoplasmata* in anthropogenic reservoir of salino-alkaline lime (Kalwasinska et al., 2019) supported their occurrence in alkaline environments. Besides pH, TOC and NH_4^+ concentration also significantly impact the relative abundances of archaeal groups inside the cave. The relative abundance of *Woesearchaeia* and *Aenigmarchaeales* negatively correlated to TOC (Figure 3A), which dominated in DW samples with a relative abundance of 1.31 ± 1.09% and 0.31 ± 0.33%, respectively (Supplementary Table 2). These anaerobes might be brought into the cave by drip water from the anoxic overlying rocks, which performed nutrient complementation with other microbes due to their prominent metabolic shortages (Castelle et al., 2015; Liu et al., 2018; Vigneron et al., 2022; Xiang et al., 2022). NH_4^+ concentration significantly impacted on the relative abundances of many archaeal and bacterial groups in the Heshang Cave (Figures 3A,B), such as the important taxa of *Thermoplasmata*, *Nitrosopumilaceae*, *Aenigmarchaeales*, *Crossiella*, *Acidothermus*, and *Solirubrobacter*, indicating the significance of NH_4^+ in cave ecosystems. Pivotal chemolithotrophy of sulfur- and ammonium-microbes, dominated by *Nitrospira* and *Candidatus* 'Nitrotoga', was reported in Movile Cave (Chen et al., 2009). Except hypogene caves, active nitrification has also be detected from cave sediments dominated by ammonia-oxidizing archaea in supergene karst cave (Zhao et al., 2016).

Microbial communities outside the cave closely correlated to pH and NO_2^- concentration (Figures 3C,D). pH has been reported to shape microbial communities in soils. However, different microbial groups show different response to pH variation. The relative abundance of Group 1.1c was positively correlated to pH (Figure 3C), which has been found in acidic soils across a pH gradient from 4.5 to 7.5 (Lehtovirta et al., 2009; Tripathi et al., 2013). The relative abundance of *Pseudonocardiaceae* negatively correlated with pH, whereas MB-A2-108 positively correlated with pH (Figures 3C,D) (Seuradge et al., 2017), which was consistent with our results. *Pseudonocardiaceae* has been isolated within a pH range of 5.0–11.0 (Basilio et al., 2003), but they grow better with neutral pH (Ningsih et al., 2019). *Candidatus* Nitrososphaera, positively correlated to pH, was isolated from arable soil with a pH of 7.5 (Ningsih et al., 2019; Nan et al., 2020), and potentially capable of ammonia oxidation as indicated by their genome information (Spang et al., 2012). NO_2^- concentration positively impacted on the relative abundances of MB-A2-108 and *Candidatus* Nitrocosmicus (Figures 3C,D), of which *Candidatus* Nitrocosmicus could oxidize ammonia in high concentration (Lehtovirta-Morley et al., 2016; St. Clair et al., 2020).

4.3. Interactions between bacteria and archaea and potential microbial functions in the karst ecosystem

Strong interactions between archaea and bacteria were observed inside the cave (Figure 4C) as indicated by the visibly direct links between microbial groups in these two domains in the co-occurrence network. For instance, archaeal OTU_42617 (affiliated to *Nitrososphaeraceae*) showed positive correlations with bacterial groups such as *Rokubacteriales*, GAL15, *Gaiella*, Acidobacterial subgroup 6, and subgroup 9 (Figure 4C). All these taxa are reported to be able to participate in nitrogen cycle (Becraft et al., 2017; de Chaves et al., 2019; Obermeier et al., 2020; Longepierre et al., 2021). *Rokubacteriale* participated in nitrogen respiration (Becraft et al., 2017) and *Gaiella* contributed to the conversion of nitrate to nitrite (Albuquerque et al., 2011; Lv et al., 2022). Moreover, GAL15, acidobacterial subgroup 6, and subgroup 9 had been reported to be sensitive to nutrient availability (Hester et al., 2017; Wang J. et al., 2021). Therefore, nitrogen cycle might serve as the vital point in the interaction of archaea and bacteria inside cave, which merits further investigation.

In the prokaryotic networks putative ammonia oxidizer *Nitrososphaeraceae* and nitrate reducer *Gaiella* were found positively correlated both inside and outside the cave (Figures 4C,G), which is also reported in the urban and agricultural ditches with nitrogen-removal (Tatariw et al., 2021). The association between *Nitrososphaeraceae* and *Solirubrobacterales* might be correlated to nutrient flow and soil function recovery in karst soils (Figure 4G) since these taxa are found in high abundance in the highly damaged soils (Wei et al., 2020; Qiu et al., 2021).

Significant different keystone taxa were identified in the inside and outside archaea-bacteria co-occurrence networks based on the top five of betweenness centrality values, which putatively played fundamental ecological functions to sustain the ecosystems. Despite that, the topological properties of bacterial networks were similar to that of the total microbial networks (Supplementary Table 4), the potential ecological functions of archaea could not be overlooked in the karst ecosystems (Supplementary Table 4).

Inside the cave, keystone taxa consisted of archaeal groups of *Candidatus* Methanoperedens (*Euryarchaeota*), *Nitrosopumilaceae* (*Thaumarchaeota*) and bacterial groups of subgroup 6 (*Acidobacteria*), *Rokubacteriales* (*Rokubacteria*) and MB-A2-108 (*Actinobacteria*) (Figure 4D; Supplementary Table 5). Archaeal *Candidatus* Methanoperedens, mainly observed in SP samples, could anaerobically oxidize methane with nitrate as the electron acceptor *via* the reverse methanogenesis pathway and was enriched from an Italian paddy field (Vaksmaa et al., 2017). The ecological trait assignment analysis in SP further confirmed methanogenesis in SP samples with the water-flooded anaerobic conditions due to the convergence of water system at the

entrance of the Heshang Cave (Figure 5A). Chemolithoautotrophic *Nitrosopumilaceae*, predominant in sediment, is able to oxidize ammonia in cave ecosystems (Hathaway et al., 2021). Acidobaterial subgroup 6 can be only enriched in the presence of *Alphaproteobacteria* and has been observed in a chemolithoautotrophically based cave ecosystem (Spring et al., 2000; Meisinger et al., 2007), suggesting that mutually beneficial trophic relationships among subgroup 6 and other taxa in caves. *Rokubacteriales*, dominated in sediment samples especially in the SD samples (11.93 ± 3.85%), may be capable of nitrogen respiration as indicated by their genomic information (Becraft et al., 2017), which is coincident with the results of ecological trait assignment dominated by nitrification and aerobic ammonia oxidation (Figure 5A).

Group 1.1c, *Nitrosophaeraceae*, and *Euryarchaeota* were the keystone taxa in the archaeal network outside the cave. Group 1.1c, dominant in acid FS soils (pH of 4.05 to 5.69), prefer acidic condition and have metabolic potential of fatty acid oxidation in deep anoxic peat (Lin et al., 2015). *Nitrosophaeraceae*, enriched in FS (15.74 ± 9.89%), is known as nitrifiers in aerobic processes (Longepierre et al., 2021), which might play roles in nitrification and aerobic ammonia oxidation in FS niches (Figure 5A). Microbial functional inference further confirmed functional niche differentiation in cave ecosystems except ecological trait assignments (Figures 5B,C). Microbial functional inferences inside the cave was dominated by energy metabolism, such as adenylate cyclase and 8-oxo-dGTP diphosphates, and ATP binding functions, which were closely correlated to DW niches (Figure 5C). In contrast, microbial functional inferences in overlying soils were related to carbohydrate metabolism such as dehydrogenase of aldehyde, long-chain acyl-CoA synthetase, succinate-semialdehyde/glutarate-semialdehyde, and 3-hydroxybutyrate, biotin metabolism and valine, leucine and isoleucine degradation (Figure 5C). It has been reported that most microbes exhibit energy metabolism due to oligotrophic conditions inside caves (Ortiz et al., 2014; Wiseschart et al., 2019), whereas carbohydrate metabolism, biotin metabolism, and degradation were found to be the pivotal functional inferences in outside soil ecosystems in our study.

5. Conclusion

Our results demonstrated differences in community structure, correlation with environmental factors, keystone taxa and potential ecological functions, and interactions between archaea and bacteria, providing new knowledge on archaeal ecology in subterranean biosphere.

1. Both archaeal and bacterial communities showed significant differences in their composition and correlations with environmental factors inside the cave and outside the cave. *Thermoplasmata*, *Nitrosopumilaceae*, *Aenigmarchaeales*, *Crossiella*, *Acidothermus*, and *Solirubrobacter* inside the cave were significantly distinguished from those in overlying soils outside the cave and these members were closely correlated to NH_4^+ concentration. In contrast, *Candidatus* Nitrososphaera, *Candidatus* Nitrocosmicus, *Thaumarchaeota* Group 1.1c, MB-A2-108, and *Pseudonocardiaceae* served as the predictors for microbial communities in the overlying karst soil ecosystems, which correlated to pH, Ca^{2+}, and NO_2^- concentrations.
2. Archaea were more connected than bacteria as indicated by the network analysis. The topological properties of bacterial networks were similar to those of the total prokaryotic networks.
3. Chemolithoautotrophic keystone taxa in the subsurface networks such as subgroup 6, *Candidatus* Methanoperedens, *Rokubacteriales*, and *Nitrosopumilaceae,* might maintain the stability of the cave ecosystem *via* obtaining energy under oligotrophic conditions. On the contrary, microbial functions in karst soils mainly involved in carbohydrate metabolism, biotin metabolism, and synthesis of fatty acid. Notably, all the keystone taxa were correlated to nitrogen cycle in karst ecosystems, indicating the fundamental role of nitrogen in the subsurface biosphere.

Data availability statement

The datasets presented in this study can be found in online repositories. The names of the repository/repositories and accession nusmber(s) can be found at: https://www.biosino.org/node, OER254939.

Author contributions

XC analyzed the data and wrote the manuscript draft. XX assisted in data analysis. YY completed the sample collection and DNA extraction. WW assisted with the partial data analysis. HW organized and conducted the sampling campaigns, obtained funded projects and supervised manuscript. PB assisted in reviewing the manuscript. All authors contributed to the article and approved the submitted version.

Funding

This work was jointly supported by the National Natural Science Foundation of China (grant numbers 91951208 and 41130207) and China Scholarship Council (grant no. 202106410099).

Conflict of interest

The authors declare that the research was conducted in the absence of any commercial or financial relationships that could be construed as a potential conflict of interest.

Publisher's note

Supplementary material

The Supplementary material for this article can be found online at: https://www.frontiersin.org/articles/10.3389/fmicb.2023.1068595/full#supplementary-material

References

Ahmed, Y. A.-R., Pichler, V., Homolák, M., Gömöryová, E., Nagy, D., Pichlerová, M., et al. (2012). High organic carbon stock in a karstic soil of the middle-European Forest Province persists after centuries-long agroforestry management. *Eur. J. Forest Res.* 131, 1669–1680. doi: 10.1007/s10342-012-0608-7

Ai, J., Guo, J., Li, Y., Zhong, X., Lv, Y., Li, J., et al. (2022). The diversity of microbes and prediction of their functions in karst caves under the influence of human tourism activities-a case study of Zhijin cave in Southwest China. *Environ. Sci. Pollut. Res. Int.* 29, 25858–25868. doi: 10.1007/s11356-021-17783-x

Albuquerque, L., Franca, L., Rainey, F. A., Schumann, P., Nobre, M. F., and da Costa, M. S. (2011). *Gaiella occulta* gen. Nov., sp. nov., a novel representative of a deep branching phylogenetic lineage within the class Actinobacteria and proposal of *Gaiellaceae* fam. Nov. and *Gaiellales* Ord. nov. *Syst. Appl. Microbiol.* 34, 595–599. doi: 10.1016/j.syapm.2011.07.001

Alonso, L., Creuze-des-Chatelliers, C., Trabac, T., Dubost, A., Moenne-Loccoz, Y., and Pommier, T. (2018). Rock substrate rather than black stain alterations drives microbial community structure in the passage of Lascaux cave. *Microbiome* 6:216. doi: 10.1186/s40168-018-0599-9

Anda, D., Krett, G., Makk, J., Márialigeti, K., and Mádl-Szőnyi, J. (2017). Comparison of bacterial and archaeal communities from different habitats of the hypogenic Molnár János cave of the Buda thermal karst system (Hungary). *J. Cave Karst Stud.* 79, 113–121. doi: 10.4311/2015mb0134

Baker, A., Hartmann, A., Duan, W., Hankin, S., Comas-Bru, L., Cuthbert, M. O., et al. (2019). Global analysis reveals climatic controls on the oxygen isotope composition of cave drip water. *Nat. Commun.* 10:2984. doi: 10.1038/s41467-019-11027-w

Barton, H. A., Giarrizzo, J. G., Suarez, P., Robertson, C. E., Broering, M. J., Banks, E. D., et al. (2014). Microbial diversity in a Venezuelan orthoquartzite cave is dominated by the *Chloroflexi* (class *Ktedonobacterales*) and *Thaumarchaeota* group I.1c. *Front. Microbiol.* 5:615. doi: 10.3389/fmicb.2014.00615

Barton, H., and Luiszer, F. (2005). Microbial metabolic structure in a sulfidic cave hot spring: potential mechanisms of biospeleogenesis. *J. Cave Karst Stud.* 67, 28–38.

Baselga, A., and Orme, C. D. L. (2012). Betapart: an R package for the study of beta diversity. *Methods Ecol. Evol.* 3, 808–812. doi: 10.1111/j.2041-210X.2012.00224.x

Basilio, A., Gonzalez, I., Vicente, M. F., Gorrochategui, J., Cabello, A., Gonzalez, A., et al. (2003). Patterns of antimicrobial activities from soil actinomycetes isolated under different conditions of pH and salinity. *J. Appl. Microbiol.* 95, 814–823. doi: 10.1046/j.1365-2672.2003.02049.x

Becraft, E. D., Woyke, T., Jarett, J., Ivanova, N., Godoy-Vitorino, F., Poulton, N., et al. (2017). Rokubacteria: genomic giants among the uncultured bacterial phyla. *Front. Microbiol.* 8:2264. doi: 10.3389/fmicb.2017.02264

Bolyen, E., Rideout, J. R., Dillon, M. R., Bokulich, N. A., Abnet, C. C., Al-Ghalith, G. A., et al. (2019). Reproducible, interactive, scalable and extensible microbiome data science using QIIME 2. *Nat. Biotechnol.* 37, 852–857. doi: 10.1038/s41587-019-0209-9

Borsodi, A. K., Knáb, M., Krett, G., Makk, J., Márialigeti, K., Erőss, A., et al. (2012). Biofilm bacterial communities inhabiting the cave walls of the Buda thermal karst system, Hungary. *Geomicrobiol J.* 29, 611–627. doi: 10.1080/01490451.2011.602801

Bradley, C., Baker, A., Jex, C. N., and Leng, M. J. (2010). Hydrological uncertainties in the modelling of cave drip-water $\delta^{18}O$ and the implications for stalagmite palaeoclimate reconstructions. *Quaternary Sci. Rev.* 29, 2201–2214. doi: 10.1016/j.quascirev.2010.05.017

Buresova-Faitova, A., Kopecky, J., Sagova-Mareckova, M., Alonso, L., Vautrin, F., Moenne-Loccoz, Y., et al. (2022). Comparison of *Actinobacteria* communities from human-impacted and pristine karst caves. *Microbiol. Open* 11:e1276. doi: 10.1002/mbo3.1276

Castelle, C. J., Wrighton, K. C., Thomas, B. C., Hug, L. A., Brown, C. T., Wilkins, M. J., et al. (2015). Genomic expansion of domain archaea highlights roles for organisms from new phyla in anaerobic carbon cycling. *Curr. Biol.* 25, 690–701. doi: 10.1016/j.cub.2015.01.014

Chalikakis, K., Plagnes, V., Guerin, R., Valois, R., and Bosch, F. P. (2011). Contribution of geophysical methods to karst-system exploration: an overview. *Hydrogeol. J.* 19, 1169–1180. doi: 10.1007/s10040-011-0746-x

Chang, F., Jia, F., Lv, R., Li, Y., Wang, Y., Jia, Q., et al. (2021). Soil bacterial communities reflect changes in soil properties during the tillage years of newly created farmland on the loess plateau. *Appl. Soil Ecol.* 161:103853. doi: 10.1016/j.apsoil.2020.103853

Chen, H., Li, D., Xiao, K., Wang, K., and Treseder, K. (2018). Soil microbial processes and resource limitation in karst and non-karst forests. *Funct. Ecol.* 32, 1400–1409. doi: 10.1111/1365-2435.13069

Chen, Y., Wu, L., Boden, R., Hillebrand, A., Kumaresan, D., Moussard, H., et al. (2009). Life without light: microbial diversity and evidence of sulfur- and ammonium-based chemolithotrophy in Movile cave. *ISME J.* 3, 1093–1104. doi: 10.1038/ismej.2009.57

Cheng, X., Liu, X., Wang, H., Su, C., Zhao, R., Bodelier, P. L. E., et al. (2021). USCγ dominated community composition and Cooccurrence network of Methanotrophs and bacteria in subterranean karst caves. *Microbiol. Spectr.* 9:e0082021. doi: 10.1128/Spectrum.00820-21

Cheng, X., Wang, H., Zeng, Z., Li, L., Zhao, R., Bodelier, P. L. E., et al. (2022). Niche differentiation of atmospheric methane-oxidizing bacteria and their community assembly in subsurface karst caves. *Environ. Microbiol. Rep.* doi: 10.1111/1758-2229.13112

Cheng, X., Yun, Y., Wang, H., Ma, L., Tian, W., Man, B., et al. (2021). Contrasting bacterial communities and their assembly processes in karst soils under different land use. *Sci. Total Environ.* 751:142263. doi: 10.1016/j.scitotenv.2020.142263

Chroňáková, A., Horák, A., Elhottová, D., and Krištůfek, V. (2009). Diverse archaeal community of a bat guano pile in Domica cave (Slovak karst, Slovakia). *Folia Microbiol.* 54, 436–446. doi: 10.1007/s12223-009-0061-2

de Chaves, M. G., Silva, G. G. Z., Rossetto, R., Edwards, R. A., Tsai, S. M., and Navarrete, A. A. (2019). Acidobacteria subgroups and their metabolic potential for carbon degradation in sugarcane soil amended with vinasse and nitrogen fertilizers. *Front. Microbiol.* 10:1680. doi: 10.3389/fmicb.2019.01680

De Waele, J., Plan, L., and Audra, P. (2009). Recent developments in surface and subsurface karst geomorphology: an introduction. *Geomorphology* 106, 1–8. doi: 10.1016/j.geomorph.2008.09.023

Di Maggio, C., Madonia, G., Parise, M., and Vattano, M. (2012). Karst of Sicily and its conservation. *J. Cave Karst Stud.* 74, 157–172. doi: 10.4311/2011jcks0209

Djemiel, C., Maron, P. A., Terrat, S., Dequiedt, S., Cottin, A., and Ranjard, L. (2022). Inferring microbiota functions from taxonomic genes: a review. *Gigascience* 11, 1–30. doi: 10.1093/gigascience/giab090

Doğruöz-Güngör, N. (2020). The microbial community structure of the Dupnisa cave in Kırklareli, Turkey. *Acta Carsologica* 49, 281–295. doi: 10.3986/ac.v49i2-3.8575

Dong, Y., Gao, J., Wu, Q., Ai, Y., Huang, Y., Wei, W., et al. (2020). Co-occurrence pattern and function prediction of bacterial community in karst cave. *BMC Microbiol.* 20:137. doi: 10.1186/s12866-020-01806-7

Engel, A. S., Meisinger, D. B., Porter, M. L., Payn, R. A., Schmid, M., Stern, L. A., et al. (2010). Linking phylogenetic and functional diversity to nutrient spiraling in microbial mats from lower Kane cave (USA). *ISME J.* 4, 98–110. doi: 10.1038/ismej.2009.91

Fan, Z., Lu, S., Liu, S., Guo, H., Wang, T., Zhou, J., et al. (2019). Changes in plant rhizosphere microbial communities under different vegetation restoration patterns in karst and non-karst ecosystems. *Sci. Rep.* 9:8761. doi: 10.1038/s41598-019-44985-8

Gabriel, C. R., and Northup, D. E. (2013). *Chapter 5: Microbial Ecology: Caves as an Extreme Habitat* London: Springer.

Ghezzi, D., Sauro, F., Columbu, A., Carbone, C., Hong, P. Y., Vergara, F., et al. (2021). Transition from unclassified *Ktedonobacterales* to *Actinobacteria* during amorphous silica precipitation in a quartzite cave environment. *Sci. Rep.* 11:3921. doi: 10.1038/s41598-021-83416-5

Gonzalez-Pimentel, J. L., Martin-Pozas, T., Jurado, V., Miller, A. Z., Caldeira, A. T., et al. (2021). Prokaryotic communities from a lava tube cave in La Palma Island (Spain) are involved in the biogeochemical cycle of major elements. *PeerJ* 9:e11386. doi: 10.7717/peerj.11386

Hartland, A., Fairchild, I. J., Lead, J. R., Borsato, A., Baker, A., Frisia, S., et al. (2012). From soil to cave: transport of trace metals by natural organic matter in karst dripwaters. *Chem. Geol.* 304-305, 68–82. doi: 10.1016/j.chemgeo.2012.01.032

Hathaway, J. J. M., Moser, D. P., Blank, J. G., and Northup, D. E. (2021). A comparison of primers in 16S rRNA gene surveys of bacteria and archaea from volcanic caves. *Geomicrobiol J.* 38, 741–754. doi: 10.1080/01490451.2021.1943727

Hershey, O. S., and Barton, H. A. (2018). *The Microbial Diversity of Caves* Cham: Springer.

Hester, E. R., Harpenslager, S. F., Diggelen, J. M. H. V., Lamers, L. L., Jetten, M. S. M., Lüke, C., et al. (2017). Linking nitrogen load to the structure and function of wetland soil and rhizosphere microbial communities. *mSystems* 3, e00214–e00217. doi: 10.1128/mSystems.00214-17

Hu, X., Liu, X., Qiao, L., Zhang, S., Su, K., Qiu, Z., et al. (2021). Study on the spatial distribution of ureolytic microorganisms in farmland soil around tailings with different heavy metal pollution. *Sci. Total Environ.* 775:144946. doi: 10.1016/j.scitotenv.2021.144946

Hu, Y., Xia, Y., Sun, Q., Liu, K., Chen, X., Ge, T., et al. (2018). Effects of long-term fertilization on phoD-harboring bacterial community in karst soils. *Sci. Total Environ.* 628-629, 53–63. doi: 10.1016/j.scitotenv.2018.01.314

Jiao, S., Liu, Z., Lin, Y., Yang, J., Chen, W., and Wei, G. (2016). Bacterial communities in oil contaminated soils: biogeography and co-occurrence patterns. *Soil Biol. Biochem.* 98, 64–73. doi: 10.1016/j.soilbio.2016.04.005

Jones, D. S., Albrecht, H. L., Dawson, K. S., Schaperdoth, I., Freeman, K. H., Pi, Y., et al. (2012). Community genomic analysis of an extremely acidophilic sulfur-oxidizing biofilm. *ISME J.* 6, 158–170. doi: 10.1038/ismej.2011.75

Kalwasinska, A., Deja-Sikora, E., Szabo, A., Felfoldi, T., Kosobucki, P., Brzezinska, M. S., et al. (2019). Salino-alkaline lime of anthropogenic origin a reservoir of diverse microbial communities. *Sci. Total Environ.* 655, 842–854. doi: 10.1016/j.scitotenv.2018.11.246

Kaufmann, G. (2014). Geophysical mapping of solution and collapse sinkholes. *J. Appl. Geophys.* 111, 271–288. doi: 10.1016/j.jappgeo.2014.10.011

Kim, E., Lee, J., Han, G., and Hwang, S. (2018). Comprehensive analysis of microbial communities in full-scale mesophilic and thermophilic anaerobic digesters treating food waste-recycling wastewater. *Bioresour. Technol.* 259, 442–450. doi: 10.1016/j.biortech.2018.03.079

Kimble, J. C., Winter, A. S., Spilde, M. N., Sinsabaugh, R. L., and Northup, D. E. (2018). A potential central role of *Thaumarchaeota* in N-cycling in a semi-arid environment, Fort

Stanton cave, Snowy River passage, New Mexico, USA. *FEMS Microbiol. Ecol.* 94, 1–17. doi: 10.1093/femsec/fiy173

Lehtovirta, L. E., Prosser, J. I., and Nicol, G. W. (2009). Soil pH regulates the abundance and diversity of group 1.1c Crenarchaeota. *FEMS Microbiol. Ecol.* 70, 367–376. doi: 10.1111/j.1574-6941.2009.00748.x

Lehtovirta-Morley, L. E., Ross, J., Hink, L., Weber, E. B., Gubry-Rangin, C., Thion, C., et al. (2016). Isolation of '*Candidatus* Nitrosocosmicus franklandus', a novel ureolytic soil archaeal ammonia oxidiser with tolerance to high ammonia concentration. *FEMS Microbiol. Ecol.* 92:fiw057. doi: 10.1093/femsec/fiw057

Li, X., Meng, D., Li, J., Yin, H., Liu, H., Liu, X., et al. (2017). Response of soil microbial communities and microbial interactions to long-term heavy metal contamination. *Environ. Pollut.* 231, 908–917. doi: 10.1016/j.envpol.2017.08.057

Liao, H., Zheng, C., Li, J., and Long, J. (2018). Dynamics of soil microbial recovery from cropland to orchard along a 20-year chronosequence in a degraded karst ecosystem. *Sci. Total Environ.* 639, 1051–1059. doi: 10.1016/j.scitotenv.2018.05.246

Lin, X., Handley, K. M., Gilbert, J. A., and Kostka, J. E. (2015). Metabolic potential of fatty acid oxidation and anaerobic respiration by abundant members of Thaumarchaeota and Thermoplasmata in deep anoxic peat. *ISME J.* 9, 2740–2744. doi: 10.1038/ismej.2015.77

Liu, X., Li, M., Castelle, C. J., Probst, A. J., Zhou, Z., Pan, J., et al. (2018). Insights into the ecology, evolution, and metabolism of the widespread Woesearchaeotal lineages. *Microbiome* 6:102. doi: 10.1186/s40168-018-0488-2

Lomakina, A., Pogodaeva, T., Kalmychkov, G., Chernitsyna, S., and Zemskaya, T. (2019). Diversity of NC10 bacteria and ANME-2d archaea in sediments of fault zones at Lake Baikal. *Diversity* 12, 1–19. doi: 10.3390/d12010010

Longepierre, M., Widmer, F., Keller, T., Weisskopf, P., Colombi, T., Six, J., et al. (2021). Limited resilience of the soil microbiome to mechanical compaction within four growing seasons of agricultural management. *ISME Commun.* 1, 1–13. doi: 10.1038/s43705-021-00046-8

Lv, H., Ji, C., Zhang, L., Jiang, C., and Cai, H. (2022). Zinc application promotes nitrogen transformation in rice rhizosphere soil by modifying microbial communities and gene expression levels. *Sci. Total Environ.* 849:157858. doi: 10.1016/j.scitotenv.2022.157858

Ma, L., Huang, X., Wang, H., Yun, Y., Cheng, X., Liu, D., et al. (2021). Microbial interactions drive distinct taxonomic and potential metabolic responses to habitats in karst cave ecosystem. *Microbiol. Spectr.* 9, e0115221–e0101121. doi: 10.1128/Spectrum.01152-21

Macalady, J. L., Jones, D. S., and Lyon, E. H. (2007). Extremely acidic, pendulous cave wall biofilms from the Frasassi cave system, Italy. *Environ. Microbiol.* 9, 1402–1414. doi: 10.1111/j.1462-2920.2007.01256.x

Martín González, A. M., Dalsgaard, B., and Olesen, J. M. (2010). Centrality measures and the importance of generalist species in pollination networks. *Ecol. Complex.* 7, 36–43. doi: 10.1016/j.ecocom.2009.03.008

Martin-Pozas, T., Cuezva, S., Fernandez-Cortes, A., Canaveras, J. C., Benavente, D., Jurado, V., et al. (2022). Role of subterranean microbiota in the carbon cycle and greenhouse gas dynamics. *Sci. Total Environ.* 831:154921. doi: 10.1016/j.scitotenv.2022.154921

Meisinger, D. B., Zimmermann, J., Ludwig, W., Schleifer, K. H., Wanner, G., Schmid, M., et al. (2007). In situ detection of novel Acidobacteria in microbial mats from a chemolithoautotrophically based cave ecosystem (lower Kane cave, WY, USA). *Environ. Microbiol.* 9, 1523–1534. doi: 10.1111/j.1462-2920.2007.01271.x

Mohagheghi, A., Grohmann, K., Himmel, M., Leighton, L., and Updegraff, D. M. (1986). Isolation and characterization of *Acidothermus cellulolyticus* gen. Nov., sp. nov., a new genus of thermophilic, acidophilic, cellulolytic bacteria. *Int. J. Syst. Bacteriol.* 36, 435–443. doi: 10.1099/00207713-36-3-435

Nan, L., Guo, Q., and Cao, S. (2020). Archaeal community diversity in different types of saline-alkali soil in arid regions of Northwest China. *J. Biosci. Bioeng.* 130, 382–389. doi: 10.1016/j.jbiosc.2020.06.001

Ningsih, F., Yokota, A., Sakai, Y., Nanatani, K., Yabe, S., Oetari, A., et al. (2019). *Gandjariella thermophila* gen. Nov., sp. nov., a new member of the family *Pseudonocardiaceae*, isolated from forest soil in a geothermal area. *Int. J. Syst. Evol. Microbiol.* 69, 3080–3086. doi: 10.1099/ijsem.0.003594

Northup, D. E., Barns, S. M., Yu, L. E., Spilde, M. N., Schelble, R. T., Dano, K. E., et al. (2003). Diverse microbial communities inhabiting ferromanganese deposits in Lechuguilla and spider caves. *Environ. Microbiol.* 5, 1071–1086. doi: 10.1046/j.1462-2920.2003.00500.x

Obermeier, M. M., Gnadinger, F., Durai Raj, A. C., Obermeier, W. A., Schmid, C. A. O., Balazs, H., et al. (2020). Under temperate climate, the conversion of grassland to arable land affects soil nutrient stocks and bacteria in a short term. *Sci. Total Environ.* 703:135494. doi: 10.1016/j.scitotenv.2019.135494

Ortiz, M., Legatzki, A., Neilson, J. W., Fryslie, B., Nelson, W. M., Wing, R. A., et al. (2014). Making a living while starving in the dark: metagenomic insights into the energy dynamics of a carbonate cave. *ISME J.* 8, 478–491. doi: 10.1038/ismej.2013.159

Pan, Y., Ni, B.-J., Liu, Y., and Guo, J. (2016). Modeling of the interaction among aerobic ammonium-oxidizing archaea/bacteria and anaerobic ammonium-oxidizing bacteria. *Chem. Eng. Sci.* 150, 35–40. doi: 10.1016/j.ces.2016.05.002

Portillo, M. C., and Gonzalez, J. M. (2009). Sulfate-reducing bacteria are common members of bacterial communities in Altamira cave (Spain). *Sci. Total Environ.* 407, 1114–1122. doi: 10.1016/j.scitotenv.2008.10.045

Qiu, L., Zhang, Q., Zhu, H., Reich, P. B., Banerjee, S., van der Heijden, M. G. A., et al. (2021). Erosion reduces soil microbial diversity, network complexity and multifunctionality. *ISME J.* 15, 2474–2489. doi: 10.1038/s41396-021-00913-1

Ribera, I., Cieslak, A., Faille, A., and Fresneda, J. (2019). *Historical and Ecological Factors Determining Cave Diversity*. Cham: Springer.

Seuradge, B. J., Oelbermann, M., and Neufeld, J. D. (2017). Depth-dependent influence of different land-use systems on bacterial biogeography. *FEMS Microbiol. Ecol.* 93, 1–17. doi: 10.1093/femsec/fiw239

Singleton, D. R., Furlong, M. A., Peacock, A. D., White, D. C., Coleman, D. C., and Whitman, W. B. (2003). *Solirubrobacter pauli* gen. Nov., sp. nov., a mesophilic bacterium within the *Rubrobacteridae* related to common soil clones. *Int. J. Syst. Evol. Microbiol.* 53, 485–490. doi: 10.1099/ijs.0.02438-0

Spang, A., Poehlein, A., Offre, P., Zumbragel, S., Haider, S., Rychlik, N., et al. (2012). The genome of the ammonia-oxidizing *Candidatus* Nitrososphaera gargensis: insights into metabolic versatility and environmental adaptations. *Environ. Microbiol.* 14, 3122–3145. doi: 10.1111/j.1462-2920.2012.02893.x

Spring, S., Schulze, R., Overmann, J., and Schleifer, K.-H. (2000). Identification and characterization of ecologically significant prokaryotes in the sediment of freshwater lakes: molecular and cultivation studies. *FEMS Microbiol. Rev.* 24, 573–590. doi: 10.1111/j.1574-6976.2000.tb00559.x

St. Clair, S., Saraylou, M., Melendez, D., Senn, N., Reitz, S., Kananipour, D., et al. (2020). Analysis of the soil microbiome of a Los Angeles urban farm. *Appl. Environ. Soil Science* 2020, 1–16. doi: 10.1155/2020/5738237

Tait, A. W., Gagen, E. J., Wilson, S. A., Tomkins, A. G., and Southam, G. (2017). Microbial populations of stony meteorites: substrate controls on first colonizers. *Front. Microbiol.* 8:1227. doi: 10.3389/fmicb.2017.01227

Tanunchai, B., Juncheed, K., Wahdan, S. F. M., Guliyev, V., Udovenko, M., Lehnert, A.-S., et al. (2021). Analysis of microbial populations in plastic–soil systems after exposure to high poly(butylene succinate-co-adipate) load using high-resolution molecular technique. *Environ. Sci. Eur.* 33, 1–17. doi: 10.1186/s12302-021-00528-5

Tatariw, C., Mason, O. U., and Mortazavi, B. (2021). Ditching nutrients: roadside drainage networks are hotspots for microbial nitrogen removal. journal of geophysical research. *Biogeosciences* 126, 1–20. doi: 10.1029/2020jg006115

Toumi, M., Abbaszade, G., Sbaoui, Y., Farkas, R., Ács, É., Jurecska, L., et al. (2021). Cultivation and molecular studies to reveal the microbial communities of Groundwaters discharge located in Hungary. *Water* 13, 1–19. doi: 10.3390/w13111533

Tripathi, B. M., Kim, M., Lai-Hoe, A., Shukor, N. A., Rahim, R. A., Go, R., et al. (2013). pH dominates variation in tropical soil archaeal diversity and community structure. *FEMS Microbiol. Ecol.* 86, 303–311. doi: 10.1111/1574-6941.12163

Vaksmaa, A., Guerrero-Cruz, S., van Alen, T. A., Cremers, G., Ettwig, K. F., Luke, C., et al. (2017). Enrichment of anaerobic nitrate-dependent methanotrophic '*Candidatus* Methanoperedens nitroreducens' archaea from an Italian paddy field soil. *Appl. Microbiol. Biotechnol.* 101, 7075–7084. doi: 10.1007/s00253-017-8416-0

Vick-Majors, T. J., Priscu, J. C., and Amaral-Zettler, L. A. (2014). Modular community structure suggests metabolic plasticity during the transition to polar night in ice-covered Antarctic lakes. *ISME J.* 8, 778–789. doi: 10.1038/ismej.2013.190

Vigneron, A., Cruaud, P., Lovejoy, C., and Vincent, W. F. (2022). Genomic evidence of functional diversity in DPANN archaea, from oxic species to anoxic vampiristic consortia. *ISME Commun.* 2, 1–10. doi: 10.1038/s43705-022-00088-6

Wan, S., Liao, X., Zhou, T. T., Wu, Y., Hu, A., Yan, D., et al. (2021). Shift in archaeal community along a soil profile in coastal wheat-maize rotation fields of different reclamation ages. *Land Degrad. Dev.* 32, 4162–4173. doi: 10.1002/ldr.4022

Wang, Y., Cheng, X., Wang, H., Zhou, J., Liu, X., and Tuovinen, O. H. (2022). The characterization of microbiome and interactions on weathered rocks in a subsurface karst cave, Central China. *Front. Microbiol.* 13:909494. doi: 10.3389/fmicb.2022.909494

Wang, J., Fu, X., Ghimire, R., Sainju, U. M., Jia, Y., and Zhao, F. (2021). Responses of soil bacterial community and enzyme activity to organic matter components under long-term fertilization on the loess plateau of China. *Appl. Soil Ecol.* 166:103992. doi: 10.1016/j.apsoil.2021.103992

Wang, B., Kuang, S., Shao, H., Cheng, F., and Wang, H. (2022). Improving soil fertility by driving microbial community changes in saline soils of Yellow River Delta under petroleum pollution. *J. Environ. Manag.* 304:114265. doi: 10.1016/j.jenvman.2021.114265

Wang, X., Li, W., Xiao, Y., Cheng, A., Shen, T., Zhu, M., et al. (2021). Abundance and diversity of carbon-fixing bacterial communities in karst wetland soil ecosystems. *Catena* 204:105418. doi: 10.1016/j.catena.2021.105418

Wang, J., Wang, D., and Wang, B. (2019). Soil bacterial diversity and its determinants in the riparian zone of the Lijiang River, China. *Curr. Sci.* 117, 1324–1332. doi: 10.18520/cs/v117/i8/1324-1332

Wei, H., Liu, Y., Chao, Y., Tsang, D. C. W., Zhao, N., Liu, K., et al. (2020). Recovery of the biological function of ethylenediaminetetraacetic acid-washed soils: roles of environmental variations and microbes. *Sci. Total Environ.* 715:137032. doi: 10.1016/j.scitotenv.2020.137032

Wemheuer, F., Taylor, J. A., Daniel, R., Johnston, E., Meinicke, P., Thomas, T., et al. (2020). Tax4Fun2: prediction of habitat-specific functional profiles and functional redundancy based on 16S rRNA gene sequences. *Environ. Microbiome* 15:11. doi: 10.1186/s40793-020-00358-7

Wen, L., Li, D., Yang, L., Luo, P., Chen, H., Xiao, K., et al. (2016). Rapid recuperation of soil nitrogen following agricultural abandonment in a karst area, Southwest China. *Biogeochemistry* 129, 341–354. doi: 10.1007/s10533-016-0235-3

Wiseschart, A., Mhuantong, W., Tangphatsornruang, S., Chantasingh, D., and Pootanakit, K. (2019). Shotgun metagenomic sequencing from Manao-pee cave, Thailand,

reveals insight into the microbial community structure and its metabolic potential. *BMC Microbiol.* 19:144. doi: 10.1186/s12866-019-1521-8

Wu, F., Zhang, Y., He, D., Gu, J.-D., Guo, Q., Liu, X., et al. (2021). Community structures of bacteria and archaea associated with the biodeterioration of sandstone sculptures at the Beishiku Temple. *Int. Biodeterior. Biodegradation* 164:105290. doi: 10.1016/j.ibiod.2021.105290

Xiang, X., Wang, H., Man, B., Xu, Y., Gong, L., Tian, W., et al. (2022). Diverse Bathyarchaeotal lineages dominate archaeal communities in the acidic Dajiuhu peatland, Central China. *Microb. Ecol.*, 1–15. doi: 10.1007/s00248-022-01990-1

Xiao, D., He, X., Zhang, W., Hu, P., Sun, M., and Wang, K. (2022). Comparison of bacterial and fungal diversity and network connectivity in karst and non-karst forests in Southwest China. *Sci. Total Environ.* 822:153179. doi: 10.1016/j.scitotenv.2022.153179

Xin, Y., Wu, N., Sun, Z., Wang, H., Chen, Y., Xu, C., et al. (2022). Methane seepage intensity distinguish microbial communities in sediments at the mid-Okinawa trough. *Sci. Total Environ.* 851:158213. doi: 10.1016/j.scitotenv.2022.158213

Yu, H., Speth, D. R., Connon, S. A., Goudeau, D., Malmstrom, R. R., Woyke, T., et al. (2022). Community structure and microbial associations in SedimentFree Methanotrophic enrichment cultures from a marine methane seep. *Appl. Environ. Microb.* 88, e0210921–e0210917. doi: 10.1128/aem.02109-21

Yun, Y. (2018). The response of microbial community in karst cave system to environmental changes - a case study of Heshang cave. Doctor degree, China University of Geosciences.

Yun, Y., Cheng, X., Wang, W., and Wang, H. (2018). Seasonal variation of bacterial community and their functional diversity in drip water from a karst cave. *Chin. Sci. Bull.* 63, 3932–3944. doi: 10.1360/N972018-00627

Yun, Y., Wang, H., Man, B., Xiang, X., Zhou, J., Qiu, X., et al. (2016). The relationship between pH and bacterial communities in a single karst ecosystem and its implication for soil acidification. *Front. Microbiol.* 7:1955. doi: 10.3389/fmicb.2016.01955

Zhao, R., Wang, H., Cheng, X., Yun, Y., and Qiu, X. (2018). Upland soil cluster gamma dominates the methanotroph communities in the karst Heshang cave. *FEMS Microbiol. Ecol.* 94, 1–13. doi: 10.1093/femsec/fiy192

Zhao, R., Wang, H., Yang, H., Yun, Y., and Barton, H. A. (2016). Ammonia-oxidizing archaea dominate ammonia-oxidizing communities within alkaline cave sediments. *Geomicrobiol. J.* 34, 511–523. doi: 10.1080/01490451.2016.1225861

Zhao, Y., Weng, Q., and Hu, B. (2022). Microbial interaction promote the degradation rate of organic matter in thermophilic period. *Waste Manag.* 144, 11–18. doi: 10.1016/j.wasman.2022.03.006

Zheng, W., Xue, D., Li, X., Deng, Y., Rui, J., Feng, K., et al. (2017). The responses and adaptations of microbial communities to salinity in farmland soils: a molecular ecological network analysis. *Appl. Soil Ecol.* 120, 239–246. doi: 10.1016/j.apsoil.2017.08.019

Zhu, H.-Z., Zhang, Z.-F., Zhou, N., Jiang, C.-Y., Wang, B.-J., Cai, L., et al. (2019). Diversity, distribution and co-occurrence patterns of bacterial communities in a karst cave system. *Front. Microbiol.* 10, 1–12. doi: 10.3389/fmicb.2019.01726

frontiers | Frontiers in Microbiology

TYPE Original Research
PUBLISHED 21 February 2023
DOI 10.3389/fmicb.2023.1111498

OPEN ACCESS

EDITED BY
Hongchen Jiang,
China University of Geosciences Wuhan, China

REVIEWED BY
Fei Yao,
Biogas Institute of Ministry of Agriculture, Chinese Academy of Agricultural Sciences, China
Yu Shi,
Institute of Soil Science (CAS), China

*CORRESPONDENCE
Hao Yang
✉ yanghao_henry@gxnu.edu.cn
Jiangming Ma
✉ mjming03@gxnu.edu.cn

†These authors have contributed equally to this work

SPECIALTY SECTION
This article was submitted to Terrestrial Microbiology, a section of the journal Frontiers in Microbiology

RECEIVED 29 November 2022
ACCEPTED 25 January 2023
PUBLISHED 21 February 2023

CITATION
Sun H, Hu W, Dai Y, Ai L, Wu M, Hu J, Zuo Z, Li M, Yang H and Ma J (2023) Moso bamboo (*Phyllostachys edulis* (Carrière) J. Houzeau) invasion affects soil microbial communities in adjacent planted forests in the Lijiang River basin, China.
Front. Microbiol. 14:1111498.
doi: 10.3389/fmicb.2023.1111498

Moso bamboo (*Phyllostachys edulis* (Carrière) J. Houzeau) invasion affects soil microbial communities in adjacent planted forests in the Lijiang River basin, China

Hongping Sun[1,2†], Wenyu Hu[2†], Yuxin Dai[1,2], Lin Ai[1,2], Min Wu[3], Jing Hu[2], Zhen Zuo[2], Mengyao Li[2], Hao Yang[1,2*] and Jiangming Ma[1,2*]

[1]Key Laboratory of Ecology of Rare and Endangered Species and Environmental Protection (Guangxi Normal University), Ministry of Education - Guangxi Key Laboratory of Landscape Resources Conservation and Sustainable Utilization in Lijiang River Basin, Guilin, China, [2]College of Life Science, Guangxi Normal University, Guilin, China, [3]College of Biology and Pharmacy, Yulin Normal University, Yulin, China

Introduction: Moso bamboo (*Phyllostachys edulis* (Carrière) J. Houz.), the most widely distributed economic bamboo species in southern China, can easily invade adjacent communities due to its clonal reproduction. However, there is little information on the effects of its establishment and expansion to adjacent forest soil communities, particularly in planted forests.

Methods: We investigated the relationships between soil properties and the microbial community during bamboo invasion under different slope directions (shady or sunny slope) and positions (bottom, middle, or top slope), in three typical stand types (bottom: pure moso bamboo, middle: mixed stands of moso bamboo and Masson pine (*Pinus massoniana* Lamb.), and top: pure Masson pine) in the Lijiang River Basin. This study aimed to explore the effects of key environmental factors on soil microbial composition, diversity, and abundance.

Results and Discussion: The results showed that the abundance of *Acidobacteria* bacterium and *Acidobacteria* bacterium 13_2_20CM_58_27, and *Verrucomicrobia* bacterium decreased as the slope increased ($p<0.05$), whereas the abundance of *Alphaproteobacteria* bacterium, *Actinobacteria* bacterium, *Trebonia kvetii*, and *Bradyrhizobium erythrophlei* increased as the slope increased ($p<0.05$). However, the difference of slope direction on microbial communities was not significant. The pH, organic matter (OM) and total phosphorus (TP) were the key soil environmental factors; most microorganisms (*Betaproteobacteria* bacterium, *Candidatus Eisenbacteria* bacterium, *Betaproteobacteria* bacterium SCGC_AG−212−J23, *Gemmatimonadetes* bacterium, *Actinobacteria* bacterium 13_2_20CM_2_66_6, and *Myxococcaceae* bacterium) showed a positive relationship with pH and a negative relationship with OM and TP. Slope position significantly affected OM, calcium (Ca), total nitrogen (TN), available phosphorus (AP), hydrolyzed nitrogen (HN), pH, and microbial abundance and composition. Slope direction significantly affected TP and magnesium (Mg). The structural equations also indicated that slope position had an effect on microbial composition, abundance, and diversity. Slope position was negatively correlated with pH ($r=-0.333$, $p=0.034$) and positively correlated with OM ($r= 0.728$, $p<0.001$), TN ($r= 0.538$, $p<0.001$) and Ca ($r= 0.672$,

$p<0.001$); pH was positively correlated with microbial composition ($r= 0.634$, $p<0.001$), abundance ($r= 0.553$, $p<0.001$) and diversity ($r= 0.412$, $p=0.002$), TN was positively correlated with microbial composition ($r= 0.220$, $p=0.014$) and abundance ($r= 0.206$, $p=0.013$), and Ca was negatively correlated with microbial composition ($r=-0.358$, $p=0.003$) and abundance ($r=-0.317$, $p=0.003$). Slope position can also influence microbial composition ($r= 0.452$, $p<0.001$) directly. In addition, slope direction had an indirect effect on microbial diversity through total potassium (TK). Therefore, we proposed that the different variations in microbial community during bamboo invasion could be related to the influence of invasion on the soil properties at different invasion stages.

KEYWORDS

moso bamboo invasion, karst soil, microbial community, Lijiang River basin, planted forests

1. Introduction

Moso bamboo (*Phyllostachys edulis* (Carrière) J. Houz.) is a widely planted herb in the forest area in southern China due to its economic value (Ouyang et al., 2022). According to the eighth national forest inventory, the existing bamboo canopy in China covers an area of about $6.01 \times 10^6 km^2$, of which moso bamboo canopy covers about $4.43 \times 10^6 km^2$ (Xu et al., 2020). Moso bamboo is able to expand rapidly because of its strong underground rhizome, which can quickly extend and invade neighboring communities, producing bamboo shoots. This enables clonal expansion of populations into new habitats and increases the area of bamboo forests, gradually leading to the replacement of existing vegetation with moso bamboo. The worldwide distribution of moso bamboo is rapidly expanding (Li et al., 2017). Previous studies have found that the invasion of moso bamboo has caused reductions in plant biodiversity (Ouyang et al., 2016), productivity (Song et al., 2017), and litter production (Song et al., 2016). In the Tianmu Mountain Nature Reserve, moso bamboo invasion caused substantial changes in plant species diversity and had strong negative effects on plant communities (Song et al., 2013). Tian et al. (2020) found that moso bamboo invasion decreased element concentrations in litter and soil as well as total microbial abundance and diversity in subtropical forests in southern China. Masson pine (*Pinus massoniana* Lamb.) forests have been planted for a long time in southern China (Chen et al., 2016). Currently, many Masson pine forests in the Lijiang River Basin have been invaded by moso bamboo, significantly affecting soil properties (Guan et al., 2017). These forests have faced many problems, including low species diversity, simplified structure (monoculture with a poorly developed shrub and herb layer), and poor resistance to natural disturbances. However, few studies have examined the effects of moso bamboo invasion on soil microbial communities of Masson pine, it is also unclear how microbial abundance, composition, and diversity respond to multiple disturbances, or whether multiple environmental changes lead to unanticipated interactive effects (Shang et al., 2021). Consequently, it is urgent to study the impact of moso bamboo invasion on Masson pine forests for ecological stability of the Lijiang River Basin.

Recently, moso bamboo invasion has been a common phenomenon in natural secondary broadleaf, and coniferous forests in the south of China (Xu et al., 2020). In addition, moso bamboo invasion can cause changes to the original soil properties. For example, Ma et al. (2022) studied the impact of moso bamboo invasion on evergreen broad-leaved forests in Anji County, Zhejiang Province, and found that the invasion of moso bamboo increased soil pH and decreased soil organic matter (OM) content. Previous studies (Fukushima et al., 2015; Shiau and Chiu, 2017) have reported the effect of moso bamboo invasion on soil properties, such as soil labile carbon (C) and nitrogen (N) contents. Liu et al. (2019) also found similar results when studying moso bamboo invasion into coniferous forests, which would lead to the decrease of soil C and N content, but had no significant difference on soil phosphorus (P) content. However, Li et al. (2017) indicated that the pH and total nitrogen (TN) levels of the soil in mixed forests during moso bamboo invasion were higher than those in uninvaded and bamboo forest soils. The invasion of adjacent hinoki (*Chamaecyparis obtusa*) forests by moso bamboo lead to an increase in soil pH, resulting in significant and sensitive changes in soil exchangeable calcium contents (Umemura and Takenaka, 2015). Plant invasions can seriously affect soil properties such as soil moisture, pH, and effectiveness of soil nutrients (N and P) (Zhang et al., 2019).

Soil microbial communities are an important component of forest ecosystems, can respond to environmental changes and are remarkably influenced by soil properties (Shang et al., 2021). Waymouth et al. (2020) indicated that microbial communities are closely related to soil properties, such as pH, total phosphorus (TP), and TN. Previous studies indicate that pH is a key factor in directly and indirectly determining organic phosphorus-mineralizing-related gene abundance, which in turn affects microbial diversity (Wan et al., 2021). Soil pH has substantial effects on soil fungi, actinomycetes, and other microorganisms, the abundance of which decreases with increasing soil pH (Shangguan et al., 2019). Widdig et al. (2020) found that TN affected microbial composition by adding TN and TP to a grassland soil. Therefore, plant invasion may impact soil microbial community by influencing soil properties and may have different effects on the abundance, composition, and diversity of the microorganisms (Shangguan et al., 2019; Widdig et al., 2020; Wan et al., 2021).

Karst surface is composed of carbonate minerals and the soil layer is shallow, easily eroded, and degenerative. Owing to the unique geographical location and topography of the Guilin National Forest Park, a sequence of various stages of moso bamboo invasion can be observed on the bottom, middle, and top slopes. This provides unique conditions to study changes in soil properties and the structure

of microbial communities. The objective of the present study was to address the following questions: (1) What are the variations in soil microorganism characteristics at different invasion stages? (2) What are the key soil environmental factors that affect the microbial community? and (3) How do the slope direction and position influence microbial communities? This study focused on the impact of moso bamboo invasion on soil microorganisms in the Lijiang River Basin. Studying the response in soil microbial community composition and diversity to variations in soil properties in different expansion stages will elucidate the key factors involved in plant invasion, thus providing scientific guidance for the restoration and sustainable management of forest vegetation.

2. Materials and methods

2.1. Sample collection and measurement

The study was conducted in the Guilin National Forest Park (25°13′31.46″ N, 110°14′51.37″E), Guangxi Province (Figure 1A). The park is located in the Lijiang River basin area of southwestern China, which is a typical karst landscape. The park has a total area of 581.5 hm^2 and a forest area of 318.1 hm^2. The climate is humid, the annual average temperature is 19.2°C, and the annual average precipitation is 1930.6 mm. The soil type is principally laterite and yellow soil based on the Chinese soil classification; this soil texture is classified as Xanthic Ferralsols in the World Reference Base for Soil Resources (Xu et al., 2020). The soil is generally thin with a coarse texture. The Masson pine forest in the park has a planting history of more than 7 years. After long-term forest closure, it has been transformed into a low-mountain bamboo experimental forest as its care measures, and the management measures are unified. We chose moso bamboo for this investigation on the basis of long-term and continuous research, because the average age of the bamboo is 5 years. Moso bamboo characteristically grows in a 2-year cycle, after 3–5 years of growth, the plant is more vigorous (Lin et al., 2022). Thus, the phenomenon of moso bamboo invading the Masson pine forest occurs at the fifth year.

Sampling of a moso bamboo invasion, in Guilin National Forest Park, was conducted on sunny and shady slopes at the bottom, middle, and top areas of a representative mountain system; sample collection was repeated three times in the same mountain. The different stages of the moso bamboo invasion could be observed on the bottom, middle, and top slopes of Guilin National Forest Park. The bottom slope was covered with moso bamboo; the middle slope was a mixed forest of moso bamboo and Masson pine; the top slope was covered with Masson pine (Figure 1B). This provides a unique condition for studying the changes of soil properties and microbial community structure. We simulated three invasion states of bamboo based on these three stand states. The top slope (T) was considered the previous invasion period, the middle slope (M) was considered the invasion period, and the bottom slope (B) was considered the late invasion period. Natural forest was used as a control group (CK). The shady and sunny slopes of the mountains are, respectively, numbered as E1, E4, and E5 with WS2, S3, and WS6, respectively (Pan et al., 2022). Therefore, the code for the previous invasion period of the shady slope from the first group, is E1_T. The mixed ratio of bamboo stand on the bottom, middle, and top slopes in different slope directions are listed in Table 1. A large 20 × 20 m sample square was set on each slope and five bamboo plants were selected from each quadrate using a five-point sampling method. Litter on the surface was removed, and fine roots (< 2 mm) were dug up with a spade. The rhizosphere soil was obtained by shaking off the fine roots, and then the soil within the quadrate was mixed evenly and kept at 4°C (Wang et al., 2018; Yang et al., 2019). All rhizosphere soil samples were divided into two parts, one was used for DNA extraction and the other was sieved (2 mm) for soil property analyses (Wang et al., 2017; Liu et al., 2018).

2.2. Analyses of soil properties

Soil organic matter (OM) content was calculated by multiplying soil organic carbon (SOC) content by the conventional Van Bemmelen factor of 1.724 (Lundmark et al., 2017; Yang et al., 2019). TP was determined following a complete sulfuric/perchloric acid digestion of unfiltered samples, and pH was determined in a soil–water slurry (ratio 1:2.5) with a combination pH electrode (Chen et al., 2012). The available potassium (AK), total potassium (TK), calcium (Ca), and magnesium (Mg) in the soil were determined by the atomic absorption method (Williams et al., 1966). Boron (B), hydrolyzed nitrogen (HN), available phosphorus (AP), and TN were determined by inductively coupled plasma mass spectrometry, acid hydrolysis, 0.05 mol/l HCL-0.025 mol/l H_2SO_4 analysis, and the semi-micro-Kjeldahl method (Xu et al., 2015), respectively.

2.3. Analysis of soil microorganisms

2.3.1. DNA extraction

DNA extraction and sequencing were conducted by the Sangon Biotech Corporation (Shang hai, China) according to the established protocols. Total community genomic DNA extraction was performed using an E.Z.N.A. Soil DNA Kit (M5635-02, Omega, United States) following the manufacturer's instructions. We measured the concentration of DNA using a Qubit 4.0 (Thermo Fisher, USA) to ensure that adequate amounts of high-quality genomic DNA were extracted.

2.3.2. Library preparation for sequencing

The total amount of DNA input for sample preparation was 500 mg. Sequencing libraries were generated using a Hieff NGS® MaxUp II DNA Library Prep Kit for Illumina® (12200ES96, YEASEN, China) following the manufacturer's instructions, and index codes were added to attribute sequences to each sample. Briefly, DNA was broken into fragments of about 500 bp using Covaris 220. The 500 bp library fragments were purified with Hieff NGS™ DNA Selection Beads DNA (12601ES56; YEASEN, China). The purified DNA was end-repaired and, adapter-ligated, followed by fragment selection. PCR of adapter-ligated DNA was then performed with 2 × Super Canace®II High-Fidelity Mix and Primer Mix (p5/p7). Finally, PCR products were purified (Hieff NGS™ DNA Selection Beads) and the library quality was assessed on the Qubit®4.0 Flurometer. The libraries were then quantified and pooled. Paired-end sequencing of the library was performed on the NovaSeq 6,000 sequencer (Illumina, United States). All sequence data were deposited on the NCBI and accessible *via* BioProject ID of PRJNA902136.

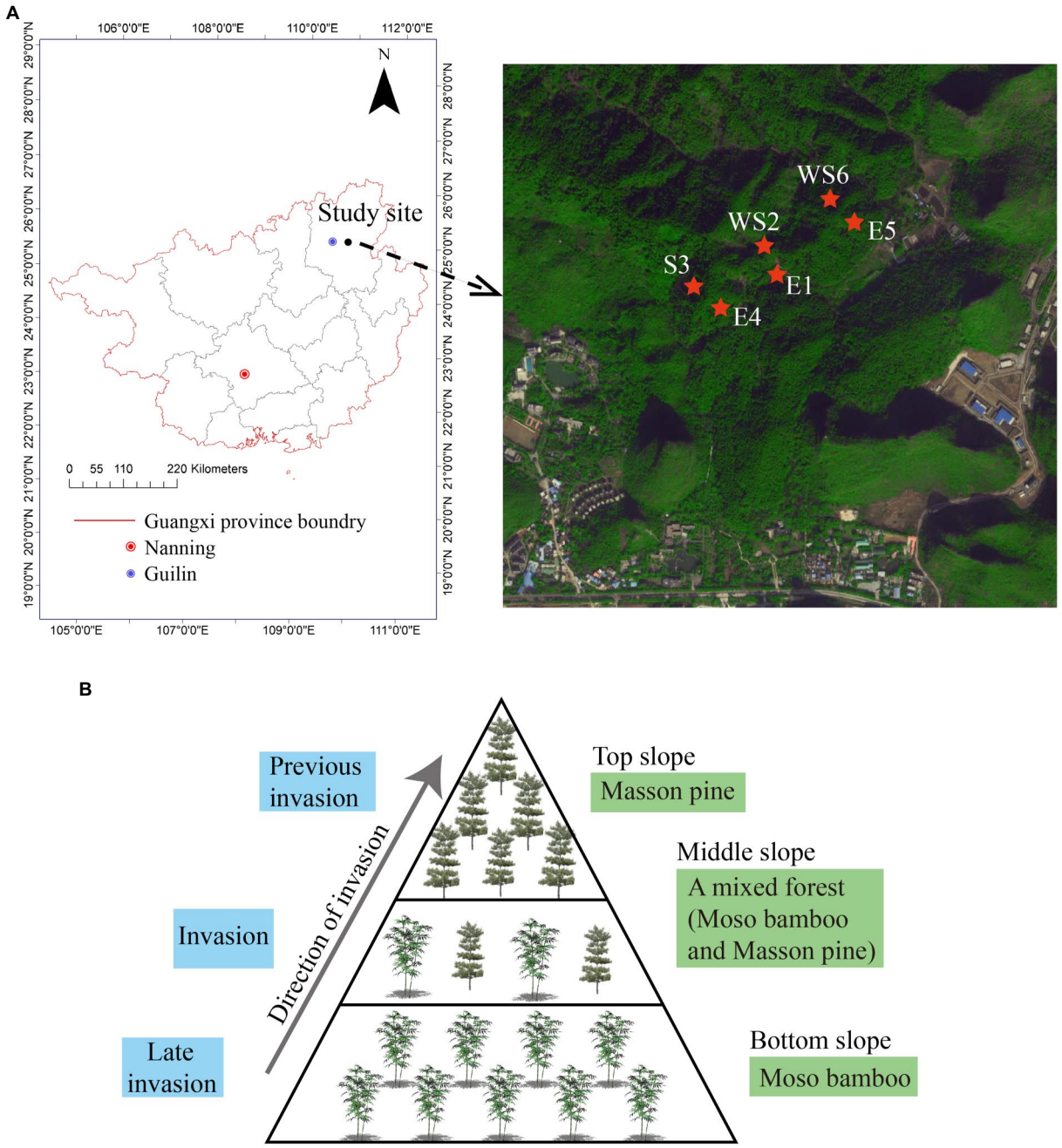

FIGURE 1
Study area settings of different slope directions **(A)** and different slope positions **(B)** in Guilin National Forest Park.

TABLE 1 Differences in bamboo standing degree of bottom slope, middle slope and top slope in different slope directions.

Item	Shady slope			Sunny slope		
	B	M	T	B	M	T
Mixed ratio (Moso bamboo:Masson pine)	22.8:1	1.31:1	0.28:1	5.56:1	0.69:1	0.28:1
Stand density of moso bamboo (tree/hm^2)	1140±140	1175±135	640±70	1390±140	995±335	810±500

B, bottom slope; M, middle slope; T, top slope.

2.3.3. Data assessment and quality control

Fastp (version 0.36) (Chen et al., 2018) was used for evaluating the quality of sequenced data. Four steps were used to filter raw reads: (1) adaptor sequences were removed; (2) low-quality bases ($Q<20$) were removed from 3′ to 5′reads using a sliding window method (window size 4 bp); (3) pairs of overlapping reads were identified and

inconsistent bases were corrected within the interval; (4) reads shorter than 35 nt and their pairing reads were removed. The remaining clean data was used for further analysis.

2.3.4. Metagenome assembly and binning

First, multi-sample mixed splicing was conducted using Megahit (version 1.2.9) (Li et al., 2015) to obtain preliminary spliced contig sequences. Then, bowite2 (version 2.1.0) was used to clean the reads and, map them back to the spliced results; unmapped reads were extracted and spliced again using SPAdes (version 3.13) to obtain low-abundance contigs. MetaWRAP (version 1.3.2) was used for a series of binning, and processes, such as bin sorting, bin purification, bin quantification, bin reassembly, and bin identification, were performed in sequence. After filtering, a draft genome of a single bacteria with high integrity and low contamination was obtained.

2.3.5. Gene prediction and non-redundant gene set construction

Prodigal (version 2.60) was used to predict the open reading frames (ORFs) (Rombel et al., 2022) of the splicing results, select genes longer than or equal to 100 bp, and translate them into amino acid sequences. For the gene prediction results of each sample, the CD-HIT (version 2.60) was used to reduce sequence de-redundancy and obtain a non-redundant gene set. Salmon (version 1.5.0) was used to construct a specific index of non-redundant gene sets and quantify gene abundance in each sample based on gene length by combing a dual-phase algorithm and a bias model.

2.3.6. Species and functional annotations

Species and functional annotation of the genes was conducted by searching against NR,[1] KEGG,[2] eggnog,[3] ARDB,[4] CAZy,[5] and SEED[6] using DIAMOND (version 0.8.20), and other databases to obtain species annotation information and functional annotation information of genes. The *E*-value of 60 was used for screening. Based on gene set abundance information and annotation information, species abundance and functional abundance were obtained, and multi-directional statistical analyses, such as species and functional composition analysis, species and functional difference analysis, and sample comparison analysis were performed.

2.4. Statistical analysis

Path analysis was used to measure the direct and indirect effects of slope direction and position. In the path analysis, a structural equation model (SEM) is designed to measure variables and analyze the relationships among these variables in a path diagram (Fanin and Bertrand, 2016). Here, we hypothesized that microbial diversity is indirectly affected by changes in soil properties, which in turn are caused by slope direction and position (Li et al., 2017). The adequacy of the model was assessed using the χ^2 tests ($p > 0.05$) and the root mean square error of approximation (RMSEA) ($p < 0.05$). These statistical tests were performed in R (version 4.2.1) using the "lavaan" package.

All data analyses were performed in R (version 4.2.1). For normally distributed data, *t*-tests were used to compare differences between two groups and one-way ANOVA to compare the differences among multiple groups. For non-normally distributed data, Wilcoxon test was used to compare the differences between two groups and Kruskal–Wallis test to compare the differences among multiple groups. Pearson's correlation coefficient and Spearman's rank correlations were used to determine the correlation between two normally and non-normally distributed variables, respectively. The Mantel test was performed to discern correlations of soil properties with microbial community composition, abundance, and diversity using the R (version 4.2.1) package "vegan" (Jiang et al., 2022b). Significant difference in all tests was considered at $p < 0.05$. We used Observed, Chao1, and Shannon indexes to represent composition, abundance, and diversity of microorganism, respectively. The SEM test was used to discern correlations among soil properties with microbial Observed, Chao1, and Shannon indexes using the R (version 4.2.1) package "Vegan" (Jiang et al., 2022b).

The collinear diagram, Venn diagram, and correlation heatmap were created using the R packages "circlize," "ggplot2," "VennDiagram," and "corrplot," respectively. The linear regression, redundancy analysis (RDA), and significant difference test were drawn using the R package "Vegan."

3. Results

3.1. Variations of the microbial communities at different invasion stages

The top 10 dominant species from all samples are shown in Figure 2, including *Acidobacteria* bacterium (53.51%), *Gammaproteobacteria* bacterium (9.88%), *Alphaproteobacteria* bacterium (8.40%), *Actinobacteria* bacterium (5.32%), *Trebonia kvetii* (5.30%), *Chloroflexi* bacterium (4.87%), *Acidobacteria* bacterium 13_2_20CM_58_27 (3.83%), *Betaproteobacteria* bacterium (3.45%), *Bradyrhizobium erythrophlei* (2.84%), and *Verrucomicrobia* bacterium (2.60%).

The variation in relative abundance of the most abundant (top 10) microbial species from the soil samples along the slope position is shown in Table 2. *Acidobacteria* bacterium and *Acidobacteria* bacterium 13_2_20CM_58_27, and *Verrucomicrobia* bacterium, had a significant difference at the bottom and top slopes ($p < 0.05$), and decreased with an increase in slope position. However, *Alphaproteobacteria* bacterium, *Actinobacteria* bacterium, *Trebonia kvetii*, and *Bradyrhizobium erythrophlei* had a significant difference at the bottom and top slopes ($p < 0.05$), which increased with an increase in slope position. However, the influence of the slope aspect on soil microbial community was not significant ($p > 0.05$) (Table 3).

Venn diagrams show the number of unique or common OTUs among different slope positions (Figure 3). In terms of the number of different OTUs, E1_B (362) < CK (462) < E1_T (548) < E1_M (601), with the highest degree of overlap between E1_ M and E1_T (492) and the lowest between E1_T and CK (157) (Figure 3A). WS2_B

1 http://ncbi.nlm.nih.gov/
2 http://www.kegg.jp
3 http://eggnogdb.embl.de/
4 https://ardb.cbcb.umd.edu/
5 http://www.cazy.org/
6 http://www.theseed.org/wiki/Main_Page

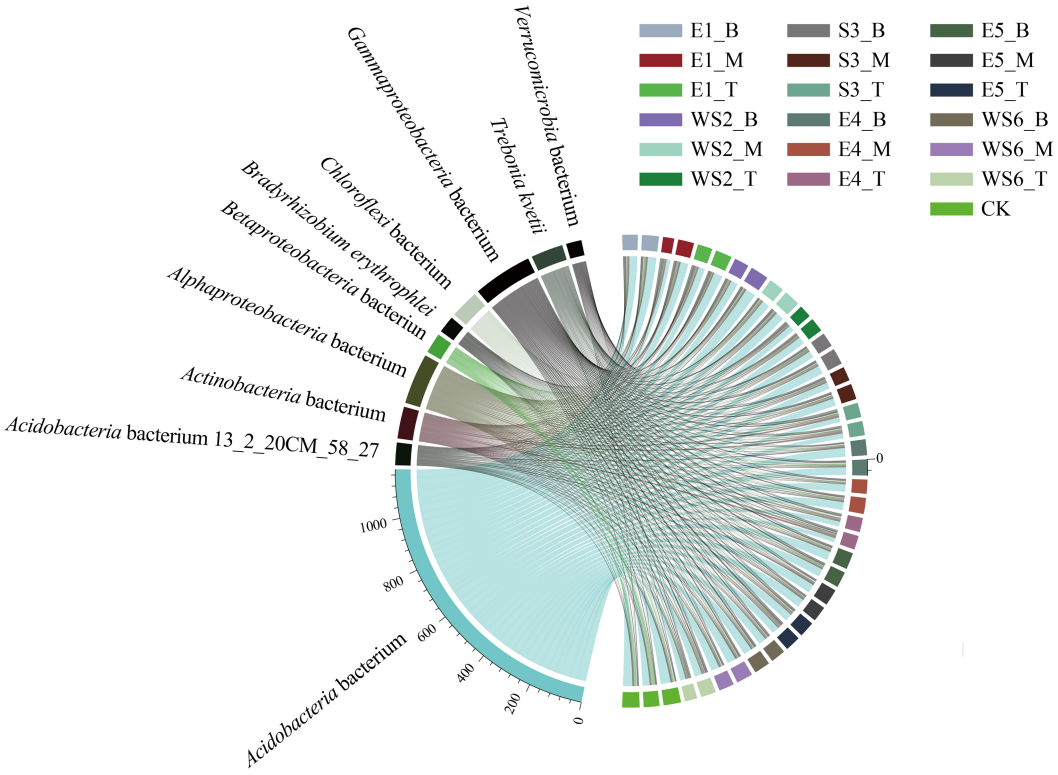

FIGURE 2
Collinear diagram of the top ten dominant microbial species from all samples.

TABLE 2 The variation in relative abundance of the most abundant (top ten) microbial species in samples along the slope position.

	Aci (%)	Gam (%)	Alp (%)	Bet (%)	Aci.27 (%)	Act (%)	Chl (%)	Tre (%)	Ver (%)	Bra (%)
B	33.21 ± 3.72a	6.21 ± 1.29a	3.99 ± 0.69bc	2.11 ± 0.97b	2.76 ± 1.07a	2.34 ± 0.40b	2.91 ± 0.86a	2.21 ± 0.93b	1.78 ± 0.37b	1.40 ± 0.49bc
M	30.75 ± 5.41ab	5.58 ± 1.40a	4.41 ± 0.87b	1.32 ± 0.82b	2.79 ± 1.41a	2.55 ± 0.48b	2.97 ± 1.10a	2.82 ± 1.27b	1.50 ± 0.28b	1.59 ± 0.59ab
T	25.47 ± 5.53b	5.77 ± 1.64a	6.46 ± 1.03a	0.83 ± 0.36b	0.60 ± 0.47b	4.47 ± 2.00a	2.23 ± 1.88a	4.69 ± 0.96a	0.92 ± 0.27c	2.18 ± 0.74a
CK	35.87 ± 5.85a	3.21 ± 0.27b	3.40 ± 0.51c	7.95 ± 3.94a	3.25 ± 1.20a	2.03 ± 0.38b	2.86 ± 1.46a	0.80 ± 0.05c	2.25 ± 0.30a	0.73 ± 0.14c

Data are given as mean ± SD. B, bottom slope; M, middle slope; T, top slope; Aci, *Acidobacteria* bacterium; Gam, *Gammaproteobacteria* bacterium; Alp, *Alphaproteobacteria* bacterium; Bet, *Betaproteobacteria* bacterium; Aci.27, *Acidobacteria* bacterium 13_2_20CM_58_27; Act, *Actinobacteria* bacterium; Chl, *Chloroflexi* bacterium; Tre, *Trebonia kvetii*; Ver, *Verrucomicrobia* bacterium; Bra; *Bradyrhizobium erythrophlei*. Values in the columns followed by the same letter(s) are not significantly different ($p < 0.05$) according to one-way ANOVA.

(273) < CK (448) < WS2_M (509) < WS2_T (966), with the highest degree of overlap between WS2_M and WS2_T (626) and the lowest between WS2_B and CK (98) (Figure 3B). S3_B (413) < CK (441) < S3_M (630) < S3_T (668), with the highest degree of overlap between S3_M and S3_T (496) and the lowest between S3_T and CK (121) (Figure 3C). E4_B (407) < CK (483) < E4_M (578) < E4_T (801), with the highest degree of overlap between E4_M and E4_T (453) and the lowest between E4_B and E4_T (199) (Figure 3D). E5_M (387) < E5_B (458) < CK (482) < E5_T (661), with the highest degree of overlap between E5_B and E5_M (408) and the lowest between E5_T and CK (189) (Figure 3E). WS6_M (321) < CK (397) < WS6_B (427) < WS6_T (654), with the highest degree of overlap between WS6_B and WS6_M (454) and the lowest between WS6_T and CK (194) (Figure 3F). Our results show that the overlap between the middle slope and the top or bottom slopes is higher than that of the top and bottom slopes.

3.2. Relationships between soil properties and microbial communities

We compared the soil properties of shady and sunny slopes (Table 4) and the results showed that the Mg content was significantly different in slope direction ($p < 0.05$), however other soil properties had no significant difference ($p > 0.05$). Table 5 indicates the difference in soil properties at different slope positions of the shady slope. The pH was significantly different at the bottom and top slopes ($p < 0.05$), and it decreased with the increase in slope position. The OM, AP, and Ca content was also significantly different at the bottom and top slopes ($p < 0.05$), however it increased with the increase in slope position. The TN content was not significantly different at the bottom and top slopes ($p > 0.05$), but it increased with the increase in slope position. The different soil properties at different slope positions of the sunny slope are shown in Table 6. The results indicated that OM, AP, Ca, TK, Mg,

TABLE 3 The variation in relative abundance of the most abundant (top ten) microbial species in samples along the slope direction.

	Aci (%)	Gam (%)	Alp (%)	Bet (%)	Aci.27 (%)	Act (%)	Chl (%)	Tre (%)	Ver (%)	Bra (%)
Shady slope	30.03 ± 30.03a	5.94 ± 1.44a	4.92 ± 1.60a	1.64 ± 1.14b	2.29 ± 1.64a	3.00 ± 1.45a	2.91 ± 1.58a	3.13±1.50a	1.41 ± 0.43b	1.71 ± 0.72a
Sunny slope	29.59 ± 29.59a	5.76 ± 1.46a	5.00 ± 1.18a	1.20 ± 0.56b	1.81 ± 1.26a	3.24 ± 1.63a	2.50 ± 1.09a	3.35 ± 1.5a	1.39 ± 0.52b	1.73 ± 0.68a
CK	35.87 ± 5.85a	3.21 ± 0.27b	3.40 ± 0.51b	7.95 ± 3.94a	3.25 ± 1.20a	2.03 ± 0.38a	2.86 ± 1.46a	0.80±0.05b	2.25 ± 0.30a	0.73 ± 0.14b

Data are given as mean ± SD. Aci, *Acidobacteria* bacterium; Gam, *Gammaproteobacteria* bacterium; Alp, *Alphaproteobacteria* bacterium; Bet, *Betaproteobacteria* bacterium; Aci.27, *Acidobacteria* bacterium 13_2_20CM_58_27; Act, *Actinobacteria* bacterium; Chl, *Chloroflexi* bacterium; Tre, *Trebonia kvetii*; Ver, *Verrucomicrobia* bacterium; Bra, *Bradyrhizobium erythrophlei*. Values in the columns followed by the same letter(s) are not significantly different ($p < 0.05$) according to one-way ANOVA.

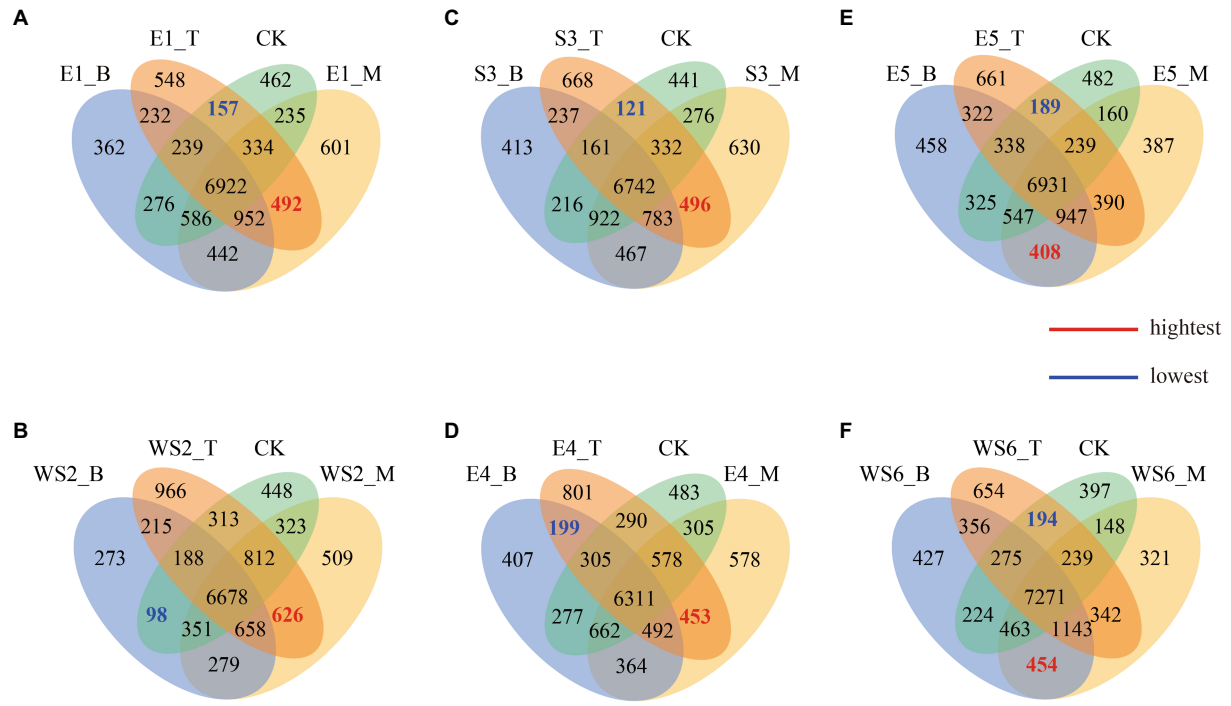

FIGURE 3
Venn diagram showing exclusive and shared OTUs of different slope positions.

and HN were significantly different at the bottom and top slopes ($p < 0.05$), and increased with the increase in slope position. The TN content was not significantly different at the bottom and top slopes ($p > 0.05$), but it increased with the increase in slope position.

Linear regression indicated the relationship between microbial abundance and soil properties (Figure 4). On the bottom slopes of the mountain (Figure 4A), microbial abundance showed a significant positive correlation with soil TP ($p < 0.001$, $F = 48.5$), but an insignificant positive correlation with AP ($p = 0.213$, $F = 1.72$). On the middle slopes of the mountain (Figure 4B), microbial diversity was positively correlated with soil Ca ($p = 0.006$, $F = 11$), pH ($p < 0.001$, $F = 35.5$) and TP ($p < 0.001$, $F = 28.9$), but negatively correlated with soil B ($p = 0.045$, $F = 4.92$), AP ($p = 0.03$, $F = 5.89$), Mg ($p < 0.001$, $F = 49.6$), and TK ($p < 0.001$, $F = 41.5$). On the top slopes of the mountain (Figure 4C), soil microbial abundance was significant positively correlated with pH ($p < 0.001$, $F = 29$). However, the correlation between microbial abundance and other soil properties was not linear.

The RDA of soil properties and the top 1% of the microbial community under every group was chosen to further investigate the relationship between environmental variables and microbial communities. The results are shown in Figure 5. Strong evidence from the first axis of the RDA two-dimensional diagram was found to explain 62.8% of the data, and the second axis accounted for 24.1%. *Betaproteobacteria* bacterium, *Candidatus Eisenbacteria* bacterium, *Betaproteobacteria* bacterium SCGC_AG-212-J23, *Gemmatimonadetes* bacterium, *Actinobacteria* bacterium 13_2_20CM_2_66_6 and *Myxococcaceae* bacterium correlated positively with pH, but negatively with OM and TP. However, *Mycobacterium* sp. 1245111.1, *Mycobacterium fragae, Mycobacterium kyorinense and Mycobacterium cookii* correlated positively with OM and TP, but negatively with pH.

In order to distinguish the effects of slope direction and position on soil properties, a significant difference analysis was performed. Correlation heat maps showed significant differences in the effects of slope direction on TK ($p = 0.008$) and Mg ($p = 0.011$), and that TK and Mg were higher on shady slopes and lower on sunny slopes

TABLE 4 The difference of soil properties in different slope directions.

	Shady slope	Sunny slope	CK
pH	4.79 ± 0.24b	4.80 ± 0.25b	5.60 ± 0.17a
OM (g/kg)	6.12 ± 2.74a	5.95 ± 3.02a	4.00 ± 1.69a
AP (mg/kg)	1.13 ± 1.13a	1.10 ± 1.1a	0.57 ± 0.57a
B (mg/kg)	94.97 ± 94.97a	90.68 ± 90.68a	78.50 ± 78.5b
Ca (g/kg)	0.88 ± 0.88b	0.86 ± 0.86b	1.29 ± 1.29a
TK (g/kg)	21.40 ± 21.4a	18.82 ± 18.82a	10.73 ± 10.73b
Mg (g/kg)	4.44 ± 0.34a	4.01 ± 0.48b	2.54 ± 0.19c
TN (g/kg)	2.07 ± 0.61a	2.01 ± 0.62a	2.21 ± 0.34a
TP (g/kg)	0.35 ± 0.05b	0.33 ± 0.06b	0.47 ± 0.02a
HN (mg/kg)	180.92 ± 45.84a	175.19 ± 48.52a	194.67 ± 21.39a
AK (mg/kg)	79.18 ± 18.28a	69.45 ± 13.23a	65.57 ± 14.72a

Data are given as mean ± SD. Values in the columns followed by the same letter(s) are not significantly different ($p < 0.05$) according to one-way ANOVA.

TABLE 5 The difference of soil properties in different slope positions of shady slope.

	B	M	T	CK
pH	4.90 ± 0.2b	4.83 ± 0.21bc	4.64 ± 0.25c	5.60 ± 0.17a
OM (g/kg)	4.17 ± 1.12b	5.39 ± 1.18b	8.79 ± 2.95a	4.00 ± 1.69b
AP (mg/kg)	0.85 ± 0.33b	0.91 ± 0.35b	1.64 ± 0.87a	0.57 ± 0.2b
B (mg/kg)	98.40 ± 7.75a	96.33 ± 10.23a	90.19 ± 9.81a	78.50 ± 3.4b
Ca (g/kg)	0.70 ± 0.18c	0.85 ± 0.29bc	1.09 ± 0.26ab	1.29 ± 0.44a
TK (g/kg)	21.53 ± 1.59a	21.62 ± 1.87a	21.05 ± 3.83a	10.73 ± 0.49b
Mg (g/kg)	4.38 ± 0.25a	4.59 ± 0.14a	4.35 ± 0.5a	2.54 ± 0.19b
TN (g/kg)	1.74 ± 0.32b	1.98 ± 0.32ab	2.48 ± 0.81ab	2.21 ± 0.3a
TP (g/kg)	0.34 ± 0.05b	0.33 ± 0.02b	0.37 ± 0.07b	0.47 ± 0.02a
HN (mg/kg)	164.00 ± 38a	169.00 ± 29a	210.00 ± 54a	195.00 ± 21a
AK (mg/kg)	85.01 ± 18.54a	82.14 ± 18.96a	70.39 ± 15.12a	60.57 ± 14.72a

Data are given as mean ± SD. B, bottom slope; M, middle slope; T, top slope. Values in the columns followed by the same letter(s) are not significantly different ($p < 0.05$) according to one-way ANOVA.

TABLE 6 The difference of soil properties in different slope positions of sunny slope.

	B	M	T	CK
pH	4.88 ± 0.18b	4.87 ± 0.25b	4.64 ± 0.25b	5.60 ± 0.17a
OM (g/kg)	3.86 ± 0.89b	5.18 ± 2.29b	8.79 ± 2.95a	4.00 ± 1.69b
AP (mg/kg)	0.80 ± 0.47b	0.86 ± 0.4b	1.64 ± 0.87a	0.57 ± 0.2b
B (mg/kg)	86.92 ± 6.78a	94.93 ± 6.24a	90.19 ± 9.81a	78.50 ± 3.4b
Ca (g/kg)	0.69 ± 0.17b	0.82 ± 0.14b	1.09 ± 0.26a	1.29 ± 0.44a
TK (g/kg)	16.45 ± 1.77b	18.97 ± 1.07ab	21.05 ± 3.83a	10.73 ± 0.49c
Mg (g/kg)	3.68 ± 0.35b	4.01 ± 0.35ab	4.35 ± 0.5a	2.54 ± 0.19c
TN (g/kg)	1.73 ± 0.28b	1.83 ± 0.35b	2.48 ± 0.81ab	2.21 ± 0.34a
TP (g/kg)	0.30 ± 0.05b	0.32 ± 0.05b	0.37 ± 0.07b	0.47 ± 0.02a
HN (mg/kg)	157.50 ± 34.43b	158.08 ± 36.94b	210.00 ± 54.39a	194.67 ± 21.39ab
AK (mg/kg)	66.13 ± 15.03a	71.84 ± 9.12a	70.39 ± 15.12a	65.57 ± 14.72a

Data are given as mean ± SD. B, bottom slope; M, middle slope; T, top slope. Values in the columns followed by the same letter(s) are not significantly different ($p < 0.05$) according to one-way ANOVA.

(Figure 6A). Significant differences were found for the effects of slope position on OM ($p < 0.001$), Ca ($p < 0.001$), TN ($p = 0.004$), AP ($p = 0.004$), HN ($p = 0.040$), and pH ($p = 0.042$). OM, Ca, TN, AP, HN content was higher on the top slope than on the bottom and middle

slopes. pH was higher on the middle slope than on the bottom slope (Figure 6B).

3.3. Slope direction and position influence soil microbial communities

In order to analyze the influence of slope direction and position on soil microbial communities, we first analyzed the significance of their influence on the three soil microbial indices. The box-plot of sample distance indicated that the differences between the effect of slope direction on microbial abundance, composition, and diversity were not significant (Figure 7A). However, the difference was significant between the effect of slope position on microbial abundance ($p = 0.029$) and composition ($p = 0.046$), but not on microbial diversity (Figure 7B).

To further understand the relationship between soil microbial indices and soil properties, we used a correlation analysis. The results showed that microbial composition was strongly and significantly correlated with pH ($r = 0.445$, $p = 0.003$), while abundance was significantly and strongly correlated with soil pH ($r = 0.563$, $p = 0.002$), TK ($r = -0.1148$, $p = 0.043$), and AP ($r = -0.484$, $p = 0.049$). Soil microbial diversity had a significant and strong correlation with pH ($r = 0.394$, $p = 0.003$) and a significant but weak correlation with Mg ($r = -0.284$, $p = 0.050$) and TK ($r = -0.253$, $p = 0.010$) (Figure 8).

The correlation analysis of soil properties showed that pH was negatively correlated with TP ($r = -0.38$, $p = 0.024$) and AP ($r = -0.47$, $p = 0.004$). OM was positively correlated with Ca ($r = 0.77$, $p < 0.001$), TN ($r = 0.57$, $p < 0.001$), HN ($r = 0.56$, $p < 0.001$), TP ($r = 0.38$, $p = 0.023$), and AP ($r = 0.49$, $p = 0.002$). B was negatively correlated with Ca ($r = -0.35$, $p = 0.036$), TN ($r = -0.39$, $p = 0.018$), HN ($r = -0.42$, $p = 0.011$), and TP ($r = -0.34$, $p = 0.046$), but positively correlated with

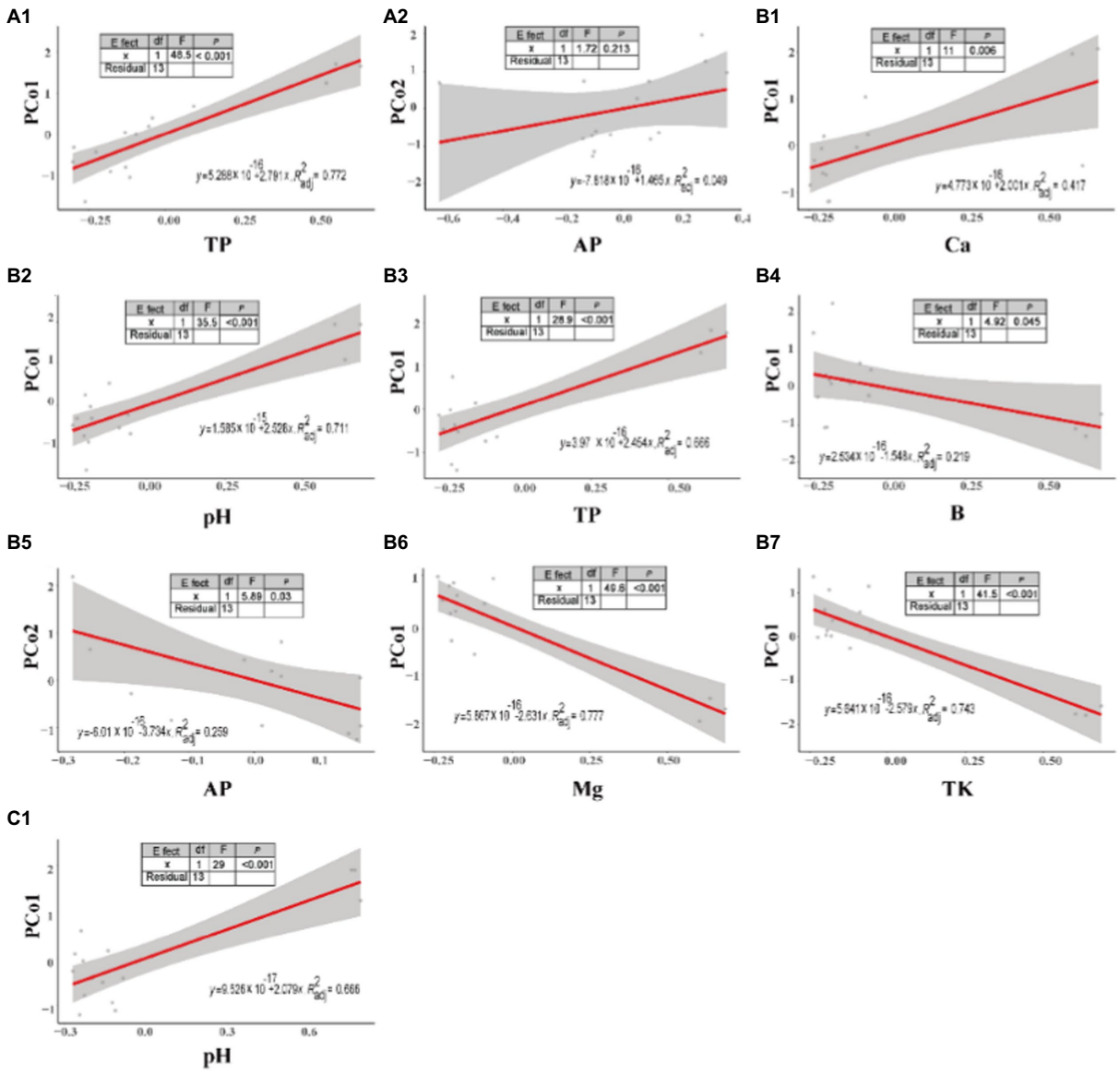

FIGURE 4
Linear regression between soil properties and microbial abundance at different slope positions. **(A)** bottom, **(B)** middle, and **(C)** top slopes.

Mg ($r = 0.51$, $p = 0.001$) and TK ($r = 0.55$, $p = 0.001$). Ca was positively correlated with TN ($r = 0.76$, $p < 0.001$), HN ($r = 0.74$, $p < 0.001$), TP ($r = 0.48$, $p = 0.003$), and AP ($r = 0.53$, $p = 0.001$). Mg was positively correlated with TK ($r = 0.91$, $p < 0.001$). TK was positively correlated with AP ($r = 0.36$, $p = 0.030$). TN was positively correlated with HN ($r = 0.83$, $p < 0.001$), TP ($r = 0.74$, $p < 0.001$), and AP ($r = 0.51$, $p = 0.001$). HN was positively correlated with TP ($r = 0.74$, $p < 0.001$) and AP ($r = 0.54$, $p = 0.001$). TP was positively correlated with AP ($r = 0.42$, $p = 0.011$) (Figure 8).

We hypothesized that changes in soil properties caused by the direction and position of the slope would have different effects on microbial composition, abundance, and diversity. We tested our hypothesis using SEM analyses. The direction and position of the slope directly induced changes in soil properties (pH: 11.1%, OM: 18.9%, TN: 53.0%, TK: 29.0%, Ca: 48.1%). Sunny or shady slopes had a significant negative relationship with TK ($r = -0.435$, $p = 0.004$) content. Slope position had a significant negative relationship with pH ($r = -0.333$, $p = 0.034$), but a positive relationship with OM ($r = 0.728$, $p < 0.001$), TN ($r = 0.538$, $p < 0.001$), and Ca ($r = 0.672$, $p < 0.001$) content. pH was significantly positively related to composition ($r = 0.634$, $p < 0.001$), abundance ($r = 0.553$, $p < 0.001$), and diversity ($r = 0.412$, $p = 0.002$). The TN content was significantly positively related to composition ($r = 0.220$, $p = 0.014$) and abundance ($r = 0.206$, $p = 0.013$), the TK content was negatively related to diversity ($r = -0.344$, $p = 0.011$), the Ca content was negatively related to composition ($r = -0.358$, $p = 0.003$) and abundance ($r = -0.317$, $p = 0.003$), and slope position significantly positively affected composition ($r = 0.452$, $p < 0.001$) (Figure 9).

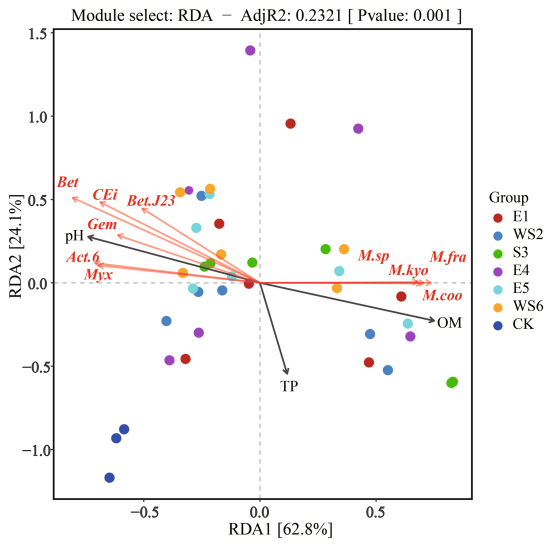

FIGURE 5
RDA analysis between microbial community and soil properties. *Bet*, *Betaproteobacteria* bacterium; *CEi*, *Candidatus Eisenbacteria* bacterium; *Bet.J23*, *Betaproteobacteria* bacterium SCGC AG–212–J23; *Gem*, *Gemmatimonadetes* bacterium; *Act.6*, *Actinobacteria* bacterium 13_2_20CM_2_66_6; *Myx*, *Myxococcaceae* bacterium; *M.sp*, *Mycobacterium* sp. 1245111.1; *M.fra*, *Mycobacterium fragae*; *M.kyo*, *Mycobacterium kyorinense*; *M.coo*, *Mycobacterium cookii*.

4. Discussion

4.1. Response of soil microbial communities variation to moso bamboo invasion

When comparing the relative abundance of the top 10 microbial species at different slope positions (Table 2), the present study found that the abundance of *Acidobacteria* bacterium and *Acidobacteria* bacterium 13_2_20CM_58_27, and *Verrucomicrobia* bacterium was significantly different between the top and the bottom slopes ($p < 0.05$), the relative abundance at the top slope was low, while the relative abundance at the bottom slope was high. The abundance of *Alphaproteobacteria* bacterium, *Actinobacteria* bacterium, *Trebonia kvetii*, and *Bradyrhizobium erythrophlei* was also significantly different between the top and bottom slopes ($p < 0.05$), but their relative abundance was higher on the top slope. *Acidobacteria* bacterium and *Acidobacteria* bacterium 13_2_20CM_58_27 belong to the *Acidobacteria* phylum. A previous study, which reported *Acidobacteria* as the dominant flora in karst areas (Jiang et al., 2022c), which are widely distributed and have specific ecological functions in forest soil (Liu et al., 2017).

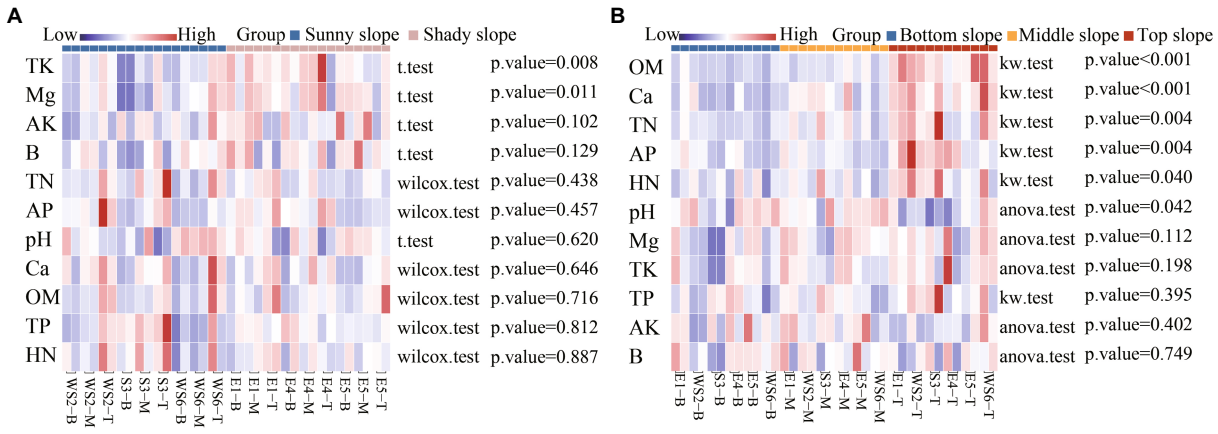

FIGURE 6
Correlation heatmap between soil properties and slope direction **(A)** and position **(B)**.

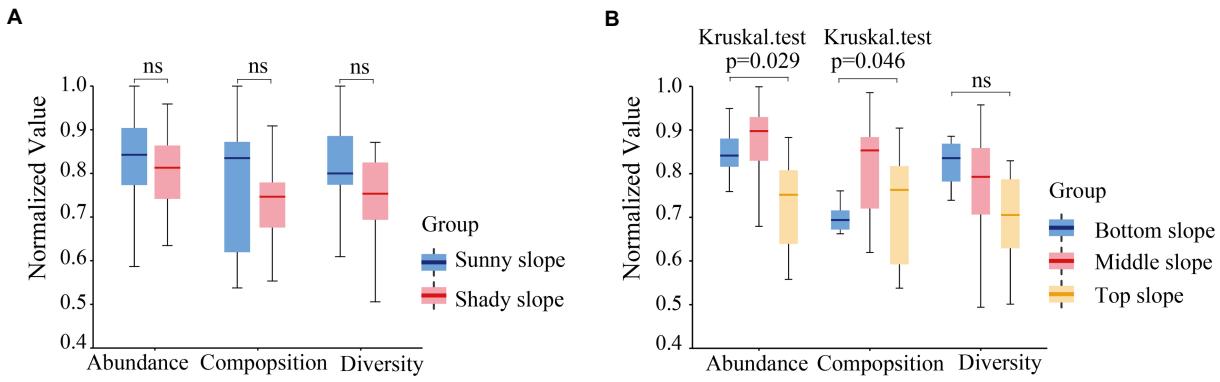

FIGURE 7
Significant difference of microbial abundance, composition, and diversity on slope direction **(A)** and position **(B)**.

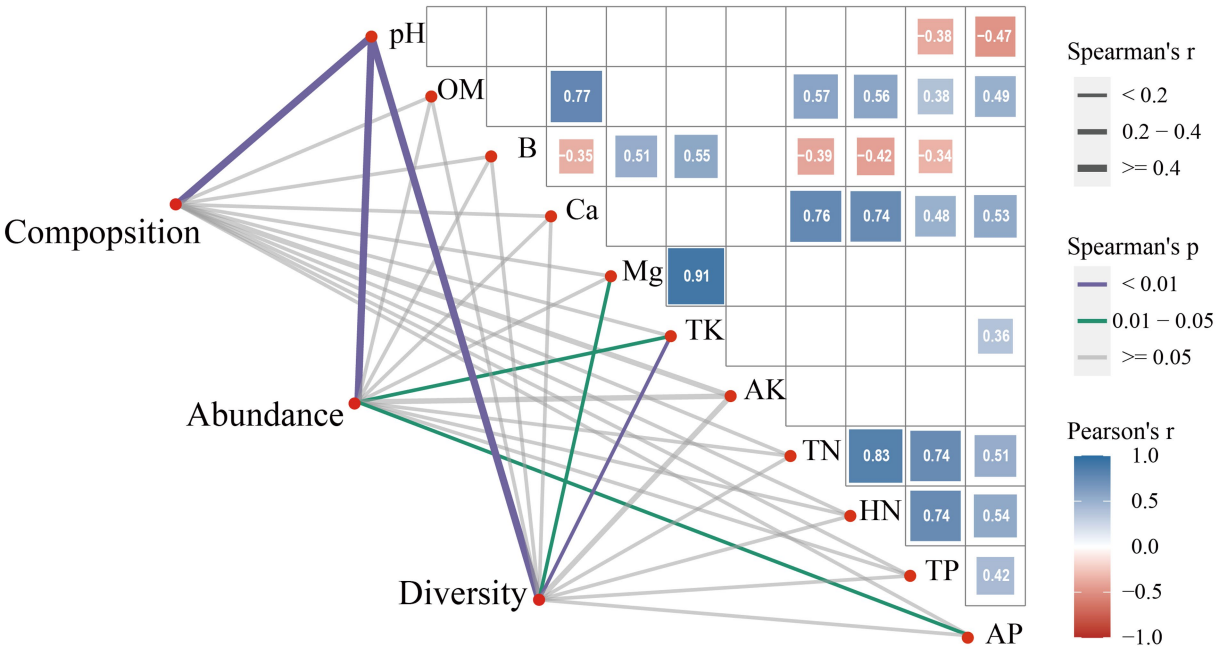

FIGURE 8
Correlation of soil properties with microbial composition, abundance, and diversity.

Acidobacteria are involved in nitrogen fixation, organic matter decomposition, and plant growth promotion and they are sensitive to soil pH, soil temperature, and plant diversity (Zhang et al., 2014; Kim et al., 2021). Our study found that the relative abundance of *Acidobacteria* was the highest in all samples, which is consistent with other studies (Liu et al., 2017; Jiang et al., 2022c). Although the pH of the bottom slope was higher than that of the top slope, both had low pH, which is suitable for the growth of *Acidobacteria*. The relative abundance of *Acidobacteria* on the bottom slope was higher because of *Acidobacteria* are oligotrophs and versatile heterotrophs (Lin et al., 2013), better adapted to extreme environments. *Alphaproteobacteria* bacterium and *Bradyrhizobium erythrophlei* belong to the *Proteobacteria* phylum. *Proteobacteria* include species attributed to nitrogen fixation, organic matter decomposition, and plant growth promotion (Zhang and Xu, 2008; Yarwood et al., 2009). *Alphaproteobacteria* bacterium and *Bradyrhizobium erythrophlei* were higher at the top slope, possibly due to the high OM content in the top slope. *Actinobacteria bacterium* and *Trebonia kvetii* belong to the *Actinobacteria* phylum. *Actinobacteria* are ubiquitous in the soil owing to their potential to grow in extreme environments by deploying a defense system that stems from their ability to produce secondary metabolites (Lee et al., 2018). *Actinobacteria* produce extracellular hydrolases that decompose the biomass of animals or plants, rendering them the central organisms in the carbon cycle. For example, decomposition of different organic substances such as cellulose, organic acids and humus is possible *via* the production of cellulase and chitinase (El-Tarabily et al., 1996; Ranjani et al., 2016; Bhatti et al., 2017). In our study, *Actinobacteria* bacterium and *Trebonia kvetii* had higher relative abundance in the top slope. This may be due to the nutrient cycling

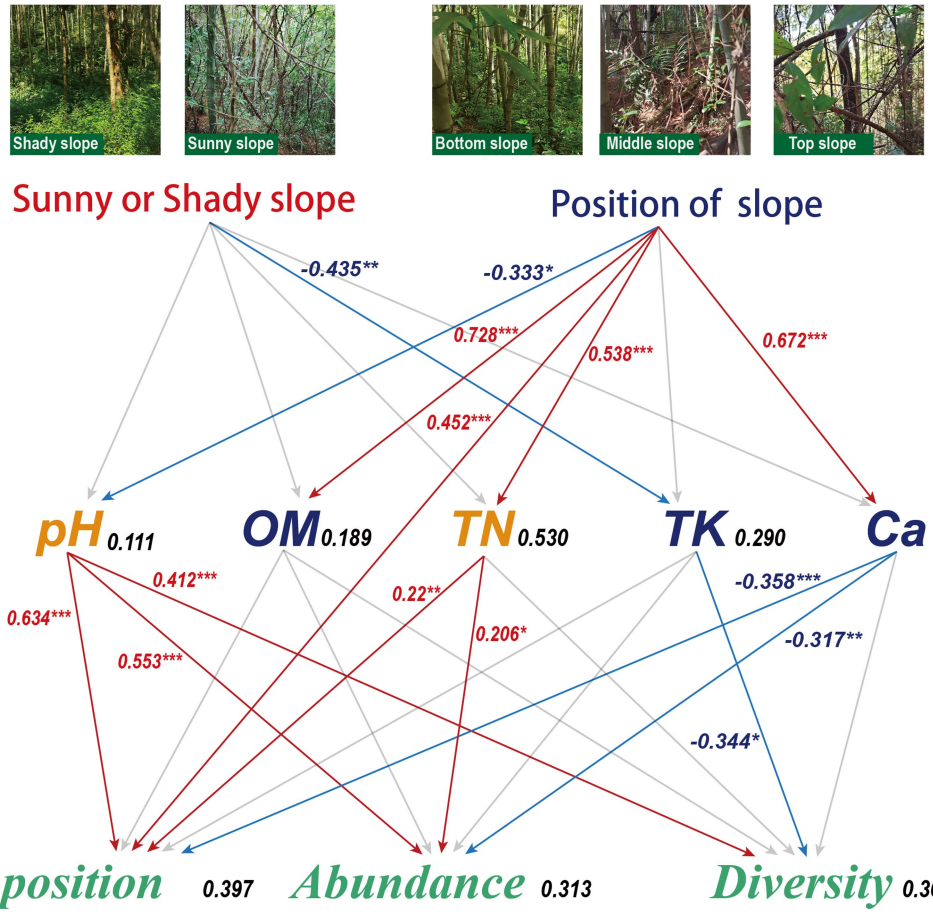

FIGURE 9
A structural equation model for the relationship between soil properties and microbial community composition, abundance, and diversity as influenced by slope direction and slope position. The number in the right of each of the soil or microbial parameter is the squared-multiple correlation, and the number on each line between these parameters is the standardized regression-weight (*: significant at $p < 0.05$; **: significant at $p < 0.01$; ***: significant at $p < 0.001$). Red solid lines indicate that the standardized regression weights are negative, blue solid lines indicate that the standardized regression weights are positive, and gray dashed lines indicate that the standardized regression weights are not significant ($p \geq 0.05$) and thus their statistics are not shown.

system of the original Masson pine forest being disturbed during the invasion of moso bamboo. *Actinobacteria* bacterium and *Trebonia kvetii* failed to adapt to new conditions, which affected their survival and decreased their relative abundance in the soil. *Verrucomicrobia* bacterium belong to the *Verrucomicrobia* phylum. Shen et al. (2017) indicated that *Verrucomicrobia* had a strong correlation with pH. However, other soil features, such as C:N ratio, soil moisture, TC, and TN, also significantly affected the *Verrucomicrobia*. In our study, *Verrucomicrobia* bacterium also showed higher abundance in the bottom slope, possibly relative to soil pH.

The Venn diagram shows that the top slope had a higher overlap with the middle slope than with the bottom slope (Figure 3), indicating that moso bamboo invasion changes the OTUs of the microbial community, probably due to the changes in the original vegetation community caused by the invasion. These changes cause differences in underground root secretions and surface apoplast, which impact the soil carbon source and nutrient cycling, leading to changes in the microbial community (Millard and Singh, 2010). Invasion of broadleaf evergreen forests by moso bamboo reduces the active organic carbon and nitrogen content of the soil, decreases the nutrient content of the original soil, and changes the structure of the original soil organic carbon and nitrogen pool (Zhang et al., 2019).

4.2. Key soil properties closely related to microbial communities

By comparing the soil properties of different slope directions, we found that Mg content showed significant differences ($p < 0.05$); and the Mg content in the shady slope was higher than that in the sunny slope (Table 4). By comparing the soil properties of different slope positions, we found that pH was significantly different on the slope position of the shady slope ($p < 0.05$), and decreased with the increase in slope position, but not significantly different on the slope position of the sunny slope ($p > 0.05$). The OM, AP, and Ca content was significantly different at the bottom and the top slope ($p < 0.05$), and increased with the increase of slope position in both shady and sunny slopes (Tables 5, 6). RDA analysis showed that pH, TP, and OM were the key factors that influenced the microbial communities

(Figure 5). This suggests that microbial abundance in the previous invasive and invasive stages of the moso bamboo invasion is positively correlated with pH. Similar results have been observed in other case studies. Numerous studies (Zhang et al., 2017; Liu et al., 2021) have shown that soil microbial communities are highly sensitive to changes in pH. Invasion of moso bamboo forests has led to changes in pH and microbial diversity, and there is strong evidence that pH is a major controlling factor of the composition of soil bacterial and fungal communities (Fierer and Jackson, 2006; Nicol et al., 2008). For example, Li et al. (2022) reported that the increase in bacterial abundance can be attributed to the increased pH in the bamboo-invaded site, because pH tends to increase bacterial diversity. Zhao et al. (2019) found that soil pH and microbial community structure are indirectly driven by plants. Plant root exudates and organic acids produced during litter decomposition were the main factors that decreased the soil pH. In addition, hot and humid climate conditions and the higher concentration of calcium in karst mountain areas promote the growth of microorganisms and decrease soil acid reactions, which affects soil microbial composition and diversity. Our study found that microbial abundance was positively correlated with TP on the bottom and middle slopes. Other studies have reported similar results, indicating that among the soil properties, TN, TP, and pH have the greatest influence on soil bacterial diversity (Guo et al., 2020). In addition, Jiang et al. (2022a) found that soil microbial communities were more limited by C and P in the karst ecosystem of Tiankeng.

4.3. Influence mechanisms of slope direction and position on soil microbial communities

The structural equation model values (chisq = 18.061, *value of* $p = 0.583$, cfi = 1.000, rmsea = 0) confirm the goodness of the model fit and the feasibility of the simulation results. Although soil microorganisms also affected soil properties, our goal was to explore the mechanism by which slope direction and slope position affected microorganisms. The results showed that slope direction indirectly affects microbial diversity through TK (Figure 9). Similar results were obtained by Bai et al. (2016), who showed that slope direction has a significant effect on the composition, structure, and function of microbial communities in karst sink holes. Soil TK plays an important role in the accumulation of biomass and the restoration of forest vegetation in karst areas, and the TK content decreases during the accumulation of biomass and the enrichment of plant species (Shen et al., 2020). Similar negative correlation between TK and microbial diversity was found in our study. Other studies have reported that slope-induced factors, such as TP, TN, TK, pH, and soil water content are important sources of ectomycorrhizal fungal richness (Wei et al., 2021). It has also been found that slope direction influences nitrogen morphology and the proportion of each nitrogen state, which differs from our findings and may be caused by differences in the study area (Huang et al., 2015). Since slope direction is a factor that indirectly affects TK variation, the analysis suggests that factors such as light and moisture may also influence microbial diversity. Differences in microbial diversity on shaded and sunny slopes may be due to differences in the microclimate created by slope direction (Chu et al., 2016).

The top, middle, and bottom slopes represent the previous invasion, invasion, and late invasion stages of moso bamboo, respectively. In general, our results showed that slope position had a significant effect on microbial composition and microbial abundance, but not on microbial diversity (Figure 7). Slope position was directly negatively correlated with pH, and positively correlated with OM, TN, and *Ca.* pH was positively correlated with microbial composition, abundance, and diversity; TN was positively correlated with microbial composition and abundance, and Ca was negatively correlated with microbial composition and abundance (Figure 9). The result indicated a positive correlation between pH and microbial diversity, which is similar to previous findings by Wan et al. (2021), who considered that spatial differences in soil microbial diversity are caused by pH-driven organic phosphorus mineralization. Previous studies (Ouyang et al., 2022) have also confirmed the increase in forest soil pH caused by bamboo invasion. Soil TN is a key soil environmental factor affecting microbial diversity. In this study, we found a positive correlation between TN and microbial composition and abundance, thus corroborating previous studies. For example, soil TN has the greatest effect on soil microbial diversity on the Loess Plateau, and greatly affects fungal community structure (Guo et al., 2020). Li et al. (2021) also found a significant positive correlation between TN and bacterial populations in their study on the Tibetan Plateau. Karst soils are characterized by a lack of nitrogen and phosphorus, but high Ca and Mg content (Li et al., 2019).The positive effect of slope position on Ca may indicate that moso bamboo exacts different limitations on soil Ca at different stages of invasion, which in turn may indirectly affect soil microbial diversity. Previous studies (Li et al., 2013) have revealed that moso bamboo affects soil nutrients and carbon inputs, which are important factors influencing the structure of the soil microbial community. A quantitative study on the variation in pH, Ca, and TN by slope position and the variation in TK by slope direction identified the key soil properties that affect the changes in microbial composition, abundance and diversity caused by moso bamboo invasion. The differences between our study and previous studies may be due to the unique nature of the high Ca and Mg content in karst soils (Li et al., 2019).

5. Conclusion

This study provides a comprehensive assessment of the composition, abundance and diversity of microorganisms during bamboo invasion in the Lijiang River Basin. Our results showed that the abundance of *Acidobacteria* bacterium, *Acidobacteria* bacterium 13_2_20CM_58_27, and *Verrucomicrobia* bacterium decreased, while that of *Alphaproteobacteria* bacterium, *Actinobacteria* bacterium, *Trebonia kvetii*, and *Bradyrhizobium erythrophlei* increased as the slope increased ($p < 0.05$). However, the difference of slope direction on microbial community was not significant. Most soil microorganisms were significantly positively correlated with soil pH and were significantly negatively correlated with soil OM and TP. The abundance and composition of microbial communities significantly differed with slope position. Slope position indirectly affects microbial composition, abundance, and diversity through pH, OM, TN, and Ca; however, it can directly influence microbial composition. Slope direction indirectly affects microbial diversity through TK. This study elucidates the response mechanisms of soil microbial composition, abundance, and

diversity to moso bamboo invasion, and these results can help with the development of management strategies for the Lijiang River Basin.

Data availability statement

The datasets presented in this study can be found in online repositories. The names of the repository/repositories and accession number(s) can be found below: https://www.ncbi.nlm.nih.gov/, PRJNA902136.

Author contributions

HY and JM: original draft preparation and methodology. HS and WH: performed experiments, analyzed data, and wrote manuscript. YD, LA, MW, JH, ZZ, and ML: conducted field sampling and plot surveys. All authors contributed to the article and approved the submitted version.

Funding

This research was funded by the Basic Ability Enhancement Program for Young and Middle-aged Teachers of Guangxi (2021KY0058), Guangxi Key Research and Development Projects (Guike AB21220057), National Natural Science Foundation (32260387), and Key R & D Projects in Guangxi (Guike AB22080071).

Acknowledgments

We are grateful to the Guilin National Forest Park for their support in field sampling and data collection.

Conflict of interest

The authors declare that the research was conducted in the absence of any commercial or financial relationships that could be construed as a potential conflict of interest.

Publisher's note

Supplementary material

The Supplementary material for this article can be found online at: https://www.frontiersin.org/articles/10.3389/fmicb.2023.1111498/full#supplementary-material

References

Bai, S. B., Conant, R. T., Zhou, G. M., Wang, Y. X., Wang, N., Li, Y. H., et al. (2016). Effects of moso bamboo encroachment into native, broad-leaved forests on soil carbon and nitrogen pools. *Sci. Rep.* 6:8. doi: 10.1038/srep31480

Bhatti, A., Haq, S., and Bhat, R. (2017). Actinomycetes benefaction role in soil and plant health. *Microb. Pathog.* 111, 458–467. doi: 10.1016/j.micpath.2017.09.036

Chen, X. M., Fang, K., and Chen, C. (2012). Seasonal variation and impact factors of available phosphorus in typical paddy soils of Taihu Lake region, China. *Water Environ. J.* 26, 392–398. doi: 10.1111/j.1747-6593.2011.00299.x

Chen, F., Yuan, Y. J., Yu, S. L., and Zhang, T. W. (2016). Influence of climate warming and resin collection on the growth of Masson pine (*pinus massoniana*) in a subtropical forest, southern China. *Trees* 30:1017. doi: 10.1007/s00468-015-1222-3

Chen, S., Zhou, Y., Chen, Y., and Gu, J. (2018). Fastp: an ultra-fast all-in-one fastq preprocessor. *Bioinformatics* 34, i884–i890. doi: 10.1093/bioinformatics/bty560

Chu, H. Y., Xiang, X. J., Yang, J., Adams, J. M., Zhang, K. P., Li, Y. T., et al. (2016). Effects of slope aspects on soil bacterial and arbuscular fungal communities in a boreal Forest in China. *Pedosphere* 26, 226–234. doi: 10.1016/s1002-0160(15)60037-6

El-Tarabily, K., Sykes, M., Kurtboke, D., Hardy, G., Hardy, A., Barbosa, R., et al. (1996). Synergistic effects of a cellulase-producing I Micromonospora carbonacea and an I antibiotic-producing Streptomyces violascens on I the suppression of Phytophthora cinnamomi root I rot of Banksia grandis. *Can. J. Bot.* 74, 618–624. doi: 10.13140/2.1.3286.1124

Fanin, N., and Bertrand, I. (2016). Aboveground litter quality is a better predictor than belowground microbial communities when estimating carbon mineralization along a land-use gradient. *Soil Biol. Biochem.* 94, 48–60. doi: 10.1016/j.soilbio.2015.11.007

Fierer, N., and Jackson, R. B. (2006). The diversity and biogeography of soil bacterial communities. *Proc. Natl. Acad. Sci. U. S. A.* 103, 626–631. doi: 10.1073/pnas.0507535103

Fukushima, K., Usui, N., Ogawa, R., and Tokuchi, N. (2015). Impacts of moso bamboo (*phyllostachys pubescens*) invasion on dry matter and carbon and nitrogen stocks in a broad-leaved secondary forest located in Kyoto, Western Japan. *Plant Species Biol.* 30, 81–95. doi: 10.1111/1442-1984.12066

Guan, F. Y., Xia, M. P., Tang, X. L., and Fan, S. H. (2017). Spatial variability of soil nitrogen, phosphorus and potassium contents in Moso bamboo forests in Yong'an City, China. *Catena* 150, 161–172. doi: 10.1016/j.catena.2016.11.017

Guo, Y. N., Liu, X. H., Tsolmon, B., Chen, J., Wei, W., Lei, S. G., et al. (2020). The influence of transplanted trees on soil microbial diversity in coal mine subsidence areas in the loess plateau of China. *Glob. Ecol. Conser.* 21:e00877. doi: 10.1016/j.gecco.2019.e00877

Huang, Y. M., Liu, D., and An, S. S. (2015). Effects of slope aspect on soil nitrogen and microbial properties in the Chinese loess region. *Catena* 125, 135–145. doi: 10.1016/j.catena.2014.09.010

Jiang, C., Li, H., and Zeng, H. (2022a). Karst tiankeng create a unique habitat for the survival of soil microbes: evidence from ecoenzymatic stoichiometry. *Front. Ecol. Evol.* 10:10. doi: 10.3389/fevo.2022.1011495

Jiang, C., Liu, Y., Li, H., Zhu, S., Sun, X., Wu, K., et al. (2022b). The characterization of microbial communities and associations in karst tiankeng. *Front. Microbiol.* 13:13. doi: 10.3389/fmicb.2022.1002198

Jiang, C., Sun, X. R., Feng, J., Zhu, S. F., and Shui, W. (2022c). Metagenomic analysis reveals the different characteristics of microbial communities inside and outside the karst tiankeng. *BMC Microbiol.* 22:115. doi: 10.1186/s12866-022-02513-1

Kim, H. S., Lee, S. H., Jo, H. Y., Finneran, K. T., and Kwon, M. J. (2021). Diversity and composition of soil *Acidobacteria* and *Proteobacteria* communities as a bacterial indicator of past land-use change from forest to farmland. *Sci. Total Environ.* 797:148944. doi: 10.1016/j.scitotenv.2021.148944

Lee, L. H., Chan, K. G., Stach, J., Wellington, E. M. H., and Goh, B. H. (2018). Editorial: the search for biological active agent(s) from *Actinobacteria*. *Front. Microbiol.* 9:4. doi: 10.3389/fmicb.2018.00824

Li, F., He, X., Sun, Y., Zhang, X., Tang, X., Li, Y., et al. (2019). Distinct endophytes are used by diverse plants for adaptation to karst regions. *Sci. Rep.* 9:5246. doi: 10.1038/s41598-019-41802-0

Li, C. Y., Li, X. L., Su, X. X., Yang, Y. W., and Li, H. L. (2021). Effects of alpine wetland degradation on soil microbial structure and diversity on the Qinghai Tibet plateau. *Eurasian Soil Sci.* 54, S33–S41. doi: 10.1134/s1064229322030097

Li, D. H., Liu, C. M., Luo, R. B., Sadakane, K., and Lam, T. W. (2015). Megahit: an ultra-fast single-node solution for large and complex metagenomics assembly via succinct de bruijn graph. *Bioinformatics* 31, 1674–1676. doi: 10.1093/bioinformatics/btv033

Li, S., Xie, D., Ge, X., Dong, W., and Luan, J. (2022). Altered diversity and functioning of soil and root-associated microbiomes by an invasive native plant. *Plant Soil* 473, 235–249. doi: 10.1007/s11104-022-05338-z

Li, Y., Zhang, J., Chang, S. X., Jiang, P., and Lin, L. (2013). Longterm intensive management effects on soil organic carbon pools and chemical composition in moso bamboo (*phyllostachys pubescens*) forests in subtropical China. *For. Ecol. Manag.* 303, 121–130. doi: 10.1016/j.foreco.2013.04.021

Li, Z. Z., Zhang, L., Deng, B. L., Liu, Y. Q., Kong, F. Q., Huang, G. X., et al. (2017). Effects of moso bamboo (*Phyllostachys edulis*) invasions on soil nitrogen cycles depend on invasion stage and warming. *Environ. Sci. Pollut. Res.* 24, 24989–24999. doi: 10.1007/s11356-017-0186-9

Lin, C. Y., Miki, T., and Kume, T. (2022). Potential factors canceling interannual cycles of shoot production in a moso bamboo (*Phyllostachys pubescens*) stand. *Front. Forests Glob. Change* 5:913426. doi: 10.3389/ffgc.2022.913426

Lin, Y. T., Tang, S. L., Pai, C. W., Whitman, W. B., Coleman, D. C., and Chiu, C. Y. (2013). Changes in the soil bacterial communities in a cedar plantation invaded by moso bamboo. *Microb. Ecol.* 67, 421–429. doi: 10.1007/s00248-013-0291-3

Liu, C. X., Dong, Y. H., Hou, L. Y., Deng, N., and Jiao, R. Z. (2017). *Acidobacteria* community responses to nitrogen dose and form in Chinese fir plantations in southern China. *Curr. Microbiol.* 74, 396–403. doi: 10.1007/s00284-016-1192-8

Liu, D., Huang, Y. M., An, S. S., Sun, H. Y., Bhople, P., and Chen, Z. W. (2018). Soil physicochemical and microbial characteristics of contrasting land-use types along soil depth gradients. *Catena* 162, 345–353. doi: 10.1016/j.catena.2017.10.028

Liu, X., Siemann, E., Cui, C., Liu, Y., Guo, X., and Zhang, L. (2019). Moso bamboo (*phyllostachys edulis*) invasion effects on litter, soil and microbial plfa characteristics depend on sites and invaded forests. *Plant Soil* 438, 85–99. doi: 10.1007/s11104-019-04010-3

Liu, C., Zhou, Y., Qin, H., Liang, C., Shao, S., Fuhrmann, J. J., et al. (2021). Moso bamboo invasion has contrasting effects on soil bacterial and fungal abundances, co-occurrence networks and their associations with enzyme activities in three broadleaved forests across subtropical China. *For. Ecol. Manag.* 498:119549. doi: 10.1016/j.foreco.2021.119549

Lundmark, H., Josefsson, T., and Östlund, L. (2017). The introduction of modern forest management and clear-cutting in Sweden: Ridö state Forest 1832–2014. *Eur. J. For. Res.* 136, 269–285. doi: 10.1007/s10342-017-1027-6

Ma, X. R., Zheng, X. L., Zheng, C. Y., Hu, Y. T., Qin, H., Chen, J. H., et al. (2022). Effects of moso bamboo (*Phyllostachys edulis*) expansion on soil microbial community in evergreen broadleaved forest. *Yingyong Shengtai Xuebao* 33, 1091–1098. doi: 10.13287/j.1001-9332.202204.030

Millard, P., and Singh, B. K. (2010). Does grassland vegetation drive soil microbial diversity? *Nutr. Cycl. Agroecosyst.* 88, 147–158. doi: 10.1007/s10705-009-9314-3

Nicol, G. W., Leininger, S., Schleper, C., and Prosser, J. I. (2008). The influence of soil pH on the diversity, abundance and transcriptional activity of ammonia oxidizing archaea and bacteria. *Environ. Microbiol.* 10, 2966–2978. doi: 10.1111/J.1462-2920.2008.01701.X

Ouyang, M., Tian, D., Pan, J. M., Chen, G. P., Su, H. J., Yan, Z. B., et al. (2022). Moso bamboo (*Phyllostachys edulis*) invasion increases forest soil pH in subtropical China. *Catena* 215:106339. doi: 10.1016/j.catena.2022.106339

Ouyang, M., Yang, Q., Chen, X., Yang, G., Shi, J., and Fang, X. (2016). Effects of the expansion of *Phyllostachys edulis* on species composition, structure and diversity of the secondary evergreen broad-leaved forests. *Biodivers. Sci.* 24, 649–657. doi: 10.17520/biods.2015290

Pan, J. B., Liu, Y. J., Yang, Y., Cheng, Z. X., Lan, X. M., Hu, W. G., et al. (2022). Slope aspect determines the abundance and composition of nitrogen-cycling microbial communities in an alpine ecosystem. *Environ. Microbiol.* 24, 3598–3611. doi: 10.1111/1462-2920.15900

Ranjani, A., Dhanasekaran, D., and Gopinath Ponnusamy, M. (2016). "An introduction to *Actinobacteria*" in *Actinobacteria*. eds. D. Dharumadurai and J. Yi (Rijeka: IntechOpen)

Rombel, I. T., Sykes, K. F., Rayner, S., and Johnston, S. A. (2022). ORF-FINDER: a vector for high-throughput gene identification. *Gene* 282, 33–41. doi: 10.1016/s0378-1119(01)00819-8

Shang, R. G., Li, S. F., Huang, X. B., Liu, W. D., Lang, X. D., and Su, J. R. (2021). Effects of soil properties and plant diversity on soil microbial community composition and diversity during secondary succession. *Forests* 12:805. doi: 10.3390/f12060805

Shangguan, Y. X., Qin, Y., Yu, H., Chen, K., Wei, Y., Zeng, X., et al. (2019). Lime application affects soil cadmium availability and microbial community composition in different soils. *Clean (Weinh)* 47:1800416. doi: 10.1002/clen.201800416

Shen, C., Ge, Y., Yang, T., and Chu, H. (2017). *Verrucomicrobial* elevational distribution was strongly influenced by soil pH and carbon/nitrogen ratio. *J. Soils Sediments* 17, 2449–2456. doi: 10.1007/s11368-017-1680-x

Shen, Y., Yu, Y., Lucas-Borja, M. E., Chen, F., Chen, Q., and Tang, Y. (2020). Change of soil K, N and P following forest restoration in rock outcrop rich karst area. *Catena* 186:104395. doi: 10.1016/j.catena.2019.104395

Shiau, Y. J., and Chiu, C. Y. (2017). Changes in soil biochemical properties in a cedar plantation invaded by moso bamboo. *Forests* 8:222. doi: 10.3390/f8070222

Song, Q. N., Lu, H., Liu, J., Yang, J., Yang, G. Y., and Yang, Q. P. (2017). Accessing the impacts of bamboo expansion on NPP and N cycling in evergreen broadleaved forest in subtropical China. *Sci. Rep.* 7:10. doi: 10.1038/srep40383

Song, Q. N., Ouyang, M., Yang, Q. P., Lu, H., Yang, G. Y., Chen, F. S., et al. (2016). Degradation of litter quality and decline of soil nitrogen mineralization after moso bamboo (*Phyllostachys pubscens*) expansion to neighboring broadleaved forest in subtropical China. *Plant Soil* 404, 113–124. doi: 10.1007/s11104-016-2835-z

Song, X. Z., Peng, C. H., Zhou, G. M., Jiang, H., Wang, W. F., and Xiang, W. H. (2013). Climate warming-induced upward shift of moso bamboo population on Tianmu Mountain, China. *J. Mt. Sci.* 10, 363–369. doi: 10.1007/s11629-013-2565-0

Tian, X. K., Wang, M. Y., Meng, P., Zhang, J. S., Zhou, B. Z., Ge, X. G., et al. (2020). Native bamboo invasions into subtropical forests alter microbial communities in litter and soil. *Forests* 11:14. doi: 10.3390/f11030314

Umemura, M., and Takenaka, C. (2015). Changes in chemical characteristics of surface soils in hinoki cypress (*Chamaecyparis obtusa*) forests induced by the invasion of exotic Moso bamboo (*Phyllostachys pubescens*) in Central Japan. *Plant Species Biol.* 30, 72–79. doi: 10.1111/1442-1984.12038

Wan, W. J., Hao, X. L., Xing, Y. H., Liu, S., Zhang, X. Y., Li, X., et al. (2021). Spatial differences in soil microbial diversity caused by pH-driven organic phosphorus mineralization. *Land Degrad. Dev.* 32, 766–776. doi: 10.1002/ldr.3734

Wang, Z., Li, T., Wen, X., Liu, Y., Han, J., Liao, Y., et al. (2017). Fungal communities in rhizosphere soil under conservation tillage shift in response to plant growth. *Front. Microbiol.* 8:11. doi: 10.3389/fmicb.2017.01301

Wang, C., Zhou, J., Liu, J., Jiang, K., Xiao, H., and Du, D. (2018). Responses of the soil fungal communities to the co-invasion of two invasive species with different cover classes. *Plant Biol.* 20, 151–159. doi: 10.1111/plb.12646

Waymouth, V., Miller, R. E., Ede, F., Bissett, A., and Aponte, C. (2020). Variation in soil microbial communities: elucidating relationships with vegetation and soil properties, and testing sampling effectiveness. *Plant Ecol.* 221, 837–851. doi: 10.1007/s11258-020-01029-w

Wei, S. P., Song, Y. J., and Jia, L. M. (2021). Influence of the slope aspect on the ectomycorrhizal fungal community of Quercus variabilis Blume in the middle part of the Taihang Mountains, North China. *J. For. Res.* 32, 385–400. doi: 10.1007/s11676-019-01083-9

Widdig, M., Heintz-Buschart, A., Schleuss, P. M., Guhr, A., and Spohn, M. (2020). Effects of nitrogen and phosphorus addition on microbial community composition and element cycling in a grassland soil. *Soil Biol. Biochem.* 151:108041. doi: 10.1016/j.soilbio.2020.108041

Williams, T. R., Wilkinson, B., Wadsworth, G. A., Barter, D. H., and Beer, W. J. (1966). Determination of magnesium in soil extracts by atomic absorption spectroscopy and chemical methods. *J. Sci. Food Agric.* 17, 344–348. doi: 10.1002/jsfa.2740170803

Xu, Q. F., Jiang, P. K., Wu, J. S., Zhou, G. M., Shen, R. F., and Fuhrmann, J. J. (2015). Bamboo invasion of native broadleaf forest modified soil microbial communities and diversity. *Biol. Invasions* 17, 433–444. doi: 10.1007/s10530-014-0741-y

Xu, Q. F., Liang, C. F., Chen, J. H., Li, Y. C., Qin, H., and Fuhrmann, J. J. (2020). Rapid bamboo invasion (expansion) and its effects on biodiversity and soil processes. *Glob. Ecol. Conserv.* 21:e00787. doi: 10.1016/j.gecco.2019.e00787

Yang, H., Miao, N., Li, S. C., Ma, R., Liao, Z. Y., Wang, W. P., et al. (2019). Relationship between stand characteristics and soil properties of two typical forest plantations in the mountainous area of Western Sichuan, China. *J. Mt. Sci.* 16, 1816–1832. doi: 10.1007/s11629-018-5265-y

Yarwood, S. A., Myrold, D. D., and Högberg, M. N. (2009). Termination of below-ground C allocation by tree alters soil fungal and bacterial communities in a boreal forest. *FEMS Microbiol. Ecol.* 70, 151–162. doi: 10.1111/j.1574-6941.2009.00733.x

Zhang, L., Chung, J., Jiang, Q., Sun, R., Zhang, J., Zhong, Y., et al. (2017). Characteristics of rumen microorganisms involved in anaerobic degradation of cellulose at various pH values. *RSC Adv.* 7, 40303–40310. doi: 10.1039/C7RA06588D

Zhang, Y. G., Cong, J., Lu, H., Li, G. L., Qu, Y. Y., Su, X. J., et al. (2014). Community structure and elevational diversity patterns of soil *Acidobacteria*. *J. Environ. Sci.* 26, 1717–1724. doi: 10.1016/j.jes.2014.06.012

Zhang, P., Li, B., Wu, J., and Hu, S. (2019). Invasive plants differentially affect soil biota through litter and rhizosphere pathways: a meta-analysis. *Ecol. Lett.* 22, 200–210. doi: 10.1111/ele.13181

Zhang, L., and Xu, Z. (2008). Assessing bacterial diversity in soil. *J. Soils Sediments* 8, 379–388. doi: 10.1007/s11368-008-0043-z

Zhao, C., Long, J., Liao, H. K., Zheng, C. L., Li, J., Liu, L. F., et al. (2019). Dynamics of soil microbial communities following vegetation succession in a karst mountain ecosystem Southwest China. *Sci. Rep.* 9:10. doi: 10.1038/s41598-018-36886-z

frontiers | Frontiers in Microbiology

TYPE Original Research
PUBLISHED 13 March 2023
DOI 10.3389/fmicb.2023.1113707

OPEN ACCESS

EDITED BY
Xiangyu Guan,
China University of Geosciences,
China

REVIEWED BY
Yuanfeng Cai,
Nanjing University,
China
Giulia Caneva,
Roma Tre University,
Italy

*CORRESPONDENCE
Kangning Xiong
xiongkn@163.com

†These authors have contributed equally to this work and share first authorship

SPECIALTY SECTION
This article was submitted to Terrestrial Microbiology, a section of the journal Frontiers in Microbiology

RECEIVED 01 December 2022
ACCEPTED 22 February 2023
PUBLISHED 13 March 2023

CITATION
Chen Q, Yan N, Xiong K and Zhao J (2023) Cyanobacterial diversity of biological soil crusts and soil properties in karst desertification area. *Front. Microbiol.* 14:1113707. doi: 10.3389/fmicb.2023.1113707

Cyanobacterial diversity of biological soil crusts and soil properties in karst desertification area

Qian Chen[1,2†], Ni Yan[1,2,3†], Kangning Xiong[1,2*] and Jiawei Zhao[1,2]

[1]School of Karst Science, Guizhou Normal University, Guiyang, China, [2]State Engineering Technology Institute for Karst Desertification Control, Guizhou Normal University, Guiyang, China, [3]School of Life Science, Guizhou Normal University, Guiyang, China

As important components of the biological soil crusts (BSCs) and of the primary stage of crust succession, cyanobacterial communities occupy an important ecological niche and play an important ecological role in desertification areas. In this study, we focused on the karst desertification area, which also belongs to the same category of desertification, and selected three study areas, Guanling-Zhenfeng Huajiang (HJ), Bijie Salaxi (SLX), and Shibing (SB), in the Guizhou Plateau, which represents the overall ecological environment of South China karst, to conduct surveys on the diversity of BSC species and soil properties. Analysis of the cyanobacterial communities and physicochemical properties using the Shannon-Wiener diversity index, principal component analysis, and redundancy analysis revealed that: (1) The three study areas had common cyanobacterial species, with a total of 200 species distributed across 22 genera, 2 classes, 5 orders, and 6 families belonging to the Oscillatoriales (39%), Scytonematales (24.5%), Chroococcales (23%), Nostocales (11.5%), and Rivulariales (2%), (2) The number of species increased with the intensity of karst desertification—while Oscillatoriaceae was the dominant family in HJ and moderate–severe desertification areas, Chroococcaceae and Scytonemataceae were dominant in the mild and potential desertification areas SLX and SB, (3) The Shannon-Wiener diversity indices followed the trend: SLX (3.56)>SB (3.08)>HJ (3.01), indicating that the species were more evenly distributed in mild desertification, (4) In the carbonate background, shrubland harbored the largest number of cyanobacterial species compared to grassland, bare land, and arbor woodland; however, the highest number was documented in arbor woodland in dolomite karst, (5) The soil is weathered limestone or yellow soil in all three areas, with pH ranging from 5.73 to 6.85, fine sand dominated, and soil nutrients increased with the intensity of desertification, and (6) Redundancy analysis showed that organic carbon, soil moisture content (0–5cm), and total nitrogen substantially influenced cyanobacterial diversity. These results reveal that differences in soil nutrient content play an important role in regulating the cyanobacterial diversity and composition, thereby establishing a foundation for further research and application of soil ecological restoration of cyanobacteria in BSCs of karst desertification areas.

KEYWORDS

biological soil crusts, cyanobacteria, species diversity, soil properties, karst desertification

1. Introduction

BSCs are an important component of desert ecosystems that have received widespread attention in desertification areas, it refers to the plant–soil complexes formed by different proportions of cyanobacteria, algae, lichens, mosses, and microorganisms cementing soil particles (Belnap and Lange, 2003; Belnap and Miller, 2004). It covers 12% of the global land area, with some arid regions covering more than 70% (Belnap and Lange, 2001). Cyanobacteria-dominated crusts have harsh environmental adaptations and are, therefore, dominant in extreme environments (Belnap et al., 2016). Research results from many different global habitats, including deserts, plateaus, mountains, savannas, and even polar regions, revealed that cyanobacterial crusts provide important ecosystem services, such as responding to climate change, dust cycling (Rodriguez-Caballero et al., 2022), hydrological change (Li et al., 2018), and enhancement of global carbon sink capacity (Zou et al., 2022). In soil ecosystems, cyanobacteria are usually the pioneers of community succession, providing carbon and nitrogen to the soil (Belnap, 2002; Housman et al., 2006) and promoting soil nutrient cycling. It also prevents soil erosion and reduces water evaporation (Felde et al., 2018), indirectly enhancing soil stability and improving ecosystem quality (Hagemann et al., 2015; Belnap et al., 2016; Chamizo et al., 2016). Soil properties reflect regional climate, bedrock, geological features, and biodiversity. Research has been conducted on the co-changes in cyanobacteria organisms and soil. Cano-Díaz et al. explored cyanobacterial diversity in gypsum soils in central Spain and revealed that gypsum soils are dominated by filamentous cyanobacteria and have lower abundance and diversity (Cano-Díaz et al., 2018). In the mountainous regions of the northern Urals, where weathering is intense, coarse sandy soils dominate steep slopes and are dominated by spherical cyanobacteria, whereas soils in depressions and gentle areas are fine-textured and dominated by filamentous cyanobacteria (Patova et al., 2018). Temraleeva (2018) explored cyanobacteria species diversity in Russian arid and desert steppe semi-desert soils, meadow soils, and chestnut calcareous soils. Roncero-Ramos et al. (2019) explored the structural diversity of cyanobacterial communities developed from clay, silty, and sandy loam of calcareous sandstones and calcareous mudstones in southeastern Spain and revealed the differences in cyanobacterial composition in soils from different geographical regions. However, more studies based on the diversity of BSCs cyanobacteria in different soil matrices are yet to be conducted.

The composition and dominance of cyanobacterial species corresponds to different soil environments. *Microcoleus*, *Scytonema*, *Phormidium*, *Trichocoleus*, *Leptolyngbya,* and *Tychonema* have been widely reported in the desert, with *Microcoleus vaginatus* being overwhelmingly dominant (Hagemann et al., 2015; Zhang et al., 2015; Etemadi-Khah et al., 2017; Fernandes et al., 2018; Zhang et al., 2021; Sosa-Quintero et al., 2022). In temperate arid steppe and dryland ecosystems, cyanobacterial crusts mainly consist of Nostocales, Oscillatoriales, Synechoccocales, and the dominant species beside *M. vaginatus*, including *Symplocastrum purpurascens*, *Scytonema* sp., *Nostoc commune*, *Phormidium* sp., with the biomass of cyanobacteria increasing with light intensity (Büdel et al., 2009; Williams et al., 2016; Büdel et al., 2018; Temraleeva, 2018; Roncero-Ramos et al., 2019). In the mountains of northeastern Europe, cyanobacteria mainly consist of *Phormidium*, *Leptolyngbya*, and *Nostoc*, with *Leptolyngbya voronichiniana*, *Leptolyngbya foveolarum*, *Trichocoleus hospitus* dominating (Gaysina et al., 2018; Novakovskaya et al., 2022). The main cyanobacteria in Brazil's tropical savanna include *Microcoleus*, *Nostoc*, *Leptolyngbya*, *Porphyrosiphon*, and *Pycnacronema* (Machado de Lima et al., 2019, 2021). In cold polar environments, Chroococcales, Pseudanabanales, and Oscillatoriales are the main cyanobacterial constituent groups but lack genera such as *Oculatella* and *Hassallia*, which are common in temperate and tropical regions and where humidity is high, and are usually covered with thicker *Nostoc* spp. with enhanced nitrogen fixation capacity (Pushkareva et al., 2015, 2016, 2018). Although there are certain similarities in genus composition, the species are different. However, whether there are differences in ecological functions between different cyanobacterial crusts remains unclear because of the lack of taxonomic information on cyanobacteria from different areas. To more accurately interpret their ecological functions from global patterns and apply their restoration value for degraded ecosystems, more attention should be paid to cyanobacteria taxonomy in karst critical zones.

Karst is the sum of the binary three-dimensional structure of landscapes and phenomena between the surface and the ground formed by erosion, dissolution, collapse, and accumulation of the affection by flowing water to soluble rocks. Karst desertification is an extreme process of ecosystem degradation (Ravbar and Šebela, 2015). South China karst is the most comprehensive, complex, and longest-developed karst landscape in the world and is one of the three largest continuous carbonate rock distribution areas worldwide (Chen et al., 2019). The expansion of rock desertification is exacerbated by the uneven spatial and temporal distribution of seasonal precipitation and overloaded economic activities due to high population loads, resulting in shallow and infertile soils, low vegetation coverage, soil erosion, and high rock exposure rates, leading to the degradation of the ecosystem and eventually presenting a karst desertification landscape such as desertification. In the desertification area in South China karst, there are completely different climatic, zonal, and non-zonal soil-forming conditions from the above desertification and temperate areas, with the soil dominated by limestone, dolomite, and other carbonate rocks and zonal yellow and brown soil (Sheng et al., 2016). In this particular context, studies based on the synergistic evolution of cyanobacteria crust species diversity and soil properties in karst desertification are still lacking. This study examined the diversity and composition of the extant cyanobacteria crust species in the three karst desertification study areas. The synergistic evolutionary relationship with cyanobacteria is discussed in terms of different habitats and soil physicochemical properties, which in turn provides data support for the study of cyanobacterial crust soils in karst desertification areas, a reference for ecological restoration of karst desertification soils, and a case study of karst desertification ecological restoration for global desertification.

2. Materials and methods

2.1. Study area

The Guizhou Plateau was selected as the study area, as it represents the overall ecological structure of South China karst, and chose the Guanling-Zhenfeng Huajiang (HJ) study area with moderate–severe desertification, the Bijie Salaxi (SLX) study area with potential-mild desertification, and the Shibing (SB) study area with no-potential

desertification (Figure 1). These areas are dominated by a subtropical humid monsoon climate with rain and heat during the same period but retain differences in lithology, soils, and vegetation. HJ is a typical plateau canyon area with an altitude of 450–1,450 m, an average annual temperature of 18°C, and an average annual precipitation of over 1,200 mm (Zhang et al., 2019). The vegetation type is mainly scrub, broad-leaved forest, and mixed coniferous forest. The altitude of SLX ranges from 1,410 to 1780 m, the average annual temperature is 12°C, the average annual precipitation is above 984.40 mm, and the vegetation type is dominated by scrubs, broad-leaved forests, and coniferous forests. SB is a typical dolomite karst area with an altitude of 526–1,576 m, an average annual temperature of 16°C, an average annual precipitation of 1,110 mm or more, and a vegetation type mainly comprised of subtropical evergreen broad-leaved forests (Wang et al., 2019); the differences in soil properties are shown in Table 1.

2.2. Sample sites

Sampling sites were identified in the three study areas, and the vegetation composition of bare land, grassland, shrubland, and arbor woodland, as well as information on key species, latitude, longitude, elevation, coverage, etc., were investigated. The major species and environmental factors of sampling sites of the same community type should be as similar as possible, with a sampling quadrat of 10 m × 10 m for bare land, grassland, and shrubland and 30 m × 30 m for arbor woodland, specific sampling quadrats information are shown in Table 2.

2.3. Crust sample collection and procession

2.3.1. Sample collection

In April 2021, BSCs were collected from different communities in the three study areas, 1 cm thickness of cyanobacteria-dominated BSCs was collected extensively and randomly with small shovels in the sampling quadrat, mixed into one sample, and placed in plastic bags. Three mixed samples were collected from each of the four community types, and 12 mixed samples were collected from one study area, resulting in a total of 36 mixed BSCs samples from the three study areas, which were placed in plastic bags and taken back to the laboratory as soon as possible.

2.3.2. Sample preservation and identification

The field-collected BSCs were placed in specimen bottles containing propanetriol-formaldehyde-water solution (1:1:8) fixative and stored at room temperature in the laboratory of the School of Karst Science, Guizhou Normal University, where cyanobacteria species identification, dominant species recording and micrographs were taken using an OLYMPUS-CX41 trinocular microscope (Yan et al., 2021).

Dominant species: a small piece of BSCs was removed with small forceps to make a temporary water mount. Three temporary slices of each sample were taken, and 10 fields of view were observed for each mount to determine the dominant cyanobacteria species based on the frequency of occurrence (Zhang et al., 2008).

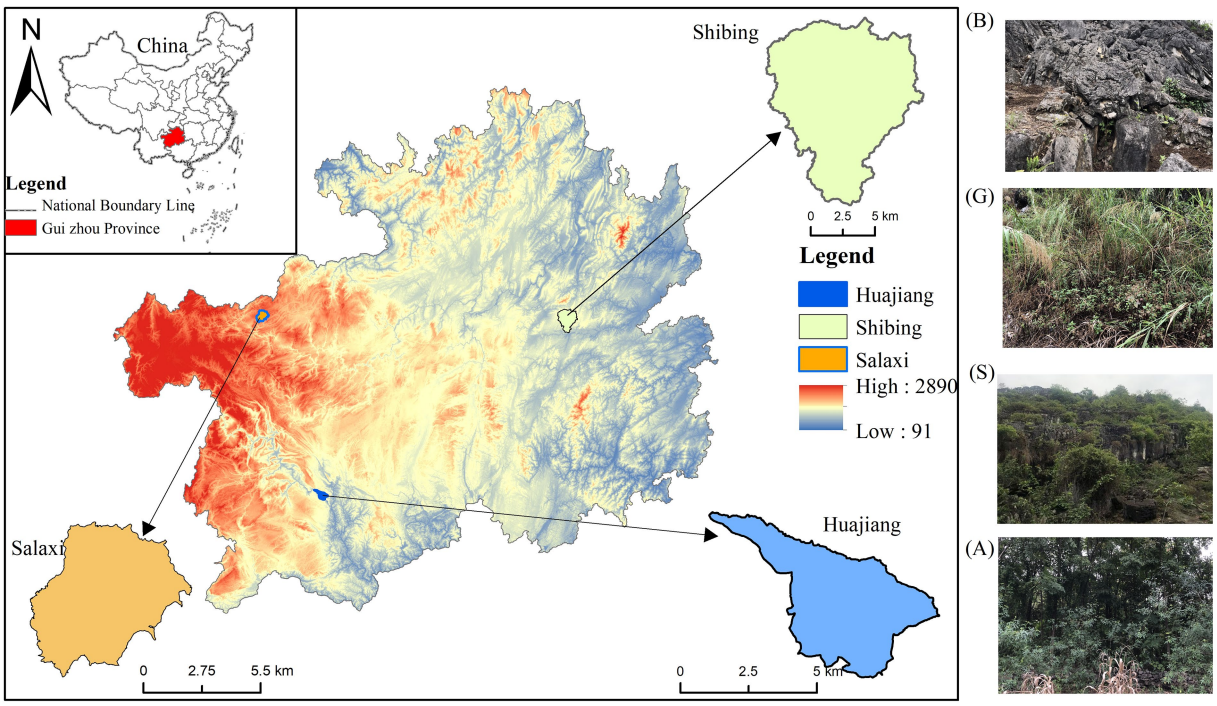

FIGURE 1
Study area and sampling community. B-Bare land; G-Grassland; S-Shrub land; A-Arbor woodland, same as below.

TABLE 1 Difference of soil factors in the study area.

	HJ	SLX	SB
Soil parent material	Limestone	Limestone, Sand shale	Dolomite
Main components	Calcite, Dolomite, Magnesite, Other carbonate minerals ($CaCO_3$)	Calcite, Dolomite, Magnesite, Other carbonate minerals ($CaCO_3$)	Dolomite, Quartz, Feldspar, Calcite, Clay mineral ($CaMg(CO_3)_2$)
Soil-forming material	Clay material rich in Al_2O_3 and Fe_2O_3	Clay material rich in Al_2O_3 and Fe_2O_3	Clay material rich in CaO and MgO
Soil type	Limestone soil, Sandy loam	Yellow soil, Yellow brown soil, Limestone soil	Black limestone soil, Yellow soil, Yellow brown soil
Soil thickness	12-50 cm	50-70 cm	60-80 cm

2.4. Soil sample collection and procession

2.4.1. Sample collection

In each community quadrate, an S-shaped random sampling method was used to collect the physical and chemical properties of different analysis targets; the ring knife sampling method was used for the physical properties of the soil, the soil with two layers of 0–5 cm and 5–10 cm was selected, and chemical properties selected 0–10 cm mixed soil. The soils were taken back to the laboratory to dry naturally, ground, and sieved through 2 and 0.15 mm soil sieves and stored in plastic bags at room temperature for later determination of indicators.

2.4.2. Methods for the determination of physical and chemical indicators

Soil moisture content was determined by the ring-knife and drying methods; pH was determined using the 1:2.5 soil/water ratio centrifugal sedimentation method and a Leici PHS-25 acidity meter; soil texture was determined by the international classification standard, which classifies soil particle size into clay (<0.002 mm), silt (0.002–0.02 mm), fine sand (0.02 ~ 0.2 mm), and coarse sand (0.2 ~ 2 mm), using the hydrometer method; soil organic carbon was determined by the potassium dichromate oxidation-external heating method; soil total nitrogen was determined by sulfuric acid-catalyst digestion and the Kjeldahl nitrogen determination method; available nitrogen was determined by the alkali-hydrolysis diffusion method; soil total phosphorus was determined by the molybdenum antimony spectrophotometric method; soil available phosphorus was determined by sodium fluoride hydrochloric acid leaching and the molybdenum antimony anti-colorimetric method (Bao, 2000).

2.5. Data statistics and analysis

2.5.1. Cyanobacterial diversity index

Using the Shannon-Wiener diversity index:

$$H = -\sum_{i=1}^{s} Pi \log_2 Pi$$

where S is the number of species in cyanobacteria, Pi is the proportion of individuals of the species among all individuals, and H is the diversity index.

2.5.2. Data analysis

The data were processed and analyzed using Excel 2013 and SPSS 22.0. One-way analysis of variance (ANOVA) and principal component analysis were used to analyze and test the soil physicochemical properties and cyanobacterial diversity using Canoco 5 software for redundancy analysis and plotting, and the remaining graphs were plotted using the Origin 2021 software.

3. Results

3.1. Taxa and diversity characteristics of cyanobacteria in karst desertification areas

3.1.1. Cyanobacteria taxa

There are 200 species of cyanobacteria in two classes, five orders, six families, and 22 genera in the three karst desertification study areas, with filamentous cyanobacteria accounting for 77.4% of the total number of cyanobacteria. Oscillatoriales (39%) accounted for the largest proportion, followed by Scytonematales (24.5%), Chroococcales (23%), Nostocales (11.5%), and Rivulariales (2%). Oscillatoriaceae and Chroococcaceae were the dominant families and only three genera of Scytonemataceae, but the number of species was second only to that of Chroococcaceae, accounting for 24.5% (Table 3). The dominant genera were *Scytonema*, *Oscillatoria*, *Lyngbya*, *Nostoc*, and *Gloeocapsa*, with filamentous cyanobacteria being overwhelmingly dominant (Figure 2).

3.1.2. Composition and distribution for each study area

The distribution and dominance of cyanobacteria families and genera differed among the different karst desertification study areas (Table 4). A total of 94 species of cyanobacteria from 5 families and 12 genera were found in HJ, with Oscillatoriaceae, the most dominant family, accounting for 54.25% of the total number of species, and Scytonemataceae, the subdominant family, accounting for 23.40%. The dominant genera were *Oscillatoria* (23), *Lyngbya* (16), and *Scytonema* (15). A total of 77 species of cyanobacteria from 5 families and 17 genera were found in SLX, with Chroococcaceae being the most dominant, accounting for 37.66% of the total number of species. Oscillatoriaceae accounted for 36.36% of the total number of species. The dominant genera were *Oscillatoria* (15), *Gloeocapsa* (10), and *Nostoc* (9). There were 80 species of cyanobacteria in 5 families and 14

TABLE 2 Sampling point information.

Study area	Community type	Sampling point	Longitude and latitude	Altitude(m)	Coverage	Main vegetation
HJ	Bare land	HB1	25°39 ′3”N; 105°40′25″E	750	/	/
		HB2	25°39 ′3”N; 105°40′25″E	760	/	
		HB3	25°39 ′3”N; 105°40′25″E	740	/	
	Grassland	HG1	25°39 ′59”N; 105°40′2″E	580	70%	*Rhus chinensis* Mill.
		HG2	25°39 ′52”N; 105°40′5″E	600	75%	*Arthraxon hispidus* (Thunb.) Makino
		HG3	25°39 ′41”N; 105°40′15″E	690	60%	*Bidens pilosa* L.
	Shrubland	HS1	25°29 ′20”N; 105°38′34″E	830	90%	*Alchornea trewioides* (Benth.) Muell. Arg.
		HS2	25°39 ′21”N; 105°38′34″E	850	85%	*Zanthoxylum bungeanum* Maxim.
		HS3	25°40 ′6”N; 105°39′15″E	840	85%	*Broussonetia papyrifera* (L.) Vent.
	Arbor woodland	HA1	25°39 ′11”N; 105°40′21″E	770	65%	*Viburnum foetidum* var. *ceanothoides* Hand. Maz.
		HA2	25°39 ′11”N; 105°40′21″E	760	60%	
		HA3	25°39 ′19”N; 105°40′32″E	770	60%	*Ailanthus altissima* (Mill.) Swingle. *Juglans regia* L.
SLX	Bare land	SB1	27°14 ′30”N; 105°5′56″E	1760	/	/
		SB2	27°15 ′20”N; 105°5′12″E	1910	/	
		SB3	27°15 ′21”N; 105°5′14″E	1890	/	
	Grassland	SG1	27°15 ′24”N; 105°5′13″E	1900	60%	*Trifolium repens* L.
		SG2	27°15′23”N; 105°5′13″E	1950	60%	*Imperata cylindrica* (L.) Beauv.
		SG3	27°15 ′20”N; 105°5′19″E	1910	60%	*Arthraxon hispidus* (Thunb.) Makino
	Shrubland	SS1	27°15 ′9”N; 105°5′31″E	1880	90%	*Rosa roxburghii* Tratt.
		SS2	27°15 ′0”N; 105°5′37″E	1890	85%	*Pyracantha fortuneana* (Maxim.) Li
		SS3	27°14 ′53”N; 105°5′47″E	1870	90%	*Cotoneaster franchetii* Bois
	Arbor woodland	SA1	27°14 ′33”N; 105°4′6″E	1920	70%	*Castanea seguinii Dode*
		SA2	25°39 ′11”N; 105°40′21″E	1850	65%	*Betula luminifera* H. Winkl.
		SA3	27°13 ′19”N; 105°4′35″E	1810	65%	*Populus alba* L.
SB	Bare land	BB1	27°6 ′49”N; 108°7′7″E	870	/	/
		BB2	27°6 ′51”N; 108°7′6″E	846	/	
		BB3	27°6 ′51”N; 108°7′6″E	870	/	
	Grassland	BG1	27°4 ′39”N;108°7′28″E	770	75%	*Miscanthus sinensis*
		BG2	27°4 ′39”N; 108°7′28″E	758	80%	*Arthraxon hispidus* (Thunb.) Makino
		BG3	27°4 ′39”N; 108°7′28″E	770	80%	*Erigeron annuus* (L.) Pers
	Shrubland	BS1	27°7 ′24”N; 108°7′31″E	890	70%	*Pyracantha fortuneana* (Maxim.) Li
		BS2	27°6 ′56”N; 108°7′2″E	870	75%	*Spiraea salicifolia* L.
		BS3	27°6 ′56”N; 108°7′2″E	870	80%	*Coriaria nepalensis* Wall
	Arbor woodland	BA1	27°6 ′58”N; 108°6′18″E	900	95%	*Platycarya longipes* Wu
		BA2	27°6 ′58”N; 108°6′20″E	900	95%	*Quercus phillyraeoides* A. Gray
		BA3	27°6 ′58”N; 108°6′51″E	910	95%	*Cinnamomum cassia* Presl

genera in SB, with Scytonemataceae being the most dominant, accounting for 33.75% of the total number of species, and Chroococcaceae being subdominant, accounting for 27.50%. The dominant genera were *Scytonema* (23), *Gloeocapsa* (16), and *Nostoc* (11) (Figure 3).

3.1.3. Number of cyanobacteria species

Under the four community habitat types in the three different desertification study areas (HJ, SLX, and SB), there were significant differences in the number of species and genera as the communities evolved from bare land, grassland, shrubland, and arbor woodland (Figure 4). HJ and SLX had the highest number of species in shrubland, with an average cover of over 85% of the community vegetation and 65% of the arbor woodland. The highest number of species was found in the arbor woodland in SB, with an average vegetation cover of 95%, whereas the other communities did not differ significantly. The number of cyanobacteria genera was highest in HJ and SB arbor woodlands and highest in SLX shrubs (Table 4).

3.1.4. Cyanobacterial diversity

The Shannon-Wiener diversity index of cyanobacteria differed among the three study areas (Figure 5), with SLX having the highest diversity index, followed by SB and HJ having the lowest, at 3.56, 3.08, and 3.01, respectively. Second, the diversity index also differed among the different types of communities in the three study areas, with HJ having the highest diversity in arbor woodland (3.19), SLX having the

TABLE 3 The statistics of the number and proportion of Family, Genus, Species of cyanobacteria.

Plylum	Order	Family	Genus	Proportion of total Genus	Species	Proportion of total Species
Cyanophyta	Oscillatoriales	Oscillatoriaceae	7	31.8%	78	39%
	Scytonematales	Scytonemataceae	3	13.6%	49	24.5%
	Chroococcales	Chroococcaceae	7	31.8%	45	22.5%
		Cyanostylonaceae	1	4.6%	1	0.5%
	Nostocales	Nostocaceae	2	9.1%	23	11.5%
	Rivulariales	Rivulariaceae	2	9.1%	4	2%
Total	5	6	22	100%	200	100%

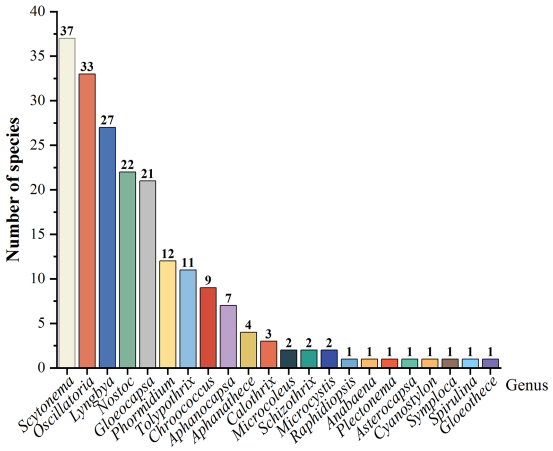

FIGURE 2
Number of Genus and Species of cyanobacteria.

highest diversity in shrubland (3.54), and SB having the highest diversity in bare land (2.93).

3.1.5. Dominant species

The dominant species differed among the three study areas and the different community types, with a total of 15 dominant cyanobacteria species identified (Table 5). The dominant species in the three study areas belonged to the genera *Oscillatoria*, *Scytonema*, and *Gloeocapsa*; in HJ, the dominant species were *Scytonema javanicum* and *Lyngbya gracilis*; in SLX, the dominant species were *Lyngbya contorta* and *Gloeocapsa montana,* and in SB, the dominant species were *Scytonema hofmanni* and *Gloeocapsa montana*.

The dominant cyanobacteria in all communities were *M. vaginatus* and *Nostoc commune*, *Scytonema* was dominant in the arbor woodlands of all three study areas, *Gloeocapsa* was dominant in the shrublands of SLX and SB, and *Lyngbya* was dominant in the shrubland of HJ, with different dominant species in the grassland and bare land.

3.2. Physicochemical properties of soils

3.2.1. Soil moisture content

There were significant differences ($p < 0.05$) in the soil physicochemical indicators between the different desertification study areas, as shown in Table 6. In the limestone-dominated study areas of HJ and SLX, the overall soil moisture content of SLX was greater than that of HJ, and the surface moisture content (0–5 cm) was greater than that of the lower layer (5–10 cm). The difference in soil moisture content between the four different community habitats was not significant, with SLX having the highest moisture content in grassland and HJ having the highest moisture content in shrubland. The dolomite-dominated study area of SB showed that the surface moisture content (0–5 cm) was less than the lower (5–10 cm) surface moisture content, with significant differences in surface moisture content and non-significant differences in lower moisture content in the community habitats, with the highest moisture content in the arbor woodland.

3.2.2. pH and soil texture

The pH of the selected karst desertification study area was neutral to acidic, with overall non-significant differences ranging from 5.93 to 6.75. The soil particles were mainly composed of sand, with the proportion of fine sand content being the largest among the soil particles in all three study areas, with an average content of HJ (66.49%) > SB (53.29%) > SLX (45.57%), with significant differences in the SLX and SB community habitats. The coarse sand content averaged 14% in the three study areas, showing SLX (23.12%) > SB (13.90%) > HJ (4.99%), with no significant differences between the HJ and SB community habitats. There was no significant difference in silt particles in the HJ community habitat, but there were significant differences in the SLX and SB community habitats, with the largest content in the SB arbor woodland and the lowest in the HJ shrubland. The clay content was below 10% in all the study areas.

3.2.3. Organic carbon, phosphorus, and nitrogen

In terms of soil nutrients, the average content of organic carbon, total phosphorus, and total nitrogen in all three study areas showed a maximum in HJ, followed by SLX, and a minimum in SB. The available nitrogen content was generally uniform with little variation. The organic carbon and total nitrogen contents did not differ significantly among the communities in the three study areas, and the average content was more uniform within the community habitats. The differences in total phosphorus content were significant in the SB communities but not in the HJ and SLX communities. The differences in available phosphorus were not significant in the communities of SLX and SB but significant in the communities of HJ, with the highest value in the arbor woodland of HJ and the lowest value in the shrubland of SB, whereas the differences in available nitrogen were not significant in the communities of SLX and SB.

10.3389/fmicb.2023.1113707

TABLE 4 Family and genus compsition of Cyanobacteria

Phylum	Families	Genera	HJ				SLX				SB			
			B	*G*	*S*	*A*	*B*	*G*	*S*	*A*	*B*	*G*	*S*	*A*
Cyanophyta	Oscillatoriaceae	*Oscillatoria*	+	+	+	+	+	+	+	+	+			+
		Lyngbya	+	+	+	+	+	+	+	+	+		+	+
		Microcoleus	+	+	+	+	+	+	+	+	+	+	+	+
		Phormidium	+		+	+	+	+						
		Schizothrix									+			
		Symploca										+		
		Spirulina					+							
	Scytonemataceae	*Tolypothrix*	+	+		+			+			+	+	+
		Scytonema	+	+	+	+	+	+	+	+	+	+	+	+
		Plectonema							+					
	Chroococcaceae	*Gloeocapsa*		+		+	+	+	+		+	+	+	+
		Aphanocapsa				+		+	+		+		+	+
		Aphanathece						+	+			+		
		Gloeothece							+					
		Chroococcus			+	+		+	+				+	
		Asterocapsa							+					+
		Microcystis		+					+	+				
	Cyanostylonaceae	*Cyanostylon*								+				
	Nostocaceae	*Nostoc*	+	+	+	+	+	+	+	+	+	+	+	+
		Anabaena							+					
	Rivulariaceae	*Calothrix*									+		+	+
		Raphidiopsis				+								
		Total	7	8	7	11	8	10	15	7	9	7	9	10

The presence of genus in communities in study areas is considered to be +, and absence is blank.

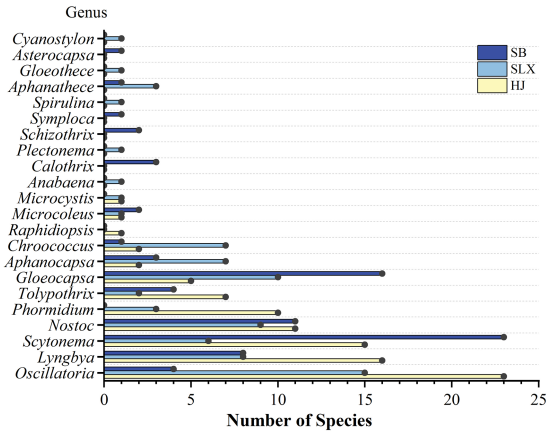

FIGURE 3
Species number of Cyanobacteria.

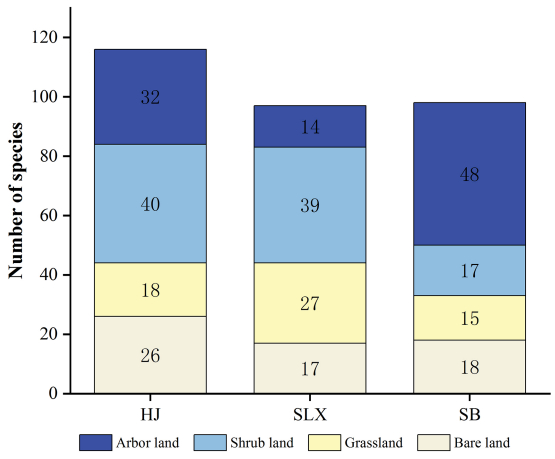

FIGURE 4
Species number of Cyanobacteria in different community types.

3.3. Cyanobacteria species diversity and soil properties

3.3.1. Soil property factors affecting the cyanobacteria species diversity

Principal component analysis (PCA) was conducted on 12 soil property factors for each community in the three study areas, with the aim of screening out the principal components that may influence cyanobacteria species diversity. The results of the PCA analysis of the soil property factors in the study areas showed that PC1 explained 34.4% of the soil property factors and PC2 explained 23.8% of the soil property factors, with differences between the soil property factors in the three study areas (Figure 6). The first principal component explained the soil property factors affecting cyanobacteria species diversity as organic carbon, total nitrogen, total phosphorus, available nitrogen, and available phosphorus, whereas the second principal

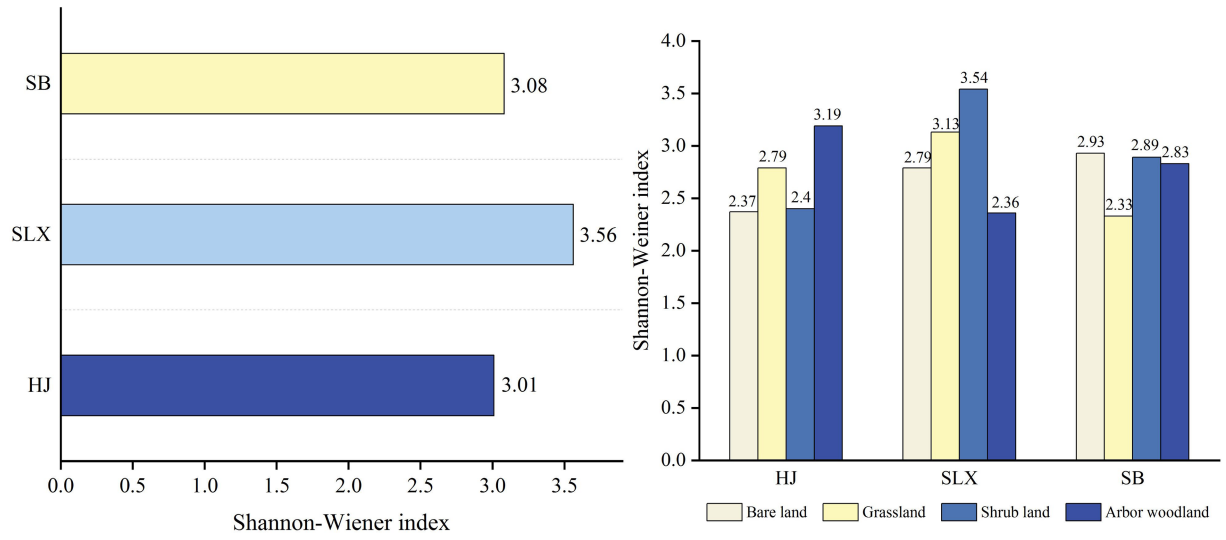

FIGURE 5
Shannon-Wiener diversity index of cyanobacteria in the study area and different community type.

TABLE 5 Dominant species of Cyanobacteria.

Dominant species	HJ				SLX				SB			
	B	*G*	*S*	*A*	*B*	*G*	*S*	*A*	*B*	*G*	*S*	*A*
Nostoc sp					+	++	++	++				
Nostoc commune	++	++	+	+	++	++	++	++	++	+	++	++
Scytonema javanicum			+	+++								
Scytonema saleyeriense										++		
Scytonema hofmanni			++					+++				+++
Scytonema julianum												++
Scytonema holstii	++									+		
Scytonema tenue				++								
Scytonema cincinnatum			++									
Lyngbya gracilis			+++									
Lyngbya contorta					+++	+++	+	+				
Microcoleus vaginatus	+++	+++	++	++	++	++	+++	++	++	+++	++	+++
Gloeocapsa montana						+	+++		+++		+++	
Gloeocapsa alpina							++					
Aphanocapsa banaresensis									++		++	

+++stands for dominant species, ++stands for subdominant species.

component explained soil moisture content (0–5 cm, 5–10 cm) and coarse and silt in the soil particle composition, thus excluding the three factors of fine sand, clay, and pH.

3.3.2. Redundancy analysis of cyanobacterial diversity and soil properties

To clarify the relationship between cyanobacterial diversity and soil properties, a redundancy analysis was conducted by combining the cyanobacterial diversity index and the number of species with nine soil property factors (Figure 7). The results showed that Axis-1 explained 56.8% of the results, with organic carbon, total nitrogen, available nitrogen, soil moisture content (0–5 cm), and soil moisture content (5–10 cm) all pointing to Axis-1. There were positive correlations (number and index) between the response factors, with the number of cyanobacteria species mainly influenced by organic carbon (contribution of 27.9%), with a significant positive correlation with organic carbon ($p <= 0.03$). The diversity index was mainly influenced by soil moisture content (0–5 cm) (contribution of 23%), with a significant positive correlation with soil water content (0–5 cm) ($p <= 0.012$), and the diversity index was also influenced by total nitrogen (contribution of 19.6%), with a significant positive correlation with total nitrogen ($p <= 0.016$). Although soil moisture content (5–10 cm) and moisture

TABLE 6 Soil physicochemical properties.

	HJ				SLX				SB			
Soil properties	*B* Mean±S.E	*G* Mean±S.E	*S* Mean±S.E	*A* Mean±S.E	*B* Mean±S.E	*G* Mean±S.E	*S* Mean±S.E	*A* Mean±S.E	*B* Mean±S.E	*G* Mean±S.E	*S* Mean±S.E	*A* Mean±S.E
Wc 0–5 (%)	6.52 ± 0.26a	6.81 ± 0.63a	14.94 ± 4.90a	9.72 ± 1.40a	20.00 ± 1.34a	24.57 ± 4.06a	21.27 ± 2.18a	21.33 ± 1.38a	7.17 ± 0.27b	5.32 ± 0.98b	8.93 ± 0.42ab	15.72 ± 4.56a
Wc 5–10(%)	6.02 ± 0.92a	7.05 ± 0.79a	12.41 ± 3.18a	8.08 ± 1.69a	19.98 ± 1.87a	18.37 ± 5.75a	19.52 ± 1.96a	19.23 ± 1.87a	7.70 ± 0.41a	6.03 ± 1.01a	10.74 ± 2.32a	15.99 ± 5.88a
pH	6.47 ± 0.12a	6.61 ± 0.14a	6.75 ± 0.07a	6.48 ± 0.21a	6.16 ± 0.17a	6.14 ± 0.18a	6.1 ± 0.24a	6.28 ± 0.13a	6.14 ± 0.13a	6.02 ± 0.26a	5.93 ± 0.12a	6.08 ± 0.18a
Cs(%)	5.08 ± 0.65a	4.32 ± 0.80a	4.87 ± 0.73a	5.72 ± 1.81a	28.20 ± 4.12ab	18.16 ± 1.07bc	16.00 ± 1.50c	30.11 ± 4.71a	12.29 ± 1.20a	14.33 ± 3.05a	16.52 ± 3.96a	12.44 ± 5.39a
Fs(%)	63.81 ± 4.20a	64.57 ± 3.39a	72.15 ± 3.0a	65.44 ± 2.0a	33.49 ± 7.65b	54.86 ± 2.61a	52.35 ± 1.33a	41.57 ± 4.23ab	61.4 ± 0.62a	49.35 ± 1.34c	55.83 ± 1.11b	46.58 ± 0.39c
S(%)	23.33 ± 4.06a	24 ± 3.06a	15.33 ± 2.67a	22 ± 1.15a	29.33 ± 3.53a	20 ± 3.06b	23.33 ± 1.33ab	20.67 ± 0.67b	16.67 ± 1.33b	27.33 ± 1.33ab	18 ± 4.16b	31.33 ± 4.81a
Sc(%)	7.78 ± 0.83a	7.11 ± 0.93a	7.65 ± 0.67a	6.85 ± 0.67a	8.98 ± 0a	6.98 ± 0b	8.31 ± 0.67ab	7.65 ± 0.67ab	9.65 ± 0.67a	8.98 ± 0a	9.65 ± 0.67a	9.65 ± 0.67a
SOC(g/kg)	25.60 ± 6.78a	14.61 ± 3.58a	29.56 ± 2.01a	30.60 ± 7.21a	20.74 ± 3.18a	28.98 ± 2.81a	24.73 ± 4.92a	20.63 ± 6.87a	27.84 ± 1.18a	14.34 ± 7.29a	12.53 ± 1.64a	30.94 ± 14.2a
TP(g/kg)	1.5 ± 0.62a	0.80 ± 0.12a	0.52 ± 0.30a	2.49 ± 0.84a	0.98 ± 0.20a	1.51 ± 0.47a	0.84 ± 0.07a	0.8 ± 0.21a	0.58 ± 0.08a	0.30 ± 0.06b	0.37 ± 0.06b	0.17 ± 0.04b
AP(mg/kg)	5.17 ± 3.64ab	1.48 ± 0.61b	1.47 ± 0.11b	10.02 ± 5.93a	5.58 ± 1.31a	1.32 ± 0.10a	7.87 ± 5.38a	1.92 ± 1.06a	1.42 ± 0.80a	2.23 ± 1.54a	0.39 ± 0.02a	1.73 ± 0.54a
TN(g/kg)	3.58 ± 0.59a	2.69 ± 0.35a	3.93 ± 0.27a	3.75 ± 0.60a	2.44 ± 0.32a	3.37 ± 0.58a	2.76 ± 0.53a	1.97 ± 0.58a	2.80 ± 0.15a	1.45 ± 0.67a	1.51 ± 0.19a	1.99 ± 0.68a
AN(g/kg)	0.35 ± 0.07b	0.22 ± 0.04b	0.45 ± 0.02a	0.4 ± 0.08ab	0.32 ± 0.04a	0.48 ± 0.08a	0.37 ± 0.09a	0.28 ± 0.07a	0.36 ± 0.03a	0.20 ± 0.10a	0.19 ± 0.02a	0.30 ± 0.11a

The data in the table represent the mean ± standard deviation; the letters a, b, c indicate the significant difference ($p < 0.05$) between different communities (bare land, grassland, shrubland, and arbor woodland) in the study area. Wc-Soil moisture content; Cs-Coarse sand; Fs-Fine sand; S-Silt; Sc-Soil clay; SOC-Soil organic carbon; TP-Total phosphorus; AP-Available phosphorus; TN-Total nitrogen; AN-Available nitrogen, same as below.

10.3389/fmicb.2023.1113707

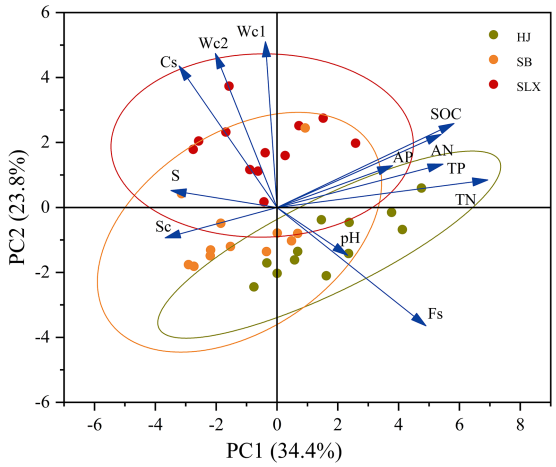

FIGURE 6
Principal component analysis of soil properties.

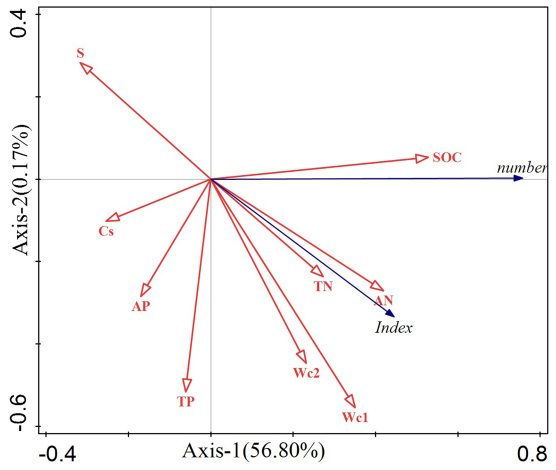

FIGURE 7
Redundancy analysis of cyanobacteria diversity and soil properties.

nitrogen also pointed to the same axis, indicating that there may also be an effect on cyanobacteria species diversity, they did not show statistical significance in the analyzes performed ($p > 0.05$).

4. Discussion

4.1. Similarities and differences in cyanobacterial diversity between karst desertification areas and desertification areas

The BSCs cyanobacteria in the karst desertification study areas were dominated by filamentous cyanobacteria, which accounted for 77.4% of the total. The main families and genera of cyanobacteria are Oscillatoriaceae (*Oscillatoria*, *Lyngbya*), Scytonemataceae (*Scytonema*), Nostocaceae (*Nostoc*), and Chroococcaceae (*Gloeocapsa*), the most common of which is *M. vaginatus* (Garcia-Pichel et al., 2001; Belnap and Lange, 2003; Zhang et al., 2015). In our study, *M. vaginatus* occurred at all sampling sites, which was generally consistent with the composition of cyanobacteria in most other types of desertification areas (Zhang et al., 2005a,b; Büdel et al., 2009; Etemadi-Khah et al., 2017; Cano-Díaz et al., 2018; Roncero-Ramos et al., 2019), indicating that *M. vaginatus* is the main cyanobacteria that make up the BSCs and plays an important ecological role, while *N. commune* also occurred in almost all sample sites and has been shown to occur most frequently among cyanobacteria (Starks et al., 1981). The cyanobacteria in this study are common to the desert ecological zone and have a wide ecological range, which again supports the fact that they are an important genus of cyanobacteria that form BSCs in the desert ecological zone, and also reflects the similarity in the cyanobacterial composition of BSCs in the karst desertification areas as a degraded desert ecological zone. There are also differences, with the genera unique to karst desertification areas being *Cyanostylon* and *Symploca*, with also differences in species, which may be related to differences in regional microhabitats and the adaptation of different cyanobacteria. Desert ecosystems are often considered to be harsh and lifeless habitats, and cyanobacteria can adapt to such extreme environmental conditions and occupy a unique ecological niche (Whitton and Potts, 2007; Perera et al., 2018), as opposed to harsh desertification areas with strong solar radiation, sandy winds, and lack of water. The warm and humid conditions in karst desertification areas provide good conditions for the growth and reproduction of filamentous cyanobacteria, and filamentous cyanobacteria are dominant in cementing fixed soil particles, which can slow down the soil loss caused by the special geomorphic structure in karst areas, improve soil stability, and have important functions in karst soil ecological restoration.

Although the species and numbers of cyanobacteria identified in the three karst desertification study areas are more convincing in this study, the classification of cyanobacteria is based only on morphological microscopic identification. It has been pointed out that the taxonomy of cyanobacteria traditionally relies heavily on morphological data, but the evolutionary relationships of cyanobacteria are more complex, and the true diversity of cyanobacteria is likely to be underestimated (Dvořák et al., 2017). The existing methods also include microscopic identification combined with culture identification, but there are cases where some cyanobacteria are not viable in culture (Dvořák et al., 2018). With the expansion of cyanobacterial gene pools and rapid development of molecular techniques, studies have shown that comprehensive evaluation of cyanobacteria in BSCs requires a combination of multiple molecular techniques, such as DNA extraction, PCR amplification, and sequencing. Molecular tools are often heavily applied to desert BSCs cyanobacteria, and some scholars have used phylogenies to study the global distribution of desert cyanobacteria, concluding that the global distribution of desert cyanobacteria is not the result of widespread dispersal but rather an ancient genetic evolution (Bahl et al., 2011). Other scholars have also argued that cyanobacterial diversity and distribution are determined by complex interactions with multiple abiotic stressors (Lacap-Bugler et al., 2017). However, it is also important to combine a multiphase approach to species description with morphology, as gene sequences can also appear to be improperly assigned to genera (Muhlsteinova et al., 2014), even though the multiphase approach does not guarantee that all cyanobacteria will be identified (Redfield et al., 2002). Therefore, in future research on karst cyanobacteria, the three karst

desertification regions also need to combine a multiphase approach to further illustrate the cyanobacterial diversity of the three sites and their intrinsic connections at the geographic scale and phylogeny.

4.2. Differences in cyanobacteria species diversity in different karst desertification areas and community habitats

In the three karst desertification study areas, there were differences in the abundance, diversity, and species composition of cyanobacteria. The overall number of species was HJ > SB > SLX, and the diversity index was SLX > SB > HJ. In the same limestone lithological background, the number of species was HJ > SLX, and the diversity index was SLX > HJ. Scholars have shown that cyanobacterial community structure is associated with different physicochemical properties of the colonized mineral matrix and petrographic properties (Khomutovska et al., 2020). The number of cyanobacteria was the highest, and the diversity index was the lowest in the HJ moderate–severe desertification study area, with the largest proportion of Oscillatoriaceae, and the species composition was relatively simple, which is consistent with the conclusion of Yang et al. (2013), and may be related to the hydrothermal combination conditions caused by the microclimate in the region since the study area of HJ in moderate–severe desertification is located in a dry and hot valley with high annual rainfall and evaporation, and high temperature, hence it is dominated by Oscillatoriaceae which is non-heterocystic, swimmable and can grow and develop while avoiding the strong sunlight and dry environment (Belnap et al., 1993). The largest number of cyanobacteria species and the highest diversity index in the SLX potential-mild desertification study area were dominated by Chroococcaceae because of the predominance of spherical cyanobacteria species with greater resilience in SLX at an average altitude of more than 1,000 m, with low mean annual temperatures and a wet and cold environment (Pushkareva et al., 2015). In the background of dolomite lithology, the number of species in the SB study area was second to that of HJ, and the diversity index was lower than that of SLX and dominated by Scytonemataceae, which is consistent with the conclusion of Yan et al. (2021) that the terrestrial algae of the dolomite karst of SB are dominated by Scytonemataceae, reflecting the richness in calcium and magnesium and poverty in nutrients of the dolomite karst and supporting the view that dolomite dominates the growth and development of heteromorphic filamentous cyanobacteria (Hu et al., 2002).

In the four community habitats of three different karst desertification study areas, in terms of species numbers, the number of species in the HJ study area was shrubland > arbor woodland > bare land > grassland; in the SLX study area, shrubland > grassland > bare land > arbor woodland, and the trends were basically the same in the two desertification study areas of the same lithology, except for the opposite positions in the number of arbor woodland and grassland. The number of species in the arbor woodland was the highest in the SB study area, whereas the rest of the communities showed little difference. In terms of diversity indices, HJ had the highest diversity in grassland and woodland, SLX had the highest diversity in grassland and shrubland, and SB had the highest diversity in bare land and shrubland. In summary, it is clear that the number of species in the study area is highest in shrubland and highest in grassland in the lithologically identical HJ and SLX study areas. The highest number of species in the dolomite study area of SB is in the arbor woodland, and the highest diversity is in the bare land, which is not only influenced by lithology, general environment, and soils but also by other factors. It has been suggested that grassland has a greater capacity to trap surface water and that vegetation coverage also affects light intensity and, thus, cyanobacterial diversity (Vijayan and Ray, 2015), combined with the community coverage information in this study.

4.3. The influence of karst desertification soil properties on cyanobacterial diversity and species composition

Soil physicochemical properties are influenced by topographic and climatic conditions, bedrock properties, land use, community vegetation, and habitat degradation, resulting in the spatial heterogeneity of regional soil properties (Quesada et al., 1998; Řeháková et al., 2011; Hakkoum et al., 2020). Karst desertification succession is considered to be an extreme land degradation process; however, in our study, soil nutrient content did not decrease with increasing desertification, in agreement with the conclusions reached by Sheng et al. (2016). The organic carbon, total nitrogen, and total phosphorus contents were greatest in the study area of moderate–severe desertification in HJ, followed by SLX, and lowest in SB, due to the increase in the rate of rock exposure as the degree of rock desertification deepened; the nutrients from atmospheric deposition, rock dissolution, and plant apoptosis cannot be absorbed and preserved by the exposed rocks and can only be washed by rain or blown by the wind into thxe surrounding soil, so the soil nutrient content increases, the soil that can be lost is limited too, and nutrient losses are minimal. The results of our study show that the soil properties that affect the cyanobacteria species diversity in the three karst desertification study areas are soil moisture content (0–5 cm), organic carbon, and total nitrogen. Organic carbon is not only positive for the growth and development of cyanobacterial crusts, but also a key factor in promoting the formation of cyanobacterial communities. Some scholars have studied the structure of Arctic cyanobacterial communities and their bearing soil substrates, showing a significant positive correlation between organic carbon and cyanobacteria abundance (Pushkareva et al., 2016). In a study of the community structure of BSCs cyanobacteria in the Tengger East Desert, Zhang et al. (2021) concluded that total nitrogen and organic carbon were the factors that significantly influenced cyanobacterial diversity and abundance, and that the highest organic carbon content and the highest number of cyanobacteria species were found in the arbor woodland of SB, while the highest diversity and total nitrogen content were found in the bare land, thus supporting this conclusion. In studying the relationship between cyanobacterial abundance and rainfall in the Atacama Desert, researchers have concluded that cyanobacterial abundance decreases with decreasing rainfall (Warren-Rhodes et al., 2006). Zhang et al. (2009) concluded that precipitation is the main factor influencing the distribution of cyanobacteria and that the higher the precipitation, the higher the soil moisture content, resulting in a finer soil texture that can

support the growth and development of more cyanobacterial communities. In a study of cyanobacteria in BSCs in the Ural Mountains, researchers pointed out that soil moisture content and total nitrogen were important soil property factors affecting cyanobacteria species diversity (Patova et al., 2018), which is generally consistent with the findings of this study. Others have shown that cyanobacterial diversity is most influenced by soil moisture content and less related to soil chemical composition (Hagemann et al., 2015), which is generally consistent with the results of this study. SLX had a significantly higher soil moisture content in all communities than the other two study areas, which, based on the analytical discussion, could be used as an explanation for the highest diversity index in SLX.

4.4. Synergistic evolution of cyanobacteria species composition and soil properties in karst desertification areas

The specific physiological and ecological characteristics of cyanobacteria allow them to occupy different ecological niches, and the dominance of cyanobacteria varies depending on habitat and soil conditions (Loza et al., 2014). A study of the cyanobacteria species composition of BSCs in the Saharan desert indicated that *Microcoleus* spp. were significantly dominant in low salinity soils, filamentous heterocystic cyanobacteria and *Acaryochloris* were dominant in high salinity soils, and non-heterocystic cyanobacteria were dominant in dry soils (Mehda et al., 2021), which is consistent with the results obtained by HJ in this study. Cyanobacteria are alkaline lovers that grow best in neutral to slightly alkaline soils (Belnap and Lange, 2003). The soil of the selected communities in karst desertification areas is neutral to acidic, but cyanobacteria species are still abundant, indicating that cyanobacteria can grow and reproduce well in acidic environments. From the analysis of our paper, it can be seen that the soils of HJ are characterized by low soil moisture content (about 7–15%), and sandy loam; the average content of organic carbon is 25.09 and total nitrogen is 3.49; the content of clay is 7.35%, resulting in low soil moisture content supporting the growth of cyanobacteria; SLX soils are characterized by rich soil moisture content (over 17%); the coarse sand content is larger than the other two study areas, and the content of clay is 7.98%, rich in organic carbon and nitrogen, and the soils of SB are characterized by low soil moisture content, similar to HJ, and relatively poor in soil nutrients. The highest organic carbon and total nitrogen content of HJ were dominated by *Oscillatoria* and *Lyngbya*, such as the unique *Oscillatoria animalis* and *Oscillatoria limosa*, etc. In addition, a unique genus *Raphidiopsis* exists. Similarly, the organic carbon and total nitrogen content of SLX was second only to that of HJ, and *Oscillatoria* was also dominant, with the unique species *Oscillatoria prolifica* and *Oscillatoria agardhii*, etc. It can be seen that soils rich in organic carbon and total nitrogen are dominated by cyanobacterial crusts of filamentous non-heterocystic *Oscillatoria*. In contrast, soils with high moisture content and coarse texture were dominated by cyanobacterial crusts of *Gloeocapsa*, such as *Gloeocapsa montana* Kütz and *Gloeocapsa montana* in SLX, in agreement with the conclusions reached by Patova et al. (2018), and the unique genera *Plectonema*, *Anabaena*, *Cyanostylon*, etc. The temperature of SB is suitable, the soil texture is fine and relatively poor in soil moisture and nutrients, and is dominated by cyanobacterial crusts of filamentous heteromorphic *Scytonema*, such as *Scytonema hofmanni* and *Scytonema julianum*, etc. In addition, there also exists the unique *Symploca* and *Calothrix* species.

5. Conclusion

1. A total of 200 species of cyanobacteria in two classes, five orders, six families, and 22 genera were identified in the three karst desertification study areas: the species composition of cyanobacteria is similar to that of desertification areas, all of which are common species, with Oscillatoriaceae, Chroococcaceae, Scytonemataceae, and Nostocaceae as common families, among which *M. vaginatus* and *N. commune* are generally dominant, which is related to the wide ecological range of generalist cyanobacteria; the dominant family and genus in the three desertification study areas were different, with Oscillatoriaceae being the dominant family in the moderate–severe desertification study area of HJ, Chroococcaceae in the potential-mild desertification study area of SLX, and Scytonemataceae in the no-potential desertification study area of SB.
2. The diversity of cyanobacteria in the karst desertification study area is related to three soil properties: soil moisture content (0–5 cm), organic carbon, and total nitrogen, but other soil properties affecting the cyanobacterial diversity need to be explored in combination with more soil properties in karst desertification areas. Cyanobacterial diversity varies between community habitats, with the highest number of species in both the HJ and SLX study areas of limestone lithology in shrubland and the highest diversity in grassland. The number of species was highest in arbor woodland, and the diversity was highest in bare land in the dolomite study area of SB. In addition to lithology and soil properties, this is also related to the increase in soil nutrients due to vegetation litter, trapping of surface water, and light intensity directly influenced by vegetation cover.
3. There is a synergistic evolution of suitable cyanobacteria in the karst desertification study area in response to changes in the soil properties. Cyanobacterial crusts of dry and hot soils (7–15% moisture content), and soils rich in organic carbon and total nitrogen, are dominated by *Oscillatoria*, reflecting the physiological adaptability of *Oscillatoria* to dry and hot environments and its carbon and nitrogen-loving properties. Cyanobacterial crusts of *Gloeocapsa* are dominant in soils with high moisture content (above 17%) and coarse texture, reflecting the resistance of *Gloeocapsa* to cold and wet conditions and influenced by coarse soil particles. *Scytonema* is influenced by dolomite lithology and is tolerant of infertile soils at suitable temperatures, so poor nutrients and low moisture content are dominated by *Scytonema* as the dominant cyanobacterial crust.

Data availability statement

The original contributions presented in the study are included in the article/supplementary material, further inquiries can be directed to the corresponding author.

Author contributions

QC and NY conceived the work, conducted data sorting, and analysis. NY, QC, and JZ collected the biocrust samples and soil samples. QC performed the microscopic study for cyanobacteria phenotypic characterization. NY performed the soil physicochemical analysis. JZ collected literature. QC wrote the manuscript and NY revised it. KX provided financial support and summarized manuscripts. All authors contributed to the article and approved the submitted version.

Funding

This research was financially supported by the Key Project of Science and Technology Program of Guizhou Province (No. 5411 2017 Qiankehe Pingtai Rencai); the China Overseas Expertise Introduction Program for Discipline Innovation (No. D17016); the National Major Research and Development Program of China (2016YFC0502607).

Conflict of interest

The authors declare that the research was conducted in the absence of any commercial or financial relationships that could be construed as a potential conflict of interest.

Publisher's note

References

Bahl, J., Lau, M. C., Smith, G. J., Vijaykrishna, D., Cary, S. C., Lacap, D. C., et al. (2011). Ancient origins determine global biogeography of hot and cold desert cyanobacteria. *Nat. Commun.* 2, 163–166. doi: 10.1038/ncomms1167

Bao, S. D. (2000). *Soil Agro-chemistrical Analysis*. China Agriculture Press, Beijing.

Belnap, J. (2002). Nitrogen fixation in biological soil crusts from Southeast Utah. *USA. Biol. Fertil. Soils.* 35, 128–135. doi: 10.1007/s00374-002-0452-x

Belnap, J., Harper, K., and Warren, S. (1993). Surface disturbance of cryptobiotic soil crusts: Nitrogenase activity, chlorophyll content, and chlorophyll degradation. *Arid Land Res. Manag.* 8, 1–8. doi: 10.1080/15324989309381373

Belnap, J., and Lange, O. L. (2001). Structure and functioning of biological soil crusts: a synthesis. *Biol. soil crusts: struct, function, Manag.* 150, 471–479. doi: 10.1007/978-3-642-56475-8_33

Belnap, J., and Lange, O. L. (2003) Biological soil crusts: structure, function, and management. *Ecol. stud.* 150.

Belnap, J., and Miller, P. (2004). Response of desert biological soil crusts to alterations in precipitation frequency. *Oecologia* 141, 306–316. doi: 10.1007/s00442-003-1438-6

Belnap, J., Weber, B., and Büdel, B. (2016). Biological soil crusts: an organizing principle in drylands. *Ecol. Studies* 226, 3–13. doi: 10.1007/978-3-319-30214-0

Büdel, B., Darienko, T., Deutschewitz, K., Mohr, K. I., and Weber, B. (2009). Southern African biological soil crusts are ubiquitous and highly diverse in drylands, being restricted by rainfall frequency. *Microb. Ecol.* 57, 229–247. doi: 10.1007/S00248-008-9449

Büdel, B., Williams, W. J., and Reichenberger, H. (2018). Annual net primary productivity of a cyanobacteria-dominated biological soil crust in the Gulf Savannah, Queensland. *Aust. Biogeosci.* 15, 491–505. doi: 10.5194/bg-15-491-2018

Cano-Díaz, C., Mateo, P., Muoz-Martín, M. A., and Maestre, F. T. (2018). Diversity of biocrust-forming cyanobacteria in a semiarid gypsiferous site from Central Spain. *J. Arid Environ.* 151, 83–89. doi: 10.1016/j.jaridenv.2017.11.008

Chamizo, S., Cantón, Y., Rodríguez-Caballero, E., and Domingo, F. (2016). Biocrusts positively affect the soil water balance in semiarid ecosystems. *Ecohydrology* 9, 1208–1221. doi: 10.1002/eco.1719

Chen, Y. B., Xiong, K. N., and Chi, Y. K. (2019). Process of rocky desertification control in karst area of southern China. *Jiangsu. J. Agric. Sci.* 47, 17–21. doi: 10.15889/j.issn.1002-1302.2019.01.004

Dvořák, P., Casamatta, D. A., Hašler, P., Jahodářová, E., Norwich, A. R., and Poulíčková, A. (2017). "Diversity of the cyanobacteria" in *Modern Topics in the Phototrophic Prokaryotes* (Cham: Springer), 3–46.

Dvořák, P., Jahodářová, E., Casamatta, D. A., Hašler, P., and Poulíčková, A. (2018). Difference without distinction? Gaps in cyanobacterial systematics; when more is just too much. *J. Czech. Phycol. Soc.* 18, 130–136. doi: 10.5507/fot.2017.023

Etemadi-Khah, A., Pourbabaee, A. A., Alikhani, H. A., Noroozi, M., and Bruno, L. (2017). Biodiversity of isolated cyanobacteria from desert soils in Iran. *Geomicrobiol J.* 34, 784–794. doi: 10.1080/01490451.2016.1271064

Felde, V. J. M. N. L., Chamizo, S., Felix-Henningsen, P., and Drahorad, S. L. (2018). What stabilizes biological soil crusts in the Negev Desert? *Plant Sci.* 429, 9–18. doi: 10.1007/s11104-017-3459-7

Fernandes, V. M. C., Machado de Lima, N. M., Roush, D., Rudgers, J., Collins, S. L., and Garcia-Pichel, F. (2018). Exposure to predicted precipitation patterns decreases population size and alters community structure of cyanobacteria in biological soil crusts from the Chihuahuan Desert. *Environ. Microbiol.* 20, 259–269. doi: 10.1111/1462-2920.13983

Garcia-Pichel, F., Lopez-Cortes, A., and Nubel, U. (2001). Phylogenetic and morphological diversity of cyanobacteria in soil desert crusts from the Colorado plateau. *Appl. Environ. Microbiol.* 67, 1902–1910. doi: 10.1128/aem.67.4.1902-1910.2001

Gaysina, L. A., Bohunicka, M., Hazukova, V., and Johansen, J. R. (2018). Biodiversity of terrestrial cyanobacteria of the South Ural region. *Cryptogam. Algol.* 39, 167–198. doi: 10.7872/crya/v39.iss2.2018.167

Hagemann, M., Henneberg, M., Felde, V. J. M. N. L., Drahorad, S. L., Berkowicz, S. M., Felix-Henningsen, P., et al. (2015). Cyanobacterial diversity in biological soil crusts along a precipitation gradient, Northwest Negev Desert. *Israel. Microb. Ecol.* 70, 219–230. doi: 10.1007/s00248-014-0533-z

Hakkoum, Z., Minaoui, F., Douma, M., Mouhri, K., and Loudiki, M. (2020). Diversity and spatial distribution of soil cyanobacteria along an altitudinal gradient in Marrakesh area (Morocco). *Appl. Ecol. Environ. Res.* 18, 5527–5545. doi: 10.15666/aeer/1804_55275545

Housman, D. C., Powers, H. H., Collins, A. D., and Belnap, J. (2006). Carbon and nitrogen fixation differ between successional stages of biological soil crusts in the Colorado plate au and Chihuahuan Desert. *J. Arid Environ.* 66, 620–634. doi: 10.1016/j.jaridenv.2005.11.014

Hu, C. X., Liu, Y. D., and Song, L. R. (2002). New development of soil algae research. *Acta. Hydrobiol. Sin.* 26, 521–528. doi: 10.3321/j.issn:1000-3207.2002.05.018

Khomutovska, N., de Los Ríos, A., and Jasser, I. (2020). Diversity and colonization strategies of endolithic cyanobacteria in the cold mountain desert of Pamir. *Microorganisms.* 9:6. doi: 10.3390/microorganisms9010006

Lacap-Bugler, D. C., Lee, K. K., Archer, S., Gillman, L. N., Lau, M. C., Leuzinger, S., et al. (2017). Global diversity of desert hypolithic cyanobacteria. *Front. Microbiol.* 8:867. doi: 10.3389/fmicb.2017.00867

Li, X. R., Jia, R. L., Zhang, Z. S., Zhang, P., and Hui, R. (2018). *Glob. Change. Biol.* 24:Hydrological response ofbiological soil crusts to global warming: A ten-year simulative study, 4960–4971. doi: 10.1111/gcb.14378

Loza, V., Perona, E., and Mateo, P. (2014). Specific responses to nitrogen and phosphorus enrichment in cyanobacteria: factors influencing changes in species dominance along eutrophic gradients. *Water Res.* 48, 622–631. doi: 10.1016/j.watres.2013.10.014

Machado de Lima, N. M., Fernandes, V. M. C., Roush, D., Velasco Ayuso, S., Rigonato, J., Garcia-Pichel, F., et al. (2019). The compositionally distinct cyanobacterial biocrusts from Brazilian savanna and their environmental drivers of community diversity. *Front. Microbiol.* 10:2798. doi: 10.3389/fmicb.2019.02798

Machado de Lima, N. M., Muñoz-Rojas, M., Vázquez-Campos, X., and Branco, L. H. Z. (2021). Biocrust cyanobacterial composition, diversity, and environmental drivers in two contrasting climatic regionsin Brazil. *Geoderma* 386:114914. doi: 10.1016/j.geoderma.2020.114914

Mehda, S., Muñoz-Martin, M. Á., Oustani, M., Hamdi-Aïssa, B., Perona, E., and Mateo, P. (2021). Microenvironmental conditions drive the differential cyanobacterial community composition of biocrusts from the Sahara Desert. *Microorganisms* 9:487. doi: 10.3390/microorganisms9030487

Muhlsteinova, R., Johansen, J. R., Pietrasiak, N., Martin, M. P., Osorio-Santos, K., and Warren, S. D. (2014). Polyphasic characterization of Trichocoleus desertorum sp. nov. (Pseudanabaenales, cyanobacteria) from desert soils and phylogenetic placement of the genus Trichocoleus. *Phytotaxa.* 163, 241–261. doi: 10.11646/phytotaxa.163.5.1

Novakovskaya, I. V., Patova, E. N., Dubrovskiy, Y. A., Novakovskiy, A. B., and Kulyugina, E. E. (2022). Distribution of algae and cyanobacteria of biological soil crusts along the elevation gradient in mountain plant communities at the northern Urals(Russian European northeast). *J. Mt. Sci.* 19, 637–646. doi: 10.1007/s11629-021-6952-7

Patova, E. N., Novakovskaya, I. V., and Deneva, S. V. (2018). The influence of edaphic and orographic factors on algal diversity in biological soil crusts on bare spots in the polar and subpolar Urals. *Eurasian Soil Sci.* 51, 309–320. doi: 10.1134/s1064229318030109

Perera, I., Subashchandrabose, S. R., Venkateswarlu, K., Naidu, R., and Megharaj, M. (2018). Consortia of cyanobacteria/microalgae and bacteria in desert soils: an underexplored microbiota. *Appl. Microbiol. Biotechnol.* 102, 7351–7363. doi: 10.1007/s00253-018-9192-1

Pushkareva, E., Johansen, J. R., and Elster, J. (2016). A review of the ecology, ecophysiology and biodiversity of microalgae in Arctic soil crusts. *Polar Biol.* 39, 2227–2240. doi: 10.1007/s00300-016-1902-5

Pushkareva, E., Pessi, I. S., Namsaraev, Z., Mano, M. J., Elster, J., and Wilmotte, A. (2018). Cyanobacteria inhabiting biological soil crusts of a polar desert: Sør Rondane Mountains. *Antarct. Syst. Appl. Microbiol.* 41, 363–373. doi: 10.1016/j.syapm.2018.01.006

Pushkareva, E., Pessi, I. S., Wilmotte, A., and Elster, J. (2015). Cyanobacterial community composition in Arctic soil crusts at different stages of development. *FEMS Microbiol. Ecol.* 91:fiv143. doi: 10.1093/femsec/fiv143

Quesada, A., Nieva, M., Leganés, F., Ucha, A., Martín, M., Prosperi, C., et al. (1998). Acclimation of Cyanophytal communities in rice fields and response of nitrogenase acti vity to light regime. *Microb. Ecol.* 35, 147–155. doi: 10.1007/s002489900069

Roncero-Ramos, B., Muñoz-Martín, M. Á., Chamizo, S., Fernández-Valbuena, L., Mendoza, D., Perona, E., et al. (2019). Polyphasic evaluation of key cyanobacteria in biocrusts from the most arid region in Europe. *PeerJ.* 7:e6169. doi: 10.7717/peerj.6169

Ravbar, N., and Šebela, S. (2015). The effectiveness of protection policies and legislative framework with special regard to karst landscapes: insights from Slovenia. *Environ. Sci. Pol.* 51, 106–116. doi: 10.1016/j.envsci.2015.02.013

Redfield, E., Barns, S. M., Belnap, J., Daane, L. L., and Kuske, C. R. (2002). Comparative diversity and composition of cyanobacteria in three predominant soil crusts of the Colorado plateau. *FEMS Microbiol. Ecol.* 40, 55–63. doi: 10.1111/j.1574-6941.2002.tb00936.x

Řeháková, K., Chlumská, Z., and Doležal, J. (2011). Soil Cyanobacterial and microalgal diversity in dry mountains of Ladakh, NW Himalaya, as related to site, altitude, and vegetation. *Microb. Ecol.* 62, 337–346. doi: 10.1007/s00248-011-9878-8

Rodriguez-Caballero, E., Stanelle, T., Egerer, S., Cheng, Y., Su, H., Canton, Y., et al. (2022). Global cycling and climate effects of aeolian dust controlled by biological soil crusts. *Nat. Geosci.* 15:458-+. doi: 10.1038/s41561-022-00942-1

Sheng, M. Y., Xiong, K. N., Wang, L. J., Li, X. N., Li, R., and Tian, X. J. (2016). Response of soil physical and chemical properties to rocky desertification succession in South China karst. *Carbonates Evaporites* 33, 15–28. doi: 10.1007/s13146-016-0295-4

Sosa-Quintero, J., Godínez-Alvarez, H., Camargo-Ricalde, S. L., Gutiérrez-Gutiérrez, M., Huber-Sannwald, E., Jiménez-Aguilar, A., et al. (2022). Biocrusts in Mexican deserts and semideserts: a review of their species composition, ecology, and ecosystem function. *J. Arid Environ.* 199:104712. doi: 10.1016/j.jaridenv.2022.104712

Starks, T. L., Shubert, L. E., and Trainor, F. R. (1981). Ecology of soil algae: a review. *Phycologia* 20, 65–80. doi: 10.2216/i0031-8884-20-1-65.1

Temraleeva, A. D. (2018). Cyanobacterial diversity in the soils of Russian dry steppesand semideserts. *Microbiology* 87, 249–260. doi: 10.1134/s0026261718020169

Vijayan, D., and Ray, J. G. (2015). Ecology and diversity of cyanobacteria in KuttanaduPaddy wetlands, Kerala. *India. Am. J. Plant. Sci.* 6, 2924–2938. doi: 10.4236/ajps.2015.618288

Wang, S., Gao, E. G., Luo, X. J., Xu, Y., and Liu, Y. L. (2019). Characteristics of forest communities of typical evergreen broad-leaved forest in Shibing. *Mol. Plant. Breed.* 17, 3432–3441. doi: 10.13271/j.mpb.017.003432

Warren-Rhodes, K. A., Rhodes, K. L., Pointing, S. B., Ewing, S. A., Lacap, D. C., Gomez-Silva, B., et al. (2006). Hypolithic cyanobacteria, dry limit of photosynthesis, and microbial ecology in the hyperarid Atacama Desert. *Microb. Ecol.* 52, 389–398. doi: 10.2307/25153391

Whitton, B. A., and Potts, M. (Eds.) (2007). *The Ecology of Cyanobacteria: Their Diversity in Time and Space* Springer Science & Business Media.

Williams, L., Loewen-Schneider, K., Maier, S., and Büdel, B. (2016). Cyanobacterial diversity of western European biological soil crusts along a latitudinal gradient. *FEMS Microbiol. Ecol.* 92:fiw157. doi: 10.1093/femsec/fiw157

Yan, N., Zhang, T., Xiong, K. N., Chen, Q., Guo, D. L., and Liu, Z. W. (2021). Terrestrial algae diversity of the two world natural heritage sites in China. *Acta Ecol. Sin.* 41, 9593–9603.

Yang, H. Y., Liang, Y. H., Fan, Y. L., Zhang, F. T., and Luo, X. Q. (2013). Characteristics of soil algae community structure in Huajiang karst area of Guizhou. *Guizhou Agric. Sci.* 41, 102–105. doi: 10.3969/j.issn.1001-3601.2013.11.027

Zhang, X. C., Li, J. Y., Liu, J. L., Yuan, C. X., Li, Y. N., Liu, B. R., et al. (2021). Temporal shifts in cyanobacterial diversity and their relationships to different types of biological soil crust in the southeastern Tengger Desert. *Rhizosphere.* 17:100322. doi: 10.1016/j.rhisph.2021.100322

Zhang, B., Li, R., Xiao, P., Su, Y., and Zhang, Y. (2015). Cyanobacterial composition and spatial distribution based on pyrosequencing data in the Gurbantunggut Desert, northwestern China. *J. Basic Microbiol.* 56, 308–320. doi: 10.1002/jobm.201500226

Zhang, N., Ye, C., An, M. T., Chen, L., and Ran, X. Z. (2019). Study on plant diversity during natural restoration of karst vegetation in Huajiang grand canyo. *Seed.* 38:64-67+71. doi: 10.16590/j.cnki.1001-4705.2019.12.064

Zhang, B. C., Zhang, Y. M., and Zhao, J. C. (2005a). Composition and ecological distribution of the algae living in the Gurbantonggut desert of Xinjiang. *Acta. Bot. Boreali-Occident. Sin.* 25, 2048–2055. doi: 10.3321/j.issn:1000-4025.2005.10.020

Zhang, B. C., Zhang, Y. M., Zhao, J. C., Chen, R. Y., and Zheng, Y. P. (2009). Variation in algal composition among different developmental stages of biological soil crusts in Gurbantunggut Desert. *Acta Ecol. Sin.* 29, 9–17. doi: 10.3321/j.issn:1000-0933.2009.01.002

Zhang, B. C., Zhang, Y. M., Zhao, J. C., and Zhang, R. C. (2005b). Study on cyanobacteria of biological soil crusts in Guerbantunggut desert, Zhungar basin, sinkiang. *Geogr. Geo-Infor. Sci.* 21, 107–109. doi: 10.10007/978-3-642-56475-8

Zhang, B. C., Zhao, J. C., Zhang, Y. M., Li, M., and Zhang, J. (2008). Vertical distribution of algae in different locations of sand dunes in the Gurbantunggut Desert, Xinjiang. *China. Chin. J. Plant. Ecol.* 32, 456–464. doi: 10.3773/j.issn.1005-264x.2008.02.025

Zou, R. S., Wang, Y. F., Rong, D., Zhu, J. F., Wang, Y. L., Liu, X. Z., et al. (2022). Research progress in how biological soil crusts improve carbon sink capacity of terrestrial ecosystems. *World For. Res.* 35, 7–12. doi: 10.13348/j.cnki.sjlyyj.2022.0044.y

frontiers | Frontiers in Microbiology

TYPE Original Research
PUBLISHED 16 March 2023
DOI 10.3389/fmicb.2023.1143900

OPEN ACCESS

EDITED BY
Qiang Li,
Chinese Academy of Geological Sciences, China

REVIEWED BY
Robin Slawson,
Wilfrid Laurier University, Canada
Joshua B. Gurtler,
Agricultural Research Service (USDA), United States

*CORRESPONDENCE
Shuaiwei Wang
✉ Tairan_W@163.com
Min Zhang
✉ minzhang205@live.cn

SPECIALTY SECTION
This article was submitted to Terrestrial Microbiology, a section of the journal Frontiers in Microbiology

RECEIVED 13 January 2023
ACCEPTED 22 February 2023
PUBLISHED 16 March 2023

CITATION
Ning Z, Wang S, Guo C and Zhang M (2023) The impact of environmental factors on the transport and survival of pathogens in agricultural soils from karst areas of Yunnan province, China: Laboratory column simulated leaching experiments.
Front. Microbiol. 14:1143900.
doi: 10.3389/fmicb.2023.1143900

The impact of environmental factors on the transport and survival of pathogens in agricultural soils from karst areas of Yunnan province, China: Laboratory column simulated leaching experiments

Zhuo Ning[1,2], Shuaiwei Wang[1]*, Caijuan Guo[1] and Min Zhang[1,2]*

[1]Institute of Hydrogeology and Environmental Geology, Chinese Academy of Geological Sciences, Shijiazhuang, China, [2]Key Laboratory of Groundwater Remediation of Hebei Province and China Geological Survey, Zhengding, China

Introduction: Groundwater is considered the best candidate for drinking water supply in the karst area. The groundwater water resources, however, are vulnerable to pathogenic microorganism contamination because of the typically thin soil layers overlying aquifers and the high permeability of the aquifer host rock, resulting in short residence times and low natural attenuation capacities. Until now, little attention has been paid to the critical environmental factors affecting the pathogenic microorganism contamination in soil-groundwater systems in the karst area.

Methods: In the study, orthogonality column experiments with controlling ambient temperatures, pH values of inlet water, and soil porosities were carried out to investigate the transport and lifespan of pathogenic microorganisms in the leachate of agricultural soils in the karst area of Yunnan province, China. The pathogenic indicators, i.e., total bacteria count (TBC) and total coliforms count (TCC), and hydrochemical parameters, i.e., pH and permanganate index (COD_{Mn}) in the leaching water, were systematically monitored.

Results and Discussion: The results showed that bacteria including coliforms can survive for prolonged periods of time in karst soils. The soils overlying the karst rocks were unable to impede the bacteria from seeping into the groundwater. The soils, in turn, likely served as both reservoirs and incubators for pathogenic bacteria. The ambient temperature was the most predominant influential factor affecting both TBC and TCC. The bacteria concentrations were proportional to the temperature in the leachate. Therefore, more attention should be paid to temperature variations in protecting the water supply, particularly in the high-temperature period, such as during the summer months.

KEYWORDS

pathogenic microorganisms, transport and survival of pathogens, leaching experiments, agricultural soils, karst area

1. Introduction

Groundwater is the best candidate for rural water supply in the karst area of Southwest China (Xia, 2016). Unfortunately, these important water resources are vulnerable to anthropogenic contamination. Because of the typically thin vadose zone soil layers and the high permeability of the host rock, the short residence time and low natural attenuation capacities may lead to the formation of infertile soils in the thin layers and the enrichment of contaminants in groundwater. Soil, water, nutrients, and contamination are easily leached *via* underground channels or conduits created by the widening of fractures in soluble rocks such as limestone or dolomite (Heinz et al., 2009). In agricultural soils, manure is frequently used to improve soil fertility. The pathogens embedded in the manure could concurrently be transferred into soils and then leach into the groundwater (Franz et al., 2008; Sharma and Reynnells, 2018; Pang et al., 2020; Chique et al., 2021). Studies have shown that pathogenic microorganisms are significant sources of anthropogenic contamination in rural villages, potentially posing a risk to water supply security, particularly in karst regions. This is due to the fact that pathogen infections are typically linked to the consumption of groundwater contaminated with pathogens (Heinz et al., 2009; Luffman and Tran, 2014; Li et al., 2020; Brad et al., 2022).

Transport of pathogens through soils is governed by several basic physical processes such as advection, dispersion, adhesion/detachment, as well as survival process growth/decay (Bitton and Harvey, 1992; Ginn et al., 2002; Sen, 2011). Most studies focused on the physical processes in the aquifer or the vadose zone relying on the column experiments (McCaulou et al., 1994; Tan et al., 1994; McCaulou et al., 1995; Schäfer et al., 1998; Ginn et al., 2006; Liu et al., 2011; Aaron, 2018; Eisfeld et al., 2022). Several studies also paid attention to the survival of pathogens in various soils or groundwater (Edmonds, 1976; Bitton et al., 1983; John and Rose, 2005; Grisey et al., 2010; Chandrasekar et al., 2021). These studies revealed that the transport and survival of pathogens are mainly affected by four factors: climate (e.g., temperature, rainfall), medium materials and conditions (e.g., texture, pH, water holding capacity, cation exchange capacity), properties of fluids (e.g., chemistry, saturation), and type of pathogen (e.g., Bacteria, fungi, protozoa, virus) (Bitton and Harvey, 1992; Franz et al., 2008; Dwivedi et al., 2016; Song et al., 2018; Pang et al., 2020). Some studies also indicate that the survival and growth of some bacteria are greatly affected by the protozoa in the soil or groundwater (King et al., 1988; England et al., 1993; Matz and Kjelleberg, 2005; Lambrecht et al., 2015).

In the karst area, previous research mainly focused on the origin of the pathogens and pointed out that agricultural activity would introduce pathogens to the karst aquifer (Pronk, 2008; Heinz et al., 2009). The survival and transport of several pathogens in various karstic aquifers have been extensively studied and found that once the pathogenic microorganisms penetrated the soil and entered into the karst aquifer, the microorganisms may migrate fast through karst channels, especially in Southwest China (Personné et al., 1998; Pronk et al., 2006; Pronk, 2008; Ward et al., 2016; Bandy et al., 2018; Buckerfield et al., 2019; Bandy et al., 2020; Oliver et al., 2020). Infiltration in the vadose zone is crucial in preventing and regulating the contamination of groundwater by pathogens. In South-Western Karst Region, most of the soils stem from limestone weathering, thus their available element contents are low, and clay and organic matter contents are high (Cao et al., 2003; Li et al., 2006; Chen and Bi, 2011). In agricultural soils, the movement and persistence of pathogens and related elements may differ from those found in typical soils. However, there have been limited studies on this subject. In our previous research, we discovered that pH, temperature, and porosity are the significant factors that influence the presence of pathogens, specifically the total bacteria count (TBC) and the total coliform count (TCC) (Wang, 2019). It is important to study the impact of these factors on the movement and survival of pathogens.

In this study, laboratory column simulated leaching experiments, with agricultural soils from karst areas of Yunnan province, China, were carried out. By altering the soil porosity, the environmental temperature, as well as the inlet water pH values, the variations of pathogenic bacteria (represented by TBC and TCC), and some hydrochemical parameters in the outlet water were monitored. With the obtained data, it is expected to uncover the mechanisms behind the formation of pathogens in groundwater that has infiltrated from agricultural soils.

2. Materials and methods

2.1. General approach

Flow-through columns packed with agricultural soils collected from the karst area of Yunnan province, China, were used to mimic runoff and infiltration of agricultural drainage in karst areas, and to evaluate changes in the total bacteria and total coliform populations during sustained water supply. A focus was placed on counting bacteria in the column effluent to concentrate on the mobile bacteria with a higher likelihood of affecting a human recipient. Along with population enumerations, pH and permanganate index (COD_{Mn}) concentration profiles were monitored along the length of the columns to know the water acid–base properties and organic matter contents that may also affect pathogens.

To understand the temporal and spatial variation of pathogenic microorganisms in the groundwater infiltrated from the selected soils, a column experiment stimulating the natural condition was carried out. The column was filled with collected soils with undisturbed natural porosity, and the pH value of the inlet water was adjusted to 7.0. Then the leaching experiment was carried out at 25°C for 42 days. To examine the temperature, pH, as well as porosity effects on the populations of pathogenic microorganisms in the groundwater infiltrated from agricultural soils, an orthogonal experiment with 3 factors and 3 levels was designed.

2.2. Flow-through columns

Flow-through glass columns (60-cm long, 25-cm inner diameter) were equipped with five sampling ports located at 10, 20, 30, 40, and 50 cm from the bottom of the column. The columns were filled with 40 cm high in a translational manner (every 10 cm correspondingly) to simulate the natural state of the agricultural soils in a karst area by controlling the density and porosity. The trapping air bubbles were precluded. The columns were wrapped in aluminum foil to minimize algal growth. The feed reservoirs were 2-L bottles wrapped in aluminum foil. Sterile deionized water amended with some inorganic

10.3389/fmicb.2023.1143900

TABLE 1 The orthogonal table with three factors and three levels.

Experimental numbers	Factors		
	Temperature (°C)	pH	Porosity
1	10	6	0.50
2	20	8	0.50
3	30	7	0.50
4	10	7	0.55
5	20	6	0.55
6	30	8	0.55
7	10	8	0.60
8	20	7	0.60
9	30	6	0.60

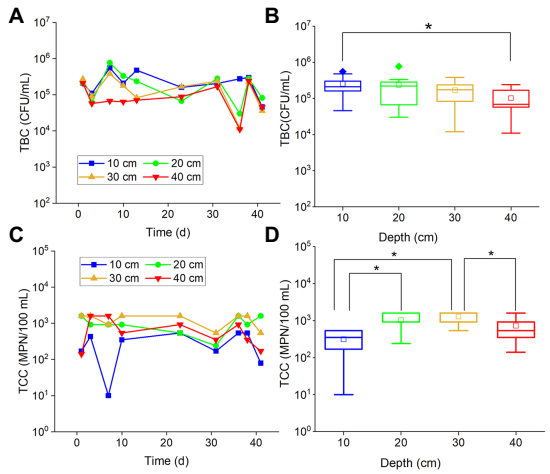

FIGURE 1
The variations of TBC and TCC with **(A,C)** time and **(B,D)** depth. The star (*) stands for there was a significant difference between the two concentrations (p<0.05). Different colors stand for different depths. The central line and square of each box are the median and mean values, respectively, while the top and bottom of each box represent the third and first quartile, respectively. Whiskers on the box plot represent maximum and minimum values, while rhombuses above or below the box plots show outliers in the data.

and organic matter (Wang, 2019) was served as rainwater and added to the columns by a peristaltic pump to produce a constant water table (10 cm above the soil top surface).

2.3. Orthogonal experiment design

Here, an orthogonal experimental design method was applied to discuss the air temperature, pH values of inlet flow, and soil porosity effects on the populations of pathogenic microorganisms in the groundwater infiltrated from agricultural soils. Temperature, pH, and porosity were determined as three factors of the orthogonal experiment and each factor had three levels. The levels of each factor were determined by the actual conditions in the study area. It was assumed that any two factors did not interact with each other. The orthogonal array of the nine experiments is shown in Table 1, designed according to the orthogonal design table L_9 (3^3).

2.4. Sampling and analyses

The water samples were collected at different depths (i.e., 10/20/30/40 cm) of each column at 0, 1, 3, 7, 10, 13, 23, 31, 36, 38, and 41 days after the soil was saturated by the inlet water in the temporal and spatial variation experiment. While in the orthogonal experiments, the effluent samples were collected at different depths at 7 and 9 days. The collected samples were stored in 100 ml sterile glass bottles at 4°C before analyses.

The pH values and COD_{Mn} concentrations in the effluent were measured by the electrode method and spectrophotometric method, respectively, (Federation and Association, 2005).

The TBC values were enumerated using the plate count method (China NHCOTPSRO, 2006). Water sample (1 ml) was inoculated onto beef extract peptone AGAR medium (Base Bio, Hangzhou, China) plate and incubated for 24 h at 37°C. Then, the colony-forming units (CFU) in the plate were enumerated and gained the TBC values (CFU/mL).

The TCC values were enumerated using the multi-tube fermentation (MTF) method (China NHCOTPSRO, 2006). A series of tubes with appropriate decimal dilutions of the water sample and lactose broth (Aobox, Beijing, China) were inoculated. Production of gas, acid formation, or abundant growth in the test tubes after 24 h of incubation at 37°C constitutes a positive presumptive reaction. All tubes with a positive presumptive reaction are subsequently subjected to a confirmation test. The formation of gas in a brilliant green lactose bile broth fermentation tube at any time within 24 h at 37°C constitutes a positive confirmation test. The results of the MTF technique are expressed in terms of the most probable number (MPN) of microorganisms present in 100 ml samples (MPN/100 ml).

2.5. Statistical evaluation

The statistical analysis was carried out in the statistical packages Origin Pro 8 and SPSS 19. Box plots were obtained from Origin Pro 8 to show each group's data distribution, such as median and interquartile values. Analysis of variance (ANOVA) and Dunnett's T3 pairwise comparison test in SPSS 19 were conducted to determine significant differences between individual treatments and to interpret the orthogonal experiments which were used to determine the significance of factors. A difference with $p \leq 0.05$ was considered statistically significant. The Pearson's correlation analysis in SPSS 19 was used to measure the relationships between every two groups.

3. Results

3.1. TBC and TCC in different soil depths and leaching times

Total bacteria count values in all examined depths fluctuated with time (Figure 1A), and most of them varied within the same order of magnitude (about 10^5 CFU/ml). Similarly, the TCC points also

fluctuated within the same order of magnitude (about 10^3 MPN/100 ml) (Figure 1C). There was no obvious attenuation or increase of TBC and TCC in the period of more than 40 days of experiments. It is suggested that a majority of the bacteria and coliforms may persist and remain in a relatively stable state in the karst soils for an extended period of time. TBC values in different depths had no significant difference, except for TBC values at 10 and 40 cm (Figure 1B). The TBC values in 40 cm were slightly less than the 30 cm values. It has been suggested that the shallow soils in the karst region, with a thickness of less than 40 cm, may not effectively block the migration of bacteria into the groundwater. As for TCC, the values in 10 cm depth were significantly smaller than the values in 20 cm ($p < 0.001$) and 30 cm ($p < 0.001$), while the values in 40 cm depth were significantly ($p < 0.001$) smaller than the values in 30 cm (Figure 1D). This result suggested that the soils may have little impact on preventing coliforms from entering the groundwater.

3.2. The results of the orthogonal experiments

The TBC and TCC values in various conditions according to the orthogonal experiment are shown in Figure 2. The TBC values in the 3, 6, and 9 tests and the TCC values in the 1, 4, and 7 tests were greater than others. Among temperature, pH, and porosity, temperature was found to have consistent values in tests 3, 6, and 9 and also in tests 1, 4, and 7. This suggests that temperature may be the primary factor impacting the bacteria community. The results of ANOVA also corroborated the speculation. The *p*-values of TBC in the test of between-subjects effects for temperature (<0.001) were the lowest relative to pH, and porosity (0.033 and 0.059, respectively). Likewise, for TCC, *p*-values of <0.001, 0.530, and 0.698 were observed for temperature, pH, and porosity, respectively, suggesting that both TBC and TCC were mainly affected by temperature, followed by pH and porosity.

3.3. Temperature effect

Total bacteria count ($r = 0.570$, $p < 0.001$) and TCC ($r = 0.677$, $p < 0.001$) were significantly positively correlated with temperature, indicating that increased temperature would promote the proliferation of bacteria and coliforms. However, the effects of temperature on TBC and TCC were non-linear. For TBC (Figure 3A), there was no significant difference between 10 and 20°C, and the same trend was found between 25 and 30°C. The TBC at 25 and 30°C were significantly greater than at both 10 and 20°C. These results suggested that 20 ~ 25°C was potentially TBC-sensitive temperature, and temperature would not affect the TBC if the temperature varied between 10 and 20°C or between 25 and 30°C. The wide range of TBC concentrations observed at 25°C suggested that this temperature acted as a transitional point for bacteria, with some becoming active and others remaining inactive. While the TCC (Figure 3B) at 10, 20, 25, and 30°C were all significantly different from each other. The average TCC followed the order: 30°C (1,189 MPN/100 ml) > 20°C (354 MPN/100 ml) > 25°C (594 MPN/100 ml) > 10°C (32 MPN/100 ml). The TCC at 20°C and 25°C were in the same order of magnitude. Therefore, the results showed a positive correlation between temperature and TCC values, with higher temperatures resulting in higher TCC. The results suggested that the propagation of coliforms was also temperature dependent.

3.4. pH effect

Despite the noticeable differences in pH levels of the recharged water, the pH values in the outflow water from the soil column at the

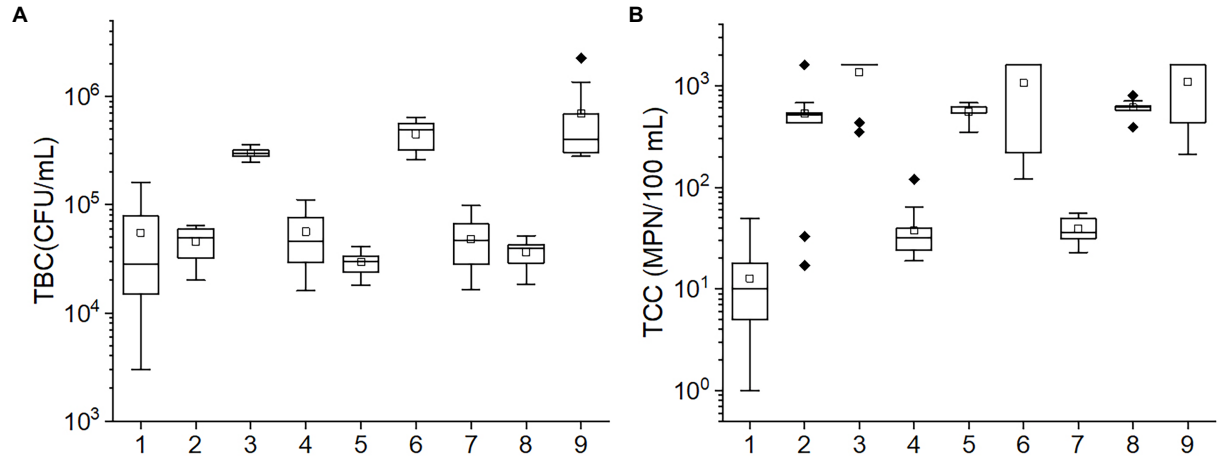

FIGURE 2
The box plots of the **(A)** TBC and **(B)** TCC concentrations in various conditions in the orthogonal experiment. The numbers in the horizontal axis stand for different conditions: 1: 10°C, pH=6, porosity=0.50; 2: 20°C, pH=8, porosity=0.50; 3: 30°C, pH=7, porosity=0.50; 4: 10°C, pH=7, porosity=0.55; 5: 20°C, pH=6, porosity=0.55; 6: 30°C, pH=8, porosity=0.55; 7: 10°C, pH=8, porosity=0.60; 8: 20°C, pH=7, porosity=0.60; 9: 30°C, pH=6, porosity=0.60. The central line and square of each box are the median and mean values, respectively, while the top and bottom of each box represent the third and first quartile, respectively. Whiskers on the box plot represent maximum and minimum values, while rhombuses above or below the box plots show outliers in the data.

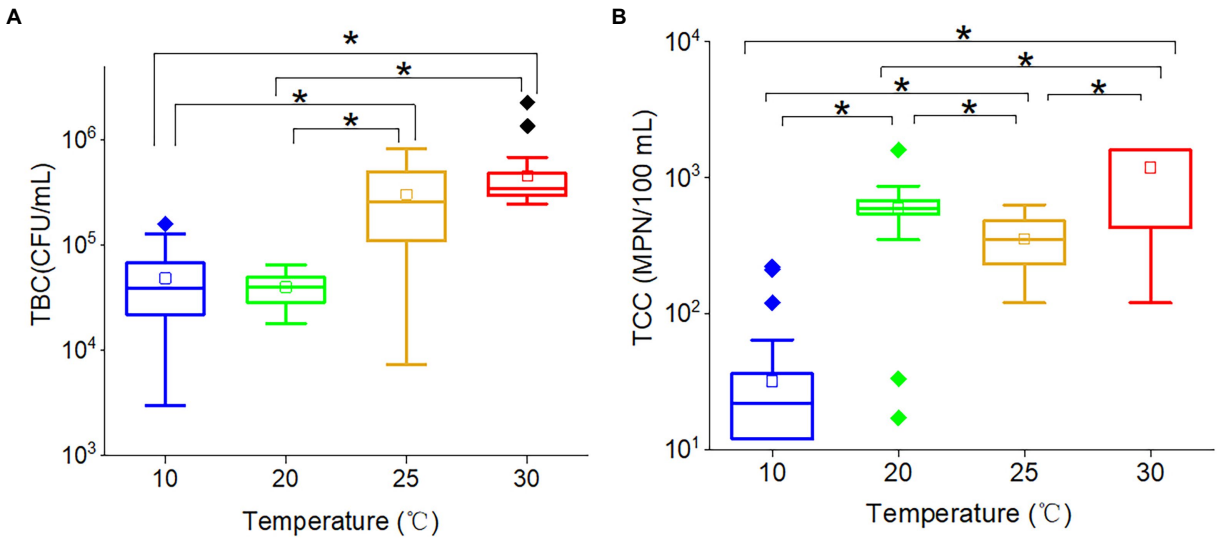

FIGURE 3
The box plots of **(A)** TBC and **(B)** TCC in various temperatures. The star (*) stands for there was a significant difference between the two concentrations (p<0.05). Different colors stand for different temperatures. The central line and square of each box are the median and mean values, respectively, while the top and bottom of each box represent the third and first quartile, respectively. Whiskers on the box plot represent maximum and minimum values, while rhombuses above or below the box plots show outliers in the data.

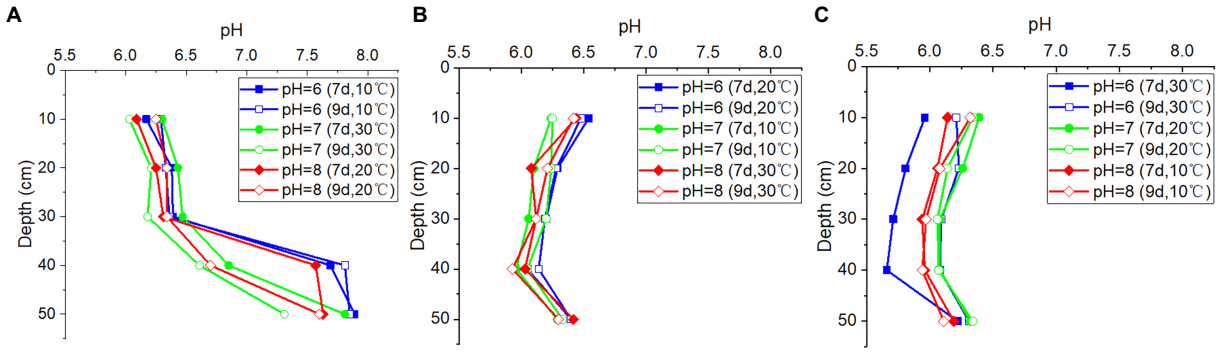

FIGURE 4
The pH values in outflow water from **(A)** column I (porosity=0.5), **(B)** column II (porosity=0.55), and **(C)** column III (porosity=0.60) at different pH values of inlet water, depths, duration time, and temperatures.

same depth remained nearly constant, regardless of temperature variations and the duration of time (Figure 4). This indicated that the variations in precipitation or other recharge would not significantly alter the groundwater pH, suggesting that the soil above the rocks had appreciable buffer capacity. However, the pH values were found to vary with the depths of the soil columns, indicating that the soil characteristics may impact the pH values of outflow water.

As shown from the results, studying the impact of different pH levels on microorganisms can be challenging due to the varying pH recharge. In order to find out the pH effect on TBC and TCC, the outflow water samples were taken into consideration. There was no significate correlation between pH and TBC ($p = 0.566$) or TCC ($p = 0.542$). As demonstrated in Figure 5, plot the TBC and TCC against pH. Most of the points were located at a position of pH less than 6.5, indicating that most of the soils were weakly acidic. The outflow water samples were divided into three groups: low ($pH \leq 6.5$), intermediate ($6.5 < pH < 7.5$) high ($pH \geq 7.5$). In the intermediate pH group, more points were located at the high values of both TBC (greater than 10^5 CFU/ml) and TCC (greater than 10^2 MPN/100 ml). In the low-pH group, for both TBC and TCC, the points were scattered in both high values and low values. In the high-pH group, more points were concentrated in low values for TBC, while more points were concentrated in high values for TCC. Taking the points in each group together for statistical analysis, the TBC values in the middle pH group were significantly greater than in the low-pH group ($p = 0.007$) and high-pH group ($p = 0.002$), while for TCC, there was no significant difference among the three groups.

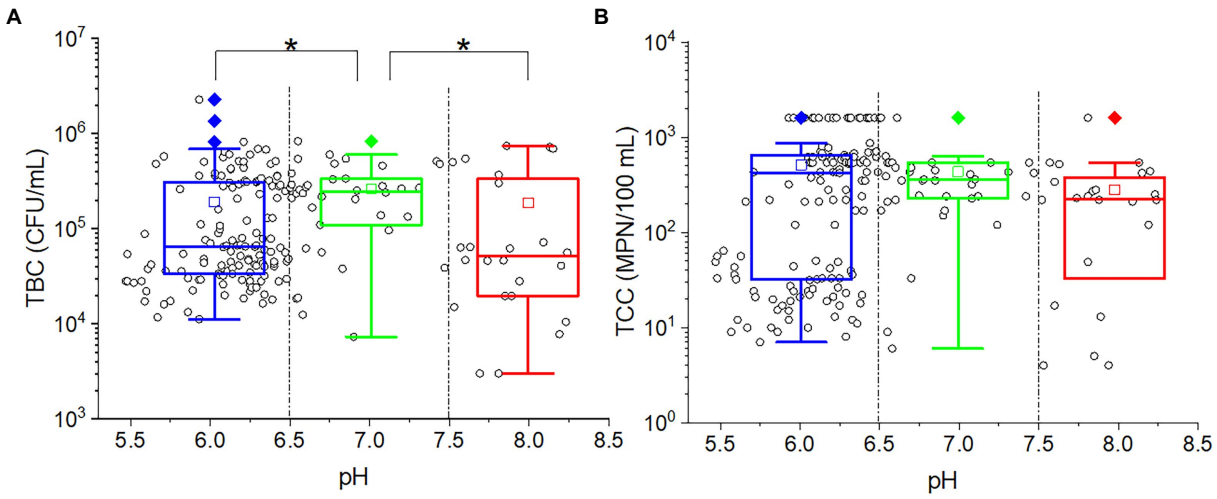

FIGURE 5
The relationship between **(A)** TBC [or **(B)** TCC] and pH. The cycles in the plots represent the measured data of each sample. The star (*) stands for there was a significant difference between the two concentrations ($p<0.05$). Different colors stand for different pH values in the effluent. The central line and square of each box are the median and mean values, respectively, while the top and bottom of each box represent the third and first quartile, respectively. Whiskers on the box plot represent maximum and minimum values, while rhombuses above or below the box plots show outliers in the data.

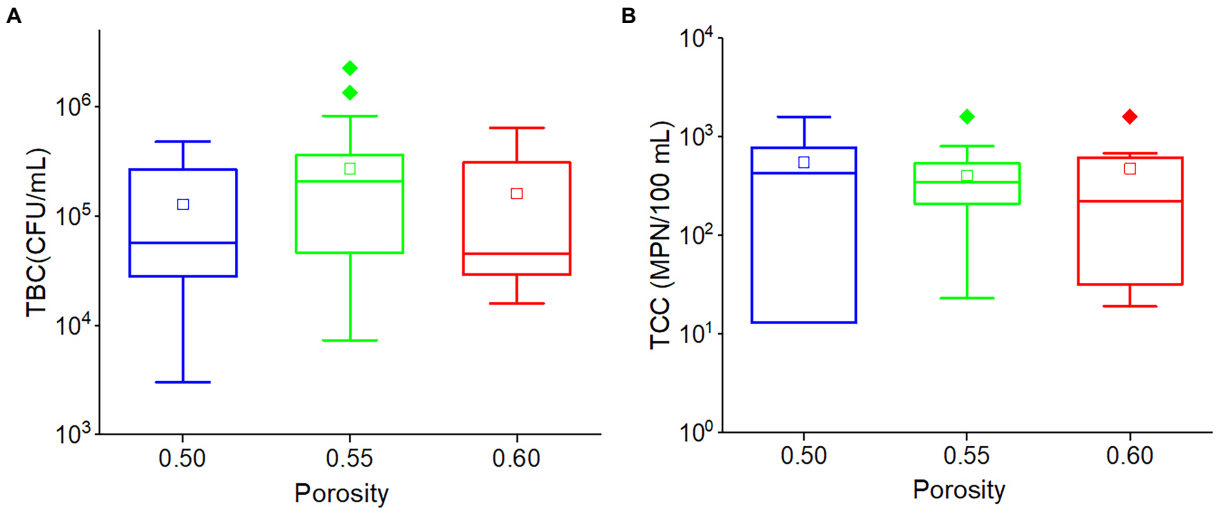

FIGURE 6
The box plots of **(A)** TBC and **(B)** TCC in various porosities. Different colors stand for different porosities. The central line and square of each box are the median and mean values, respectively, while the top and bottom of each box represent the third and first quartile, respectively. Whiskers on the box plot represent maximum and minimum values, while rhombuses above or below the box plots show outliers in the data.

3.5. Porosity effect

There was no significant relationship between porosity and TBC ($r=0.102$, $p=0.148$) or TCC ($r=-0.078$, $p=0.274$). Although the average TBC value in the outflow of 0.55 porosity soil was greater than others, and the average TCC value in the outflow of 0.50 porosity soil was greater than others, there was no significant difference in TBC and TCC values among the three porosities (0.50, 0.55, and 0.60) soils (Figure 6). This indicated that porosity would have a limited impact on TCC and TBC levels in the outflow water in this karst region.

3.6. The relationship between TBC and TCC

The TCC values were significantly positively correlated with TBC ($r=0.365$, $p<0.001$). Among the plots of the relationship between TBC and TCC values, the samples collected at the same temperature were grouped together (Figure 7A). Both the TBC and TCC displayed lower values at 10°C and more at 30°C. At 20°C, only higher TCC was found, and this resulted in higher ratios of TCC to TBC. While at 25°C, the TBC values increased with nearly constant TCC values compared with those at 20°C. For the impact of pH, as shown in

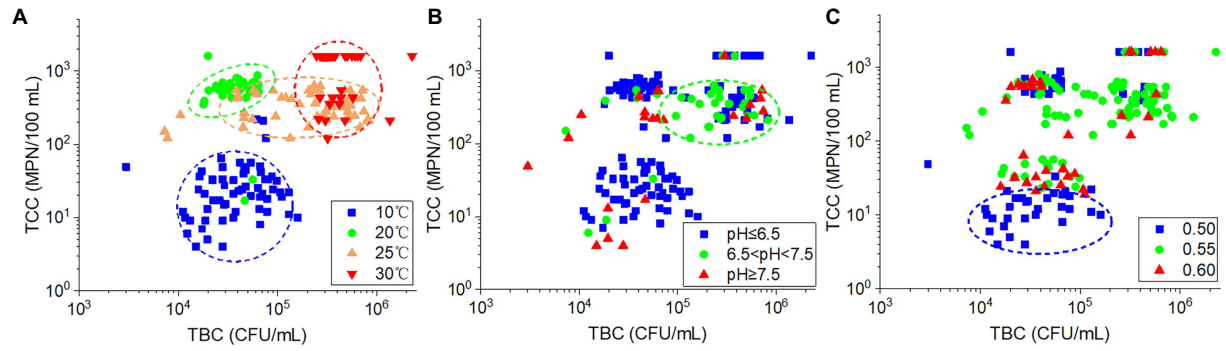

FIGURE 7
The relationship between TCC and TBC according to different **(A)** ambient temperatures, **(B)** effluent pH values, and **(C)** soil porosities.

Figure 7B, the samples with low-pH values (pH ≤ 6.5) and high-pH values (pH ≥ 7.5) were dispersed, whereas the majority of samples with intermediate pH values (6.5 < pH < 7.5) were concentrated in an area of higher TCC and TBC. With regard to porosity (Figure 7C), samples with lower TCC value (in the cycle of the plot) were mostly found in soils with 0.5 porosity. The remaining samples were dispersed throughout the plot, indicating a lack of clear relationship between porosity and TBC or TCC in these samples. As a result, the variation of TBC and TCC in the samples appears to be influenced by temperature, pH, and porosity in a similar but also somewhat diverse manner.

4. Discussion

4.1. The temperature effect on microorganisms

As mentioned in the introduction, the temperature, pH, and porosity are considered to be the critical factors impacting the pathogen in the karst soil. The results of the present study have demonstrated that temperature was the most significant factor. Previous studies have identified two distinct impacts of temperature on soil bacteria, particularly coliforms. The first one is that higher temperatures may increase the soil's hydraulic conductivity, and promote the desorption of bacteria from soil particles, and resulted in increased concentrations of bacteria in groundwater (Acea et al., 1988; Gharabaghi et al., 2015). The other one is that high temperatures create unfavorable conditions for the bacteria, leading to a rapid decline in their numbers, which is the common trend (Blaustein et al., 2013; Chandrasena et al., 2014).

Our results evinced that both the TBC and TCC increased due to the elevated temperatures, which supported the first possibility. However, previous studies have found that the effect of temperature on adsorption and hydraulic conductivity is not as pronounced (Acea et al., 1988). It should be noted that soil is not only an aggregation consisting predominantly of particulate matter, but also a growth medium (Aleklett et al., 2018).Therefore, the higher TBC and TCC values observed at relatively higher temperatures could be mainly attributed to an increase in bacterial populations in the soil. In the column soils, there was enough organic matter (represented by COD_{Mn}, see Supplementary Figure S1), which can meet the demand for carbon and energy sources for bacteria (Wen et al., 2022). Most the coliforms are always deemed as the prevalent commensal inhabitants of the gastrointestinal tracts of humans and warm-blooded animals (Allocati et al., 2013); however, there was no such animal in the soil. Previous studies revealed that the multiplying of some coliforms in the soil may be caused by the soil protozoan, such as *Acanthamoeba polyphaga*, in which the coliforms and other pathogens survive and replicate (Barker et al., 1999). The elevated temperature stimulated the growth of bacteria (Kirchman et al., 2005), as well as protozoan (Müller and Geller, 1993), and may also indirectly stimulate the presence of coliforms.

It is generally acknowledged that 37°C is the optimum temperature for coliforms and some bacteria, and therefore, in most cases, the TBC and TCC increased with the elevating temperature in the laboratory medium (Jones et al., 1987; Raghubeer and Matches, 1990). However, it was not the case in the present study. Accordingly, the TBC and TCC increased with elevated temperature asynchronously. The TBC concentrations almost reached a maximum at 25°C, whereas the TCC peaked at 20°C. The phenomena may be caused by the protozoa in the soils. The optimum temperature for most protozoa is 18 ~ 25°C (Littleford, 1960). We speculated that at 20°C, the protozoa thrived, while the bacteria including coliforms were being preyed by the thriving protozoa (Bott and Kaplan, 1990). Most bacteria and some coliforms are digested as a food source, while most coliforms are able to resist lysosomal attack and therefore multiplied within membrane-bound vacuoles (Barker et al., 1999; Van Elsas et al., 2011; George et al., 2020; Mungroo et al., 2021). Previous studies have noted that protozoa, such as *Acanthamoeba,* can inhibit bacterial growth through the release of free radicals in their lysates (Connor et al., 1993), but have no inhibitory effect on certain coliforms, such as *E. coli*. On the contrary, those protozoa are an abundant source of amino acids, enzymes, fatty acids, and lipids and clearly provided coliforms with nutrients for growth (Van Elsas et al., 2011; Geisen et al., 2018; Gambushe et al., 2022). Therefore, the thriving of protozoa would lead to an increase in the number of coliforms and a decrease in other bacteria that are susceptible to predation by protozoa in the soil environment (Matin and Jung, 2011; Iqbal et al., 2014). This is consistent with our findings of lower TBC and higher TCC values at 20°C. Another possible reason is that some environmentally adapted coliforms may thrive at ambient temperatures (about 20°C) other than other temperatures.

4.2. The pH and porosity effects on microorganisms

Several studies illustrate that higher pH values produced longer survival time for coliforms in acidic soil, especially in south China (Jiang et al., 2002; Wang et al., 2014; Xing et al., 2019), while pH may negatively affect the persistence of the strains in soils with pH greater than 7 (Ma et al., 2012). Therefore, a neutral pH is desirable for most bacteria and protozoa (Rousk et al., 2010). In the present study, the intermediate pH groups ($6.5 < pH < 7.5$) had relatively high TBC and TCC, which exemplified the theory. Additionally, pH may affect the desorption of attached bacteria in the soil. Several studies found that bacterial retention in the columns was greatest in acidic soil and decreased with increasing pH (Scholl et al., 1990; Scholl and Harvey, 1992). However, the dissolved organic matter has been shown to alter the surface charge on suspended particulate matter, and therefore change the behavior of sorption (Scholl and Harvey, 1992). The wide range of dissolved organic matter (represented by COD_{Mn}, see Supplementary Figure S1) in the column water might account for the wide range of values observed for both TBC and TCC. Combined with other factors, such as temperature, the pH effect was obscured in low-pH and high-pH groups' samples.

The porosity variation altered the permeability of the soil. Generally, for the same texture soil, the more porosity, the greater the permeability coefficient. Under the same hydraulic gradient, the groundwater flow velocity in the greater porosity soil would be greater, and therefore, the water infiltrated through the greater porosity soil would have a higher concentration of bacteria (Smith et al., 1985; Huysman and Verstraete, 1993; Sepehrnia et al., 2019; Liu et al., 2020). In the present study, the lower TCC value samples were almost collected in the 0.5 porosity soils at 10°C, indicating that the soils with less porosity would retard the migration of coliforms, which could be observed at low temperature, while at high temperature, the retardation effect might be obscured by temperature effect. Therefore, there was no significant difference in TBC and TCC among different porosity soils.

Therefore, the pH and porosity might have affected the behavior of bacteria including coliforms in the karst soils, but the affected variations of TBC and TCC might be covered by the temperature effect.

4.3. The origination of the microorganisms in the groundwater

Previous studies on microorganism migration in aquifers have primarily centered that the microorganisms come from the soil surface and thus, when conducting related studies, these bacteria or similar organisms are added to the soil. Typically, the added microorganisms were retarded by the adsorption of soil and resulted in fewer microorganisms in outflow of groundwater (Castro and Tufenkji, 2007; Passmore et al., 2010; Wen et al., 2016; Bandy et al., 2018). However, in the present study, the outflow of groundwater infiltrated from the soil column contained higher level of TBC and TCC than the inlet water, indicating that the collected soil in the karst area may be a source of bacteria in the groundwater.

The TBC and TCC values in the outflow remained relatively unchanged for over 40 days, demonstrating that the bacteria, including the coliforms, remained active throughout that time in the soil. This is in contrast to prior studies, where coliform counts were observed to decrease significantly within a few days in various soils (Fremaux et al., 2008). Previous studies revealed that most bacteria concentrations would decline in several days if the soil condition was not suitable (Acea et al., 1988). However, in the present study, there was no introduction of foreign organisms and the environmental conditions remained relatively constant, providing a suitable environment for the survival of the studied bacteria.

Through the discussion about the temperature effect, only the survival of the bacteria cannot fully explain the phenomena of the study, the multiplied bacteria may be the main contributor of TBC and TCC in the outflow water. The TBC or TCC values in different depths were mostly in the same order of magnitude, indicating that the bacteria migration with groundwater flow played negligible roles for bacterial concentrations. Instead, the bacteria in the outflow water may stem from the thin-layer soils near the outlet.

Therefore, the soil in the study area may serve as both reservoirs and incubators for pathogenic bacteria. These bacteria can easily spread into the underground water, becoming a significant contributor to the contamination of groundwater pathogens.

4.4. Implication

The thin soil in the karst cannot effectively block coliforms and other pathogens from infiltrating groundwater through the seepage of rainfall. Instead, the soils served as both reservoirs and incubators for pathogenic bacteria. Accordingly, to reduce the pathogens concentrations in the infiltrated water, several approaches can be carried out, including slowing down the migration of pathogens, reducing the input of pathogens, and changing the environmental condition to inhibit the growth and multiplying of pathogens. In the soils, as discussed above, the migration velocity was not the primary factor for introducing bacteria to the groundwater, and therefore changing the structure of the soil, such as compressing or loosening the soil, would not reduce the TBC and TCC values. Whereas the multiplying of pathogens played a crucial role in controlling the TBC and TCC. Therefore, creating an uninviting and inhospitable environment for pathogens' growth would be beneficial. For example, by acidizing or alkalizing the soil, or reducing the amount of organic matter input when planting crops.

Our results suggested that elevated temperature may help for breeding more pathogens. Therefore, in similar areas, it is vital to pay closer attention to the pathogens in areas with similar climate during hot weather, especially in the summer days.

5. Conclusion

In the study, the orthogonality column experiments were used to investigate how environmental factors, including ambient temperature, pH values of inlet water, and soil porosities, affect the microbiological indices in the leachate of agricultural soils from karst areas of Yunnan province, China. Results revealed that ambient temperature was the most crucial factor that affected the effluent bacteria, with higher temperature leading to the greater values of TBC and TCC. Although the neutral pH appeared to be suitable for the survival of bacteria, and the lower porosity may block the coliforms

into the effluent, they did not significantly impact the bacteria. There was no obvious decay of TBC and TCC in the effluent for more than 40 days, indicating the bacteria including the coliforms remained active in the soils. As temperature increased, the TBC and TCC also increased, suggesting that agricultural soils in the study area likely served as both reservoirs and incubators for bacteria including coliforms, which may readily migrate into the groundwater and become an important source of groundwater pathogen contamination. The behavior of the bacteria in the soil with water seepage is intricate, and tightly related to the soil characteristics, hydrogeology condition, as well as other factors. In the present study, we suspected that temperature was the key factor for pathogens microorganisms, and protozoa might play a role in multiplying some pathogens. To validate the speculation, future studies, such as batch experiments, microscopic imaging, as well as metagenomic analysis, should be carried out.

Data availability statement

The raw data supporting the conclusions of this article will be made available by the authors, without undue reservation.

Author contributions

SW and MZ contributed to the conception and design of the study. SW carried out the experiments. ZN and CG performed the statistical analysis and wrote the first draft of the manuscript. All authors contributed to the manuscript revision, read, and approved the submitted version.

Funding

This research was supported by Hebei Natural Science Foundation, D2022504009.

Conflict of interest

The authors declare that the research was conducted in the absence of any commercial or financial relationships that could be construed as a potential conflict of interest.

The handling editor QL declared a shared affiliation with the authors at the time of review.

Publisher's note

All claims expressed in this article are solely those of the authors and do not necessarily represent those of their affiliated organizations, or those of the publisher, the editors and the reviewers. Any product that may be evaluated in this article, or claim that may be made by its manufacturer, is not guaranteed or endorsed by the publisher.

Supplementary material

The Supplementary material for this article can be found online at: https://www.frontiersin.org/articles/10.3389/fmicb.2023.1143900/full#supplementary-material

References

Aaron, L.M. (2018) *Movement of bacteria in the subsurface*. In The Microbiology of the Terrestrial Deep Subsurface Boca Raton: CRC Press, 225–244.

Acea, M. J., Moore, C. R., and Alexander, M. (1988). Survival and growth of bacteria introduced into soil. *Soil Biol. Biochem.* 20, 509–515. doi: 10.1016/0038-0717(88)90066-1

Aleklett, K., Kiers, E. T., Ohlsson, P., Shimizu, T. S., Caldas, V. E., and Hammer, E. C. (2018). Build your own soil: exploring microfluidics to create microbial habitat structures. *ISME J* 12, 312–319. doi: 10.1038/ismej.2017.184

Allocati, N., Masulli, M., Alexeyev, M. F., and Di Ilio, C. (2013). *Escherichia coli* in Europe: an overview. *Int. J. Environ. Res. Public Health* 10, 6235–6254. doi: 10.3390/ijerph10126235

Bandy, A., Cook, K., Fryar, A. E., and Polk, J. (2018). Use of molecular markers to compare *Escherichia coli* transport with traditional groundwater tracers in epikarst. *J. Environ. Qual.* 47, 88–95. doi: 10.2134/jeq2017.10.0406

Bandy, A. M., Cook, K., Fryar, A. E., and Zhu, J. (2020). Differential transport of *Escherichia coli* isolates compared to abiotic tracers in a karst aquifer. *Groundwater* 58, 70–78. doi: 10.1111/gwat.12889

Barker, J., Humphrey, T. J., and Brown, M. W. R. (1999). Survival of *Escherichia coli* 0157 in a soil protozoan: implications for disease. *FEMS Microbiol. Lett.* 173, 291–295. doi: 10.1111/j.1574-6968.1999.tb13516.x

Bitton, G., Farrah, S. R., Ruskin, R. H., Butner, J., and Chou, Y. J. (1983). Survival of pathogenic and indicator organisms in ground water. *Groundwater* 21, 405–410. doi: 10.1111/j.1745-6584.1983.tb00741.x

Bitton, G., and Harvey, R. W. (1992). Transport of pathogens through soils and aquifers. *Environ. Microbiol.* 19, 103–123.

Blaustein, R. A., Pachepsky, Y., Hill, R. L., Shelton, D. R., and Whelan, G. (2013). Escherichia coli survival in waters: temperature dependence. *Water Res.* 47, 569–578. doi: 10.1016/j.watres.2012.10.027

Bott, T. L., and Kaplan, L. A. (1990). Potential for protozoan grazing of bacteria in streambed sediments. *J. N. Am. Benthol. Soc.* 9, 336–345. doi: 10.2307/1467901

Brad, T., Bizic, M., Ionescu, D., Chiriac, C. M., Kenesz, M., Roba, C., et al. (2022). Potential for natural attenuation of domestic and agricultural pollution in karst groundwater environments. *Water* 14:1597. doi: 10.3390/w14101597

Buckerfield, S. J., Waldron, S., Quilliam, R. S., Naylor, L. A., Li, S., and Oliver, D. M. (2019). How can we improve understanding of faecal indicator dynamics in karst systems under changing climatic, population, and land use stressors? – research opportunities in SW China. *Sci. Total Environ.* 646, 438–447. doi: 10.1016/j.scitotenv.2018.07.292

Cao, J. H., Yuan, D. X., and Pan, G. X. (2003). Some soil features in karst ecosystem. *Adv. Earth Sci.* 18, 37–44. doi: 10.11867/j.issn.1001-8166.2003.01.0037

Castro, F. D., and Tufenkji, N. (2007). Relevance of nontoxigenic strains as surrogates for *Escherichia coli* O157:H7 in groundwater contamination potential: role of temperature and cell acclimation time. *Environ. Sci. Technol.* 41, 4332–4338. doi: 10.1021/es0701558

Chandrasekar, A., Binder, M., Liedl, R., and Berendonk, T. U. (2021). Reactive-transport modelling of Enterococcus faecalis JH2-2 passage through water saturated sediment columns. *J. Hazard. Mater.* 413:125292. doi: 10.1016/j.jhazmat.2021.125292

Chandrasena, G. I., Deletic, A., and McCarthy, D. T. (2014). Survival of *Escherichia coli* in stormwater biofilters. *Environ. Sci. Pollut. Res.* 21, 5391–5401. doi: 10.1007/s11356-013-2430-2

Chen, R., and Bi, K. (2011). Correlation of karst agricultural geo-environment with non-karst agricultural geo-environment with respect to nutritive elements in Guizhou. *Chin. J. Geochem.* 30, 563–568. doi: 10.1007/s11631-011-0540-4

China NHCOTPSRO (2006). "Standard examination methods for drinking water" in *Microbiological Indices*. State Administration for Market Regulation of China & Standardization Administration of China (Beijing: Standards Press of China).

Chique, C., Hynds, P., Burke, L., Morris, D., Ryan, M. P., and O'Dwyer, J. (2021). Contamination of domestic groundwater systems by verotoxigenic Escherichia coli (VTEC), 2003–2019: a global scoping review. *Water Res.* 188:116496. doi: 10.1016/j.watres.2020.116496

Connor, R., Hay, J., Mead, A., and Seal, D. (1993). Reversal of inhibitory effects of *Acanthamoeba castellanii* lysate for *Legionella pneumophila* using catalase. *J. Microbiol. Methods* 18, 311–316. doi: 10.1016/0167-7012(93)90012-7

Dwivedi, D., Mohanty, B. P., and Lesikar, B. J. (2016). Impact of the linked surface water-soil water-groundwater system on transport of *E. coli* in the subsurface. *Water Air Soil Pollut.* 227, 1–16. doi: 10.1007/s11270-016-3053-2

Edmonds, R. L. (1976). Survival of coliform bacteria in sewage sludge applied to a forest clearcut and potential movement into groundwater. *Appl. Environ. Microbiol.* 32, 537–546. doi: 10.1128/aem.32.4.537-546.1976

Eisfeld, C., Schijven, J. F., van der Wolf, J. M., Medema, G., Kruisdijk, E., and van Breukelen, B. M. (2022). Removal of bacterial plant pathogens in columns filled with quartz and natural sediments under anoxic and oxygenated conditions. *Water Res.* 220:118724. doi: 10.1016/j.watres.2022.118724

England, L. S., Lee, H., and Trevors, J. T. (1993). Bacterial survival in soil: effect of clays and protozoa. *Soil Biol. Biochem.* 25, 525–531. doi: 10.1016/0038-0717(93)90189-I

Federation, W.E., and Association, A. (2005) *Standard Methods for the Examination of Water and Wastewater*. American Public Health Association (APHA) Washington, DC.

Franz, E., Semenov, A. V., Termorshuizen, A. J., De Vos, O. J., Bokhorst, J. G., and Van Bruggen, A. H. C. (2008). Manure-amended soil characteristics affecting the survival of E. coli O157:H7 in 36 Dutch soils. *Environ. Microbiol.* 10, 313–327. doi: 10.1111/j.1462-2920.2007.01453.x

Fremaux, B., Prigent-Combaret, C., Delignette-Muller, M. L., Mallen, B., Dothal, M., Gleizal, A., et al. (2008). Persistence of Shiga toxin-producing *Escherichia coli* O26 in various manure-amended soil types. *J. Appl. Microbiol.* 104, 296–304. doi: 10.1111/j.1365-2672.2007.03532.x

Gambushe, S. M., Zishiri, O. T., and El Zowalaty, M. E. (2022). Review of *Escherichia coli* O157: H7 prevalence, pathogenicity, heavy metal and antimicrobial resistance, African perspective. *Infect. Drug Resist.* 15, 4645–4673. doi: 10.2147/IDR.S365269

Geisen, S., Mitchell, E. A., Adl, S., Bonkowski, M., Dunthorn, M., Ekelund, F., et al. (2018). Soil protists: a fertile frontier in soil biology research. *FEMS Microbiol. Rev.* 42, 293–323. doi: 10.1093/femsre/fuy006

George, A. S., Rehfuss, M. Y. M., Parker, C. T., and Brandl, M. T. (2020). The transcriptome of *Escherichia coli* O157: H7 reveals a role for oxidative stress resistance in its survival from predation by Tetrahymena. *FEMS Microbiol. Ecol.* 96:fiaa014. doi: 10.1093/femsec/fiaa014

Gharabaghi, B., Safadoust, A., Mahboubi, A. A., Mosaddeghi, M. R., Unc, A., Ahrens, B., et al. (2015). Temperature effect on the transport of bromide and *E. coli* NAR in saturated soils. *J. Hydrol.* 522, 418–427. doi: 10.1016/j.jhydrol.2015.01.003

Ginn, T. R., Camesano, T., Scheibe, T. D., Nelson, K. E., Clement, T. P., and Wood, B. D. (2006). "105. Microbial Transport in the Subsurface: Ecological and Hydrological Interactions" in *Encyclopedia of Hydrological Sciences*.

Ginn, T. R., Wood, B. D., Nelson, K. E., Scheibe, T. D., Murphy, E. M., and Clement, T. P. (2002). Processes in microbial transport in the natural subsurface. *Adv. Water Resour.* 25, 1017–1042. doi: 10.1016/S0309-1708(02)00046-5

Grisey, E., Belle, E., Dat, J., Mudry, J., and Aleya, L. (2010). Survival of pathogenic and indicator organisms in groundwater and landfill leachate through coupling bacterial enumeration with tracer tests. *Desalination* 261, 162–168. doi: 10.1016/j.desal.2010.05.007

Heinz, B., Birk, S., Liedl, R., Geyer, T., Straub, K., Andresen, J., et al. (2009). Water quality deterioration at a karst spring (Gallusquelle, Germany) due to combined sewer overflow: evidence of bacterial and micro-pollutant contamination. *Environ. Geol.* 57, 797–808. doi: 10.1007/s00254-008-1359-0

Huysman, F., and Verstraete, W. (1993). Water-facilitated transport of bacteria in unsaturated soil columns: influence of cell surface hydrophobicity and soil properties. *Soil Biol. Biochem.* 25, 83–90. doi: 10.1016/0038-0717(93)90245-7

Iqbal, J., Siddiqui, R., and Khan, N. A. (2014). Acanthamoeba and bacteria produce antimicrobials to target their counterpart. *Parasit. Vectors* 7, 1–6. doi: 10.1186/1756-3305-7-56

Jiang, X., Morgan, J., and Doyle, M. P. (2002). Fate of *Escherichia coli* O157: H7 in manure-amended soil. *Appl. Environ. Microbiol.* 68, 2605–2609. doi: 10.1128/AEM.68.5.2605-2609.2002

John, D. E., and Rose, J. B. (2005). Review of factors affecting microbial survival in groundwater. *Environ. Sci. Technol.* 39, 7345–7356. doi: 10.1021/es047995w

Jones, P. G., VanBogelen, R. A., and Neidhardt, F. C. (1987). Induction of proteins in response to low temperature in *Escherichia coli*. *J. Bacteriol.* 169, 2092–2095. doi: 10.1128/jb.169.5.2092-2095.1987

King, C. H., Shotts, E. B. Jr., Wooley, R. E., and Porter, K. G. (1988). Survival of coliforms and bacterial pathogens within protozoa during chlorination. *Appl. Environ. Microbiol.* 54, 3023–3033. doi: 10.1128/aem.54.12.3023-3033.1988

Kirchman, D. L., Malmstrom, R. R., and Cottrell, M. T. (2005). Control of bacterial growth by temperature and organic matter in the Western Arctic. *Deep-Sea Res. II Top. Stud. Oceanogr.* 52, 3386–3395. doi: 10.1016/j.dsr2.2005.09.005

Lambrecht, E., Baré, J., Chavatte, N., Bert, W., Sabbe, K., and Houf, K. (2015). Protozoan cysts act as a survival niche and protective shelter for foodborne pathogenic bacteria. *Appl. Environ. Microbiol.* 81, 5604–5612. doi: 10.1128/AEM.01031-15

Li, J., Chen, Q., Li, H., Li, S., Liu, Y., Yang, L., et al. (2020). Impacts of different sources of animal manures on dissemination of human pathogenic bacteria in agricultural soils. *Environ. Pollut.* 266:115399. doi: 10.1016/j.envpol.2020.115399

Li, Y.-B., Wang, S.-J., and Wang, J. (2006). Soil properties in karst ecosystem and further study. *Carsol. Sin.* 25, 285–289.

Littleford, R. A. (1960). Culture of protozoa in the classroom. *Am. Biol. Teach.* 22, 551–559. doi: 10.2307/4439448

Liu, G., Fang, Z., Zhong, H., Shi, L., Yang, X., and Liu, Z. (2020). Transport of *Pseudomonas aeruginosa* in porous media mediated by low-concentration surfactants: the critical role of surfactant to change cell surface hydrophobicity. *Water Resour. Res.* 56:e2019WR026103. doi: 10.1029/2019WR026103

Liu, J., Ford, R. M., and Smith, J. A. (2011). Idling time of motile bacteria contributes to retardation and dispersion in sand porous medium. *Environ. Sci. Technol.* 45, 3945–3951. doi: 10.1021/es104041t

Luffman, I., and Tran, L. (2014). Risk factors for *E. coli* O157 and cryptosporidiosis infection in individuals in the karst valleys of East Tennessee, USA. *Geosciences* 4, 202–218. doi: 10.3390/geosciences4030202

Ma, J., Ibekwe, A. M., Crowley, D. E., and Yang, C.-H. (2012). Persistence of *Escherichia coli* O157:H7 in major leafy green producing soils. *Environ. Sci. Technol.* 46, 12154–12161. doi: 10.1021/es302738z

Matin, A., and Jung, S.-Y. (2011). Interaction of *Escherichia coli* K1 and K5 with *Acanthamoeba castellanii* trophozoites and cysts. *Korean J. Parasitol.* 49, 349–356. doi: 10.3347/kjp.2011.49.4.349

Matz, C., and Kjelleberg, S. (2005). Off the hook – how bacteria survive protozoan grazing. *Trends Microbiol.* 13, 302–307. doi: 10.1016/j.tim.2005.05.009

McCaulou, D. R., Bales, R. C., and Arnold, R. G. (1995). Effect of temperature-controlled motility on transport of bacteria and microspheres through saturated sediment. *Water Resour. Res.* 31, 271–280. doi: 10.1029/94WR02569

McCaulou, D. R., Bales, R. C., and McCarthy, J. F. (1994). Use of short-pulse experiments to study bacteria transport through porous media. *J. Contam. Hydrol.* 15, 1–14. doi: 10.1016/0169-7722(94)90007-8

Müller, H., and Geller, W. (1993). Maximum growth rates of aquatic ciliated protozoa: the dependence on body size and temperature reconsidered. *Archiv. Hydrobiol.* 126, 315–327. doi: 10.1127/archiv-hydrobiol/126/1993/315

Mungroo, M. R., Siddiqui, R., and Khan, N. A. (2021). War of the microbial world: *Acanthamoeba* spp. interactions with microorganisms. *Folia Microbiol.* 66, 689–699. doi: 10.1007/s12223-021-00889-7

Oliver, D. M., Zheng, Y., Naylor, L. A., Murtagh, M., Waldron, S., and Peng, T. (2020). How does smallholder farming practice and environmental awareness vary across village communities in the karst terrain of Southwest China? Agriculture. *Ecosyst. Environ.* 288:106715. doi: 10.1016/j.agee.2019.106715

Pang, H., Mokhtari, A., Chen, Y., Oryang, D., Ingram, D. T., Sharma, M., et al. (2020). A predictive model for survival of *Escherichia coli* O157: H7 and generic *E. coli* in soil amended with untreated animal manure. *Risk Anal.* 40, 1367–1382. doi: 10.1111/risa.13491

Passmore, J. M., Rudolph, D. L., Mesquita, M. M., Cey, E. E., and Emelko, M. B. (2010). The utility of microspheres as surrogates for the transport of *E. coli* RS2g in partially saturated agricultural soil. *Water Res.* 44, 1235–1245. doi: 10.1016/j.watres.2009.10.010

Personné, J., Poty, F., Vaute, L., and Drogue, C. (1998). Survival, transport and dissemination of *Escherichia coli* and enterococci in a fissured environment. Study of a flood in a karstic aquifer. *J. Appl. Microbiol.* 84, 431–438. doi: 10.1046/j.1365-2672.1998.00366.x

Pronk, M. (2008). *Origin and Behaviour of Microorganisms and Particles in Selected Karst Aquifer Systems*. Canberra: Université de Neuchâtel.

Pronk, M., Goldscheider, N., and Zopfi, J. (2006). Dynamics and interaction of organic carbon, turbidity and bacteria in a karst aquifer system. *Hydrogeol. J.* 14, 473–484. doi: 10.1007/s10040-005-0454-5

Raghubeer, E. V., and Matches, J. R. (1990). Temperature range for growth of Escherichia coli serotype O157: H7 and selected coliforms in *E. coli* medium. *J. Clin. Microbiol.* 28, 803–805. doi: 10.1128/jcm.28.4.803-805.1990

Rousk, J., Bååth, E., Brookes, P. C., Lauber, C. L., Lozupone, C., Caporaso, J. G., et al. (2010). Soil bacterial and fungal communities across a pH gradient in an arable soil. *ISME J.* 4, 1340–1351. doi: 10.1038/ismej.2010.58

Schäfer, A., Ustohal, P., Harms, H., Stauffer, F., Dracos, T., and Zehnder, A. J. B. (1998). Transport of bacteria in unsaturated porous media. *J. Contam. Hydrol.* 33, 149–169. doi: 10.1016/S0169-7722(98)00069-2

Scholl, M. A., and Harvey, R. W. (1992). Laboratory investigations on the role of sediment surface and groundwater chemistry in transport of bacteria through a contaminated sandy aquifer. *Environ. Sci. Technol.* 26, 1410–1417. doi: 10.1021/es00031a020

Scholl, M. A., Mills, A. L., Herman, J. S., and Hornberger, G. M. (1990). The influence of mineralogy and solution chemistry on the attachment of bacteria to representative aquifer materials. *J. Contam. Hydrol.* 6, 321–336. doi: 10.1016/0169-7722(90)90032-C

Sen, T. K. (2011). Processes in pathogenic biocolloidal contaminants transport in saturated and unsaturated porous media: a review. *Water Air Soil Pollut.* 216, 239–256. doi: 10.1007/s11270-010-0531-9

Sepehrnia, N., Bachmann, J., Hajabbasi, M. A., Rezanezhad, F., Lichner, L., Hallett, P. D., et al. (2019). Transport, retention, and release of Escherichia coli and

Rhodococcus erythropolis through dry natural soils as affected by water repellency. *Sci. Total Environ.* 694:133666. doi: 10.1016/j.scitotenv.2019.133666

Sharma, M., and Reynnells, R. (2018). Importance of soil amendments: survival of bacterial pathogens in manure and compost used as organic fertilizers. *Preharvest Food Safety*, 159–175. doi: 10.1128/9781555819644.ch9

Smith, M., Thomas, G., White, R., and Ritonga, D. (1985). Transport of Escherichia coli through intact and disturbed soil columns. *J. Environ. Qual* 14, 87–91. doi: 10.2134/jeq1985.00472425001400010017x

Song, A., Liang, Y.-M., and Li, Q. (2018). Influence of precipitation on bacterial structure in a typical karst spring, SW China. *J. Groundw. Sci. Eng.* 5, 193–204. doi: 10.19637/j.cnki.2305-7068.2018.03.005

Tan, Y., Gannon, J., Baveye, P., and Alexander, M. (1994). Transport of bacteria in an aquifer sand: experiments and model simulations. *Water Resour. Res.* 30, 3243–3252. doi: 10.1029/94WR02032

Van Elsas, J. D., Semenov, A. V., Costa, R., and Trevors, J. T. (2011). Survival of Escherichia coli in the environment: fundamental and public health aspects. *ISME J.* 5, 173–183. doi: 10.1038/ismej.2010.80

Wang, S. (2019) *Microbial-Toxicological Combined Response Mechanism and Simulation of Groundwater Polluted by Farming in Desertification Areas*. Beijing: Chinese Academy of Geological Sciences.

Wang, H. Z., Wei, G., Yao, Z. Y., Lou, J., Xiao, K. C., Wu, L. S., et al. (2014). Response of Escherichia coli O157:H7 survival to pH of cultivated soils. *J. Soils Sediments* 14, 1841–1849. doi: 10.1007/s11368-014-0944-y

Ward, J. W., Warden, J. G., Bandy, A. M., Fryar, A. E., Brion, G. M., Macko, S. A., et al. (2016). Use of nitrogen-15-enriched *Escherichia coli* as a bacterial tracer in karst aquifers. *Groundwater* 54, 830–839. doi: 10.1111/gwat.12426

Wen, J., Li, J.-S., and Li, Y.-F. (2016). Wetting patterns and bacterial distributions in different soils from a surface point source applying effluents with varying *Escherichia coli* concentrations. *J. Integr. Agric.* 15, 1625–1637. doi: 10.1016/S2095-3119(15)61249-7

Wen, L., Li, D., Xiao, X., and Tang, H. (2022). Alterations in soil microbial phospholipid fatty acid profile with soil depth following cropland conversion in karst region, Southwest China. *Environ. Sci. Pollut. Res.* 30, 1502–1519. doi: 10.1007/s11356-022-22178-7

Xia, R. (2016). Groundwater resources in karst area in southern China and sustainable utilization pattern. *J. Groundw. Sci. Eng.* 4, 301–309.

Xing, J., Wang, H., Brookes, P. C., Salles, J. F., and Xu, J. (2019). Soil pH and microbial diversity constrain the survival of *E. coli* in soil. *Soil Biol. Biochem.* 128, 139–149. doi: 10.1016/j.soilbio.2018.10.013

frontiers | Frontiers in Microbiology

TYPE Original Research
PUBLISHED 23 March 2023
DOI 10.3389/fmicb.2023.1133938

OPEN ACCESS

EDITED BY
Zhenjiang Jin,
Guilin University of Technology,
China

REVIEWED BY
Zongqiang Zhu,
Guilin University of Technology,
China
Hailong Sun,
Institute of Geochemistry (CAS),
China

*CORRESPONDENCE
Fei Liu
✉ feiliu@cugb.edu.cn

SPECIALTY SECTION
This article was submitted to Terrestrial Microbiology, a section of the journal Frontiers in Microbiology

RECEIVED 29 December 2022
ACCEPTED 03 March 2023
PUBLISHED 23 March 2023

CITATION
Guan X, He R, Zhang B, Gao C and Liu F (2023) Seasonal variations of microbial community structure, assembly processes, and influencing factors in karst river.
Front. Microbiol. 14:1133938.
doi: 10.3389/fmicb.2023.1133938

Seasonal variations of microbial community structure, assembly processes, and influencing factors in karst river

Xiangyu Guan[1], Ruoxue He[1,2], Biao Zhang[1], Chengjie Gao[3] and Fei Liu[4]*

[1]School of Ocean Sciences, China University of Geosciences, Beijing, China, [2]Department of Discipline Construction and Technology Development, Chengdu Technological University, Chengdu, China, [3]Beijing Municipal Research Institute of Eco-Environmental Protection, Beijing, China, [4]Key Laboratory of Groundwater Conservation of MWR, China University of Geosciences, Beijing, China

The physicochemical properties and microbial communities have significant annual and seasonal changes in karst aquifers. To explore the changes of microbial community and their relationships with environmental factors, water samples were collected from a typical karst river. Microbial communities in winter (Jan-2017 and Jan-2019) were stable with high similarity in spite of the 2 years sampling interval, but the microbial communities in Aug-2017 was different from that in Aug-2018. In four sampling times, there were 275 shared genera, whose average relative abundance ranging from 89.04 to 96.27%. The winter and summer specific genera were mainly from the recharge of tributary site K6 and discharge of waste water treatment plant (K2 and K3), respectively. The deterministic processes had a more significant effect on the microbial community assembly in winter than that in summer, which was affected by environmental pressure from pollution. Furthermore, antibiotics and inorganic nitrogen pollution affected element cycles of nitrogen and sulfur indirectly through microbial ecological modules in karst river, and the denitrification and desulfurization processes were potentially inhibited. These findings contributed to understand the changes and its assembly mechanism of microbial community, as well as the feedback to environment in polluted karst river.

KEYWORDS

karst river, microbial community, assembly, nitrogen, antibiotic

1. Introduction

Approximately 15% of the continents are karst terrain (Yuan, 1997). The water cycle was rapid in the karst system because of its underground-surface double-layered structure and high hydraulic conductivity (Torres et al., 2018). Due to the uneven distribution of karst aquifer fissures and tubes, rapid discharge, and significant seasonal flow velocity variation, the hydrological processes and hydrochemical characteristics exhibit substantial spatial and temporal variability (He et al., 2018; Sun et al., 2019, 2021). Karst water provided drinking water for about 25% of the global population (Dodgen et al., 2017). With the strengthening human activities, however, pollutants such as nitrogen, phosphorus, heavy metals, and organic matter (Wu et al., 2018; Huang F. et al., 2019; Qin et al., 2020, 2021) are continuously introduced into karst aquifers, which have altered the karst ecosystem and element cycles.

As the most active component of the aquatic ecosystem, microorganisms acquire nutrients and energy to survive in an oligotrophic environment *via* numerous metabolic pathways, which are crucial to the elemental cycling of the karst ecosystem (Webster et al., 2018; Xue et al., 2020; Zhu et al., 2022). According to several studies, Proteobacterium, Bacteroides, and Firmicutes were the most common phyla in karst aquifers (Li et al., 2017; Danczak et al., 2018; Tang et al., 2019; Li Q. et al., 2020), and there were shifts in both geographical and seasonal composition of microbial communities (Opalički Slabe et al., 2021). Deterministic and stochastic processes jointly govern the assembly of microbial communities (Chave, 2004). Previous studies have demonstrated that the relationship between these processes varies across different spatial and temporal scales due to the intensity of environmental change and the threshold of microbial tolerance (Liu et al., 2019). In karst aquifer, the relatively steady hydrodynamic circumstances during the dry season resulted in the distinct microbial communities in individual aquifers because of their distinct physicochemical conditions (Shabarova, 2013; Shabarova et al., 2014), whereas the rapid recharge during the rainy season enabled the passive migration of isolated species in densely connected aquifers, reducing the environmental selection on microbial communities and resulting in their convergence in karst aquifer (Yan et al., 2020). In addition to the aquifer connectivity, different hydrochemical conditions affected the composition and distribution of "permanent inhabitants" and specific species in different seasons in microbial communities. In the unexplored karst aquifer, pH, temperature (Yun et al., 2016; Li H. et al., 2021), salinity (Park et al., 2021; Fang et al., 2022), and organic matter (Iker et al., 2010) were the most impacted factors on the microbial communities. With increasing human activities, the constant input of nitrogen, phosphorus and emerging pollutants such as antibiotics had disrupted the physicochemical properties, the structure and interactions of microbial communities, as well as their carbon and nitrogen cycles (Zhang et al., 2013; Xi et al., 2015; Mahana et al., 2016; Zhernakova et al., 2016; Subirats et al., 2019; Roose-Amsaleg et al., 2021). Not only had antibiotics affected the microbial community structure, but also influenced their metabolic mechanisms, such as carbon sequestration, nitrification and denitrification (Gonzalez-Martinez et al., 2014; Xiong et al., 2015; Li H. et al., 2020; Slipko et al., 2021). Different bacteria acquired resistance genes variously under the selection pressure caused by antibiotics, which regulated their metabolic strategies and the efficiency of element cycles (Ming et al., 2020; Yang et al., 2020; Zhang et al., 2022). However, karst aquifers with intense human activities were often influenced by more than one pollutant (Zhu et al., 2019), which would have more complex effects on the community structure and function of microbial community.

The elements cycles were driven by biogeochemical processes in karst system, which would further influence the role of karst system in global climate change (Mahler et al., 2021). However, the microbial assembly and ecological roles in polluted karst rivers at annual and seasonal scales, as well as their feedback to environment were less studied. In this study, we focused on: (1) the physicochemical properties and pollution characteristics of typical karst river in dry and rainy seasons; (2) the variation and assembly mechanisms of microbial communities in polluted karst river; and (3) the response of microbial community composition and functions to environmental factors, especially the pollutants from human activities.

2. Materials and methods

2.1. Study area and sample collection

The study area, Kaiyang, is situated in Guizhou Province, southwest China, in a typical subtropical monsoon climate zone with an annual average temperature of 14.4°C and precipitation primarily concentrated from June to September. There were two karst rivers from west to east, the south river and the north river, with three underground entrances (K4, K8, K9) and three underground exits (K5, K7, and KX) (Figure 1). A total 40 samples were collected. Each 10 samples were collected in January 2017 (Jan-2017), August 2017 (Aug-2017) (Xiang et al., 2020), August 2018 (Aug-2018) and January 2019 (Jan-2019) (Zhang et al., 2021), respectively.

Except for K9 and KX, all sampling sites were in the south river. K1 to K4 were located in the surface river from upstream; K1 was located in a reservoir; K2 and K3 were situated upstream and downstream of a waste water treatment plant (WWTP), respectively; and K4 was situated in a resort. There were agricultural fields and a small amount of livestock activity between K5 and K8. K5 was an outlet of underground river, with evident domestic wastes. K8 was an underground entrance. K6 and K7 were located in the upstream tributaries of K5 and K8, respectively. K6 was a surface river site with domestic wastes, and K7 was the outlet of an underground river. K9 was a sinkhole in the scenic region of the north river, while KX was the confluence of the north and south rivers.

2.2. Hydrochemistry monitoring and analyses

Temperature (T) and pH value of karst river water samples were determined by pH meter (pH30, CLEAN, CA, United States). Electronic conductivity (EC) and dissolved oxygen (DO) were determined by EC meter (CON, CLEAN, CA, United States) and DO meter (CON30, CLEAN, CA, United States), respectively. The total organic carbon (TOC) was determined by TOC analyzer (Shimadzu, Japan). HCO_3^- was tested by potentiometric titrator (Metrohm 877 Titrino plus, Swiss), and Cl^-, SO_4^{2-} were measured by ion chromatograph (DIONEX ICS-900, Sunnyvale, CA, United States). Ca^{2+}, Mg^{2+}, K^+, and Na^+ were measured by ICP-OES (SPECTRO Blue Sop, Germany). And the spectrophotometer UV-1800 (Shimadzu, Japan) was used to determine dissolved inorganic nitrogen (DIN) - NH_4^+, NO_3^- and NO_2^-. Following our previous studies (Huang H. et al., 2019), auto-solid phase extraction (SPE) instrument (Auto SPE-06C, Reeko Instrument, TX, United States) with an Oasis HLB SPE column (6 mL, 500 mg, Waters, MA, United States) was used to extract antibiotics from water samples of karst river. Samples were collected and immediately chilled in 4°C and transported *via* overnight express to the laboratory for further test. The sampling process was followed our previous study (Xiang et al., 2020).

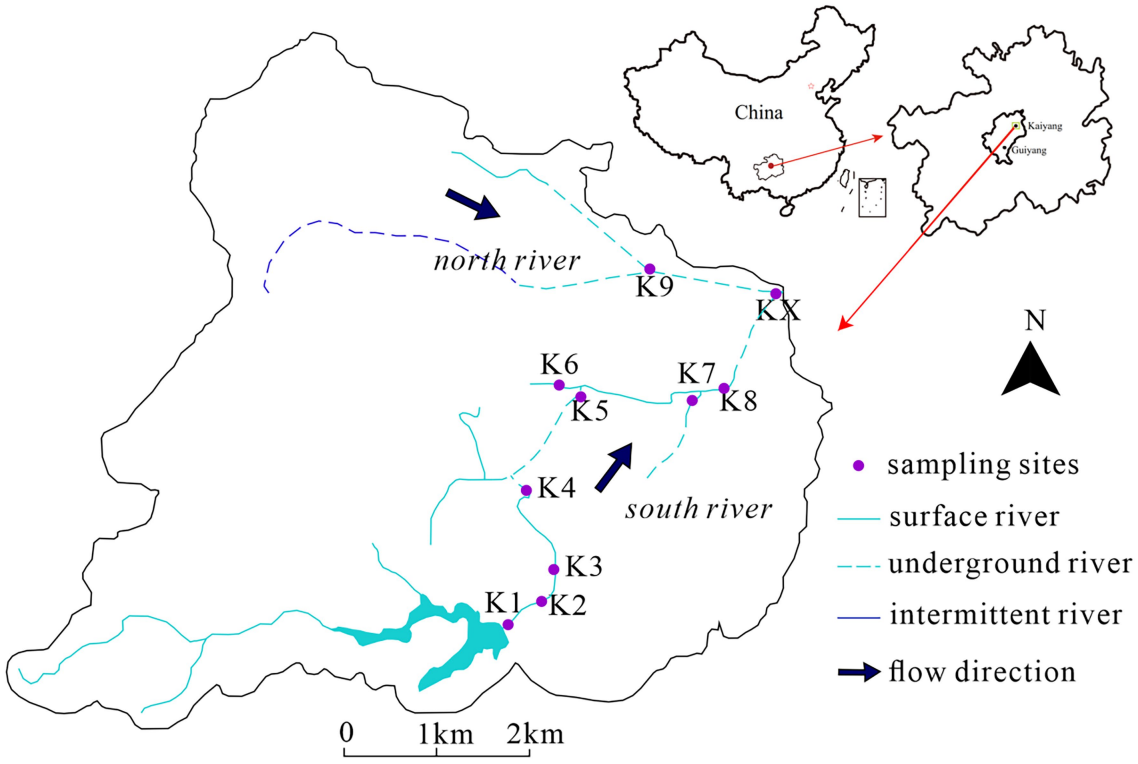

FIGURE 1
The sampling sites in study area.

2.3. DNA extraction and 16S rRNA gene sequencing

The bacteria in each sample were filtered through a 0.22 μm Millipore GSWP membrane for 1.0 l water and then suspended in 10 mL of physiological saline for 6 h. The mentioned suspensions were separated and kept for DNA extraction using a PowerSoil DNA Extraction Kit (MoBio Laboratories, Carlsbad, CA, United States). The extracted DNA was stored at −20°C for further analysis and at −80°C for permanent preservation. Using a NanoDrop ND-2000 spectrophotometer (Thermo Fisher Scientific, Wilmington, DE, United States) and agarose gel electrophoresis (Bio-Rad, Hercules, CA, United States), the quantity and quality of the extracted DNA were established.

The primers 338F and 806R (338F: 5′-barcode-ACTCCTAC GGGAGGCAGCAG-3′ and 806R: 5′-barcode-GGACTACHVGG GTWTCTAAT-3′) were used to amplify the V3-V4 regions of the bacterial 16S ribosomal RNA gene (16S rRNA gene). The PCR amplification method was referred to our previous study (Zhang et al., 2020). Raw fastq files were demultiplexed, then quality-filtered using QIIME (Version 1.17). All clusters were subsampled by the minimum reads (19,551 reads), and operational taxonomic units (OTUs) were clustered with a 97% similarity cutoff by Uparse.[1] Mothur[2] was used to compute the alpha diversity. The Kyoto Encyclopedia of Genes and Genomes (KEGG) functional profiling was predicted using PICRUSt2.[3] The clustered sequence datasets in this study were deposited in the NCBI Genbank with the accession number PRJNA908735 and PRJNA936825.

2.4. Statistical analysis

The data were normalized except for pH value. Spearman correlation analysis and its significance test among each factor were completed by "corrplot" package.[4] The ordinary least squares (OLS) analysis among ammonium, nitrate, sulfate, and other environmental factors were calculated by "car" package.[5] Principal co-ordinates analysis (PCoA) based on Bray-Curtis distance and variance partitioning analysis (VPA) were both performed by "vegan" package.[6] Venn diagram at genus level was plotted by "vennDiagram" package. The Kruskal-Wallis test ($p < 0.05$) was completed by "nparcomp" package, and corrected p-values were calculated using Dunn's test. The microbial community assembly processes were analyzed by "iCAMP" package.[7] And the heatmap figure was plotted by "pheatmap" package.[8]

1 http://www.drive5.com/uparse/
2 http://www.mothur.org/wiki/Classify.seqs
3 https://github.com/picrust/picrust2/
4 https://github.com/taiyun/corrplot
5 https://callr.r-lib.org/
6 https://github.com/vegandevs/vegan
7 https://github.com/DaliangNing/iCAMP1
8 https://cran.rstudio.com/package=pheatmap

All the above data analysis were implemented in R.[9] The co-occurrence network of bacteria at genus level was visualized with Gephi 0.9.2,[10] and ecological modules were identified using the Louvain algorithm. The saturation index of gypsum (SIg) and saturation index of calcite (*SIc*) were calculated by PHREEQC (Version 3.6.2). Structural equation model (SEM) was performed by SPSS AMOS (Version 24.0) to discuss the environmental factors effect on ecological module and element metabolic module.

3. Results and discussion

3.1. Characteristics of physicochemical properties of karst river

The pH value of karst river water was ranging from 7.70 to 8.82, and the temperature was ranging from 4.0°C to 26.1°C (Supplementary Table 1). DO ranged from 1.88 to 9.93 mg/L, and TOC ranged from 1.09 to 30.63 mg/L. Ca^{2+} and HCO_3^- were the major cation and anion due to the abundant carbonate rocks in the study area (Sun et al., 2019). For carbonate rock weathering involving only carbonic acid, the equivalent ratio of $[Ca^{2+}+Mg^{2+}]/[HCO_3^-]$ is typically around 1. But the average value of our study was 1.23, while the mean value of $[Ca^{2+}+Mg^{2+}]/[HCO_3^- + NO_3^- + SO_4^{2-}]$ was 0.93, indicating that the carbonate weathering was influenced by both carbonic acid and sulfuric/nitric acids (Martin, 2017; Sun et al., 2021).

The concentration of NO_3^- varied from 0.74 to 45.82 mg/L, with an average value of 18.23 mg/L, and the concentration of SO_4^{2-} varied from 20.14 to 74.25 mg/L. There were severe NH_4^+ and NO_2^- pollution, with NH_4^+ amounting from 0.02 to 45.35 mg/L and NO_2^- amounting from 0.01 to 9.51 mg/L. The concentrations of both NH_4^+ and NO_3^- showed seasonal variations with higher in winter and lower in summer, mainly influenced by the dilution effect of precipitation recharge in rainy season. Meanwhile, the NH_4^+ were higher in upstream, particularly from K1 to K4, while NO_3^- concentrated downstream from K7 to KX, due to nitrification and the NO_3^- accumulation for its high solubility (Li X. et al., 2021; Li H. et al., 2021). The negative correlations between NH_4^+ and NO_3^- also supported this hypothesis (Eqs 1, 2):

$$\begin{aligned} NH_4^+ = & -0.35NO_3^- + 0.17TOC - 0.31T \\ & +0.20DO + 0.50Antibiotics \\ & +a1\left(R^2 = 0.56,\ p < 0.01,\ a1 < 0.0001\right) \end{aligned} \quad \text{(Equation 1)}$$

$$\begin{aligned} NO_3^- = & -0.42NH_4^+ + 0.54NO_2^- - 0.60T + 0.27pH \\ & +a2\left(R^2 = 0.48,\ p < 0.01,\ a2 < 0.0001\right). \end{aligned} \quad \text{(Equation 2)}$$

As shown in Eq.1, The concentration of NH_4^+ was positively correlated with antibiotics, as well as its correlation coefficients with macrolides, lincomycin, tetracyclines were 0.78, 0.71 and 0.66 ($p < 0.01$), respectively. The concentrations of NH_4^+ and antibiotics showed a similar spatial variation trend, displayed higher upstream. As one of the most prevalent forms of nitrogen pollution in WWTP, NH_4^+ originated primarily from wastewater plant discharges, the same source of antibiotics.

SO_4^{2-} is mainly derived from both natural (dissolution of soluble sulfate, oxidation of sulfide minerals, and atmospheric precipitation) and anthropogenic inputs(agricultural fertilizers, domestic sewage, industrial wastewater, and mine waste water)(Li et al., 2018). In the study area, the $[Mg^{2+}]/[Ca^{2+}]$ values ranged from 0.39 to 1.14 with average 0.65, which indicated that the chemical composition is mainly influenced by low-magnesium minerals such as calcite and gypsum. Furthermore, the SIg values were −2.43 ~ −1.75 while *SIc* were −0.79 ~ 1.28, implied that the dissolution of gypsum were the main source of sulfate. Additional, SO_4^{2-} were positively correlated with antibiotics ($R = 0.66$, $p < 0.01$), which implied that SO_4^{2-} also originated from WWTP, which was consistent with its concentration spatial distribution of higher in upstream.

A total of 28 antibiotics were detected, with total concentrations ranging from 9.13 to 1411.33 ng/L (Supplementary Table 2). The mean concentrations of four sampling times from high to low were Jan-2019 (average value of 514.15 ng/L), Jan-2017 (472.60 ng/L), Aug-2017 (392.44 ng/L), and Aug-2018 (199.37 ng/L), with a seasonal trend of higher in winter and lower in summer (Figure 2), due to the dilution effect of precipitation recharge, which was consistent with our previous study (Huang F. et al., 2019; Huang H. et al., 2019). The maximum value for each time was frequently recorded at K2 and K3, suggesting that WWTP effluent discharge was the major source of antibiotics in karst river, which indicated the anthropogenic inputs. Antibiotic demonstrated a spatial changes that fluctuates and decreases along the stream, which was affected by the adsorption of soil and sediment and the degradation of bacteria (Zhao et al., 2012). Moreover, antibiotic concentrations in tributaries K6 and K7 were lower than those in the mainstream.

Quinolones (QNs), lincomycin (LIN), and macrolides (MLs) were the major antibiotics, accounting on average for 43.45, 34.58, and 13.99% of total concentration, respectively, which were consistent with their frequent use in southwest China (Sun et al., 2015; Zeng et al., 2019). QNs ranged from 3.10 to 994.13 ng/L (Figure 2A) with a 95% detection frequency. QNs were persistent pollutants due to their high chemical stability and prolonged half-life (Andriole, 1999). Ofloxacin and norfloxacin, as the maximum content subclass of QNs in most WWTP (Dinh et al., 2017), also dominated in karst river, ranging from 4.60 to 486.00 ng/L and 4.09 to 204.00 ng/L, respectively. The detection frequency of LIN was 95%, and the concentration was 4.77–227.53 ng/L (Figure 2B). The detection frequency of MLs was 88%, with concentration ranging from 0.83 to 205.13 ng/L (Figure 2C). Erythromycin and roxithromycin were the main subclasses of MLs. While antibiotics were transferred underground by continuous precipitation recharge in summer, their natural degradation was weakened due to weak light and then accumulated (Liu et al., 2021). However, the high connectivity of karst aquifers enabled rapid hydration and a more quickly response to contaminants.

The concentrations of tetracyclines (TCs), chloramphenicols (CAP), and sulfonamides (SAs) were ranged from 3.43 to 177.80 ng/L (Figure 2D), 1.70 to 76.20 ng/L (Figure 2E), and 0.65

9 https://www.r-project.org
10 https://gephi.org/

10.3389/fmicb.2023.1133938

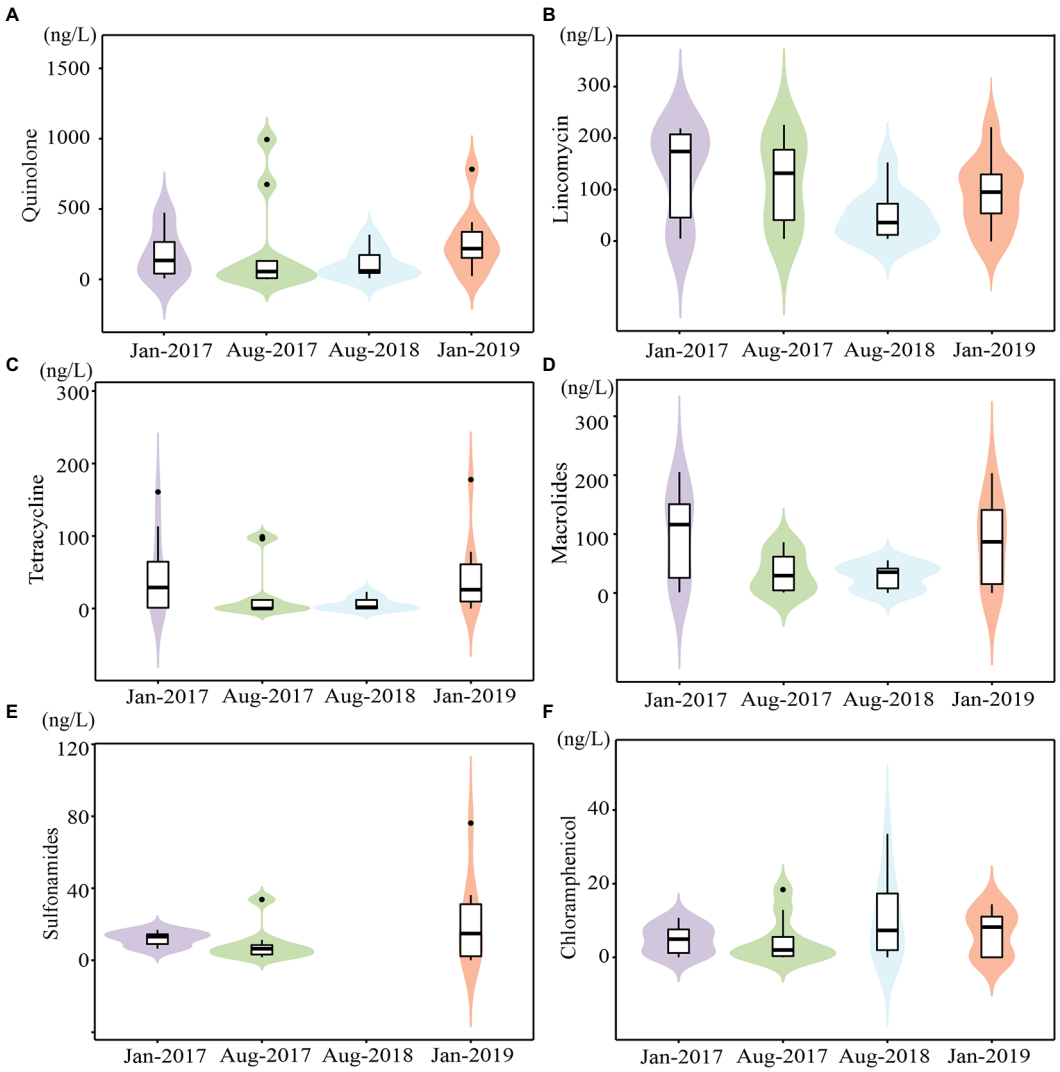

FIGURE 2
The concentrations of main antibiotics in karst river at four sampling times (Jan-2017, Aug-2017, Aug-2018 and Jan-2019). **(A–F)** The concentrations of quinolones, lincomycin, macrolides, tetracyclines, sulfonamides and Chloramphenicol.

to 33.56 ng/L (Figure 2F), respectively. The detection rate of TCs was 60%, with tetracycline and oxytetracycline being the most commonly used antibiotics. The detection frequency of CAP was 53%. Both TCs and CAP were higher in winter. The detection rate of SAs was 75%, with sulfapyridine being the most common subclass. The maximum content and the most subclasses of SAs were observed in Aug-2018. Only samples from Aug-2018 contained sulfadimethoxine and sulfadimidin, both of which were widely applied in veterinary medicine. Increased livestock vaccination in study area in 2018 may result in an increase use of veterinary drugs.[11] As a notable veterinary drug, enrofloxacin was also detected only in Aug-2018.

3.2. The structure of bacterial community in karst river

A total of 3,955,799 optimum sequences were obtained in 40 samples (Supplementary Table 3). After subsampling by the minimum sequences, 5,242 OTUs were obtained. The species richness in Aug-2017 was the lowest. Nonetheless, the Shannon index had no significant difference at four sampling times (Supplementary Table 3).

Proteobacteria (relative abundance ranged from 36.03 to 61.15%), Bacteroidetes (18.97 to 38.03%), Cyanobacteria (6.14 to 13.85%), and five other phyla with relative abundance greater than 5% were the dominant phyla. *Flavobacterium*, *Arcobacter*, norank_c_Cyanobacteria, *Pseudomonas* and *Acinetobacter* were prevalent in a total 945 genera, with the relative abundance of 12.68, 5.78, 5.18, 4.41 and 4.35%, respectively.

PC1 and PC2 explained 22.65% of the variance in community structure together (Figure 3A). The bacterial communities of Jan-2017 and Jan-2019 were similar. The bacterial community structures of Aug-2017 and Aug-2018 were divided from each other, which apparently differed from samples taken in winter.

11 http://nynct.guizhou.gov.cn/xwzx/zwdt/201712/t20171205250414433.html

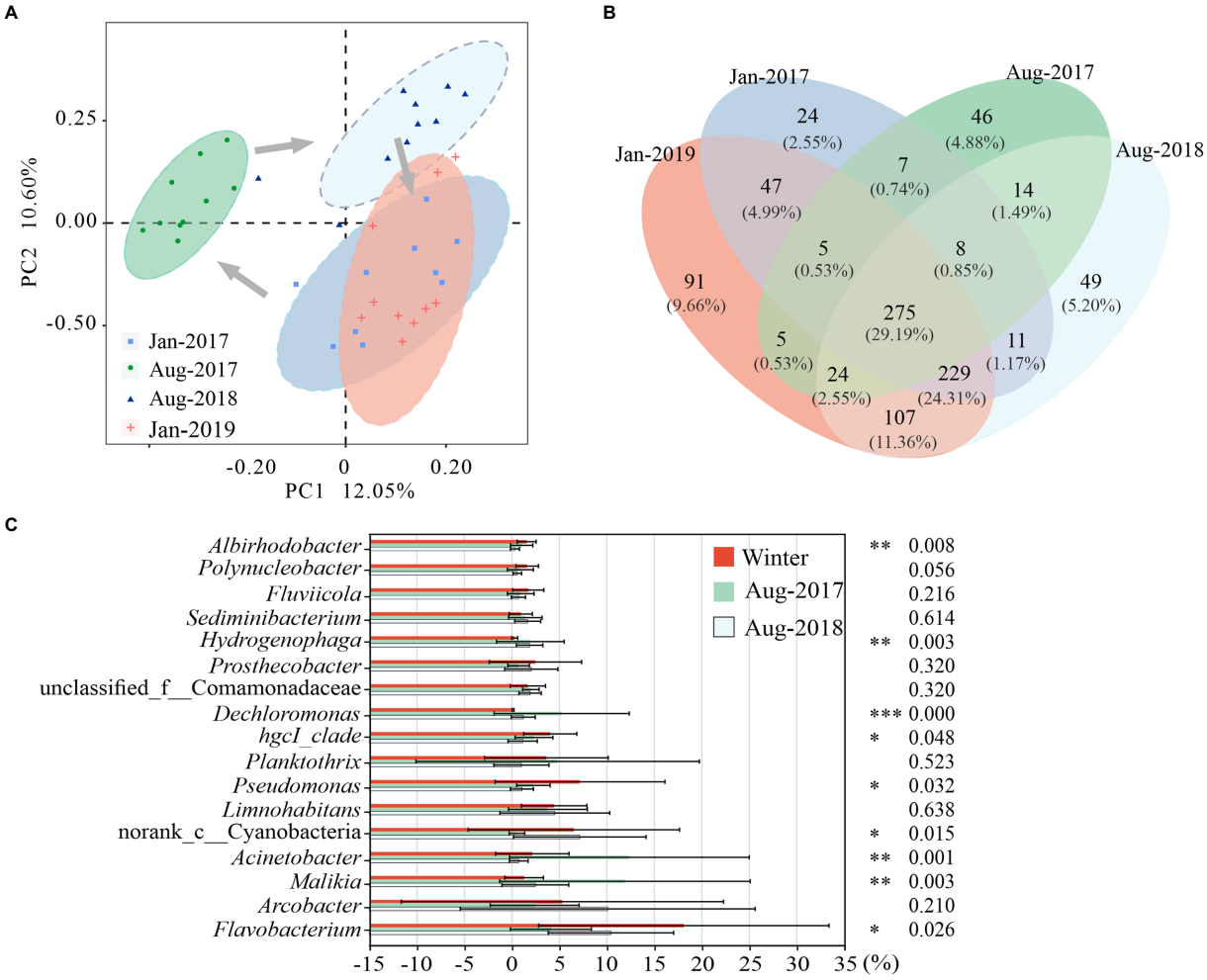

FIGURE 3
Differences of microbial communities in karst rivers among four sampling times (Jan-2017, Aug-2017, Aug-2018 and Jan-2019). **(A)** Principal co-ordinates analysis (PCoA) of microbial community structure based on Bray-Curtis distance at genus level. **(B)** Venn diagram of microbial community at genus level. **(C)** Significantly Different of genus among two winter, Aug-2017 and Aug-2018. Kruskal-Wallis test with *p*-values were *$p<0.05$, **$p<0.01$, ***$p<0.001$.

The relative abundance of 275 shared genera varied from 89.04 to 96.27% (Figure 3B). Most of them showed obvious seasonal characteristics. Seven genera were mainly distributed in winter, including *Flavobacterium*, *Pseudomonas* and *hgcI_clade*. In previous study, we observed strong correlations between ARGs and *Flavobacterium*, *Pseudomonas* (Zhang et al., 2021), which were more likely to survive in winter with higher antibiotic concentrations. Six genera were enriched in summer, including *Dechloromonas*, *Hydrogenophaga* and *Cloacibacterium*. The relative abundance of unclassified_f__Comamonadaceae gradually increased while *Limnohabitans* showed no noticeable trend in this study. Nine out of the nineteen dominant genera (relative abundance above 1%) (Supplementary Figure 1) exhibited statistically significant differences ($p<0.05$) (Figure 3C). *Flavobacterium*, *Pseudomonas*, *hgcI_clade* and *Albirhodobacter* were considerably enriched in winter with average relative abundances varying from 8.15 to 28.06%, 6.26% to 8.08, 3.53 to 4.54% and 1.49 to 1.62%, respectively. *Acinetobacter*, *Malikia*, *Dechloromonas* and *Hydrogenophaga* were highly expressed in Aug-2017 with average relative abundances of 12.37, 11.90, 5.24 and 1.94%, respectively. And the relative abundance of norank_c_Cyanobacteria (7.15%) was the highest in Aug-2018.

Compared with shared genera, the richness and abundance of specific genera were lower. Forty seven genera only presented in winter, with relative abundances of 0.23 and 0.24% in Jan-2017 and Jan-2019, including Candidatus_Azambacteria, *Empedobacter*, etc. The winter genera were mainly distributed at K4 and K6 in Jan-2017 and at K6 in Jan-2019. As a sampling site in the tributary, there might be a relatively higher flow at K6 that introduce a great number of exotic species in winter. Forty six genera were only found in Aug-2017, with an average relative abundance of 1.13%, and distributed mainly at K2 and K3, such as *Macromonas*, Candidatus_Aquiluna. Forty nine genera such as *Sporacetigenium* and *Desulfitobacterium* were only found in Aug-2018, with an average relative abundance of 1.73% and primarily enriched at K8.

Five clusters (MOD0-MOD4) were obtained through co-occurrence network analysis of genera with relative abundance above 0.1% (Figure 4A). Twenty one genera were included in

MOD0, primarily *Flavobacterium*, *Malikia*, *Dechloromonas*, etc., each of which exhibited distinct seasonal differences. Thus, there was no discernible seasonal trend in MOD0 but a peak value in Jan-2019 (Figure 4C), where *Flavobacterium* concentrated. Twenty three genera of MOD1 were mainly included *Limnohabitans* and *Planktothrix*, which concentrated in summer. Twenty five genera were included in MOD2, such as *Arcobactor*, *Pseudomonas*, *Cyanobacteria*. MOD3 was consisted of 17 genera, such as *hgcI_clade* and *Hydrogenophaga*, etc., which were abundant in winter. *Prosthecobacter*, *Nitromonas* and *Nitrospira* were dominant in MOD4 among the total 24 genera.

The co-occurrence network of major microorganisms helped to reveal functional group structure and potential interactions between bacteria (Curtis et al., 2002; Cardona et al., 2016). There were 165 positive and 68 negative edges among five MODs (Figure 4B), with a modularity of 0.41, suggesting a strongly associated community among the major communities which were mainly positive synergies. MOD0, MOD3 and MOD4 were strongly connected with other MODs with 100, 98 and 65 positive edges, respectively. There were more negative edges between MOD1 and MOD4, indicating a negatively competitive relationship among genera. Genera involved in carbon, nitrogen and sulfur metabolism were widely distributed in each module. *Flavobacterium*, *Dechloromonas*, *Massilia* in MOD0 participated in denitrification, nitrogen reduction and sulfate reduction (Tanikawa et al., 2018; Chang et al., 2019). The diversity of metabolic function makes it most closely related to other MODs. MOD3 were primarily denitrifying bacteria, such as *hgcI_clade* (Herrmann et al., 2015; Luo et al., 2018). Conversely, ecological modules with different functions often exhibit a tendency to compete for limiting nutrients (Tate, 2020). This competitive relationship may also exist between MOD1 and MOD4. MOD1 was dominated by *Limnohabitans*, *Planktothrix*, and other genera with both carbon and nitrogen metabolism function, whereas the MOD4 was ruled by nitrifying bacteria such as *Prosthecobacter*, *Nitrosomonas*, and *Nitrospira*. In addition, *Hydrogenophaga* and *Limnohabitans* in MOD1 and MOD4 participate in sulfur metabolism (Herrmann et al., 2015; Luo et al., 2018). Conjecturally, bacterial communities participated in nitrogen and sulfur cycles were potentially affected by the pollution of antibiotics and nitrogen in karst river.

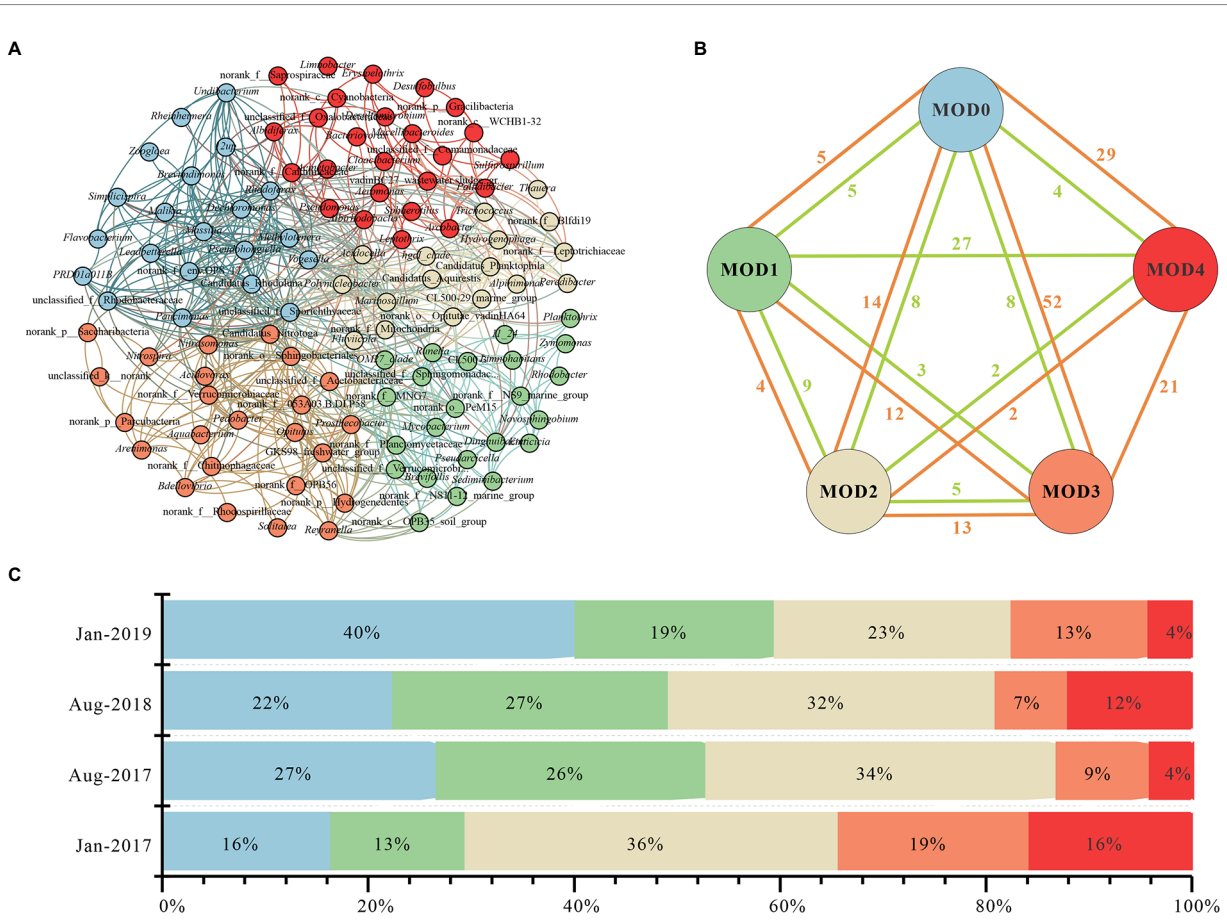

FIGURE 4
Interactions of microbial community in karst river. **(A)** Co-occurrence network of genus with relative abundance above 0.1%. Genus with relative abundance above 0.1% were selected to calculate their correlations. Each node represented a genus, the nodes were colored by module, and the connection between nodes represented a significant correlation (Spearman, $p<0.05$, $|r|>0.6$). **(B)** Connections of modules. The correlation of each genus in every module, negative relations were represented in green edges and positive relations were represented in orange edges. **(C)** Stacked histogram of five modules in Jan-2017, Aug-2017, Aug-2018, and Jan-2019. Relative abundance of each module was represented in different color.

3.3. Assembly mechanisms of bacterial community in karst river

The bacterial community assembly processes were consisted of deterministic processes (heterogeneous selection and homogeneous selection) and stochastic processes (dispersal limitation, homogenizing dispersal and drift) (Stegen et al., 2013). Deterministic processes represented the influence of environmental factors such as physical and chemical indicators on microbial community, while stochastic processes were related to spatial variation. In general, deterministic processes were dominant in small spatial scale while stochastic processes dominated in a larger spatial scale (Dini-Andreote et al., 2015). However, frequent anthropogenic impacts and intense variation in karst hydrodynamic conditions produced high variance and increased the influence of stochastic processes.

In Figure 5, stochastic processes had more advantage in Aug-2017 (56.96%) and Aug-2018 (50.66%), and primarily affected by dispersal limitation and drift effects. Stochastic processes played a major role in microbial community assembly with less environmental pressure (Dini-Andreote et al., 2015). Lower antibiotic concentrations in summer reduced the survival pressure for less resistant bacteria, which increased their relative abundance. The type of antibiotics in Aug-2017 and Aug-2018 were remarkable different, and their additive, synergistic and antagonistic effects led to greater differences in community structure (De Liguoro et al., 2018; Liang et al., 2022). The rapid surface-underground exchange and the drastic environmental changes in karst river resulted in short adaptation and rapid turnover in summer, which benefited distinguishable bacterial communities as well. Deterministic processes enhanced in winter, and homogeneous selection was predominant, with 49.51 and 68.14% in Jan-2017 and Jan-2019, respectively, which was caused by the survival pressure of high concentration of antibiotics and DIN. Therefore, we suggested that the environmental selection caused by the multiple pressure of antibiotics and DIN created a more stable bacterial community with antibiotic resistance in winter. Consequently, despite the two-year sampling interval between Jan-2017 and Jan-2019, the structure of bacterial community showed a highly similarity, while the stronger survival pressure from pollutions led to a decline in the relative abundance of specific genera. The proportion of dispersal limitation in the stochastic processes decreased gradually, while the proportion of homogenizing dispersal increased, indicating that the composition of microbial community tended to be more similar over time.

3.4. Effects of environmental factors on the functions of bacterial community in karst river

Variations in microbial community were accompanied by alterations in community function (Zhong et al., 2018). The results of KEGG functional profiling revealed that the average relative abundance of 16 functional genes exceeded 1%, which were mainly sub-functions of metabolism, environmental information processing, and genetic information processing and so on (Figure 6). Among them, the average relative abundance of energy metabolism ranged from 5.58 to 5.79% and was higher in summer, possibly due to nutrient limitation (Cline and Zak, 2015; Jiang et al., 2022). In winter, the copious nutrients conditions made nutrients more accessible to microorganisms, and hence the corresponding metabolism gene was less prevalent. However, nutrient availability was restricted by dilution effects in summer, and microorganisms maintained their growth by increasing the metabolic function gene (Jiang et al., 2022).

From the results of function profiling, 13 carbon fixation pathways, 5 nitrogen metabolism pathways, and 2 sulfur metabolism pathways were annotated (Figure 7; Supplementary Table 4). The carbon fixation pathways mainly included 7 carbon fixation pathways in prokaryotes (average relative abundance ranged from 5.98 to 6.58%) and 8 pathways in photosynthetic organisms (from 3.01 to 3.26%), such as reductive citrate cycle (M00173), dicarboxylate-hydroxybutyrate cycle (M00374), and reductive pentose phosphate cycle (Calvin cycle) (M00165), etc. The nitrogen metabolism pathways included nitrogen fixation (M00175), nitrification (M00528), denitrification (M00529), and 2 nitrate reduction to ammonium pathways (M00530 and M00531), with average relative abundances from

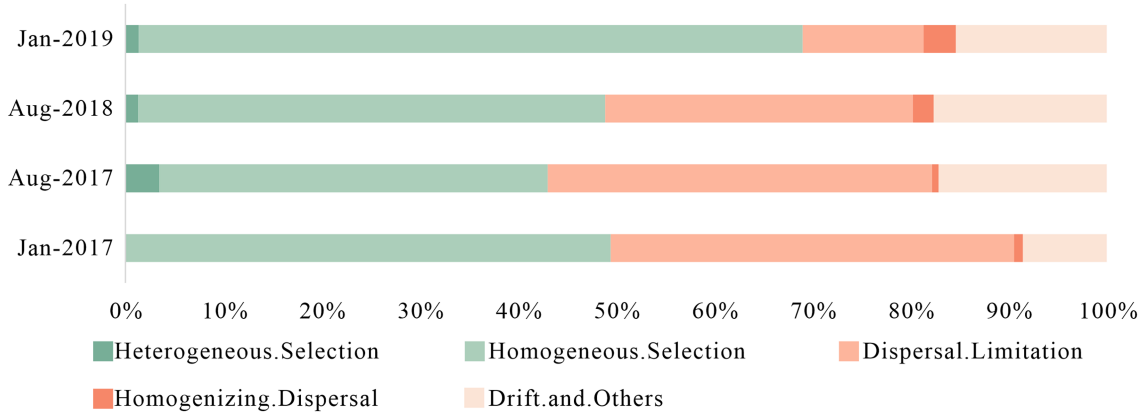

FIGURE 5
Assembly processes of bacteria community in karst river at four sampling times (Jan-2017, Aug-2017, Aug-2018, and Jan-2019) in karst river. Deterministic processes were composed of heterogeneous selection and homogeneous selection, and stochastic processes were composed of dispersal limitation, homogenizing dispersal, drift and other effects.

0.43 to 0.81%. The sulfur metabolism pathways included 2 sulfate reduction pathways (M00176 and M00596), with relative abundance ranging from 0.55 to 0.66%. But all the metabolism pathways above showed no clear seasonal variations.

SEM showed that MOD0, MOD3 and MOD4 contributed significantly to nitrogen and sulfur metabolism (Figure 8A). MOD0 was mainly composed of denitrification and nitrate reduction bacteria, so the denitrification was significantly influenced directly by MOD0, with path coefficient value of 0.95, and the nitrate reduction was not significantly influenced directly by MOD0. MOD3 also directly contributed significantly to nitrate reduction and denitrification, with coefficients of 0.84 and 0.44, respectively. Meanwhile, MOD4 played an important role in sulfate reduction.

On the other hand, the microbial community function was indirectly affected by environmental factors through certain ecological modules. Consistent with the result of VPA (Figure 8B), the antibiotics and DIN had significant impacts on microbial communities (with 5.34 and 0.53% explanation, respectively). MOD3 and MOD4 were resistant and promoted by the antibiotics. *Trichococcus* and norank_f__ Leptotrichiaceae in MOD3 and *Acidovorax* and norank_p_ Saccharibacteria in MOD4 carried resistance genes of tetracycline and multidrugs (Zhang et al., 2021), providing a stronger survival advantage in winter with higher concentration of antibiotics. DIN showed negative influence to MOD0, MOD3 and MOD4. The high nitrate content would produce significant inhibition or toxicity to bacteria (Cua and Stein, 2011), as well as to sulfate-reducing bacteria (He et al., 2010; Zhou and Xing, 2021). Besides, the high nitrate suppression to sulfate-reducing bacteria was diminished by the denitrifier (Zhou and Xing, 2021), which also explained the strong correlation between MOD4 and MOD0.

Denitrification, nitrate reduction and sulfur reduction were indirectly promoted by antibiotics *via* MOD3 and MOD4, whereas they were inhibited by DIN. As the substrate of nitrogen metabolism, DIN also indirectly promoted the process of nitrification, denitrification and nitrate reduction. SEM results showed that the total effect value of environmental factors on nitrification and nitrate reduction was −2.53 and 20.39, respectively. We suggested that the antibiotics and DIN inhibited nitrification, but strongly promoted the nitrate reduction, which lead a further accumulation of NH_4^+. Although the effects of antibiotics and inorganic nitrogen pollution on microbial ecological modules and their functions in karst rivers was indicated, the influence relationship of different ecological groups on environmental factors and the possible environmental utility was identified, the influence on metabolic process and the fluxes of nitrogen and sulfur still requires further researches such as long-term monitoring, isotope tests and other experimental methods.

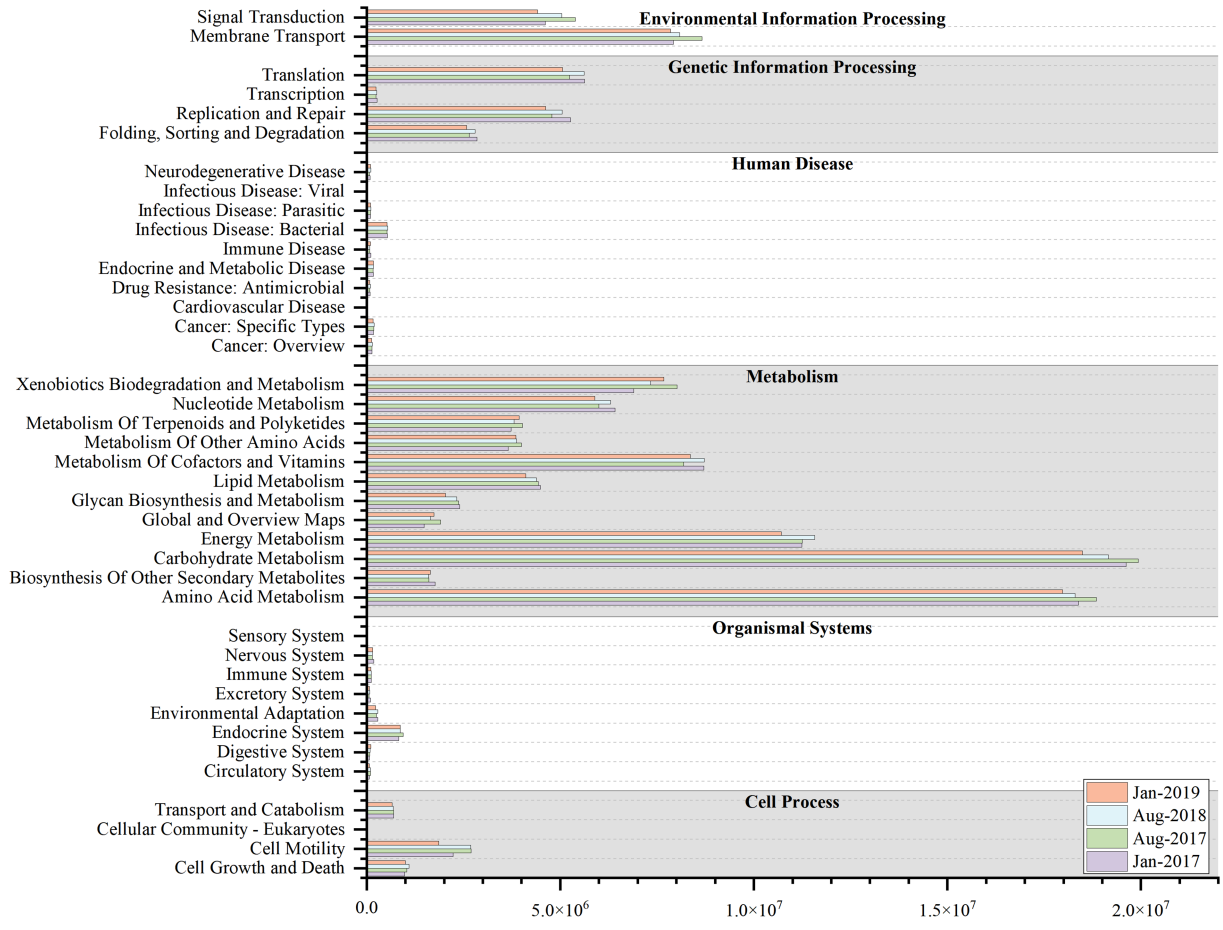

FIGURE 6
The Kyoto Encyclopedia of Genes and Genomes (KEGG) functional profiling at level-2 at four sampling time (Jan-2017, Aug-2017, Aug-2018 and Jan-2019).

10.3389/fmicb.2023.1133938

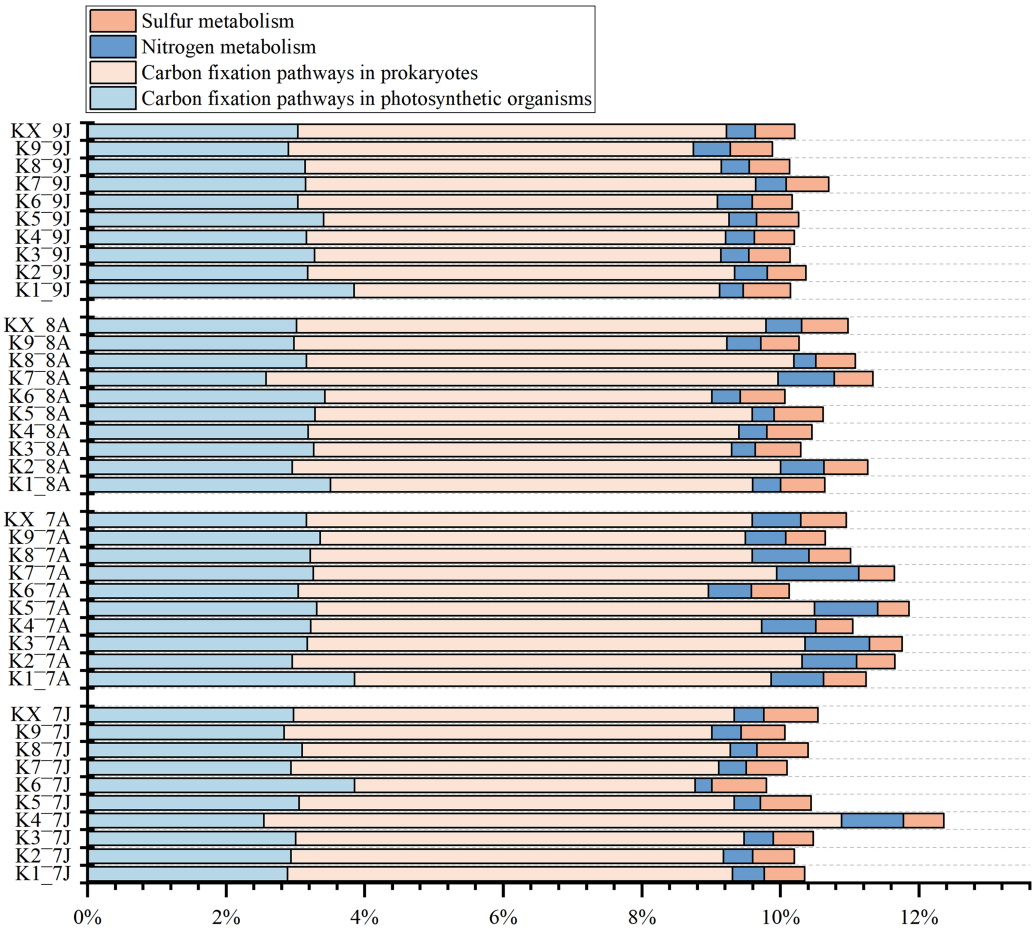

FIGURE 7
The stacked histogram of carbon, nitrogen, sulfur metabolic modules of Kyoto Encyclopedia of Genes and Genomes (KEGG) functional profiling at four sampling time (Jan-2017, Aug-2017, Aug-2018 and Jan-2019).

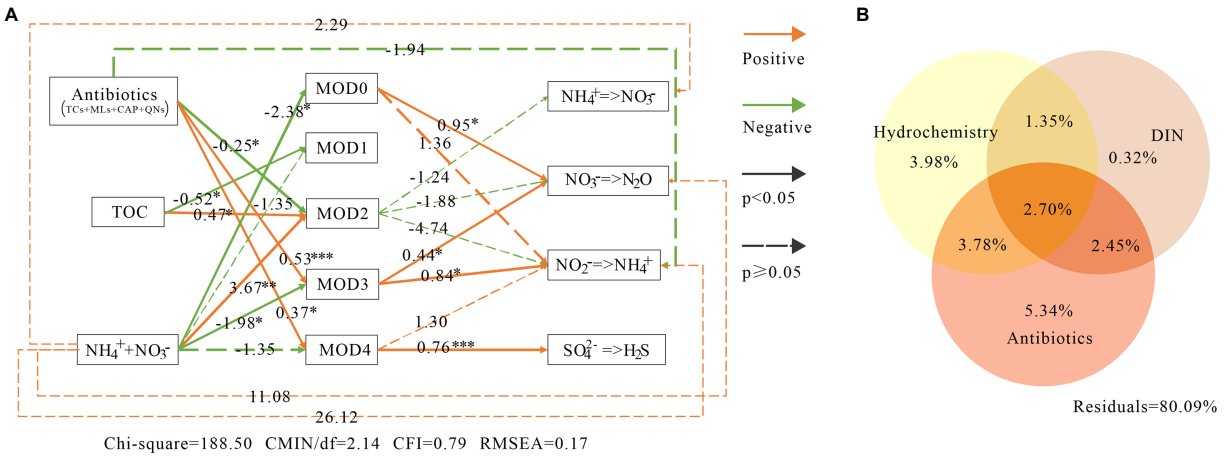

FIGURE 8
The environmental impacts on bacterial communities and their metabolic function in karst river. **(A)** Structure equation model (SEM) among environmental factors, modules and metabolic functions. Antibiotics were including tetracyclines, macrolides, chloramphenicol and quinolones. Green lines, orange lines indicated negative and positive impacts, respectively, and the associated numbers were the path coefficient value with p-values *p<0.05, **p<0.01, ***p<0.001. **(B)** Variance partitioning analysis (VPA) diagram. The impact of antibiotics, DIN and hydrochemical factors on microbial communities. DIN included ammonium, nitrate and nitrite. Antibiotics included quinolones, lincomycin, tetracyclines, macrolides, sulfonamides and chloramphenicol. Hydrochemistry included temperature, pH, electronic conductivity, dissolved oxygen and total organic carbon.

4. Conclusion

The structure of microbial community with physicochemical properties altered considerably from winter to summer in karst ecosystem. Pollution such as antibiotics and inorganic nitrogen were introduced by anthropogenic activities from WWTP and agricultural discharges. Microbial communities in winter of 2 years interval were stable with higher similarity than those in summer of different year. Deterministic processes, homogeneous selection process specifically, occupied in winter due to the environmental pressure of high pollutants content, while stochastic processes had more advantages in summer with a significant extent of spatial heterogeneity due to intensive human activities and karst hydrodynamic condition. Pollution would indirectly affect the nitrogen and sulfur metabolism *via* microbial functional group. Furthermore, the environmental response and feedback of microbial communities' element cycles needs more attentions and further measurable research.

Data availability statement

The datasets presented in this study can be found in the NCBI repository (https://www.ncbi.nlm.nih.gov/), accession numbers PRJNA908735 and PRJNA936825.

Author contributions

XG: contributed to the conceptualization, methodology, and writing. RH and BZ: participated in the formal analysis and discussion. CG: participated in the investigation. FL: participated in the topic and discussion of the whole study. All authors contributed to the article and approved the submitted version.

Funding

This research was supported by the National Natural Science Foundation of China (Grant no. 42172336 awarded to XG), Guangxi key R & D program support (Grand no. Guike AB22080070 awarded to FL) and the Fundamental Research Funds for Central Universities (Grant no. 2652019077 awarded to XG).

Conflict of interest

The authors declare that they have no known competing financial interests or personal relationships that could have appeared to influence the work reported in this paper.

Publisher's note

Supplementary material

The Supplementary material for this article can be found online at: https://www.frontiersin.org/articles/10.3389/fmicb.2023.1133938/full#supplementary-material

References

Andriole, V. T. (1999). The Future of the Quinolones. *Drugs* 58, 1–5. doi: 10.2165/00003495-199958002-00001

Cardona, C., Weisenhorn, P., Henry, C., and Gilbert, J. A. (2016). Network-based metabolic analysis and microbial community modeling. *Curr. Opin. Microbiol.* 31, 124–131. doi: 10.1016/j.mib.2016.03.008

Chang, M., Wang, Y., Pan, Y., Zhang, K., Lyu, L., Wang, M., et al. (2019). Nitrogen removal from wastewater via simultaneous nitrification and denitrification using a biological folded non-aerated filter. *Bioresour. Technol.* 289:121696. doi: 10.1016/j.biortech.2019.121696

Chave, J. (2004). Neutral theory and community ecology: Neutral theory and community ecology. *Ecol. Lett.* 7, 241–253. doi: 10.1111/j.1461-0248.2003.00566.x

Cline, L. C., and Zak, D. R. (2015). Soil microbial communities are shaped by plant-driven changes in resource availability during secondary succession. *Ecology* 96, 3374–3385. doi: 10.1890/15-0184.1

Cua, L. S., and Stein, L. Y. (2011). Effects of nitrite on ammonia-oxidizing activity and gene regulation in three ammonia-oxidizing bacteria: Effects of nitrite on ammonia-oxidizing bacteria. *FEMS Microbiol. Lett.* 319, 169–175. doi: 10.1111/j.1574-6968.2011.02277.x

Curtis, T. P., Sloan, W. T., and Scannell, J. W. (2002). Estimating prokaryotic diversity and its limits. *Proc. Natl. Acad. Sci. U. S. A.* 99, 10494–10499. doi: 10.1073/pnas.142680199

Danczak, R. E., Johnston, M. D., Kenah, C., Slattery, M., and Wilkins, M. J. (2018). Microbialcommunity cohesion mediates community turnover in unperturbed aquifers. *mSystems*, 3, e00066–e00018. doi: 10.1128/mSystems.00066-18

De Liguoro, M., Riga, A., and Fariselli, P. (2018). Synergistic toxicity of some sulfonamide mixtures on Daphnia magna. *Ecotoxicol. Environ. Saf.* 164, 84–91. doi: 10.1016/j.ecoenv.2018.08.011

Dinh, Q., Moreau Guigon, E., Labadie, P., Alliot, F., Teil, M. J., Blanchard, M., et al. (2017). Fate of antibiotics from hospital and domestic sources in a sewage network. *Sci. Total Environ.* 575, 758–766. doi: 10.1016/j.scitotenv.2016.09.118

Dini-Andreote, F., Stegen, J. C., van Elsas, J. D., and Salles, J. F. (2015). Disentangling mechanisms that mediate the balance between stochastic and deterministic processes in microbial succession. *Proc. Natl. Acad. Sci. U. S. A.* 112, E1326–E1332. doi: 10.1073/pnas.1414261112

Dodgen, L. K., Kelly, W. R., Panno, S. V., Taylor, S. J., Armstrong, D. L., Wiles, K. N., et al. (2017). Characterizing pharmaceutical, personal care product, and hormone contamination in a karst aquifer of southwestern Illinois, USA, using water quality and stream flow parameters. *Sci. Total Environ.* 578, 281–289. doi: 10.1016/j.scitotenv.2016.10.103

Fang, Y., Liu, J., Yang, J., Wu, G., Hua, Z., Dong, H., et al. (2022). Compositional and metabolic responses of autotrophic microbial community to salinity in lacustrine. *Environments* 7:e0033522. doi: 10.1128/msystems.00335-22

Gonzalez-Martinez, A., Rodriguez-Sanchez, A., Martinez-Toledo, M. V., Garcia-Ruiz, M.-J., Hontoria, E., Osorio-Robles, F., et al. (2014). Effect of ciprofloxacin antibiotic on the partial-nitritation process and bacterial community structure of a submerged biofilter. *Sci. Total Environ.* 476-477, 276–287. doi: 10.1016/j.scitotenv.2014.01.012

He, Q., He, Z., Joyner, D. C., Joachimiak, M., Price, M. N., Yang, Z. K., et al. (2010). Impact of elevated nitrate on sulfate-reducing bacteria: a comparative study of Desulfovibrio vulgaris. *ISME J.* 4, 1386–1397. doi: 10.1038/ismej.2010.59

He, Z., Liang, H., Yang, C., Huang, F., and Zeng, X. (2018). Temporal–spatial evolution of the hydrologic drought characteristics of the karst drainage basins in South China. *Int. J. Appl. Earth Obs. Geoinform.* 64, 22–30. doi: 10.1016/j.jag.2017.08.010

Herrmann, M., Rusznyák, A., Akob, D. M., Schulze, I., Opitz, S., Totsche, K. U., et al. (2015). Large Fractions of CO_2 -Fixing Microorganisms in Pristine Limestone Aquifers Appear To Be Involved in the Oxidation of Reduced Sulfur and Nitrogen Compounds. *Appl. Environ. Microbiol.* 81, 2384–2394. doi: 10.1128/AEM.03269-14

Huang, H., Chen, Z., Wang, T., Xiang, C., Zhang, L., Zhou, G., et al. (2019). Nitrate distribution and dynamics as indicators to characterize karst groundwater flow in a mined mineral deposit in southwestern China. *Hydrogeol. J.* 27, 2077–2089. doi: 10.1007/s10040-019-01987-0

Huang, F., Zou, S., Deng, D., Lang, H., and Liu, F. (2019). Antibiotics in a typical karst river system in China: Spatiotemporal variation and environmental risks. *Sci. Total Environ.* 650, 1348–1355. doi: 10.1016/j.scitotenv.2018.09.131

Iker, B. C., Kambesis, P., Oehrle, S. A., Groves, C., and Barton, H. A. (2010). Microbial Atrazine Breakdown in a Karst Groundwater System and Its Effect on Ecosystem Energetics. *J. Environ. Qual.* 39, 509–518. doi: 10.2134/jeq2009.0048

Jiang, C., Sun, X., Feng, J., Zhu, S., and Shui, W. (2022). Metagenomic analysis reveals the different characteristics of microbial communities inside and outside the karst tiankeng. *BMC Microbiol.* 22:115. doi: 10.1186/s12866-022-02513-1

Li, X., Gao, D., Hou, L., Qian, W., Liu, M., Zeng, H., et al. (2021). Nitrogen loads alter the N2 production between denitrification and anammox in Min River Estuary, a highly impacted estuary in southeast China. *Environ. Pollut.* 277:116757. doi: 10.1016/j.envpol.2021.116757

Li, Q., Huang, Y., Xin, S., and Li, Z. (2020). Comparative analysis of bacterioplankton assemblages from two subtropical karst reservoirs of southwestern China with contrasting trophic status. *Sci. Rep.* 10:22296. doi: 10.1038/s41598-020-78459-z

Li, Q., Song, A., Peng, W., Jin, Z., Müller, W. E. G., and Wang, X. (2017). Contribution of aerobic anoxygenic phototrophic bacteria to total organic carbon pool in aquatic system of subtropical karst catchments, Southwest China: evidence from hydrochemical and microbiological study. *FEMS Microbiol. Ecol.* 93, fix065. doi: 10.1093/femsec/fix065

Li, H., Song, H.-L., Xu, H., Lu, Y., Zhang, S., Yang, Y.-L., et al. (2020). Effect of the coexposure of sulfadiazine, ciprofloxacin and zinc on the fate of antibiotic resistance genes, bacterial communities and functions in three-dimensional biofilm-electrode reactors. *Bioresour. Technol.* 296:122290. doi: 10.1016/j.biortech.2019.122290

Li, X., Wu, P., Han, Z., Zha, X., Ye, H., and Qin, Y. (2018). Effects of mining activities on evolution of water quality of karst waters in Midwestern Guizhou, China: evidences from hydrochemistry and isotopic composition. *Environ. Sci. Pollut. Res.* 25, 1220–1230. doi: 10.1007/s11356-017-0488-y

Li, H., Yang, S., Semenov, M. V., Yao, F., Ye, J., Bu, R., et al. (2021). Temperature sensitivity of SOM decomposition is linked with a K-selected microbial community. *Glob. Change Biol.* 27, 2763–2779. doi: 10.1111/gcb.15593

Liang, D., Hu, Y., Huang, R., Cheng, J., and Chen, Y. (2022). Effects of various antibiotics on aerobic nitrogen removal and antibiotic degradation performance: Mechanism, degradation pathways, and microbial community evolution. *J. Hazard. Mater.* 422:126818. doi: 10.1016/j.jhazmat.2021.126818

Liu, J., Meng, Z., Liu, X., and Zhang, X.-H. (2019). Microbial assembly, interaction, functioning, activity and diversification: a review derived from community compositional data. *Mar. Life Sci. Technol.* 1, 112–128. doi: 10.1007/s42995-019-00004-3

Liu, X., Wang, Z., Zhang, L., Fan, W., Yang, C., Li, E., et al. (2021). Inconsistent seasonal variation of antibiotics between surface water and groundwater in the Jianghan Plain: Risks and linkage to land uses. *J. Environ. Sci.* 109, 102–113. doi: 10.1016/j.jes.2021.03.002

Luo, J., Tan, X., Liu, K., and Lin, W. (2018). Survey of sulfur-oxidizing bacterial community in the Pearl River water using soxB, sqr, and dsrA as molecular biomarkers. *3 Biotech* 8:73. doi: 10.1007/s13205-017-1077-y

Mahana, D., Trent, C. M., Kurtz, Z. D., Bokulich, N. A., Battaglia, T., Chung, J., et al. (2016). Antibiotic perturbation of the murine gut microbiome enhances the adiposity, insulin resistance, and liver disease associated with high-fat diet. *Genome Med.* 8:48. doi: 10.1186/s13073-016-0297-9

Mahler, B. J., Jiang, Y., Pu, J., and Martin, J. B. (2021). Editorial: Advances in hydrology and the water environment in the karst critical zone under the impacts of climate change and anthropogenic activities. *J. Hydrol.* 595:125982. doi: 10.1016/j.jhydrol.2021.125982

Martin, J. B. (2017). Carbonate minerals in the global carbon cycle. *Chem. Geol.* 449, 58–72. doi: 10.1016/j.chemgeo.2016.11.029

Ming, X., Groves, C., Wu, X., Chang, L., Zheng, Y., and Yang, P. (2020). Nitrate migration and transformations in groundwater quantified by dual nitrate isotopes and hydrochemistry in a karst World Heritage site. *Sci. Total Environ.* 735:138907. doi: 10.1016/j.scitotenv.2020.138907

Opalički Slabe, M., Danevčič, T., Hug, K., Fillinger, L., Mandic-Mulec, I., Griebler, C., et al. (2021). Key drivers of microbial abundance, activity, and diversity in karst spring waters across an altitudinal gradient in Slovenia. *Aquat. Microb. Ecol.* 86, 99–114. doi: 10.3354/ame01956

Park, Y., Yu, J., Nguyen, V. K., Park, S., Kim, J., and Lee, T. (2021). Understanding complete ammonium removal mechanism in single-chamber microbial fuel cells based on microbial ecology. *Sci. Total Environ.* 764:144231. doi: 10.1016/j.scitotenv.2020.144231

Qin, W., Han, D., Song, X., and Liu, S. (2021). Sources and migration of heavy metals in a karst water system under the threats of an abandoned Pb–Zn mine. *Southwest China. Environ. Pollut.* 277:116774. doi: 10.1016/j.envpol.2021.116774

Qin, Y., Hao, F., Zhang, D., Lang, Y., and Wang, F. (2020). Accumulation of organic carbon in a large canyon reservoir in Karstic area, Southwest China. *Environ. Sci. Pollut. Res.* 27, 25163–25172. doi: 10.1007/s11356-020-08724-1

Roose-Amsaleg, C., David, V., Alliot, F., Guigon, E., Crouzet, O., and Laverman, A. M. (2021). Synergetic effect of antibiotic mixtures on soil bacterial N2O-reducing communities. *Environ. Chem. Lett.* 19, 1873–1878. doi: 10.1007/s10311-020-01117-3

Shabarova, T. (2013). Life in subsurface pools: Insight into microbial diversity and dynamics in the endokarst environment zur Erlangung der naturwissenschaftlichen Doktorwürde

Shabarova, T., Villiger, J., Morenkov, O., Niggemann, J., Dittmar, T., and Pernthaler, J. (2014). Bacterial community structure and dissolved organic matter in repeatedly flooded subsurface karst water pools. *FEMS Microbiol. Ecol.* 89, 111–126. doi: 10.1111/1574-6941.12339

Slipko, K., Marano, R. B., Cytryn, E., Merkus, V., Wögerbauer, M., Krampe, J., et al. (2021). Effects of subinhibitory quinolone concentrations on functionality, microbial community composition, and abundance of antibiotic resistant bacteria and qnrS in activated sludge. *J. Environ. Chem. Eng.* 9:104783. doi: 10.1016/j.jece.2020.104783

Stegen, J. C., Lin, X., Fredrickson, J. K., Chen, X., Kennedy, D. W., Murray, C. J., et al. (2013). Quantifying community assembly processes and identifying features that impose them. *ISME J.* 7, 2069–2079. doi: 10.1038/ismej.2013.93

Subirats, J., Di Cesare, A., Varela Della Giustina, S., Fiorentino, A., Eckert, E. M., Rodriguez-Mozaz, S., et al. (2019). High-quality treated wastewater causes remarkable changes in natural microbial communities and intI1 gene abundance. *Water Res.* 167:114895. doi: 10.1016/j.watres.2019.114895

Sun, P., He, S., Yu, S., Pu, J., Yuan, Y., and Zhang, C. (2021). Dynamics in riverine inorganic and organic carbon based on carbonate weathering coupled with aquatic photosynthesis in a karst catchment. *Southwest China. Water Res.* 189:116658. doi: 10.1016/j.watres.2020.116658

Sun, P., He, S., Yuan, Y., Yu, S., and Zhang, C. (2019). Effects of aquatic phototrophs on seasonal hydrochemical, inorganic, and organic carbon variations in a typical karst basin, Southwest China. *Environ. Sci. Pollut. Res.* 26, 32836–32851. doi: 10.1007/s11356-019-06374-6

Sun, J., Luo, Q., Wang, D., and Wang, Z. (2015). Occurrences of pharmaceuticals in drinking water sources of major river watersheds. *China. Ecotoxicol. Environ. Saf.* 117, 132–140. doi: 10.1016/j.ecoenv.2015.03.032

Tang, J., Tang, X., Qin, Y., He, Q., Yi, Y., and Ji, Z. (2019). Karst rocky desertification progress: Soil calcium as a possible driving force. *Sci. Total Environ.* 649, 1250–1259. doi: 10.1016/j.scitotenv.2018.08.242

Tanikawa, D., Nakamura, Y., Tokuzawa, H., Hirakata, Y., Hatamoto, M., and Yamaguchi, T. (2018). Effluent treatment in an aquaponics-based closed aquaculture system with single-stage nitrification–denitrification using a down-flow hanging sponge reactor. *Int. Biodeterior. Biodegrad.* 132, 268–273. doi: 10.1016/j.ibiod.2018.04.016

Tate, R.L. (2020). *Soil Microbiology*, *1st* New York: Wiley.

Torres, N. I., Yu, X., Padilla, I. Y., Macchiavelli, R. E., Ghasemizadeh, R., Kaeli, D., et al. (2018). The influence of hydrogeological and anthropogenic variables on phthalate contamination in eogenetic karst groundwater systems. *Environ. Pollut.* 237, 298–307. doi: 10.1016/j.envpol.2018.01.106

Webster, K. D., Drobniak, A., Etiope, G., Mastalerz, M., Sauer, P. E., and Schimmelmann, A. (2018). Subterranean karst environments as a global sink for atmospheric methane. *Earth Planet. Sci. Lett.* 485, 9–18. doi: 10.1016/j.epsl.2017.12.025

Wu, X., Wu, L., Liu, Y., Zhang, P., Li, Q., Zhou, J., et al. (2018). Microbial Interactions With Dissolved Organic Matter Drive Carbon Dynamics and Community Succession. *Front. Microbiol.* 9:1234. doi: 10.3389/fmicb.2018.01234

Xi, X., Wang, M., Chen, Y., Yu, S., Hong, Y., Ma, J., et al. (2015). Adaption of the microbial community to continuous exposures of multiple residual antibiotics in sediments from a salt-water aquacultural farm. *J. Hazard. Mater.* 290, 96–105. doi: 10.1016/j.jhazmat.2015.02.059

Xiang, S., Wang, X., Ma, W., Liu, X., Zhang, B., Huang, F., et al. (2020). Response of microbial communities of karst river water to antibiotics and microbial source tracking for antibiotics. *Sci. Total Environ.* 706:135730. doi: 10.1016/j.scitotenv.2019.135730

Xiong, W., Sun, Y., Zhang, T., Ding, X., Li, Y., Wang, M., et al. (2015). Antibiotics, Antibiotic Resistance Genes, and Bacterial Community Composition in Fresh Water Aquaculture Environment in China. *Microb. Ecol.* 70, 425–432. doi: 10.1007/s00248-015-0583-x

Xue, Y., Tian, J., Quine, T. A., Powlson, D., Xing, K., Yang, L., et al. (2020). The persistence of bacterial diversity and ecosystem multifunctionality along a disturbance intensity gradient in karst soil. *Sci. Total Environ.* 748:142381. doi: 10.1016/j.scitotenv.2020.142381

Yan, L., Herrmann, M., Kampe, B., Lehmann, R., Totsche, K. U., and Küsel, K. (2020). Environmental selection shapes the formation of near-surface groundwater microbiomes. *Water Res.* 170:115341. doi: 10.1016/j.watres.2019.115341

Yang, X., Song, X., Hallerman, E., and Huang, Z. (2020). Microbial community structure and nitrogen removal responses of an aerobic denitrification biofilm system exposed to tetracycline. *Aquaculture* 529:735665. doi: 10.1016/j.aquaculture.2020.735665

Yuan, D. X. (1997). Rock desertification in the subtropical karst of South China. *Ztschrift Geomorphol.* 108:81–90.

Yun, Y., Wang, H., Man, B., Xiang, X., Zhou, J., Qiu, X., et al. (2016). The Relationship between pH and Bacterial Communities in a Single Karst Ecosystem and Its Implication for Soil Acidification. *Front. Microbiol*, 7: 1955. doi: 10.3389/fmicb.2016.01955

Zeng, S., Xu, Z., Wang, X., Liu, W., Qian, L., Chen, X., et al. (2019). Time series analysis of antibacterial usage and bacterial resistance in China: observations from a tertiary hospital from 2014 to 2018. *Infect. Drug Resist.* 12, 2683–2691. doi: 10.2147/IDR.S220183

Zhang, Y., Ji, T., Jiang, Y., Zheng, C., Yang, H., and Liu, Q. (2022). Long-term effects of three compound probiotics on water quality, growth performances, microbiota distributions and resistance to Aeromonas veronii in crucian carp Carassius auratus gibelio. *Fish Shellfish Immunol.* 120, 233–241. doi: 10.1016/j.fsi.2021.11.036

Zhang, B., Li, Y., Xiang, S., Yan, Y., Yang, R., Lin, M., et al. (2020). Sediment Microbial Communities and Their Potential Role as Environmental Pollution Indicators in Xuande Atoll. *South China Sea. Front. Microbiol.* 11:1011. doi: 10.3389/fmicb.2020.01011

Zhang, B., Qin, S., Guan, X., Jiang, K., Jiang, M., and Liu, F. (2021). Distribution of Antibiotic Resistance Genes in Karst River and Its Ecological Risk. *Water Res.* 203:117507. doi: 10.1016/j.watres.2021.117507

Zhang, Y., Xie, J., Liu, M., Tian, Z., He, Z., van Nostrand, J. D., et al. (2013). Microbial community functional structure in response to antibiotics in pharmaceutical wastewater treatment systems. *Water Res.* 47, 6298–6308. doi: 10.1016/j.watres.2013.08.003

Zhao, Y., Gu, X., Gao, S., Geng, J., and Wang, X. (2012). Adsorption of tetracycline (TC) onto montmorillonite: Cations and humic acid effects. *Geoderma* 183-184, 12–18. doi: 10.1016/j.geoderma.2012.03.004

Zhernakova, A., Kurilshikov, A., Bonder, M. J., Tigchelaar, E., Schirmer, M., Vatanen, T., et al. (2016). Population-based metagenomics analysis reveals markers for gut microbiome composition and diversity. *Science* 352, 565–569. doi: 10.1126/science.aad3369

Zhong, Y., Yang, Q., Fu, G., Xu, Y., Cheng, Y., Chen, C., et al. (2018). Denitrifying microbial community with the ability to bromate reduction in a rotating biofilm-electrode reactor. *J. Hazard. Mater.* 342, 150–157. doi: 10.1016/j.jhazmat.2017.08.019

Zhou, J., and Xing, J. (2021). Haloalkaliphilic denitrifiers-dependent sulfate-reducing bacteria thrive in nitrate-enriched environments. *Water Res.* 201:117354. doi: 10.1016/j.watres.2021.117354

Zhu, H., Jiang, C., and Liu, S. (2022). Microbial roles in cave biogeochemical cycling. *Front. Microbiol.* 13:950005. doi: 10.3389/fmicb.2022.950005

Zhu, Z., Wang, J., Hu, M., and Jia, L. (2019). Geographical detection of groundwater pollution vulnerability and hazard in karst areas of Guangxi Province. *China Environ. Pollut.* 245, 627–633. doi: 10.1016/j.envpol.2018.10.017

frontiers | Frontiers in Microbiology

TYPE Original Research
PUBLISHED 17 April 2023
DOI 10.3389/fmicb.2023.1103550

OPEN ACCESS

EDITED BY
Qiang Li,
Chinese Academy of Geological Sciences, China

REVIEWED BY
Yuejun He,
Institute of Soil Science, Guizhou University, China
Sara Fareed Mohamed Wahdan,
Suez Canal University, Egypt

*CORRESPONDENCE
Xiankun Li
xiankunli@163.com

SPECIALTY SECTION
This article was submitted to Terrestrial Microbiology, a section of the journal Frontiers in Microbiology

RECEIVED 20 November 2022
ACCEPTED 15 March 2023
PUBLISHED 17 April 2023

CITATION
Zhang X, Wang B, Chen T, Guo Y and Li X (2023) Revealing the relative importance among plant species, slope positions, and soil types on rhizosphere microbial communities in northern tropical karst and non-karst seasonal rainforests of China.
Front. Microbiol. 14:1103550.
doi: 10.3389/fmicb.2023.1103550

Revealing the relative importance among plant species, slope positions, and soil types on rhizosphere microbial communities in northern tropical karst and non-karst seasonal rainforests of China

Xingming Zhang[1,2], Bin Wang[1,3], Ting Chen[1,3], Yili Guo[1,3] and Xiankun Li[1,3]*

[1]Guangxi Key Laboratory of Plant Conservation and Restoration Ecology in Karst Terrain, Guangxi Institute of Botany, Guangxi Zhuang Autonomous Region and Chinese Academy of Sciences, Guilin, China, [2]College of Urban Construction, Wuchang Shouyi University, Wuhan, China, [3]Nonggang Karst Ecosystem Observation and Research Station of Guangxi, Chongzuo, Guangxi, China

Rhizosphere microbes have an extremely close relationship with plants and the study on the relationship between rhizosphere microorganisms and their influencing factors is conducive to the protection of vegetation and the maintenance of biodiversity. Here we investigated how plant species, slope positions and soil types affect the rhizosphere microbial community. Slope positions and soil types were collected from northern tropical karst and non-karst seasonal rainforests. The results indicated that soil types played a predominant role in the development of rhizosphere microbial communities (28.3% of separate contribution rate), more than plant species identity (10.9% of separate contribution rate) and slope position (3.5% of separate contribution rate). Notably, environmental factors closely related to soil properties were the major influence factors that controlling the rhizosphere bacterial community structure in the northern tropical seasonal rainforest, especially pH. Additionally, plant species also influenced the rhizosphere bacterial community. In low nitrogen content soil environments, rhizosphere biomarkers of dominant plant species were often nitrogen-fixing strains. It suggested that plants might have a selective adaptation mechanism to rhizosphere microorganisms to obtain the advantages of nutrient supply. Overall, soil types exerted the biggest influence on rhizosphere microbial community structure, followed by plant species and finally slope positions.

KEYWORDS

rhizosphere microbial community, northern tropical seasonal rainforest, soil types, plant species, slope positions, relative importance

1. Introduction

The rhizosphere, a small volume of soil surrounding and influenced by plant roots, is the most dynamic habitat and is regarded as the most important zone and one of the most complicated ecosystems on Earth (Hinsinger et al., 2009; Mendes et al., 2013). Rhizosphere microbes have an extremely close relationship with plants. Due to this, they are thought to be the

second genome of the plant (Berendsen et al., 2012; Saleem et al., 2016). The development of plants is subjected to internal signals, depending on the provided mineral nutrients through the rhizosphere (from soil to the roots) (Dakora and Phillips, 2002). Thus, the rhizosphere environment provides unique and fundamental points of plant-microbial symbioses (Hao et al., 2016). Bacteria, as the primary component of rhizosphere microbiome food webs, play an important role in the nutrient cycle in the rhizosphere. This is the key to the isolation of prospective biotransformation strains, agricultural practices, and potential biocontrol strains (Maurhofer et al., 2004; Hao et al., 2008, 2009). Despite the importance of rhizosphere microbes, the relative importance of various factors and combined effects affecting the structure of rhizosphere microbial communities are still poorly understood (Igwe and Vannette, 2019).

Plants can produce an effect on the rhizosphere microbial community structure and activity. This is based on their behavior of secreting photosynthetically fixed carbon in the rhizosphere (Berendsen et al., 2012). Furthermore, plant rhizosphere exudates can also play a regulating role in the type and composition of microorganisms. For example, studies on potato rhizosphere exudates have shown that the photosynthetic products of rhizosphere exudates are different in different varieties of potatoes and different growth stages, which in turn have a greater impact on the rhizosphere microbial community (Gschwendtner et al., 2011). Plants also affect rhizosphere microorganisms through the generation of biological signals. Studies have shown that when the leaves of *Arabidopsis thaliana* are infected, they conduct biological signals to their roots and induce the release of malic acid, and the aggregation of malic acid in the rhizosphere promotes the aggregation of beneficial bacteria, thereby enhancing the disease resistance of *Arabidopsis thaliana* (Lakshmanan et al., 2012). In addition to plant traits, such as plant species characteristics and rhizosphere secretions, which have significant influences on rhizosphere microbial community structure, other investigations have shown that the physicochemical properties of rhizosphere soil also play a key decisive role.

Indeed, rhizosphere microbes are highly dependent on soil abiotic environmental factors. Previous studies have investigated the relationships between soil biogeochemical properties and microbial community, such as ammonium nitrogen (AN), soil organic matter, available K and N, pH, and nutrient content (Gu et al., 2018; Nan et al., 2020). Some scholars studied the effects of three types of slope aspects on soil bacteria and arbuscular mycorrhizal fungal communities in a boreal forest of the Greater Khingan Mountains and found that soil pH and substratum shrub biomass were significantly correlated with bacterial communities, and soil available phosphorus and shrub biomass were significantly correlated with arbuscular mycorrhizal fungal communities. In addition, they found that slope aspects affected bacterial and AMF communities, mediated by aspect-induced changes in plant community and soil chemical properties (Chu et al., 2016). Thus, in addition to the plant traits, such as plant species characteristics and rhizosphere secretions, soil biogeochemical properties and slope aspects also have a considerable impact on the rhizosphere microbial community, a better understanding of the relative importance of these three factors and their combined effect is essential. Although some of the previous studies have addressed the effect of plant species or rhizosphere biogeochemical properties on rhizosphere microbial community composition and diversity, they have mostly emphasized crop plants with cultivation-based approaches in long-term treated soils (Pii et al., 2016; Leff et al., 2018). The rhizosphere microbial community is very complicated, so only a few studies based on the culture-independent approach have focused on natural plant species (Hao et al., 2016). Recently, with the introduction of PCR-based and high-throughput sequencing technologies, a new molecular view of the microbial world is rendered on the ground that it has improved the feature of natural microbial communities in complex environments such as rhizosphere soil (Lynch and Neufeld, 2015).

Northern tropical seasonal rain forest includes karst seasonal rain forest and non-karst seasonal rain forest. It is a unique and huge treasure pool of biological diversity in the southwest karst area of China and one of the global biodiversity hotspots (Myers et al., 2000). The same period of rain and heat climatic conditions, the low soil formation rate, and other natural processes in this region have given rise to serious soil erosion in the karst area as well as difficulty in vegetation restoration (Jiang et al., 2014). Since there is no anthropogenic disturbance for over 100 years, this reserve has the most typical and aboriginal karst seasonal rainforest in China (Guo et al., 2018). The study of the northern tropical karst seasonal rainforest could help deepen the conservation and maintenance of the seasonal rainforest biodiversity. However, as to the northern tropical seasonal rainforest, there is very limited knowledge on the relationship of the rhizosphere microbial community composition with diversity with the dominant species in virgin forests. Moreover, it is still unclear about the combined effects and relative importance of various factors that affect the structure of the rhizosphere microbial community (Liu et al., 2020).

In this study, based on the high-throughput sequencing technology and multiple regression analysis, the relative importance and effects of plant species, slope positions, and soil types on the rhizosphere microbial community of the northern tropical seasonal rainforest were studied. This research would enhance the conservation and maintenance of the seasonal rainforest biodiversity in the southwest karst area of China.

2. Materials and methods

2.1. Sample site

The northern tropical seasonal rainforest of China is a zonal vegetation type of northern tropics in south Guangxi (Wang et al., 2001), which include karst and non-karst seasonal rainforest in the acid soil region. At the end of August 2016, 48 soil samples, including 39 rhizosphere soil samples and nine non-rhizosphere soil samples, were collected from the northern tropical seasonal rainforest of China at two sites in Guangxi Province: (a) Nonggang Northern Tropical Karst Seasonal Rainforest Dynamics Plot (106.95°E, 22.43°N, 15 ha, Figure 1) and (b) Fangcheng Northern Tropical Seasonal Rainforest Dynamics Plot (108.136°E, 21.775°N, 1 ha, Figure 1). Site A was located inside Nongang National Nature Reserve, which was typical karst peak-cluster depression landform with karst lime soil (Wang et al., 2014). Sample site B was located inside Fangcheng *Camellia nitidissima Chi* National Nature Reserve, which was a non-karst area. The landform type was coastal hills and mesas (Huang et al., 2013), and the soil type was laterite and brick red soil formed from granite, sand shale, mudstone, and conglomerate (Huang, 2000).

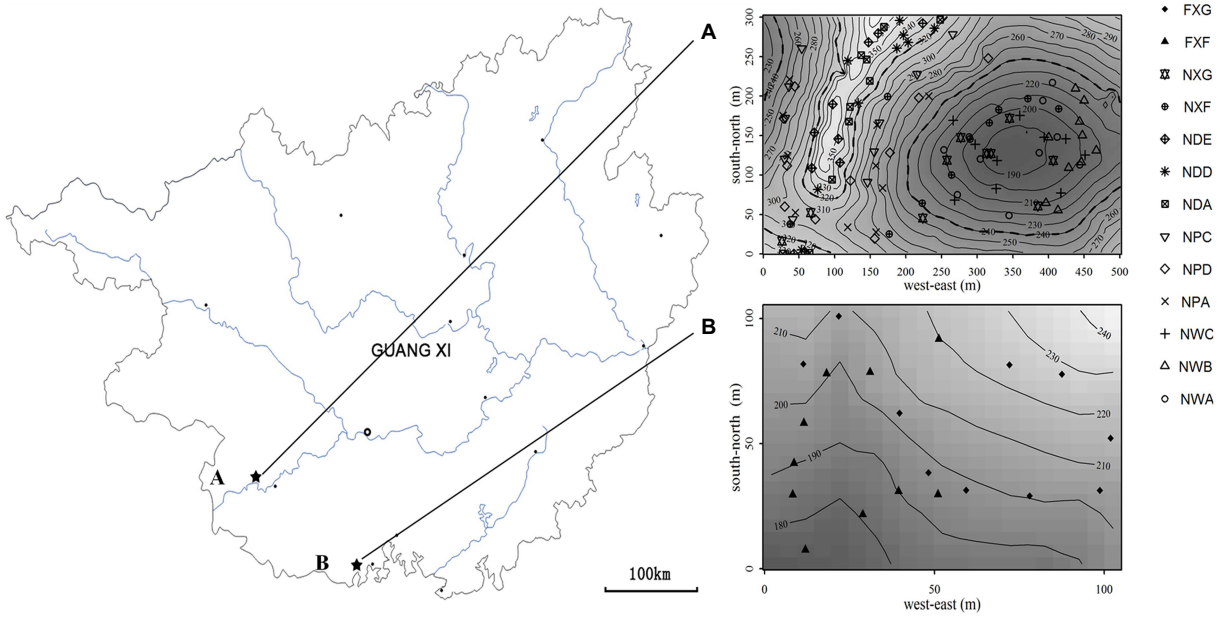

FIGURE 1
Locations of the sampling sites in two plots in Guangxi province (R software (version 3.3.0) was employed to produce Maps). A: Nonggang northern tropical karst seasonal rainforest dynamics plot; **(A)**: sampling points of the Nonggang plot. B: Fangcheng northern tropical seasonal rainforest dynamics plot; **(B)**: sampling points of the Fangcheng plot.

2.2. Experimental design

Sample site A was divided into the following three slope positions: around the shoulder, the back slope, and the toe slope. The rhizosphere soil was collected from the dominant species and common species in each slope position. Two common species of rhizosphere soil were gathered at both sites (Table 1). The experimental groups were as follows: (1) NWA, NWB, and NWC, which were sampled around the toe slope in site A and represented the rhizosphere of *Sterculia monosperma*, *Saraca dives*, and *Catunaregam spinosa*, respectively; (2) NPA, NPD, and NPC, which were sampled in the back slope and represented the rhizosphere of *Sterculia monosperma*, *Excentrodendron tonkinensis*, and *Catunaregam spinosa*, respectively; (3) NDA, NDD, and NDE, which were sampled around the shoulder and represented the rhizosphere of *Sterculia monosperma*, *Excentrodendron tonkinensis*, and *Boniodendron minius*, respectively; (4) NXF and NXG, which were sampled from site A and represented the rhizosphere of *Wendlandia uvariifolia* and *Bridelia balansae*; (5) FXF and FXG, which were sampled from site B and represented the rhizosphere of *Wendlandia uvariifolia* and *Bridelia balansae*; (6) NWK, NPK, and NDK represented non-rhizosphere soil samples and were collected for each slope position in site A as control groups.

2.3. Sample collection and DNA extraction

The plants are aged 8–20 years. Roots, rock, and large chunks of non-rooted soil were moved away. The collection of rhizosphere samples was made in triplicate from 10 individual plants of each species within the field of 15 ha and 1 ha (Figure 1). The control groups at each slope position were sampled at 10 spots in triplicate using the "S"-shaped sampling method. Rhizosphere samples and control samples were divided into two parts, one part for the analysis of biogeochemical properties and the other stored at −80°C for nucleic acid analyses. Genomic DNA from soil samples was extracted by applying the PowerSoil DNA Isolation Kit (MoBio Laboratories, Carlsbad, CA). Agarose gel electrophoresis was applied to examine DNA, and the NanoDrop spectrophotometer was employed to check its purity.

2.4. Analysis method

From each sampling site, a composite sample was obtained by gathering and mixing three soil samples. After oven drying part of the samples at 105°C to a constant weight, it was weighed for the determination of moisture content (MC). For pH, soil organic carbon (SOC), total nitrogen (TN), total phosphorus (TP), hydrolyzable nitrogen (HN), and available phosphate (AP) measurements, part of the soil samples were manually separated to visually remove stones, plant roots, and litter, and then sieved through a 0.25 mm mesh. An FE20 pH meter (Mettler Toledo, Shanghai, China) was adopted to measure soil pH values at a soil-to-water (deionized) ratio of 1: 2.5. The $K_2Cr_2O_7/H_2SO_4$ oxidation method was employed to determine SOC concentrations. The Kjeldahl method was employed to determine TN concentrations, and the sodium hydroxide (NaOH) fusion and Mo–Sb colorimetric methods were used to measure TP concentrations (Jiang et al., 2017). HN was determined using the Illinois Soil N Test (ISNT) method (Roberts et al., 2009). AP was determined by the $NaHCO_3$ procedure and heteropoly molybdenum blue method (Mussa et al., 2009). Calcium (Ca) and magnesium (Mg) were determined based on chemical methods (Lu, 2000). Each experiment

TABLE 1 Samples description.

Groups	Samples sites	Slope positions	Soil types	Cover plants
NWA	Nonggang Northern Tropical Karst Seasonal Rainforest Dynamics Plot	Toe slope	Lime soil	*Sterculia monosperma*
NWB	Nonggang Northern Tropical Karst Seasonal Rainforest Dynamics Plot	Toe slope	Lime soil	*Saraca dives*
NWC	Nonggang Northern Tropical Karst Seasonal Rainforest Dynamics Plot	Toe slope	Lime soil	*Catunaregam spinosa*
NWK	Nonggang Northern Tropical Karst Seasonal Rainforest Dynamics Plot	Toe slope	Lime soil	none
NPA	Nonggang Northern Tropical Karst Seasonal Rainforest Dynamics Plot	Back slope	Lime soil	*Sterculia monosperma*
NPD	Nonggang Northern Tropical Karst Seasonal Rainforest Dynamics Plot	Back slope	Lime soil	*Excentrodendron tonkinense*
NPC	Nonggang Northern Tropical Karst Seasonal Rainforest Dynamics Plot	Back slope	Lime soil	*Catunaregam spinosa*
NPK	Nonggang Northern Tropical Karst Seasonal Rainforest Dynamics Plot	Back slope	Lime soil	none
NDA	Nonggang Northern Tropical Karst Seasonal Rainforest Dynamics Plot	Shoulder	Lime soil	*Sterculia monosperma*
NDD	Nonggang Northern Tropical Karst Seasonal Rainforest Dynamics Plot	Shoulder	Lime soil	*Excentrodendron tonkinense*
NDE	Nonggang Northern Tropical Karst Seasonal Rainforest Dynamics Plot	Shoulder	Lime soil	*Boniodendron minius*
NDK	Nonggang Northern Tropical Karst Seasonal Rainforest Dynamics Plot	Shoulder	Lime soil	none
NXF	Nonggang Northern Tropical Karst Seasonal Rainforest Dynamics Plot	Toe slope	Lime soil	*Wendlandia uvariifolia*
NXG	Nonggang Northern Tropical Karst Seasonal Rainforest Dynamics Plot	Toe slope	Lime soil	*Bridelia balansae*
FXF	Fangcheng Northern Tropical Seasonal Rainforest Dynamics Plot	Back slope	Laterite and brick red soil	*Wendlandia uvariifolia*
FXG	Fangcheng Northern Tropical Seasonal Rainforest Dynamics Plot	Toe slope	Laterite and brick red soil	*Bridelia balansae*

was conducted three times in parallel, and the results are indicated in Table 2.

2.5. Sequencing by synthesis

PCR used primers 341F-806R with the barcode was employed to amplify the variable region V3-4 of the 16S rRNA gene. The resulting amplicons were sequenced on the Illumina HiSeq2500 platform, and Novogene Bioinformatics Technology Co. (Beijing, China) generated 250 bp paired-end reads (Caporaso et al., 2011, 2012).

2.6. Sequence analysis

Paired-end reads were distributed to samples based on their unique barcode and merged by adopting FLASH (V1.2.7). The high-quality clean tags (Bokulich et al., 2013) were gained according to QIIME (V1.7.0) (Caporaso et al., 2010) quality-controlled process under specific filtering conditions. Effective tags were finally gained by filtering chimera sequences (Edgar et al., 2011). Uparse software (Uparse v7.0.1001) (Edgar, 2013) was employed to carry out sequence analyses, and taxonomic information was annotated by adopting GreenGene Database (DeSantis et al., 2006) based on the RDP classifier (version 2.2) (Wang et al., 2007). Sequences with at least 97% similarity were clustered into the same OTUs. MUSCLE software (version 3.8.3) was used to make multiple sequence alignments to research the phylogenetic relationships among different OTUs and the difference of the predominant species in different samples (Edgar, 2004).

2.7. Diversity and statistical analysis

The calculation of alpha-diversity measures, including the Shannon diversity index (Magurran, 1988), Chao1 richness estimator

TABLE 2 Mean biogeochemical properties of samples collected in two plots.

Sample sites	Moisture content (%)	Total nitrogen (gkg^{-1})	Total phosphorus (gkg^{-1})	Organic Carbon (%)	Hydrolyzable nitrogen ($mgkg^{-1}$)	Available phosphate ($mgkg^{-1}$)	pH water (1:2.5)	Calcium (gkg^{-1})	Magnesium (gkg^{-1})
NWA	39.37 ± 0.13	14.64 ± 0.03	2.87 ± 0.02	6.99 ± 0.03	234.5 ± 3.97	5.16 ± 0.10	7.99 ± 0.05	18.89 ± 0.14	10.24 ± 0.03
NWB	39.91 ± 0.60	13.86 ± 0.12	1.88 ± 0.03	5.95 ± 0.04	254.1 ± 8.48	22.23 ± 0.06	7.69 ± 0.04	17.93 ± 0.03	12.07 ± 0.05
NWC	41.32 ± 0.99	14.51 ± 0.07	3.37 ± 0.09	7.19 ± 0.06	368.2 ± 3.80	17.91 ± 0.09	7.83 ± 0.02	20.98 ± 0.08	11.51 ± 0.08
NWK	37.48 ± 0.10	13.47 ± 0.02	1.88 ± 0.05	5.07 ± 0.03	273.0 ± 6.37	18.90 ± 0.11	7.99 ± 0.03	18.96 ± 0.03	9.68 ± 0.04
NPA	38.08 ± 0.14	15.94 ± 0.06	0.40 ± 0.05	5.87 ± 0.02	287.0 ± 1.68	5.14 ± 0.09	8.07 ± 0.01	20.12 ± 0.10	6.52 ± 0.05
NPD	29.67 ± 0.05	13.60 ± 0.09	0.40 ± 0.01	5.78 ± 0.01	203.0 ± 2.76	0.83 ± 0.08	8.05 ± 0.02	17.98 ± 0.08	10.90 ± 0.20
NPC	33.82 ± 0.08	17.75 ± 0.10	0.89 ± 0.02	6.50 ± 0.01	303.8 ± 7.18	6.17 ± 0.11	8.59 ± 0.03	15.87 ± 0.03	6.01 ± 0.06
NPK	31.94 ± 0.27	17.62 ± 0.06	0.89 ± 0.05	6.08 ± 0.02	266.0 ± 5.60	1.17 ± 0.07	8.23 ± 0.02	18.98 ± 0.06	7.87 ± 0.07
NDA	29.23 ± 0.37	18.14 ± 0.06	2.38 ± 0.04	11.21 ± 0.01	318.5 ± 4.20	1.50 ± 0.05	8.31 ± 0.03	22.99 ± 0.06	7.88 ± 0.03
NDD	30.25 ± 0.81	18.66 ± 0.13	0.40 ± 0.02	11.82 ± 0.11	326.2 ± 0.46	1.08 ± 0.12	8.27 ± 0.03	28.28 ± 0.04	3.98 ± 0.06
NDE	25.95 ± 0.13	18.14 ± 0.08	1.39 ± 0.02	9.97 ± 0.05	293.3 ± 0.53	1.08 ± 0.09	8.22 ± 0.03	19.94 ± 0.11	3.63 ± 0.04
NDK	25.75 ± 0.11	18.79 ± 0.17	0.89 ± 0.03	6.12 ± 0.02	266.0 ± 17.58	0.50 ± 0.02	8.29 ± 0.03	15.90 ± 0.14	7.23 ± 0.02
NXF	32.50 ± 0.05	18.92 ± 0.09	0.40 ± 0.03	7.17 ± 0.03	302.4 ± 4.88	1.05 ± 0.04	8.29 ± 0.02	21.71 ± 0.07	7.97 ± 0.12
NXG	43.92 ± 0.10	20.22 ± 0.05	2.38 ± 0.10	11.24 ± 0.01	360.5 ± 2.25	8.71 ± 0.05	8.39 ± 0.02	24.97 ± 0.13	10.29 ± 0.05
FXF	32.90 ± 0.10	18.53 ± 0.10	0.89 ± 0.03	6.56 ± 0.02	308.0 ± 11.65	1.51 ± 0.08	5.76 ± 0.03	17.95 ± 0.07	6.04 ± 0.08
FXG	31.35 ± 0.06	16.97 ± 0.04	3.37 ± 0.04	4.75 ± 0.02	270.2 ± 4.48	0.63 ± 0.07	5.79 ± 0.04	15.57 ± 0.11	7.50 ± 0.07

10.3389/fmicb.2023.1103550

TABLE 3 Mean bacteria diversity index of the samples.

Sample name	OTUs	Shannon	Simpson	Ace	Chao1 richness estimator	PD whole tree	Good's coverage (%)
NWA	3311.33	9.27	0.9930	3347.80	3237.887	198.5860	97.13
NWB	3280.33	9.24	0.9943	3495.23	3392.368	191.6597	96.83
NWC	3108.00	9.18	0.9947	3141.87	3061.604	182.4097	97.27
NWK	3664.33	9.54	0.9947	4143.75	4072.341	222.0557	96.07
NPA	3464.00	9.65	0.9957	4390.37	5271.669	217.6163	95.73
NPD	3389.00	9.59	0.9957	3782.18	3718.123	209.1093	96.53
NPC	3265.00	9.45	0.9953	3283.17	3223.533	203.1617	97.17
NPK	3659.33	9.58	0.9953	3895.75	3755.389	215.9177	96.40
NDA	3362.67	9.69	0.9970	3511.51	3428.952	200.0757	97.00
NDD	3093.67	9.52	0.9967	3016.51	2996.649	183.8223	97.53
NDE	3216.33	9.64	0.9963	3459.30	3428.717	207.4817	97.00
NDK	3791.00	9.89	0.9970	3889.85	3804.239	215.0593	96.60
NXF	3709.67	9.71	0.9970	3978.43	3860.708	214.5317	96.30
NXG	3534.00	9.55	0.9960	3791.51	3708.465	202.2613	96.50
FXF	3728.00	9.16	0.9937	4090.29	3949.574	220.0440	96.07
FXG	2829.67	8.13	0.9877	2967.08	2831.888	166.9200	97.13

(Chao and Bunge, 2002), phylogenetic diversity (PD) index (Lozupone and Knight, 2008), and Good's coverage (Good, 1953), was made. All indices were shown with R software (version 2.15.3) and calculated with QIIME (version 1.7.0). An unweighted pair group approach with arithmetic means (UPGMA) was carried out to cluster samples by weighted UniFrac distances (Johnson et al., 2003). Principal coordinates analysis (PCoA) applying unweighted UniFrac metrics was carried out to distinguish the distribution patterns of the bacterial community composition among the samples. The Mantel test and CCA were adopted to assess the linkages of the rhizosphere bacterial community structure with rhizosphere biogeochemical properties. CCA was conducted by applying functions in the Vegan package (version 2.3–0) of the R project (version 3.2.2).

2.8. Accession number(s)

The nucleotide sequences observed during this research have been stored in the NCBI database under the accession number SRP158785.

3. Results

3.1. General statistics analysis for 16S rRNA gene sequences and taxonomic compositions of the microbe communities

The total number of 16S rRNA tags gained from the 48 samples, after splicing, quality control, and filtering chimera, was 2,674,104, which were clustered into 163,219 operational taxonomic units (OTUs) with at least 97% sequence similarity in nucleotide identity, and those data were subjected for further statistical analyses (Table 3). The results suggested that Chao1 and ACE indices were between 2831.888–5271.669 and 2967.08–4390.37, respectively. It indicated a good richness of samples. Goods coverage was more than 0.955, indicating that the sequencing results could represent the sample microbial real situation.

There were small gaps among rhizospheres microbial community richness index, ACE, and Chao1 of three plants under the same slope position(NWA, NWB, and NWC)in site A, while these indices of the same plant at different slope positions(NWA, NPA, and NDA)had a greater gap, but the indices of NPA were the highest. Shannon and Simpson diversity indices integrating evenness and species richness were comparable in NWA, NWB, and NWC. These two indices were higher in NDA and NPA than in NWA ones (Table 3). These results showed that slope positions could generate an effect on rhizosphere microbial diversity. By comparing the ACE and Chao1 indices of the same plant in the different soil types (NXF and FXF), we discovered that the indices of NXF were higher than those of FXF. In addition, the Shannon diversity indices of NXF (9.71) were higher than FXF (9.16), and the Shannon diversity indices of NXG (9.55) were greater than FXG (8.13). Such results indicated that soil types might have a significant relation with the rhizosphere microbial diversity.

Operational taxonomic units were further classified into different taxa, and the estimation of their relative taxonomic abundance was made across different rhizospheres. A total of 100 bacteria classes were belonging to at least 48 phyla identified, including several unknown groups. The top 10 phyla with the highest relative abundance were *Acidobacteria, Proteobacteria, Actinobacteria, Nitrospirae, Thaumarchaeota, Verrucomicrobia, Latescibacteria, Gemmatimonadetes, Chloroflexi,* and *Bacteroidetes*. The *Proteobacteria* stood for the highest number of tags in rhizospheres and occupied at least 45.66% of the total bacteria population in samples, followed by *Acidobacteria* (34.21%), *Actinobacteria* (10.40%), and *Nitrospirae*

(9.73%) (Figure 2). In the lime soil samples (NXF and NXG), *Proteobacteria* was the most abundant phylum with a content of 48.19 and 46.44%, respectively. In the laterite and brick red soil samples (FXF and FXG), *Acidobacteria* was the most abundant phylum with 42.12 and 53.58%, respectively. The foregoing results showed that there might be a causal relationship between various soil types with the dominant communities of rhizosphere microorganisms.

Further PCoA analysis (Figure 3) was done based on OTUs, and it showed that microbial communities in the laterite and brick red soil samples (FXF and FXG) were separated from the cluster representing microbial communities of the lime soil samples (NXF and NXG). In addition, the bacteria community compositions in the toe slope of site A were similar to that of the back slope and these two were very different from the shoulder in the same soil type, and those resulting from the planting of different plant species in the same slope position were also significantly different (NPA, NPC, and NPD). PERMANOVA and VPA analyses showed that rhizosphere microbial communities were significantly affected by plant species ($p < 0.001$), slope position ($p < 0.01$), and soil type ($p < 0.001$), and that the relative importance of soil type on microbial communities was the greatest, followed by plant species and slope position (Figure 4).

3.2. LEfSe (LDA effect size) analysis of bacterial communities among plant species, slope positions, and soil types

Linear discriminant analysis effect size was applied to the microbial data of the nine rhizosphere groups. Statistically different taxonomic clades with an LDA score higher than 4.0 (Figure 5) were found. The cladogram (Figures 5D–F) indicated that many taxa were common (shown in yellow), but some specific differences also existed.

The rhizosphere microbe of the *Sterculia monosperma*, *Saraca dives*, and *Catunaregam spinosa* (NWA, NWB, and NWC) were compared together to identify the impact of the different plant species in the same slope position and soil type on the bacterial community compositions (Figure 5A). The results suggested that the most differentially abundant bacterial taxa in these groups belonged to *unidentified_Acidobacteria*, *Betaproteobacteria*, and *Nitrospira* at the class level, respectively. At the order level, the enrichments of NWA, NWB, and NWC were *B1_7BS*, *Sh765B_TzT_29*, and *Nitrospirales*. It revealed that the influence of plant species on rhizosphere microbial community structure was still worth some attention.

The rhizosphere microbe of the *Sterculia monosperma* (NWA, NPA, and NDA) was compared together to identify the effect of the same plant species and soil type in different slope positions on the rhizosphere bacterial composition (Figure 5B). The outcomes revealed that the most differentially abundant bacterial taxa in NWA were *B1_7BS* and *Sh765B_TzT_29*, and in NDA were *Subgroup_6*, *Solirubrobacterales*, and *Sphingomonadales* at the order level. NPA enriched the family *0319_6A21* and the genus *Geobacter*. It indicated that slope positions might affect the rhizosphere microbial community structure of the same plant.

The rhizosphere microbe of the *Wendlandia uvariifolia* (NXF and FXF) and *Bridelia balansae* (NXG and FXG) in sites A and B were compared together to evaluate the difference in bacterial communities when the same species of plants lived in the different soil types (Figure 5C). NXF and FXF were located at different slope positions, while NXG and FXG were located at the same slope positions. The NXF rhizosphere generated a greatly higher relative abundance of the *Proteobacteria* phylum and *SC_I_84*, *Myxococcales*, and *Subgroup_4* orders, while the FXF rhizosphere had a higher relative abundance of the *Subgroup_3* and *Rhizobiales* orders, *unidentified_Acidobacteria* family, and *Candidatus_Solibacter* genus. The NXG rhizosphere enhanced the relative abundance of *Nitrospirae*, *Actinobacteria*, *Latescibacteria* Phyla, *Betaproteobacteria*, *Nitrospira*, *Deltaproteobacteria* and *Thermoleophilia* classes, *Subgroup_6*, *Nitrospirales*, *Sh765B_TzT_29*, *B1_7BS*, *Gaiellales* orders, and *0319_6A21* family. However, the FXG rhizosphere exhibited a higher relative abundance of the *Acidobacteria* phylum, the class *unidentified_Acidobacteria*, *Acidobacteriales*, and *Subgroup_2* orders, *DA111* and *Acidobacteriaceae__Subgroup_1* families, *Candidatus_Koribacter*, and *Acidibacter* genera. This result suggested that soil types could also affect the rhizosphere microbial community structure of the same plant.

3.3. CCA analysis of the biogeochemical properties of rhizosphere soil and bacterial community diversity

Nine variables, including pH, moisture content (MC), total nitrogen (TN), total phosphorus (TP), soil organic carbon (SOC), hydrolyzable nitrogen (HN), available phosphate (AP), calcium (Ca), and magnesium (Mg), were used in further CCA analysis. pH, MC, TN, TP, SOC, AP, Ca, and Mg were significant at all taxonomic levels ($p < 0.05$), except in the case of the TP at the genus level ($p = 0.085$). However, HN did not have a significant effect on the community structure ($p > 0.05$). HN was not a major factor for any of the groups at any taxonomic level (Figure 6). CCA of the relationships between the nine variables of biogeochemical properties in the rhizosphere and the bacteria community composition at different taxonomic levels revealed that community structures were most greatly influenced by pH. Among the explanatory variables, the order of influence was pH ($p < 0.01$) > MC ($p < 0.01$) > Mg ($p < 0.01$) > SOC ($p < 0.01$) (Figure 6).

4. Discussion

4.1. Plant species, slope positions, and soil types have different determinant roles in the rhizosphere microbial community structure

Under combined variations of plant species, slope positions, and soil types identity, the phenomenon was observed that the soil type was found to play a predominant role in the development of rhizosphere microbial communities (28.3% of separate contribution rate for bacteria), more than plant species identity (10.9% of separate contribution rate for bacteria) and slope position (3.5% of separate contribution rate for bacteria) (Figure 4). A few published reports have indicated that soil types have a greater effect on the root microbiota profiles than the plant species did (Bulgarelli et al., 2012; Lundberg et al., 2012; Veach

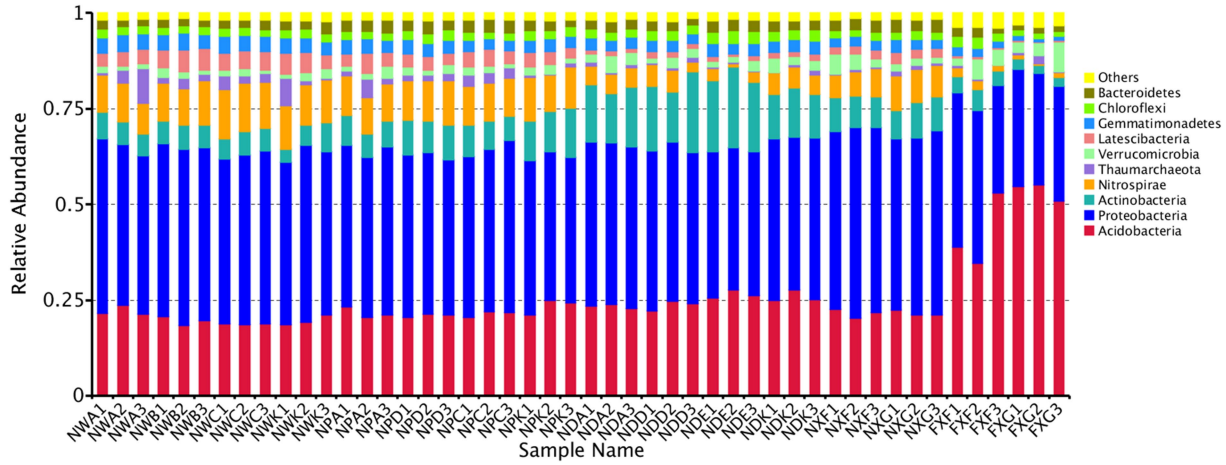

FIGURE 2
Microbe community structure is the 10 most abundant phyla in the 48 samples. All phyla were within the domain of *Bacteria*, except for the *Thaumarchaeota*, which was within the *Archaea*.

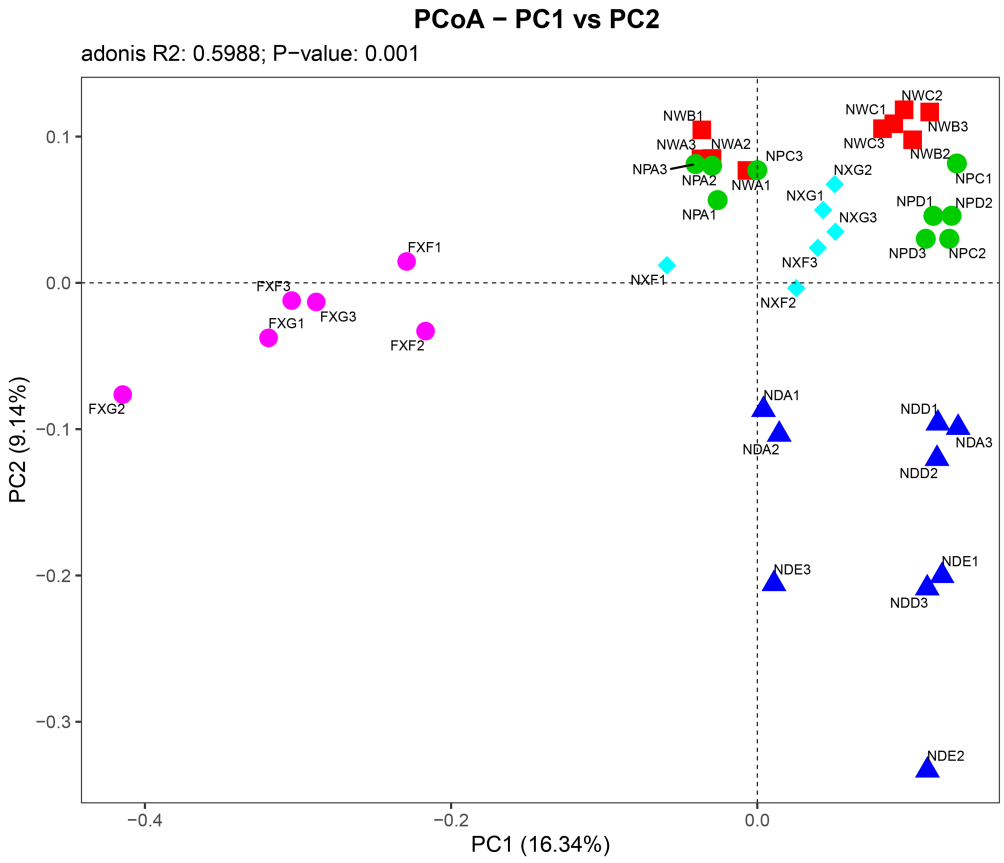

FIGURE 3
Associations between individual samples were explained by PCoA analysis. Symbols of the same color show sample from a similar habitat type and the distance between symbols display their dissimilarity. The detailed meaning of each sample was shown in Table 1, 1~3 represented three biological replicates.

et al., 2019). These reports were consistent with our results. However, many previous studies have shown that the influence of plant species on the rhizosphere microbial community is stronger than that of soil abiotic environment, or the influence of both is comparable. For example, Miethling et al. conducted experiments by collecting rhizosphere microorganisms of two plant species,

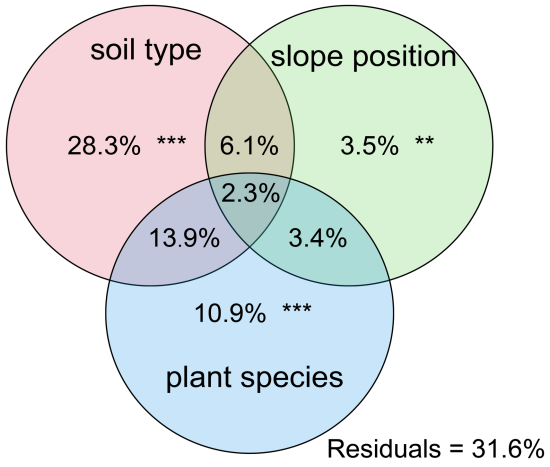

FIGURE 4
Contributions of soil type, slope position, and plant species on the assembly of soil bacterial communities were calculated based on variance partitioning analyses (VPAss), and *p*-value was determined by PERMANOVA.

alfalfa (Medicago sativa) and rye (Secale cereale), which grew on two kinds of soil collected from farmland in different locations, to compare the effects of plant species and soil types on plant root microbial communities. It was determined that plant species was the main determinant of microbial community characteristics, and soil was of minor importance (Miethling et al., 2000). Some scholars investigated the importance of pH, soil type, soil amendment, nutritional status of the plant, plant species, and plant age on the structure of the bacterial community in the rhizosphere by growing several kinds of different plant species (cucumber, barley, chickpea, canola, and Sudan grass) in three different soil types (sand, loam, and clay) and observed that many different factors will contribute to shaping the species composition in the rhizosphere, but that the plant itself exerts a highly selective effect that is at least as great as that of the soil(Marschner et al., 2004). Igwe and Vannette observed that plant species and soil type had comparable effects in structuring rhizoplane bacterial communities (Igwe and Vannette, 2019). Some researchers revealed that the soil type had a larger effect than plant species on fungal community composition, but the opposite was true for bacterial communities with a trap-plant bioassay experiment (Bonito et al., 2014). Our findings here are possibly due to (1) the influence of soil types on the rhizosphere microbial community structure under different geological backgrounds might be caused by the differences of nutrient elements, pH value, and other factors, which have more shaping effects than plants species and slope position; (2) different plants adaptively changed the composition of root exudates to absorb different microorganisms according to different slope environments, and the shaping effect was greater than that of slope environment (Figures 5A,B,D,E); and (3) although slope position has the least influence, it is worth noting that due to severe rain erosion and little soil retention, the rhizosphere microbial community compositions in the shoulder in karst areas were different from those of the back slope and toe slope (Figure 3).

4.2. The pH-based environmental factors were the main factors affecting the rhizosphere microbial community structure in the northern tropical seasonal rainforest

Microbial diversity analysis showed that the rhizosphere bacterial diversity was mostly affected by soil types. In further CCA analysis of rhizosphere soil biogeochemical properties and rhizosphere microbial community structure, pH was considered the most important variable factor governing the variation of the bacteria community structures in 48 samples gained from different types of northern tropical seasonal rainforests in China. Our results discovered great correlations between variable factors (pH, MC, Mg, and SOC) and the distributions of community composition (Figure 6). In those parameters, pH showed positive correlations with MC, Mg, and SOC across all samples. It was reported that microbial biogeography was controlled mainly by edaphic variables, and the biodiversity of soil bacterial communities differed by ecosystem type. Furthermore, these differences could largely be illustrated by soil pH (Fierer and Jackson, 2006), which produced a complicated effect on microbial communities by affecting the nutrients, microbial adsorption, etc. The pH value of the soil environment affected the migration and morphology of elements in the soil and was an important determinant of soil nutrient distribution.

Regarding microbial compositions of rhizospheres that developed in both sites, we found that the most dominant microbes showed significantly different relative abundances in the two soil types. This was observed for microbial phyla (Figure 2)，such as *Acidobacteria, Proteobacteria, Actinobacteria, Nitrospirae, Thaumarchaeota, Verrucomicrobia, Latescibacteria,* and *Gemmatimonadetes*, indicating that these phyla were sensitive to the soil biogeochemical properties factors even if the same plant species. For example, the relative abundance of *Acidobacteria* doubled. Since the soil at site B was laterite and brick red soil (pH <7), the *Acidobacteria* could adapt to the foregoing acidic environment. However, the core bacterial species did not change much. *Proteobacteria*, *Acidobacteria*, and *Actinobacteria* still occupied the top three positions. It was similar to the rhizosphere microorganisms of sugar beet plants analyzed by PhiloChip, except that the dominant ones were *Proteobacteria*, *Firmicutes*, and *Actinobacteria* (Mendes et al., 2011), which confirmed our conclusion. Previous studies have suggested that soil abiotic environmental factors affected rhizosphere microorganisms, which might be due to differences in the nutrient distribution in different habitats (Shi et al., 2011). In short, these results indicate that different soil biogeochemical property factors have distinct effects on rhizosphere microbial community structures.

4.3. Some plants in the northern tropical seasonal rainforest might resist the adverse effects of nutrient tolerance and gain ecological advantages by coexisting with specific rhizosphere microorganisms

The rhizosphere microbial population of *Catunaregam spinosa* (NWC) in site A had its specific biomarker *Nitrospirae*. We noted that *Nitrospirae* could convert ammonia and nitrite into nitrates in nature that could be used directly by plants and provide nitrogen for plants

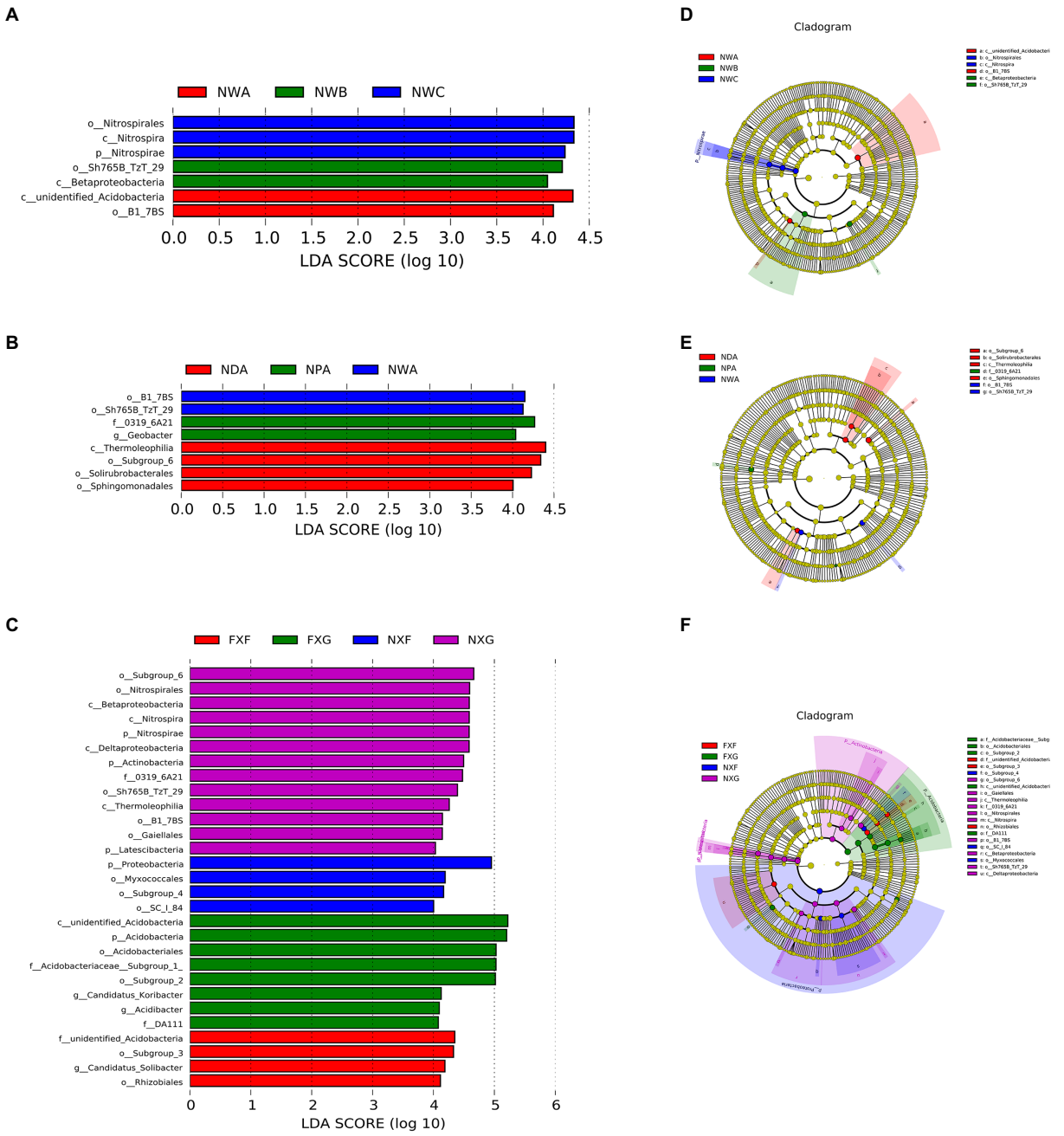

FIGURE 5
LDA value distribution histogram and evolutionary branches of LEfSe analysis. In the evolutionary cladogram, circles from inside to outside represented the classification level from the phylum to the species. Coloring principle: Species without great differences were uniformly colored yellow, and the Biomarker followed the group for coloration. The red node indicated that the microbial group played a significant role in the red group, and the green node indicated that the microbial group played a significant role in the green group. The blue node indicated that the microbial group played a significant role in the blue group, and the purple node indicated that the microbial group played a significant role in the purple group. **(A)**: LDA value distribution histogram of NWA, NWB, and NWC groups; **(B)**: LDA value distribution histogram of NDA, NPA, and NWA groups; **(C)**: LDA value distribution histogram of FXF, FXG, NXF, and NXG groups; **(D)**: Evolutionary cladogram of NWA, NWB, and NWC groups; **(E)**: Evolutionary cladogram of NDA, NPA, and NWA groups; **(F)**: Evolutionary cladogram of FXF, FXG, NXF, and NXG groups.

(Attard et al., 2010; Daebeler et al., 2014). The reason for the earlier phenomenon might be due to the low MC in the shoulder (Table 2), in which the rainfall was particularly rapid (Liu et al., 2004; Shen et al., 2017), and the shrubs and herbaceous plants were scarce so that the consumption of nitrogen in the soil was less, and the high nitrogen content was sufficient for trees. Therefore, it was not necessary to additionally increase the supply of nitrogen by symbiosis with *Nitrospirae*. At the toe slope, this situation was just the opposite. Due to the high MC in the toe slope, the vegetation was rich, resulting in severe consumption of nitrogen (Table 2). In the absence of nitrogen, plants might form symbiotic relationships with *Nitrospirae* by providing them with carbon sources and others to obtain additional

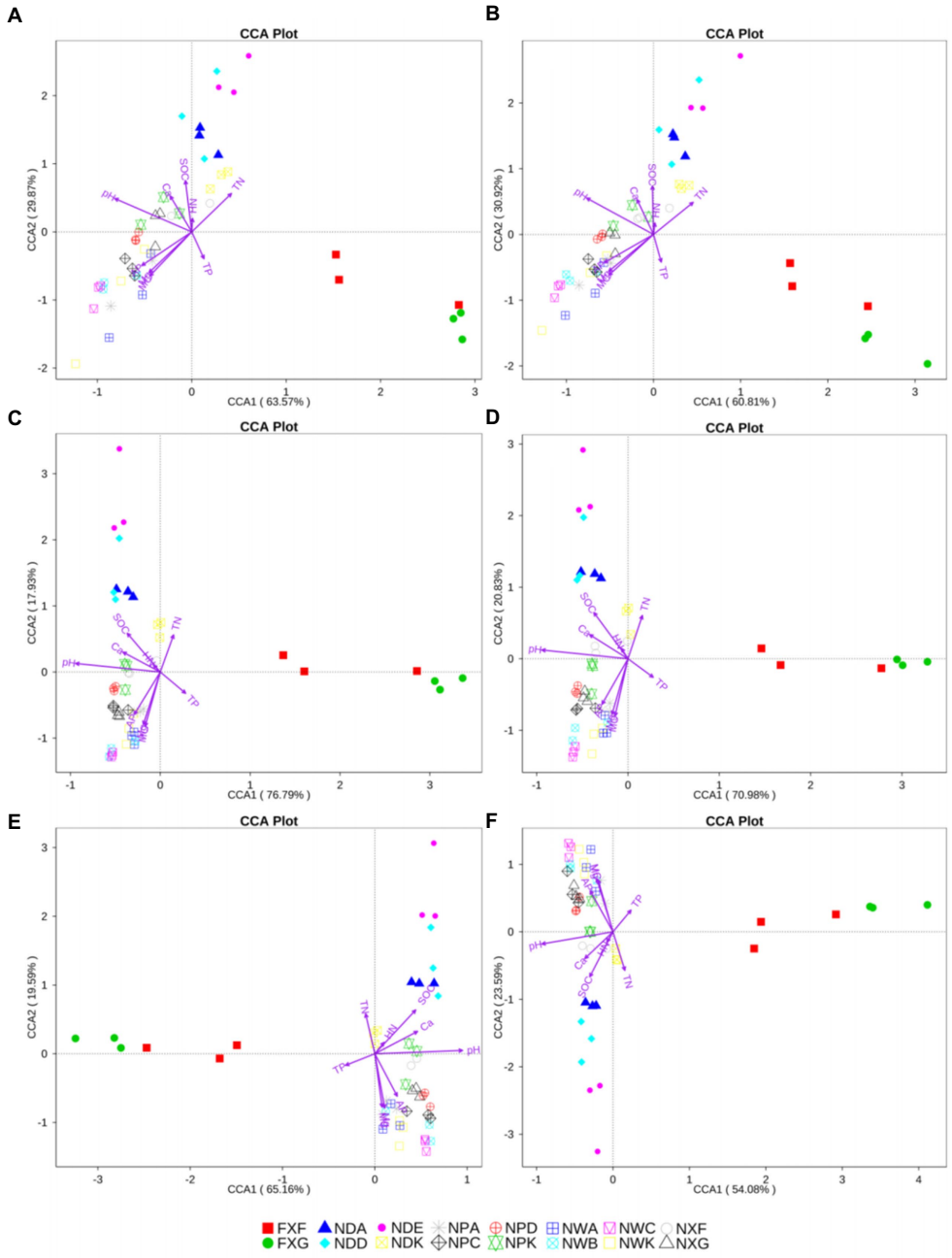

FIGURE 6
CCA analysis at the phylum **(A)**, class **(B)**, order **(C)**, family **(D)** genus **(E)**, and species **(F)** levels. The same symbols and colors indicated samples from the same group. Environmental parameters were demonstrated by purple arrows. The axes showed the percentages of variation in the distribution of microbe communities.

nitrogen and gain a competitive advantage. According to previous investigations, in the toe slope of the nitrogen deficiency, *Catunaregam spinosa* was, indeed, the dominant species (Huang et al., 2014). The earlier results suggested that the nitrogen-fixing or nitrogen-transforming ability of rhizosphere microorganisms was likely to be a decisive factor for plants to become dominant species in nitrogen-deficient habitats. The theory that microorganisms could co-produce nitrogen with plants and provide nitrogen to plants has been widely accepted (Delgado et al., 1998; Popescu, 1998). Our result revealed a new perspective that the formation of plant-dominant species might be related to rhizosphere microorganisms with nitrogen conversion ability. This phenomenon might due to the mutualism between plants and microorganisms. Plants could get benefits from mutualistic partnerships with a wide variety of bacteria, fungi, and animals. In the northern tropical seasonal rainforest, reciprocity with specific microorganisms provided benefits to plants such as nitrogen fixation, which might result in plant species being dominant. It also indicated that soil and hydrological changes that were associated with topography played a significant role in the habitat allocation of heterogeneous karst forests. The niche separation has major effects on

keeping the diversity of this heterogeneous karst forest (Guo et al., 2017).

In addition, the earlier relationship might be dominated by plants. One of the rhizosphere biomarkers of the NWA group was *Sh765B_TzT_29*, and the *Geobacter* enriched in the NPA group, which belonged to the *Deltaproteobacteria*. It was reported that *Sh765B_TzT_29* could reduce the sulfur element in the zinc-rich arsenic environment (Baldwin et al., 2015), while *Geobacter* could reduce Fe^{3+} ions (Magnuson et al., 2000). Such microorganisms preferred an anaerobic environment and a lower redox potential. In the environment of shallow rhizosphere soil, it was hard to achieve such conditions. But the *Sterculia monosperma* might just be able to provide this environment, thus causing the *Sterculia monosperma rhizosphere* microorganisms to converge inhabit. It could be seen that the influence of plants on the rhizosphere environment might have a certain dominant position. Previous studies have shown that plants could regulate mycorrhizal fungi by regulating the supply of carbohydrates to resist nutritional constraints (Johnson et al., 2003). The results of this study suggested that there might be a similar mechanism that plants could regulate rhizosphere microbes.

In short, due to climate and topography, the soil nutrient distribution in the northern tropical seasonal rainforest was uneven. Plants might selectively adapt their rhizosphere microorganisms under such pressure to form symbiotic nitrogen fixation patterns and other possible ways to resist the lack of nutrients. This adaptation mechanism was likely to be the decisive factor in determining whether a plant could become a dominant species. Plants were likely to be the dominant players in this adaptation process. This relationship between plants and rhizosphere microorganisms could be used to help protect the diversity of karst forests.

5. Conclusion

Through the study, the factors influencing the development of rhizosphere microbial communities were explained in multiple scales. On the medium and small scale, plant species and slope position could explain part of it (site A). Meanwhile, on a large scale (sites A and B), it is mainly reflected in different soil types caused by different geological backgrounds (karst and non-karst). Overall, soil types had the greatest influence on rhizosphere microbial diversity, followed by plant species and finally slope positions. These differences could largely be illustrated by soil pH, which had a complicated effect on microbial communities by affecting the nutrients, microbial adsorption, and so on. In studying the plant diversity of the northern tropical seasonal rainforest, more attention should be paid to rhizosphere soil types, physicochemical properties, and rhizosphere microbial community. Moreover, plants might selectively adapt themselves to rhizosphere microorganisms *via* secretions and other ways to gain advantages of getting nitrogen and other characteristic nutrients. This adaptation mechanism would help the plants to use the resources and living space effectively and have great significance to ecological restoration and agricultural production.

Data availability statement

The datasets presented in this study can be found in online repositories. The names of the repository/repositories and accession number(s) can be found below: https://www.ncbi.nlm.nih.gov/sra/SRP158785.

Author contributions

XZ and XL: conceptualization and writing—original draft preparation. YG, BW, and TC: investigation. XZ, YG, BW, TC, and XL: writing—review and editing. XZ: visualization. XL: supervision. All authors have read and agreed to the published version of the manuscript.

Funding

This research was supported by the National Natural Science Foundation of China (32271599, 32260276, and 31660130) and the Key Laboratory of Ecology of Rare and Endangered Species and Environmental Protection (Guangxi Normal University), Ministry of Education, China (ERESEP2021K03).

Acknowledgments

The authors thank Dr Taiming Shen for providing valuable advice, Yong Xu (Guangxi Pfomic info Co., Ltd.) for technical assistance with data processing, as well as reviewers for their constructive comments.

Conflict of interest

The authors declare that the research was conducted in the absence of any commercial or financial relationships that could be construed as a potential conflict of interest.

Publisher's note

References

Attard, E., Poly, F., Commeaux, C., Laurent, F., Terada, A., Smets, B. F., et al. (2010). Shifts between nitrospira–and nitrobacter–like nitrite oxidizers underlie the response of soil potential nitrite oxidation to changes in tillage practices. *Environ. Microbiol.* 12, 315–326. doi: 10.1111/j.1462-2920.2009.02070.x

Baldwin, S. A., Khoshnoodi, M., Rezadehbashi, M., Taupp, M., Hallam, S., Mattes, A., et al. (2015). The microbial community of a passive biochemical reactor treating arsenic, zinc, and sulfate–rich seepage. *Front. Bioeng. Biotechnol.* 3:27. doi: 10.3389/fbioe.2015.00027

Berendsen, R. L., Pieterse, C. M., and Bakker, P. A. (2012). The rhizosphere microbiome and plant health. *Trends Plant Sci.* 17, 478–486. doi: 10.1016/j.tplants.2012.04.001

Bokulich, N. A., Subramanian, S., Faith, J. J., Gevers, D., Gordon, J. I., Knight, R., et al. (2013). Quality–filtering vastly improves diversity estimates from Illumina amplicon sequencing. *Nat. Methods* 10, 57–59. doi: 10.1038/nmeth.2276

Bonito, G., Reynolds, H., Robeson, M. S., Nelson, J., Hodkinson, B. P., Tuskan, G. A., et al. (2014). Plant host and soil origin influence fungal and bacterial assemblages in the roots of woody plants. *Mol. Ecol.* 23, 3356–3370. doi: 10.1111/mec.12821

Bulgarelli, D., Rott, M., Schlaeppi, K., Loren, V., van Themaat, E., Ahmadinejad, N., et al. (2012). Revealing structure and assembly cues for Arabidopsis root–inhabiting bacterial microbiota. *Nature* 488, 91–95. doi: 10.1038/nature11336

Caporaso, J. G., Kuczynski, J., Stombaugh, J., Bittinger, K., Bushman, F. D., Costello, E. K., et al. (2010). QIIME allows analysis of high–throughput community sequencing data. *Nat. Methods* 7, 335–336. doi: 10.1038/nmeth.f.303

Caporaso, J. G., Lauber, C. L., Walters, W. A., Berq-Lyons, D., Huntley, J., Fierer, N., et al. (2012). Ultra–high–throughput microbial community analysis on the Illumina HiSeq and MiSeq platforms. *J. Multidiscip. J. Microb. Ecol.* 6, 1621–1624. doi: 10.1038/ismej.2012.8

Caporaso, J. G., Lauber, C. L., Walters, W. A., Berq-Lyons, D., Lozupone, C. A., Turnbauqh, P. J., et al. (2011). Global patterns of 16s rRNA diversity at a depth of millions of sequences per sample. *Proc. Natl. Acad. Sci. U. S. A.* 108, 4516–4522. doi: 10.1073/pnas.1000080107

Chao, A., and Bunge, J. (2002). Estimating the number of species in a stochastic abundance model. *Biometrics* 58, 531–539. doi: 10.1111/j.0006-341X.2002.00531.x

Chu, H. Y., Xiang, X. J., Yang, J., Jonathan, M. A., Zhang, K. P., Li, Y. T., et al. (2016). Effects of slope aspects on soil bacterial and arbuscular fungal communities in a boreal Forest in China[J]. *Pedosphere* 26, 226–234. doi: 10.1016/S1002-0160(15)60037-6

Daebeler, A., Bodelier, P. L., Yan, Z., Hefting, M. M., Jia, Z., and Laanbroek, H. J. (2014). Interactions between Thaumarchaea, Nitrospira and methanotrophs modulate autotrophic nitrification in volcanic grassland soil. *ISME J.* l 8, 2397–2410. doi: 10.1038/ismej.2014.81

Dakora, F. D., and Phillips, D. A. (2002). Root exudates as mediators of mineral acquisition in low–nutrient environments. *Plant Soil* 245, 35–47. doi: 10.1023/A:1020809400075

Delgado, M. J., Bedmar, E. J., and Downie, J. A. (1998). Genes involved in the formation and assembly of Rhizobial cytochromes and their role in symbiotic nitrogen fixation. *Adv. Microb. Physiol.* 40, 191–231. doi: 10.1016/S0065-2911(08)60132-0

DeSantis, T. Z., Hugenholtz, P., Larsen, N., Rojas, M., Brodie, E. L., Keller, K., et al. (2006). Greengenes, a chimera–checked 16S rRNA gene database and workbench compatible with ARB. *Appl. Environ. Microbiol.* 72, 5069–5072. doi: 10.1128/AEM.03006-05

Edgar, R. C. (2004). MUSCLE: multiple sequence alignment with high accuracy and high throughput. *Nucleic Acids Res.* 32, 1792–1797. doi: 10.1093/nar/gkh340

Edgar, R. C. (2013). UPARSE: highly accurate OTU sequences from microbial amplicon reads. *Nat. Methods* 10, 996–998. doi: 10.1038/nmeth.2604

Edgar, R. C., Haas, B. J., Clemente, J. C., Quince, C., and Knight, R. (2011). UCHIME improves sensitivity and speed of chimera detection. *Bioinformatics* 27, 2194–2200. doi: 10.1093/bioinformatics/btr381

Fierer, N., and Jackson, R. B. (2006). The diversity and biogeography of soil bacterial communities. *Proc. Natl. Acad. Sci. U. S. A.* 103, 626–631. doi: 10.1073/pnas.0507535103

Good, I. J. (1953). The population frequencies of species and the estimation of population parameters. *Biometrika* 40, 237–264. doi: 10.1093/biomet/40.3-4.237

Gschwendtner, S., Esperschütz, J., Buegger, F., Reichmann, M., Muiller, M., Munch, J. C., et al. (2011). Effects of genetically modified starch metabolism in potato plants on photosynthate fluxes into the rhizosphere and on microbial degraders of root exudates[J]. *FEMS Microbiol. Ecol.* 76, 564–575. doi: 10.1111/j.1574-6941.2011.01073.x

Gu, M. Y., XU, W. L., Zhang, Z. D., Tang, G. M., Liu, H. L., Li, Z. Q., et al. (2018). Relationships between fungi diversity, physicochemical properties and verticillium wilt in continuous cropping cotton rhizosphere soil with cotton Stover biochar[J]. *Xinjiang Agric. Sci.* 55, 1698–1709. doi: 10.6048/j.issn.1001-4330.2018.09.016

Guo, Y. L., Wang, B., Mallik, A. U., Huang, F. Z., Xiang, W. S., Ding, T., et al. (2017). Topographic species–habitat associations of tree species in a heterogeneous tropical karst seasonal rain forest. *China. J. Plant Ecol.* 10, 450–460. doi: 10.1093/jpe/rtw057

Guo, Y. L., Xiang, W. S., Wang, B., Li, D. X., Mallik, A. U., Han, Y. H. C., et al. (2018). Partitioning beta diversity in a tropical karst seasonal rainforest in southern China. *Sci. Rep.* 8:17408. doi: 10.1038/s41598-018-35410-7

Hao, D. C., Chen, S. L., and Xiao, P. G. (2009). Study of rhizosphere microbe based on molecular biology and genomics. *Microbiology* 36, 892–899.

Hao, D. C., Ge, G. B., and Yang, L. (2008). Bacterial diversity of Taxus rhizosphere: culture–independent and culture–dependent approaches. *FEMS Microbiol. Lett.* 284, 204–212. doi: 10.1111/j.1574-6968.2008.01201.x

Hao, D. C., Song, S. M., Mu, J., Hu, W. L., and Xiao, P. G. (2016). Unearthing microbial diversity of Taxus rhizosphere via MiSeq high–throughput amplicon sequencing and isolate characterization. *Sci. Rep.* 6:22006. doi: 10.1038/srep22006

Hinsinger, P., Bengough, A. G., Vetterlein, D., and Young, L. M. (2009). Rhizosphere: biophysics, biogeochemistry and ecological relevance. *Plant Soil* 321, 117–152. doi: 10.1007/s11104-008-9885-9

Huang, F. P. (2000). Study on soil biochemical characteristics of Camellia nitidissima chi woodland in Fangcheng. *Guangxi Forest. Sci.* 29, 178–181.

Huang, M. C., Shi, Y. C., Wei, X., Wu, L. F., Wu, R. H., Pan, Z. P., et al. (2013). Point pattern analysis of rare and endangered plant Camellia nitidissima chi. *Chin. J. Ecol.* 32, 1127–1134. doi: 10.13292/j.1000-4890.2013.0200

Huang, F. Z., Wang, B., Ding, T., Xiang, W. S., Li, X. K., and Zhou, A. P. (2014). Numerical classification of associations in a northern tropical karst seasonal rain forest and the relationships of these associations with environmental factors. *Biodivers. Sci.* 27, 295–298. doi: 10.1006/jhge.2001.0316

Igwe, A., and Vannette, R. L. (2019). Bacterial communities differ between plant species and soil type, and differentially influence seedling establishment on serpentine soils. *Plant Soil* 441, 423–437. doi: 10.1007/s11104-019-04135-5

Jiang, Z. C., Lian, Y. Q., and Qin, X. Q. (2014). Rocky desertification in Southwest China: impacts, causes, and restoration. *Earth. Rev.* 132, 1–12. doi: 10.1016/j.earscirev.2014.01.005

Jiang, F., Wu, X. H., Xiang, W. H., Fang, X., Zeng, Y. L., Shuai, O. Y., et al. (2017). Spatial variations in soil organic carbon, nitrogen and phosphorus concentrations related to stand characteristics in subtropical areas. *Plant Soil* 413, 289–301. doi: 10.1007/s11104-016-3101-0

Johnson, N. C., Rowland, D. L., Corkidi, L., Egerton-Warburton, L. M., and Allen, E. B. (2003). Nitrogen enrichment alters mycorrhizal allocation at five Mesic to semiarid grasslands. *Ecology* 84, 1895–1908. doi: 10.1890/0012-9658(2003)084[1895:NEAMAA]2.0.CO;2

Lakshmanan, V., Kitto, S. L., Caplan, J. L., Hsueh, Y.-H., Kearns, D. B., Wu, Y.-S., et al. (2012). Microbe-associated molecular patterns-triggered root responses mediate beneficial Rhizobacterial recruitment in Arabidopsis[J]. *Plant Physiol.* 160, 1642–1661. doi: 10.1104/pp.112.200386

Leff, J. W., Bardgett, R. D., Wilkinson, A., Jackson, B. G., Pritchard, W. J., de Long, J. R., et al. (2018). Predicting the structure of soil communities from plant community taxonomy, phylogeny, and traits. *ISME J.* 12, 1794–1805. doi: 10.1038/s41396-018-0089-x

Liu, Z. H., Groves, C., Yuan, D. X., and Li, Q. (2004). Hydrochemical variations during flood pulses in the south–West China peak cluster karst: impacts of CaCO3–H2O–CO2 interactions. *Hydrol. Process.* 18, 2423–2437. doi: 10.1002/hyp.1472

Liu, L. L., Huang, X. Q., Zhang, J. B., Cai, Z. C., Jiang, K., and Chang, Y. Y. (2020). Deciphering the combined effect and relative importance of soil and plant traits on the development of rhizosphere microbial communities. *Soil Biol. Biochem.* 148:107909. doi: 10.1016/j.soilbio.2020.107909

Lozupone, C. A., and Knight, R. (2008). Species divergence and the measurement of microbial diversity. *FEMS Microbiol. Rev.* 32, 557–578. doi: 10.1111/j.1574-6976.2008.00111.x

Lu, R. K. *Soil chemical analysis methods in agriculture*. Beijing: China Agricultural Science and Technology Press (2000).

Lundberg, D. S., Lebeis, S. L., Paredes, S. H., Yourstone, S., Gehring, J., Malfatti, S., et al. (2012). Defining the core Arabidopsis thaliana root microbiome. *Nature* 488, 86–90. doi: 10.1038/nature11237

Lynch, M. D., and Neufeld, J. D. (2015). Ecology and exploration of the rare biosphere. *Nat. Rev. Microbiol.* 13, 217–229. doi: 10.1038/nrmicro3400

Magnuson, T. S., Hodges-Myerson, A. L., and Lovley, D. R. (2000). Characterization of a membrane–bound NADH–dependent Fe^{3+} reductase from the dissimilatory Fe^{3+}–reducing bacterium Geobacter sulfurreducens. *FEMS Microbiol. Lett.* 185, 205–211. doi: 10.1111/j.1574-6968.2000.tb09063.x

Magurran, A. E. *Ecological diversity and its measurement*. Princeton: Princeton University Press (1988).

Marschner, P., Crowley, D. E., and Yang, C. H. (2004). Development of specific rhizosphere bacterial communities in relation to plant species, nutrition and soil type. *Plant Soil* 261, 199–208. doi: 10.1023/B:PLSO.0000035569.80747.c5

Maurhofer, M., Baehler, E., Notz, R., Martinez, V., and Keel, C. (2004). Cross talk between 2, 4–Diacetylphloroglucinol–producing biocontrol pseudomonads on wheat roots. *Appl. Environ. Microbiol.* 70, 1990–1998. doi: 10.1128/AEM.70.4.1990-1998.2004

Mendes, R., Garbeva, P., and Raaijmakers, J. M. (2013). The rhizosphere microbiome: significance of plant beneficial, plant pathogenic, and human pathogenic microorganisms. *FEMS Microbiol. Rev.* 37, 634–663. doi: 10.1111/1574-6976.12028

Mendes, R., Kruijt, M., de Bruijn, I., Dekkers, E., van der Voort, M., Schneider, J. H., et al. (2011). Deciphering the rhizosphere microbiome for disease–suppressive bacteria. *Science* 332, 1097–1100. doi: 10.1126/science.1203980

Miethling, R., Wieland, G., Backhaus, H., and Tebbe, C. (2000). Variation of microbial rhizosphere communities in response to crop species, soil origin, and inoculation with Sinorhizobium meliloti L33. *Microb. Ecol.* 40, 43–56. doi: 10.1007/s002480000021

Mussa, S. A. B., Elferjani, H. S., Haroun, F. A., and Abdelnabi, F. F. (2009). Determination of available nitrate, phosphate and sulfate in soil samples. *Int. J. PharmTech Res.* 1, 598–604.

Myers, N., Mittermeier, R. A., Mittermeier, C. G., da Fonseca, G. A., and Kent, J. (2000). Biodiversity hotspots for conservation priorities. *Nature* 403, 853–858. doi: 10.1038/35002501

Nan, J., Chao, L. M., Ma, X. D., Xu, D. L., Mo, L., Zhang, X. D., et al. (2020). Microbial diversity in the rhizosphere soils of three Stipa species from the eastern inner Mongolian grasslands[J]. *Glob. Ecol. Conserv.* 22:e00992. doi: 10.1016/j.gecco.2020.e00992

Pii, Y., Borruso, L., Brusetti, L., Crecchio, C., Cesco, S., and Mimmo, T. (2016). The interaction between iron nutrition, plant species and soil type shapes the rhizosphere microbiome. *Plant Physiol. Biochem.* 99, 39–48. doi: 10.1016/j.plaphy.2015.12.002

Popescu, A. (1998). Contributions and limitations to symbiotic nitrogen fixation in common bean (Phaseolus vulgaris L.) in Romania. *Plant Soil* 204, 117–125. doi: 10.1023/A:1004339313310

Roberts, T. L., Norman, R. J., Slaton, N. A., Wilson, C. E., Ross, W. J., and Bushong, J. T. (2009). Direct steam distillation as an alternative to the Illinois soil nitrogen test. *Soil Sci. Soc. Am. J.* 73, 1268–1275. doi: 10.2136/sssaj2008.0165

Saleem, M., Law, A. D., and Moe, L. A. (2016). Nicotiana, roots recruit rare rhizosphere taxa as major root–inhabiting microbes. *Microb. Ecol.* 71, 469–472. doi: 10.1007/s00248-015-0672-x

Shen, T. M., Li, W., Pan, W. Z., Lin, S. Y., Zhu, M., and Yu, L. J. (2017). Role of bacterial carbonic anhydrase during CO_2 capture in the CO_2–H_2O–carbonate system. *Biochem. Eng. J.* 123, 66–74. doi: 10.1016/j.bej.2017.04.003

Shi, J. Y., Yuan, X. F., Lin, H. R., Yang, Y. Q., and Li, Z. Y. (2011). Differences in soil properties and bacterial communities between the rhizosphere and bulk soil and among different production areas of the medicinal plant Fritillaria thunbergii. *Int. J. Mol. Sci.* 12, 3770–3785. doi: 10.3390/ijms12063770

Veach, A. M., Morris, R., Yip, D. Z., Yang, Z. K., and Schadt, C. W. (2019). Rhizosphere microbiomes diverge among Populus trichocarpa plant–host genotypes and chemotypes, but it depends on soil origin. *Microbiome* 7:76. doi: 10.1186/s40168-019-0668-8

Wang, Q., Garrity, G. M., Tiedje, J. M., and Cole, J. R. (2007). Naive Bayesian classifier for rapid assignment of rRNA sequences into the new bacterial taxonomy. *Appl. Environ. Microbiol.* 73, 5261–5267. doi: 10.1128/AEM.00062-07

Wang, B., Huang, Y. S., Li, X. K., and He, L. J. (2014). Species composition and spatial distribution of a 15 ha northern tropical karst seasonal rain forest dynamics study plot in Nonggang, Guangxi, southern China. *Biodivers. Sci.* 22, 141–156. doi: 10.3724/SP.J.1003.2014.13195

Wang, X. P., Li, J. Q., and Li, X. X. (2001). The study of seasonal rain forest classification in acid soil region of Guangxi. *Bull. Bot. Res.* 21, 456–469. doi: 10.3969/j.issn.1673-5102.2001.03.030

frontiers | Frontiers in Microbiology

TYPE Original Research
PUBLISHED 25 July 2023
DOI 10.3389/fmicb.2023.1111383

OPEN ACCESS

EDITED BY
Xiangyu Guan,
China University of Geosciences, China

REVIEWED BY
Yang Liu,
Shenzhen University, China
Gaozhong Pu,
Independent Researcher, Guilin, China

*CORRESPONDENCE
Bin Li
✉ see-libin@pku.edu.cn

RECEIVED 29 November 2022
ACCEPTED 26 June 2023
PUBLISHED 25 July 2023

CITATION
Zhong S, Hou B, Zhang J, Wang Y, Xu X, Li B and Ni J (2023) Ecological differentiation and assembly processes of abundant and rare bacterial subcommunities in karst groundwater. *Front. Microbiol.* 14:1111383. doi: 10.3389/fmicb.2023.1111383

Ecological differentiation and assembly processes of abundant and rare bacterial subcommunities in karst groundwater

Sining Zhong[1,2,3], Bowen Hou[4], Jinzheng Zhang[1], Yichu Wang[2,3,5], Xuming Xu[2,3], Bin Li[2,3]* and Jinren Ni[2,3]

[1]Fujian Provincial Key Laboratory of Soil Environment Health and Regulation, College of Resources and Environment, Fujian Agriculture and Forestry University, Fuzhou, China, [2]College of Environmental Sciences and Engineering, Peking University, Beijing, China, [3]State Environmental Protection Key Laboratory of All Material Fluxes in River Ecosystems, College of Environmental Sciences and Engineering, Peking University, Beijing, China, [4]State Key Laboratory of Eco-hydraulics in Northwest Arid Region of China, Xi'an University of Technology, Xi'an, China, [5]College of Water Sciences, Beijing Normal University, Beijing, China

The ecological health of karst groundwater has been of global concern due to increasing anthropogenic activities. Bacteria comprising a few abundant taxa (AT) and plentiful rare taxa (RT) play essential roles in maintaining ecosystem stability, yet limited information is known about their ecological differentiation and assembly processes in karst groundwater. Based on a metabarcoding analysis of 64 groundwater samples from typical karst regions in southwest China, we revealed the environmental drivers, ecological roles, and assembly mechanisms of abundant and rare bacterial communities. We found a relatively high abundance of potential functional groups associated with parasites and pathogens in karst groundwater, which might be linked to the frequent regional anthropogenic activities. Our study confirmed that AT was dominated by Proteobacteria and Campilobacterota, while Patescibacteria and Chloroflexi flourished more in the RT subcommunity. The node-level topological features of the co-occurrence network indicated that AT might share similar niches and play more important roles in maintaining bacterial community stability. RT in karst groundwater was less environmentally constrained and showed a wider environmental threshold response to various environmental factors than AT. Deterministic processes, especially homogeneous selection, tended to be more important in the community assembly of AT, whereas the community assembly of RT was mainly controlled by stochastic processes. This study expanded our knowledge of the karst groundwater microbiome and was of great significance to the assessment of ecological stability and drinking water safety in karst regions.

KEYWORDS

bacterial community, abundant and rare taxa, karst groundwater, assembly processes, environmental thresholds

1. Introduction

Karst landforms are broadly distributed in the world and represent 7–12% of the Earth's continental area (Zhang et al., 2018). More than 25% of the global population relies on karst groundwater for domestic drinking and irrigation purposes (Hartmann et al., 2014). Karst aquifers are characterized by unique features such as large voids, high flow

velocities, and rapid infiltrations due to strong dissolution processes (White, 2002), leading to their high ecological sensitivity in response to climate changes and human activities (Ollivier et al., 2019; Olarinoye et al., 2020). Varieties of anthropogenic contaminants, such as pharmaceuticals, flame retardants, microplastics, and antibiotics (Reberski et al., 2022), have been widely detected in karstic aquifers. Due to the increasing pressure from these environmental issues, the ecological health and drinking water sustainability of karst groundwater has become a global concern (Tang et al., 2022).

Diversified microbes that colonize aquifers constitute the sole ecological community in groundwater ecosystems (Whitman et al., 1998; Magnabosco et al., 2018) and pivotally participate in multiple biogeochemical processes (e.g., carbon, nitrogen, sulfur, and phosphorus; Probst et al., 2018; Wang S. et al., 2019; Wang Y. et al., 2019). Bacterial communities are normally uneven in abundance and distribution, with a few species with high abundance (abundant taxa) and the majority with low abundance (rare taxa; Pedros-Alio, 2012; He et al., 2022; Zhao et al., 2022). Rare taxa, considered a crucial microbial "seed bank," are ecological insurance for microbial diversity and community stability and provide disproportionately important functions (Shade et al., 2014; Liu et al., 2015a; Jiao and Lu, 2020). Generally, dominant taxa tend to exhibit strong environmental adaptation, but rare taxa would become dominant under suitable environmental conditions (Reddin et al., 2015; Kurm et al., 2019). The variety of "rare-to-prevalent" dynamics could be explained by the priority effects, awakening from dormancy, and heterogeneity of environmental preference (Lee et al., 2021; Zhang et al., 2022). Previous studies have documented the distinct spatial patterns and functional traits of abundant and rare bacteria in surface water such as rivers (Yi et al., 2022), lakes (Zhang et al., 2022), and oceans (Li et al., 2021). However, the biogeographic patterns and assembly mechanisms of abundant and rare bacterial subcommunities in groundwater remained unclear.

Rapid advances in sequencing and multi-omics technologies have made it possible to identify biogeographic patterns of bacterial diversity and structure at large scales, promoting our understanding of the ecological and evolutionary processes in natural ecosystems (Liu et al., 2018; Shi et al., 2018). Meta-analyses revealed that the substantially different bacterial communities between distinct habitats were driven by multiple environmental factors (e.g., salinity, nutrients, and heavy metals; Power et al., 2018; Carlson et al., 2019; Liu et al., 2020). Habitat specialization is usually the consequence of adaptive and metabolic evolution via natural selection (environmental filtering; Wang et al., 2013). Meanwhile, variation in bacterial communities is also influenced by stochastic processes (e.g., ecological drift, dispersal limitation, mass effects, and historical contingency; Bahram et al., 2016; Fodelianakis et al., 2017; Archer et al., 2019). To date, there is a consensus that both deterministic (niche-based) and stochastic (neutral) processes would simultaneously shape microbial community assembly but disentangling the balance between these two processes is still a complicated issue.

Southwest China harbors the largest karst landscapes in the world and is one of the hotspots of global biodiversity (Li et al., 2022). As the main driver of groundwater ecosystems, the bacterial community affects the material and energy fluxes of the karst subterranean environments. Understanding the spatial variations, ecological drivers, and assembly processes of abundant and rare bacteria in karst groundwater is beneficial to assess its vulnerability and sustainable potential relevant to various human disturbances. In this study, we collected 64 groundwater samples from a karst area in southwest China (Figure 1A) and aimed to (a) reveal the bacterial diversity, structures, and potential functions of karst groundwater; (b) determine the composition and environmental adaptability of rare and abundant bacterial taxa; and (c) elucidate the ecological processes involved in shaping the abundant and rare subcommunities.

2. Materials and methods

2.1. Study area description and sampling

Southwest China (97°38′-113°40′ E, 21°03′-34°57′ N) has a subtropical/tropical humid monsoon climate with abundant annual rainfall ranging from 1,013 to 1,607 mm (Li et al., 2022). The continuous dissolution of widely distributed carbonate and sulfate rocks facilitates the development of stone forests and karst caves (Liu et al., 2021), thereby leading to the formation of the largest karst landform in the world (5.5×10^4 km^2). Considering typical topographic types, major rocky desertification zones, and potential ecologically fragile regions, we collected 64 groundwater samples from three provinces (i.e., Yunnan, Guizhou, and Guangxi) in southwest China during 2016–2017. Based on groundwater types identified by the China Geological Survey (https://geocloud.cgs.gov.cn/), these sampling sites included karst fissure water (42), pore-fissure water in red bed (5), bedrock fissure water (10), and pore water in loose rock (7), classified based on National Geological Survey (https://geocloud.cgs.gov.cn/). All groundwater samples were first-hand data from newly constructed wells according to the procedures of national standards (HJ/T 164-2004).

Before sample collection, groundwater was pumped out using a submersible sampling pump at a controlled discharge below 100 ml/min. Physicochemical properties (i.e., pH, conductivity, and oxidation–reduction values) of outflowing groundwater were measured with a portable tester for 15 min until three consecutive measurements were consistent (standard deviation < 5%). Following this purge, more than 3,000 L of groundwater were formally extracted and filtered by 0.01 μm hollow fiber membranes (Toray, Japan) to enrich microbial cells. All filtered membranes were immediately transported with dry ice to the designated laboratories. Then, the substances on the membranes were further extracted by ultrasonication, filtered by 0.22 μm polycarbonate membranes (Millipore, USA), and stored at −80°C before DNA extraction.

2.2. Groundwater physicochemical analysis

The longitude and latitude of each groundwater sample were recorded through a handheld GPS (Magellan, USA) during sampling. Groundwater samples for physicochemical analysis were collected in 5 L sterile bottles and transported to the laboratory at 4°C within 24 h. Standard methods were adopted to measure an array of physicochemical properties. The major metals [e.g.,

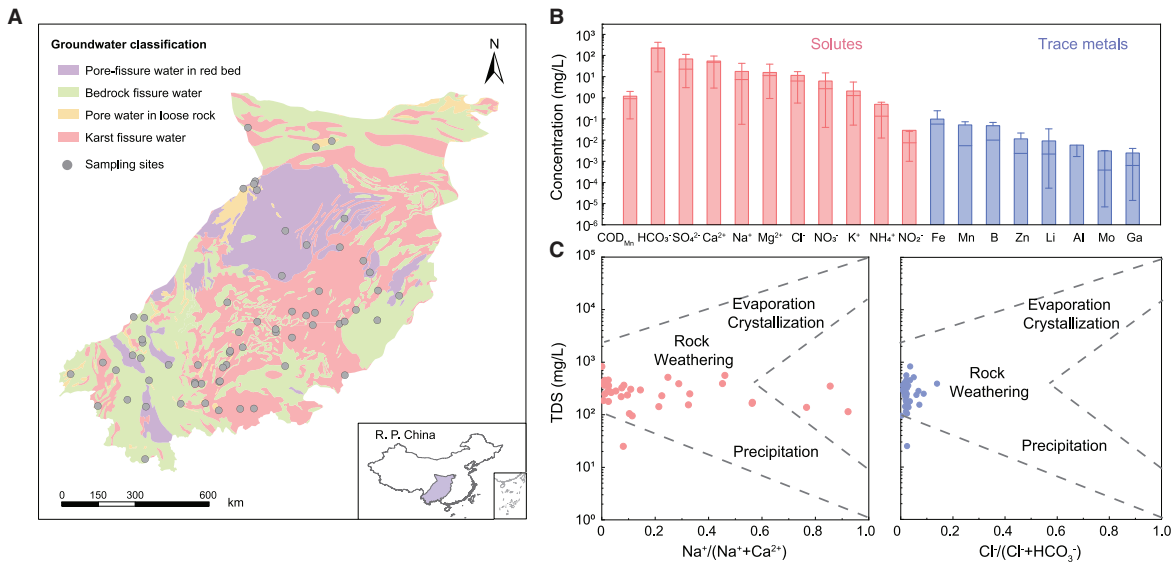

FIGURE 1
Physicochemical characteristics of karst groundwater in southwest China. **(A)** Map of typical karst areas showing the sampling sites in southwest China. **(B)** The content of main solutes and metals in karst groundwater. **(C)** Gibbs diagrams showing the dominant hydrochemical processes for karst groundwater.

calcium (Ca), sodium (Na), magnesium (Mg), and potassium (K)] were measured by ICP-MS (Thermo Fisher Scientific, USA), while trace metals [e.g., manganese (Mn), iron (Fe), arsenic (As), and copper (Cu)] were determined by ICP-OES (Leeman, USA). The water samples were collected in 5 L sterile bottles for further analysis of total organic carbon (TOC; HJ 501–2009), ammonia nitrogen (NH_4-N; HJ 535–2009), nitrate nitrogen (NO_3-N; HJ/T 346–2007), and nitrite nitrogen (NO_2-N; GB 7493–87).

2.3. DNA extraction and sequencing

The genomic DNA of each groundwater sample was extracted using the MoBio PowerSoil® Kit (MoBio Laboratories, Carlsbad, CA, USA), according to the manufacturer's protocols. The DNA concentration and quality of mixed duplicate extracts were evaluated by a NanoDrop Spectrophotometer (NanoDrop Technologies Inc., Wilmington, DE, USA). The barcoded primer pairs 338F (ACTCCTACGGGAGG-CAGCAG) and 806R (GGACTACHVGGGTWTCTAAT-3) were used to amplify the bacterial 16S rRNA genes (Caporaso et al., 2011). Based on the concentration to generate amplicon libraries, PCR products were mixed in equal amounts and sequenced on the Illumina MiSeq PE300 platform (Illumina, San Diego, USA) at Shanghai Majorbio Bio-Pharm Technology Company Co., Ltd. (Shanghai, China).

2.4. Bioinformatics and statistical analyses

Bioinformatic analysis of the next-generation DNA sequencing data was performed using QIIME on the Majorbio cloud platform (https://cloud.majorbio.com/). Operational taxonomic units (OTUs) were clustered with 97% identity using UPARSE (Edgar, 2013), and chimeric sequences were removed using UCHIME. Bacterial OTUs were assigned using the RDP classifier (Wang et al., 2007) against the SILVA 16S rRNA database (http://www.arb-silva.de/). Bacteria were classified into different metabolic functional groups based on the FAPROTAX database (Louca et al., 2016; Sansupa et al., 2021). To account for the uneven sequencing depth among samples, the OTU table for subsequent comparative analysis was rarefied to the same sequencing depth, according to the minimum read count. We defined the abundant taxa as the average relative abundance of OTUs $>$ 0.1%, the rare taxa as the relative abundance of $<$ 0.01%, and the intermediate OTUs as the relative abundance between 0.01 and 0.1% (Jiao and Lu, 2020). All the raw sequencing datasets in this study have been deposited in the NCBI Sequence Read Archive, under accession number PRJNA692269.

Non-metric multidimensional scaling (NMDS) was used to visualize the dissimilarity of bacterial communities based on the Bray–Curtis distance, and similarity analysis (ANOSIM) was calculated to test the significance of differences in community structures. Variance partitioning analysis (VPA) was performed using pairwise Bray–Curtis dissimilarity to quantify the relative contribution of environmental and geographic factors, in addition to their combined effect on the spatial turnover of bacterial communities. A constrained correspondence analysis (CCA) with environmental variables was performed to interpret community distribution. NMDS, ANOSIM, CCA, and VPA were performed with the *vegan* packages in R software (https://www.r-project.org/). Mantel tests were used to evaluate the significance of Spearman's rank correlations between the Bray–Curtis dissimilarity and geographic distance matrices. The

differences in bacterial composition were examined at $p < 0.05$, with Wilcoxon rank-sum tests. To calculate the threshold values of rare and abundant subcommunities responding to various environmental factors, we applied threshold indicator taxa analysis (TITAN) using the *TITAN2* R package (Jiao and Lu, 2020).

Pairwise Spearman's correlation coefficients based on the relative abundances were calculated only between OTUs that occurred in > 20% of samples. Then, the robust (Spearman's $r > 0.60$) and significant correlations ($p < 0.01$) were selected to filter the data for reduced network complexity. The network visualization and modular analyses were conducted with the interactive platform Gephi (version 0.9.2), and node-level topological features (i.e., degree, betweenness, and closeness centrality) were characterized with the igraph package in R software. The topological roles of nodes in the networks were classified by the threshold values of Zi (within-module connectivity) and Pi (among-module connectivity; Guimera and Amaral, 2005). Node attributes can be divided into four types, namely, module hubs (Zi > 2.5), network hubs (Zi > 2.5 and Pi > 0.62), connectors (Pi > 0.62), and peripherals (Zi < 2.5 and Pi < 0.62).

The neutral model of Sloan et al. was used to estimate the potential role of neutral processes in shaping microbial community structure by describing the relationship between the observed frequency of occurrence and the abundance of OTUs (Sloan et al., 2007). To quantify the relative importance of deterministic and stochastic processes in microbial community assembly, the normalized stochasticity ratio (NST) was estimated using the "tNST" and "nst.boot" functions with the NST package in R software, with 50% taken as the boundary point between more deterministic (<50%) and more stochastic (>50%) assemblies (Guo et al., 2018; Ning et al., 2019). The null model framework was calculated with the picante and vegan packages in R software to estimate the relative importance of five ecological processes (i.e., homogenizing selection, variable selection, dispersal limitation, homogenizing dispersal, and ecological drift) in bacterial community assembly (Stegen et al., 2013).

3. Results

3.1. Physicochemical characteristics of karst groundwater in southwest China

Most groundwater samples (85.0%) were weakly alkaline with an average pH of 7.51 (6.31–11.35), which was mainly related to chemical erosion of carbonate minerals and accumulation of HCO_3^- in the study area (average 232.97 mg/L; Li et al., 2018). According to the standard for Groundwater Quality of China (GB/T 14848–2017), 78.1–100% of groundwater samples were satisfied with a fairly good level (I, II, or III). NO_3^--N, NH_4^+-N, F^-, and Mn could be identified as potential threats to groundwater quality, with >10% of samples at the poor level (IV or V; Figure 1B and Supplementary Table 1). High concentrations of NO_3^--N (average 13.2 mg/L) and NH_4^+-N (average 0.45 mg/L) in karst groundwater were potentially attributed to anthropogenic loadings considering the high permeability of karst rocks (Opsahl et al., 2017) and extensive agricultural fertilization in southwest China (Zhang, 2020). Fe (0.13 mg/L), B (0.07 mg/L), and Mn (0.05 mg/L) were the dominant trace metals in karst groundwater, which are closely related to the regional geological environments (Peng et al., 2022).

The concentration of total dissolved solids (TDS) ranged from 25 to ~1.792 mg/L with an average value of 361.79 mg/L, indicating low salinity in karat groundwater. Ca^{2+} (45.99 mg/L), Na^+ (26.93 mg/L), and Mg^{2+} (12.77 mg/L) were identified as major cations while HCO_3^- (232.97 mg/L) and SO_4^{2-} (97.31 mg/L) were dominant anions. Piper analysis further showed that the hydrochemical types of the groundwater samples were assigned to Mg^{2+}-Ca^{2+}-HCO_3^- category, which suggested a remarkable leaching process in karst regions (Supplementary Figure 1). Gibbs diagrams indicated that the chemical evolution of most groundwater samples (93.5%) was mainly controlled by rock weathering (Figure 1C), reflecting the chronological impacts of soluble rocks on karst groundwater (Li et al., 2018).

3.2. Diversity, structure, and potential function of the bacterial community

After quality filtering and the removal of chimeric sequences, high-throughput Illumina sequencing yielded a total of 24,321 OTUs from 64 karst groundwater samples in southwest China. The rarefaction curves (Supplementary Figure 2) and high Good's coverage values (0.973 ± 0.002, Supplementary Table 2) of each sample illustrated that the majority of bacterial taxa were well-covered by the current sequencing depth. The bacterial alpha diversity in karst groundwater, including Chao1, Shannon diversity, and phylogenetic diversity (pd), exhibited a more significant relationship with geographic factors (i.e., longitude, latitude, and well depth) than with environmental variables (Supplementary Figure 3).

Among the 67 identified phyla, Proteobacteria was the most dominant phylum, accounting for 21.55% of the total OTUs and 63.5% of the total sequences, followed by Campylobacterota, Bacteroidota, Actinobacteriota, Patescibacteria, Firmicutes, and Desulfobacterota (Supplementary Figure 4). As the most concerned superphylum in recent years (Herrmann et al., 2019; Chaudhari et al., 2021; Ruiz-Gonzalez et al., 2022), Patescibacteria had abundant phylotypes in karst groundwater (18.7% of the total OTUs), second only to Proteobacteria. The NMDS and ANOSIM analyses illustrated the significant discrepancy in bacterial composition (Supplementary Figure 5A) between phreatic and confined water, classified based on the burial condition of the karst region. Community similarity among samples in phreatic water was much higher than that in confined water (Wilcoxon rank-sum test: $p < 0.01$). At the genus level, *Aquabacterium*, *Acidovorax*, *Cavicella*, *Simplicispira*, and *Polaromonas* all belonging to Proteobacteria, preferred the phreatic water, whereas *Acetobacterium* (Firmicutes), *Perlucidibaca* (Proteobacteria), and *Desulfovibrio* (Desulfobacterota) were relatively abundant in confined water (Supplementary Figure 6).

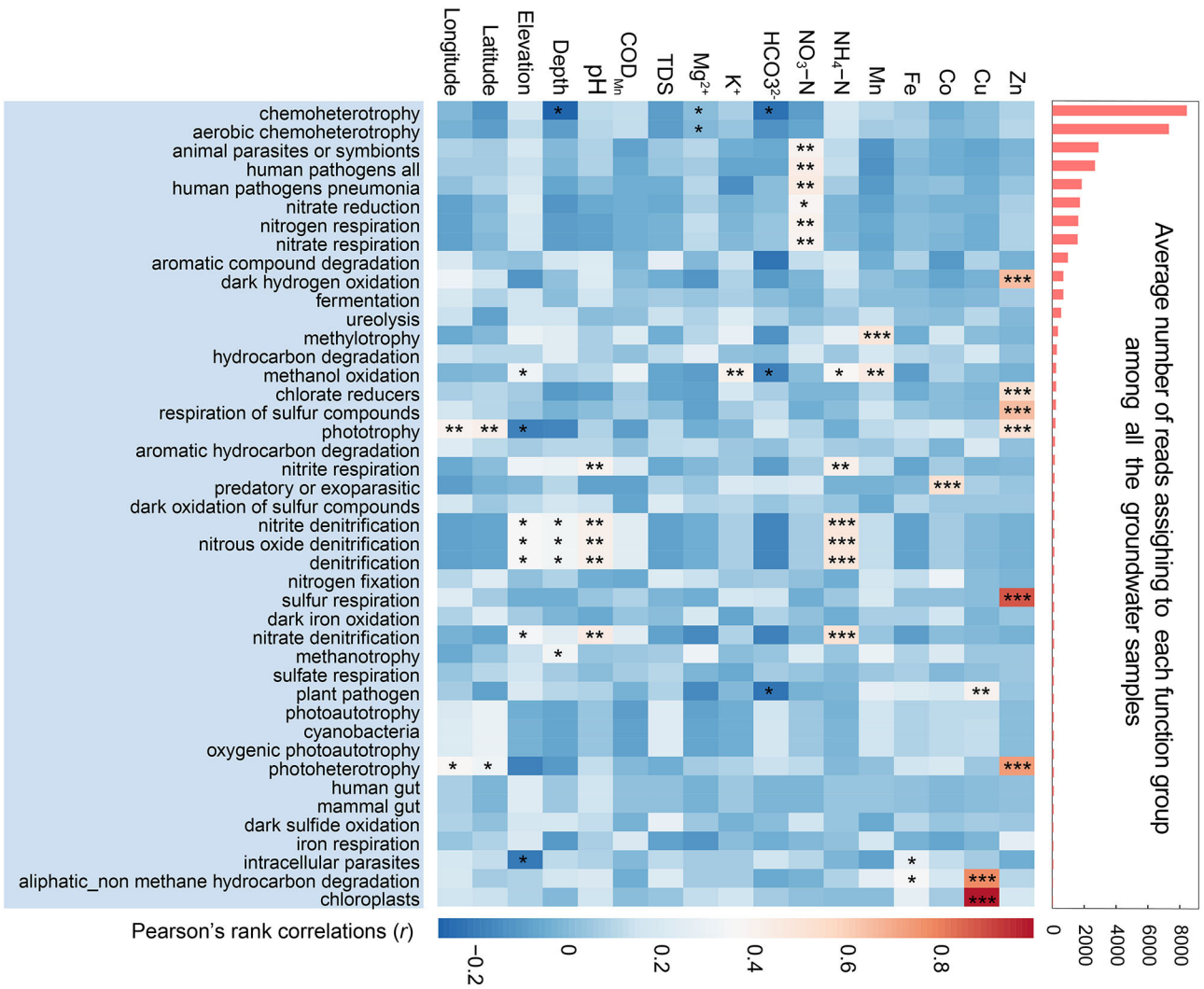

FIGURE 2
Bacterial functional profiles in karst groundwater. The bar chart on the right indicates the average number of reads assigned to each functional group predicted by FAPROTAX. The heatmap on the left shows Spearman's correlations between the abundances of functional groups and environmental variables. The asterisks denoted the significance of statistical tests: ***$p < 0.001$, **$0.001 < p < 0.01$, and *$0.01 < p < 0.05$.

Moreover, CCA results suggested that longitude, well depth, and some geochemical variables (e.g., K^+, Mg^{2+}, and HCO_3^-) significantly impacted the spatial patterns of bacterial communities in karst groundwater (Supplementary Figure 5B).

The results of potential function predicted by FAPROTAX (Figure 2) showed that chemoheterotrophy, especially aerobic chemoheterotrophy, was the most abundant functional group even in such oligotrophic and anoxic subterranean environments, negatively associated with well depth and HCO_3^-. The relatively high abundance of potential functional groups associated with animal parasites and human pathogens in karst groundwater was strongly and positively correlated with the content of NO_3-N. In terms of the functional groups relevant to nitrogenous compound cycles, nitrate reduction, nitrogen respiration, and nitrate respiration were correlated with NO_3-N, while nitrite denitrification, nitrous oxide denitrification, and denitrification were strongly associated with NH_4-N.

3.3. Rare/abundant subcommunities and their environmental responses

Only 151 OTUs (0.62% of total OTUs) were identified as abundant taxa (AT), yet they accounted for 66.0% of the average relative abundance. Conversely, rare taxa (RT) accounted for more than 96.5% of the total OTUs with an average relative abundance of merely 13.6% (Figure 3A). Proteobacteria was the most abundant phylum in both abundant and rare subcommunities, though the proportion richness and relative abundance of AT (73.9 and 66.2% of the sequence and OTUs, separately) were much higher than those of RT (29.0 and 20.0%, $p < 0.05$). Most members of Campilobacterota were identified as AT (5.2%) rather than RT (0.3%), while Patescibacteria and Chloroflexi flourished more in RT (26.6%) than in AT (3.3%).

As shown in Figure 3B, the community similarity of AT was significantly higher than that of total taxa (Wilcoxon rank-sum

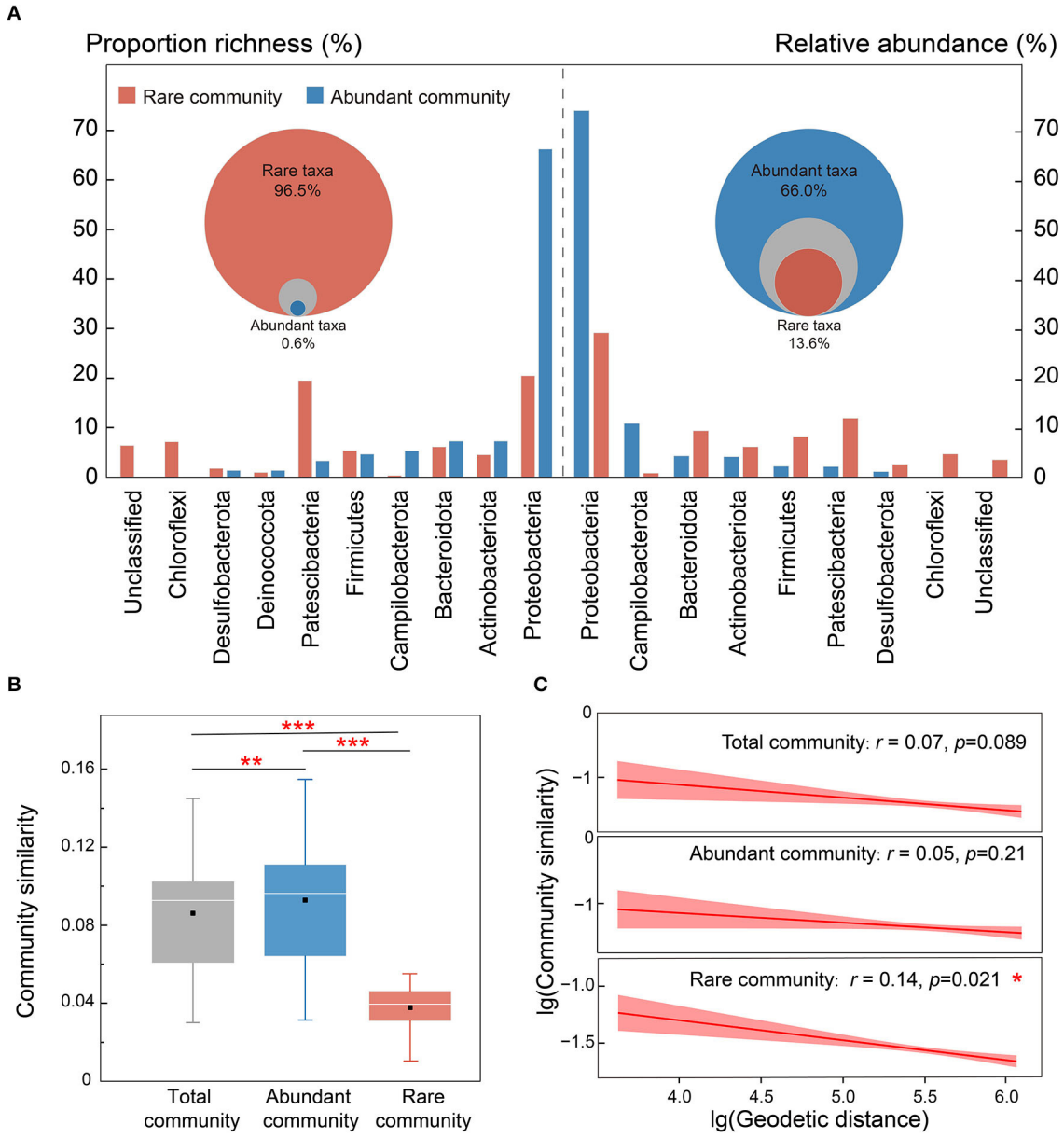

FIGURE 3
The compositional differentiation of rare and abundant subcommunities in karst groundwater. **(A)** Relative abundances of the major phyla in rare and abundant subcommunities. Only the phyla with mean proportional richness or relative abundances of > 1% are shown. Bacterial compositional differences. **(B)** The discrepancy in community similarity between total and abundant taxa in karst groundwater. **(C)** Geodetic distance–decay curves of total and abundant communities based on Bray–Curtis similarities. The colored solid lines indicate the ordinary least squares linear regressions, with the shaded areas representing 95% confidence intervals. Mantel Spearman's *r* and *p*-values are stated. The asterisks denote the significance of statistical tests: $^{***}p < 0.001$, $^{**}0.001 < p < 0.01$, and $^{*}0.01 < p < 0.05$.

test, $p < 0.01$) and RT ($p < 0.001$), suggesting that rare taxa were the main driver of community differences in karst groundwater. The rare subcommunity showed a significant distance-decay relationship (DDR), in which community similarity decreased with increasing geographic distance (Wu et al., 2019), while no significant DDR was observed for the abundant subcommunity (Figure 3C), indicating that AT was less constrained by geographic distance in karst groundwater. The rare subcommunity exhibited broader environmental threshold ranges in response to most environmental variables than the abundant subcommunity, based on the TITAN2 analysis (Figure 4A and Supplementary Figure 7). Notably, the environmental threshold ranges of Na^+ (Valuerare = 4.47; Valueabundant = 1.0) and Cl^- (Valuerare = 3.2; Valueabundant =0.75) for the rare subcommunity were most significantly higher than those of the abundant subcommunity, whereas only those of SO_4^{2-} were higher for the abundant subcommunity (Valuerare = 1.1; Valueabundant = 8.9). As the results of VPA (Figure 4B), 3.5%, 1.8%, and 20.3% of the variation of the abundant subcommunity were explained by geographic distance, environmental variables, and their interactions respectively, and the proportions of explaining were much higher than that of the rare subcommunity (2.5, 1.0, and

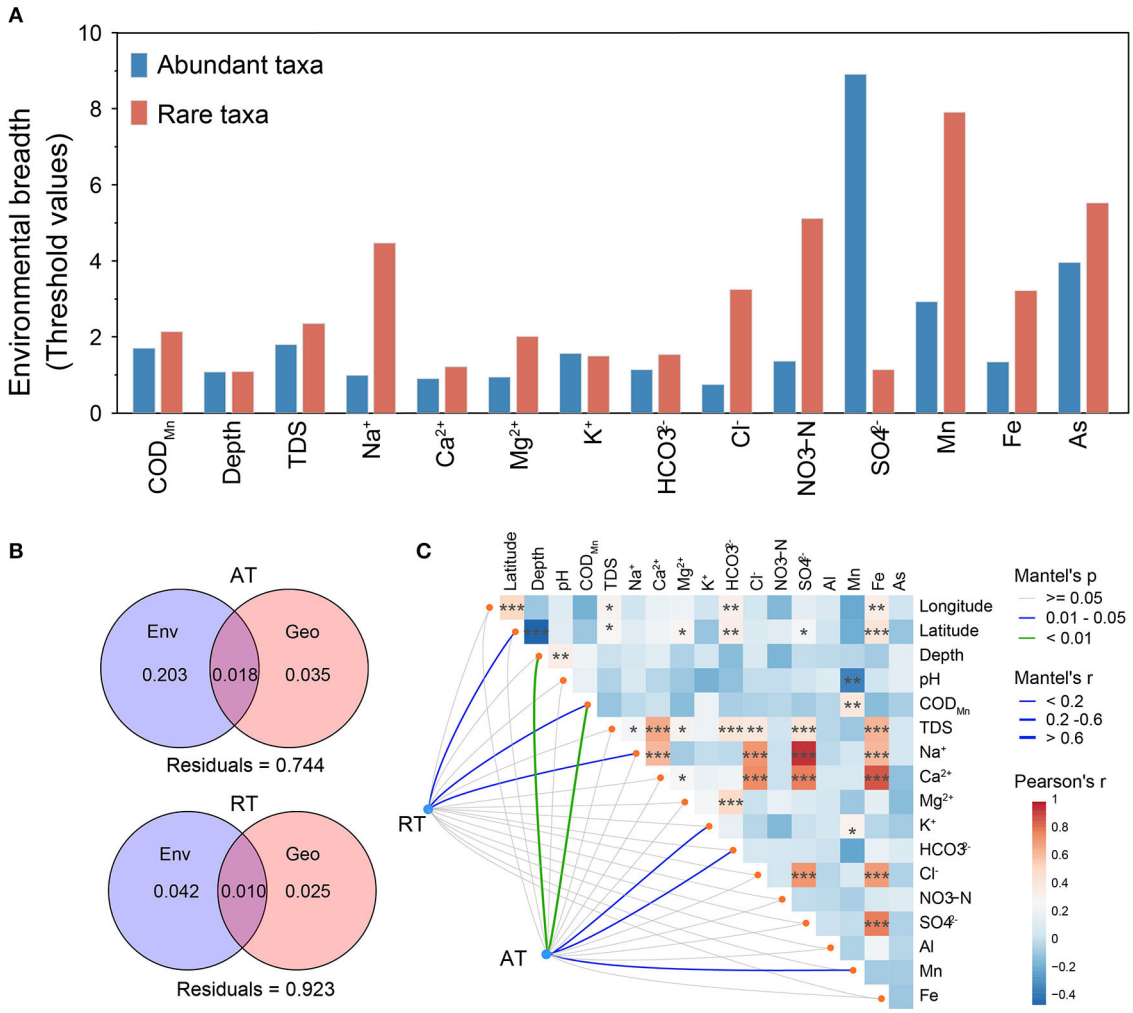

FIGURE 4
Environmental drivers of abundant and rare subcommunities in karst groundwater. **(A)** The environmental breadth of groundwater physicochemical variables for abundant and rare subcommunities is estimated through threshold indicator taxon analyses (TITAN). The threshold value ranges were standardized to non-dimensionalize selected physicochemical variables. **(B)** Variance partition analysis shows the relative contributions of environmental (Env.) and geographic (Geo.) factors and their combined effect on community variations. **(C)** The response of the rare and abundant subcommunities to environmental variables based on Mantel tests. The edge color indicates Mantel's *p*-value, and the width of the edges indicates Mantel's *r*-value. Pearson's correlation coefficients between environmental variables are displayed with the color gradient. All the asterisks denote the significance of statistical tests: ***$p < 0.001$, **$0.001 < p < 0.01$, and *$0.01 < p < 0.05$.

4.2%, respectively). Mantel and CCA results further confirmed that the structures of rare subcommunity were significantly affected by geographic factors (i.e., latitude and longitude) rather than hydrochemical factors, while well depth, K^+, HCO_3^-, NO_3-N, COD_{Mn}, and some metals (e.g., Mn and As) impacted the spatial distribution of abundant subcommunity in karst groundwater (Figure 4C and Supplementary Figure 8).

3.4. Co-occurrence network of bacterial communities in karst groundwater

A bacterial co-occurrence network was constructed based on Spearman's correlations among total OTUs ($|r| > 0.6$ and FDR-adjusted $p < 0.01$, Figure 5A) to reveal the ecological roles and interrelationships of abundant and rare taxa in karst groundwater. The network degree of the bacterial community was distributed according to the power-law distribution pattern, which suggested that the co-occurrence network was reliable, scale-free, and non-random (Bergman and Siegal, 2003; Steele et al., 2011; Barberán et al., 2012). Intermediate OTUs dominated bacterial co-occurrence networks (44.9% of nodes) and connected more closely than rare and abundant taxa (75.6% of edges). The inter-connections between rare and abundant taxa only accounted for 5.1% of total edges, suggesting poor rare-abundant interactions in karst groundwater. AT exhibited stronger inter-connectivity than RT, characterized by a higher average degree of betweenness and clustering coefficient (Figure 5B), which indicated that AT might share similar niches and play more important roles in maintaining bacterial community stability in karst groundwater.

Based on the values of Zi and Pi, the network hub (Zi > 2.5 and Pi > 0.62), module hub (Zi > 2.5), and connector (Pi >

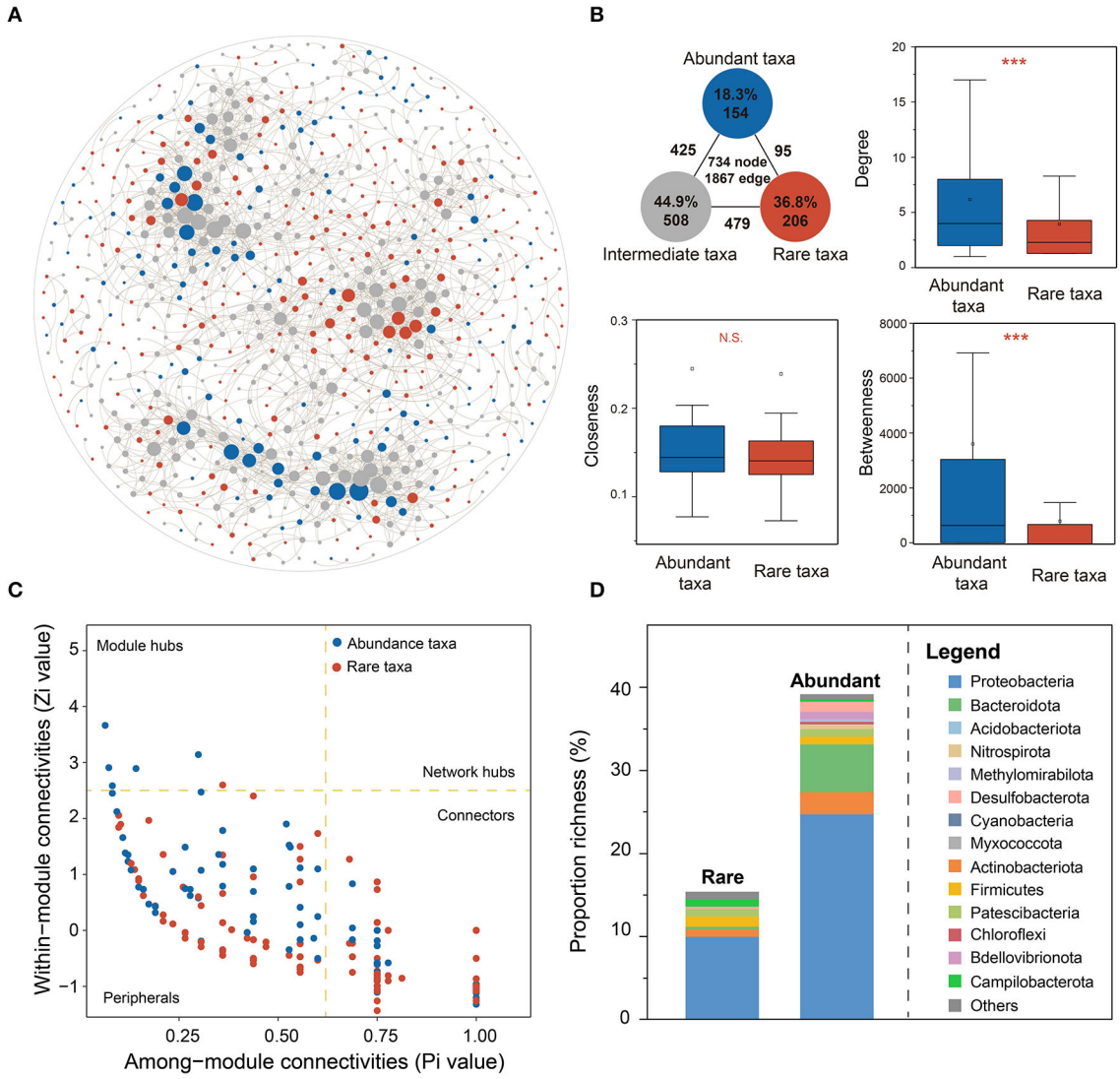

FIGURE 5
Ecological roles of AT and RT in the bacterial co-occurrence network. **(A)** The bacterial co-occurrence network was constructed based on a strong (Spearman's $r > 0.6$) and significant (FDR-adjusted $p < 0.05$) correlation among total OTUs. **(B)** The node-level topological features of AT and RT include degree, betweenness centrality, and closeness centrality. **(C)** Network roles of AT and RT based on the values of Zi and Pi. **(D)** The composition of keystone species for AT and RT. The asterisks denote the significance of statistical tests: $^{***}p < 0.001$, $^{**}0.001 < p < 0.01$, and $^{*}0.01 < p < 0.05$.

0.62) could be identified as the keystone taxa of the co-occurrence network (Figure 5C and Supplementary Table 3). Of 15 module hubs and 332 connectors, more RTs were identified as connectors, while more module hubs were ATs than RTs. The keystone taxa of AT were primarily composed of Proteobacteria (33), Acidobacteriota (4), Patescibacteria (3), and Campilobacterota (3) (Figure 5D), while those of RT mostly belonged to Proteobacteria (82), Bacteroidota (19), Actinobacteriota (9), Desulfobacterota (4), Firmicutes (3), Patescibacteria (3), and Bdellovibrionota (3). Furthermore, we explored how environmental variables influence community stability by unraveling the responses of module hubs to environmental changes (Supplementary Figure 9). As a result, the module hubs of AT exhibited similar responses to environmental variation, which were strongly correlated with well depth, total hardness, TDS, Na^+, Ca^{2+}, Cl^-, and Fe, while module hubs belonging to rare and intermediate taxa were little affected by environmental factors.

3.5. Assembly processes of abundant and rare subcommunities

To investigate the underlying mechanisms of coexistence and spatial distribution of bacterial communities in karst groundwater, we assessed the contributions of deterministic and stochastic processes in the community assembly of abundant and rare taxa by the ecological models (Figure 6). The neutral interpretation of the bacterial community in karst groundwater ($R^2 = 0.424$)

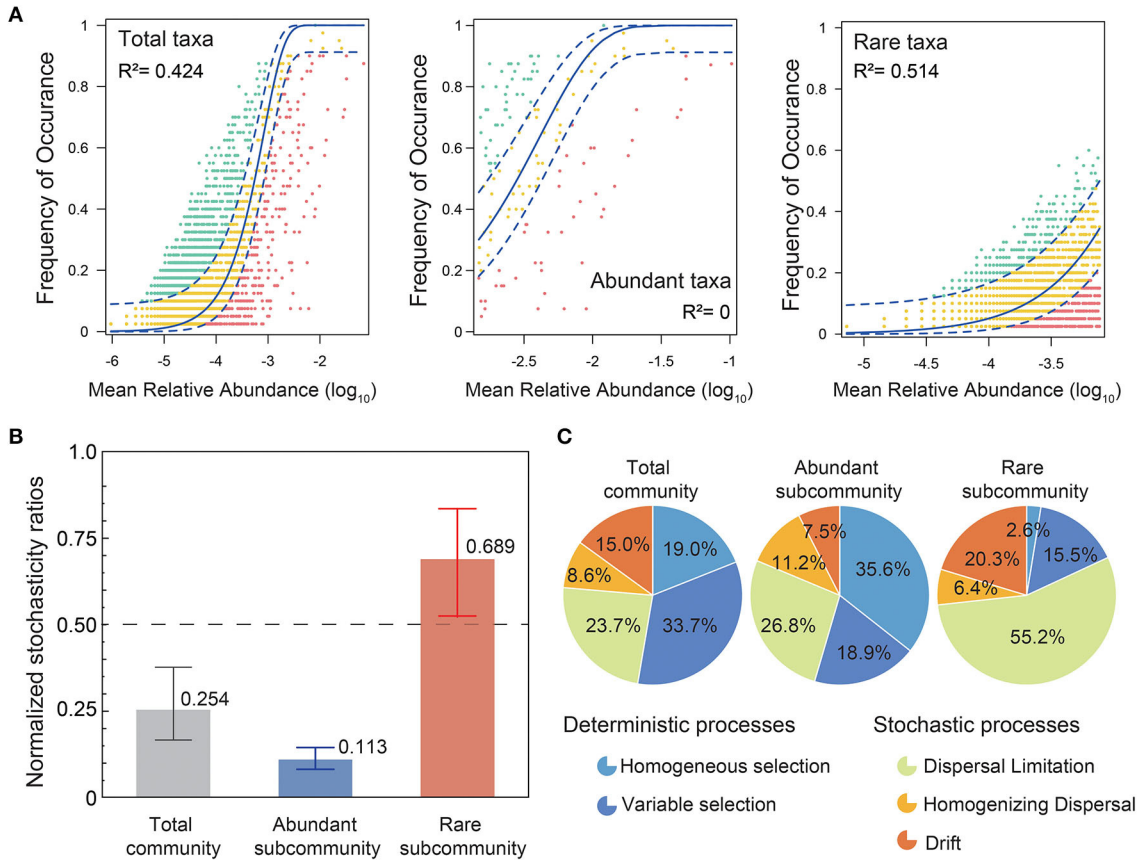

FIGURE 6
Assembly processes of abundant and rare subcommunities. **(A)** The neutral interpretations of total, abundant, and rare subcommunities are based on the neutral community model (NCM). R^2 denotes the fitting goodness of the neutral model. Green circles indicate that OTUs occur more frequently than predicted by the NCM, while red circles represent those that occur less frequently than predicted. The solid blue line shows the best-fitting neutral models and the dashed lines depict the 95% confidence intervals for the models. **(B)** Mean values of normalized stochasticity ratios (NST) of total, abundant, and rare subcommunities, with 0.5 taken as the boundary point between more deterministic (<0.5) and more stochastic (>0.5) assemblies. **(C)** Null model analysis of deterministic and stochastic processes in the community assemblies of total, abundant, and rare subcommunities. Deterministic processes include variable selection and homogeneous selection, while stochastic processes include dispersal limitation, homogenizing dispersal, and drift.

was much lower than in other natural surface ecosystems (Burns et al., 2016; Liu et al., 2018), which indicated that bacteria in karst groundwater suffered a stronger dispersal limitation than in surface ecosystems. The neutral interpretation (R^2 = 0.514) of rare subcommunities was much higher than that of abundant subcommunities. Based on NST, the total community, especially the abundant subcommunity, was mainly governed by deterministic processes (total: 0.254, abundance: 0.113), while the rare subcommunity was more regulated by stochasticity (mean NSTs = 0.689; Figure 5B). Furthermore, the null model analysis suggested that deterministic processes (54.5%) prevailed primarily in abundant subcommunity assemblies, while the majority of rare taxa (81.9%) were controlled by stochastic processes (Figure 5C). Particularly, dispersal limitation contributed a larger proportion to the assembly of rare subcommunities (55.2%) compared with abundant ones (26.8%), while homogeneous selection influenced the abundant taxa (35.6%) more than the rare taxa (2.6%). Homogenizing dispersal had less influence on both rare and abundant taxa.

4. Discussion

4.1. Potential impacts of hydrogeological properties and human activities on bacterial structure

Revealing the distribution pattern, environmental drivers, and assembly processes of bacterial communities is crucial for understanding the ecological function and health of karst groundwater (Gao et al., 2021; Tang et al., 2022). In this study, we conducted a comprehensive investigation of the distribution of groundwater bacterial communities based on 64 pristine groundwater samples across southwest China, one of the largest karst landforms in the world. The burial condition of groundwater primarily determines the hydrological connectivity and chemical characteristics of karst groundwater (Hill and Polyak, 2010; Larned, 2012). We observed a significant discrepancy in bacterial composition between phreatic and confined water, and the community similarity in phreatic water was significantly higher

than that in confined water ($p < 0.01$). Confined aquifers are regarded as strictly anaerobic, oligotrophic, and isolated environments, providing ideal targets for the study of microbial evolution and environmental adaptation (Yan et al., 2021), while phreatic aquifers are usually closer to the Earth's surface, where groundwater is directly recharged by rainfall or snowmelt (Oliver et al., 2022). Thus, it was not surprising to observe the discrepancy in microbial structures between the two groundwater types. Meanwhile, the community similarity in phreatic water was higher than that in confined water, which could be attributed to the difference in hydrological connectivity between phreatic and confined water. Generally, phreatic aquifers in the karst region with characterized large voids, high flow velocities, and rapid infiltrations tend to strengthen microbial dispersal, while confined aquifers overlined by relatively impermeable rock or clay would reduce hydraulic connection and limit microbial diffusion (Flynn et al., 2012).

The specific hydraulic and hydrogeologic characteristics of karst aquifers render them highly vulnerable to pollution from human activities (Kacaroglu, 1999; Katsanou et al., 2013). Subject to the impacts of increasing pressure from heavy subterranean resource exploitation and anthropogenic contamination (Reberski et al., 2022), the potential ecological consequences (e.g., biodiversity loss) of karst aquifers have received extensive attention (Tang et al., 2022). In this study, we found that the potential functional groups associated with parasites and pathogens were much higher in karst groundwater than in other groundwater habitats (Liu et al., 2022), which were positively correlated with groundwater NO_3-N content. Given that nitrate in groundwater is a typical anthropogenic pollutant and is widely used to indicate anthropogenic influences (Liu et al., 2015b; Opsahl et al., 2017), the prevalence of potential pathogen functional groups in karst groundwater could be closely linked to the footprints of anthropogenic activities (Stokdyk et al., 2020). Over the past decades, various antimicrobials, antibiotic-resistance genes, hormones, and microbial pathogens have been found widely distributed in groundwater (Manamsa et al., 2016) and are highly relevant to livestock and clinical waste (Hubbard et al., 2020). This study highlighted that bacteria would be a potential indicator for human impact evaluation of groundwater pathogen risk and drinking water safety. However, given the limitations of the potential functions predicted by FAPROTAX, the complementary confirmatory experiments combined with metabolome or transcriptome analyses would be further used to verify the feasibility of the bacterial indicator.

4.2. Ecological differentiation of rare and abundant taxa in karst groundwater

The bacterial community of karst groundwater in southwest China consists of a few abundant taxa and a high proportion of rare taxa, which is consistent with the most natural ecosystems (He et al., 2022; Zhao et al., 2022). As the most typical habitat generalist (Tully et al., 2018), Proteobacteria was observed to be the most abundant phylum in karst groundwater, with a higher proportion of abundant rather than rare subcommunities. These abundant taxa in karst groundwater may share some phenotypic traits or life history strategies to adapt to harsh subterranean habitats. For example, the genus Pseudomonas with the highest relative abundance (12.0%) in karst groundwater has been reported to have low nutritional requirements and can use various refractory organics (Vasquez-Ponce et al., 2018). On the contrary, the rare subcommunity harbored much higher phenotypic diversity and abundance of Patescibacteria and Chloroflexi than the abundant subcommunity. The newly defined superphylum Patescibacteria was prevalent in varying aquifer environments (Herrmann et al., 2019; Chaudhari et al., 2021; Ruiz-Gonzalez et al., 2022). In the absence of numerous biosynthetic capacities and stress response systems, it is confirmed that most Patescibacteria cannot live alone but be mutualists with other microbes, limiting their relative abundance in groundwater (Nelson and Stegen, 2015; Lemos et al., 2019). The majority of Chloroflexi members were classically phototrophic and were found to be abundant in surface water (Burganskaya et al., 2018; Gaisin et al., 2019). Although most Chloroflexi were rare taxa in groundwater, intensive study of these Chloroflexi members may provide a novel phototrophic mechanism in the deep biosphere (Zheng et al., 2022).

Revealing the underlying mechanisms of species coexistence within a specific ecological niche is of great importance for ecosystem restoration and environmental management (Yang Y. et al., 2022; Yang Z. et al., 2022). Based on bacterial co-occurrence networks in karst groundwater (Figure 6C), the positive correlations of mutualism, parasitism, or commensalism were prevalent among groundwater bacteria, whereas the negative correlations of competition for space and resources less occurred, indicating that bacterial co-occurrence based on cooperative interrelation was vital to community stability even in oligotrophic environments (Herren and McMahon, 2017). The node-level topological features of AT were significantly higher than those of RT, indicating that AT was more frequently central in the network. The key taxa of the abundant subcommunity mainly were module hubs, which were regarded as integral elements within distinct modules and may mediate important functions (Shi et al., 2020). The keystone species of RT were mainly identified as connectors, which contribute to community recovery under disturbance and might provide a buffer against environmental fluctuations (Yang Y. et al., 2022; Yang Z. et al., 2022). Previous studies found that rare taxa representing a substantial amount of ecological potential might achieve "rare-to-prevalent" dynamics over time as a response to disturbance events to maintain community stability and ecological function (Lynch and Neufeld, 2015; Nyirabuhoro et al., 2020). Generally, connectors are more conserved than module hubs (Guimera and Amaral, 2005). The keystone species of AT were more sensitive to various environments than those of the rare subcommunity, which supported the view that RT has a disproportionately large effect on ecological stability relative to its abundance (Shade et al., 2014; Jiao and Lu, 2020).

4.3. Higher environmental adaptation and stochasticity of rare than abundant taxa

Our results revealed that RT in karst groundwater was environmentally less constrained and showed wider environmental thresholds in response to most hydrochemical factors compared

with AT. The results were consistent with those studies carried out in regions that suffered strong changes (He et al., 2022), but in contrast to most studies on surface soil, which tends to be rich in nutrients (Jiao and Lu, 2020). He et al. found that the stronger environmental adaptability of RT than AT during the reforestation ecological succession process was mainly associated with soil electrical conductivity (He et al., 2022). In general, rare taxa are regarded as a vital repository of specialists, while abundant taxa mainly comprise generalists (Xu et al., 2021). Specialists could be more competitive within a narrow niche breadth (Friedman et al., 2017), while generalists are more adaptable to habitat variations (Wang S. et al., 2019; Wang Y. et al., 2019). Karst aquifers in southeast China with anisotropic hydraulic connections would provide enough wide niche breadth for various specialists to survive (Opsahl et al., 2017), which increased the diversity of the rare subcommunity and may further enhance the important roles of rare taxa against environmental fluctuations (Yang Y. et al., 2022; Yang Z. et al., 2022). Therefore, the higher proportion of RT (specialists) would provide an important adaptability strategy for the bacterial community in extreme environments (e.g., karst groundwater), which is of great significance to broadening environmental threshold ranges and maintaining community stability.

Nowadays, there is still an ongoing debate about the relative contributions of deterministic and stochastic processes in the community assembly of rare and abundant taxa (Li et al., 2021; Yang Y. et al., 2022; Yang Z. et al., 2022). In this study, bacterial community assembly in karst groundwater was dominated by deterministic processes. More specifically, community assembly is mainly governed by variable selection (33.7%) rather than homogeneous selection (19.0%). Previous studies have demonstrated that variable selection (i.e., heterogeneous selection) caused by environmental heterogeneity would result in community divergence across localities and has been regarded as the most important ecological process of community assembly in natural habitats, especially in extreme environments (Wang et al., 2013; Evans et al., 2017). Meanwhile, we found that neutral processes had a significant impact on shaping the RT compared with the AT. Deterministic processes, especially homogeneous selection (35.6%), tended to be more important in shaping the subcommunity assembly of AT, while stochastic processes dominated by dispersal limitation (55.2%) and drift (20.3%) were the main assembly processes of rare subcommunities. Homogeneous selection could result in low compositional turnover (Zhou et al., 2013; Wang et al., 2020), which supported the result of much higher community similarity among abundant than rare subcommunities, whereas stochastic processes, such as ecological drift driven by stochastic demographic events, could result in dissimilar communities among localities even though sharing similar environmental conditions; thus, RT exhibited more randomness in phylogenetic clustering (Zhou et al., 2013; Stegen et al., 2015). Furthermore, higher dispersal limitations of RT could enhance the distance–decay relationship and result in high spatial species turnover (Zhou and Ning, 2017; Wang et al., 2020).

5. Conclusion

Our study provided a comprehensive investigation of the bacterial communities in karst groundwater in southwest China. Proteobacteria was the most abundant phylum in both AT and RT, while Patescibacteria and Chloroflexi flourished more in RT than AT. AT was more frequently central in the network and played important roles in maintaining bacterial community stability. Compared with AT, RT in karst groundwater exhibited stronger environmental adaptability and might contribute to community recovery under disturbance and provide a buffer against environmental fluctuations. Homogeneous selection belonging to deterministic processes dominated the abundant bacterial assembly, whereas dispersal limitation and drift belonging to stochastic processes governed the rare taxa. Meanwhile, we linked the high abundance of potential functional groups associated with parasites and pathogens in karst groundwater to frequent regional anthropogenic activities. This study significantly advances the knowledge of ecological differentiation and assembly processes of rare and abundant bacteria in typical karst aquifers and contributes to the microbial ecological prediction of ecosystem health and drinking water safety in karst regions.

Data availability statement

The datasets presented in this study can be found in online repositories. The names of the repository/repositories and accession number(s) can be found below: NCBI - PRJNA692269.

Author contributions

SZ and BL designed the research and wrote the manuscript. SZ performed the research with the help of BH, JZ, YW, XX, and JN. All authors contributed new ideas and participated in the interpretation of the findings. All authors contributed to the article and approved the submitted version.

Funding

Financial support was from the National Natural Science Foundation of China under Grant Nos. 51721006 and 91647211.

Acknowledgments

The authors are grateful for support from Majorbio Company (Shanghai, China) and the Geo-Cloud Database of the China Geological Survey.

Conflict of interest

The authors declare that the research was conducted in the absence of any commercial or financial relationships that could be construed as a potential conflict of interest.

Publisher's note

All claims expressed in this article are solely those of the authors and do not necessarily represent those of

their affiliated organizations, or those of the publisher, the editors and the reviewers. Any product that may be evaluated in this article, or claim that may be made by its manufacturer, is not guaranteed or endorsed by the publisher.

Supplementary material

The Supplementary Material for this article can be found online at: https://www.frontiersin.org/articles/10.3389/fmicb.2023.1111383/full#supplementary-material

References

Archer, S. D. J., Lee, K. C., Caruso, T., Maki, T., Lee, C. K., Carys, S. C., et al. (2019). Airborne microbial transport limitation to isolated Antarctic soil habitats. *Nat. Microbiol.* 4, 925–932. doi: 10.1038/s41564-019-0370-4

Bahram, M., Kohout, P., Anslan, S., Harend, H., Abarenkov, K., and Tedersoo, L. (2016). Stochastic distribution of small soil eukaryotes resulting from high dispersal and drift in a local environment. *ISME J.* 10, 885–896. doi: 10.1038/ismej.2015.164

Barberán, A., Bates, S. T., Casamayor, E. O., and Fierer, N. (2012). Using network analysis to explore co-occurrence patterns in soil microbial communities. *ISME J.* 6, 343–351. doi: 10.1038/ismej.2011.119

Bergman, A., and Siegal, M. L. (2003). Evolutionary capacitance as a general feature of complex gene networks. *Nature* 424, 549–552. doi: 10.1038/nature01765

Burganskaya, E. I., Bryantseva, I. A., Gaisin, V. A., Grouzdev, D. S., Rysina, M. S., Barkhutova, D. D., et al. (2018). Benthic phototrophic community from Kiran soda lake, south-eastern Siberia. *Extremophiles* 22, 211–220. doi: 10.1007/s00792-017-0989-0

Burns, A. R., Stephens, W. Z., Stagaman, K., Wong, S., Rawls, J. F., Guillemin, K., et al. (2016). Contribution of neutral processes to the assembly of gut microbial communities in the zebrafish over host development. *ISME J.* 10, 655–664. doi: 10.1038/ismej.2015.142

Caporaso, J. G., Lauber, C. L., Walters, W. A., Berg-Lyons, D., Lozupone, C. A., Turnbaugh, P. J., et al. (2011). Global patterns of 16S rRNA diversity at a depth of millions of sequences per sample. *Proc. Natl. Acad. Sci. U. S. A.* 108, 4516–4522. doi: 10.1073/pnas.1000080107

Carlson, H. K., Price, M. N., Callaghan, M., Aaring, A., Chakraborty, R., Liu, H., et al. (2019). The selective pressures on the microbial community in a metal-contaminated aquifer. *ISME J.* 13, 937–949. doi: 10.1038/s41396-018-0328-1

Chaudhari, N. M., Overholt, W. A., Figueroa-Gonzalez, P. A., Taubert, M., Bornemann, T. L. V., Probst, A. J., et al. (2021). The economical lifestyle of CPR bacteria in groundwater allows little preference for environmental drivers. *Environ. Microbiol.* 16, 395. doi: 10.1186/s40793-021-00395-w

Edgar, R. C. (2013). UPARSE: highly accurate OTU sequences from microbial amplicon reads. *Nat. Methods* 10, 996–998. doi: 10.1038/nmeth.2604

Evans, S., Martiny, J. B. H., and Allison, S. D. (2017). Effects of dispersal and selection on stochastic assembly in microbial communities. *ISME J.* 11, 176–185. doi: 10.1038/ismej.2016.96

Flynn, T. M., Sanford, R. A., Santo Domingo, J. W., Ashbolt, N. J., Levine, A. D., and Bethke, C. M. (2012). The active bacterial community in a pristine confined aquifer. *Water Resour. Res.* 48, 11568. doi: 10.1029/2011WR011568

Fodelianakis, S., Moustakas, A., Papageorgiou, N., Manoli, O., Tsikopoulou, I., Michoud, G., et al. (2017). Modified niche optima and breadths explain the historical contingency of bacterial community responses to eutrophication in coastal sediments. *Mol. Ecol.* 26, 2006–2018. doi: 10.1111/mec.13842

Friedman, J., Higgins, L. M., and Gore, J. (2017). Community structure follows simple assembly rules in microbial microcosms. *Nat. Ecol. Evol.* 1, 109. doi: 10.1038/s41559-017-0109

Gaisin, V. A., Burganskaya, E. I., Grouzdev, D. S., Ashikhmin, A. A., Kostrikinal, N. A., Bryantseva, I. A., et al. (2019). "Candidatus Viridilinea mediisalina", a novel phototrophic *Chloroflexi bacterium* from a Siberian soda lake. *FEMS Microbiol. Lett.* 366, fnz043. doi: 10.1093/femsle/fnz043

Gao, J., Zuo, L., and Liu, W. (2021). Environmental determinants impacting the spatial heterogeneity of karst ecosystem services in Southwest China. *Land Degrad. Dev.* 32, 1718–1731. doi: 10.1002/ldr.3815

Guimera, R., and Amaral, L. A. N. (2005). Functional cartography of complex metabolic networks. *Nature* 433, 895–900. doi: 10.1038/nature03288

Guo, X., Feng, J., Shi, Z., Zhou, X., Yuan, M., Tao, X., et al. (2018). Climate warming leads to divergent succession of grassland microbial communities. *Nat. Clim. Change* 8, 813–818. doi: 10.1038/s41558-018-0254-2

Hartmann, A., Goldscheider, N., Wagener, T., Lange, J., and Weiler, M. (2014). Karst water resources in a changing world: review of hydrological modeling approaches. *Rev. Geophys.* 52, 218–242. doi: 10.1002/2013RG000443

He, Z., Liu, D., Shi, Y., Wu, X., Dai, Y., Shang, Y., et al. (2022). Broader environmental adaptation of rare rather than abundant bacteria in reforestation succession soil. *Sci. Total Environ.* 828, 154364. doi: 10.1016/j.scitotenv.2022.154364

Herren, C. M., and McMahon, K. D. (2017). Cohesion: a method for quantifying the connectivity of microbial communities. *ISME J.* 11, 2426–2438. doi: 10.1038/ismej.2017.91

Herrmann, M., Wegner, C. E., Taubert, M., Geesink, P., Lehmann, K., Yan, L., et al. (2019). Predominance of Cand. Patescibacteria in groundwater is caused by their preferential mobilization from soils and flourishing under oligotrophic conditions. *Front. Microbiol.* 10, 1407. doi: 10.3389/fmicb.2019.01407

Hill, C. A., and Polyak, V. J. (2010). Karst hydrology of Grand Canyon, Arizona, USA. *J. Hydrol.* 390, 169–181. doi: 10.1016/j.jhydrol.2010.06.040

Hubbard, L. E., Givens, C. E., Griffin, D. W., Iwanowicz, L. R., Meyer, M. T., and Kolpin, D. W. (2020). Poultry litter as potential source of pathogens and other contaminants in groundwater and surface water proximal to large-scale confined poultry feeding operations. *Sci. Total Environ.* 735, 139459. doi: 10.1016/j.scitotenv.2020.139459

Jiao, S., and Lu, Y. (2020). Abundant fungi adapt to broader environmental gradients than rare fungi in agricultural fields. *Glob. Chang. Biol.* 26, 4506–4520. doi: 10.1111/gcb.15130

Kacaroglu, F. (1999). Review of groundwater pollution and protection in karst areas. *Water Air Soil Pollut.* 113, 337–356. doi: 10.1023/A:1005014532330

Katsanou, K., Siavalas, G., and Lambrakis, N. (2013). Geochemical controls on fluoriferous groundwaters of the Pliocene and the more recent aquifers: the case of Aigion region, Greece. *J. Contam. Hydrol.* 155, 55–68. doi: 10.1016/j.jconhyd.2013.08.009

Kurm, V., Geisen, S., and Hol, W. H. G. (2019). A low proportion of rare bacterial taxa responds to abiotic changes compared with dominant taxa. *Environ. Microb.* 21, 750–758. doi: 10.1111/1462-2920.14492

Larned, S. T. (2012). Phreatic groundwater ecosystems: research frontiers for freshwater ecology. *Freshw. Biol.* 57, 885–906. doi: 10.1111/j.1365-2427.2012.02769.x

Lee, S. H., Kim, T. S., and Park, H. D. (2021). Transient-rare bacterial taxa are assembled neutrally across temporal scales. *Microbes Environ.* 36, 20110. doi: 10.1264/jsme2.ME20110

Lemos, L. N., Medeiros, J. D., Dini-Andreote, F., Fernandes, G. R., Varani, A. M., Oliveira, G., et al. (2019). Genomic signatures and co-occurrence patterns of the ultra-small Saccharimonadia (phylum CPR/Patescibacteria) suggest a symbiotic lifestyle. *Mol. Ecol.* 28, 4259–4271. doi: 10.1111/mec.15208

Li, H., Wang, S., Bai, X., Luo, W., Tang, H., Cao, Y., et al. (2018). Spatiotemporal distribution and national measurement of the global carbonate carbon sink. *Sci. Total Environ.* 643, 157–170. doi: 10.1016/j.scitotenv.2018.06.196

Li, L., Pujari, L., Wu, C., Huang, D., Wei, Y., Guo, C., et al. (2021). Assembly processes and co-occurrence patterns of abundant and rare bacterial community in the Eastern Indian Ocean. *Front. Microbiol.* 12, 616956. doi: 10.3389/fmicb.2021.616956

Li, Y., Song, T., Lai, Y., Huang, Y., Fang, L., and Chang, J. (2022). Status, mechanism, suitable distribution areas and protection countermeasure of invasive species in the karst areas of Southwest China. *Front. Environ. Sci.* 10, 957216. doi: 10.3389/fenvs.2022.957216

Liu, L., Luo, D. L., Wang, L., Huang, Y. D., and Chen, F. F. (2021). Dynamics of freezing/thawing indices and frozen ground from 1900 to 2017 in the upper Brahmaputra River Basin, Tibetan Plateau. *Adv. Clim. Chang. Res.* 12, 6–17. doi: 10.1016/j.accre.2020.10.003

Liu, L., Yang, J., Yu, Z., and Wilkinson, D. M. (2015a). The biogeography of abundant and rare bacterioplankton in the lakes and reservoirs of China. *ISME J.* 9, 2068–2077. doi: 10.1038/ismej.2015.29

Liu, M., Xu, X., and Sun, A. (2015b). Decreasing spatial variability in precipitation extremes in southwestern China and the local/large-scale influencing factors. *J. Geophys. Res.* 120, 6480–6488. doi: 10.1002/2014JD022886

Liu, S., Chen, Q., Li, J., Li, Y., Zhong, S., Hu, J., et al. (2022). Different spatiotemporal dynamics, ecological drivers and assembly processes of bacterial, archaeal and

fungal communities in brackish-saline groundwater. *Water Res.* 214, 118193–118193. doi: 10.1016/j.watres.2022.118193

Liu, S., Wang, H., Chen, L., Wang, J., Zheng, M., Liu, S., et al. (2020). ComammoxNitrospirawithin the Yangtze River continuum: community, biogeography, and ecological drivers. *ISME J.* 14, 2488–2504. doi: 10.1038/s41396-020-0701-8

Liu, T., Zhang, A. N., Wang, J., Liu, S., Jiang, X., Dang, C., et al. (2018). Integrated biogeography of planktonic and sedimentary bacterial communities in the Yangtze River. *Microbiome* 6, 388. doi: 10.1186/s40168-017-0388-x

Louca, S., Parfrey, L. W., and Doebeli, M. (2016). Decoupling function and taxonomy in the global ocean microbiome. *Science* 353, 1272–1277. doi: 10.1126/science.aaf4507

Lynch, M. D. J., and Neufeld, J. D. (2015). Ecology and exploration of the rare biosphere. *Nat. Rev. Microbiol.* 13, 217–229. doi: 10.1038/nrmicro3400

Magnabosco, C., Lin, L. H., Dong, H., Bomberg, M., Ghiorse, W., Stan-Lotter, H., et al. (2018). The biomass and biodiversity of the continental subsurface. *Nat. Geosci.* 11, 707–717. doi: 10.1038/s41561-018-0221-6

Manamsa, K., Lapworth, D. J., and Stuart, M. E. (2016). Temporal variability of micro-organic contaminants in lowland chalk catchments: new insights into contaminant sources and hydrological processes. *Sci. Total Environ.* 568, 566–577. doi: 10.1016/j.scitotenv.2016.01.146

Nelson, W. C., and Stegen, J. C. (2015). The reduced genomes of Parcubacteria (OD1) contain signatures of a symbiotic lifestyle. *Front. Microb.* 6, 713. doi: 10.3389/fmicb.2015.00713

Ning, D., Deng, Y., Tiedje, J. M., and Zhou, J. (2019). A general framework for quantitatively assessing ecological stochasticity. *Proc. Natl. Acad. Sci. U. S. A.* 116, 16892–16898. doi: 10.1073/pnas.1904623116

Nyirabuhoro, P., Liu, M., Xiao, P., Liu, L., Yu, Z., Wang, L., et al. (2020). Seasonal variability of conditionally rare taxa in the water column bacterioplankton community of subtropical reservoirs in China. *Microb. Ecol.* 80, 14–26. doi: 10.1007/s00248-019-01458-9

Olarinoye, T., Gleeson, T., Marx, V., Seeger, S., Adinehvand, R., Allocca, V., et al. (2020). Global karst springs hydrograph dataset for research and management of the world's fastest-flowing groundwater. *Sci. Data* 7, 5. doi: 10.1038/s41597-019-0346-5

Oliver, K., Cyril, M., Bla,Ž, K., Marko, V., Jaanus, T., and Andres, M. (2022). Surface water and groundwater hydraulics of lowland karst aquifers of Estonia. *J. Hydrol.* 610, 127908. doi: 10.1016/j.jhydrol.2022.127908

Ollivier, C., Lecomte, Y., Chalikakis, K., Mazzilli, N., Danquigny, C., and Emblanch, C. (2019). A QGIS plugin based on the PaPRIKa method for Karst aquifer vulnerability mapping. *Groundwater* 57, 201–204. doi: 10.1111/gwat.12855

Opsahl, S. P., Musgrove, M., and Slattery, R. N. (2017). New insights into nitrate dynamics in a karst groundwater system gained from in situ high-frequency optical sensor measurements. *J. Hydrol.* 546, 179–188. doi: 10.1016/j.jhydrol.2016.12.038

Pedros-Alio, C. (2012). The rare bacterial biosphere. *Ann. Rev. Mar. Sci.* 4. 449–466. doi: 10.1146/annurev-marine-120710-100948

Peng, H., Yang, W., Xiong, S., Li, X., Niu, G., Lu, T., et al. (2022). Hydrochemical characteristics and health risk assessment of groundwater in karst areas of southwest China: a case study of Bama, Guangxi. *J. Clean. Prod.* 341, 130872. doi: 10.1016/j.jclepro.2022.130872

Power, J. F., Carere, C. R., Lee, C. K., Wakerley, G. L. J., Evans, D. W., Button, M., et al. (2018). Microbial biogeography of 925 geothermal springs in New Zealand. *Nat. Commun.* 9, 5020. doi: 10.1038/s41467-018-05020-y

Probst, A. J., Ladd, B., Jarett, J. K., Geller-McGrath, D. E., Sieber, C. M. K., Emerson, J. B., et al. (2018). Differential depth distribution of microbial function and putative symbionts through sediment- hosted aquifers in the deep terrestrial subsurface. *Nat. Microb.* 3, 328–336. doi: 10.1038/s41564-017-0098-y

Reberski, J. L., Terzic, J., Maurice, L. D., and Lapworth, D. J. (2022). Emerging organic contaminants in karst groundwater: a global level assessment. *J. Hydrol.* 604. doi: 10.1016/j.jhydrol.2021.127242

Reddin, C. J., Bothwell, J. H., and Lennon, J. J. (2015). Between-taxon matching of common and rare species richness patterns. *Glob. Ecol. Biogeogr.* 24, 1476–1486. doi: 10.1111/geb.12372

Ruiz-Gonzalez, C., Rodriguez-Pie, L., Maister, O., Rodellas, V., Alorda-Keinglass, A., Diego-Feliu, M., et al. (2022). High spatial heterogeneity and low connectivity of bacterial communities along a Mediterranean subterranean estuary. *Mol. Ecol.* 31, 5745–5764. doi: 10.1111/mec.16695

Sansupa, C., Wahdan, S. F. M., Hossen, S., Disayathanoowat, T., Wubet, T., and Purahong, W. (2021). Can we use functional annotation of prokaryotic taxa (FAPROTAX) to assign the ecological functions of soil bacteria? *Appl. Sci.* 11, 688. doi: 10.3390/app11020688

Shade, A., Jones, S. E., Caporaso, J. G., Handelsman, J., Knight, R., Fierer, N., et al. (2014). Conditionally rare taxa disproportionately contribute to temporal changes in microbial diversity. *Mbio* 5, 14. doi: 10.1128/mBio.01371-14

Shi, Y., Delgado-Baquerizo, M., Li, Y., Yang, Y., Zhu, Y.-G., Penuelas, J., et al. (2020). Abundance of kinless hubs within soil microbial networks are associated with high functional potential in agricultural ecosystems. *Environ. Int.* 142, 105869. doi: 10.1016/j.envint.2020.105869

Shi, Y., Li, Y., Xiang, X., Sun, R., Yang, T., He, D., et al. (2018). Spatial scale affects the relative role of stochasticity versus determinism in soil bacterial communities in wheat fields across the North China Plain. *Microbiome* 6, 4. doi: 10.1186/s40168-018-0409-4

Sloan, W. T., Woodcock, S., Lunn, M., Head, I. M., and Curtis, T. P. (2007). Modeling taxa-abundance distributions in microbial communities using environmental sequence data. *Microb. Ecol.* 53, 443–455. doi: 10.1007/s00248-006-9141-x

Steele, J. A., Countway, P. D., Xia, L., Vigil, P. D., Beman, J. M., Kim, D. Y., et al. (2011). Marine bacterial, archaeal and protistan association networks reveal ecological linkages. *ISME J.* 5, 1414–1425. doi: 10.1038/ismej.2011.24

Stegen, J. C., Lin, X., Fredrickson, J. K., Chen, X., Kennedy, D. W., Murray, C. J., et al. (2013). Quantifying community assembly processes and identifying features that impose them. *ISME J.* 7, 2069–2079. doi: 10.1038/ismej.2013.93

Stegen, J. C., Lin, X., Fredrickson, J. K., and Konopka, A. E. (2015). Estimating and mapping ecological processes influencing microbial community assembly. *Front. Microbiol.* 6, 370. doi: 10.3389/fmicb.2015.00370

Stokdyk, J. P., Firnstahl, A. D., Walsh, J. F., Spencer, S. K., de Lambert, J. R., Anderson, A. C., et al. (2020). Viral, bacterial, and protozoan pathogens and fecal markers in wells supplying groundwater to public water systems in Minnesota, USA. *Water Res.* 178, 115814. doi: 10.1016/j.watres.2020.115814

Tang, X., Xiao, J., Ma, M., Yang, H., Li, X., Ding, Z., et al. (2022). Satellite evidence for China's leading role in restoring vegetation productivity over global karst ecosystems. *For. Ecol. Manag.* 507, 12. doi: 10.1016/j.foreco.2021.120000

Tully, B. J., Wheat, C. G., Glazer, B. T., and Huber, J. A. (2018). A dynamic microbial community with high functional redundancy inhabits the cold, oxic subseafloor aquifer. *ISME J.* 12, 1–16. doi: 10.1038/ismej.2017.187

Vasquez-Ponce, F., Higuera-Llanten, S., Pavlov, M. S., Marshall, S. H., and Olivares-Pacheco, J. (2018). Phylogenetic MLSA and phenotypic analysis identification of three probable novel Pseudomonas species isolated on King George Island, South Shetland, Antarctica. *Braz. J. Microbiol.* 49, 695–702. doi: 10.1016/j.bjm.2018.02.005

Wang, J., Shen, J., Wu, Y., Tu, C., Soininen, J., Stegen, J. C., et al. (2013). Phylogenetic beta diversity in bacterial assemblages across ecosystems: deterministic versus stochastic processes. *ISME J.* 7, 1310–1321. doi: 10.1038/ismej.2013.30

Wang, P., Li, S.-P., Yang, X., Zhou, J., Shu, W., and Jiang, L. (2020). Mechanisms of soil bacterial and fungal community assembly differ among and within islands. *Environ. Microbiol.* 22, 1559–1571. doi: 10.1111/1462-2920.14864

Wang, Q., Garrity, G. M., Tiedje, J. M., and Cole, J. R. (2007). Naive Bayesian classifier for rapid assignment of rRNA sequences into the new bacterial taxonomy. *Appl. Microbiol. Biotechnol.* 73, 5261–5267. doi: 10.1128/AEM.00062-07

Wang, S., Zhu, G., Zhuang, L., Li, Y., Liu, L., Lavik, G., et al. (2019). Anaerobic ammonium oxidation is a major N-sink in aquifer systems around the world. *ISME J.* 14, 151–163. doi: 10.1038/s41396-019-0513-x

Wang, Y., Kou, Y., Li, C., Tu, B., Wang, J., Yao, M., et al. (2019). Contrasting responses of diazotrophic specialists, opportunists, and generalists to steppe types in Inner Mongolia. *Catena* 182, 104168. doi: 10.1016/j.catena.2019.104168

White, W. B. (2002). Karst hydrology: recent developments and open questions. *Eng. Geol.* 65, 85–105. doi: 10.1016/S0013-7952(01)00116-8

Whitman, W. B., Coleman, D. C., and Wiebe, W. J. (1998). Prokaryotes: the unseen majority. *Proc. Natl. Acad. Sci. U. S. A.* 95, 6578–6583. doi: 10.1073/pnas.95.12.6578

Wu, L., Ning, D., Zhang, B., Li, Y., Zhang, P., Shan, X., et al. (2019). Global diversity and biogeography of bacterial communities in wastewater treatment plants. *Nat. Microbiol.* 4, 1183–1195. doi: 10.1038/s41564-019-0426-5

Xu, J., Gao, W., Zhao, B., Chen, M., Ma, L., Jia, Z., et al. (2021). Bacterial community composition and assembly along a natural sodicity/salinity gradient in surface and subsurface soils. *Appl. Soil Ecol.* 157, 103731. doi: 10.1016/j.apsoil.2020.103731

Yan, L., Hermans, S. M., Totsche, K. U., Lehmann, R., Herrmann, M., and Küsel, K. (2021). Groundwater bacterial communities evolve over time in response to recharge. *Water Res.* 201, 117290. doi: 10.1016/j.watres.2021.117290

Yang, Y., Cheng, K., Li, K., Jin, Y., and He, X. (2022). Deciphering the diversity patterns and community assembly of rare and abundant bacterial communities in a wetland system. *Sci. Total Environ.* 838, 156334. doi: 10.1016/j.scitotenv.2022.156334

Yang, Z., Peng, C., Cao, H., Song, J., Gong, B., Li, L., et al. (2022). Microbial functional assemblages predicted by the FAPROTAX analysis are impacted by physicochemical properties, but C, N and S cycling genes are not in mangrove soil in the Beibu Gulf, China. *Ecol. Indic.* 139, 108887. doi: 10.1016/j.ecolind.2022.108887

Yi, M., Fang, Y., Hu, G., Liu, S., Ni, J., and Liu, T. (2022). Distinct community assembly processes underlie significant spatiotemporal dynamics of abundant and rare bacterioplankton in the Yangtze River. *Front. Environ. Sci. Eng.* 16, 4. doi: 10.1007/s11783-021-1513-4

Zhang, C. (2020). Moisture sources for precipitation in Southwest China in summer and the changes during the extreme droughts of 2006 and 2011. *J. Hydrol.* 591, 125333. doi: 10.1016/j.jhydrol.2020.125333

Zhang, R., Xu, X., Liu, M., Zhang, Y., Xu, C., Yi, R., et al. (2018). Comparing evapotranspiration characteristics and environmental controls for three agroforestry ecosystems in a subtropical humid karst area. *J. Hydrol.* 563, 1042–1050. doi: 10.1016/j.jhydrol.2018.06.051

Zhang, W., Wan, W., Lin, H., Pan, X., Lin, L., and Yang, Y. (2022). Nitrogen rather than phosphorus driving the biogeographic patterns of abundant bacterial taxa in a eutrophic plateau lake. *Sci. Total Environ.* 806, 150947. doi: 10.1016/j.scitotenv.2021.150947

Zhao, H., Brearley, F. Q., Huang, L., Tang, J., Xu, Q., Li, X., et al. (2022). Abundant and rare taxa of planktonic fungal community exhibit distinct assembly patterns along coastal eutrophication gradient. *Microb. Ecol.* 22, 1976. doi: 10.1007/s00248-022-01976-z

Zheng, R., Cai, R., Wang, C., Liu, R., and Sun, C. (2022). Characterization of the first cultured representative of "candidatus thermofonsia" clade 2 within chloroflexi reveals its phototrophic lifestyle. *Mbio* 13, 22. doi: 10.1128/mbio.00657-22

Zhou, J., Liu, W., Deng, Y., Jiang, Y. H., Xue, K., He, Z., et al. (2013). Stochastic assembly leads to alternative communities with distinct functions in a bioreactor microbial community. *Mbio* 4, 12. doi: 10.1128/mBio.00584-12

Zhou, J., and Ning, D. (2017). Stochastic community assembly: does it matter in microbial ecology? *Microbiol. Molecul. Biol. R.* 81, 17. doi: 10.1128/MMBR.00002-17

Frontiers in Microbiology

Explores the habitable world and the potential of microbial life

The largest and most cited microbiology journal which advances our understanding of the role microbes play in addressing global challenges such as healthcare, food security, and climate change.

Discover the latest Research Topics

See more →

Frontiers

Avenue du Tribunal-Fédéral 34
1005 Lausanne, Switzerland
frontiersin.org

Contact us

+41 (0)21 510 17 00
frontiersin.org/about/contact